

CISM International Centre for Mechanical Sciences 572
Courses and Lectures

Holm Altenbach
Victor Eremeyev *Editors*

Shell-like Structures

Advanced Theories and Applications



International Centre
for Mechanical Sciences



Springer

CISM International Centre for Mechanical Sciences

Courses and Lectures

Volume 572

Series editors

The Rectors

Friedrich Pfeiffer, Munich, Germany

Franz G. Rammerstorfer, Vienna, Austria

Elisabeth Guazzelli, Marseille, France

The Secretary General

Bernhard Schrefler, Padua, Italy

Executive Editor

Paolo Serafini, Udine, Italy



The series presents lecture notes, monographs, edited works and proceedings in the field of Mechanics, Engineering, Computer Science and Applied Mathematics. Purpose of the series is to make known in the international scientific and technical community results obtained in some of the activities organized by CISM, the International Centre for Mechanical Sciences.

More information about this series at <http://www.springer.com/series/76>

Holm Altenbach · Victor Eremeyev
Editors

Shell-like Structures

Advanced Theories and Applications

 Springer

Editors

Holm Altenbach
Faculty of Mechanical Engineering
Otto-von-Guericke-University Magdeburg
Magdeburg
Germany

Victor Eremeyev
Department of Mechanical Engineering
and Avionics
Rzeszów University of Technology
Podkarpacie, Rzeszów
Poland

ISSN 0254-1971 ISSN 2309-3706 (electronic)
CISM International Centre for Mechanical Sciences
ISBN 978-3-319-42275-6 ISBN 978-3-319-42277-0 (eBook)
DOI 10.1007/978-3-319-42277-0

Library of Congress Control Number: 2016945776

© CISM International Centre for Mechanical Sciences 2017

This work is subject to copyright. All rights are reserved by the Publisher, whether the whole or part of the material is concerned, specifically the rights of translation, reprinting, reuse of illustrations, recitation, broadcasting, reproduction on microfilms or in any other physical way, and transmission or information storage and retrieval, electronic adaptation, computer software, or by similar or dissimilar methodology now known or hereafter developed.

The use of general descriptive names, registered names, trademarks, service marks, etc. in this publication does not imply, even in the absence of a specific statement, that such names are exempt from the relevant protective laws and regulations and therefore free for general use.

The publisher, the authors and the editors are safe to assume that the advice and information in this book are believed to be true and accurate at the date of publication. Neither the publisher nor the authors or the editors give a warranty, express or implied, with respect to the material contained herein or for any errors or omissions that may have been made.

Printed on acid-free paper

This Springer imprint is published by Springer Nature
The registered company is Springer International Publishing AG Switzerland

Preface

Shell-like structures are widely used in engineering as basic structural elements. Such structures are also used in other branches of science as a model of analysis, e.g., in medicine, biology, nanotechnology, etc. New applications are primarily related to new materials—for example, instead of steel or concrete, now one has to analyze laminates, foams, functionally graded materials, shape memory thin films, fullerenes, nanofilms, biological membranes, soft tissues, etc. The new trends in applications demand the improvements of the theoretical foundations of shell theory, since new effects must be taken into account. For example, in the case of small-size shell-like structures (thin films, multi-walled nanotubes), the surface effect plays an important role in the mechanical analysis of these structural elements. On the other hand, the theoretical achievements must be supplemented with the development of consistent numerical tool.

The aim of the CISM course, *Shell-like Structures—Advanced Theories and Applications*, was to present together mathematical aspects of the theory of plates and shells, applications in civil, aerospace and mechanical engineering, as well as other areas. The focus of the course relates to the following problems:

- comprehensive review of the most popular theories of plates and shells;
- relation between 3D and 2D theories;
- presentation of recently developed new refined plates and shells theories such as for example, micropolar theory, or gradient-type theories;
- applications in modeling of complex structures (multi-folded, branching and/or self-intersecting shells, plates and shells made of foams, functionally graded materials, etc.);
- modeling of coupled effects in shells and plates related to electromagnetic and temperature fields, phase transitions, diffusion, etc.;
- applications in modeling of non-classical objects as thin- and nanofilms, nanotubes, and nanoparticles, and biological membranes;
- presentation of actual numerical tools based on finite elements approach.

- During the course the following lectures were presented:
- Holm Altenbach: Thin-walled Structural Elements—Classification, Classical and Advanced Theories, New Applications;
- Victor Eremeyev: Mechanics and Thermodynamics of Micropolar Shells;
- Gennady Mikhasev: Non-Classical Problems on Localized Vibrations and Waves in Thin Shells;
- Paolo Podio-Guidugli: How to Deduce Structure Theories from 3D Elasticity;
- Karam Sab: The Bending-Gradient Theory for Heterogeneous In-Plane Periodic Plates;
- Krzysztof Wisniewski: Selected Topics on Finite Elements for Finite Rotation Shells

In this sense the course was an overview about the theories of plate and shells, the history, and some new developments. In the following chapters the basic material of the course was slightly changed. The chapter names are not always the same like the lecture names.

Finally, the authors of these proceedings acknowledge Prof. Paolo Serafini and Mrs. Silvia Schilgerius from Springer-Austria for supporting the publication and last but not least, Mrs. Paola Agnola from the CISM Secretariat fulfilling all organizing duties.

Magdeburg, Germany
Rzeszów, Poland

Holm Altenbach
Victor Eremeyev

Contents

Thin-Walled Structural Elements: Classification, Classical and Advanced Theories, New Applications	1
Holm Altenbach and Victor Eremeyev	
Basics of Mechanics of Micropolar Shells	63
Victor Eremeyev and Holm Altenbach	
The Bending-Gradient Theory for Laminates and In-Plane Periodic Plates	113
Arthur Lebéé and Karam Sab	
Some Problems on Localized Vibrations and Waves in Thin Shells	149
Gennadi Mikhasev	
Six Lectures in the Mechanics of Elastic Structures	211
Paolo Podio-Guidugli	
Selected Topics on Mixed/Enhanced Four-Node Shell Elements with Drilling Rotation	247
K. Wisniewski and E. Turska	

Thin-Walled Structural Elements: Classification, Classical and Advanced Theories, New Applications

Holm Altenbach and Victor Eremeyev

Abstract Thin structures were existing from the ancient time. From observations of the nature the people understood that thinner means lighter, but stiffness and stability problems arose. This was the starting point for the elaboration of theories analyzing these structures. At that time applications were limited to civil engineering. At present they are used in aerospace engineering as basic elements. Such structures are applied as a model of analysis in other branches too, e.g. mechanical engineering. With the necessity to substitute classical material by new (advanced) materials—instead of steel or concrete, now laminates, foams, nano-films, biological membranes, etc. are used. The new trends in applications demand improvements of the theoretical foundations of the plate and shell theories, since new effects (for example, transverse shear or surface effects) must be taken into account. This contribution is mainly an introduction to the CISM-Course *SHELL-LIKE STRUCTURES: ADVANCED THEORIES AND APPLICATIONS*. After some introduction to the history some examples concerning new applications are discussed. After that main directions in the theory of plates and shells are presented. Finally, various advanced theories are briefly introduced. Other advanced theories are presented in the following chapter.

H. Altenbach (✉)

Chair of Engineering Mechanics, Faculty of Mechanical Engineering,
Otto-von-Guericke-University Magdeburg, Magdeburg, Germany
e-mail: holm.altenbach@ovgu.de

V. Eremeyev

Department of Mechanical Engineering and Avionics,
Rzeszów University of Technology, Podkarpacie, Rzeszów, Poland
e-mail: veremeyev@prz.edu.pl

V. Eremeyev

South Scientific Center of Russian Academy of Science, Rostov on Don, Russia

V. Eremeyev

Department of Mathematics, Mechanics and Computer Science,
South Federal University, Rostov on Don, Russia



Fig. 1 First (simplest) beam theory: **a** Daniel Bernoulli, **b** Leonhard Euler

1 Introduction: Historical Remarks

The starting point for the development of any plate or shell analysis was given by two mathematicians: Daniel Bernoulli¹ and Leonhard Euler² (Fig. 1). They presented a beam theory containing all necessary elements: kinematics, reaction to external loadings and equilibrium statements based on the balances of momentum and of moment of momentum. At the same time they introduce two crucial items

- geometrical linearization and kinematical hypotheses and
- independence of forces and moments (both are the stress resultants) resulting in the independence of the above mentioned balance equations.³

By this way the first engineering theory was formulated. This is an approximate theory and application bounds are not clear. But at the same time the resulting beam equation or the set of coupled equations allows analytical solutions.

Any mechanical theory is related also to some experimental investigations. In the case of plates and shells the studies of Ernst Florens Friedrich Chladni⁴ (Fig. 2) were

¹*January 29 (jul.)/February 8 (greg.) 1700 in Groningen, †March 17, 1782 in Basel.

²*April 15, 1707 in Basel, †September 18, 1783 in St. Petersburg.

³This was analyzed by Clifford Ambrose Truesdell III (*February 18, 1919, †January 14, 2000) in Truesdell 1964.

⁴*November 30, 1756 in Wittenberg, †April 3, 1827 Breslau.

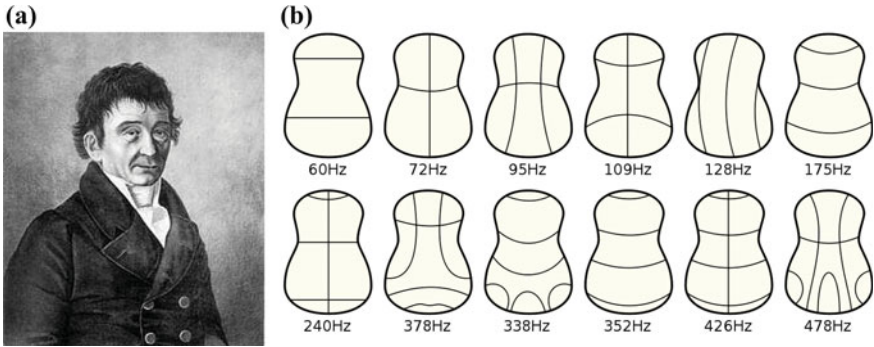


Fig. 2 Music and mechanics: **a** Ernst Florens Friedrich Chladni, **b** Chladni's patterns of a guitar backplate

related to the verification of the theory. At the same time they had relations to the practice. Chladni was a physicist and musician. It was well-known that the sound music results in vibrations. For thin bodies this are mainly deflections. The patterns are the lines of vanishing deflections.

The theory for the analysis of thin plates was not ready when Chladni obtained his results. Only Sophie Germain⁵ (Fig. 3a) had presented the first closed theory. In her paper *Recherches sur la théorie des surfaces élastique* submitted to the Paris Academy of Sciences she offered the first vibration equation for a thin plate

$$N^2 \left(\frac{\partial^4 z}{\partial x^4} + \frac{\partial^4 z}{\partial x^2 \partial y^2} + \frac{\partial^4 z}{\partial y^4} \right) + \frac{\partial^2 z}{\partial t^2} = 0 \quad (1)$$

The submission was checked by the members of the Academy and Joseph-Louis Lagrange⁶ had indicated an error. After improving Sophie Germain was elected as the first female prize winner from the Paris Academy of Sciences (8 January 1816).

The analysis of plates is a part of the general structural analysis the founder of which was Claude Louis Marie Henri Navier⁷ (Fig. 4a). He introduced not only a special type of elastic solutions, but also was able to specify the meaning of N in Germain's equation (1) establishing in 1826 the elastic modulus as a property of materials independent of the second moment of area (with other words he introduced the bending stiffness). At that time it was obvious that any theory of thin bodies is a theory of two coordinates. In 1828 Navier and Siméon-Denis Poisson⁸ (Fig. 4b) were the first who performed a mathematical reduction of three- to two-dimensional equations using power series representations. By this way they deduced equations

⁵* April 1, 1776 in Paris, † June 27, 1831 in Paris.

⁶* January 25, 1736 in Turin as Giuseppe Lodovico Lagrangia or Giuseppe Luigi Lagrangia, † April 10, 1813 in Paris.

⁷* February 10, 1785 in Dijon, † August 21, 1836 in Paris.

⁸* June 21, 1781, † April 25, 1840.

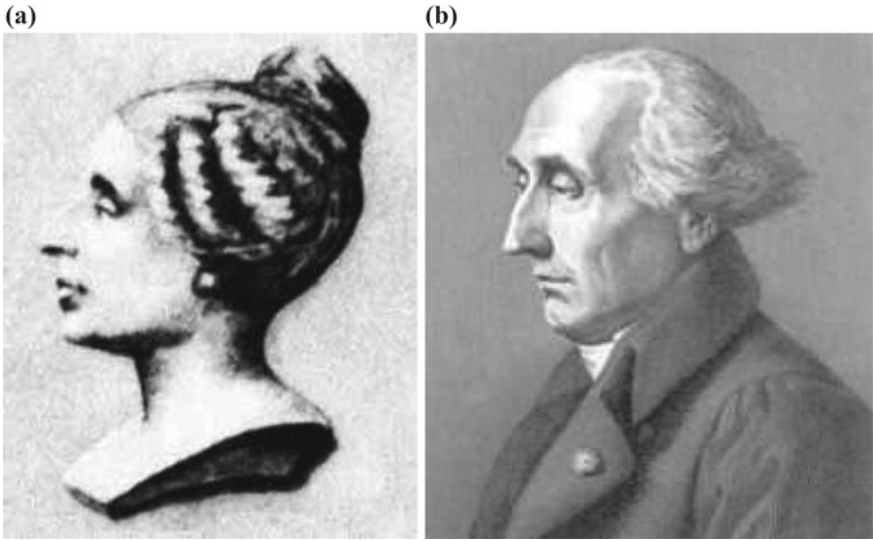


Fig. 3 Beginning of the plate theory in the Paris Academy of Sciences: **a** Sophie German, **b** Joseph-Louis Lagrange

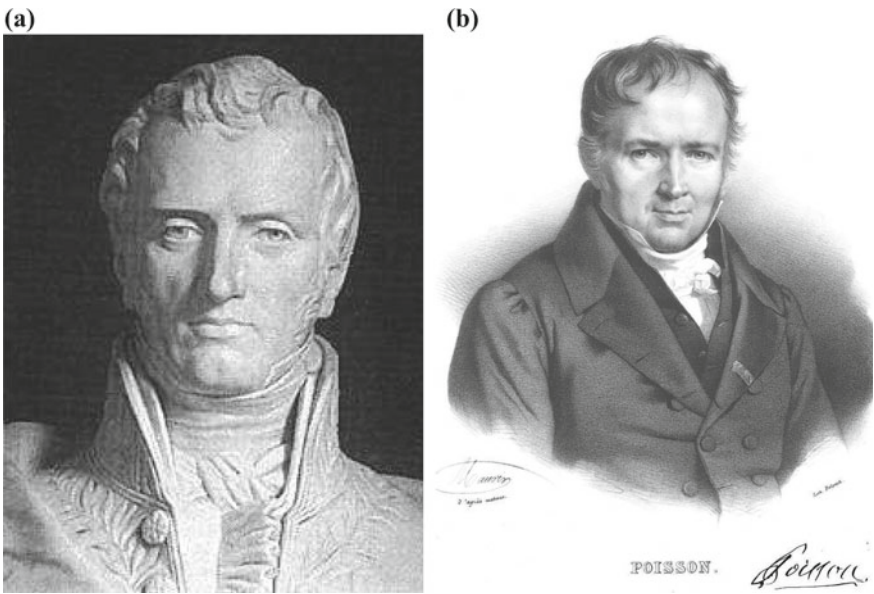


Fig. 4 Bending stiffness and power series: **a** Claude Louis Marie Henri Navier, **b** Siméon-Denis Poisson

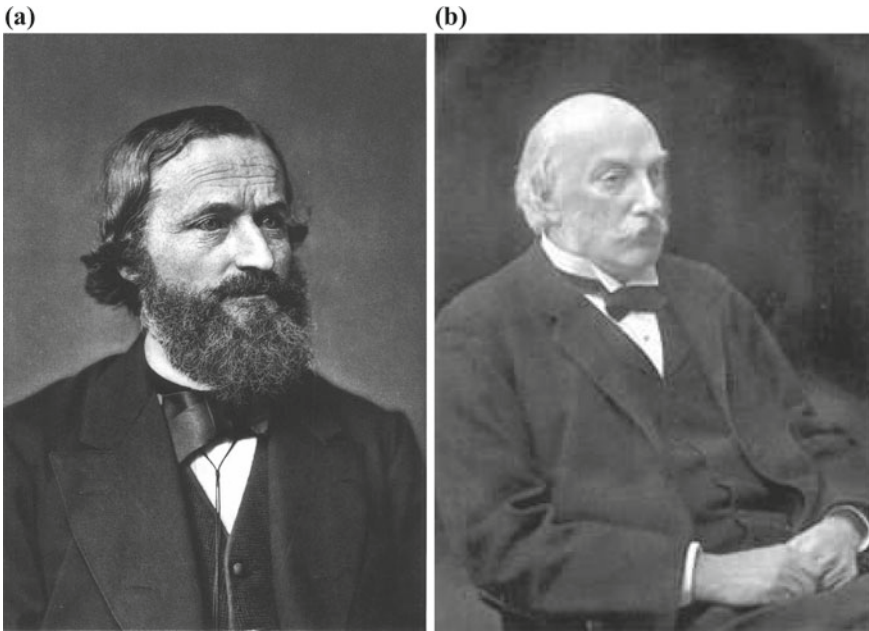


Fig. 5 First plate theory and approximate solution: **a** Gustav Robert Kirchhoff, **b** John William Strutt, 3rd Baron Rayleigh

of equilibrium and free vibrations. From that time we had the scientific dispute concerning Poisson's boundary conditions (see, for example, Todhunter and Pearson 1960; Zhilin 1992).

The first complete plate theory was proposed by the German physicist Gustav Robert Kirchhoff⁹ (Fig. 5a). He contributes a lot fundamental understanding to different branches of physics like

- electrical circuits,
- spectroscopy, and
- emission of black-body radiation.

The Kirchhoff's plate theory (Kirchhoff 1850) was based on a few basic hypotheses allowing the reduction of the three-dimensional equations to two-dimensional. These hypotheses are usually formulated that a straight line orthogonal to the undeformed midplane of the plate will be after the deformation straight and orthogonal to the deformed midplane and during the deformation the length of the straight line is unchanged. These simple assumptions result in

$$\Delta\Delta w = \frac{q}{D} \quad \text{with} \quad D = \frac{Eh^3}{12(1-\nu^2)}$$

⁹*March 12, 1824 in Königsberg, East Prussia, †October 17, 1887 in Berlin.



Fig. 6 “Founders” of the FEM: **a** Walter Ritz, **b** Boris Grigor’evic Galërkin

Here Δ is the two-dimensional Laplace operator, w denotes the deflection which depends only on the midplane coordinates and q is the transverse surface load. The results for many practical problems agreed with experimental measurements in a satisfying manner. But the Kirchhoff’s theory yields in a governing 4th order partial differential equation and on in each boundary only two boundary conditions can be satisfied. This is not enough in some situations when the transverse force, the bending moment and the torque are given. For this case Kirchhoff introduced a mechanical equivalent force (named *Ersatzkraft*) which is the combination of the transverse force and the torque at the boundary.

John William Strutt, 3rd Baron Rayleigh¹⁰ (Fig. 5b) was English physicist and Nobel Prize winner (1904). One of his research topics was the theory of sounds (Strutt 1877). He introduced a direct method to find an approximate solution for boundary value problems which is now named Rayleigh-Ritz method. The Swiss mathematician Walter Ritz¹¹ (Fig. 6a) suggested a generalization in 1908 (Ritz 1908). The Ritz’ method together with the approach developed by Boris Grigor’evic Galërkin¹² (Fig. 6b) belong to the basics of the finite element method.

The Kirchhoff’s theory started with an undeformed plane midsurface. In practice one has also two-dimensional bearing structures which are curved. The first extension

¹⁰*November 12, 1842, Langford Grove, Maldon, †June 30, 1919, Terlins Place near Witham.

¹¹*February 22, 1878, Sion, † July 7, 1909, Göttingen.

¹²*March 4, 1871, Polozk, † July 12, 1945, Leningrad.

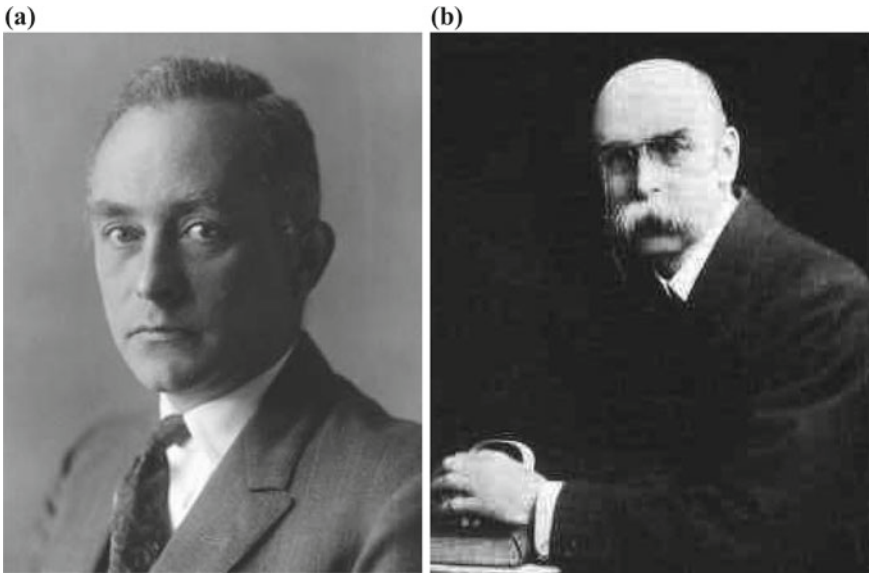


Fig. 7 Simplest shell theory: **a** Hermann Aron, **b** Augustus Edward Hough Love

of the Kirchhoff's theory to this case was given by Hermann Aron¹³ (Fig. 7a). He was a German physician and businessman. As a scientist he discussed problems of the shell theory (Aron 1874), but also of electrical engineering. Later Augustus Edward Hough Love¹⁴ (Fig. 7b) suggested a shell theory by analogy to Kirchhoff's theory which in our days is named Kirchhoff-Love shell theory. Love was an English mathematician making a lot of contributions to the mathematical theory of elasticity, see, for example, Love (1906).

Any plate or shell theory, which is presented by two-dimensional partial differential equation, is approximate and based on some assumptions, for example, kinematical hypotheses. Improvements of the approximations can be made introducing new assumption. Stephen (Stepan) Timoshenko¹⁵ (Fig. 8a) introduced a kinematical hypotheses for beams (Timoshenko 1921) allowing to take into account the transverse shear (and rotational inertia effects). This approach can be easily extended to plates and shells. Timoshenko was also the founder of the modern engineering education in the U.S. universities and wrote a lot of textbooks in mechanics, for example Timoshenko and Woinowsky-Krieger (1985).

Another approach was suggested by Theodore von Kármán¹⁶ (Fig. 8b). With respect to the thinness of the plate he assumed that the deflection can huge and this

¹³*October 1, 1845, Kempen (Kępnó), †August 29, 1913, Charlottenburg.

¹⁴*April 17, 1863, Weston-super-Mare, †June 5, 1940, Oxford.

¹⁵*December 22, 1878, Shpotivka, Russia, †May 29, 1972, Wuppertal.

¹⁶*Mai 11, 1881, Budapest, Austria-Hungary, †May 6, 1963, Aachen.

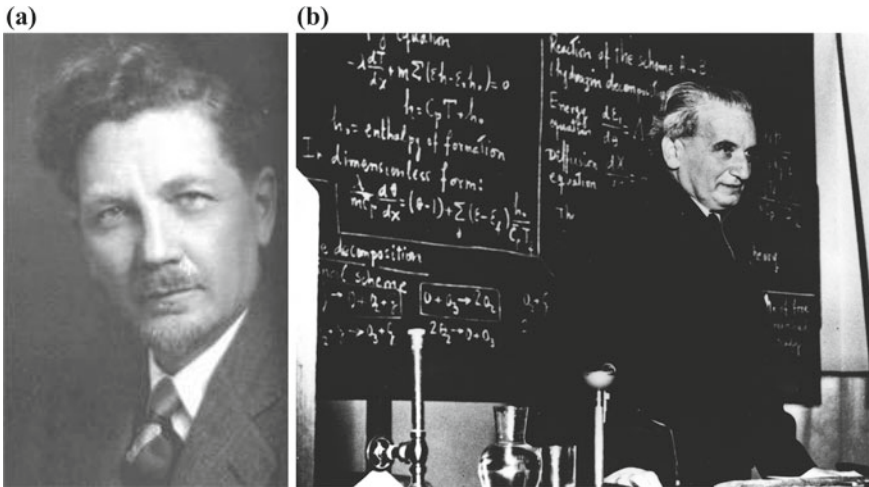


Fig. 8 Improvements of the kinematical assumptions: **a** Stephen (Stepan) Timoshenko, **b** Theodore von Kármán

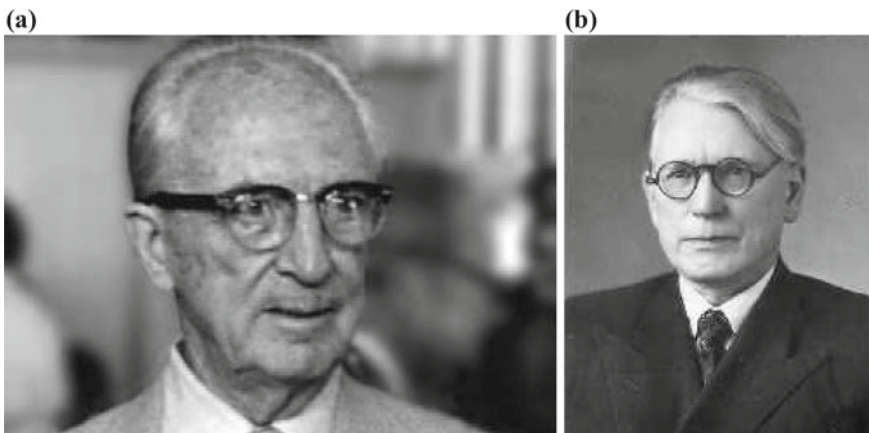


Fig. 9 Improvements of the shell theory: **a** Lloyd Hamilton Donnell, **b** Khamid Mushtari

results partly in nonlinear strains. At first this idea was published in von Kármán (1910).

The development of the nonlinear shell theory was connected with the demands from the aircraft industries. For example, Lloyd Hamilton Donnell¹⁷ (Fig. 9a) and Khamid Mushtari¹⁸ (Fig. 9b) developed refined theories for aerospace applications.

¹⁷*May 20, 1895, Kent’s Hill, Maine, †November 7, 1997, Palo Alto, Texas.

¹⁸*July 22, 1900, Orenburg, Russia, †January 23, 1981, Kazan, Soviet Union.

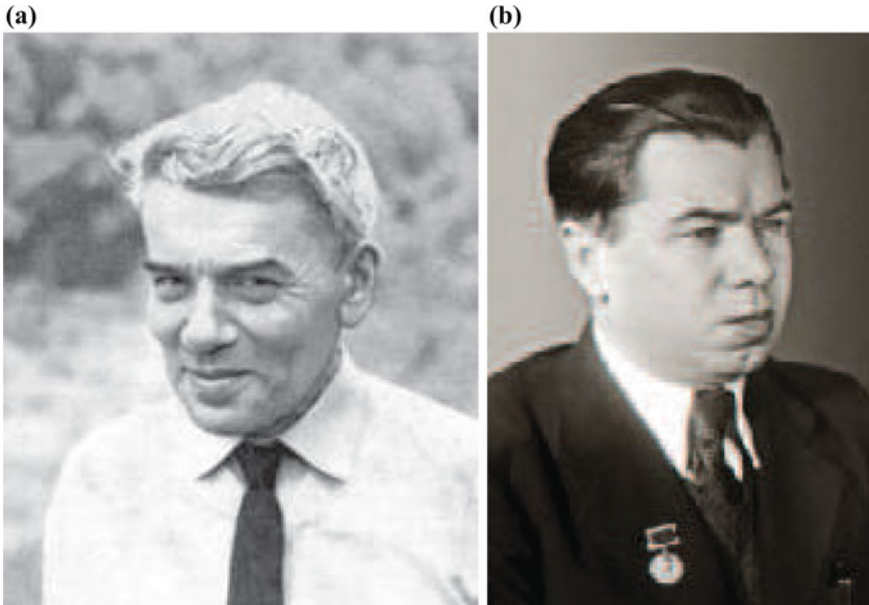


Fig. 10 Theoretical and engineering approaches to the shell theory: **a** Anatoly Isakovich Lurie, **b** Vasily Zakharovich Vlasov

In addition, Donnel suggested monocoques (structures that supports loads through an object's external skin, similar to an egg shell) for air planes and cars. He summarized his main results in Donnel (1976). At the same time he was the founding editor of journal "Applied Mechanics Reviews". The Tatarian scientist Mushtari mostly published in Russian, but one book was translated into English (Mushtari and Galimov 1961).

Anatoly Isakovich Lurie¹⁹ (Fig. 10a) was the founder of the plate and shell theory school at the Leningrad Polytechnic Institute. He worked in the field of theoretical and applied mechanics and control theory. He published the first monograph devoted to the shell theory authored by a Russian scientist (Lurie 1947). One of the main results was also published in English (Lurie 1961). Vasily Zakharovich Vlasov²⁰ (Fig. 10b) was a Soviet civil engineer, mathematician and mechanic. His main contributions to the theory of thin-walled structures were presented in Vlasov (1949), which was later translated into German (Wlassow 1958) and English (1964).

Aleksey L'vovich Gol'denveizer²¹ (Fig. 11a) was a Russian/Soviet mechanic working in the field theory of shells. He applied the asymptotic integration method (Gol'denveizer 1962, 1963) for the formulation of plate and shell theories. The starting point is the appropriate scaling of the coordinates. The components of the

¹⁹* July 19, 1901, Mogilev, Russia, † February 12, 1980, Leningrad.

²⁰* February 24, 1906, Kareevo, Russia, † August 7, 1958, Moscow.

²¹* January 12, 1911, Moscow, † January 12, 2003, Moscow.

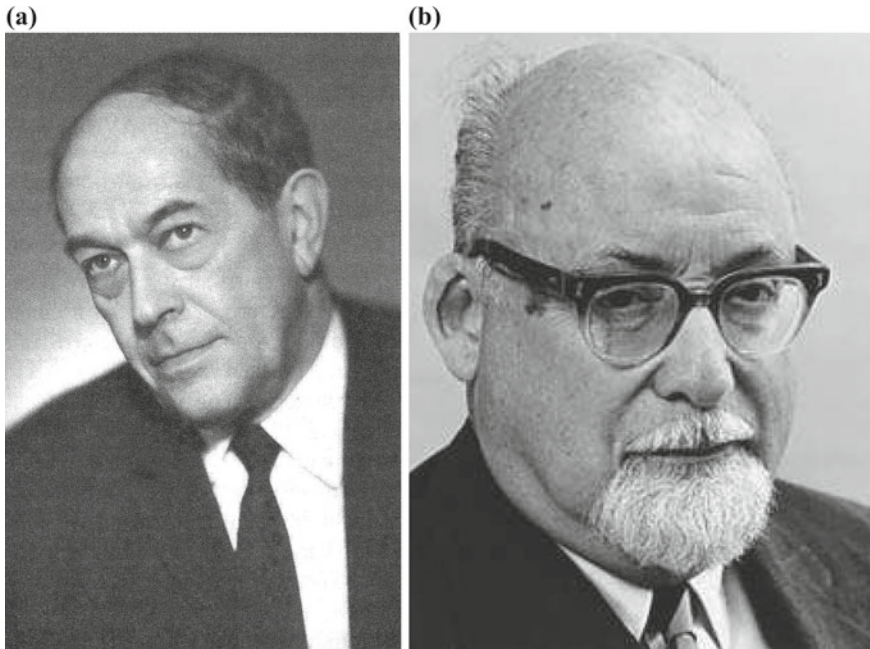


Fig. 11 Shell theories of different parameters: **a** Aleksey L'vovich Gol'denveizer, **b** Eric Reissner (Max Erich Reissner)

stress tensor and the displacement vector are obtained as asymptotic power series of a characteristic small parameter. Introducing these expansions into the equilibrium equations and boundary conditions of the theory of elasticity, and collecting terms with the same powers of the small parameter, one obtains sets of two-dimensional equations and boundary conditions which do not contain the small parameter and which can be solved much easier in comparison with the three-dimensional problem (van der Heijden 1976).

Eric Reissner²² (Fig. 11b) was a civil engineer and mechanician. In 1944/5 he improved the classical plate theory introducing hypotheses different from Kirchhoff's one as the starting point. By this way he obtained partial differential equations of 6th order (instead of 4th order in the Kirchhoff theory) allowing to satisfy three boundary conditions on each boundary. The basic ideas and some principal reference were presented in Reissner (1985).

Raymond David Mindlin²³ (Fig. 12a) has made a lot of fundamental contributions to various branches of mechanics. Among them there were publications to the micropolar theory which is based on the Cosserat model in continuum mechanics. His approach to the improvement of the Kirchhoff plate theory was different from

²²*January 5, 1913, Aachen, †November 1, 1996, La Jolla, California.

²³*September 17, 1906, New York, †November 12, 1987, Hanover, New Hampshire.



Fig. 12 Various formulation principles: **a** Raymond David Mindlin, **b** Ilia Nestorovich Vekua

Reissner's papers. His starting point was a dynamic problem (Mindlin 1951), in the case of Reissner the starting point was statics. With respect to this the formulated theories are different and the shear correction factor introduced by both takes different values (which are in the engineering sense are very close). With respect to the similarities of both theories especially in the finite element references the term "Reissner-Mindlin theory" is used. The Georgian mathematician Ilia Nestorovich Vekua²⁴ (Fig. 12b) formulated lower-dimensional theories from the three-dimensional theory of elasticity using a displacement ansatz with truncated series expansion of Legendre polynomials (Vekua 1955, 1985).

Valentin Valentinovich Novozhilov²⁵ (Fig. 13a) was a Russian scientist working mostly in Solid Mechanics, but at the end of his life he investigated also Fluid Mechanics problems. Since 1945, he has been a professor in the subdepartment of the theory of elasticity, department of mathematics and mechanics, Leningrad University. He published in 1951 a book on thin shells which was translated into English (Novozhilov 1959).

Warner Tjardus Koiter²⁶ (Fig. 13b) was a mechanical engineer and the Professor of Applied Mechanics at Delft University of Technology in the Netherlands from 1949 to 1979. Koiter is primarily known for his asymptotic theory of initial

²⁴* April 23, 1907, Sheshelety, †December 2, 1977, Tbilisi.

²⁵* May 18, 1910, Lublin, †June 14, 1987, Leningrad.

²⁶* June 16, 1914, Amsterdam, †September 2, 1997, Delft.

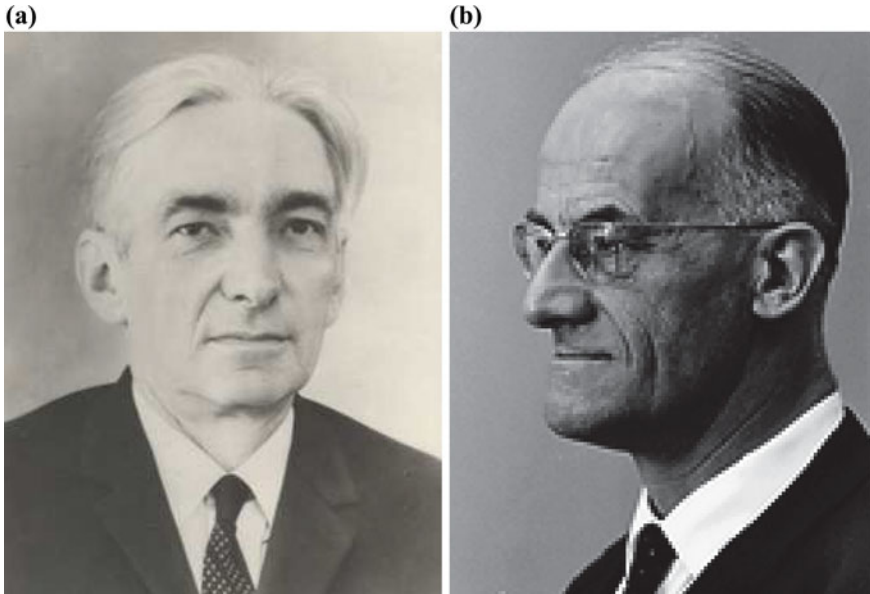


Fig. 13 Love’s approach is enough: **a** Valentin Valentinovich Novozhilov, **b** Warner Tjardus Koiter

post-buckling stability. Other contributions are in linear and non-linear thin shell theory. For one of his contributions on the “best” linear thin shell theory he paraphrased the Beatle’s song title *All you need is Love*.

Sergei Alexandrovich Ambarcumyan²⁷ (Fig. 14a) is an Armenian scientist working in the field of Solid Mechanics. He makes his own proposal for a kinematical hypothesis in the theory of plates. His famous book on the theory of anisotropic plates was translated into English (Ambarcumyan 1991).

Paul Mansur Naghdi²⁸ (Fig. 14b) was an Iranian-American civil engineer and professor at the University of Berkeley. Naghdi’s work on Continuum Mechanics extended over a period of more than forty years. Various aspects of the mechanical behavior of solids and fluids were in his focus. His contributions to the shell theory were based on a new approach—the Cosserat surface. His main contributions in this field were published in a review article (Naghdi 1972).

Richard Hugo Gallagher²⁹ (Fig. 15a) was an American civil engineer with research focus on structure mechanics. He was one of the founders of the finite element method (FEM), an engineering computation technique for solving coupled systems of partial differential equations. This method is now widely used and well established in the analysis of plate- or shell-like structures.

²⁷*March 17, 1922, Gumry.

²⁸*March 24, 1924, Teheran, †July 9, 1994, Berkeley, California.

²⁹*November 17, 1927, Manhattan, New York, †September 30, 1997, Tuscon, Arizona.

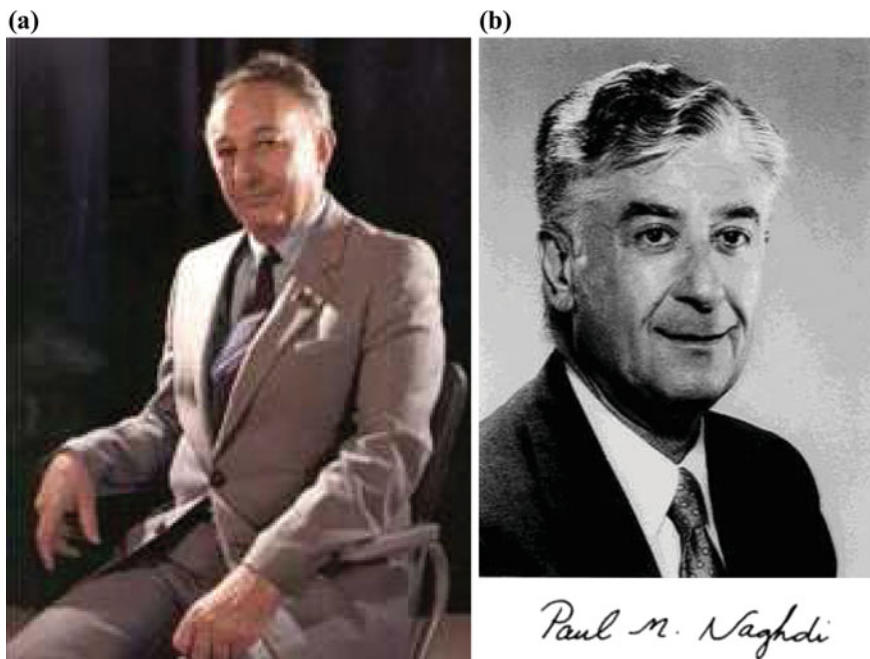


Fig. 14 Love's approach is enough: **a** Sergei Alexandrovich Ambarcumyan, **b** Paul Mansur Naghdi

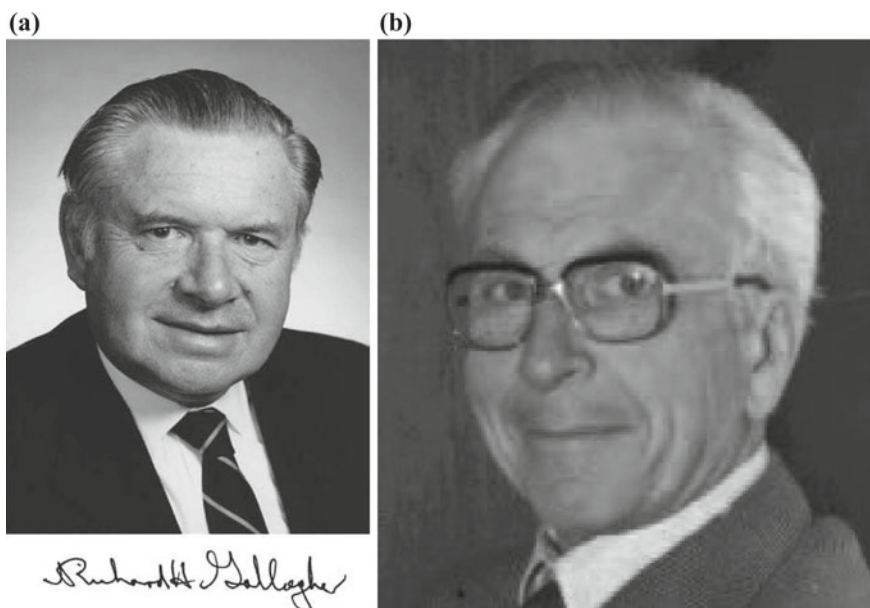


Fig. 15 Finite Element Method: **a** Richard Hugo Gallagher, **b** John Hadji Argyris

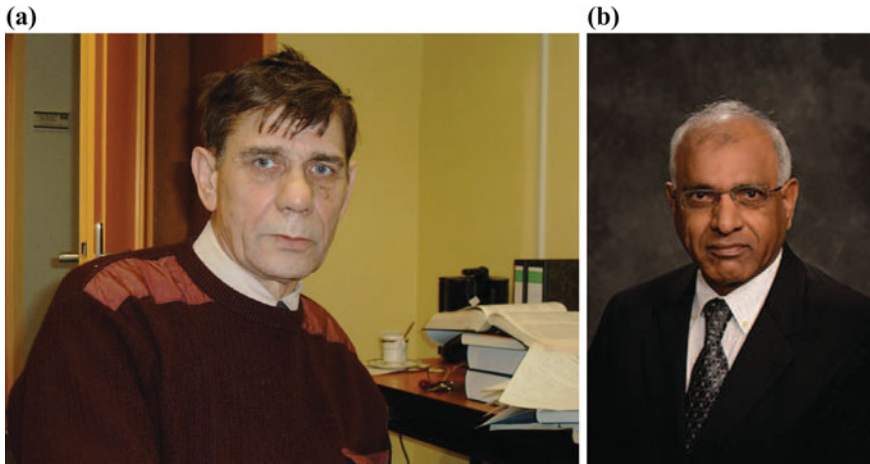


Fig. 16 Hypotheses versus direct approach: **a** Pavel Andreievich Zhilin, **b** Junutula Narasinha Reddy

John Hadji Argyris³⁰ (Fig. 15b) was a pioneer of computer applications in science and engineering and among the creators of the finite element method (FEM). He pioneered computer mechanics and established in the early 1950s the matrix structural theory introducing the first finite elements concepts including effects of material and geometrical nonlinearities

Pavel Andreievich Zhilin³¹ (Fig. 16a) was a professor of Rational Mechanics at the Leningrad Polytechnical Institute (now St. Petersburg State Polytechnical University “Peter the Great”). He delivered various interesting results to Continuum Mechanics, among them

- formulation of the fundamental laws of mechanics,
- direct tensor calculus,
- rigid body dynamics,
- nonlinear rod and shell theory,
- general theory of inelastic media.

He applied the direct approach in the formulation of the rod or shell theory (see, for example, Zhilin 1976).

Junutula Narasinha Reddy³² (Fig. 16b) is an Indian/American scientist in the field of theoretical and computational mechanics. He established a class of third- and higher-order theories (Reddy 1984). In addition, he published some fundamental books on plates and shells (Reddy 2004, 2007; Wang et al. 2000)

³⁰* August 19, 1913, Volos, Greece, †April 2, 2004, Stuttgart, Germany.

³¹*February 8, 1942, Velikiy Ustyug (Vologda region), Soviet Union, †December 4, 2005, St. Petersburg, Russia.

³²* August 12, 1945, Warangal, Andhra Pradesh.

This short review of the history of the theory of plates is not complete. More information one can get, for example, from Altenbach (1988); Altenbach et al. (2010b); Becchi et al. (2003); Grigolyuk and Seleznev (1973); Kurrer (2008); Léwinski (1987); Lo et al. (1977); Maugin (2013); Naghdi (1972); Panc (1975); Reddy (2004); Reissner (1985); Timoshenko (1953); Todhunter and Pearson (1960). The recent developments in the theory of shells and plates are reported in Altenbach and Eremeyev (2011); Jaiani and Podio-Guidugli (2008); Kienzler et al. (2003); Altenbach and Mikhasev (2014).

2 Some Examples of New Applications

Thin-walled structures as plates and shells have a lot of applications. One of the first were related to the aerospace developments—airplanes and rockets can be modelled as shell-like structures—another possibility to model such structures are thin-walled beam models. Two examples of space launching systems are shown in Fig. 17. The US space station “Skylab” was launched on a Saturn V rocket (Fig. 17a) with a height of 85 m, a diameter of 6.6 m and a launching mass of 2934.8 t. For the Soviet/Russian Proton M rocket (Fig. 17b) the following data are valid: height of 53 m, a diameter of 7.4 m and a launching mass of 712.8 t. It is obvious that in both cases also thin-walled beam structure models can be used.

The next examples of thin-walled shell-like structures are two modern airplanes (Fig. 18). The length of the Airbus A 380 (Fig. 18a) is 73 m, the diameter 7.14 m \times 8.40 m, the span 80 m and the launch weight 590 t. For the Boeing 787 Dreamliner (Fig. 18b) the parameters are: length 69 m, diameter 5.74 m, span 60 m and the launch weight 250 t. It should be mentioned that both airplanes are produced

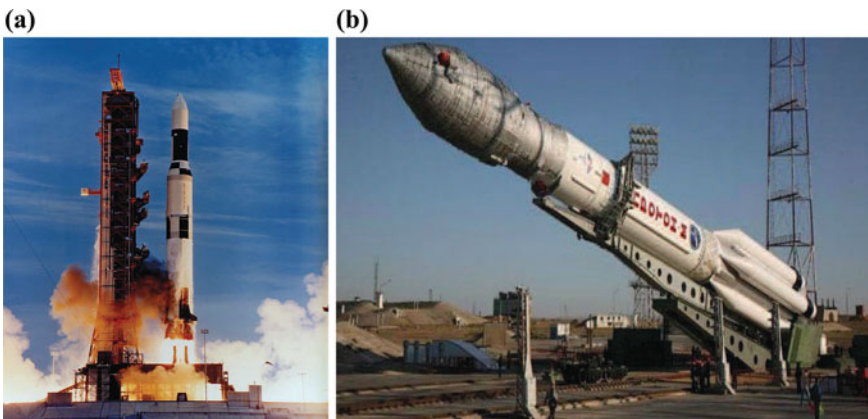


Fig. 17 Space launching system: **a** Saturn V, **b** Proton M

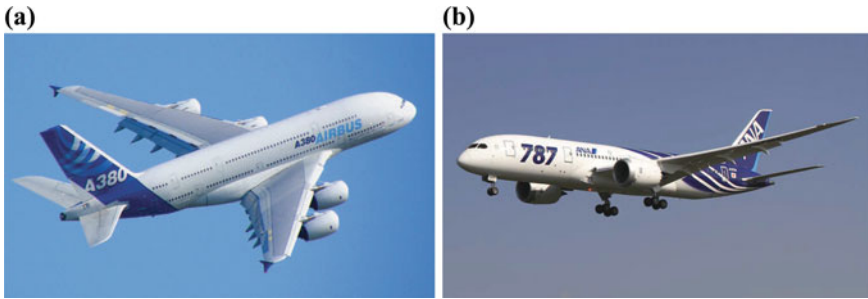


Fig. 18 Modern airplanes: **a** Airbus A 380, **b** Boeing 787 Dreamliner

Fig. 19 Sydney opera house



using a huge amount of composites. The Dreamliner has an airframe comprising nearly 50% carbon fiber reinforced plastic and other composites.

Another field of shell-like structures is related to Civil Engineering. The first example is shown in Fig. 19. This building features a modern expressionist design, with a series of large precast concrete “shells”, each composed of sections of a sphere of 75.2 m radius, forming the roofs of the structure, set on a monumental podium. The roof structure is commonly referred to as “shells”, but they are precast concrete panels supported by precast concrete ribs. Such structures are not shells in the sense of the common definitions (Başar and Krätzig 1985; Gol’denveizer 1962; Naghdi 1972; Novozhilov 1959; Timoshenko and Woinowsky-Krieger 1985).

The design of cooling towers (Fig. 20) has a great influence on the theory of shells. The reason for that were some spectacular disasters based on in-complete mechanical analysis of such shell-like structures. In addition, it should be mentioned that the cooling towers are hyperboloid shells. Hyperbolic structures have a negative Gaussian curvature.

The next example from Civil Engineering is the so-called hyperbolic paraboloid shell structure (Fig. 21). Hyperbolic paraboloid geometry is often used in saddle roof constructions.

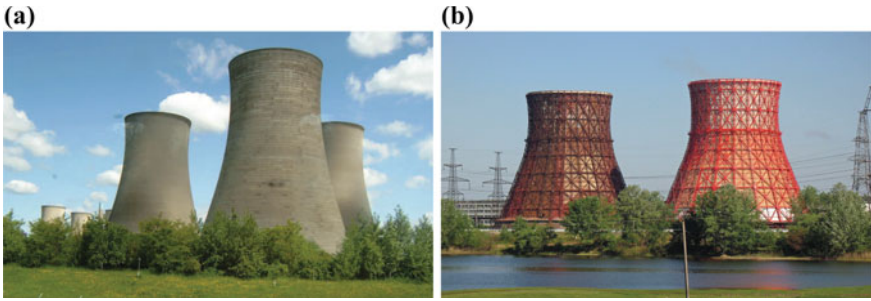


Fig. 20 Cooling towers: **a** Didcot Power Station (UK), **b** Kharkiv Power Station

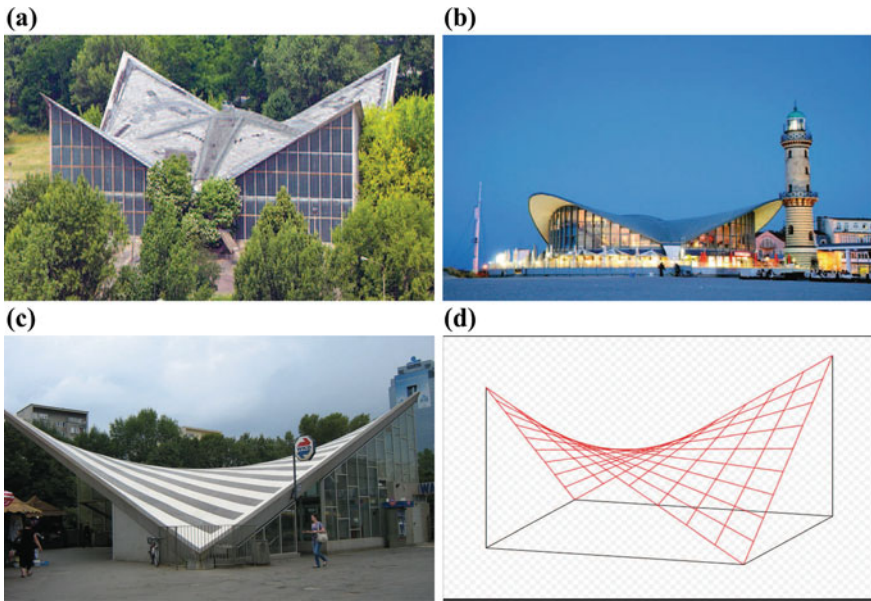


Fig. 21 Hyperbolic paraboloid shell structure: **a** Exhibition hall in Magdeburg (Germany), **b** Restaurant in Warnemünde (Germany), **c** Railway station Warszawa-Ochota (Poland), **d** design principle

Sandwich structures belongs to the plate- and shell-like structural elements (Fig. 22). Honeycomb has the highest strength to weight ratio (in a sandwich form) of any known material. In modern applications the core layer is composed by short fibre reinforced composites (Fig. 23) or foams.

Many biological systems can be modeled as thin-walled structures. Two examples are given in Fig. 24.

In the recent year a new application field for plate- or shell-like structures was established. With the increasing miniaturization nanoplates and nanoshells are applied in special applications. One example is shown in Fig. 25.



Fig. 22 Honeycomb sandwich plate

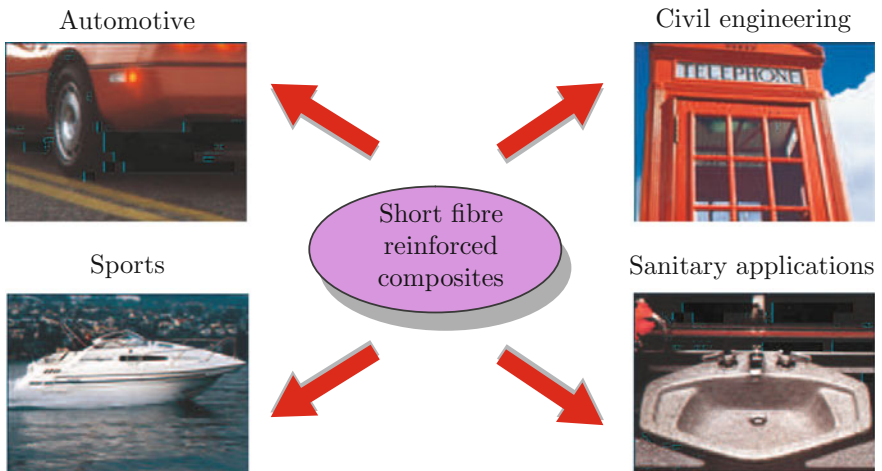


Fig. 23 Short fibre composites applications

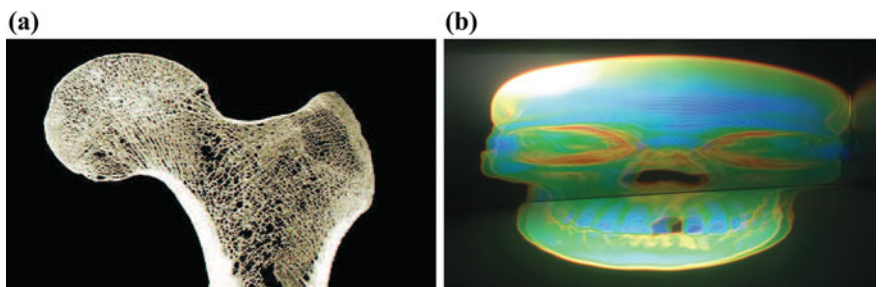


Fig. 24 Biological shell structures: a Femur, b Human skull

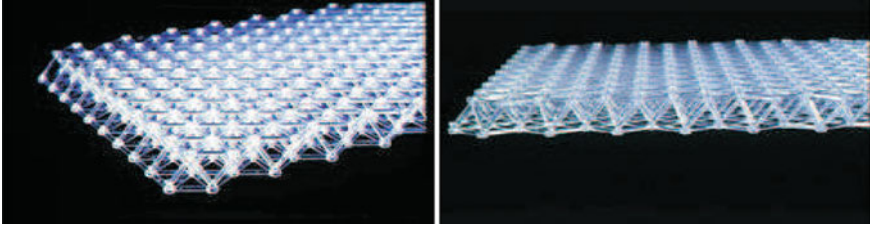


Fig. 25 Lattice structures

3 Main Directions in the Theory of Plates and Shells

Let us introduce at first some requirements to a plate or shell theory. In general such theory should take into account

- the thinness hypothesis which allows to present the approximate theory using only two coordinates,
- different types of deformability, for example, shear-rigid or shear-deformable,
- geometrical nonlinearities,
- physical nonlinearities,
- etc.

In general, we distinguish the following formulation concepts in the theory of plates and shells:

- the engineering approach (based on hypotheses about the stress state and/or the kinematics),
- the direct approach,
- the consistent approach, and
- the asymptotic approach.

The first two and the fourth approach were widely discussed in the 70th of the last century (see, for example, Grigolyuk and Seleznev 1973; Naghdi 1972; Rothert 1973), the third one was introduced only some years ago (Kienzler 2002; Kienzler and Schneider 2016; Schneider and Kienzler 2011; Schneider et al. 2014).

In dependence from the introduced kinematical assumption below, three classical variants of the plate theory are briefly discussed: the Kirchhoff theory, the Mindlin theory and the von Kármán theory. The three mentioned theories are a brief description of some basic statements. For more details see Altenbach et al. (2016).

3.1 Kirchhoff Theory

In the case of the Kirchhoff theory (Kirchhoff 1850, 1883) for the thickness h we assume that $h \ll L$, where L is a characteristic length (for example, in the case of

rectangular plates the minimum of the side length L_1, L_2 or in the case of circular plates the radius R).

Let us assume for the further discussions that we have only rectangular plates. They can be presented in the Cartesian coordinate system x_1, x_2, z . x_1, x_2 are the in-plane coordinates. z is the coordinate in the thickness direction. The plate has the following dimensions: $0 \leq x_1 \leq L_1, 0 \leq x_2 \leq L_2$ and $|z| \leq h/2$. The Kirchhoff theory is based on the following assumptions:

- The plate is made of a homogeneous, isotropic, linear-elastic material. The generalized Hooke's law is assumed.
- Kinematical assumptions
 - The mid surface of the plate is, in the case of bending, the neutral plane. The points of the midsurface have the displacements

$$u_1(x_1, x_2, 0) = 0, u_2(x_1, x_2, 0) = 0, u_3(x_1, x_2, 0) = w \neq 0$$

The deflections w are assumed to be small $w \ll h$. The derivatives of the deflections w.r.t. x_1 and x_2 (angle of slope of the surface in the case of bending) is so small that the squares can be neglected in comparison with 1. The curvatures of the surface can be linearized

$$\kappa_{11} = \frac{-w_{,11}}{[1 + (w_{,1})^2]^{3/2}} \approx -w_{,11}, \quad \kappa_{22} = \frac{-w_{,22}}{[1 + (w_{,2})^2]^{3/2}} \approx -w_{,22}$$

Here $(\dots)_i$ denotes the derivative w.r.t. $x_i, i = 1, 2$, This is the kinematical model of a shear-rigid plate.

- All points of the normal to the undeformed midsurface are points of the normal to the deformed midsurface (generalization of the Bernoulli hypothesis in the beam theory). In the thickness direction the plate is rigid (no normal strains). Then we have the following displacements

$$u_1(x_1, x_2, x_3) = x_3 \psi_1(x_1, x_2),$$

$$u_2(x_1, x_2, x_3) = x_3 \psi_2(x_1, x_2),$$

$$u_3(x_1, x_2, x_3) = w(x_1, x_2)$$

ψ_1 and ψ_2 are the rotations of the cross-sections of the plate w.r.t. to the x_2 - and x_1 -Axis, respectively. From the strain-displacement equations it follows: $\varepsilon_{33} = 0$, and γ_{13}, γ_{23} are independent from x_3 . In addition, one has $\psi_1 = -w_{,1}$, $\psi_2 = -w_{,2}$ and $\gamma_{13} = \gamma_{23} = 0$.

- Static hypothesis
 - The normal stress σ_{33} much smaller in comparison with σ_{11} and σ_{22}

$$\sigma_{33} \ll \sigma_{11}, \sigma_{22}$$

In the classical plate theory it is assumed $\sigma_{33} \approx 0$ (static hypothesis). This contradicts to the case of localized loading with high intensity since this results in significant contact stresses σ_{33} .

- Kinematic hypothesis

- The kinematic hypothesis $\varepsilon_{33} = 0$ following from $u_3 = w$ and the static hypothesis $\sigma_{33} = 0$ are incompatible within the theory of elasticity. For thin plates the error is small. The shear stresses σ_{13} and σ_{23} should be non equal to zero (equilibrium conditions). Because of the kinematic hypothesis $\gamma_{13} = \gamma_{23} = 0$ this results in $G \rightarrow \infty$ (shear-rigid plate).

From the static and kinematic hypothesis follows that in the classical plate theory the plane stress state can be assumed: the Hooke's law contains only the stresses $\sigma_{11}, \sigma_{22}, \sigma_{12}$, the shear stresses σ_{13} and σ_{23} can be computed with the help of the equilibrium conditions. The stresses σ_{33}, σ_{13} and σ_{23} does not influence the strain energy of the shear-rigid plate, where G is the shear modulus.

Remark 3.1 The original Kirchhoff theory was developed for the bending problem only. That means the plate exhibit only deflections w , in-plane displacements are disregarded.

The Kirchhoff theory is for small deflections valid. In this case we get the following approximations

$$\begin{aligned}\cos \varphi_1 &\approx \cos \varphi_2 \approx 1, \\ \sin \varphi_1 &\approx \varphi_1 \approx \tan \varphi_1 = w_{,1}, \\ \sin \varphi_2 &\approx \varphi_2 \approx \tan \varphi_2 = w_{,2}\end{aligned}$$

The displacements can be computed as follows

$$\begin{aligned}u_1(x_1, x_2, x_3) &= -x_3 w_{,1}(x_1, x_2), \\ u_2(x_1, x_2, x_3) &= -x_3 w_{,2}(x_1, x_2), \\ u_3(x_1, x_2, x_3) &= w(x_1, x_2),\end{aligned}$$

and finally we obtain the strain-displacement equations

$$\begin{aligned}\varepsilon_{11} = u_{1,1} &= -x_3 w_{,11} = x_3 \kappa_{11}, \\ \varepsilon_{22} = u_{2,2} &= -x_3 w_{,22} = x_3 \kappa_{22}, \\ \gamma_{12} = u_{1,2} + u_{2,1} &= -2x_3 w_{,12} = 2x_3 \kappa_{12}, \\ \gamma_{21} = u_{2,1} + u_{1,2} &= -2x_3 w_{,21} = 2x_3 \kappa_{21}\end{aligned}$$

The stress resultants are integrals over the plate thickness. The in-plane stress resultants follow as

$$\int_{-h/2}^{h/2} \sigma_{11} dz = n_{11}, \quad \int_{-h/2}^{h/2} \sigma_{22} dz = n_{22}, \quad \int_{-h/2}^{h/2} \sigma_{12} dz = n_{12}, \quad \int_{-h/2}^{h/2} \sigma_{21} dz = n_{21},$$

the out-of-plane stress resultants as

$$\begin{aligned} \int_{-h/2}^{h/2} \sigma_{11} x_3 dz &= m_{11}(x_1, x_2), & \int_{-h/2}^{h/2} \sigma_{22} x_3 dz &= m_{22}(x_1, x_2), \\ \int_{-h/2}^{h/2} \sigma_{12} x_3 dz &= m_{12}(x_1, x_2), & \int_{-h/2}^{h/2} \sigma_{21} x_3 dz &= m_{21}(x_1, x_2), \\ \int_{-h/2}^{h/2} \sigma_{13} dz &= q_1(x_1, x_2), & \int_{-h/2}^{h/2} \sigma_{23} dz &= q_2(x_1, x_2) \end{aligned}$$

These formal definitions are valid since the stress distributions are not specified. In the above mentioned equations σ_{ij} , $i = 1, 2$, $j = 1, 2, 3$ are the components of the stress tensor. n_{11} , n_{22} are the in-plane tension forces, n_{12} , n_{21} are the in-plane shear forces, m_{11} , m_{22} are the bending moments, m_{12} , m_{21} are the torsion moments and q_1 , q_2 denotes the shear forces. If we assume a classical (Cauchy) continuum the following constrain is valid: $\sigma_{12} = \sigma_{21}$. From this follow: $n_{12} = n_{21}$ and $m_{12} = m_{21}$. The further discussions are related to the classical continuum only.

Remark 3.2 Even in the case of the classical continuum this simplification for shells is not valid in the general case since the shell curvatures are included in the stress resultants. Only if the both principal curvatures are the same (and they coincide with the coordinate system) or the contribution from the curvatures can be neglected w.r.t. 1, the symmetry conditions for the stress resultants can be used also for shells.

If we assume constant plane stress state, then the out-of-plane resultants are vanishing. If we assume linear stress state, then the in-plane resultants are vanishing. The further discussion concerning the Kirchhoff and the Mindlin theories will be restricted to the out-of-plane behaviour, that means

$$\int_{-h/2}^{h/2} \sigma_{11} dz = n_{11} = 0, \quad \int_{-h/2}^{h/2} \sigma_{22} dz = n_{22} = 0, \quad \int_{-h/2}^{h/2} \sigma_{12} dz = n_{12} = n_{21} = 0$$

The equilibrium equations can be established as follows

- force equilibrium in z -direction

$$q_{1,1} + q_{2,2} + q = 0,$$

- moments equilibrium around x_1 -axis

$$-m_{22,2} - m_{12,1} + q_2 = 0,$$

- moments equilibrium around x_2 -axis

$$-m_{11,1} - m_{21,2} + q_1 = 0$$

Note that $m_{12} = m_{21}$.

This is a system of three equations with five unknowns. Expressing the shear forces as

$$q_2 = m_{12,1} + m_{22,2}, \quad q_1 = m_{11,1} + m_{21,2}$$

one gets from the first equilibrium equation

$$m_{11,11} + 2m_{12,12} + m_{22,22} = -q$$

This is one equation with three unknowns. It is obvious that the Kirchhoff equilibrium equations result in a statically indeterminate problem. That means for solving boundary value problems additional equations should be introduced.

Remark 3.3 The simplest way to get dynamic equations (equations of motion) is the use of the d'Alambert principle which means that the static equilibrium equations are added by inertia terms.

Let us introduce the following constitutive equations

$$\begin{aligned} \varepsilon_{11} &= \frac{1}{E}(\sigma_{11} - \nu\sigma_{22}) & \text{or} & \quad \sigma_{11} = \frac{E}{1-\nu^2}(\varepsilon_{11} + \nu\varepsilon_{22}), \\ \varepsilon_{22} &= \frac{1}{E}(\sigma_{22} - \nu\sigma_{11}) & \text{or} & \quad \sigma_{22} = \frac{E}{1-\nu^2}(\varepsilon_{22} + \nu\varepsilon_{11}), \\ \gamma_{12} &= \frac{2(1+\nu)}{E}\sigma_{12} & \text{or} & \quad \sigma_{12} = \frac{E}{2(1+\nu)}\gamma_{12}, \end{aligned}$$

where E , ν denotes Young's modulus and Poisson's ration. Both are assumed to be constant w.r.t. the thickness coordinate. Substituting the strains

$$\begin{aligned} \sigma_{11}(x_1, x_2, x_3) &= -\frac{Ex_3}{1-\nu^2}(w_{,11} + \nu w_{,22}), \\ \sigma_{22}(x_1, x_2, x_3) &= -\frac{Ex_3}{1-\nu^2}(w_{,22} + \nu w_{,11}), \\ \sigma_{12}(x_1, x_2, x_3) &= -\frac{Ex_3}{1+\nu}w_{,12} = -(1-\nu)\frac{Ex_3}{1-\nu^2}w_{,12} \end{aligned}$$

the following constitutive equations for the stress resultants can be computed

$$\begin{aligned}
 m_{11}(x_1, x_2) &= -\frac{Eh^3}{12(1-\nu^2)}(w_{,11} + \nu w_{,22}) = -K(w_{,11} + \nu w_{,22}), \\
 m_{22}(x_1, x_2) &= -\frac{Eh^3}{12(1-\nu^2)}(w_{,22} + \nu w_{,11}) = -K(w_{,22} + \nu w_{,11}), \\
 m_{12}(x_1, x_2) &= -(1-\nu)\frac{Eh^3}{12(1-\nu^2)}w_{,12} = -K(1-\nu)w_{,12}
 \end{aligned}$$

K denotes the classical Kirchhoff's bending stiffness which is presented in standard textbooks (see Timoshenko and Woinowsky-Krieger 1985, among others)

$$K = \frac{Eh^3}{12(1-\nu^2)}$$

As any stiffness the bending stiffness contains information on the geometry of the structure (here thickness) and the material behavior.

The shear forces cannot be estimated by constitutive equations since in the case of the Kirchhoff theory the transverse shear rigidity is assumed (no transverse shear strains results assuming isotropic material behavior in zero shear stresses). The shear forces follow from the equilibrium equations

$$\begin{aligned}
 q_1(x_1, x_2) &= m_{11,1} + m_{21,2} = -\frac{\partial}{\partial x_1}[K(w_{,11} + \nu w_{,22})] - \frac{\partial}{\partial x_2}[K(1-\nu)w_{,12}], \\
 q_2(x_1, x_2) &= m_{22,2} + m_{12,1} = -\frac{\partial}{\partial x_2}[K(w_{,22} + \nu w_{,11})] - \frac{\partial}{\partial x_1}[K(1-\nu)w_{,12}]
 \end{aligned}$$

if the deflections are known.

Finally, if the thickness is constant and material behavior is homogeneous the following set of governing equations is valid

$$\begin{aligned}
 \Delta \Delta w(x_1, x_2) &= \frac{q(x_1, x_2)}{K}, \\
 m_{11}(x_1, x_2) &= -K[w_{,11}(x_1, x_2) + \nu w_{,22}(x_1, x_2)], \\
 m_{22}(x_1, x_2) &= -K[w_{,22}(x_1, x_2) + \nu w_{,11}(x_1, x_2)], \\
 m_{12}(x_1, x_2) &= -K(1-\nu)w_{,12}(x_1, x_2), \\
 q_1(x_1, x_2) &= -K[\Delta w(x_1, x_2)]_{,1}, \\
 q_2(x_1, x_2) &= -K[\Delta w(x_1, x_2)]_{,2}
 \end{aligned}$$

For the rectangular plate with constant bending stiffness it is easy to get some special cases

- Bending equation for simply supported plate

$$K \Delta \Delta w(x_1, x_2) = q(x_1, x_2)$$

- Bending equation for elastically supported plate

$$K \Delta \Delta w(x_1, x_2) = q(x_1, x_2) - cw(x_1, x_2)$$

- Bending vibration equation for simply supported plate

$$K \Delta \Delta w(x_1, x_2, t) + \rho h \ddot{w}(x_1, x_2, t) = q(x_1, x_2, t)$$

- Bending vibration equation for elastically supported plate

$$K \Delta \Delta w(x_1, x_2, t) + \rho h \ddot{w}(x_1, x_2, t) = q(x_1, x_2, t) - cw(x_1, x_2, t)$$

($\dot{}$) denotes the time (t) derivative.

3.2 Mindlin Plate Theory

The Mindlin theory is a shear deformable plate theory (Mindlin 1951). The material is assumed again to be homogeneous and isotropic. The midplane is in the case of bending the “neutral plane” that means we have the following displacements

$$u_1(x_1, x_2, 0) = 0, \quad u_2(x_1, x_2, 0) = 0, \quad u_3(x_1, x_2, 0) = w(x_1, x_2) \neq 0$$

The displacements are small in comparison to the plate thickness and the curvatures are linearized of the bending surface

$$\kappa_{11} \approx \psi_{1,1}, \quad \kappa_{22} \approx \psi_{2,2}, \quad \kappa_{12} \approx \psi_{1,2} + \psi_{2,1}$$

ψ_1 and ψ_2 are the rotations of the cross-sections. They are independent variables and each point of the midsurface of the Mindlin plate has five degrees of freedom. The following assumptions are valid

- All point of the line element are orthogonal to the undeformed midsurface and the line elements are inextensible ($\varepsilon_{33} \approx 0$)

$$u_1(x_1, x_2, x_3) \approx x_3 \psi_1(x_1, x_2),$$

$$u_2(x_1, x_2, x_3) \approx x_3 \psi_2(x_1, x_2),$$

$$u_3(x_1, x_2, x_3) \approx w(x_1, x_2)$$

- The normal stresses $\sigma_{33} \ll \text{Max}(\sigma_{11}, \sigma_{22})$ can be neglected even for the shear-deformable plate that means $\sigma_{33} \approx 0$. In the theory of elasticity one gets from the assumption $\sigma_{33} = 0$ the plane stress state. From $\varepsilon_{33} = 0$ one gets the plane strain state. Both assumptions results like in the case of the classical plate in inconsistant conditions. In many applications the error from this inconsistency is relatively small.

Considering these assumptions the kinematic and equilibrium equations can be based on the following approximations of the displacements

$$\begin{aligned} u_1(x_1, x_2, x_3) &\approx x_3\psi_1(x_1, x_2), \\ u_2(x_1, x_2, x_3) &\approx x_3\psi_2(x_1, x_2), \\ u_3(x_1, x_2, x_3) &\approx w(x_1, x_2) \end{aligned}$$

The strain-displacement/rotation equations are

$$\begin{aligned} \varepsilon_{11} = u_{1,1} &= x_3\psi_{1,1}, \quad \gamma_{12} = u_{1,2} + u_{2,1} = x_3(\psi_{1,2} + \psi_{2,1}), \\ \varepsilon_{22} = u_{2,2} &= x_3\psi_{2,2}, \quad \gamma_{31} = w_{,1} + u_{1,3} = w_{,1} + \psi_1, \\ \varepsilon_{33} = w_{,3} &= 0, \quad \gamma_{23} = u_{2,3} + w_{,2} = \psi_2 + w_{,2} \end{aligned}$$

The equilibrium equations are the same like in the case of the Kirchhoff theory

$$\begin{aligned} q_{1,1} + q_{2,2} + q &= 0, \\ m_{12,1} + m_{22,2} - q_2 &= 0 \quad \text{or} \quad q_2 = m_{12,1} + m_{22,2}, \\ m_{11,1} + m_{21,2} - q_1 &= 0 \quad \text{or} \quad q_1 = m_{11,1} + m_{21,2} \end{aligned}$$

This is a system of three equations with five unknowns. That means we need again constitutive equations. With $\sigma_{33} = 0$ one gets from the generalized Hookean law

$$\begin{aligned} \varepsilon_{11} &= \frac{1}{E}(\sigma_{11} - \nu\sigma_{22}), & \sigma_{11} &= \frac{E}{1 - \nu^2}(\varepsilon_{11} + \nu\varepsilon_{22}), \\ \varepsilon_{22} &= \frac{1}{E}(\sigma_{22} - \nu\sigma_{11}), & \sigma_{22} &= \frac{E}{1 - \nu^2}(\varepsilon_{22} + \nu\varepsilon_{11}), \\ \gamma_{12} &= \frac{1}{G}\sigma_{12} = \frac{2(1 + \nu)}{E}\sigma_{12}, & \sigma_{12} &= G\gamma_{12} = \frac{E}{2(1 + \nu)}\gamma_{12}, \\ \gamma_{23} &= \frac{1}{G}\sigma_{23} = \frac{2(1 + \nu)}{E}\sigma_{23}, & \sigma_{23} &= G\gamma_{23} = \frac{E}{2(1 + \nu)}\gamma_{23}, \\ \gamma_{31} &= \frac{1}{G}\sigma_{31} = \frac{2(1 + \nu)}{E}\sigma_{31}, & \sigma_{31} &= G\gamma_{31} = \frac{E}{2(1 + \nu)}\gamma_{31} \end{aligned}$$

With the strain-displacement and the constitutive equations

$$\begin{aligned} \sigma_{11} &= \frac{Ex_3}{1 - \nu^2}(\psi_{1,1} + \nu\psi_{2,2}), & \sigma_{23} &= \frac{E}{2(1 + \nu)}(\psi_2 + w_{,2}), \\ \sigma_{22} &= \frac{Ex_3}{1 - \nu^2}(\psi_{2,2} + \nu\psi_{1,1}), & \sigma_{31} &= \frac{E}{2(1 + \nu)}(\psi_1 + w_{,1}), \\ \sigma_{12} &= \frac{Ex_3}{2(1 + \nu)}(\psi_{1,2} + \psi_{2,1}) \end{aligned}$$

the constitutive equations for the stress resultants can be established

$$\begin{aligned}
m_{11} &= K(\psi_{1,1} + \nu\psi_{2,2}), & m_{22} &= K(\psi_{2,2} + \nu\psi_{1,1}), \\
m_{12} &= \frac{1-\nu}{2}K(\psi_{1,2} + \psi_{2,1}), \\
q_1 &= Gh_s(\psi_1 + w_{,1}), & q_2 &= Gh_s(\psi_2 + w_{,2})
\end{aligned}$$

The constitutive equations for the shear forces should be corrected. This can be done by introducing shear correction. The complementary strain energy W_f^* based on the parabolic shear stress distribution

$$\sigma_{23}(x_3) = \frac{q_2 S(x_3)}{I}, \quad S(x_3) = \frac{1}{2} \left[\left(\frac{h}{2} \right)^2 - x_3^2 \right], \quad I = \frac{h^3}{12}$$

and $W_{f_2}^*$ with a constant distribution $\sigma_{23} = q_2/h$ modified by shear stress factor k_s can be expressed as it follows

$$W_{f_1}^* = \frac{1}{2} \int_{-h/2}^{h/2} \frac{\sigma_{23}^2(x_3)}{G} dx_3 = \frac{1}{2} \frac{q_2^2}{Gh} \frac{6}{5}, \quad W_{f_2}^* = \frac{1}{2} \int_{-h/2}^{h/2} \frac{q_2^2}{k_s h^2 G} dx_3 = \frac{1}{2} \frac{q_2^2}{k_s Gh}$$

With $W_{f_1}^* = W_{f_2}^*$

$$\frac{1}{k_s} = \frac{6}{5}, \quad \text{that means } k_s = \frac{5}{6} \quad \text{or } h_s = k_s h = \frac{h}{1,2}.$$

This shear correction corresponds to Reissner's estimate (Reissner 1944). Other estimates of shear correction factors are discussed in Mindlin (1951); Vlachoutsis (1992).

Let us develop a suitable set of governing equations in kinematical variables. At first, we introduce the abbreviations

$$\psi_{1,1} + \psi_{2,2} = \Phi(x_1, x_2), \quad \psi_{2,1} - \psi_{1,2} = \Psi(x_1, x_2)$$

With

$$m_{11,11} + 2m_{12,12} + m_{22,22} = -q$$

and

$$\begin{aligned}
m_{11} &= K(\psi_{1,1} + \nu\psi_{2,2}), & m_{22} &= K(\psi_{2,2} + \nu\psi_{1,1}), \\
m_{12} &= \frac{1-\nu}{2}K(\psi_{1,2} + \psi_{2,1})
\end{aligned}$$

one gets

$$K[\psi_{1,111} + \nu\psi_{2,112} + (1-\nu)(\psi_{2,112} + \psi_{1,122}) + \psi_{2,222} + \nu\psi_{1,122}] = -q$$

and finally

$$K \Delta(\psi_{1,1} + \psi_{2,2}) = -q \quad \text{or} \quad K \Delta \Phi = -q$$

The constitutive equations for the stress resultants and the equilibrium equations results in

$$\begin{aligned} w_{,1} &= -\psi_1 + \frac{K}{Gh_s} \left(\Phi_{,1} - \frac{1-\nu}{2} \Psi_{,2} \right), \\ w_{,2} &= -\psi_2 + \frac{K}{Gh_s} \left(\Phi_{,2} + \frac{1-\nu}{2} \Psi_{,1} \right) \end{aligned}$$

With $w_{,11} + w_{,22} = \Delta w$ and $w_{,12} - w_{,21} = 0$ follows

$$\Delta w = -\Phi + \frac{K}{Gh_s} \Delta \Phi, \quad \Psi - \frac{K}{Gh_s} \frac{1-\nu}{2} \Delta \Psi = 0$$

Finally, we obtain the plate equations for shear deformable plates

$$K \Delta \Phi = -q, \quad \Delta w = -\Phi + \frac{K}{Gh_s} \Delta \Phi, \quad \frac{1-\nu}{2} \frac{K}{Gh_s} \Delta \Psi - \Psi = 0$$

The special case of the shear-rigid plate follows from $Gh_s \rightarrow \infty$. Then $K \Delta \Phi = -q$, $\Delta w = -\Phi$ and $\Psi = 0$ and

$$K \Delta \Delta w = q$$

In addition, with $Gh_s \rightarrow \infty$

$$\psi_1 = -w_{,1}, \quad \psi_2 = -w_{,2}.$$

These are for the Kirchhoff plate the kinematic hypotheses.

Introducing \tilde{w}

$$\tilde{w} = w - \frac{K}{Gh_s} \Phi,$$

the equations can be decoupled. From $K \Delta \Phi = -q$ and

$$\Delta w - \frac{K}{Gh_s} \Delta \Phi = \Delta \tilde{w} = -\Phi$$

one gets one differential equation of fourth order

$$\Delta \Delta \tilde{w} = -\Delta \Phi = \frac{q}{K}$$

and one of second order

$$\frac{1-\nu}{2} \frac{K}{Gh_s} \Delta \Psi - \Psi = 0$$

Now the boundary conditions are

- clamped edge

$$w = 0, \psi_n = -\tilde{w}_{,n} - \frac{K}{Gh_s} \frac{1-\nu}{2} \Psi_{,t} = 0,$$

$$\psi_t = -\tilde{w}_{,t} - \frac{K}{Gh_s} \frac{1-\nu}{2} \Psi_{,n} = 0$$

- free edge

$$m_{nn} = K(\psi_{n,n} + \nu\psi_{t,t})$$

$$= -K \left(\tilde{w}_{,nn} + \nu\tilde{w}_{,tt} + \frac{K}{Gh_s} \frac{1-\nu^2}{2} \Psi_{,nt} \right) = 0,$$

$$m_{nt} = \frac{1-\nu}{2} K(\psi_{t,n} + \psi_{n,t})$$

$$= -K \left[(1-\nu)\tilde{w}_{,nt} - \frac{K}{Gh_s} \frac{(1-\nu)^2}{4} (\Psi_{,nn} + \Psi_{,tt}) \right] = 0,$$

$$q_n = Gh_s(\psi_n + w_{,n}) = -K \left[(\Delta\tilde{w})_{,n} + \frac{1-\nu}{2} \Psi_{,t} \right] = 0$$

The dynamic Mindlin plate equations (equations of motion) can be introduced adding the inertia terms to the equilibrium equations

$$q_{1,1}(x_1, x_2, t) + q_{2,2}(x_1, x_2, t) + q(x_1, x_2, t) = \rho h \ddot{w}(x_1, x_2, t),$$

$$m_{11,1}(x_1, x_2, t) + m_{12,2}(x_1, x_2, t) - q_1(x_1, x_2, t) = \frac{\rho h^3}{12} \ddot{\psi}_1(x_1, x_2, t),$$

$$m_{12,1}(x_1, x_2, t) + m_{22,2}(x_1, x_2, t) - q_2(x_1, x_2, t) = \frac{\rho h^3}{12} \ddot{\psi}_2(x_1, x_2, t)$$

With the stress resultants

$$Gh_s(\psi_{1,1} + w_{,11} + \psi_{2,2} + w_{,22}) + q = \rho h \ddot{w},$$

$$K \left(\psi_{1,11} + \frac{1-\nu}{2} \psi_{1,22} + \frac{1+\nu}{2} \psi_{2,12} \right) - Gh_s(\psi_1 + w_{,1}) = \frac{\rho h^3}{12} \ddot{\psi}_1,$$

$$K \left(\frac{1+\nu}{2} \psi_{1,12} + \frac{1-\nu}{2} \psi_{2,11} + \psi_{2,22} \right) - Gh_s(\psi_2 + w_{,2}) = \frac{\rho h^3}{12} \ddot{\psi}_2$$

With $\Phi = \psi_{1,1} + \psi_{2,2}$ we obtain

$$Gh_s(\Delta w + \Phi) + q = \rho h \ddot{w},$$

$$\frac{K}{2}[(1 - \nu)\Delta\psi_1 + (1 + \nu)\Phi_{,1}] - Gh_s(\psi_1 + w_{,1}) = \frac{\rho h^3}{12}\ddot{\psi}_1,$$

$$\frac{K}{2}[(1 - \nu)\Delta\psi_2 + (1 + \nu)\Phi_{,2}] - Gh_s(\psi_2 + w_{,2}) = \frac{\rho h^3}{12}\ddot{\psi}_2$$

The initial conditions are

$$w(x_1, x_2, t = 0) = w_0, \psi_1(x_1, x_2, t = 0) = \psi_{10}, \psi_2(x_1, x_2, t = 0) = \psi_{20},$$

$$\dot{w}(x_1, x_2, t = 0) = \dot{w}_0, \dot{\psi}_1(x_1, x_2, t = 0) = \dot{\psi}_{10}, \dot{\psi}_2(x_1, x_2, t = 0) = \dot{\psi}_{20}$$

After eliminating ψ_1 and ψ_2 we have

$$\left(K \Delta - Gh_s - \frac{\rho h^3}{12} \frac{\partial^2}{\partial t^2} \right) \Phi = Gh_s \Delta w$$

After some manipulations Φ can be eliminated and the Mindlin equation for the deflections can be written

$$\left(\Delta - \frac{\rho h}{Gh_s} \frac{\partial^2}{\partial t^2} \right) \left(K \Delta - \frac{\rho h^3}{12} \frac{\partial^2}{\partial t^2} \right) w + \rho h \frac{\partial^2 w}{\partial t^2} = \left(1 - \frac{K}{Gh_s} \Delta + \frac{\rho h^3}{12Gh_s} \frac{\partial^2}{\partial t^2} \right) q$$

The following special cases can be assumed:

- Neglecting the rotational inertia ($\rho h^3 \rightarrow 0$)

$$K \left(\Delta - \frac{\rho h}{Gh_s} \frac{\partial^2}{\partial t^2} \right) \Delta w + \rho h \frac{\partial^2 w}{\partial t^2} = \left(1 - \frac{K}{Gh_s} \Delta \right) q$$

- Neglecting the shear stiffness ($Gh_s \rightarrow \infty$)

$$\left(K \Delta - \frac{\rho h^3}{12} \frac{\partial^2}{\partial t^2} \right) \Delta w + \rho h \frac{\partial^2 w}{\partial t^2} = q$$

- Neglecting both the rotational inertia and the shear stiffness

$$K \Delta \Delta w + \rho h \frac{\partial^2 w}{\partial t^2} = q.$$

3.3 Reissner Plate Theory

The starting point are the equilibrium equations (like in the classical theory)

$$\begin{aligned}
q_{1,1} + q_{2,2} + q &= 0, \\
m_{12,1} + m_{22,2} - q_2 &= 0 \quad \text{or} \quad q_2 = m_{12,1} + m_{22,2}, \\
m_{11,1} + m_{21,2} - q_1 &= 0 \quad \text{or} \quad q_1 = m_{11,1} + m_{21,2}
\end{aligned}$$

Stress distributions are like in the classical theory (linear for the moments, parabolic for the shear forces)

$$\begin{aligned}
\sigma_{11} &= \frac{6}{h^2} m_{11} \frac{2x_3}{h}, & \sigma_{22} &= \frac{6}{h^2} m_{22} \frac{2x_3}{h}, \\
\tau_{12} &= \frac{3}{h^2} m_{12} \frac{2x_3}{h} = \tau_{21}, \\
\tau_{32} &= \frac{3}{2h} q_2 \left[1 - \left(\frac{2x_3}{h} \right)^2 \right], & \tau_{31} &= \frac{3}{2h} q_1 \left[1 - \left(\frac{2x_3}{h} \right)^2 \right]
\end{aligned}$$

In addition, the normal stress distribution follows from the three-dimensional equilibrium state

$$\sigma_{33} = - \int \frac{\partial \tau_{31}}{\partial x_1} dx_3 - \int \frac{\partial \tau_{32}}{\partial x_2} dx_3 + \phi(x_1, x_2)$$

With the expressions for τ_{31} and τ_{32}

$$\sigma_{33} = - \frac{3}{2h} \left[\frac{\partial q_1}{\partial x_1} + \frac{\partial q_2}{\partial x_2} \right] \int \left[1 - \left(\frac{2x_3}{h} \right)^2 \right] dx_3 + \phi(x_1, x_2)$$

and w.r.t. the third equilibrium equation for the resultants one has

$$\sigma_{33} = \frac{3}{4} p \frac{2x_3}{h} - \frac{1}{4} \left(\frac{2x_3}{h} \right)^3 p + \phi(x_1, x_2)$$

The boundary conditions are

$$\sigma_{33}(-h/2) = -p(x_1, x_2), \quad \sigma_{33}(h/2) = 0$$

The solution is

$$\phi(x_1, x_2) = -\frac{1}{2} p \quad \Rightarrow \quad \sigma_{33} = \frac{3}{4} p \left[\frac{2x_3}{h} - \frac{1}{3} \left(\frac{2x_3}{h} \right)^3 - \frac{2}{3} \right]$$

With the estimated stresses σ_{11} , σ_{22} , σ_{33} , τ_{12} , τ_{23} , τ_{13} the following strains can be computed

$$\begin{aligned}
\varepsilon_{11} &= \frac{\partial u_1}{\partial x_1} = \frac{1}{E}[\sigma_{11} - \nu(\sigma_{22} + \sigma_{33})], \\
\varepsilon_{22} &= \frac{\partial u_2}{\partial x_1} = \frac{1}{E}[\sigma_{22} - \nu(\sigma_{11} + \sigma_{33})], \\
\gamma_{12} &= \frac{\partial u_1}{\partial x_2} + \frac{\partial u_2}{\partial x_1} = \frac{1}{G}\tau_{12}, \\
\gamma_{23} &= \frac{\partial u_2}{\partial x_3} + \frac{\partial u_3}{\partial x_2} = \frac{1}{G}\tau_{23}, \\
\gamma_{13} &= \frac{\partial u_1}{\partial x_3} + \frac{\partial u_3}{\partial x_1} = \frac{1}{G}\tau_{13}
\end{aligned}$$

Performing the following averaging procedure

$$\begin{aligned}
\int_{-h/2}^{+h/2} \tau_{13} u_3 dx_3 = q_1 w &\Rightarrow w = \frac{3}{2h} \int_{-h/2}^{+h/2} u_3 \left[1 - \left(\frac{2x_3}{h} \right)^2 \right] dx_3, \\
\int_{-h/2}^{+h/2} \sigma_{11} u_1 dx_3 = m_{11} \psi_1 &\Rightarrow \psi_1 = \frac{6}{h^2} \int_{-h/2}^{+h/2} u_1 \frac{2x_3}{h} dx_3, \\
\int_{-h/2}^{+h/2} \tau_{12} u_2 dx_3 = m_{12} \psi_2 &\Rightarrow \psi_2 = \frac{6}{h^2} \int_{-h/2}^{+h/2} u_2 \frac{2x_3}{h} dx_3
\end{aligned}$$

This approximation is not the same like in Mindlin's theory: instead of a plane inextensible, not normal cross-section, now a curved inextensible cross-section can assumed. The governing equations consist of a coupled system of partial differential equations w.r.t. q_1 , q_2 , w :

$$\begin{aligned}
K \Delta \Delta w &= p - \frac{h^2}{10} \frac{2-\nu}{1-\nu} \Delta p, \\
q_1 &= -D \frac{\partial \Delta w}{\partial x_1} + \frac{h^2}{10} \Delta q_1 - \frac{h^2}{10} \frac{1}{1-\nu} \frac{\partial p}{\partial x_1}, \\
q_2 &= -D \frac{\partial \Delta w}{\partial x_2} + \frac{h^2}{10} \Delta q_2 - \frac{h^2}{10} \frac{1}{1-\nu} \frac{\partial p}{\partial x_2}
\end{aligned}$$

The decoupled system follows again after some manipulations

$$K \Delta \Delta \left(1 - \frac{h^2}{10} \Delta \right) w = \left[\left(\frac{h^2}{10} \right)^2 \frac{2-\nu}{1-\nu} \Delta \Delta - \frac{h^2}{10} \frac{3-2\nu}{1-\nu} \Delta + 1 \right] p,$$

$$\begin{aligned}\Delta\Delta\left(1-\frac{h^2}{10}\Delta\right)q_1 &= -\frac{\partial}{\partial x_1}\Delta\left(1-\frac{h^2}{10}\Delta\right)p, \\ \Delta\Delta\left(1-\frac{h^2}{10}\Delta\right)q_2 &= -\frac{\partial}{\partial x_2}\Delta\left(1-\frac{h^2}{10}\Delta\right)p.\end{aligned}$$

3.4 Reddy Plate Theory

In the Reddy theory (Reddy 1984, 2007) the kinematics is given as the following displacement approximation

$$\begin{aligned}u_1(x_1, x_2, x_3) &\approx u(x_1, x_2) + x_3\psi_1(x_1, x_2) - \frac{4x_3^3}{3h^2}\left(\psi_1(x_1, x_2) + \frac{\partial w(x_1, x_2)}{\partial x_1}\right), \\ u_2(x_1, x_2, x_3) &\approx v(x_1, x_2) + x_3\psi_2(x_1, x_2) - \frac{4x_3^3}{3h^2}\left(\psi_2(x_1, x_2) + \frac{\partial w(x_1, x_2)}{\partial x_2}\right), \\ u_3(x_1, x_2, x_3) &\approx w(x_1, x_2)\end{aligned}$$

ψ_1 and ψ_2 are the slopes of the transverse normal at $x_3 = 0$

$$\psi_1 = \frac{\partial u_1}{\partial x_1}, \quad \psi_2 = \frac{\partial u_2}{\partial x_2}$$

Stress-free boundary conditions are assumed

$$\sigma_{13}\left(x_1, x_2, \pm\frac{h}{2}\right) = \sigma_{23}\left(x_1, x_2, \pm\frac{h}{2}\right) = 0$$

The theory is characterized by

- no shear correction factor,
- higher order stress resultants,
- higher order “moments of area”.

Remark 3.4 Since the physical meaning of higher order moments is not clear the formulation of physically motivated boundary conditions is not trivial and the question of the consistency of the approximation is not clear.

The last question is discussed with respect of other plate theories in Kienzler (2002).

3.5 Föppl-von Kármán Plate Theory

Let us introduce the following assumptions

- thin linear-isotropic elastic shear-rigid plates,

- infinite strains, but finite deflections,
- in-plane and out-of-plane behavior cannot be decoupled, and
- $h/\text{Min}(l_1, l_2) < 0, 1; 0, 2 \leq w/h \leq 5$.

Further details are in Föppl (1907); von Kármán (1910); Meenen and Altenbach (2001).

The nonlinear kinematics $u_i = u_i(x_1, x_2, x_3)$, $i = 1, 2, 3$ can be presented by

$$\varepsilon_{11}(x_1, x_2, x_3) = u_{1,1} + \frac{1}{2} \underline{(u_{1,1}^2 + u_{2,1}^2 + u_{3,1}^2)},$$

$$\varepsilon_{22}(x_1, x_2, x_3) = u_{2,2} + \frac{1}{2} \underline{(u_{1,2}^2 + u_{2,2}^2 + u_{3,2}^2)},$$

$$\varepsilon_{33}(x_1, x_2, x_3) = u_{3,3} + \frac{1}{2} \underline{(u_{1,3}^2 + u_{2,3}^2 + u_{3,3}^2)},$$

$$\gamma_{12}(x_1, x_2, x_3) = u_{1,2} + u_{2,1} + \underline{u_{1,1}u_{1,2} + u_{2,1}u_{2,2} + u_{3,1}u_{3,2}},$$

$$\gamma_{23}(x_1, x_2, x_3) = u_{2,3} + u_{3,2} + \underline{u_{1,2}u_{1,3} + u_{2,2}u_{2,3} + u_{3,2}u_{3,3}},$$

$$\gamma_{31}(x_1, x_2, x_3) = u_{3,1} + u_{1,3} + \underline{u_{1,3}u_{1,1} + u_{2,3}u_{2,1} + u_{3,3}u_{3,1}}$$

The underlined terms are the contributions from the geometrical nonlinearity. In addition, some terms are small with respect to the different order of u_1, u_2, u_3 : $u_1, u_2 \ll u_3$ and no derivative with respect to x_3 : $u_3(x_1, x_2, x_3) \approx w(x_1, x_2)$. The classical assumptions: $\varepsilon_{33} \approx 0$, $\gamma_{23} \approx 0$, $\gamma_{31} \approx 0$ are valid.

The kinematical approximations are

- in-plane displacements u_1, u_2 are much smaller in comparison with the deflections u_3

$$\begin{aligned} u_{1,1}^2, u_{2,1}^2 &\ll u_{3,1}^2, & u_{1,2}^2, u_{2,2}^2 &\ll u_{3,2}^2, \\ u_{1,1}u_{1,2}, u_{2,1}u_{2,2} &\ll u_{3,1}u_{3,2}, \end{aligned}$$

- rotations of the normal are very small

$$\psi_1^2, \psi_2^2 \ll 1,$$

which results in

$$\begin{aligned} \sin \psi_1 &\approx \psi_1, & \cos \psi_1 &\approx 1, & \psi_1 &\approx -w_{,1}, \\ \sin \psi_2 &\approx \psi_2, & \cos \psi_2 &\approx 1, & \psi_2 &\approx -w_{,2}, \end{aligned}$$

- displacements

$$\begin{aligned} u_1(x_1, x_2, x_3) &= u(x_1, x_2) - x_3 w_{,1}(x_1, x_2), \\ u_2(x_1, x_2, x_3) &= v(x_1, x_2) - x_3 w_{,2}(x_1, x_2), \\ u_3(x_1, x_2, x_3) &\approx w(x_1, x_2), \end{aligned}$$

- strains

$$\begin{aligned}\varepsilon_{11}(x_1, x_2, x_3) &= u_{,1}(x_1, x_2) + \frac{1}{2}w_{,1}^2(x_1, x_2) + x_3\kappa_{11}(x_1, x_2), \\ \varepsilon_{22}(x_1, x_2, x_3) &= v_{,2}(x_1, x_2) + \frac{1}{2}w_{,2}^2(x_1, x_2) + x_3\kappa_{22}(x_1, x_2), \\ \gamma_{12}(x_1, x_2, x_3) &= u_{,2}(x_1, x_2) + v_{,1}(x_1, x_2) + w_{,1}(x_1, x_2)w_{,2}(x_1, x_2) \\ &\quad + 2x_3\kappa_{12}(x_1, x_2)\end{aligned}$$

with

$$\kappa_{11} = -w_{,11}, \quad \kappa_{22} = -w_{,22}, \quad \kappa_{12} = -w_{,12}$$

- strains in the midsurface

$$\begin{aligned}\epsilon_{11}(x_1, x_2) &= u_{,1}(x_1, x_2) + \frac{1}{2}w_{,1}^2(x_1, x_2), \\ \epsilon_{22}(x_1, x_2) &= v_{,2}(x_1, x_2) + \frac{1}{2}w_{,2}^2(x_1, x_2), \\ 2\epsilon_{12}(x_1, x_2) &= u_{,2}(x_1, x_2) + v_{,1}(x_1, x_2) + w_{,1}(x_1, x_2)w_{,2}(x_1, x_2),\end{aligned}$$

- strains in the distance x_3 from the midsurfaces

$$\begin{aligned}\varepsilon_{11}(x_1, x_2, x_3) &= \epsilon_{11}(x_1, x_2) + x_3\kappa_{11}(x_1, x_2), \\ \varepsilon_{22}(x_1, x_2, x_3) &= \epsilon_{22}(x_1, x_2) + x_3\kappa_{22}(x_1, x_2), \\ \gamma_{12}(x_1, x_2, x_3) &= 2\epsilon_{12}(x_1, x_2) + 2x_3\kappa_{12}(x_1, x_2),\end{aligned}$$

- compatibility conditions

$$\varepsilon_{11,22} + \varepsilon_{22,11} - 2\varepsilon_{12,12} = (w_{,12})^2 - w_{,11}w_{,22}$$

Now the equilibrium equations will be formulated for the deformed configuration (in all previous cases this was performed for the undeformed configuration):

- equilibrium of forces in x_3 -direction assuming the smallness of higher order terms, $w_{,12} = w_{,21}$

$$q_{1,1} + q_{2,2} + (n_{11}w_{,1} + n_{12}w_{,2})_{,1} + (n_{21}w_{,1} + n_{22}w_{,2})_{,2} + q = 0,$$

- equilibrium of forces in x_1 - and x_2 -direction

$$n_{11,1} + n_{12,2} = 0, \quad n_{12,1} + n_{22,2} = 0,$$

- taking into account the last equation we get the simplified equilibrium equations for the forces in x_3 -direction (the underlined terms are related to the extensions of

the Kirchhoff theory)

$$q_{1,1} + q_{2,2} + \underline{n_{11}w_{,11} + n_{22}w_{,22} + 2n_{12}w_{,12}} + q = 0,$$

- equilibrium of the moments

$$m_{12,1} + m_{22,2} - q_2 = 0, \quad m_{11,1} + m_{21,2} - q_1 = 0$$

The constitutive equations are assuming plane stress state

$$\begin{aligned} \sigma_{11} &= \frac{E}{1-\nu^2} [\epsilon_{11} + \nu\epsilon_{22} + x_3(\kappa_{11} + \nu\kappa_{22})], \\ \sigma_{22} &= \frac{E}{1-\nu^2} [\epsilon_{22} + \nu\epsilon_{11} + x_3(\kappa_{22} + \nu\kappa_{11})], \\ \sigma_{12} &= \frac{E}{1+\nu} (\epsilon_{12} + x_3\kappa_{12}) \end{aligned}$$

From this follow the constitutive equations in stress resultants

$$\begin{aligned} n_{11} &= D(\epsilon_{11} + \nu\epsilon_{22}), \\ n_{22} &= D(\epsilon_{22} + \nu\epsilon_{11}), \\ n_{12} &= D(1-\nu)\epsilon_{12}, \\ m_{11} &= K(\kappa_{11} + \nu\kappa_{22}), \\ m_{22} &= K(\kappa_{22} + \nu\kappa_{11}), \\ m_{12} &= K(1-\nu)\kappa_{12} \end{aligned}$$

Let us introduce the governing equations in displacements. From the two equilibrium equations of the in-plane forces

$$\begin{aligned} u_{,11} + \frac{1-\nu}{2}u_{,22} + \frac{1+\nu}{2}v_{,12} + w_{,1}w_{,11} + \frac{1-\nu}{2}w_{,1}w_{,22} + \frac{1+\nu}{2}w_{,2}w_{,12} &= 0, \\ v_{,22} + \frac{1-\nu}{2}v_{,11} + \frac{1+\nu}{2}u_{,12} + w_{,2}w_{,22} + \frac{1-\nu}{2}w_{,2}w_{,11} + \frac{1+\nu}{2}w_{,1}w_{,12} &= 0 \end{aligned}$$

The derivation of the third equation is based the other three equilibrium equations

$$m_{11,11} + 2m_{12,12} + m_{22,22} + n_{11}w_{,11} + n_{22}w_{,22} + 2n_{12}w_{,12} + q = 0$$

With the constitutive equations

$$\begin{aligned} -K\Delta\Delta w + \frac{Eh}{1-\nu^2} \left(u_{,1}w_{,11} + \frac{1}{2}w_{,1}^2w_{,11} + v_{,2}w_{,22} + \frac{1}{2}w_{,2}^2w_{,22} \right. \\ \left. + \nu v_{,2}w_{,11} + \frac{1}{2}\nu w_{,2}^2w_{,11} + \frac{1}{2}\nu w_{,1}^2w_{,22} + \nu u_{,1}w_{,22} \right) \\ + \frac{Eh}{1+\nu} (u_{,2}w_{,12} + v_{,1}w_{,12} + w_{,1}w_{,2}w_{,12}) + q = 0 \end{aligned}$$

we obtain the final set of governing equations in displacements. The smallness of $w_{,1}^2 w_{,11}$, $w_{,2}^2 w_{,22}$, $w_{,2}^2 w_{,11}$, $w_{,1}^2 w_{,22}$ and $w_{,1} w_{,12} w_{,2}$ results in

$$\begin{aligned} u_{,11} + \frac{1-\nu}{2} u_{,22} + \frac{1+\nu}{2} v_{,12} &= -w_{,1} w_{,11} - \frac{1-\nu}{2} w_{,1} w_{,22} - \frac{1+\nu}{2} w_{,2} w_{,12}, \\ v_{,22} + \frac{1-\nu}{2} v_{,11} + \frac{1+\nu}{2} u_{,12} &= -w_{,2} w_{,22} - \frac{1-\nu}{2} w_{,2} w_{,11} - \frac{1+\nu}{2} w_{,1} w_{,12}, \\ \Delta \Delta w &= \frac{q}{K} + \frac{12}{h^2} [u_{,1} w_{,11} + v_{,2} w_{,22} + (1-\nu)(u_{,2} + v_{,1}) w_{,12} + \nu(v_{,2} w_{,11} + u_{,1} w_{,22})] \end{aligned}$$

The following boundary conditions can be established

- in displacements

$$u|_{\Gamma} = \bar{u}, \quad v|_{\Gamma} = \bar{v}, \quad w|_{\Gamma} = \bar{w}, \quad w_{,n}|_{\Gamma} = \bar{w}_{,n}$$

- in-plane forces

$$n_{11}|_{\Gamma} \cos \alpha + n_{12}|_{\Gamma} \sin \alpha = \bar{n}_1, \quad n_{21}|_{\Gamma} \cos \alpha + n_{22}|_{\Gamma} \sin \alpha = \bar{n}_2$$

with

$$\begin{aligned} n_{11} &= \frac{Eh}{1-\nu^2} \left[u_{,1} + \nu v_{,2} + \frac{1}{2}(w_{,1}^2 + \nu w_{,2}^2) \right], \\ n_{22} &= \frac{Eh}{1-\nu^2} \left[v_{,2} + \nu u_{,1} + \frac{1}{2}(w_{,2}^2 + \nu w_{,1}^2) \right], \\ n_{12} &= \frac{Eh}{2(1+\nu)} (u_{,2} + v_{,1} + w_{,1} w_{,2}) \end{aligned}$$

For arbitrary boundaries we obtain the following boundary conditions

- shear forces:

$$q_n^*|_{\Gamma} + (n_{11}|_{\Gamma} \cos \alpha + n_{12}|_{\Gamma} \sin \alpha) w_{,1}|_{\Gamma} + (n_{21}|_{\Gamma} \cos \alpha + n_{22}|_{\Gamma} \sin \alpha) w_{,2}|_{\Gamma} = \bar{q}_n^*$$

or

$$q_n^*|_{\Gamma} + n_{nn}|_{\Gamma} w_{,n}|_{\Gamma} + n_{nt}|_{\Gamma} w_{,t}|_{\Gamma} = \bar{q}^*$$

- moments

$$m_{nn}|_{\Gamma} = \bar{m}$$

- kinematical conditions

– clamped boundary: $u = 0, v = 0, w = 0, w_{,1} = 0$

– support: $u = 0, v = 0, w = 0, m_{11} = 0$

– free boundary: $n_{11} = 0, n_{12} = 0, q_1^* = 0, m_{11} = 0$

Finally we introduce the governing equations in mixed form. With the Airy's stress function Φ

$$n_{11} = \Phi_{,22}, \quad n_{22} = \Phi_{,11}, \quad n_{12} = -\Phi_{,12}$$

the in-plane equilibrium is satisfied. The constitutive equations

$$\begin{aligned} \epsilon_{11} &= \frac{1}{Eh}(n_{11} - \nu n_{22}) = \frac{1}{Eh}(\Phi_{,22} - \nu\Phi_{,11}), \\ \epsilon_{22} &= \frac{1}{Eh}(n_{22} - \nu n_{11}) = \frac{1}{Eh}(\Phi_{,11} - \nu\Phi_{,22}), \\ \epsilon_{12} &= \frac{1+\nu}{Eh}n_{12} = -\frac{1+\nu}{Eh}\Phi_{,12} \end{aligned}$$

and the compatibility condition results in

$$\frac{1}{Eh}\Delta\Delta\Phi = (w_{,12})^2 - w_{,11}w_{,22}$$

From the equilibrium for the shear forces and moments

$$K\Delta\Delta w = q + \Phi_{,22}w_{,11} + \Phi_{,11}w_{,22} - 2\Phi_{,12}w_{,12}$$

Finally we get

$$\begin{aligned} K\Delta\Delta w &= L(w, \Phi) + q, \\ \frac{1}{Eh}\Delta\Delta\Phi &= -\frac{1}{2}L(w, w) \end{aligned}$$

with

$$L(f, g) = f_{,11}g_{,22} + f_{,22}g_{,11} - 2f_{,12}g_{,12}$$

The boundary conditions are

$$\begin{aligned} \Phi_{,22} \cos \alpha - \Phi_{,12} \cos \alpha &= \bar{n}_1, \\ -\Phi_{,12} \cos \alpha + \Phi_{,11} \cos \alpha &= \bar{n}_2 \end{aligned}$$

or

$$\Phi_{,mn} = \bar{n}_{nn}, \quad -\Phi_{,nt} = \bar{n}_{nt}$$

Remark 3.5 Extension to shear deformable behavior is possible.

Remark 3.6 Ciarlet's statement (Ciarlet 1990) that the von Kármán theory cannot be derived from the non-linear continuum mechanics, may be, should be corrected (Meenen and Altenbach 2001; Podio-Guidugli 2003)

Remark 3.7 While the Föppl-von Kármán equations are of interest from a purely mathematical point of view, the physical validity of these equations is questionable.

Remark 3.8 (Ciarlet) The two-dimensional von Kármán equations for plates, originally proposed by von Kármán (1910), play a mythical role in applied mathematics. While they have been abundantly, and satisfactorily, studied from the mathematical standpoint, as regards notably various questions of existence, regularity, and bifurcation, of their solutions, their physical soundness has been often seriously questioned.

Remark 3.9 (Truesdell 1978) An analyst may regard that theory [v. Kármán's theory of plates] as handed out by some higher power (a Hungarian wizard, say) and study it as a matter of pure analysis. To do so for v. Kármán theory is particularly tempting because nobody can make sense out of the 'derivations' ...

Remark 3.10 (Antman) Reasons for trouble include the facts that

1. the theory depends on an approximate geometry which is not clearly defined
2. a given variation of stress over a cross-section is assumed arbitrarily
3. a linear constitutive relation is used that does not correspond to a known relation between well defined measures of stress and strain
4. some components of strain are arbitrarily ignored
5. there is a confusion between reference and deformed configurations which makes the theory inapplicable to the large deformations for which it was apparently devised.

Conditions under which these equations are actually applicable and will give reasonable results when solved are discussed by Ciarlet (1980, 1990).

4 Direct Approach to the Theory of Shells

The *Direct Approach* in the theories of plates and shells first time was discussed in the monograph of Cosserat and Cosserat (1909). Here we are following Zhilin (1976). Let us introduce the following definition.

Definition 4.1 (*Simple shell*) A simple shell is a two-dimensional continuum in which the interaction between neighboring parts is due to forces and moments.

In this sense the shell is modeled as a deformable surface with material points for which we can prescribe physical properties. The definition is valid for homogeneous and inhomogeneous in the thickness direction shells. Below we are discussing the simplest case: each material point of the surface is an infinitesimal body with 5

degrees of freedom (three translations and two rotations) which means that we have a Timoshenko-Reissner-Mindlin-type theory.

Let us introduce briefly the material independent equations. Below the direct tensor notation will be used (for further details see Lebedev et al. 2010, among others) The kinematical model will be given in two configurations. In the reference configuration (undeformed state) we have

$$\{\mathbf{r}(q^1, q^2); \mathbf{d}_k(q^1, q^2)\}, \quad \mathbf{d}_k \cdot \mathbf{d}_m = \delta_{km}$$

$\mathbf{r}(q^1, q^2)$ is the position vector, $\mathbf{d}_k(q^1, q^2)$ are orthonormal vectors. Then for the actual configuration (deformed state) one has

$$\{\mathbf{R}(q^1, q^2, t); \mathbf{D}_k(q^1, q^2, t)\}, \quad \mathbf{D}_k \cdot \mathbf{D}_m = \delta_{km}$$

The capital letters denote the same quantities as in the reference configuration. The motion of the directed surface is defined by

$$\mathbf{R}(q, t), \quad \mathbf{P}(q, t) \equiv \mathbf{D}^k(q, t) \otimes \mathbf{d}_k(q)$$

$\mathbf{P}(q, t) \equiv \mathbf{P}(q^1, q^2, t)$ denotes a rotation tensor with $\text{Det } \mathbf{P} = +1$. The linear and angular velocities $\mathbf{v}(q, t)$, $\boldsymbol{\omega}(q, t)$ can be presented by

$$\mathbf{v} = \dot{\mathbf{R}}, \quad \dot{\mathbf{P}} = \boldsymbol{\omega} \times \mathbf{P}, \quad \mathbf{P}(q^1, q^2, 0) = \mathbf{P}_0, \quad \dot{f} \equiv \frac{df}{dt}$$

With the help of these quantities local equations of motion are given as follows

- First EULER equation of motion

$$\tilde{\nabla} \cdot \mathbf{T} + \rho \mathbf{F}_* = \rho(\mathbf{v} + \boldsymbol{\Theta}_1^T \cdot \boldsymbol{\omega})'$$

$\mathbf{T} = \mathbf{R}_\alpha \otimes \mathbf{T}^\alpha$ is the force tensor, \mathbf{F}_* is mass density of the external forces, ρ , $\rho \boldsymbol{\Theta}_1$ are the density and the first tensor of inertia, $\tilde{\nabla} \equiv \mathbf{R}^\alpha(q^1, q^2, t) \frac{\partial}{\partial q^\alpha}$ denotes the Nabla operator

- Second EULER equation of motion

$$\tilde{\nabla} \cdot \mathbf{M} + \mathbf{T}_\times + \rho \mathbf{L} = \rho(\boldsymbol{\Theta}_1 \cdot \mathbf{v} + \boldsymbol{\Theta}_2 \cdot \boldsymbol{\omega})' + \rho \mathbf{v} \times \boldsymbol{\Theta}_1^T \cdot \boldsymbol{\omega}$$

$\mathbf{M} = \mathbf{R}_\alpha \otimes \mathbf{M}^\alpha$ is the moment tensor, $\mathbf{T}_\times \equiv \mathbf{R}_\alpha \times \mathbf{T}^\alpha$, \mathbf{L} is the mass density of the external moments, $\rho \boldsymbol{\Theta}_2$ is the second tensor of inertia

The local form of the balance of energy can be presented as

$$\rho \dot{\mathcal{L}} = \mathbf{T}^T \cdot \tilde{\nabla} \mathbf{v} - \mathbf{T}_\times \cdot \boldsymbol{\omega} - \mathbf{M}^T \cdot \tilde{\nabla} \boldsymbol{\omega}$$

\mathfrak{U} is the mass density of the internal energy. Introducing the energetic tensors (Lurie 2005)

$$\mathbf{T}_e = (\tilde{\mathbf{V}}\mathbf{r})^T \cdot \mathbf{T} \cdot \mathbf{P}, \quad \mathbf{M}_e = (\tilde{\mathbf{V}}\mathbf{r})^T \cdot \mathbf{M} \cdot \mathbf{P}$$

we obtain another form of the balance of energy

$$\rho \dot{\mathfrak{U}} = \mathbf{T}_e^T \cdot \dot{\mathbf{E}} + \mathbf{M}_e^T \cdot \dot{\mathbf{F}}$$

\mathbf{E} , \mathbf{F} are the first and the second deformation tensors

$$\mathbf{E} = \nabla \mathbf{R} \cdot \mathbf{P} - \mathbf{a}, \quad \mathbf{F} = (\Phi_\alpha \cdot \mathbf{D}_k) \mathbf{r}^\alpha \otimes \mathbf{d}^k$$

with $\partial_\alpha \mathbf{P} = \Phi_\alpha \times \mathbf{P} \Rightarrow 2\Phi_\alpha = -[\partial_\alpha \mathbf{P} \cdot \mathbf{P}^T]_\times$. The strain energy $\mathfrak{U} = \mathfrak{U}(\mathbf{E}, \mathbf{F})$ contains 12 scalar arguments. The number of arguments can be reduced due to some restrictions:

- simple shells of constant thickness
- non-polar materials

The following restrictions are valid

$$\mathbf{L} \cdot \mathbf{D}_3 = \mathbf{0}, \quad \mathbf{M} \cdot \mathbf{D}_3 = \mathbf{0}, \quad \mathbf{M}_e^T \cdot [(\mathbf{F} - \mathbf{b} \cdot \mathbf{c}) \cdot \mathbf{c}] + \mathbf{T}_e^T \cdot [(\mathbf{E} + \mathbf{a}) \cdot \mathbf{c}] = \mathbf{0}$$

The specific energy \mathfrak{U} must satisfy

$$\left(\frac{\partial \mathfrak{U}}{\partial \mathbf{E}} \right)^T \cdot [(\mathbf{E} + \mathbf{a}) \cdot \mathbf{c}] + \left(\frac{\partial \mathfrak{U}}{\partial \mathbf{F}} \right)^T \cdot [(\mathbf{F} - \mathbf{b} \cdot \mathbf{c}) \cdot \mathbf{c}] = 0, \quad \frac{\partial \rho \mathfrak{U}}{\partial (\mathbf{F} \cdot \mathbf{n})} = \mathbf{0}$$

The characteristic system of the first equation is a system of 12th order

$$\frac{d}{ds} \mathbf{E} = (\mathbf{E} + \mathbf{a}) \cdot \mathbf{c}, \quad \frac{d}{ds} \mathbf{F} = (\mathbf{F} - \mathbf{b} \cdot \mathbf{c}) \cdot \mathbf{c},$$

having 11 independent integrals. The independent integrals are the strain measures. Four strain measures can be established

$$\begin{aligned} \mathfrak{E} &= \frac{1}{2} [(\mathbf{E} + \mathbf{a}) \cdot \mathbf{a} \cdot (\mathbf{E} + \mathbf{a})^T - \mathbf{a}], \\ \Phi &= (\mathbf{F} - \mathbf{b} \cdot \mathbf{c}) \cdot \mathbf{a} \cdot (\mathbf{E} + \mathbf{a})^T + \mathbf{b} \cdot \mathbf{c} \cdot \mathfrak{E} + \mathbf{b} \cdot \mathbf{c}, \\ \gamma &= \mathbf{E} \cdot \mathbf{n}, \\ \gamma_* &= \mathbf{F} \cdot \mathbf{n} \end{aligned}$$

- The arbitrary function $\mathfrak{U}(\mathfrak{E}, \Phi, \gamma, \gamma_*)$ satisfies the first equation of the characteristic system.
- From the second equation follows that \mathfrak{U} does not depend on γ_* .
- Tensors $\mathfrak{E}, \Phi, \gamma$ are called the reduced deformation tensors.

- $\boldsymbol{\epsilon}$ denote plane tensile and shear strains, $\boldsymbol{\Phi}$ denotes the bending and torsional strains and γ denotes the transverse shear.

The introduced equations contain more unknown than equations. Additional equations are the constitutive equations presenting the individual response of the given material. Lets start with the strain energy of the simple shells. For a shell made from an elastic material we can assume that the strains are relatively small while the displacements and rotations can be relatively large. In such a case the following quadratic approximation takes place

$$\begin{aligned} 2\rho_0\mathcal{U} = & 2\mathbf{T}_0 \cdot \boldsymbol{\epsilon} + 2\mathbf{M}_0^T \cdot \boldsymbol{\Phi} + 2\mathbf{N}_0 \cdot \gamma \\ & + \boldsymbol{\epsilon} \cdot \cdot {}^{(4)}\mathbf{C}_1 \cdot \boldsymbol{\epsilon} + 2\boldsymbol{\epsilon} \cdot \cdot {}^{(4)}\mathbf{C}_2 \cdot \boldsymbol{\Phi} + 2\boldsymbol{\Phi} \cdot \cdot {}^{(4)}\mathbf{C}_3 \cdot \boldsymbol{\Phi} \\ & + \gamma \cdot \boldsymbol{\Gamma} \cdot \gamma + 2\gamma \cdot {}^{(3)}\boldsymbol{\Gamma}_1 \cdot \boldsymbol{\epsilon} + {}^{(3)}\boldsymbol{\Gamma}_2 \cdot \boldsymbol{\Phi} \end{aligned}$$

$\mathbf{T}_0, \mathbf{M}_0, \mathbf{N}_0, {}^{(4)}\mathbf{C}_1, {}^{(4)}\mathbf{C}_2, {}^{(4)}\mathbf{C}_3, {}^{(3)}\boldsymbol{\Gamma}_1, {}^{(3)}\boldsymbol{\Gamma}_2, \boldsymbol{\Gamma}$ are stiffness tensors of different rank. They express the effective elastic properties of the simple shell. The differences between various classes of simple shells are connected with different expressions of the stiffness tensors. The stiffness tensors do not depend on the deformations. Thus they may be found from tests based on the linear shell theory.

After the formulation of the governing equations there exists one open question—the identification of the effective properties (stiffness, etc.). Various solutions of this problem are existing in the literature (Altenbach 2000; Zhilin 1976). To find the general structure of stiffness tensors the theory of symmetry must be applied Nye (2000). The classical theory of symmetry is not sufficient because it is valid for Euclidean tensors only. In the shell theory non-Euclidean tensors are involved. The following types of tensors in the shell theory used.

- Polar tensors $\rho, \mathcal{U}, \mathcal{W}, \mathbf{u}, \mathbf{u}, \mathbf{E}, \mathbf{T}, \mathbf{a}, \rho\boldsymbol{\Theta}_2, \mathbf{T}_0, {}^{(4)}\mathbf{C}_1, {}^{(4)}\mathbf{C}_3, \boldsymbol{\Gamma}$
- Axial tensors $\rho\boldsymbol{\Theta}_1, \boldsymbol{\varphi}, \boldsymbol{\omega}, \mathbf{F}, \boldsymbol{\Phi}, \mathbf{b} \cdot \mathbf{c}, \mathbf{M}_0, {}^{(4)}\mathbf{C}_2$
- Polar \mathbf{n} -oriented tensors $\mathbf{b}, \mathbf{B}, \boldsymbol{\gamma}, \mathbf{Q} = \mathbf{T} \cdot \mathbf{n}, {}^{(3)}\boldsymbol{\Gamma}_1, \mathbf{N}_0$
- Axial \mathbf{n} -oriented tensors $\mathbf{c} = -\mathbf{a} \times \mathbf{n}, {}^{(3)}\boldsymbol{\Gamma}_2$

For the orthogonal transformations of an arbitrary tensor of rank p is valid

$$\begin{aligned} \otimes_1^p \mathbf{Q} \cdot {}^{(p)}\mathbf{S} & \equiv S^{i_1 \dots i_p} \mathbf{Q} \cdot \mathbf{g}_{i_1} \otimes \mathbf{Q} \cdot \mathbf{g}_{i_2} \otimes \dots \otimes \mathbf{Q} \cdot \mathbf{g}_{i_p}, \\ {}^{(p)}\mathbf{S}' & \equiv (\mathbf{n} \cdot \mathbf{Q} \cdot \mathbf{n})^\beta (\text{Det}\mathbf{Q})^\alpha \otimes_1^p \mathbf{Q} \cdot {}^{(p)}\mathbf{S}, \end{aligned}$$

For polar tensors $\alpha = 0, \beta = 0$, axial tensors $\alpha = 1, \beta = 0$, polar \mathbf{n} -oriented tensors $\alpha = 0, \beta = 1$, axial \mathbf{n} -oriented tensors $\alpha = 1, \beta = 1$. Symmetries can be described in terms of the geometric operations which produce identical configurations. The set of symmetry operations and results of their combinations define a mathematical structure called a group. The symmetry operations which involve only rotations, reflections and inversion define the point group. The symmetries are described by orthogonal tensors

- Reflection (\mathbf{n} is the unit normal to the mirror plane)

$$\mathbf{Q} = \mathbf{I} - 2\mathbf{n} \otimes \mathbf{n}, \quad \det \mathbf{Q} = -1$$

- Rotation (\mathbf{m} represents the axis and ψ is the angle of rotation)

$$\mathbf{Q}(\psi \mathbf{m}) = \mathbf{m} \otimes \mathbf{m} + \cos \psi (\mathbf{I} - \mathbf{m} \otimes \mathbf{m}) + \sin \psi \mathbf{m} \times \mathbf{I},$$

$$-\pi < \psi < \pi, \quad \det \mathbf{Q} = 1,$$

- Inversion

$$-\mathbf{I}$$

How do the symmetries of the microstructure affect the physical properties? The answer follows from Curie-Neumann's principle in the physics of crystals:

- Any type of symmetry exhibited by the point group of a crystal is possessed by every physical property of the crystal.
- For a material element and for any of its physical properties, every material symmetry transformation of the material element is a physical symmetry transformation of the physical property.
- The symmetry group of the reason belongs to the symmetry group of the consequence.

The reasons in the case of simple shells are the intersection of:

- symmetry of the material of the shell (fibre-reinforced material, rolled sheets),
- symmetry of the surface shape (shell or plate), and
- symmetry of the internal structure of the shell (laminated plates—symmetry of the layer structure with respect to the mid-surface)

The identification is based on some relations between two- and three-dimensional properties:

- forces and moments with stress tensor of the classical theory of elasticity

$$\mathbf{T} = \langle \mu^{-1} \cdot \boldsymbol{\sigma} \rangle, \quad \mathbf{M} = \langle \mu^{-1} \cdot \boldsymbol{\sigma} \cdot \mathbf{cz} \rangle,$$

- displacements and rotations with the three-dimensional displacement vector

$$\rho_0(\mathbf{u} + \boldsymbol{\Theta}_1^T \cdot \boldsymbol{\varphi}) \cdot \langle \rho_0^* \mathbf{u}_* \rangle, \quad \rho_0(\boldsymbol{\Theta}_1 \cdot \mathbf{u} + \boldsymbol{\Theta}_2^T \cdot \boldsymbol{\varphi}) = \langle \rho_0^* \mathbf{u}_* \cdot \mathbf{cz} \rangle$$

- external force and moment

$$\rho_0 \mathbf{F}_* = \langle \rho_0^* \mathbf{F}^* \rangle + \mu^+ \boldsymbol{\sigma}_n^+ + \mu^- \boldsymbol{\sigma}_n^-,$$

$$\rho_0 \mathbf{L} = \mathbf{n} \times \langle \rho_0^* \mathbf{F}^* z \rangle + (h/2) \mathbf{n} \times (\mu^+ \boldsymbol{\sigma}_n^+ - \mu^- \boldsymbol{\sigma}_n^-)$$

$\mu^{+(-)} = 1 - (+)hH + (h^2/4)G$, $\sigma_n^{+(-)}$ are stress vectors on the upper and lower face surfaces of the shell.

Let us assume orthotropic material behavior and a plane mid-surface $({}^{(4)}\mathbf{C}_1 = \mathbf{A}$, $({}^{(4)}\mathbf{C}_2 = \mathbf{B}$, $({}^{(4)}\mathbf{C}_3 = \mathbf{C})$

$$\begin{aligned}\mathbf{A} &= A_{11}\mathbf{a}_1\mathbf{a}_1 + A_{12}(\mathbf{a}_1\mathbf{a}_2 + \mathbf{a}_2\mathbf{a}_1) + A_{22}\mathbf{a}_2\mathbf{a}_2 + A_{44}\mathbf{a}_4\mathbf{a}_4, \\ \mathbf{B} &= B_{13}\mathbf{a}_1\mathbf{a}_3 + B_{14}\mathbf{a}_1\mathbf{a}_4 + B_{23}\mathbf{a}_2\mathbf{a}_3 + B_{24}\mathbf{a}_2\mathbf{a}_4 + B_{42}\mathbf{a}_4\mathbf{a}_2, \\ \mathbf{C} &= C_{22}\mathbf{a}_2\mathbf{a}_2 + C_{33}\mathbf{a}_3\mathbf{a}_3 + C_{34}(\mathbf{a}_3\mathbf{a}_4 + \mathbf{a}_4\mathbf{a}_3) + C_{44}\mathbf{a}_4\mathbf{a}_4, \\ \boldsymbol{\Gamma} &= \Gamma_1\mathbf{a}_1 + \Gamma_2\mathbf{a}_2, \quad \boldsymbol{\Gamma}_1 = \mathbf{0}, \quad \boldsymbol{\Gamma}_2 = \mathbf{0}\end{aligned}$$

with

$$\begin{aligned}\mathbf{a}_1 &= \mathbf{a} = \mathbf{e}_1\mathbf{e}_1 + \mathbf{e}_2\mathbf{e}_2, & \mathbf{a}_2 &= \mathbf{e}_1\mathbf{e}_1 - \mathbf{e}_2\mathbf{e}_2, \\ \mathbf{a}_3 &= \mathbf{c} = \mathbf{e}_1\mathbf{e}_2 - \mathbf{e}_2\mathbf{e}_1, & \mathbf{a}_4 &= \mathbf{e}_1\mathbf{e}_2 + \mathbf{e}_2\mathbf{e}_1\end{aligned}$$

$\mathbf{e}_1, \mathbf{e}_2$ are unit basic vectors. In addition, one obtains the orthogonality condition for \mathbf{a}_i ($i = 1, 2, 3, 4$)

$$\frac{1}{2}\mathbf{a}_i \cdot \mathbf{a}_j = \delta_{ij}, \quad \delta_{ij} = \begin{cases} 1, & i = j, \\ 0, & i \neq j \end{cases}$$

The elastic orthotropic law is valid in the following cases:

Case 1: Homogeneous plates—all properties are constant (no dependency from z).

Case 2: Inhomogeneous plates (sandwich, multilayered, functionally graded)—all properties are functions of z , e.g., $E_i = E_i(z)$.

The identification of the effective properties can be performed with the help of static boundary value problems (two-dimensional, three-dimensional) and the comparison of the forces and moments (in the sense of averaged stresses or stress resultants)

$$\mathbf{T} = \langle \mathbf{a} \cdot \boldsymbol{\sigma} \rangle, \quad \mathbf{M} = \langle \mathbf{a} \cdot \boldsymbol{\sigma} z \cdot \mathbf{c} \rangle$$

$\boldsymbol{\sigma}$ is the stress tensor, $\langle (\dots) \rangle = \int_{-h/2}^{h/2} (\dots) dz$. With the help of three problems (tension and bending, plane shear and torsion) the effective stiffness tensors can be computed

$$\begin{aligned}
A_{11} &= \frac{1}{4} \left\langle \frac{E_1 + E_2 + 2E_1\nu_{21}}{1 - \nu_{12}\nu_{21}} \right\rangle, & A_{12} &= \frac{1}{4} \left\langle \frac{E_1 - E_2}{1 - \nu_{12}\nu_{21}} \right\rangle, \\
A_{22} &= \frac{1}{4} \left\langle \frac{E_1 + E_2 - 2E_1\nu_{21}}{1 - \nu_{12}\nu_{21}} \right\rangle, \\
B_{13} &= -\frac{1}{4} \left\langle \frac{E_1 + E_2 + 2E_1\nu_{21}}{1 - \nu_{12}\nu_{21}} z \right\rangle, & -B_{23} = B_{14} &= \frac{1}{4} \left\langle \frac{E_1 - E_2}{1 - \nu_{12}\nu_{21}} z \right\rangle, \\
B_{24} &= \frac{1}{4} \left\langle \frac{E_1 + E_2 - 2E_1\nu_{21}}{1 - \nu_{12}\nu_{21}} z \right\rangle, \\
C_{33} &= \frac{1}{4} \left\langle \frac{E_1 + E_2 + 2E_1\nu_{21}}{1 - \nu_{12}\nu_{21}} z^2 \right\rangle, & C_{34} &= -\frac{1}{4} \left\langle \frac{E_1 - E_2}{1 - \nu_{12}\nu_{21}} z^2 \right\rangle, \\
C_{44} &= \frac{1}{4} \left\langle \frac{E_1 + E_2 - 2E_1\nu_{21}}{1 - \nu_{12}\nu_{21}} z^2 \right\rangle
\end{aligned}$$

$$A_{44} = \langle G_{12} \rangle, \quad B_{42} = - \langle G_{12}z \rangle, \quad C_{22} = \langle G_{12}z^2 \rangle$$

$$\Gamma_1 = \frac{1}{2}(\lambda^2 + \eta^2) \frac{A_{44}C_{22} - B_{42}^2}{A_{44}}, \quad \Gamma_2 = \frac{1}{2}(\eta^2 - \lambda^2) \frac{A_{44}C_{22} - B_{42}^2}{A_{44}},$$

where λ follows from two Sturm-Liouville problems

$$\frac{d}{dz} \left(G_{2n} \frac{dZ}{dz} \right) + \lambda_*^2 G_{12} Z = 0, \quad \frac{dZ}{dz} \Big|_{|z|=\frac{h}{2}} = 0$$

and

$$\frac{d}{dz} \left(G_{1n} \frac{dZ^*}{dz} \right) + \eta^2 G_{12} Z^* = 0, \quad \frac{dZ^*}{dz} \Big|_{|z|=\frac{h}{2}} = 0$$

The details are given in Altenbach (2000). The classical stiffness tensors for homogeneous plates (the basic geometrical property is the thickness h , the plate is symmetrically with respect to the mid-plane which results in $\mathbf{B} \equiv \mathbf{0}$ and the following material data—Young's modulus E , shear modulus $G = E/2(1 + \nu)$, Poisson's ratio ν , all material properties are constant)

$$\begin{aligned}
A_{11} &= \frac{Eh}{2(1 - \nu)}, & A_{22} &= \frac{Eh}{2(1 + \nu)} = A_{44} = Gh, \\
C_{33} &= \frac{Eh^3}{24(1 - \nu)}, & C_{44} &= \frac{Eh^3}{24(1 + \nu)} = C_{22} = \frac{Gh^3}{12}
\end{aligned}$$

The classical plate (bending) stiffness (Timoshenko and Woinowsky-Krieger 1985) follows as

$$C_{33} + C_{44} = \frac{Eh^3}{12(1 - \nu^2)}$$

The transverse shear stiffness for the homogeneous plate follows from

$$\Gamma = \lambda^2 C_{22} \quad \text{with} \quad \frac{d^2 Z}{dz^2} + \lambda^2 Z = 0, \quad \left. \frac{dZ}{dz} \right|_{|z|=\frac{h}{2}} = 0$$

The λ value can be computed analytically. From $\cos \lambda z = 0$ yields the smallest eigenvalue

$$\lambda = \frac{\pi}{h}$$

and finally we have

$$\Gamma = \frac{\pi^2}{h^2} \frac{Gh^3}{12} = \frac{\pi^2}{12} Gh$$

$\pi^2/12$ is similar to the shear correction factor first presented in Mindlin (1951). The estimate of Reissner (1944) slightly differs (5/6).

Summarizing the presented results here:

- The classical stiffness tensors are in all approaches the same.
- Mindlin's estimate of the transverse shear stiffness coincide with our estimate. But Mindlin used a dynamic problem, we have a static problem for the computing of the transverse shear stiffness.
- Reissner's static approach coincide with our approach in the case of sandwich structures.
- For functionally graded materials we can make the following conclusions: Reissner's solution gives understated values of the transverse stiffness when the difference between elastic moduli is big enough. On the other hand, Reissner's solution gives overstated values when the elastic moduli do not differ.

5 Examples of Advanced Theories

5.1 Nanoeffects

Let discuss at first the formulation of theories for nano-plates and -shells.

- The development of nanotechnologies extends the field of application of the classical or non-classical theories of plates and shells towards the new thin-walled structures.
- In general, modern nanomaterials have physical properties which are different from the bulk material.
- The classical linear elasticity can be extended to the nanoscale by implementation of the theory of elasticity taking into account the surface stresses.

- In particular, the surface stresses are responsible for the size-effect, that means the material properties of a specimen depend on its size. For example, Young's modulus of a cylindrical specimen increases significantly, when the cylinder diameter becomes very small.
- The surface stresses are the generalization of the scalar surface tension which is well-known phenomenon in the theory of capillarity.

Previous investigations

- were related to investigations of the surface phenomena which were initiated by Gibbs (1928); Laplace (1805, 1806); Young (1805).
- resulted in several reviews by Duan et al. (2008); Finn (1986); Orowan (1970); Podstrigach and Povstenko (1985); Rusanov (2005a, b), ...
- taking into account surface stresses: Gurtin and Murdoch (1975a, b); Podstrigach and Povstenko (1985); Steigmann and Ogden (1999),
- applied the theory of elasticity with surface stresses to the modifications of the two-dimensional theories of nanosized plates in Altenbach and Eremeyev (2011); Altenbach et al. (2009, 2010a, 2012); Eremeyev et al. (2009); Huang (2008); Lu et al. (2006).

Various theories of plates are formulated. The approaches can be classified, for example, by the starting point of the derivation. This can be the well-known three-dimensional continuum mechanics equations. In contrast, one can introduce à priori a two-dimensional deformable surface which is the basis for a more natural formulation of the two-dimensional governing equations. This so-called direct approach should be supplemented by the theoretical or experimental determination of the material parameters included in the constitutive equations.

Here we use the general theory of shells presented in

- Libai and Simmonds (1998) and
- Chróścielewski et al. (2004)

for the modification of the constitutive equations taking into account the surface stresses.

We show that both the stress and the couple stress resultant tensors may be represented as a sum of two terms. The first term is the volume stress resultant while the second one determined by the surface stresses and the shell geometry. In the linear case this modification reduces to the addition of new terms to the elastic stiffness parameters. The influence of these terms on the bending stiffness of a shell is discussed. We show that the surface elasticity makes a shell more stiffer in comparison with the shell without surface stresses.

The strain energy function can be presented as

$$\begin{aligned}
 \mathcal{W} &= \mathcal{W}(\mathbf{F}, \mathbf{Q}, \nabla \mathbf{Q}), \quad \mathbf{F} \triangleq \nabla \mathbf{r}, \quad \mathbf{Q} \triangleq \mathbf{D}^k \otimes \mathbf{d}_k, \\
 \nabla(\dots) &\triangleq \mathbf{R}^\alpha \otimes \partial(\dots)/\partial q^\alpha, \quad \alpha, \beta = 1, 2, \\
 \mathbf{R}^\alpha \cdot \mathbf{R}_\beta &= \delta_\beta^\alpha, \quad \mathbf{R}^\alpha \cdot \mathbf{N} = 0, \quad \mathbf{R}_\alpha = \frac{\partial \mathbf{R}}{\partial q^\alpha},
 \end{aligned} \tag{2}$$

where \mathbf{Q} is an orthogonal tensor which is named the microrotation tensor, and \mathbf{N} is the unit normal to the surface Ω in the reference configuration. After application of the principle of the frame indifference \mathcal{W} takes the form

$$\begin{aligned} \mathcal{W} &= \mathcal{W}(\mathbf{E}, \mathbf{K}), \\ \mathbf{E} &\triangleq \mathbf{F} \cdot \mathbf{Q}^T, \quad \mathbf{K} \triangleq \frac{1}{2} \mathbf{R}^\alpha \otimes \left(\frac{\partial \mathbf{Q}}{\partial q^\alpha} \cdot \mathbf{Q}^T \right)_{\times} \end{aligned} \quad (3)$$

The Lagrangian equilibrium equations are

$$\begin{aligned} \nabla \cdot \mathbf{D} + \mathbf{q} &= \mathbf{0}, \quad \nabla \cdot \mathbf{H} + [\mathbf{F}^T \cdot \mathbf{D}]_{\times} + \mathbf{c} = \mathbf{0}, \\ \mathbf{D} &\triangleq \partial \mathcal{W} / \partial \mathbf{E} \cdot \mathbf{Q}, \quad \mathbf{H} \triangleq \partial \mathcal{W} / \partial \mathbf{K} \cdot \mathbf{Q}. \end{aligned} \quad (4)$$

Here \mathbf{D} and \mathbf{H} the surface stress resultant and stress couple tensors of the first Piola-Kirchhoff type, while \mathbf{q} and \mathbf{c} are the external surface force and moment vectors, respectively. The strain measures \mathbf{E} and \mathbf{K} are work-conjugate to the respective stress measures \mathbf{D} and \mathbf{H} .

For three-dimensional shell-like body we have if taking into account surface stresses (Gurtin and Murdoch 1975a, b)

$$\begin{aligned} \nabla_{\mathbf{x}} \cdot \mathbf{P} + \rho \mathbf{f} &= \mathbf{0}, \quad (\mathbf{n}_{\pm} \cdot \mathbf{P} - \nabla_{\pm} \cdot \mathbf{S}_{\pm})|_{\Omega_{\pm}} = \mathbf{t}_{\pm}, \\ \mathbf{u}|_{\Omega_u} &= \mathbf{0}, \quad \mathbf{n} \cdot \mathbf{P}|_{\Omega_f} = \mathbf{t}. \end{aligned} \quad (5)$$

Here \mathbf{P} is the first Piola-Kirchhoff stress tensor, \mathbf{S}_{\pm} is the surface stress tensors of the first Piola-Kirchhoff type acting on the surfaces Ω_{\pm} , $\mathbf{u} = \mathbf{x} - \mathbf{X}$ is the displacement vector, \mathbf{f} and \mathbf{t}_{\pm} , \mathbf{t} are the body force and surface loads vectors, respectively, ρ is the density. We assume that the part of body surface Ω_u is fixed, while on Ω_f the surface stresses are absent. In the theory of (Gurtin and Murdoch 1975a, b) the tensors \mathbf{S}_{\pm} are similar to the membrane stress resultants. $\mathbf{S}_{\pm} = \partial U_{\pm} / \partial \mathbf{F}$, where U_{\pm} are the surface strain energy densities. The reduction from 3D to 2D is performed in the sense of Chróścielewski et al. (2004); Libai and Simmonds (1998): for the nonlinear elastic body without surface stresses, i.e. when $\mathbf{S}_{\pm} = \mathbf{0}$, this technique gives the following relations between \mathbf{D} , \mathbf{H} , and \mathbf{P} :

$$\begin{aligned} \mathbf{D} &= \int \mathbf{G} \cdot \mathbf{P} d\zeta, \\ \mathbf{H} &= - \int \mathbf{G} \cdot \mathbf{P} \times \mathbf{z} d\zeta \end{aligned} \quad (6)$$

where \mathbf{z} is the base reference deviation, $\zeta \in [-h/2, h/2]$ and \mathbf{G} the geometrical tensor defined by Libai and Simmonds (1998).

The surface loads \mathbf{q} and \mathbf{c} in (4) are also determined by the through-the-thickness integration procedure. The boundary value problem (5) is linear with respect to the surface stresses \mathbf{S}_{\pm} . The through-the-thickness integration procedure is linear too. This means that the stress resultants for the shell with surface stresses can be

represented as a sum of two terms

$$\mathbf{D}^* = \mathbf{D} + \mathbf{D}_S \quad \mathbf{H}^* = \mathbf{H} + \mathbf{M}_S \quad (7)$$

\mathbf{D} , \mathbf{H} is the classical stress and couple stress resultant tensors (6), \mathbf{D}_S , \mathbf{H}_S are resultant tensors induced by \mathbf{S}_\pm

$$\begin{aligned} \mathbf{D}_S &= G_+ \nabla \cdot \mathbf{S}_+ + G_- \nabla \cdot \mathbf{S}_- \\ \mathbf{M}_S &= -h/2 [G_+ (\nabla \cdot \mathbf{S}_+) \times \mathbf{z}_+ - G_- (\nabla \cdot \mathbf{S}_-) \times \mathbf{z}_-]. \end{aligned} \quad (8)$$

Here G is the geometric scale factor, and $G_\pm = G|_{\zeta=\pm h/2}$. It may be shown that the tensors \mathbf{D}_S and \mathbf{H}_S have a structure of the constitutive equations of nonlinear Kirchhoff-Love-type theory. Further we restrict ourself assuming the linear theory.

Let us assume isotropic elastic material behavior. The theory is simplified in the case of plates and infinitesimal strains. The surface strain energy density is given by

$$\begin{aligned} 2W &= \alpha_1 \text{tr}^2 \mathbf{E}_\parallel + \alpha_3 \text{tr} (\mathbf{E}_\parallel \cdot \mathbf{E}_\parallel^T) + \alpha_4 \mathbf{N} \cdot \mathbf{E}^T \cdot \mathbf{E} \cdot \mathbf{N} \\ &+ \beta_1 \text{tr}^2 \mathbf{K}_\parallel + \beta_3 \text{tr} (\mathbf{K}_\parallel \cdot \mathbf{K}_\parallel^T) + \beta_4 \mathbf{N} \cdot \mathbf{K}^T \cdot \mathbf{K} \cdot \mathbf{N}. \end{aligned} \quad (9)$$

$\mathbf{E}_\parallel = \mathbf{E} \cdot \mathbf{A}$, $\mathbf{K}_\parallel = \mathbf{K} \cdot \mathbf{A}$, $\mathbf{A} = \mathbf{I} - \mathbf{N} \otimes \mathbf{N}$, α_i, β_i are the elastic constants

$$\begin{aligned} \alpha_1 &= C\nu, \quad \alpha_3 = C(1-\nu), \quad \alpha_4 = \alpha_s C(1-\nu), \\ \beta_1 &= D\nu, \quad \beta_3 = D(1-\nu), \quad \beta_4 = \alpha_t D(1-\nu), \\ C &= \frac{Eh}{1-\nu^2}, \quad D = \frac{Eh^3}{12(1-\nu^2)} \end{aligned} \quad (10)$$

E, ν are Young's modulus and Poisson's ratio of the bulk material, α_s, α_t are dimensionless coefficients, h is the shell thickness, α_s is similar to the shear correction factor introduced by Reissner (1944) ($\alpha_s = 5/6$) and Mindlin (1951) ($\alpha_s = \pi^2/12$). The value $\alpha_t = 0.7$ was proposed by Pietraszkiewicz (1979).

The surface stress tensors \mathbf{S}_\pm can be introduced following Duan et al. (2008); Gurtin and Murdoch (1975a, b)

$$\begin{aligned} \mathbf{S}_\pm &= \lambda_S^\pm \mathbf{A} \text{tr} \mathbf{e}_\pm + 2\mu_S^\pm \mathbf{e}_\pm, \\ 2\mathbf{e}_\pm &= \nabla \mathbf{u}_\pm \cdot \mathbf{A} + \mathbf{A} \cdot (\nabla \mathbf{u}_\pm)^T, \end{aligned} \quad (11)$$

$\mathbf{u}_\pm = \mathbf{u}|_{\zeta=\pm h/2}$, λ_S^\pm, μ_S^\pm —"surface Lamé's constants". For the sake of simplicity let us assume the symmetric case: $\lambda_S^\pm = \lambda_S$ and $\mu_S^\pm = \mu_S$.

Taking into account (11)

$$\begin{aligned} \alpha_1 &= C\nu + 2\lambda_S, \quad \alpha_3 = C(1-\nu) + 4\mu_S, \\ \beta_1 &= D\nu + h^2\lambda_S/2, \quad \beta_3 = D(1-\nu) + h^2\mu_S, \\ C^* &= C + 4\mu_S + 2\lambda_S, \\ D^* &= D + h^2\mu_S + h^2\lambda_S/2. \end{aligned} \quad (12)$$

C^* and D^* are the effective in-plane and bending stiffness of the plate with surface stresses. $C^* > C$ and $D^* > D$, i.e. the plate with surface stresses is stiffer. α_4, β_4 do not depend on λ_S and μ_S .

5.2 Direct Approach to Viscoelastic Plates

Since the direct approach is a natural way to describe the behavior of plates (the stress resultants which are used in most of plate theories can be interpreted as forces and moments) a two-dimensional plate theory which allows to model homogeneous and inhomogeneous plates can be presented also for the viscoelastic case. The equations of motions are the same as in the elastic case:

- balance of momentum

$$\nabla \cdot \mathbf{T} + \mathbf{q} = \rho \ddot{\mathbf{u}} + \rho \Theta_1 \cdot \ddot{\varphi}$$

- balance of moment of momentum

$$\nabla \cdot \mathbf{M} + \mathbf{T}_\times + \mathbf{m} = \rho \Theta_1^T \cdot \ddot{\mathbf{u}} + \rho \Theta_2 \cdot \ddot{\varphi}$$

\mathbf{T}, \mathbf{M} are tensors of forces and moments, \mathbf{q}, \mathbf{m} are surface loads (forces and moments), \mathbf{u}, φ are displacements and rotations, Θ_1, Θ_2 are first and second tensor of inertia, ρ is the density (effective property of the deformable surface). In addition, kinematical relations $\boldsymbol{\mu} = (\nabla \mathbf{u} \cdot \mathbf{a})^{\text{sym}}$, $\boldsymbol{\gamma} = \nabla \mathbf{u} \cdot \mathbf{n} + \mathbf{c} \cdot \varphi$, $\boldsymbol{\kappa} = \nabla \varphi$, $\boldsymbol{\mu}, \boldsymbol{\gamma}$ and $\boldsymbol{\kappa}$ are strain tensors and initial/boundary conditions. The boundary conditions are

- static and kinematic conditions

$$\boldsymbol{\nu} \cdot \mathbf{T} = \mathbf{f}, \quad \boldsymbol{\nu} \cdot \mathbf{M} = \mathbf{l} \quad (\mathbf{l} \cdot \mathbf{n} = 0) \quad \text{or} \quad \mathbf{u} = \mathbf{u}^0, \quad \varphi = \varphi^0 \quad \text{along } S$$

Here \mathbf{f} and \mathbf{l} are external force and moment vectors acting along the boundary S of the plate, while \mathbf{u}^0 and φ^0 are given functions describing the displacements and rotations of the plate boundary, respectively. $\boldsymbol{\nu}$ is the unit outer normal vector to the boundary S ($\boldsymbol{\nu} \cdot \mathbf{n} = 0$).

- boundary conditions corresponding to a hinge

$$\boldsymbol{\nu} \cdot \mathbf{M} \cdot \boldsymbol{\tau} = 0, \quad \mathbf{u} = \mathbf{0}, \quad \varphi \cdot \boldsymbol{\tau} = 0.$$

Here $\boldsymbol{\tau}$ is the unit tangent vector in the tangential plane to the boundary S ($\boldsymbol{\tau} \cdot \mathbf{n} = \boldsymbol{\tau} \cdot \boldsymbol{\nu} = 0$).

The constitutive behavior can be presented as follow

- in-plane forces

$$\mathbf{T} \cdot \mathbf{a} = \mathcal{A}\boldsymbol{\mu} + \mathcal{B}\boldsymbol{\kappa} \equiv \int_{-\infty}^t \mathbf{A}(t - \tau) \cdot \dot{\boldsymbol{\mu}}(\tau) d\tau + \int_{-\infty}^t \mathbf{B}(t - \tau) \cdot \dot{\boldsymbol{\kappa}}(\tau) d\tau,$$

- transverse shear forces

$$\mathbf{T} \cdot \mathbf{n} = \mathcal{G}\boldsymbol{\gamma} \equiv \Gamma(t - \tau) \cdot \dot{\boldsymbol{\gamma}}(\tau) d\tau,$$

- moments

$$\mathbf{M}^T = \hat{\mathcal{B}}\boldsymbol{\mu} + \mathcal{C}\boldsymbol{\kappa} \equiv \int_{-\infty}^t \dot{\boldsymbol{\mu}}(\tau) \cdot \mathbf{B}(t - \tau) d\tau + \int_{-\infty}^t \mathbf{C}(t - \tau) \cdot \dot{\boldsymbol{\kappa}}(\tau) d\tau$$

$\mathcal{A}, \mathcal{B}, \hat{\mathcal{B}}, \mathcal{C}, \mathcal{G}$ are linear viscoelastic operators, $\mathbf{A}(t), \mathbf{B}(t), \mathbf{C}(t)$ are 4th rank tensors, $\boldsymbol{\Gamma}(t)$ is a 2nd rank tensor. The effective stiffness properties (relaxation functions for the plate) can be compute like in the elastic case. They depend on the material properties and the cross-section geometry

$$\begin{aligned} \mathbf{A} &= A_{11}\mathbf{a}_1\mathbf{a}_1 + A_{12}(\mathbf{a}_1\mathbf{a}_2 + \mathbf{a}_2\mathbf{a}_1) + A_{22}\mathbf{a}_2\mathbf{a}_2 + A_{44}\mathbf{a}_4\mathbf{a}_4, \\ \mathbf{B} &= B_{13}\mathbf{a}_1\mathbf{a}_3 + B_{14}\mathbf{a}_1\mathbf{a}_4 + B_{23}\mathbf{a}_2\mathbf{a}_3 + \mathbf{B}_{24}\mathbf{a}_2\mathbf{a}_4 + B_{42}\mathbf{a}_4\mathbf{a}_2, \\ \mathbf{C} &= C_{22}\mathbf{a}_2\mathbf{a}_2 + C_{33}\mathbf{a}_3\mathbf{a}_3 + C_{34}(\mathbf{a}_3\mathbf{a}_4 + \mathbf{a}_4\mathbf{a}_3) + C_{44}\mathbf{a}_4\mathbf{a}_4, \\ \boldsymbol{\Gamma} &= \Gamma_1\mathbf{a}_1 + \Gamma_2\mathbf{a}_2, \end{aligned}$$

$$\mathbf{a}_1 = \mathbf{a} = \mathbf{e}_1\mathbf{e}_1 + \mathbf{e}_2\mathbf{e}_2, \quad \mathbf{a}_2 = \mathbf{e}_1\mathbf{e}_1 - \mathbf{e}_2\mathbf{e}_2,$$

$$\mathbf{a}_3 = \mathbf{c} = \mathbf{e}_1\mathbf{e}_2 - \mathbf{e}_2\mathbf{e}_1, \quad \mathbf{a}_4 = \mathbf{e}_1\mathbf{e}_2 + \mathbf{e}_2\mathbf{e}_1$$

Isotropic and symmetric over the thickness plates

$$\mathbf{A} = A_{11}\mathbf{a}_1\mathbf{a}_1 + A_{22}(\mathbf{a}_2\mathbf{a}_2 + \mathbf{a}_4\mathbf{a}_4), \quad \mathbf{C} = C_{22}(\mathbf{a}_2\mathbf{a}_2 + \mathbf{a}_4\mathbf{a}_4) + C_{33}\mathbf{a}_3\mathbf{a}_3,$$

$$\boldsymbol{\Gamma} = \Gamma\mathbf{a}$$

The viscoelastic orthotropic law is valid in the following cases:

Case 1: Homogeneous plates—all properties are constant (no dependency from z).

Case 2: Inhomogeneous plates (sandwich, multilayered, functionally graded)—all properties are functions of z .

The identification of the effective properties can be performed with the help of quasi-static boundary value problems (two-dimensional, three-dimensional) and the comparison of the forces and moments (in the sense of averaged stresses or stress resultants).

$$\mathbf{T} = \langle \mathbf{a} \cdot \boldsymbol{\sigma} \rangle, \quad \mathbf{M} = \langle \mathbf{a} \cdot \boldsymbol{\sigma}_z \cdot \mathbf{c} \rangle$$

$\boldsymbol{\sigma}$ is the stress tensor, $\langle (\dots) \rangle = \int_{-h/2}^{h/2} (\dots) dz$. The three-dimensional viscoelasticity is presented by

$$\boldsymbol{\sigma} = \int_{-\infty}^t \mathbf{R}(t - \tau) \cdot \dot{\boldsymbol{\varepsilon}}(\tau) d\tau \quad \text{or} \quad \boldsymbol{\varepsilon} = \int_{-\infty}^t \mathbf{J}(t - \tau) \cdot \dot{\boldsymbol{\sigma}} d\tau,$$

$\mathbf{R}(t)$ and $\mathbf{J}(t)$ are 4th rank tensors of relaxation and creep functions.

Let us consider that all properties are functions of the thickness coordinate z :

$$\mathbf{R} = \mathbf{R}(z, t), \quad \mathbf{J} = \mathbf{J}(z, t)$$

The density depends only on the thickness coordinate $\rho_0 = \rho_0(z)$

With the help of the Laplace transform

$$\bar{f}(s) = \int_0^{\infty} f(t) e^{-st} dt \quad \Rightarrow \quad \bar{\boldsymbol{\sigma}} = s \bar{\mathbf{R}}(s) \cdot \bar{\boldsymbol{\varepsilon}} \quad \text{or} \quad \bar{\boldsymbol{\varepsilon}} = s \bar{\mathbf{J}}(s) \cdot \bar{\boldsymbol{\sigma}}$$

one can perform the identification. Applying the correspondence principle one can use the identification procedure presented in Altenbach (1988). There are again basic test problems:

- tension/compression with superposed bending,
- in-plan shear, and
- torsion at the plate boundaries

The on-zero components of the stiffness tensors are for the isotropic case

$$\begin{aligned} \bar{A}_{11} &= \frac{1}{2} \left\langle \frac{\bar{E}}{1 - \bar{\nu}} \right\rangle, & \bar{A}_{22} &= \frac{1}{2} \left\langle \frac{\bar{E}}{1 + \bar{\nu}} \right\rangle = \bar{A}_{44} = \langle \bar{\mu} \rangle, \\ \bar{B}_{13} &= -\frac{1}{2} \left\langle \frac{\bar{E}}{1 - \bar{\nu}} z \right\rangle, & \bar{B}_{24} &= \frac{1}{2} \left\langle \frac{\bar{E}}{1 + \bar{\nu}} z \right\rangle = -\bar{B}_{42} = \langle \bar{\mu} z \rangle, \\ \bar{C}_{33} &= \frac{1}{2} \left\langle \frac{\bar{E}}{1 - \bar{\nu}} z^2 \right\rangle, & \bar{C}_{44} &= \frac{1}{2} \left\langle \frac{\bar{E}}{1 + \bar{\nu}} z^2 \right\rangle = \bar{C}_{22} = \langle \bar{\mu} z^2 \rangle, \\ \bar{\Gamma}_1 = \bar{\Gamma} &= \lambda^2 \frac{\bar{A}_{44} \bar{C}_{22} - \bar{B}_{42}^2}{\bar{A}_{44}}, \end{aligned}$$

λ is again the minimal nonzero eigen-value of a Sturm-Liouville problem

$$\frac{d}{dz} \left(\bar{\mu} \frac{dZ}{dz} \right) + \lambda^2 \bar{\mu} Z = 0, \quad \frac{dZ}{dz} \Big|_{|z|=\frac{h}{2}} = 0$$

The relaxation functions for the case of orthotropic material behavior are

$$\begin{aligned} \bar{A}_{11} &= \frac{1}{4} \left\langle \frac{\bar{E}_1 + \bar{E}_2 + 2\bar{E}_1 \bar{\nu}_{21}}{1 - \bar{\nu}_{12} \bar{\nu}_{21}} \right\rangle, & \bar{A}_{12} &= \frac{1}{4} \left\langle \frac{\bar{E}_1 - \bar{E}_2}{1 - \bar{\nu}_{12} \bar{\nu}_{21}} \right\rangle, \\ \bar{A}_{22} &= \frac{1}{4} \left\langle \frac{\bar{E}_1 + \bar{E}_2 - 2\bar{E}_1 \bar{\nu}_{21}}{1 - \bar{\nu}_{12} \bar{\nu}_{21}} \right\rangle, & \bar{A}_{44} &= \langle \bar{G}_{12} \rangle, \\ \bar{B}_{13} &= -\frac{1}{4} \left\langle \frac{\bar{E}_1 + \bar{E}_2 + 2\bar{E}_1 \bar{\nu}_{21}}{1 - \bar{\nu}_{12} \bar{\nu}_{21}} z \right\rangle, & -\bar{B}_{23} = \bar{B}_{14} &= \frac{1}{4} \left\langle \frac{\bar{E}_1 - \bar{E}_2}{1 - \bar{\nu}_{12} \bar{\nu}_{21}} z \right\rangle, \\ \bar{B}_{24} &= \frac{1}{4} \left\langle \frac{\bar{E}_1 + \bar{E}_2 - 2\bar{E}_1 \bar{\nu}_{21}}{1 - \bar{\nu}_{12} \bar{\nu}_{21}} z \right\rangle, & \bar{B}_{42} &= -\langle \bar{G}_{12} z \rangle, \\ \bar{C}_{33} &= \frac{1}{4} \left\langle \frac{\bar{E}_1 + \bar{E}_2 + 2\bar{E}_1 \bar{\nu}_{21}}{1 - \bar{\nu}_{12} \bar{\nu}_{21}} z^2 \right\rangle, & \bar{C}_{34} &= -\frac{1}{4} \left\langle \frac{\bar{E}_1 - \bar{E}_2}{1 - \bar{\nu}_{12} \bar{\nu}_{21}} z^2 \right\rangle, \\ \bar{C}_{44} &= \frac{1}{4} \left\langle \frac{\bar{E}_1 + \bar{E}_2 - 2\bar{E}_1 \bar{\nu}_{21}}{1 - \bar{\nu}_{12} \bar{\nu}_{21}} z^2 \right\rangle, & \bar{C}_{22} &= \langle \bar{G}_{12} z^2 \rangle, \\ \bar{\Gamma}_1 &= \frac{1}{2} (\lambda^2 + \eta^2) \frac{\bar{A}_{44} \bar{C}_{22} - \bar{B}_{42}^2}{\bar{A}_{44}}, & \bar{\Gamma}_2 &= \frac{1}{2} (\eta^2 - \lambda^2) \frac{\bar{A}_{44} \bar{C}_{22} - \bar{B}_{42}^2}{\bar{A}_{44}} \end{aligned}$$

where λ and η are minimal non-zero eigen-values of the problems

$$\begin{aligned} \frac{d}{dz} \left(\bar{G}_{2n} \frac{dZ}{dz} \right) + \lambda^2 \bar{G}_{12} Z &= 0, & \frac{dZ}{dz} \Big|_{|z|=\frac{h}{2}} &= 0, \\ \frac{d}{dz} \left(\bar{G}_{1n} \frac{d\tilde{Z}}{dz} \right) + \eta^2 \bar{G}_{12} \tilde{Z} &= 0, & \frac{d\tilde{Z}}{dz} \Big|_{|z|=\frac{h}{2}} &= 0 \end{aligned}$$

The following conclusions can be given:

- For a plate which is symmetrically to the midplane the relation $\bar{\mathbf{B}} = \mathbf{0}$ holds true.
- The relaxation functions of the isotropic viscoelastic plate with symmetric cross-section were considered in Altenbach and Eremeyev (2008).
- For isotropic viscoelastic material we introduced three functions $\bar{E}(s)$, $\bar{\mu}(s)$ and $\bar{\nu}(s)$. They are interlinked by

$$\bar{E} = 2\bar{\mu}(1 + \bar{\nu})$$

This is the definition of the Poisson's ratio for the viscoelastic material (Lakes and Wineman 2006).

- In the theory of viscoelasticity of solids the assumption $\nu(t) = \nu = \text{const}$ is often used. It is fulfilled in many applications (Christensen 1971; Drozdov 1996) concerning $\nu(t) \approx \text{const}$, for example, $\nu = 1/2$ for an incompressible viscoelastic material.
- In the general case, ν is a function of t . $\nu(t)$ was considered as an increasing function (Tschoegl 1989) or non-monotonous function (Lakes 1992) of t . The latter case may be realized for cellular materials or foams.
- Further we investigate the influence of $\nu(t)$ on the deflexion of a viscoelastic plate and its effective relaxation functions.

In the case of homogeneous plates with the assumption $\nu(t) = \nu = \text{const}$ we get $E(t) = 2\mu(t)(1 + \nu)$. In addition, we obtain

$$\begin{aligned} A_{11}(t) &= \frac{E(t)h}{2(1-\nu)}, & A_{22}(t) &= \frac{E(t)h}{2(1+\nu)} = \mu(t)h, \\ C_{33}(t) &= \frac{E(t)h^3}{24(1-\nu)}, & C_{22}(t) &= \frac{E(t)h^3}{24(1+\nu)} = \frac{\mu(t)h^3}{12} \end{aligned}$$

and the bending “stiffness”

$$D(t) = \frac{E(t)h^3}{12(1-\nu^2)}$$

The density and the rotation inertia are

$$\rho = \rho_0 h, \quad \Theta = \frac{\rho_0 h^3}{12} \quad (13)$$

For the Sturm-Liouville problem we obtain $\lambda = \pi/h$ and finally we have

$$\Gamma(t) = \lambda^2 C_{22} = \frac{\pi^2}{h^2} \frac{\mu(t)h^3}{12} = \frac{\pi^2}{12} \mu(t)h \quad (14)$$

For $\nu = \nu(t)$ we get

$$\bar{D} = \frac{\bar{E}h^3}{12(1-\bar{\nu}^2)}$$

and

$$D(t) = \int_{-\infty}^t \frac{E(t-\tau)h^3}{12[1-\nu^2(\tau)]} d\tau$$

Using formulas $f(0) = \lim_{s \rightarrow \infty} s \bar{f}(s)$ and $\lim_{t \rightarrow \infty} f(t) = \lim_{s \rightarrow 0} s \bar{f}(s)$, we obtain

$$D(0) = \frac{E(0)h^3}{12(1 - \nu_0^2)}, \quad D(\infty) = \frac{E(\infty)h^3}{12(1 - \nu_\infty^2)},$$

where

$$\nu_0 = \frac{E(0)}{2\mu(0)} - 1, \quad \nu_\infty = \frac{E(\infty)}{2\mu(\infty)} - 1, \quad f(\infty) = \lim_{t \rightarrow \infty} f(t)$$

In the case of the standard viscoelastic body we have

$$E(t) = E_\infty + (E_0 - E_\infty)e^{-t/\tau_E}, \quad \mu(t) = \mu_\infty + (\mu_0 - \mu_\infty)e^{-t/\tau_\mu},$$

$E_\infty < E_0$, $\mu_\infty < \mu_0$, τ_E , and τ_μ are the material constants. The transformed values are

$$\begin{aligned} \bar{E} &= \frac{E_\infty}{s} + \frac{E_0 - E_\infty}{s + \tau_E}, \quad \bar{\mu} = \frac{\mu_\infty}{s} + \frac{\mu_0 - \mu_\infty}{s + \tau_\mu}, \quad E_\infty < E_0, \quad \mu_\infty < \mu_0 \\ \bar{\nu} &= \frac{(s + \tau_\mu)(E_\infty \tau_E + E_0 s)}{2(s + \tau_E)(\mu_\infty \tau_\mu + \mu_0 s)} - 1 \end{aligned}$$

If $\bar{\nu} = \text{const}$ we get $E_\infty/E_0 = \mu_\infty/\mu_0$, $\tau_E = \tau_\mu$. The bending “stiffness” can be computed as

$$\bar{D} = \frac{\bar{\mu}^2 h^3}{3(4\bar{\mu} - \bar{E})} = \frac{(\mu_\infty + \mu_0 \tau_\mu s)^2 h^3}{s^2 (s \tau_\mu + 1)^2 \left[12 \frac{\mu_\infty + \mu_0 \tau_\mu s}{s(s \tau_\mu + 1)} - 3 \frac{E_\infty + E_0 \tau_E s}{s(s \tau_E + 1)} \right]},$$

which results in

$$D(0) = \frac{E_0 h^3}{12(1 - \nu_0^2)}, \quad D(\infty) = \frac{E_\infty h^3}{12(1 - \nu_\infty^2)},$$

and

$$\nu_0 = \frac{E_0}{2\mu_0} - 1, \quad \nu_\infty = \frac{E_\infty}{2\mu_\infty} - 1$$

For the panel made from a porous polymer foam the distribution of the pores over the thickness can be inhomogeneous. Let us introduce h as the thickness of the panel, ρ_s as the density of the bulk material and ρ_p as the minimum value of the density of the foam. For the description of the symmetric distribution of the porosity we assume the power law

$$V(z) = \alpha + (1 - \alpha) \left| \frac{2z}{h} \right|^n,$$

where $\alpha = \rho_p/\rho_s$ is the minimal relative density, n is the power. $n = 0$ corresponds to the homogeneous plate described in the previous paragraph. For the polymer foam the modification of the standard linear viscoelastic solid is proposed (Gibson and Ashby 1997)

$$\dot{\sigma} + \tau_E \sigma = \kappa(z) [E_\infty \tau_E \varepsilon + E_0 \dot{\varepsilon}]$$

For open-cell foams

$$\kappa(z) = C_1 V(z)^2,$$

for closed-cell foams

$$\kappa(z) = C_2 [\phi^2 V(z)^2 + (1 - \phi) V(z)]$$

$C_1 \approx 1$, $C_2 \approx 1$, ϕ describes the relative volume of the solid polymer concentrated near the cell ribs. Usually, $\phi = 0.6 \dots 0.7$. E_∞ , E_0 , τ_E are material constants of the polymer used in manufacturing of the foam. The corresponding relaxation function are

$$E = E(z, t) = E(t) \kappa(z), \quad E(t) = E_\infty + (E_0 - E_\infty) e^{-t/\tau_E},$$

Here E_∞ and E_0 are the equilibrium and the short-time Young's moduli ($E_\infty < E_0$), while τ_E is the relaxation time for tension.

By analogy the following relation can be established for the shear relaxation function

$$\mu = \mu(z, t) = \mu(t) m(z)$$

These equations have the meaning that the viscoelastic properties of the foam, for example, the time of relaxation, do not depend on the porosity distribution. Note that the representations are only rough approximation for spatial nonhomogeneous foams.

Further approximations can be given using experimental data of Ashby et al. (2000). One can assume $\nu = \text{const}$:

$$A_{11} = \frac{1 + \nu}{1 - \nu} A_{22}, \quad C_{33} = \frac{1 + \nu}{1 - \nu} C_{22},$$

$$\{A_{22}, C_{22}, \Gamma\} = \{A_{22}^\circ, C_{22}^\circ, \lambda^2 C_{22}^\circ\} \mu(t)$$

For the closed-cell foam A_{22}° and C_{22}° we obtain

$$A_{22}^\circ = h \left\{ \phi^2 \left[\alpha^2 + \frac{2\alpha(1-\alpha)}{n+1} + \frac{(1-\alpha)^2}{2n+1} \right] + (1-\phi) \left[\alpha + \frac{1-\alpha}{n+1} \right] \right\},$$

$$C_{22}^\circ = \frac{h^3}{12} \left\{ \phi^2 \left[\alpha^2 + \frac{6\alpha(1-\alpha)}{n+3} + \frac{3(1-\alpha)^2}{2n+3} \right] + (1-\phi) \left[\alpha + \frac{3(1-\alpha)}{n+3} \right] \right\},$$

while for the open-cell foam $\phi = 1$. Here we assume that $C_1 = 1$, $C_2 = 1$, and that ϕ does not depend on z . Let us summarize the results:

- It is easy to see that the classical relaxation functions differ only by factors from the shear relaxation function.
- Note that one can easily extend the suggested equation to the case of general constitutive equations.
- Thus, using assumption that $\nu = \text{const}$, one can calculate the classical effective stiffness relaxation functions for general viscoelastic constitutive equations multiplying the shear relaxation function with the corresponding factor.
- In the more general situation with $\nu = \nu(t)$ or taking into account other viscoelastic phenomena, for example, the filtration of a fluid in the saturated foam, the effective stiffness relaxation functions may be more complex than for the pure solid polymer discussed here.
- Finally, we should mention that in the case of constant Poisson's ratio and with the introduced assumption the determination of the effective in-plane, bending and transverse shear stiffness tensors of a symmetric viscoelastic plate made of a polymer foam can be realized by the same method as for elastic plates.
- The relaxation functions for viscoelastic plates can be found from the values of the corresponding effective stiffness of an elastic plate by multiplication with the normalized shear relaxation function of the polymer solid.

Let us consider a bending of viscoelastic plate with simple-support boundary conditions

$$s \overline{D}_{\text{eff}} \Delta \Delta \overline{w} = \overline{q}_n - \frac{\overline{D}_{\text{eff}}}{\overline{I}} \Delta \overline{q}_n,$$

where $\overline{D}_{\text{eff}} = \overline{C}_{22} + \overline{C}_{33}$ is Laplace transform of the effective bending stiffness relaxation function. Note that here $\overline{D}_{\text{eff}} = D_{\text{eff}}^0 \overline{\mu}(s)$, so we obtain that $D_{\text{eff}} = (C_{22}^0 + C_{33}^0) \mu(t)$. Using the assumption that $\nu = \text{const}$ we get the relation $\frac{\overline{D}_{\text{eff}}}{\overline{I}} = \frac{2}{\lambda^2(1-\nu)}$. We are looking for the solution in the form

$$w = \sum_{k=1}^{\infty} c_k(t) w_k(x, y),$$

where w_k are eigen-functions satisfying of the equation $\Delta \Delta w_k = \omega_k^2 w_k$ with simple-support boundary conditions, while c_k are unknown functions, we obtain that

$$\overline{c}_k(s) = \frac{1}{s \overline{D}_{\text{eff}} \omega_k^2} \left(\overline{q}_n - \frac{2}{\lambda^2(1-\nu)} \Delta \overline{q}_n, w_k \right), \quad (f, g) = \iint f g \, dx dy$$

This solution differs from the case of viscoelastic Kirchhoff plate (underlined terms). For the case of rectangular plate, it was shown that the maximal deflection may be on 20% larger than in the case of Kirchhoff plate. The deflection of a homogeneous rectangular plate is

$$w_{\max}(t) = Q_0 \frac{12(1-\nu^2)}{h^3\eta^4} \left[1 - \frac{2h^2 \left(\frac{1}{a^2} + \frac{1}{b^2} \right)}{1-\nu} \right] \left[\frac{1}{E_0} + \left(\frac{1}{E_0} - \frac{1}{E_\infty} \right) e^{-tE_0/(E_\infty\tau_E)} \right]$$

The deflection of a FGM rectangular plate can be computed as

$$\bar{w} = \frac{K}{\eta^4 h^4} \frac{Q}{s\bar{\mu}(s)} \sin \frac{\pi h x}{a} \sin \frac{\pi h y}{b}, \quad K = 1 + \frac{2\eta^2}{1-\nu} \frac{1}{\lambda^2}$$

$$K = K_K \equiv 1, \quad K = K_M \equiv 1 + \frac{2\eta}{1-\nu} \frac{1}{\pi^2}$$

The bounds are

$$1 + \frac{2\eta}{1-\nu} \frac{L^2 m_{\min}^2}{\pi^2 h^2} \leq K \leq 1 + \frac{2\eta}{1-\nu} \frac{L^2 m_{\max}^2}{\pi^2 h^2}$$

For example, if $\nu = 0.3$, $a = b$, $h = 0.05a$, $\alpha = 0.9$ it follows that $\lambda = 0.83/h$ for $n = 2$, and $\lambda = 0.82/h$ for $n = 5$. Then

$$K_M \approx 1.014, \quad K \approx 1.20 \quad (n = 2), \quad K \approx 1.21 \quad (n = 5)$$

For detailed analysis we refer to Altenbach and Eremeyev (2009).

References

- Altenbach, H. (1988). Eine direkt formulierte lineare Theorie für viskoelastische Platten und Schalen. *Ing.-Arch.*, 58, 215–228.
- Altenbach, H. (2000). An alternative determination of transverse shear stiffnesses for sandwich and laminated plates. *International Journal of Solid and Structure*, 37(25), 3503–3520.
- Altenbach, H., & Eremeyev, V. A. (2008). Analysis of the viscoelastic behavior of plates made of functionally graded materials. *ZAMM*, 88(5), 332–341.
- Altenbach, H., & Eremeyev, V. A. (2009). On the bending of viscoelastic plates made of polymer foams. *Acta Mechanica*, 204(3–4), 137–154.
- Altenbach, H., & Eremeyev, V. A. (2011). *Shell-like Structures: Non-classical Theories and Applications*. Advanced Structured Materials Berlin, Heidelberg: Springer Science & Business Media.
- Altenbach, H., & Mikhasev, G. (2014). *Shell and Membrane Theories in Mechanics and Biology: From Macro- to Nanoscale Structures*. Advanced Structured Materials Cham: Springer.
- Altenbach, H., Eremeyev, V. A., & Morozov, N. F. (2009). Linear theory of shells taking into account surface stresses. *Doklady Physics*, 54(12), 531–535.

- Altenbach, H., Eremeev, V. A., & Morozov, N. F. (2010a). On equations of the linear theory of shells with surface stresses taken into account. *Mechanics of Solids*, 45(3), 331–342.
- Altenbach, H., Eremeyev, V. A., & Morozov, N. F. (2012). Surface viscoelasticity and effective properties of thin-walled structures at the nanoscale. *International Journal of Engineering Science*, 59, 83–89.
- Altenbach, H., Altenbach, J., & Naumenko, K. (2016). *Ebene Flächentragwerke* (2nd ed.). Cham: Springer.
- Altenbach, J., Altenbach, H., & Eremeyev, V. A. (2010b). On generalized Cosserat-type theories of plates and shells: a short review and bibliography. *Archive of Applied Mechanics*, 80(1), 73–92.
- Ambarcumyan, S. A. (1991). *Theory of Anisotropic Plates: Strength, Stability, and Vibrations*. Washington: Hemisphere Publishing.
- Aron, H. (1874). Das Gleichgewicht und die Bewegung einer unendlich dünnen, beliebig gekrümmten elastischen Schale. *Journal für die reine und angewandte Mathematik*, 78, 136–174.
- Ashby, M. F., Evans, T., Fleck, N. A., Hutchinson, J. W., Wadley, H. N. G., & Gibson, L. J. (2000). *Metal Foams: A Design Guide*. Boston: Butterworth-Heinemann.
- Başar, Y., & Krätzig, W. B. (1985). *Mechanik der Flächentragwerke*. Braunschweig/Wiesbaden: Vieweg.
- Becchi, A., Corradi, M., Foce, F., & Pedemonte, O. (Eds.). (2003). *Essays on the History of Mechanics—In Memory of Clifford Ambrose Truesdell and Edoardo Benvenuto*. Basel: Birkhäuser.
- Christensen, R. M. (1971). *Theory of Viscoelasticity. An Introduction*. New York: Academic Press.
- Chróscielewski, J., Makowski, J., & Pietraszkiewicz, W. (2004). *Statics and Dynamics of Multi-folded Shells. Nonlinear theory and Finite Element Method*. Warsaw: IPPT PAN.
- Ciarlet, P. G. (1980). A justification of the von Kármán equations. *The Archive for Rational Mechanics and Analysis*, 73(4), 349–389.
- Ciarlet, P. G. (1990). *Plates and Junctions in Elastic Multi-Structures: An Asymptotic Analysis.*, Collection Recherches en Mathématiques Appliquées Paris: Masson.
- Cosserat, E., & Cosserat, F. (1909). *Théorie des corps déformables*. Paris: Herman et Fils.
- Donnel, L. H. (1976). *Beams, Plates, and Shells.*, Engineering Societies Monographs Series New York: McGraw-Hill.
- Drozдов, A. D. (1996). *Finite Elasticity and Viscoelasticity*. Singapore: World Scientific.
- Duan, H. L., Wang, J., & Karihaloo, B. L. (2008). Theory of elasticity at the nanoscale. *Advances in Applied Mechanics* (pp. 1–68). San Diego: Elsevier.
- Eremeyev, V. A., Altenbach, H., & Morozov, N. F. (2009). The influence of surface tension on the effective stiffness of nanosize plates. *Doklady Physics*, 54(2), 98–100.
- Finn, R. (1986). *Equilibrium Capillary Surfaces*. New-York: Springer.
- Föppl, A. (1907). *Vorlesungen über technische Mechanik* (Vol. 5). Leipzig: B.G. Teubner.
- Gibbs, J. W. (1928). On the equilibrium of heterogeneous substances. *The Collected Works of J. Willard Gibbs* (pp. 55–353). New York: Longmans, Green & Co.
- Gibson, L. J., & Ashby, M. F. (1997). *Cellular Solids: Structure and Properties*. Cambridge: Cambridge University Press.
- Gol'denveizer, A. L. (1962). Derivation of an approximate theory of bending of a plate by the methods of asymptotic integration of the equations of the theory of elasticity. *Prikl. Matem. Mekh.*, 26(4), 1000–1025.
- Gol'denveizer, A. L. (1963). Derivation of an approximate theory of shells by means of asymptotic integration of the equations of the theory of elasticity. *Prikl. Matem. Mekh.*, 27(4), 903–924.
- Grigolyuk, E. I., & Seleznev, I. T. (1973). *Nonclassical Theories of Oscillations of Rods, Plates, and Shells.*, togi Nauki i Tekhniki. Ser. Mekh. Tverdogo Deformir. Tela Moscow: VINITI.
- Gurtin, M. E., & Murdoch, A. I. (1975a). A continuum theory of elastic material surfaces. *Archive for Rational Mechanics and Analysis*, 57(4), 291–323.
- Gurtin, M. E., & Murdoch, A. I. (1975b). Addenda to our paper A continuum theory of elastic material surfaces. *Archive for Rational Mechanics and Analysis*, 59(4), 389–390.

- Huang, D. W. (2008). Size-dependent response of ultra-thin films with surface effects. *International Journal of Solids and Structures*, 45(2), 568–579.
- Jaiani, G., Podio-Guidugli, P. (2008). *IUTAM Symposium on Relations of Shell, Plate, Beam and 3D Models: Proceedings of the IUTAM Symposium on the Relations of Shell, Plate, Beam, and 3D Models Dedicated to the Centenary of Ilia Vekua's Birth, held Tbilisi, Georgia, April 23–27, 2007*, Vol. 9. Springer Science & Business Media.
- Kienzler, R. (2002). On consistent plate theories. *Archive of Applied Mechanics*, 72, 229–247.
- Kienzler, R., & Schneider, P. (2016). Direct approach versus consistent theory. In K. Naumenko & M. Abmus (Eds.), *Advances Methods of Continuum Mechanics for Materials and Structures* (Vol. 60, pp. 415–433)., Advanced Structured Materials Singapore: Springer.
- Kienzler, R., Altenbach, H., & Ott, I. (2003). *Theories of Plates and Shells: Critical Review and New Applications*., Lecture Notes in Applied and Computational Mechanics Berlin, Heidelberg: Springer.
- Kirchhoff, G. (1883). *Vorlesungen über Mathematische Physik* (3rd ed.). Leipzig: B. G. Teubner.
- Kirchhoff, G. R. (1850). Über das Gleichgewicht und die Bewegung einer elastischen Scheibe. *Crelles Journal für die reine und angewandte Mathematik*, 40, 51–88.
- Kurrer, K.-E. (2008). *The History of the Theory of Structures*., From Arch Analysis to Computational Mechanics Berlin: Ernst & Sohn.
- Lakes, R. S. (1992). The time-dependent Poisson's ratio of viscoelastic materials can increase or decrease. *Cellular Polymers*, 11, 466–469.
- Lakes, R. S., & Wineman, A. (2006). On Poisson's ratio in linearly viscoelastic solids. *Journal of Elasticity*, 85, 45–63.
- Laplace, P. S. (1805). Sur l'action capillaire. supplément à la théorie de l'action capillaire. *Traité de mécanique céleste* (Vol. 4, pp. 771–777)., Supplement 1, livre X Paris: Gauthier-Villars et fils.
- Laplace, P. S. (1806). À la théorie de l'action capillaire. supplément à la théorie de l'action capillaire. *Traité de mécanique céleste* (Vol. 4, pp. 909–945)., Supplement 2, Livre X Paris: Gauthier-Villars et fils.
- Lebedev, L. P., Cloud, M. J., & Eremeyev, V. A. (2010). *Tensor Analysis with Applications in Mechanics*. New Jersey: World Scientific.
- Léwinski, T. (1987). On refined plate models based on kinematical assumptions. *Ing.-Arch.*, 57, 133–146.
- Libai, A., & Simmonds, J. G. (1998). *The Nonlinear Theory of Elastic Shells* (2nd ed.). Cambridge: Cambridge University Press.
- Lo, K. H., Christensen, R. M., & Wu, E. M. (1977). A higher-order theory of plate deformation, part 1: Homogeneous plates. *Journal of Applied Mechanics Transactions of the ASME*, 44, 663–668.
- Love, A. E. H. (1906). *A Treatise on the Mathematical Theory of Elasticity* (2nd ed.). Cambridge: University Press.
- Lu, P., He, L. H., Lee, H. P., & Lu, C. (2006). Thin plate theory including surface effects. *International Journal of Solids and Structures*, 43(16), 4631–4647.
- Lurie, A. I. (1947). *Statics of the Thin Elastic Shells (in Russ.)*. Moscow: Gostekhizdat.
- Lurie, A. I. (1961). On the static-geometric analogy of the theory of shells. *Muschilishvili Anniversary Volume*. Philadelphia: SIAM.
- Lurie, A. I. (2005). *Theory of Elasticity*., Foundations of Engineering Mechanics Berlin: Springer.
- Maugin, G. (2013). *Continuum Mechanics Through the Twentieth Century*. Cham: Springer.
- Meenen, J., & Altenbach, H. (2001). A consistent deduction of von Kármán-type plate theories from three-dimensional non-linear continuum mechanics. *Acta Mechanica*, 147, 1–17.
- Mindlin, R. D. (1951). Influence of rotatory inertia and shear on flexural motions of isotropic elastic plates. *Journal of Applied Mechanics Transactions of the ASME*, 18, 31–38.
- Mushtari, K. M., & Galimov, K. Z. (1961). *Nonlinear Theory of Thin Elastic Shells*. Washington: NSF-NASA.
- Naghdi, P. M. (1972). The Theory of Shells and Plates. In S. Flügge (Ed.), *Handbuch der Physik* (pp. 425–640)., volume VIa/2 New York: Springer.
- Novozhilov, V. V. (1959). *The Theory of Thin Shells*. Groningen: Noordhoff.

- Nye, J. F. (2000). *Physical Properties of Crystals, their Representation by Tensors und Matrices*. Clarendon: Oxford, reprint edition.
- Orowan, E. (1970). Surface energy and surface tension in solids and fluids. *Proceedings of the Royal Society of London A*, 316(1527), 473–491.
- Panc, V. (1975). *Theories of Elastic Plates*. Leyden: Nordhoff Int. Publ.
- Pietraszkiewicz, W. (1979). *Finite Rotations and Lagrangian Description in the Non-linear Theory of Shells*. Warszawa-Poznań: Polish Scientific Publishers.
- Podio-Guidugli, P. (2003). A new quasilinear model for plate buckling. *Journal of Elasticity*, 71, 157–182.
- Podstrigach, Y. S., & Povstenko, Y. Z. (1985). *Introduction to Mechanics of Surface Phenomena in Deformable Solids (in Russ.)*. Kiev: Naukova Dumka.
- Reddy, J. N. (1984). A simple higher-order theory for laminated composite plates. *Journal of Applied Mechanics Transactions of the ASME*, 51(4), 745–752.
- Reddy, J. N. (2007). *Theory and Analysis of Elastic Plates and Shells* (2nd ed.). Boca Raton: CRC Press.
- Reddy, J. N. (2004). *Mechanics of Laminated Composite Plates: Theory and Analysis* (2nd ed.). Boca Raton: CRC Press.
- Reissner, E. (1944). On the theory of bending of elastic plates. *Journal of Mathematics and Physics*, 23, 184–191.
- Reissner, E. (1985). Reflection on the theory of elastic plates. *Applied Mechanics Review*, 38(11), 1453–1464.
- Ritz, W. (1908). Über eine neue Methode zur Lösung gewisser Variationsprobleme der mathematischen Physik. *Journal für die reine und angewandte Mathematik*, 135, 1–61.
- Rothert, H. (1973). Direkte Theorie von Linien- und Flächentragwerken bei viskoelastischen Werkstoffverhalten. Techn.-Wiss. Mitteilungen des Instituts für Konstruktiven Ingenieurbau 73-2, Ruhr-Universität, Bochum
- Rusanov, A. I. (2005a). Thermodynamics of solid surfaces. *Surface Science Reports*, 23(6–8), 173–247.
- Rusanov, A. I. (2005b). Surface thermodynamics revisited. *Surface Science Reports*, 58(5–8), 111–239.
- Schneider, P., & Kienzler, R. (2011). An algorithm for the automatization of pseudo reductions of PDE systems arising from the uniform-approximation technique. In H. Altenbach & V. A. Eremeyev (Eds.), *Shell-like Structures: Non-classical Theories and Applications* (pp. 377–390). Berlin, Heidelberg: Springer.
- Schneider, P., Kienzler, R., & Böhm, M. (2014). Modeling of consistent second-order plate theories for anisotropic materials. *ZAMM—Journal of Applied Mathematics and Mechanics / Zeitschrift für Angewandte Mathematik und Mechanik*, 94(1–2), 21–42.
- Steigmann, D. J., & Ogden, R. W. (1999). Elastic surface-substrate interactions. *Proc. R. Soc. London, Ser. A—Math. Phys. Engg. Sci.*, 455(1982), 437–474.
- Strutt, J. W. (1877). *The Theory of Sound* (Vol. 1). London: MacMillan and Co.
- Timoshenko, S. P. (1953). *History of Strength of Materials*. New York: McGraw-Hill.
- Timoshenko, S. P. (1921). On the correction for shear of the differential equation for transverse vibrations of prismatic bars. *Philosophical Magazine Series 6*(245), 41, 744–746.
- Timoshenko, S. P., & Woinowsky-Krieger, S. (1985). *Theory of Plates and Shells*. New York: McGraw Hill.
- Todhunter, I., & Pearson, K. (1960). *A History of the Theory of Elasticity and of the Strength of Materials: from Galilei to Lord Kelvin*. New York: Dover.
- Truesdell, C. A. (1964). Die Entwicklung des Drallsatzes. *ZAMM*, 44(4/5), 149–158.
- Truesdell, C. (1978). Comments on rational continuum mechanics. In G. M. de la Penha & L. A. Medeiros (Eds.), *Contemporary Developments in Continuum Mechanics and Partial Differential Equations* (pp. 495–603). North-Holland, Amsterdam.
- Tschoegl, N. W. (1989). *The Phenomenological Theory of Linear Viscoelastic Behavior. An Introduction*. Berlin: Springer.

- van der Heijden, A.M.A. (1976). *On modified boundary conditions for the free edge of a shell*. Ph.D. thesis, TH Delft, Delft.
- Vekua, I. N. (1955). On one method of calculating prismatic shells (in Russ.). *Trudy Tbilis. Mat. Inst.*, 21, 191–259.
- Vekua, I. N. (1985). *Shell Theory: General Methods of Construction*. Boston-London-Melbourne: Advanced Publishing Program. Pitman Advanced Publishing Program.
- Vlachoutsis, S. (1992). Shear correction factors for plates and shells. *International Journal for Numerical Methods in Engineering*, 33, 1537–1552.
- Vlasov, V. Z. (1949). *General Theory for Shells and its Application in Engineering (in Russ.)*. Moscow: Gostekhizdat.
- von Kármán, T. (1910). Festigkeitsprobleme im Maschinenbau. *Encyklopedie der Mathematischen Wissenschaften* (pp. 311–385). Leipzig: B.G. Teubner.
- Wang, C. M., Reddy, J. N., & Lee, K. H. (2000). *Shear Deformation Theories of Beams and Plates Dynamics Relationships with Classical Solution*. London: Elsevier.
- Wlassow, W. S. (1958). *Allgemeine Schalentheorie und ihre Anwendung in der Technik*. Berlin: Akademie-Verlag.
- Young, T. (1805). An essay on the cohesion of fluids. *Philosophical Transactions of the Royal Society of London*, 95, 65–87.
- Zhilin, P. A. (1976). Mechanics of deformable directed surfaces. *International Journal of Solids and Structures*, 12, 635–648.
- Zhilin, P. A. (1992). On the theories of Poisson and Kirchhoff from the point of view of modern plate theories (in Russ.). *Mekhanika Tverdogo Tela (Mechanics of Solids)*, 3, 49–64.

Basics of Mechanics of Micropolar Shells

Victor Eremeyev and Holm Altenbach

Abstract The chapter is devoted to the introduction to the nonlinear theory of micropolar shells called also six-parametric shell theory. Within the theory a shell is described as a deformable directed material surface each point of which has six degrees of freedom (DOF), i.e. three translational and three rotational DOF. In other words the shell kinematics coincides with the kinematics of a two-dimensional (2D) micropolar or Cosserat body. Here we present the basic equations of the micropolar shell theory including variational statements, compatibility conditions, etc.

1 Introduction

Theory of plates and shells is one of the oldest branches of mechanics. First scientific publications in the field belong to Euler who published paper in 1767, to the paper by J. Bernoulli in 1789, see the bibliography collected by Jemielita (2001) and the first chapter in this book. Nowadays there are theories of plates and shells related with the names by Kirchhoff, Love, Cosserat, Timoshenko, Reissner, Mindlin, Koiter, Naghdi, Donnell, Vekua and many others. So, many models may be considered as refinement or extension of the classical Kirchhoff-Love theory of shells. Nowadays, various refined 2D theories are implemented in commercial FEM software and widely used in contemporary engineering practice. Nevertheless, the refinement of plate and shell

V. Eremeyev (✉)

Department of Mechanical Engineering and Avionics,
Rzeszów University of Technology, Podkarpacie, Rzeszów, Poland
e-mail: veremeyev@prz.edu.pl

V. Eremeyev

South Scientific Center of Russian Academy of Science, Rostov on Don, Russia

V. Eremeyev

Department of Mathematics, Mechanics and Computer Science,
South Federal University, Rostov on Don, Russia

H. Altenbach

Chair of Engineering Mechanics, Faculty of Mechanical Engineering,
Otto-von-Guericke-University Magdeburg, Magdeburg, Germany
e-mail: holm.altenbach@ovgu.de

© CISM International Centre for Mechanical Sciences 2017
H. Altenbach and V. Eremeyev (eds.), *Shell-like Structures*,
CISM International Centre for Mechanical Sciences 572,
DOI 10.1007/978-3-319-42277-0_2

theories are still required in various directions, see brief discussion by Eremeyev and Pietraszkiewicz (2014). In particular, the following directions in the field of thin-walled structures are very actual:

- refinement of 2D governing relations for better accuracy;
- application to modelling of new materials and phenomena;
- development of efficient numerical tools.

For various methods of derivations of plates and shells equations we refer to Ambartsumyan (1970), Naghdi (1972), Goldenveizer (1976), Reissner (1985), Novozhilov et al. (1991), Libai and Simmonds (1998), Ciarlet (1997, 2000), Wang et al. (2000), Tovstik and Smirnov (2001), Kabrits et al. (2002), Reddy (2003), Kreja (2007), Amabili (2008), Carrera et al. (2011), Jaiani (2011). The current state of the art in the field can be found in recent paper collections and reviews (Pietraszkiewicz and Szymczak 2005; Jaiani and Podio-Guidugli 2008; Pietraszkiewicz and Kreja 2010; Altenbach and Eremeyev 2011c; Altenbach and Mikhasev 2014; Alijani and Amabili 2014; Pietraszkiewicz and Górski 2014).

In this chapter we discuss the nonlinear micropolar shell theory using the direct approach and its applications. Within the direct approach the basic governing equations are derived for a 2D continuum. The discussed model coincides kinematically with the general resultant nonlinear six-parameter theory of shells derived using the through-the-thickness integrations of the motion equations of the nonlinear elasticity. The basics of this theory is presented in Libai and Simmonds (1983, 1998), Chróścielewski et al. (2004a), Eremeyev and Zubov (2008), Lebedev et al. (2010), Eremeyev et al. (2013), Altenbach and Eremeyev (2013b), Pietraszkiewicz (2015). Within the micropolar shell theory the kinematics of the shell is determined by two kinematically independent fields of translations and rotations. The surface stress and couple stress tensors are introduced in the theory. Each point of the micropolar shell base surface has six degrees of freedom as in rigid body dynamics. This means that the drilling moment is taken in account. The advantage of the six-parameter shell model is the correct description of multifolded shells, of interaction of a shell with a rigid body, etc., see Konopińska and Pietraszkiewicz (2007), Pietraszkiewicz and Konopińska (2011), Pietraszkiewicz and Konopińska (2015) and the references therein. The full micropolar kinematics may be important for proper modelling of piezoelectric or piezomagnetic shells since electromagnetics fields produce forces and moments including the drilling ones, see Eringen and Maugin (1990), Maugin (1988). In addition, this gives the possibility of description of the contact interaction of shells with distributed on its surface nano-objects Eremeyev (2005a), Eremeyev et al. (2015a) or sensors, actuators, absorbers, etc., see Koç et al. (2005), Akay et al. (2005), Carcaterra et al. (2012), Andreaus et al. (2004), Vidoli and dell'Isola (2001), dell'Isola and Vidoli (1998), dell'Isola et al. (2003), Maurini et al. (2004).

This chapter is almost based on recent works by Altenbach and Eremeyev (2013a, 2014a, b), Eremeyev et al. (2013, 2015b), Eremeyev and Zubov (2007). In what follows we use the direct tensor calculus as in (Lebedev et al. 2010; Eremeyev et al. 2013). Here vectors and tensors are denoted by semi-bold font shape.

2 On Rigid Body Dynamics

In this section we recall basic notions of rigid body dynamics such as the moments, the inertia tensors, the kinetic energy and others which are also used in continuum mechanics and mechanics of structures. For details we can refer to various textbooks, see e.g. Lurie (2001).

The *rigid body* \mathcal{P} can be considered as a collection of mass points (material particles) and can be defined as follows.

Definition 2.1 A set of material points for which the mutual distances between the points remain unchanged in motion, is called rigid body.

The kinematics of the rigid body is determined by six parameters, by three translations of an arbitrary point of the rigid body and by three rotations. Let $o \in \mathcal{P}$ be a point of the body called the pole and $\mathbf{r}_0(t)$ is its position vector at instant t . This vector describes translations of the rigid body. For description of rotations we consider embedded the coordinate trihedron with unit vectors $\mathbf{d}_1(t), \mathbf{d}_2(t), \mathbf{d}_3(t)$, $\mathbf{d}_i \cdot \mathbf{d}_j = \delta_{ij}$, see Fig. 1, here δ_{ij} is the Kronecker symbol. Using $\mathbf{r}_0(t)$ and $\mathbf{d}_k(t)$ the position of any point $z \in \mathcal{P}$ is determined by

$$\mathbf{r}(t) = \mathbf{r}_0(t) + \mathbf{z}(t), \quad \mathbf{z}(t) = z_i \mathbf{d}_i(t). \tag{1}$$

For the body, we fix an initial configuration \varkappa . For example, we can take the body position at instant $t = 0$ as the initial configuration. The position of the pole o , the point z and the embedded trihedron of the coordinate axes that are $\mathbf{R}_0, \mathbf{R} = \mathbf{R}_0 + \mathbf{Z}, \mathbf{D}_1, \mathbf{D}_2, \mathbf{D}_3$, respectively, in the initial configuration, define the body position uniquely at any instant. As the body is rigid, $\mathbf{Z} = z_i \mathbf{D}_i$.

To describe the body rotation, instead of vectors \mathbf{d}_i we can introduce a proper orthogonal tensor $\mathbf{Q} = \mathbf{d}_i \otimes \mathbf{D}_i$, where \otimes is the tensor product. Then Eq. (1) takes

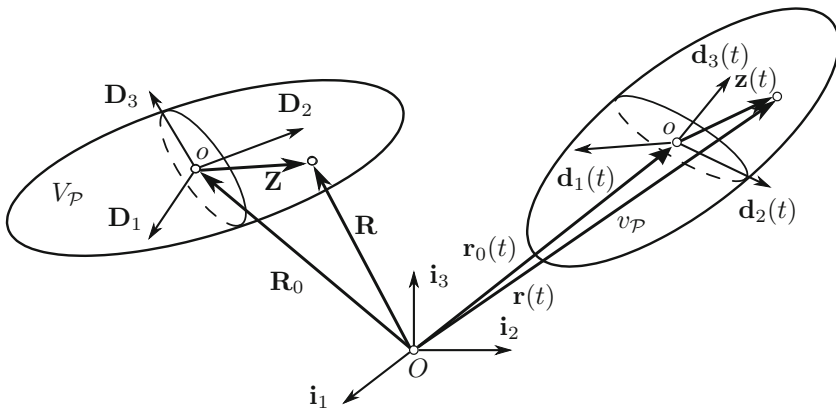


Fig. 1 Rigid body motion

the form

$$\mathbf{r}(t) = \mathbf{R}_0 + \mathbf{u}(t) + \mathbf{Q}(t) \cdot \mathbf{Z}. \quad (2)$$

Hence the rigid body motion is determined by two quantities, one of which is the translation vector of point o , i.e. $\mathbf{u}(t) = \mathbf{r}_0(t) - \mathbf{R}_0$, and another is the rotation tensor $\mathbf{Q}(t)$. To describe the motion, we also can use *Rodrigues's finite rotation vector* $\boldsymbol{\theta}$, cf. Lurie (2001) that we see in the representation of the proper orthogonal tensor

$$\mathbf{Q} = \frac{1}{(4 + \theta^2)} [(4 - \theta^2)\mathbf{I} + 2\boldsymbol{\theta} \otimes \boldsymbol{\theta} - 4\mathbf{I} \times \boldsymbol{\theta}], \quad \theta^2 = \boldsymbol{\theta} \cdot \boldsymbol{\theta}. \quad (3)$$

Here \times stands for the cross product while centered dot \cdot denotes the scalar (inner) product.

The other known vectorial parameterizations of an orthogonal tensor are presented by Pietraszkiewicz and Eremeyev (2009b), Bauchau and Trainelli (2003), Bauchau (2010), Wiśniewski (2010). By Eq. (3), vector $\boldsymbol{\theta}$ is determined by proper orthogonal tensor \mathbf{Q} as follows

$$\boldsymbol{\theta} = 2(1 + \text{tr } \mathbf{Q})^{-1} \mathbf{Q}_\times, \quad (4)$$

where $\text{tr } \mathbf{Q}$ is the trace of the second-order tensor, and we introduced the vector invariant \mathbf{Q}_\times by the formula

$$\mathbf{Q}_\times = (Q_{mn} \mathbf{e}^m \otimes \mathbf{e}^n)_\times \stackrel{\Delta}{=} Q_{mn} \mathbf{e}^m \times \mathbf{e}^n \quad (5)$$

for any base vectors \mathbf{e}^k . In particular, for a dyad $\mathbf{a} \otimes \mathbf{b}$ we have

$$(\mathbf{a} \otimes \mathbf{b})_\times = \mathbf{a} \times \mathbf{b}.$$

Differentiating (2) we find the velocity

$$\dot{\mathbf{r}}(t) = \dot{\mathbf{u}}(t) + \dot{\mathbf{Q}}(t) \cdot \mathbf{Z}. \quad (6)$$

Hereinafter, the overdot denotes the derivative with respect to time. \mathbf{Q} is orthogonal so tensor $\dot{\mathbf{Q}} \cdot \mathbf{Q}^T$ is skew-symmetric. As any skew-symmetric tensor, it can be represented in the form

$$\dot{\mathbf{Q}} \cdot \mathbf{Q}^T = \boldsymbol{\omega} \times \mathbf{I}, \quad (7)$$

where $\boldsymbol{\omega}$ is called the angular velocity of \mathcal{P} . Vector $\boldsymbol{\omega}$ can be determined from (7) as follows

$$\boldsymbol{\omega} = -\frac{1}{2}(\dot{\mathbf{Q}} \cdot \mathbf{Q}^T)_\times, \quad (8)$$

Thus the velocity vector of a body point takes the form

$$\mathbf{v}(t) = \dot{\mathbf{u}}(t) + \boldsymbol{\omega}(t) \times \mathbf{Z}, \quad (9)$$

The rigid body can be considered as a system of mass-points and so we introduce the following definitions.

Definition 2.2 The momentum and the moment of momentum with respect to the pole o for a rigid body are the quantities

$$\mathfrak{P} = \iiint_{v_{\mathcal{P}}} \rho \mathbf{v} \, dv, \quad \mathfrak{M} = \iiint_{v_{\mathcal{P}}} \rho (\mathbf{r} - \mathbf{r}_0) \times \mathbf{v} \, dv,$$

respectively.

Here ρ is the mass density of \mathcal{P} so its mass m is given by the integral over the domain $v_{\mathcal{P}} \subset \mathbb{R}^3$ taken by the body in the space,

$$m(\mathcal{P}) = \iiint_{v_{\mathcal{P}}} \rho \, dv.$$

Let us take as a pole the body mass center, that is the point whose radius vector \mathbf{r}_0 satisfies the relation

$$\iiint_{v_{\mathcal{P}}} \rho (\mathbf{r} - \mathbf{r}_0) \, dv = \mathbf{0}.$$

Then the momentum and the moment of momentum of the rigid body take the form

$$\mathfrak{P} = m \mathbf{v}_0, \quad \mathfrak{M} = \iiint_{v_{\mathcal{P}}} \rho \mathbf{z} \times \dot{\mathbf{z}} \, dv = \iiint_{v_{\mathcal{P}}} \rho \mathbf{z} \times (\boldsymbol{\omega} \times \mathbf{z}) \, dv = \mathbf{J} \cdot \boldsymbol{\omega}, \quad (10)$$

where $\mathbf{v}_0 = \dot{\mathbf{u}}$ and \mathbf{J} is the *inertia tensor*:

$$\mathbf{J} \triangleq \iiint_{v_{\mathcal{P}}} \rho [(\mathbf{z} \cdot \mathbf{z}) \mathbf{I} - \mathbf{z} \otimes \mathbf{z}] \, dv. \quad (11)$$

It is seen that \mathbf{J} possesses the following property

$$\mathbf{J} = \mathbf{Q} \cdot \mathbf{J}_0 \cdot \mathbf{Q}^T, \quad \mathbf{J}_0 \triangleq \iiint_{V_{\mathcal{P}}} \rho [(\mathbf{Z} \cdot \mathbf{Z}) \mathbf{I} - \mathbf{Z} \otimes \mathbf{Z}] \, dv, \quad (12)$$

where the volume integral is taken over $V_{\mathcal{P}}$ in the initial body configuration. The constant tensor \mathbf{J}_0 can be called the inertia tensor in the initial configuration. For example, for a solid homogeneous sphere of radius a , \mathbf{J} is a spherical tensor

$$\mathbf{J} = \frac{2}{5} m a^2 \mathbf{I} = \mathbf{J}_0.$$

If the directors \mathbf{d}_k are unit vectors along the principle axes of the inertia tensor, we see that \mathbf{J} and \mathbf{J}_0 are diagonal

$$\mathbf{J} = J_1 \mathbf{d}_1 \otimes \mathbf{d}_1 + J_2 \mathbf{d}_2 \otimes \mathbf{d}_2 + J_3 \mathbf{d}_3 \otimes \mathbf{d}_3,$$

$$\mathbf{J}_0 = J_1 \mathbf{D}_1 \otimes \mathbf{D}_1 + J_2 \mathbf{D}_2 \otimes \mathbf{D}_2 + J_3 \mathbf{D}_3 \otimes \mathbf{D}_3,$$

where J_1, J_2, J_3 are moments of inertia with respect to the principal axes.

With regard to (7) and (12) it can be shown that the derivative of \mathbf{J} satisfies the relation

$$\dot{\mathbf{J}} = \boldsymbol{\omega} \times \mathbf{J} - \mathbf{J} \times \boldsymbol{\omega}. \quad (13)$$

Taking the mass center as a pole we can rewrite the *kinetic energy* of the rigid body as follows

$$K \triangleq \frac{1}{2} \iiint_{v_P} \rho \mathbf{v} \cdot \mathbf{v} \, dv = \frac{1}{2} m \mathbf{v}_0 \cdot \mathbf{v}_0 + \frac{1}{2} \boldsymbol{\omega} \cdot \mathbf{J} \cdot \boldsymbol{\omega}. \quad (14)$$

The following identities are valid

$$\mathfrak{P} = \frac{\partial K}{\partial \mathbf{v}_0}, \quad \mathfrak{M} = \frac{\partial K}{\partial \boldsymbol{\omega}}. \quad (15)$$

To a rigid body we can apply the forces and torques (couples or moments). The forces relates with the translation of the body whereas the torques involve body rotation.

The rigid body motion is described by two Euler's laws of motion.

1. *The time rate of the rigid body momentum is equal to the resultant vector of forces \mathfrak{F} , acting on the body:*

$$\frac{d}{dt} \mathfrak{P} = \mathfrak{F}, \quad \mathfrak{F} \triangleq \iiint_{v_P} \rho \mathbf{f} \, dv. \quad (16)$$

2. *The time rate of the rigid body moment of momentum with respect to pole o is equal to the resultant moment of all forces with respect to the pole and the body moments:*

$$\frac{d}{dt} \mathfrak{M} = \mathfrak{C}, \quad \mathfrak{C} \triangleq \iiint_{v_P} \rho [(\mathbf{r} - \mathbf{r}_0) \times \mathbf{f} + \mathbf{m}] \, dv. \quad (17)$$

Here \mathbf{f} and \mathbf{m} are the densities of the forces and the moments acting on the body, respectively.

In equilibrium, these laws reduce to the equality to zero of the resultant vector of the forces and the resultant moment:

$$\mathfrak{F} = \mathbf{0}, \quad \mathfrak{C} = \mathbf{0}. \quad (18)$$

Substituting (10) to (17) and taking account (13), we get the motion equations of the rigid body

$$m\dot{\mathbf{v}}_0 = \mathfrak{F}, \quad \mathbf{J} \cdot \dot{\boldsymbol{\omega}} + \boldsymbol{\omega} \times \mathbf{J} \cdot \boldsymbol{\omega} = \mathfrak{C}. \quad (19)$$

In mechanics, Eqs. (16) and (17) constitute the foundation of classic mechanics as well as of continuum mechanics. For example, in equilibrium state of a deformable media Eqs. (18) should be fulfilled for ant part of the media.

3 Kinematics of a Micropolar Shell

In what follows we consider a shell as a material surface and apply Euler's motion laws to an arbitrary part of the shell. Each point (particle) of the shell is considered as infinitesimal rigid body with six degrees of freedom. The deformation of the shell is described by a mapping from a fixed reference configuration into an actual configuration. In other words, we consider a mapping between two directed surfaces including rotations of their particles. Let Σ be a base surface of the micropolar shell in the reference configuration \varkappa , q^α ($\alpha = 1, 2$) Gaussian coordinates on Σ , and $\mathbf{P}(q^1, q^2)$ the position vector of the points of Σ , see Fig. 2. Usually but not necessary, one uses undeformed shell state as a initial configuration. In the actual, deformed, configuration χ the base surface is denoted by σ , and the position of its material points (infinitesimal point-bodies) is given by vector $\boldsymbol{\rho}(q^1, q^2, t)$. The point-body orientation is described by the *microrotation tensor* $\mathbf{Q}(q^1, q^2, t)$ that is a proper orthogonal tensor. Introducing three orthonormal vectors \mathbf{D}_k ($k = 1, 2, 3$) describing the orientation in the reference configuration, and three orthonormal vectors \mathbf{d}_k determining the orientation in the actual configuration, we get tensor \mathbf{Q} in the form $\mathbf{Q} = \mathbf{d}_k \otimes \mathbf{D}_k$. Thus the micropolar shell is described by two kinematically independent fields

$$\boldsymbol{\rho} = \boldsymbol{\rho}(q^\alpha, t) \quad \text{and} \quad \mathbf{Q} = \mathbf{Q}(q^\alpha, t). \quad (20)$$

Instead of \mathbf{Q} one can use vectorial representation (3) of \mathbf{Q} or other vectorial representations of a rotation tensor, see Pietraszkiewicz and Eremeyev (2009b), Wiśniewski (2010).

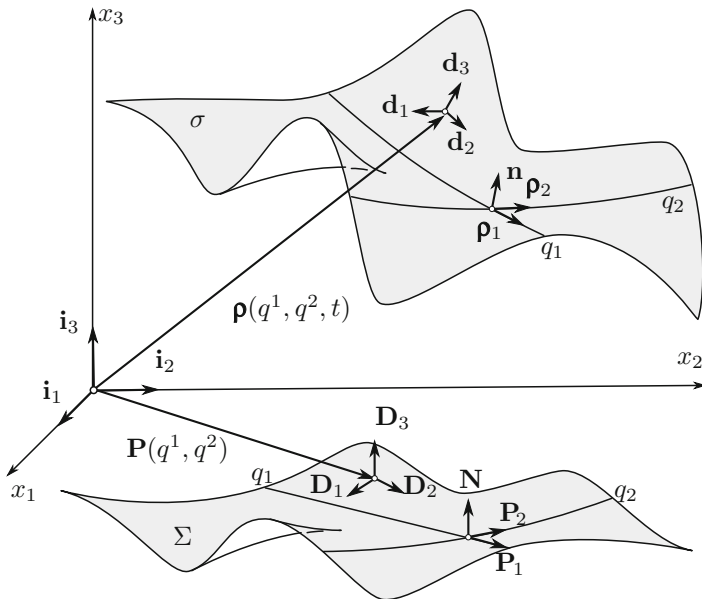


Fig. 2 Kinematics of a micropolar shell

4 Euler's Motion Laws of a Micropolar Shell

The shell motion equations can be introduced using two-dimensional analogues of Euler's motion laws. Here we use the referential (Lagrangian) description, so we introduce quantities using the reference configuration. Let us define the momentum \mathfrak{P} and moment of momentum \mathfrak{M} of an arbitrary shell part \mathcal{P} as follows

$$\mathfrak{P}(\mathcal{P}) \triangleq \iint_{\Sigma_{\mathcal{P}}} \rho \mathbf{K}_1 d\Sigma, \quad \mathfrak{M}(\mathcal{P}) \triangleq \iint_{\Sigma_{\mathcal{P}}} \rho \{(\boldsymbol{\rho} - \boldsymbol{\rho}_0) \times \mathbf{K}_1 + \mathbf{K}_2\} d\Sigma, \quad (21)$$

where \mathbf{K}_1 and \mathbf{K}_2 are defined by formulae

$$\mathbf{K}_1 \triangleq \frac{\partial K}{\partial \mathbf{v}} = \mathbf{v} + \boldsymbol{\Theta}_1^T \cdot \boldsymbol{\omega}, \quad \mathbf{K}_2 \triangleq \frac{\partial K}{\partial \boldsymbol{\omega}} = \boldsymbol{\Theta}_1 \cdot \mathbf{v} + \boldsymbol{\Theta}_2 \cdot \boldsymbol{\omega}, \quad (22)$$

$$K(\mathbf{v}, \boldsymbol{\omega}) = \frac{1}{2} \mathbf{v} \cdot \mathbf{v} + \boldsymbol{\omega} \cdot \boldsymbol{\Theta}_1 \cdot \mathbf{v} + \frac{1}{2} \boldsymbol{\omega} \cdot \boldsymbol{\Theta}_2 \cdot \boldsymbol{\omega}, \quad (23)$$

$\Sigma_{\mathcal{P}} \subset \Sigma$ is the part of Σ corresponding to \mathcal{P} in the reference configuration, see Fig. 3.

Here

$$\mathbf{v} = \frac{d\boldsymbol{\rho}}{dt}, \quad \boldsymbol{\omega} = \frac{1}{2} \left(\mathbf{Q}^T \cdot \frac{d\mathbf{Q}}{dt} \right)_{\times}$$

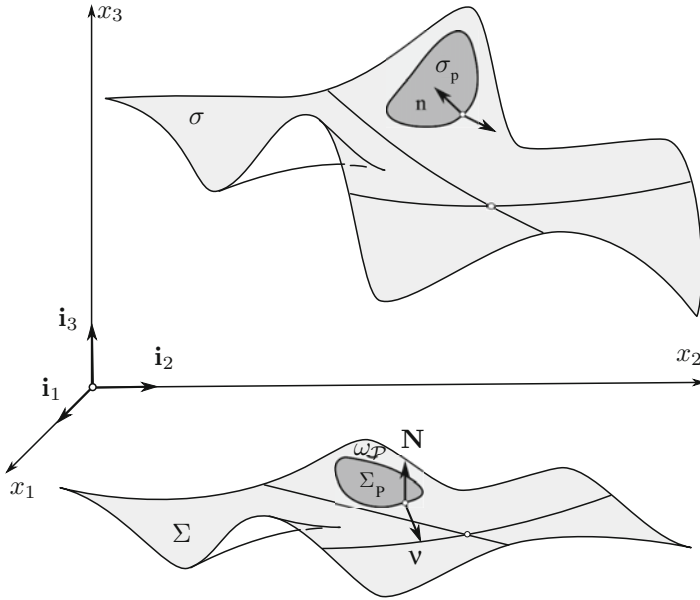


Fig. 3 Part \mathcal{P} of the shell in reference and actual configurations

are the linear and angular velocities, respectively, ρ is the surface mass density in the reference configuration, ρK is the surface density of the kinetic energy, and $\rho\Theta_1, \rho\Theta_2$ are the rotatory inertia tensors ($\Theta_2^T = \Theta_2$). We assume that K is a quadratic form of velocities \mathbf{v} and $\boldsymbol{\omega}$.

Equations (22) are called the kinetic constitutive equations of the micropolar shell. A more general form of the kinetic constitutive equations is discussed by Pietraszkiewicz (2011). Presented here definitions of momentum and moment of momentum for a part of the shell are straightforward generalizations of momentum and moment of momentum of a rigid body.

In a similar way, Euler’s motion laws for the shell are analogues of Eqs. (16) and (17), they are formulated as follows:

1. Balance of momentum. First Euler’s law of motion of the shell. *The time rate of change of the momentum of an arbitrary shell part \mathcal{P} is equal to the total force acting on \mathcal{P} :*

$$\frac{d}{dt} \mathfrak{P}(\mathcal{P}) = \mathfrak{F}, \quad \mathfrak{F} \triangleq \iint_{\Sigma_{\mathcal{P}}} \mathbf{f} \, d\Sigma + \int_{\omega_{\mathcal{P}}} \mathbf{t} \, d\omega. \tag{24}$$

Here \mathbf{f} is the surface force density distributed on $\Sigma_{\mathcal{P}}$ and \mathbf{t} is the linear density of forces distributed along corresponding parts of the contour $\omega_{\mathcal{P}}$, respectively.

2. Balance of moment of momentum. Second Euler's law of motion of the shell. *The time rate of change of the moment of momentum of an arbitrary shell part \mathcal{P} about a fixed point ρ_0 is equal to the total moment about ρ_0 acting on \mathcal{P} :*

$$\frac{d}{dt} \mathfrak{M}(\mathcal{P}) = \mathfrak{C}, \quad (25)$$

$$\mathfrak{C} \triangleq \iint_{\Sigma_{\mathcal{P}}} \{(\rho - \rho_0) \times \mathbf{f} + \mathbf{m}\} d\Sigma + \int_{\omega_{\mathcal{P}}} \{(\rho - \rho_0) \times \mathbf{t} + \boldsymbol{\mu}\} d\omega.$$

The quantities \mathbf{m} and $\boldsymbol{\mu}$ introduced here are the surface and linear densities of couples distributed along corresponding parts of $\Sigma_{\mathcal{P}}$ and $\omega_{\mathcal{P}}$, respectively.

So, here as in the case of rigid body dynamics we have forces and couples as basic loading parameters. Unlike a rigid body for a shell we have surface and linear densities of forces and couples. In other words, we assume that the interaction between shell and its environment or between shell parts is described only by forces and couples (moments).

As for 3D Cosserat continuum (Eremeyev et al. 2013), using (24) and (25) we can prove two-dimensional analogues to the Cauchy lemma and Cauchy theorem and afterwards introduce the surface stress measures and derive the motion equations of a micropolar shell. As the result we introduce the nonsymmetric second-order tensors \mathbf{D} and \mathbf{G} which relate to \mathbf{t} and $\boldsymbol{\mu}$ by formulas

$$\mathbf{t} = \mathbf{v} \cdot \mathbf{D}, \quad \boldsymbol{\mu} = \mathbf{v} \cdot \mathbf{G},$$

where \mathbf{v} is the external unit normal to the boundary curve $\omega_{\mathcal{P}}$ such that $\mathbf{v} \cdot \mathbf{N} = 0$. \mathbf{D} and \mathbf{G} are the *surface stress and couple stress tensors* of the 1st Piola-Kirchhoff type.

The following relations are valid:

$$\mathbf{N} \cdot \mathbf{D} = \mathbf{0} = \mathbf{N} \cdot \mathbf{G}. \quad (26)$$

In what follows we use the *divergence theorem* on the surface

$$\iint_{\Sigma} (\nabla_s \cdot \mathbf{T} + 2HN \cdot \mathbf{T}) d\Sigma = \int_{\partial\Sigma} \mathbf{v} \cdot \mathbf{T} ds, \quad (27)$$

where \mathbf{T} is an arbitrary tensor field, ∇_s is the *surface nabla-operator* on Σ defined by the formula

$$\nabla_s = \mathbf{P}^\alpha \frac{\partial}{\partial q^\alpha}, \quad \mathbf{P}_1 = \frac{\partial \mathbf{P}}{\partial q^1}, \quad \mathbf{P}_2 = \frac{\partial \mathbf{P}}{\partial q^2}, \quad \mathbf{P}_\alpha \cdot \mathbf{P}^\beta = \delta_\alpha^\beta \quad (\alpha, \beta = 1, 2).$$

\mathbf{v} is the unit external normal to contour $\partial\Sigma$, lying in the tangent plane to Σ , that is $\mathbf{v} \cdot \mathbf{N} = 0$, \mathbf{N} is the normal to the surface Σ , and H is the mean curvature of Σ .

From (24) and (25) we obtain the Lagrangian *motion equations* of the micropolar shell

$$\begin{aligned} \nabla_s \cdot \mathbf{D} + \mathbf{f} &= \rho \frac{d\mathbf{K}_1}{dt}, \\ \nabla_s \cdot \mathbf{G} + [\mathbf{F}^T \cdot \mathbf{D}]_x + \mathbf{m} &= \rho \left(\frac{d\mathbf{K}_2}{dt} + \mathbf{v} \times \Theta_1^T \cdot \boldsymbol{\omega} \right). \end{aligned} \quad (28)$$

Here $\mathbf{F} = \nabla_s \boldsymbol{\rho}$ is the *surface deformation gradient*. These equations are presented also by Chróscielewski et al. (2004b), Eremeyev and Zubov (2008), Libai and Simmonds (1998).

5 Strain Energy Density and Strain Measures

For a micropolar hyper-elastic shell we can introduce a strain energy density W . With regard for the local action principle by Truesdell and Noll (1965), W takes the form

$$W = W(\boldsymbol{\rho}, \nabla_s \boldsymbol{\rho}, \mathbf{Q}, \nabla_s \mathbf{Q}).$$

Here we recall that

$$\nabla_s \boldsymbol{\psi} \triangleq \mathbf{P}^\alpha \otimes \frac{\partial \boldsymbol{\psi}}{\partial q^\alpha} \quad (\alpha, \beta = 1, 2), \quad \mathbf{P}^\alpha \cdot \mathbf{P}_\beta = \delta_\beta^\alpha, \quad \mathbf{P}^\alpha \cdot \mathbf{N} = 0, \quad \mathbf{P}_\beta = \frac{\partial \mathbf{P}}{\partial q^\beta}.$$

Here vectors \mathbf{P}_β and \mathbf{P}^α denote the natural and reciprocal bases on Σ respectively, \mathbf{N} is the unit normal to Σ , ∇_s is the surface nabla operator on Σ , and $\boldsymbol{\psi}$ is an arbitrary differentiable tensor field given on Σ .

From the principle of material frame-indifference by Truesdell and Noll (1965) we can deduce that W depends on two surface strain measures \mathbf{E} and \mathbf{K} of Cosserat type:

$$W = W(\mathbf{E}, \mathbf{K}),$$

where

$$\mathbf{E} = \mathbf{F} \cdot \mathbf{Q}^T - \mathbf{A}, \quad \mathbf{K} = \frac{1}{2} \mathbf{P}^\alpha \otimes \left(\frac{\partial \mathbf{Q}}{\partial q^\alpha} \cdot \mathbf{Q}^T \right)_x, \quad \mathbf{F} = \nabla_s \boldsymbol{\rho}. \quad (29)$$

Here \mathbf{F} is the surface deformation gradient, $\mathbf{A} \triangleq \mathbf{I} - \mathbf{N} \otimes \mathbf{N}$, and \mathbf{I} is the 3D unit tensor.

The proper orthogonal tensor describing the rotation about axis \mathbf{e} for angle φ can be represented with use of the Gibbs's formula

$$\mathbf{Q} = (\mathbf{I} - \mathbf{e} \otimes \mathbf{e}) \cos \varphi + \mathbf{e} \otimes \mathbf{e} - \mathbf{e} \times \mathbf{I} \sin \varphi, \quad (30)$$

where φ is the rotation angle about the axis with the unit vector \mathbf{e} .

Introducing the finite rotation vector $\boldsymbol{\theta} = 2\mathbf{e} \tan \varphi/2$ we get a representation of \mathbf{Q} in the form (3) that does not contain trigonometric functions. By Eq. (3), a proper orthogonal tensor \mathbf{Q} defines uniquely vector $\boldsymbol{\theta}$

$$\boldsymbol{\theta} = 2(1 + \text{tr } \mathbf{Q})^{-1} \mathbf{Q}_\times. \quad (31)$$

Using the *finite rotation vector* $\boldsymbol{\theta}$ we can express \mathbf{K} as follows

$$\mathbf{K} = \mathbf{P}^\alpha \otimes \mathbf{L}_\alpha = \frac{4}{4 + \theta^2} \nabla_s \boldsymbol{\theta} \cdot \left(\mathbf{I} + \frac{1}{2} \mathbf{I} \times \boldsymbol{\theta} \right). \quad (32)$$

The strain measures \mathbf{E} and \mathbf{K} are two-dimensional analogues of the strain measures used in 3D Cosserat continuum, see Pietraszkiewicz and Eremeyev (2009a, b).

6 Constitutive Equations of an Elastic Isotropic Shell

For an elastic shell, the constitutive equations are defined by the surface strain energy density as the function of two strain measures. An example we present the model of a *physically linear isotropic shell*, see Chróścielewski et al. (2004b), Eremeyev and Pietraszkiewicz (2006), Eremeyev and Zubov (2008), whose energy is given by the quadratic form

$$2W = \alpha_1 \text{tr } {}^2\mathbf{E}_\parallel + \alpha_2 \text{tr } \mathbf{E}_\parallel^2 + \alpha_3 \text{tr } (\mathbf{E}_\parallel \cdot \mathbf{E}_\parallel^T) + \alpha_4 \mathbf{N} \cdot \mathbf{E}^T \cdot \mathbf{E} \cdot \mathbf{N} \\ + \beta_1 \text{tr } {}^2\mathbf{K}_\parallel + \beta_2 \text{tr } \mathbf{K}_\parallel^2 + \beta_3 \text{tr } (\mathbf{K}_\parallel \cdot \mathbf{K}_\parallel^T) + \beta_4 \mathbf{N} \cdot \mathbf{K}^T \cdot \mathbf{K} \cdot \mathbf{N}, \quad (33)$$

where $\mathbf{E}_\parallel \triangleq \mathbf{E} \cdot \mathbf{A}$, $\mathbf{K}_\parallel \triangleq \mathbf{K} \cdot \mathbf{A}$. In Eq. (33) there is no term that is bilinear in \mathbf{E} and \mathbf{K} , it is a consequence of the fact that the surface wryness tensor \mathbf{K} is a axial tensor that changes the sign on a space mirror reflection. Discussion on axial and polar tensors can be found for example in Eremeyev et al. (2013). Note the constitutive equations contain 8 parameters, α_k, β_k $k = 1, 2, 3, 4$.

With respect to Eq. (33) \mathbf{P}_1 and \mathbf{P}_2 have the form

$$\mathbf{P}_1 = \alpha_1 (\text{tr } \mathbf{E}_\parallel) \mathbf{A} + \alpha_2 \mathbf{E}_\parallel^T + \alpha_3 \mathbf{E}_\parallel + \alpha_4 (\mathbf{E} \cdot \mathbf{N}) \otimes \mathbf{N}, \quad (34)$$

$$\mathbf{P}_2 = \beta_1 (\text{tr } \mathbf{K}_\parallel) \mathbf{A} + \beta_2 \mathbf{K}_\parallel^T + \beta_3 \mathbf{K}_\parallel + \beta_4 (\mathbf{K} \cdot \mathbf{N}) \otimes \mathbf{N}. \quad (35)$$

Introducing the fourth-order tensors \mathbf{C}_1 and \mathbf{C}_2 by the formulae

$$\mathbf{C}_1 = \alpha_1 \mathbf{A} \otimes \mathbf{A} + \alpha_2 \mathbf{P}_\alpha \otimes \mathbf{A} \otimes \mathbf{P}^\alpha + \alpha_4 \mathbf{P}_\alpha \otimes \mathbf{N} \otimes \mathbf{P}^\alpha \otimes \mathbf{N},$$

$$\mathbf{C}_2 = \beta_1 \mathbf{A} \otimes \mathbf{A} + \beta_2 \mathbf{P}_\alpha \otimes \mathbf{A} \otimes \mathbf{P}^\alpha \mathbf{P}^\beta + \beta_4 \mathbf{P}_\alpha \otimes \mathbf{N} \otimes \mathbf{P}^\alpha \otimes \mathbf{N}$$

we re-write (34) and (35) in a more compact form

$$\mathbf{P}_1 = \mathbf{C}_1 : \mathbf{E}, \quad \mathbf{P}_2 = \mathbf{C}_2 : \mathbf{K}, \quad (36)$$

where “:” denotes the inner product in the space of second-order tensors, for example

$$(\mathbf{a} \otimes \mathbf{b} \otimes \mathbf{c} \otimes \mathbf{d}) : (\mathbf{x} \otimes \mathbf{y}) = (\mathbf{c} \cdot \mathbf{x})(\mathbf{d} \cdot \mathbf{y})\mathbf{a} \otimes \mathbf{b}.$$

For the elastic moduli in Eq. (33) Chróścielewski et al. (2004b) proposed the relations:

$$\begin{aligned} \alpha_1 &= C\nu, \quad \alpha_2 = 0, \quad \alpha_3 = C(1 - \nu), \quad \alpha_4 = \alpha_s C(1 - \nu), \\ C &= \frac{Eh}{1 - \nu^2}, \\ \beta_1 &= D\nu, \quad \beta_2 = 0, \quad \beta_3 = D(1 - \nu), \quad \beta_4 = \alpha_t D(1 - \nu), \\ D &= \frac{Eh^3}{12(1 - \nu^2)}, \end{aligned}$$

where E is the Young modulus, ν is the Poisson ratio of the bulk material, and h is the shell thickness. Parameter α_s is the dimensionless shear correction factor. Reissner (1944) used $\alpha_s = 5/6$ in his plate theory, by Mindlin (1951) $\alpha_s = \pi^2/12$. For the couple stresses parameter α_t plays a role similar to α_s for the stresses. The value $\alpha_t = 0.7$ was proposed by Pietraszkiewicz (1979a, b), also see Chróścielewski et al. (2010). In Chróścielewski et al. (2004b), Chróścielewski and Witkowski (2010), Chróścielewski et al. (2010) the influence of α_s and α_t on the solution is investigated numerically for several boundary value problems.

For some types of anisotropy, other representations of shell energy density W were constructed by Eremeyev and Pietraszkiewicz (2006) using material symmetry groups. Let us note that the definition of the material symmetry group for shells is more complex than in the case of simple materials (Truesdell 1984) and even for micropolar elastic materials (Eremeyev and Pietraszkiewicz 2012, 2016).

7 The Virtual Work Principle and Formulation of Boundary Value Problems

Another way of derivation of motion and equilibrium equation is based on the virtual work principle. For formulations of the principle of virtual power for media with microstructure we refer to the landmark papers by Sedov (1968) and by Germain (1973a, b) see also Berdichevsky (2009). Lagrangian equilibrium equations for a micropolar shell can be derived from *the virtual work principle*

$$\delta \iint_{\Sigma} W \, d\Sigma = \delta' A, \quad (37)$$

where

$$\delta' A = \iint_{\Sigma} (\mathbf{f} \cdot \delta \boldsymbol{\rho} + \mathbf{m} \cdot \delta' \boldsymbol{\psi}) d\Sigma + \int_{\omega_2} \mathbf{t} \cdot \delta \boldsymbol{\rho} ds + \int_{\omega_4} \boldsymbol{\mu} \cdot \delta' \boldsymbol{\psi} ds,$$

$$\mathbf{I} \times \delta' \boldsymbol{\psi} = -\mathbf{Q}^T \cdot \delta \mathbf{Q}.$$

In Eq. (37), δ is the symbol of variation, $\delta' \boldsymbol{\psi}$ the virtual rotation vector, \mathbf{f} and \mathbf{m} the surface force density and the surface couple density distributed on Σ , respectively, \mathbf{t} force distributed along $\omega_2 \subset \partial \Sigma$, and $\boldsymbol{\mu}$ the couples distributed on $\omega_4 \subset \partial \Sigma$. Here we used the symbol δ' to underline that $\delta' A$ and $\delta' \boldsymbol{\psi}$ are not variations, in general.

Using the formulae suggested in Eremeyev and Zubov (2008),

$$\delta W = \frac{\partial W}{\partial \mathbf{E}} : \delta \mathbf{E} + \frac{\partial W}{\partial \mathbf{K}} : \delta \mathbf{K},$$

$$\delta \mathbf{E} = (\nabla_s \delta \boldsymbol{\rho}) \cdot \mathbf{Q}^T + \mathbf{F} \cdot \delta \mathbf{Q}^T, \quad \delta \mathbf{K} = (\nabla_s \delta' \boldsymbol{\psi}) \cdot \mathbf{Q}^T,$$

$$\delta' \boldsymbol{\psi} = \frac{4}{4 + \theta^2} \left(\delta \boldsymbol{\theta} + \frac{1}{2} \boldsymbol{\theta} \times \delta \boldsymbol{\theta} \right)$$

and Eq. (37), we obtain the *Lagrangian shell equations*:

$$\nabla_s \cdot \mathbf{D} + \mathbf{f} = \mathbf{0}, \quad \nabla_s \cdot \mathbf{G} + [\mathbf{F}^T \cdot \mathbf{D}]_{\times} + \mathbf{m} = \mathbf{0}, \quad (38)$$

$$\mathbf{D} = \mathbf{P}_1 \cdot \mathbf{Q}, \quad \mathbf{G} = \mathbf{P}_2 \cdot \mathbf{Q}, \quad \mathbf{P}_1 = \frac{\partial W}{\partial \mathbf{E}}, \quad \mathbf{P}_2 = \frac{\partial W}{\partial \mathbf{K}}. \quad (39)$$

They are supplemented by the boundary conditions:

$$\begin{aligned} \text{on } \omega_1 : \boldsymbol{\rho} &= \boldsymbol{\rho}_0(s), & \text{on } \omega_2 : \mathbf{v} \cdot \mathbf{D} &= \mathbf{t}(s), \\ \text{on } \omega_3 : \mathbf{Q} &= \mathbf{h}(s), \quad \mathbf{h} \cdot \mathbf{h}^T = \mathbf{I}, & \text{on } \omega_4 : \mathbf{v} \cdot \mathbf{G} &= \boldsymbol{\mu}(s). \end{aligned} \quad (40)$$

Here $\boldsymbol{\rho}_0(s)$, $\mathbf{h}(s)$ are given vector and tensor functions, and \mathbf{v} is the external unit normal to the boundary curve ω ($\mathbf{v} \cdot \mathbf{N} = 0$). Equations (38) are the equilibrium equations for the linear momentum and angular momentum at any shell point. The stress measures \mathbf{P}_1 and \mathbf{P}_2 in Eqs. (38) are the referential stress and couple stress tensors, respectively, $\mathbf{N} \cdot \mathbf{P}_1 = \mathbf{N} \cdot \mathbf{P}_2 = \mathbf{0}$. The strain measures \mathbf{E} and \mathbf{K} are work-conjugate to the 1st Piola-Kirchhoff stress measures \mathbf{D} and \mathbf{G} . The boundary ω of Σ is divided into two parts in such a way that $\omega = \omega_1 \cup \omega_2 = \omega_3 \cup \omega_4$.

The *equilibrium equations* (38) may be transformed to the *Eulerian form* using the surface analogue of the Piola transformation

$$\tilde{\nabla}_s \cdot \mathbf{T} + J^{-1} \mathbf{f} = \mathbf{0}, \quad \tilde{\nabla}_s \cdot \mathbf{M} + \mathbf{T}_{\times} + J^{-1} \mathbf{m} = \mathbf{0}, \quad (41)$$

where

$$\tilde{\nabla}_s \cdot \boldsymbol{\psi} \triangleq \boldsymbol{\rho}^{\alpha} \cdot \frac{\partial \boldsymbol{\psi}}{\partial q^{\alpha}}, \quad \boldsymbol{\rho}^{\alpha} \cdot \boldsymbol{\rho}^{\beta} = \delta_{\beta}^{\alpha}, \quad \boldsymbol{\rho}^{\alpha} \cdot \mathbf{n} = 0, \quad \boldsymbol{\rho}^{\beta} = \frac{\partial \boldsymbol{\rho}}{\partial q^{\beta}},$$

$$\mathbf{T} = J^{-1} \mathbf{F}^T \cdot \mathbf{D}, \quad \mathbf{M} = J^{-1} \mathbf{F}^T \cdot \mathbf{G}, \quad (42)$$

$$J = \sqrt{\frac{1}{2} \left\{ [\text{tr} (\mathbf{F} \cdot \mathbf{F}^T)]^2 - \text{tr} [(\mathbf{F} \cdot \mathbf{F}^T)^2] \right\}}.$$

Here \mathbf{T} and \mathbf{M} are Cauchy-type surface stress and couple stress tensors, $\tilde{\nabla}_s$ is the surface nabla operator on σ related with ∇_s by the formula

$$\nabla_s = \mathbf{F} \cdot \tilde{\nabla}_s,$$

and \mathbf{n} is the unit normal to σ .

Under some natural restrictions, the equilibrium problem for a micropolar shell can be transformed to the system with respect to the strain measures:

$$\nabla_s \cdot \mathbf{P}_1 - (\mathbf{P}_1^T \cdot \mathbf{K})_{\times} + \mathbf{f}^* = \mathbf{0}; \quad (43)$$

$$\nabla_s \cdot \mathbf{P}_2 - (\mathbf{P}_2^T \cdot \mathbf{K} + \mathbf{P}_1^T \cdot \mathbf{E})_{\times} + \mathbf{m}^* = \mathbf{0}, \quad (44)$$

$$\omega_2 : \mathbf{v} \cdot \mathbf{P}_1 = \mathbf{t}^*, \quad \omega_4 : \mathbf{v} \cdot \mathbf{P}_2 = \boldsymbol{\mu}^*, \quad (45)$$

$$\mathbf{f}^* \triangleq \mathbf{f} \cdot \mathbf{Q}^T, \quad \mathbf{m}^* \triangleq \mathbf{m} \cdot \mathbf{Q}^T, \quad \mathbf{t}^* \triangleq \mathbf{t} \cdot \mathbf{Q}^T, \quad \boldsymbol{\mu}^* \triangleq \boldsymbol{\mu} \cdot \mathbf{Q}^T.$$

Let the vectors \mathbf{f}^* , \mathbf{m}^* , and \mathbf{t}^* , $\boldsymbol{\mu}^*$ be given as some functions of coordinates q^1 , q^2 , and s . From the physical point of view, it means that the shell is loaded by tracking forces and couples. Then Eqs. (43)–(45) depend on \mathbf{E} , \mathbf{K} that are the only independent fields.

For the dynamic problem (28), the initial conditions are

$$\boldsymbol{\rho}|_{t=0} = \boldsymbol{\rho}^\circ, \quad \mathbf{v}|_{t=0} = \mathbf{v}^\circ, \quad \mathbf{Q}|_{t=0} = \mathbf{Q}^\circ, \quad \boldsymbol{\omega}|_{t=0} = \boldsymbol{\omega}^\circ,$$

with given initial values $\boldsymbol{\rho}^\circ$, \mathbf{v}° , \mathbf{Q}° , $\boldsymbol{\omega}^\circ$.

8 Compatibility Conditions

Let us consider how to determine the position-vector $\boldsymbol{\rho}(q^1, q^2)$ of σ from the surface stretch tensor \mathbf{E} and micro-rotation tensor \mathbf{Q} , which are assumed to be given as continuously differentiable functions on Σ . By using the equation

$$\mathbf{F} = (\mathbf{E} + \mathbf{A}) \cdot \mathbf{Q} \quad (46)$$

the problem is reduced to

$$\nabla_s \boldsymbol{\rho} = \mathbf{F}. \quad (47)$$

The necessary and sufficient condition for solvability of Eq. (47) is given by the relation

$$\operatorname{div}(\mathbf{e} \cdot \mathbf{F}) = \mathbf{0}, \quad \mathbf{e} \triangleq -\mathbf{I} \times \mathbf{N}, \quad (48)$$

which we call the compatibility condition for the distortion tensor \mathbf{F} . Here \mathbf{e} is the skew-symmetric discriminant tensor on the surface Σ . For a simply-connected region Σ , if the condition (48) is satisfied, the vector field $\boldsymbol{\rho}$ may be deduced from Eq. (47) only up to an additive vector.

Let us consider a more complex problem of determination of both the translations and rotations of the micropolar shell from the given fields of \mathbf{E} and \mathbf{K} . At first, let us deduce the field $\mathbf{Q}(q^1, q^2)$ by using the system of equations following from definition (29) of \mathbf{K}

$$\frac{\partial \mathbf{Q}}{\partial q^\alpha} = -\mathbf{K}_\alpha \times \mathbf{Q}, \quad \mathbf{K}_\alpha \triangleq \mathbf{P}_\alpha \cdot \mathbf{K}. \quad (49)$$

The integrability conditions for the system (49) are given by the relation

$$\frac{\partial \mathbf{K}_\alpha}{\partial q^\beta} - \frac{\partial \mathbf{K}_\beta}{\partial q^\alpha} = \mathbf{K}_\alpha \times \mathbf{K}_\beta \quad (\alpha, \beta = 1, 2). \quad (50)$$

Equations (50) were obtained by Pietraszkiewicz (1979a, 1989), Libai and Simmonds (1983) as the conditions of existence of the rotation field of the shell. They may be written in the following coordinate-free form

$$\operatorname{div}(\mathbf{e} \cdot \mathbf{K}) + \mathbf{K}^\perp \cdot \mathbf{n} = \mathbf{0}, \quad (51)$$

where

$$\mathbf{K}^\perp \triangleq \frac{1}{2} (\mathbf{K}_\alpha \times \mathbf{K}_\beta) \otimes (\mathbf{P}^\alpha \times \mathbf{P}^\beta) = \mathbf{K}^2 - \mathbf{K} \operatorname{tr} \mathbf{K} + \frac{1}{2} (\operatorname{tr}^2 \mathbf{K} - \operatorname{tr} \mathbf{K}^2) \mathbf{I}.$$

Using Eqs. (46) and (29) we transform the compatibility condition (48) into the coordinate-free form

$$\operatorname{div}(\mathbf{e} \cdot \mathbf{E}) + [(\mathbf{E} + \mathbf{A})^T \cdot \mathbf{e} \cdot \mathbf{K}]_\times = \mathbf{0}. \quad (52)$$

Two coordinate-free vector equations (51) and (52) are the compatibility conditions for the nonlinear micropolar shell. These conditions and the system of equations (43)–(45) constitute the complete boundary-value problem of statics of micropolar shells expressed entirely in terms of the surface strain measures \mathbf{E} and \mathbf{K} .

9 Variational Statements

The presented above static and dynamic boundary-value problems of the micropolar shell theory have corresponding variational statements. Some of them for statics and for dynamics are presented below.

9.1 Lagrange-Type Principle

Let us assume that the external forces and couples are conservative. In the Lagrange-type variational principle

$$\delta \mathcal{E}_1 = 0$$

we use the total energy functional

$$\mathcal{E}_1[\boldsymbol{\rho}, \mathbf{Q}] = \iint_{\Sigma} W \, d\Sigma - \mathcal{A}[\boldsymbol{\rho}, \mathbf{Q}], \quad (53)$$

where \mathcal{A} is the potential of the external loads.

Here the translations and the rotations have to satisfy the kinematic boundary conditions (40)₁ and (40)₃ on ω_1 and ω_3 , respectively. The stationarity of \mathcal{E}_1 is equivalent to the equilibrium equations (38), (39) and the static boundary conditions (40)₂ and (40)₄ on ω_2 and ω_4 .

9.2 Hu-Washizu-Type Principle

For this principle the functional is given by

$$\begin{aligned} \mathcal{E}_2[\boldsymbol{\rho}, \mathbf{Q}, \mathbf{E}, \mathbf{K}, \mathbf{D}, \mathbf{P}_2] = & \iint_{\Sigma} \left\{ W(\mathbf{E}, \mathbf{K}) - \mathbf{D} : (\mathbf{E} \cdot \mathbf{Q} - \nabla_s \boldsymbol{\rho}) \right. \\ & \left. - \mathbf{P}_2 : \left[\mathbf{K} - \frac{1}{2} \mathbf{P}^\alpha \otimes \left(\frac{\partial \mathbf{Q}}{\partial q^\alpha} \cdot \mathbf{Q}^T \right) \right] \right\} d\Sigma \\ & - \int_{\omega_1} \boldsymbol{\nu} \cdot \mathbf{D} \cdot (\boldsymbol{\rho} - \boldsymbol{\rho}_0) \, ds - \mathcal{A}[\boldsymbol{\rho}, \mathbf{Q}]. \end{aligned}$$

From the condition $\delta \mathcal{E}_2 = 0$ the equilibrium equations (38) and (39), the constitutive equations, and the relations (29) can be deduced. For this principle the natural boundary conditions are given by the relations (40)₁, (40)₂ and (40)₄, respectively.

Several other variational statements are given in Eremeyev and Zubov (2008). Mixed variational functionals are constructed in Chróścielewski et al. (2004b). They

are used for the development of a family of finite elements with six degrees of freedom in each node. A number of nonlinear simulations of complex multifold shell structures were performed on the base of these elements Chróścielewski et al. (2004b, 2010), Chróścielewski and Witkowski (2010).

9.3 Hamilton-Type Principle

The *kinetic energy of micropolar shells* can be expressed as

$$\mathcal{K} = \iint_{\Sigma} \rho K(\mathbf{v}, \boldsymbol{\omega}) d\Sigma. \quad (54)$$

It is obvious that we should assume the kinetic energy to be a positive definite function that imposes some restriction on the form of the inertia tensors.

The Hamilton principle is a variational principle of dynamics. In real motion, the functional

$$\mathcal{E}_3[\boldsymbol{\rho}, \mathbf{Q}] = \int_{t_0}^{t_1} (\mathcal{K} - \mathcal{E}_1) dt \quad (55)$$

takes a stationary value on the set of all possible shell motions that at the range t_0, t_1 take given values of the real motion values and satisfy the kinematic boundary values. In other words, its first variation on a real motion is zero. From condition $\delta\mathcal{E}_3 = 0$, Eqs. (28) can be established.

10 Linear Theory of Micropolar Shells

For small strains the shell equations can be simplified significantly. In geometrically linear version, Eulerian and Lagrangian shell descriptions do not differ as the difference between σ and Σ is considered to be infinitesimal. Here we do not distinguish the operators $\tilde{\nabla}_s$ and ∇_s as well as the types of stress and couple stress tensors in different configurations.

Let us introduce the *vector of infinitesimal translations* \mathbf{u} and the *vector of infinitesimal rotations* $\boldsymbol{\mathfrak{d}}$ such that

$$\boldsymbol{\rho} \approx \mathbf{P} + \mathbf{u}, \quad \mathbf{Q} \approx \mathbf{I} - \mathbf{I} \times \boldsymbol{\mathfrak{d}}. \quad (56)$$

The formula for \mathbf{Q} follows from the representation of a proper orthogonal tensor through the finite rotation vector (3) for $|\boldsymbol{\mathfrak{d}}| \ll 1$.

The stretch measure \mathbf{E} and the wryness tensor \mathbf{K} can be expressed in terms of the *linear stretch tensor* $\boldsymbol{\varepsilon}$ and the *linear wryness tensor* $\boldsymbol{\varkappa}$ up to a linear addendum:

$$\mathbf{E} \approx \mathbf{I} + \boldsymbol{\varepsilon}, \quad \mathbf{K} \approx \boldsymbol{\varkappa}, \quad \boldsymbol{\varepsilon} = \nabla_s \mathbf{u} + \mathbf{A} \times \boldsymbol{\vartheta}, \quad \boldsymbol{\varkappa} = \nabla_s \boldsymbol{\vartheta}. \quad (57)$$

$\boldsymbol{\varepsilon}$ and $\boldsymbol{\varkappa}$ are used in the linear theory of micropolar shells, cf. Chróścielewski et al. (2004b), Eremeyev and Zubov (2008), Lebedev et al. (2010), Zhilin (1976), Zubov (1997). As a consequence of (57) in the linear shell theory, the stress tensors \mathbf{D} , \mathbf{P}_1 , and \mathbf{T} coincide, the couple tensors \mathbf{G} , \mathbf{P}_2 , \mathbf{M} do not differ as well. In what follows, we will denote the stress tensor by \mathbf{T} and the couple stress tensor by \mathbf{M} .

For a linearly elastic shell, the constitutive equations can be represented through the strain energy density $W = W(\boldsymbol{\varepsilon}, \boldsymbol{\varkappa})$ as it follows

$$\mathbf{T} = \frac{\partial W}{\partial \boldsymbol{\varepsilon}}, \quad \mathbf{M} = \frac{\partial W}{\partial \boldsymbol{\varkappa}}. \quad (58)$$

The equilibrium equations in the linear theory are

$$\nabla_s \cdot \mathbf{T} + \mathbf{f} = \mathbf{0}, \quad \nabla_s \cdot \mathbf{M} + \mathbf{T}_\times + \mathbf{m} = \mathbf{0}, \quad (59)$$

whereas the boundary conditions transform to

$$\begin{aligned} \text{on } \omega_1 : \quad \mathbf{u} &= \mathbf{u}_0(s), & \text{on } \omega_2 : \quad \mathbf{v} \cdot \mathbf{T} &= \mathbf{t}(s), \\ \text{on } \omega_3 : \quad \boldsymbol{\vartheta} &= \boldsymbol{\vartheta}_0(s), & \text{on } \omega_4 : \quad \mathbf{v} \cdot \mathbf{M} &= \boldsymbol{\mu}(s), \end{aligned} \quad (60)$$

where $\mathbf{u}_0(s)$ and $\boldsymbol{\vartheta}_0(s)$ are given functions of the arclength s ; the conditions define the translations and rotations on contour parts ω_k .

For small strains, an example of constitutive equations is defined by the following quadratic form

$$\begin{aligned} 2W &= \alpha_1 \text{tr}^2 \boldsymbol{\varepsilon}_\parallel + \alpha_2 \text{tr} \boldsymbol{\varepsilon}_\parallel^2 + \alpha_3 \text{tr} (\boldsymbol{\varepsilon}_\parallel \cdot \boldsymbol{\varepsilon}_\parallel^T) + \alpha_4 \mathbf{N} \cdot \boldsymbol{\varepsilon}^T \cdot \boldsymbol{\varepsilon} \cdot \mathbf{N} \\ &+ \beta_1 \text{tr}^2 \boldsymbol{\varkappa}_\parallel + \beta_2 \text{tr} \boldsymbol{\varkappa}_\parallel^2 + \beta_3 \text{tr} (\boldsymbol{\varkappa}_\parallel \cdot \boldsymbol{\varkappa}_\parallel^T) + \beta_4 \mathbf{N} \cdot \boldsymbol{\varkappa}^T \cdot \boldsymbol{\varkappa} \cdot \mathbf{N} \end{aligned} \quad (61)$$

that describes a *linear isotropic shell*. Here α_k and β_k , $k = 1, 2, 3, 4$, are elastic constants, and $\boldsymbol{\varepsilon}_\parallel \triangleq \boldsymbol{\varepsilon} \cdot \mathbf{A}$, $\boldsymbol{\varkappa}_\parallel \triangleq \boldsymbol{\varkappa} \cdot \mathbf{A}$.

By Eqs. (58) and (61), the stress tensor and the couple stress tensor are

$$\mathbf{T} = \alpha_1 \mathbf{A} \text{tr} \boldsymbol{\varepsilon}_\parallel + \alpha_2 \boldsymbol{\varepsilon}_\parallel^T + \alpha_3 \boldsymbol{\varepsilon}_\parallel + \alpha_4 \boldsymbol{\varepsilon} \cdot \mathbf{N} \otimes \mathbf{N}, \quad (62)$$

$$\mathbf{M} = \beta_1 \mathbf{A} \text{tr} \boldsymbol{\varkappa}_\parallel + \beta_2 \boldsymbol{\varkappa}_\parallel^T + \beta_3 \boldsymbol{\varkappa}_\parallel + \beta_4 \boldsymbol{\varkappa} \cdot \mathbf{N} \otimes \mathbf{N}. \quad (63)$$

Supplemented with Eqs. (59) and (60), the linear constitutive equations (62) and (63) constitute the setup of the linear boundary value problem with respect to the fields of translations and rotations. It describes micropolar shell equilibrium when the strains are infinitesimal.

11 Linearized Boundary-Value Problems

Let $\boldsymbol{\rho}_0$ and \mathbf{Q}_0 are the known static solution of (28) and (40). The corresponding state of the shell we will call the basic actual configuration and denote it by χ_0 . In addition, let us consider the actual configuration χ_* , which differs from χ_0 by infinitesimal deformation, and derive the linearized boundary-value problem. Denoting quantities related to χ_* by the lower index $*$ we have

$$\boldsymbol{\rho}_* = \boldsymbol{\rho}_0 + \delta\boldsymbol{\rho}, \quad \mathbf{Q}_* = \mathbf{Q}_0 + \delta\mathbf{Q},$$

where we use the symbol δ for infinitesimal increments of corresponding quantities. Since \mathbf{Q} is an orthogonal tensor, the tensor $\mathbf{Q}^T \cdot \delta\mathbf{Q}$ is a skew-symmetric tensor and can be represented as follows

$$\mathbf{Q}^T \cdot \delta\mathbf{Q} = -\mathbf{I} \times \boldsymbol{\psi},$$

where $\boldsymbol{\psi}$ is the infinitesimal rotation vector. It can be expressed by the increment of the finite rotation vector as follows

$$\boldsymbol{\psi} = \frac{4}{4 + \theta^2} \left(\delta\boldsymbol{\theta} + \frac{1}{2}\boldsymbol{\theta} \times \delta\boldsymbol{\theta} \right).$$

The increments of the strain measures are given by the formulae (Eremeyev and Zubov 2008)

$$\delta\mathbf{E} = (\nabla_s \delta\boldsymbol{\rho}) \cdot \mathbf{Q}_0^T + \mathbf{F}_0 \cdot \delta\mathbf{Q}^T = \mathbf{F}_0 \cdot \boldsymbol{\varepsilon} \cdot \mathbf{Q}_0^T, \quad (64)$$

$$\delta\mathbf{K} = (\nabla_s \boldsymbol{\psi}) \cdot \mathbf{Q}^T = \mathbf{F}_0 \cdot \boldsymbol{\varkappa} \cdot \mathbf{Q}_0^T, \quad (65)$$

where $\boldsymbol{\varepsilon}$ and $\boldsymbol{\varkappa}$ are the linear strain measures given by

$$\boldsymbol{\varepsilon} = \nabla_\chi \mathbf{w} + \mathbf{A} \times \boldsymbol{\psi}, \quad \boldsymbol{\varkappa} = \nabla_\chi \boldsymbol{\psi}, \quad (66)$$

$\mathbf{w} = \delta\boldsymbol{\rho}$ and $\mathbf{F}_0 = \nabla_\varkappa \boldsymbol{\rho}_0$. Here ∇_χ is the surface nabla-operator in the basic actual configuration χ_0 . Assuming that $\delta\mathbf{f} = \mathbf{0}$ and $\delta\mathbf{m} = \mathbf{0}$ the linearization leads to the Lagrangian linearized equations of motion

$$\nabla_s \cdot \delta\mathbf{D} = \rho \frac{d^2 \mathbf{w}}{dt^2}, \quad (67)$$

$$\nabla_s \cdot \delta\mathbf{G} + [(\nabla_s \mathbf{w})^T \cdot \mathbf{D} + \mathbf{F}_0^T \cdot \delta\mathbf{D}]_\times = \rho\gamma \frac{d^2 \boldsymbol{\psi}}{dt^2}. \quad (68)$$

Here for simplicity we assume that $\boldsymbol{\Theta}_1 = \mathbf{0}$ and $\boldsymbol{\Theta}_2 = \gamma\mathbf{I}$.

The increments of the stress and couple stress tensors are calculated by the relations

$$\delta \mathbf{D} = \delta \mathbf{P}_1 \cdot \mathbf{Q}_0 + \mathbf{P}_1 \cdot \delta \mathbf{Q} = \delta \mathbf{P}_1 \cdot \mathbf{Q}_0 - \mathbf{D} \times \boldsymbol{\psi}, \quad (69)$$

$$\delta \mathbf{G} = \delta \mathbf{P}_2 \cdot \mathbf{Q}_0 + \mathbf{P}_2 \cdot \delta \mathbf{Q} = \delta \mathbf{P}_2 \cdot \mathbf{Q}_0 - \mathbf{G} \times \boldsymbol{\psi}, \quad (70)$$

$$\delta \mathbf{P}_1 = \frac{\partial^2 W}{\partial \mathbf{E} \partial \mathbf{E}} : \delta \mathbf{E} + \frac{\partial^2 W}{\partial \mathbf{E} \partial \mathbf{K}} : \delta \mathbf{K}, \quad (71)$$

$$\delta \mathbf{P}_2 = \frac{\partial^2 W}{\partial \mathbf{K} \partial \mathbf{E}} : \delta \mathbf{E} + \frac{\partial^2 W}{\partial \mathbf{K} \partial \mathbf{K}} : \delta \mathbf{K}. \quad (72)$$

Using (36) for the physically linear shell we have

$$\delta \mathbf{P}_1 = \mathbf{C}_1 : \delta \mathbf{E} = \mathbf{D}_1 : \boldsymbol{\varepsilon}, \quad \delta \mathbf{P}_2 = \mathbf{C}_2 : \delta \mathbf{K} = \mathbf{D}_2 : \boldsymbol{\varkappa},$$

where \mathbf{D}_1 and \mathbf{D}_2 are fourth-order tensors given by

$$\begin{aligned} \mathbf{D}_1 &= \alpha_1 \mathbf{A} \otimes \mathbf{F}_0^T \cdot \mathbf{P}_\alpha \otimes \mathbf{Q}_0^T \cdot \mathbf{P}^\alpha + \alpha_2 \mathbf{P}_\alpha \otimes \mathbf{P}_\beta \otimes \mathbf{F}_0^T \cdot \mathbf{P}^\beta \otimes \mathbf{Q}_0^T \cdot \mathbf{P}^\alpha \\ &\quad + \alpha_3 \mathbf{P}_\alpha \otimes \mathbf{P}_\beta \otimes \mathbf{F}_0^T \cdot \mathbf{P}^\alpha \otimes \mathbf{Q}_0^T \cdot \mathbf{P}^\beta + \alpha_4 \mathbf{P}_\alpha \otimes \mathbf{N} \otimes \mathbf{F}_0^T \cdot \mathbf{P}^\alpha \otimes \mathbf{Q}_0^T \cdot \mathbf{N}, \\ \mathbf{D}_2 &= \beta_1 \mathbf{A} \otimes \mathbf{F}_0^T \cdot \mathbf{P}_\alpha \otimes \mathbf{Q}_0^T \cdot \mathbf{P}^\alpha + \beta_2 \mathbf{P}_\alpha \otimes \mathbf{P}_\beta \otimes \mathbf{F}_0^T \cdot \mathbf{P}^\beta \otimes \mathbf{Q}_0^T \cdot \mathbf{P}^\alpha \\ &\quad + \beta_3 \mathbf{P}_\alpha \otimes \mathbf{P}_\beta \otimes \mathbf{F}_0^T \cdot \mathbf{P}^\alpha \otimes \mathbf{Q}_0^T \cdot \mathbf{P}^\beta + \beta_4 \mathbf{P}_\alpha \otimes \mathbf{N} \otimes \mathbf{F}_0^T \cdot \mathbf{P}^\alpha \otimes \mathbf{Q}_0^T \cdot \mathbf{N}. \end{aligned}$$

Assuming that $\delta \mathbf{t} = \mathbf{0}$, $\delta \boldsymbol{\mu} = \mathbf{0}$, $\delta \mathbf{r}_0 = \mathbf{0}$, and $\delta \mathbf{h} = \mathbf{0}$, we obtain the linearized boundary conditions

$$\begin{aligned} \text{on } \omega_1 : \mathbf{w} &= \mathbf{0}, & \text{on } \omega_2 : \mathbf{v} \cdot \delta \mathbf{D} &= \mathbf{0}, \\ \text{on } \omega_3 : \boldsymbol{\psi} &= \mathbf{0}, & \text{on } \omega_4 : \mathbf{v} \cdot \delta \mathbf{G} &= \mathbf{0}. \end{aligned} \quad (73)$$

Introducing the tensors

$$\boldsymbol{\Phi}_1 = J_0^{-1} \mathbf{F}_0^T \cdot \delta \mathbf{D}, \quad \boldsymbol{\Phi}_2 = J_0^{-1} \mathbf{F}_0^T \cdot \delta \mathbf{G}, \quad (74)$$

where $J_0 = J(\mathbf{F}_0)$, we transform Eqs. (67) and (68) into the linearized equations of motion in the actual configuration χ_0

$$\nabla_\chi \cdot \boldsymbol{\Phi}_1 = \rho \frac{d^2 \mathbf{w}}{dt^2}, \quad (75)$$

$$\nabla_\chi \cdot \boldsymbol{\Phi}_2 + [(\nabla_\chi \mathbf{w})^T \cdot \mathbf{T} + \boldsymbol{\Phi}_1]_\times = \rho \gamma \frac{d^2 \boldsymbol{\psi}}{dt^2}. \quad (76)$$

For the physically linear isotropic micropolar shell $\boldsymbol{\Phi}_1$ and $\boldsymbol{\Phi}_2$ are given by relations

$$\begin{aligned} \boldsymbol{\Phi}_1 &= \mathbf{H}_1 : \boldsymbol{\varepsilon} - \mathbf{T} \times \boldsymbol{\psi}, & \boldsymbol{\Phi}_2 &= \mathbf{H}_2 : \boldsymbol{\varkappa} - \mathbf{M} \times \boldsymbol{\psi}, \\ \mathbf{H}_1 &= J_0^{-1} \mathbf{F}_0^T \cdot \tilde{\mathbf{D}}_1, & \mathbf{H}_2 &= J_0^{-1} \mathbf{F}_0^T \cdot \tilde{\mathbf{D}}_2, \end{aligned}$$

where

$$\begin{aligned}
\tilde{\mathbf{D}}_1 &= \alpha_1 \mathbf{P}_\alpha \otimes \mathbf{Q}_0^T \cdot \mathbf{P}^\alpha \otimes \mathbf{F}_0^T \cdot \mathbf{P}_\beta \otimes \mathbf{Q}_0^T \cdot \mathbf{P}^\beta \\
&\quad + \alpha_2 \mathbf{P}_\alpha \otimes \mathbf{Q}_0^T \cdot \mathbf{P}_\beta \otimes \mathbf{F}_0^T \cdot \mathbf{P}^\beta \otimes \mathbf{Q}_0^T \cdot \mathbf{P}^\alpha \\
&\quad + \alpha_3 \mathbf{P}_\alpha \otimes \mathbf{Q}_0^T \cdot \mathbf{P}_\beta \otimes \mathbf{F}_0^T \cdot \mathbf{P}^\alpha \otimes \mathbf{Q}_0^T \cdot \mathbf{P}^\beta \\
&\quad + \alpha_4 \mathbf{P}_\alpha \otimes \mathbf{Q}_0^T \cdot \mathbf{N} \otimes \mathbf{F}_0^T \cdot \mathbf{P}^\alpha \otimes \mathbf{Q}_0^T \cdot \mathbf{N}, \\
\tilde{\mathbf{D}}_2 &= \beta_1 \mathbf{P}_\alpha \otimes \mathbf{Q}_0^T \cdot \mathbf{P}^\alpha \otimes \mathbf{F}_0^T \cdot \mathbf{P}_\beta \otimes \mathbf{Q}_0^T \cdot \mathbf{P}^\beta \\
&\quad + \beta_2 \mathbf{P}_\alpha \otimes \mathbf{Q}_0^T \cdot \mathbf{P}_\beta \otimes \mathbf{F}_0^T \cdot \mathbf{P}^\beta \otimes \mathbf{Q}_0^T \cdot \mathbf{P}^\alpha \\
&\quad + \beta_3 \mathbf{P}_\alpha \otimes \mathbf{Q}_0^T \cdot \mathbf{P}_\beta \otimes \mathbf{F}_0^T \cdot \mathbf{P}^\alpha \otimes \mathbf{Q}_0^T \cdot \mathbf{P}^\beta \\
&\quad + \beta_4 \mathbf{P}_\alpha \otimes \mathbf{Q}_0^T \cdot \mathbf{N} \otimes \mathbf{F}_0^T \cdot \mathbf{P}^\alpha \otimes \mathbf{Q}_0^T \cdot \mathbf{N}.
\end{aligned}$$

The fourth-order tensors \mathbf{H}_1 and \mathbf{H}_2 are tangent stiffness tensors in the non-linear theory of shells which have the same properties as in the three-dimensional non-linear elasticity, see Fu and Ogden (1999), Ogden (1997), Lurie (1990), Altenbach and Eremeyev (2010). The components of \mathbf{H}_1 and \mathbf{H}_2 depend on initial deformations and, as a result, have symmetry properties which are different from ones of \mathbf{C}_1 and \mathbf{C}_2 , in general.

The linearized Eulerian boundary conditions are

$$\begin{aligned}
&\text{on } \ell_1 : \mathbf{w} = \mathbf{0}, \quad \text{on } \ell_2 : \boldsymbol{\eta} \cdot \boldsymbol{\Phi}_1 = \mathbf{0}, \\
&\text{on } \ell_3 : \boldsymbol{\psi} = \mathbf{0}, \quad \text{on } \ell_4 : \boldsymbol{\eta} \cdot \boldsymbol{\Phi}_2 = \mathbf{0}.
\end{aligned} \tag{77}$$

Here $\boldsymbol{\eta}$ is the unit vector normal to the shell contour $\ell = \partial\sigma$, $\boldsymbol{\eta} \cdot \mathbf{n} = 0$, $\ell = \ell_1 \cup \ell_2 = \ell_3 \cup \ell_4$, ℓ_1 , ℓ_2 , ℓ_3 , and ℓ_4 are the parts of the shell contour in the actual configuration corresponding to ω_1 , ω_2 , ω_3 , and ω_4 , respectively.

The boundary-value problems (67), (68), (73), and (75)–(77) describe the motion of the prestressed micropolar shell. For $\chi_0 = \varkappa$ we have

$$\mathbf{F}_0 = \mathbf{A}, \quad \mathbf{Q}_0 = \mathbf{I}.$$

Assuming in addition the absence of initial stresses

$$\mathbf{T} = \mathbf{M} = \mathbf{0}$$

the linearized boundary-value problems coincide with the equations of motion of linear isotropic micropolar shells discussed in Chróścielewski et al. (2004b), Eremeyev and Zubov (2008), Lebedev et al. (2010), Eremeyev and Lebedev (2011), Eremeyev et al. (2015b).

12 Eigen-Vibrations of Prestressed Micropolar Shells

Let us consider eigen-vibrations of a prestressed shell. By linearity, eigen-solutions are proportional to $e^{i\Omega t}$:

$$\mathbf{w} = \mathbf{W}(q^1, q^2)e^{i\Omega t}, \quad \boldsymbol{\psi} = \boldsymbol{\Psi}(q^1, q^2)e^{i\Omega t}.$$

Substituting the latter relations into (75) and (77) we obtain the boundary-value problem for the physically linear isotropic prestressed micropolar shell

$$\nabla_{\chi} \cdot \boldsymbol{\Phi}_1 = -\rho\Omega^2 \mathbf{W}, \quad (78)$$

$$\nabla_{\chi} \cdot \boldsymbol{\Phi}_2 + [(\nabla_{\chi} \mathbf{w})^T \cdot \mathbf{T} + \boldsymbol{\Phi}_1]_{\chi} = -\rho\gamma\Omega^2 \boldsymbol{\Psi}, \quad (79)$$

$$\begin{aligned} \text{on } \ell_1 : \mathbf{W} &= \mathbf{0}, & \text{on } \ell_2 : \boldsymbol{\eta} \cdot \boldsymbol{\Phi}_1 &= \mathbf{0}, \\ \text{on } \ell_3 : \boldsymbol{\Psi} &= \mathbf{0}, & \text{on } \ell_4 : \boldsymbol{\eta} \cdot \boldsymbol{\Phi}_2 &= \mathbf{0}, \end{aligned} \quad (80)$$

where

$$\begin{aligned} \boldsymbol{\Phi}_1 &= \mathbf{H}_1 : \boldsymbol{\varepsilon} - \mathbf{T} \times \boldsymbol{\Psi}, & \boldsymbol{\Phi}_1 &= \mathbf{H}_2 : \boldsymbol{\varkappa} - \mathbf{M} \times \boldsymbol{\Psi}, \\ \boldsymbol{\varepsilon} &= \nabla_{\chi} \mathbf{W} + \mathbf{A} \times \boldsymbol{\Psi}, & \boldsymbol{\varkappa} &= \nabla_{\chi} \boldsymbol{\Psi}. \end{aligned} \quad (81)$$

Additionally we consider the linear boundary-value problem of the micropolar shell without initial deformation, that is when $\chi_0 = \varkappa$, which is given by

$$\nabla_{\chi} \cdot \boldsymbol{\Phi}_1^0 = -\rho\Omega^2 \mathbf{W}, \quad \nabla_{\chi} \cdot \boldsymbol{\Phi}_2^0 + \boldsymbol{\Phi}_{1 \times}^0 = -\rho\gamma\Omega^2 \boldsymbol{\Psi}, \quad (82)$$

$$\begin{aligned} \text{on } \ell_1 : \mathbf{W} &= \mathbf{0}, & \text{on } \ell_2 : \boldsymbol{\eta} \cdot \boldsymbol{\Phi}_1^0 &= \mathbf{0}, \\ \text{on } \ell_3 : \boldsymbol{\Psi} &= \mathbf{0}, & \text{on } \ell_4 : \boldsymbol{\eta} \cdot \boldsymbol{\Phi}_2^0 &= \mathbf{0}, \end{aligned} \quad (83)$$

$$\boldsymbol{\Phi}_1^0 = \mathbf{C}_1 : \boldsymbol{\varepsilon}, \quad \boldsymbol{\Phi}_1^0 = \mathbf{C}_2 : \boldsymbol{\varkappa}. \quad (84)$$

The comparison of $\boldsymbol{\Phi}_1^0$ and $\boldsymbol{\Phi}_1$, $\boldsymbol{\Phi}_2^0$ and $\boldsymbol{\Phi}_2$ shows that difference between these boundary-value problems consists of

1. the difference between the elastic moduli tensors \mathbf{C}_{α} and \mathbf{H}_{α} , $\alpha = 1, 2$, and
2. the existence of initial stress tensors \mathbf{T} and \mathbf{M} in $\boldsymbol{\Phi}_1$ and $\boldsymbol{\Phi}_2$.

In what follows we show the influence on eigen-frequencies of the prestressed shell using the variational approach.

12.1 Rayleigh Principle

In the linear and linearized shell theories presented above there is a variational principle for eigen-vibrations called the Rayleigh variational principle. To formulate it we consider the second variation of the functional of the total energy of the micropolar

shell. Suppose that $\mathbf{m} = \boldsymbol{\mu} = \mathbf{0}$ and the external forces are “dead”. This means that \mathbf{f} and \mathbf{t} do not depend on \mathbf{u} and \mathbf{Q} . Thus the functional of the total potential energy of the shell is

$$\Pi = \iint_{\Sigma} W \, d\Sigma - \iint_{\Sigma} \mathbf{f} \cdot \mathbf{u} \, d\Sigma - \int_{\omega_2} \mathbf{t} \cdot \mathbf{u} \, ds.$$

The first variation of Π is given by

$$\begin{aligned} \delta\Pi = & \iint_{\Sigma} [\operatorname{tr} (\mathbf{D}^T \cdot \nabla_s \mathbf{w}) + \operatorname{tr} (\mathbf{D}^T \cdot \mathbf{F}_0 \times \boldsymbol{\psi}) + \operatorname{tr} (\mathbf{G}^T \cdot \nabla_s \boldsymbol{\psi})] \, d\Sigma \quad (85) \\ & - \iint_{\Sigma} \mathbf{f} \cdot \mathbf{w} \, d\Sigma - \int_{\omega_2} \mathbf{t} \cdot \mathbf{w} \, ds. \end{aligned}$$

Since $\boldsymbol{\rho}_0$ and \mathbf{Q}_0 are assumed to satisfy equilibrium equations and boundary conditions (40), the first variation of the energy vanishes

$$\delta\Pi = 0.$$

The second variation of the energy takes the form

$$\begin{aligned} \delta^2\Pi = & \iint_{\Sigma} \{ \operatorname{tr} (\delta\mathbf{D}^T \cdot \nabla_s \mathbf{w}) + \operatorname{tr} (\delta\mathbf{D}^T \cdot \mathbf{F}_0 \times \boldsymbol{\psi}) + \operatorname{tr} [\mathbf{D}^T \cdot (\nabla_s \mathbf{w}) \times \boldsymbol{\psi}] \\ & + \operatorname{tr} (\delta\mathbf{G}^T \cdot \nabla_s \boldsymbol{\psi}) \} \, d\Sigma. \end{aligned}$$

Using identities $\nabla_{\chi} = \mathbf{F} \cdot \nabla_s$, $d\sigma = J \, d\Sigma$, and (74), we transform $\delta^2\Pi$ to

$$\begin{aligned} \delta^2\Pi = & \iint_{\sigma} \{ \boldsymbol{\Phi}_1 : (\nabla_{\chi} \mathbf{w} + \mathbf{A} \times \boldsymbol{\psi}) + \boldsymbol{\Phi}_1 : \nabla_{\chi} \boldsymbol{\psi} \\ & + \operatorname{tr} [\mathbf{T}^T \cdot (\nabla_{\chi} \mathbf{w}) \times \boldsymbol{\psi}] \} \, d\sigma \\ = & \iint_{\sigma} \{ \boldsymbol{\Phi}_1 : \boldsymbol{\varepsilon} + \boldsymbol{\Phi}_2 : \boldsymbol{\varkappa} \\ & + \operatorname{tr} [\mathbf{T}^T \cdot (\nabla_{\chi} \mathbf{w}) \times \boldsymbol{\psi}] \} \, d\sigma. \end{aligned}$$

Finally, with Eqs. (81), the second energy variation takes the form

$$\delta^2\Pi = 2 \iint_{\sigma} w \, d\sigma, \quad w = w_1 + w_2, \quad (86)$$

where

$$\begin{aligned} w_1(\boldsymbol{\varepsilon}, \boldsymbol{\varkappa}) &= \frac{1}{2} \boldsymbol{\varepsilon} : \mathbf{H}_1 : \boldsymbol{\varepsilon} + \frac{1}{2} \boldsymbol{\varkappa} : \mathbf{H}_2 : \boldsymbol{\varkappa}, \\ w_2(\boldsymbol{\psi}, \boldsymbol{\varepsilon}, \boldsymbol{\varkappa}) &= \text{tr} (\boldsymbol{\psi} \times \mathbf{T}^T \cdot \boldsymbol{\varepsilon}) - \frac{1}{2} \text{tr} (\boldsymbol{\psi} \times \mathbf{T}^T \times \boldsymbol{\psi}) + \frac{1}{2} \text{tr} (\boldsymbol{\psi} \times \mathbf{M}^T \cdot \boldsymbol{\varkappa}). \end{aligned} \quad (87)$$

Let us note that w is the increment of the elastic energy density of the initially prestressed shell under additional infinitesimal deformations. By Eqs. (86) and (87), w splits into two terms. The first term, w_1 , is similar to the strain energy density of the linear shell. w_1 is the quadratic form of $\boldsymbol{\varepsilon}$ and $\boldsymbol{\varkappa}$ with the elastic moduli tensors \mathbf{H}_1 and \mathbf{H}_2 . w_2 is also a quadratic form but depending on $\boldsymbol{\psi}$, $\boldsymbol{\varepsilon}$ and $\boldsymbol{\varkappa}$. The coefficients in the quadratic form w_2 are expressed in terms of the initial stress and couple stress tensors only, they do not depend on the properties of shell material.

If $\chi_0 = \varkappa$, that is $\mathbf{T} = \mathbf{M} = \mathbf{0}$, then the energy density w is a quadratic form of tensors $\boldsymbol{\varepsilon}$ and $\boldsymbol{\varkappa}$ having the form

$$w = w_0 \equiv \frac{1}{2} \boldsymbol{\varepsilon} : \mathbf{C}_1 : \boldsymbol{\varepsilon} + \frac{1}{2} \boldsymbol{\varkappa} : \mathbf{C}_2 : \boldsymbol{\varkappa}.$$

Here w_0 is the strain energy density of an isotropic linear micropolar shell under infinitesimal deformations, see Chróścielewski et al. (2004b), Eremeyev and Zubov (2008), Eremeyev et al. (2013), Eremeyev and Lebedev (2011).

Now the Rayleigh variational principle can be formulated as follows. The modes of shell eigen-oscillations are stationary points of the energy functional

$$\mathcal{E}[\mathbf{W}, \boldsymbol{\Psi}] = \iint_{\sigma} [w_1(\boldsymbol{\varepsilon}, \boldsymbol{\varkappa}) + w_2(\boldsymbol{\Psi}, \boldsymbol{\varepsilon}, \boldsymbol{\varkappa})] d\sigma, \quad (88)$$

where

$$\boldsymbol{\varepsilon} = \nabla_{\chi} \mathbf{W} + \mathbf{A} \times \boldsymbol{\Psi}, \quad \boldsymbol{\varkappa} = \nabla_{\chi} \boldsymbol{\Psi},$$

on the set of functions that satisfy the kinematic boundary conditions

$$\text{on } \ell_1 : \mathbf{W} = \mathbf{0} \quad \text{and on } \ell_3 : \boldsymbol{\Psi} = \mathbf{0} \quad (89)$$

and the restriction

$$\mathcal{K}(\mathbf{W}, \boldsymbol{\Psi}) \equiv \frac{1}{2} \iint_{\sigma} \rho (\mathbf{W} \cdot \mathbf{W} + \gamma \boldsymbol{\Psi} \cdot \boldsymbol{\Psi}) d\sigma = 1. \quad (90)$$

Here the functions \mathbf{W} , $\boldsymbol{\Psi}$ are the oscillation amplitudes for the translations and rotations, respectively.

The Rayleigh variational principle is equivalent to the stationary principle for the Rayleigh quotient

$$\mathcal{R}[\mathbf{W}, \boldsymbol{\Psi}] = \frac{\mathcal{E}[\mathbf{W}, \boldsymbol{\Psi}]}{\mathcal{K}(\mathbf{W}, \boldsymbol{\Psi})}, \quad (91)$$

that is defined on kinematically admissible functions $\mathbf{W}, \boldsymbol{\Psi}$.

The proof of the principle in the case of a prestressed shell is standard and mimics one which can be found for example in Berdichevsky (2009) or in the case of the micropolar shell theory in Eremeyev and Lebedev (2011). For comparison purposes we introduce the Rayleigh quotient of the shell without initial stresses

$$\mathcal{R}_0[\mathbf{W}, \boldsymbol{\Psi}] = \frac{\mathcal{E}_0[\mathbf{W}, \boldsymbol{\Psi}]}{\mathcal{K}(\mathbf{W}, \boldsymbol{\Psi})}, \quad \mathcal{E}_0[\mathbf{W}, \boldsymbol{\Psi}] = \iint_{\sigma} w_0(\boldsymbol{\varepsilon}, \boldsymbol{\varkappa}) \, d\sigma. \quad (92)$$

Note that the least squared eigenfrequencies of the shell correspond to the minimal values of \mathcal{R} and \mathcal{R}_0

$$\Omega_{\min}^2 = \inf \mathcal{R}[\mathbf{W}, \boldsymbol{\Psi}], \quad \Omega_{0\min}^2 = \inf \mathcal{R}_0[\mathbf{W}, \boldsymbol{\Psi}]$$

on $\mathbf{W}, \boldsymbol{\Psi}$ that satisfy (89). By the Courant minimax principle, see Courant and Hilbert (1991), Berdichevsky (2009), the Rayleigh quotient (91) allows us to estimate the values of higher eigen-frequencies. For this we should consider \mathcal{R} on the set of functions that are orthogonal to the previous modes of eigen-oscillations in some functional energy space.

12.2 Influence of Initial (Residual) Stresses

To analyze the influence of initial (residual) stresses we compare the functionals \mathcal{R} and \mathcal{R}_0 that is equivalent to comparison of \mathcal{E} and \mathcal{E}_0 . It is obvious that the difference between \mathcal{E} and \mathcal{E}_0 consist of two terms: the difference in elastic moduli, that is the difference between \mathbf{C}_1 and \mathbf{H}_1 , \mathbf{C}_2 and \mathbf{H}_2 , and the term w_2 depending on initial stress and couple stress tensors.

Let us consider first w_1 and w_0 . In the linear theory of shell it is assumed that w_0 is a positive definite quadratic form of $\boldsymbol{\varepsilon}$ and $\boldsymbol{\varkappa}$. We also assume that $w_1(\boldsymbol{\varepsilon}, \boldsymbol{\varkappa})$ is a positive definite quadratic form. This means that w_1 satisfies the following inequality

$$w_1(\boldsymbol{\varepsilon}, \boldsymbol{\varkappa}) \geq c_1 \|\boldsymbol{\varepsilon}\|^2 + c_2 \|\boldsymbol{\varkappa}\|^2$$

with positive constants c_1 and c_2 depending on the shell geometry. This restriction plays the same role as the generalized Coleman-Noll inequality used in the non-linear elasticity, see Eremeyev and Zubov (2007). This case is similar to the dependence of the eigen-frequency of a spring on its stiffness: the increase of stiffness leads to the increase of eigen-frequency.

To analyze the influence of w_2 let us assume that $\mathbf{C}_1 = \mathbf{H}_1$, $\mathbf{C}_2 = \mathbf{H}_2$. This means that we neglect in influence of initial strains on the elastic moduli of the shell. Here we have $w - w_0 = w_2$. It is obvious that w_2 is not a positive definite function, in general. Indeed, let us consider as an example the uniform stretching of the shell with $\mathbf{T} = T\mathbf{A}$, $\mathbf{M} = \mathbf{0}$, T is the uniform tension. We have

$$\begin{aligned} w_2(\boldsymbol{\Psi}, \boldsymbol{\varepsilon}, \boldsymbol{\varkappa}) &= T \operatorname{tr} (\boldsymbol{\Psi} \times \mathbf{A} \cdot \boldsymbol{\varepsilon}) - \frac{T}{2} \operatorname{tr} (\boldsymbol{\Psi} \times \mathbf{A} \times \boldsymbol{\Psi}) \\ &= T \operatorname{tr} (\boldsymbol{\Psi} \times \nabla_\chi \mathbf{W}) + \frac{T}{2} \operatorname{tr} (\boldsymbol{\Psi} \times \mathbf{A} \times \boldsymbol{\Psi}) \\ &= T \operatorname{tr} (\boldsymbol{\Psi} \times \nabla_\chi \mathbf{W}) + \frac{T}{2} [\boldsymbol{\Psi} \cdot \boldsymbol{\Psi} + (\boldsymbol{\Psi} \cdot \mathbf{N})^2]. \end{aligned}$$

Assuming $\nabla_\chi \mathbf{W} = \mathbf{0}$ we obtain

$$w_2 = \frac{T}{2} [\boldsymbol{\Psi} \cdot \boldsymbol{\Psi} + (\boldsymbol{\Psi} \cdot \mathbf{N})^2].$$

Thus, the sign of w_2 coincides with the sign of T . As a result we have

$$\mathcal{E}[\mathbf{0}, \boldsymbol{\Psi}] - \mathcal{E}_0[\mathbf{0}, \boldsymbol{\Psi}] = \frac{T}{2} \iint_{\sigma} [\boldsymbol{\Psi} \cdot \boldsymbol{\Psi} + (\boldsymbol{\Psi} \cdot \mathbf{N})^2] d\sigma.$$

Positive values of T leads to an increase of Ω . This case is similar to the dependence of eigen-frequency of a string on tension (Courant and Hilbert 1991): stretching ($T > 0$) leads to the increase while compression ($T < 0$) leads to the decrease of the eigen-frequencies in comparison with the unstressed shell. Moreover, since initial stresses and couple stresses may lead to instability of the shell that is when $\delta^2\Pi$ becomes non-positive their influence on eigen-oscillations is more important than the change of elastic moduli tensors.

A few examples showing the influence of initial stresses on the least eigen-frequencies of a prestressed six-parameter shell are given by Altenbach and Eremeyev (2014a). Eremeyev et al. (2015b) presented extension of the eigen-frequencies analysis for higher eigen-frequencies using the Courant variational principle.

13 Constitutive Restrictions for Micropolar Shells

As in 3D elasticity, in the theory of micropolar shells we should supplement the equilibrium/motion equations with constitutive restrictions. We will do that in the frame of general nonlinear shell theory similarly to what was done in 3D elasticity. Following Eremeyev and Zubov (2007) we will formulate the generalized Coleman-Noll inequality (GCN-condition), the strong ellipticity condition for the equilibrium equations and the Hadamard inequality. The inequalities impose some restrictions

on constitutive equations of elastic shells under finite deformation. We also will prove that the Coleman-Noll inequality implies strong ellipticity of shell equilibrium equations. We begin with the linear theory.

13.1 Linear Theory of Micropolar Shell

Suppose that specific strain energy $W(\boldsymbol{\varepsilon}, \boldsymbol{\kappa})$ is positive definite. W is a quadratic form depending on the linear strain tensor and linear bending strain tensor. For an isotropic shell, W takes the form (61). Positivity of the quadratic form (61) with respect to $\boldsymbol{\varepsilon}$ and $\boldsymbol{\kappa}$ is equivalent to the following set of inequalities

$$2\alpha_1 + \alpha_2 + \alpha_3 > 0, \quad \alpha_2 + \alpha_3 > 0, \quad \alpha_3 - \alpha_2 > 0, \quad \alpha_4 > 0, \quad (93)$$

$$2\beta_1 + \beta_2 + \beta_3 > 0, \quad \beta_2 + \beta_3 > 0, \quad \beta_3 - \beta_2 > 0, \quad \beta_4 > 0.$$

The inequality

$$W(\boldsymbol{\varepsilon}, \boldsymbol{\kappa}) > 0, \quad \forall \boldsymbol{\varepsilon}, \boldsymbol{\kappa} \neq \mathbf{0}$$

and the inequalities for elastic constants of isotropic material (93) that are its consequences, present the simplest example of additional inequalities in the shell theory. If the inequalities fail this leads to a number of pathological consequences. For example boundary value problems of linear shell theory can have few solutions or can have no solution for some loads. Next, the propagation of waves in some directions becomes impossible that is not natural from the physical point of view. Note that for finite strains, the positive definiteness of specific energy $W(\mathbf{E}, \mathbf{K})$ is not a warranty that the desired properties of boundary value problems or wave propagation hold, here we should introduce some additional restrictions.

13.2 Coleman-Noll Inequality for Elastic Shells

Suppose a solution of equilibrium problem for a nonlinear elastic shell of Cosserat type is known. Let us call it the initial or basic stressed state. The state is defined by vector field $\boldsymbol{\rho}(q^\alpha)$ and tensor field $\mathbf{Q}(q^\alpha)$. Now we consider some equilibrium shell state that perturbs the basic state. If the difference between the state is infinitesimal we can linearize the equations with respect to the quantities characterizing the difference between the states. Let us denote the small increment of various quantities characterizing the perturbed equilibrium with the dot superscript like \mathbf{D}^\cdot . This quantity can be calculated by the formula:

$$\mathbf{D}^\cdot = \left. \frac{d}{d\tau} \mathbf{D} [\nabla_s(\boldsymbol{\rho} + \tau \mathbf{u}, \mathbf{Q} - \tau \mathbf{Q} \times \boldsymbol{\theta}, \nabla_s(\mathbf{Q} - \tau \mathbf{Q} \times \boldsymbol{\theta}))] \right|_{\tau=0}, \quad (94)$$

where \mathbf{u} is the vector of additional infinitesimal translation and $\boldsymbol{\theta}$ is the vector of additional infinitesimal rotation characterizing the small rotation with respect to the initial stressed state. The following relations are valid

$$\boldsymbol{\rho}' = \mathbf{u}, \quad \mathbf{Q}' = -\mathbf{Q} \times \boldsymbol{\theta}, \quad \mathbf{E}' = \mathbf{F} \cdot \boldsymbol{\varepsilon} \cdot \mathbf{Q}^T, \quad \mathbf{K}' = \mathbf{F} \cdot \boldsymbol{\kappa} \cdot \mathbf{Q}^T, \quad (95)$$

$$\boldsymbol{\varepsilon} = \nabla_s \mathbf{u} + \mathbf{A} \times \boldsymbol{\theta}, \quad \boldsymbol{\kappa} = \nabla_s \boldsymbol{\theta}, \quad (96)$$

where $\boldsymbol{\varepsilon}$ and $\boldsymbol{\kappa}$ are the linear stretch tensor and linear wryness tensor introduced in (57).

As a reference configuration it can be chosen any stressed shell state. To avoid awkward expressions and to simplify the calculations, we assume the reference configuration to be the initial (basic) stressed state of the shell. This means that in the reference configuration $\mathbf{F} = \mathbf{E} = \mathbf{I} - \mathbf{N} \otimes \mathbf{N}$, $\mathbf{Q} = \mathbf{I}$, $\mathbf{K} = \mathbf{0}$. Under this choice, using Eqs. (39), (42), (94)–(96) we have

$$\begin{aligned} \mathbf{D}' &= \frac{\partial^2 W}{\partial \mathbf{E} \partial \mathbf{E}} : \boldsymbol{\varepsilon} + \frac{\partial^2 W}{\partial \mathbf{E} \partial \mathbf{K}} : \boldsymbol{\kappa} - \mathbf{T} \times \boldsymbol{\theta}, \\ \mathbf{G}' &= \frac{\partial^2 W}{\partial \mathbf{K} \partial \mathbf{E}} : \boldsymbol{\varepsilon} + \frac{\partial^2 W}{\partial \mathbf{K} \partial \mathbf{K}} : \boldsymbol{\kappa} - \mathbf{M} \times \boldsymbol{\theta}. \end{aligned} \quad (97)$$

Suppose that in the initial and perturbed stressed shell states the external couples are zero $\mathbf{m} = \boldsymbol{\mu} = \mathbf{0}$ and the external forces are “dead”. Then the total potential energy of the shell is

$$\Pi = \iint_{\Sigma} W \, d\Sigma - \iint_{\Sigma} \mathbf{f} \cdot (\boldsymbol{\rho} - \mathbf{P}) \, d\Sigma - \int_{\omega_2} \mathbf{t} \cdot (\boldsymbol{\rho} - \mathbf{P}) \, ds.$$

Let us consider the energy increment for the perturbed equilibrium state with respect to the initial energy taking into account the members of the second order of smallness

$$\Pi - \Pi_0 = \tau \left(\frac{d\Pi}{d\tau} \right)_{\tau=0} + \frac{1}{2} \tau^2 \left(\frac{d^2\Pi}{d\tau^2} \right)_{\tau=0} + \dots$$

By the constitutive relations (39) and Eqs. (95), (96), we get

$$\begin{aligned} \frac{d\Pi}{d\tau} &= \iint_{\Sigma} [\text{tr} (\mathbf{D}^T \cdot \nabla_s \mathbf{u}) + \text{tr} (\mathbf{D}^T \cdot \mathbf{F} \times \boldsymbol{\theta}) + \text{tr} (\mathbf{G}^T \cdot \nabla_s \boldsymbol{\theta})] \, d\Sigma \\ &\quad - \iint_{\Sigma} \mathbf{f} \cdot \mathbf{u} \, d\Sigma - \int_{\omega_2} \boldsymbol{\varphi} \cdot \mathbf{u} \, ds. \end{aligned} \quad (98)$$

We recall that the basic stressed shell state is the reference configuration of the shell. Differentiating Eq. (98) with respect to parameter τ and using Eqs. (95) we obtain

$$\begin{aligned} \left. \frac{d^2 \Pi}{d\tau^2} \right|_{\tau=0} &= \iint_{\Sigma} [\operatorname{tr} (\mathbf{D}^T \cdot \nabla_s \mathbf{u}) + \operatorname{tr} (\mathbf{D}^T \times \boldsymbol{\theta}) \\ &\quad + \operatorname{tr} (\mathbf{T}^T \cdot (\nabla_s \mathbf{u}) \times \boldsymbol{\theta}) + \operatorname{tr} (\mathbf{G}^T \cdot \boldsymbol{\kappa})] d\Sigma. \end{aligned}$$

As we have chosen equilibrium of shell as the basic state, with use of Eqs. (38) and (40) we get that the first variation of the energy vanishes

$$\left. \frac{d\Pi}{d\tau} \right|_{\tau=0} = 0.$$

By Eqs. (96) and (97), the second energy variation takes the form

$$\left. \frac{d^2 \Pi}{d\tau^2} \right|_{\tau=0} = 2 \iint_{\Sigma} w d\Sigma, \quad w = w' + w'', \quad (99)$$

where

$$\begin{aligned} w' &= \frac{1}{2} \boldsymbol{\varepsilon} : \frac{\partial^2 W}{\partial \mathbf{E} \partial \mathbf{E}} : \boldsymbol{\varepsilon} + \boldsymbol{\varepsilon} : \frac{\partial^2 W}{\partial \mathbf{E} \partial \mathbf{K}} : \boldsymbol{\kappa} + \frac{1}{2} \boldsymbol{\kappa} : \frac{\partial^2 W}{\partial \mathbf{K} \partial \mathbf{K}} : \boldsymbol{\kappa}, \\ w'' &= \operatorname{tr} (\boldsymbol{\theta} \times \mathbf{T}^T \cdot \boldsymbol{\varepsilon}) - \frac{1}{2} \operatorname{tr} (\boldsymbol{\theta} \times \mathbf{T}^T \times \boldsymbol{\theta}) + \frac{1}{2} \operatorname{tr} (\boldsymbol{\theta} \times \mathbf{M}^T \cdot \boldsymbol{\kappa}). \end{aligned} \quad (100)$$

w is the increment of the elastic energy of the initially prestressed shell under additional infinitesimal deformations. By Eqs. (99) and (100), this incremental energy splits into two parts: the pure strain energy, w' , and the energy of rotations w'' . The coefficients in the quadratic form w'' are expressed in terms of the stress and couple stress tensors of the initially prestressed state, they do not depend on the properties of shell material. If the basic stressed state of the shell is natural, that is $\mathbf{T} = \mathbf{M} = \mathbf{0}$, then $w = w'$ and the energy is a quadratic form of tensors $\boldsymbol{\varepsilon}$ and $\boldsymbol{\kappa}$. It is easily seen that the decomposition (86) and Eqs. (87) coincide with the corresponding quantities for the increment of the strain energy density of 3D micropolar body (Eremeyev and Zubov 1994) up to the notation.

The Coleman-Noll constitutive inequality is one of well-known in nonlinear elasticity (Truesdell and Noll 1965; Truesdell 1977, 1984). Its differential form, a so-called GCN-condition, expresses the property that for any reference configuration, the increment of the elastic energy density for arbitrary infinitesimal non-zero strains should be positive. Note that the Coleman–Noll inequality in 3D elasticity does not restrict the constitutive equations with respect to the rotations.

Taking into account the decomposition (86) of the energy we obtain an analogue of the *Coleman-Noll inequality* for micropolar elastic shells

$$w'(\boldsymbol{\varepsilon}, \boldsymbol{\kappa}) > 0 \quad \forall \boldsymbol{\varepsilon} \neq \mathbf{0}, \quad \boldsymbol{\kappa} \neq \mathbf{0}. \quad (101)$$

Using Eqs. (87) we rewrite (101) in the equivalent form

$$\left. \frac{d^2}{d\tau^2} W(\mathbf{E} + \tau\boldsymbol{\varepsilon}, \mathbf{K} + \tau\boldsymbol{\kappa}) \right|_{\tau=0} > 0 \quad \forall \boldsymbol{\varepsilon} \neq \mathbf{0}, \quad \boldsymbol{\kappa} \neq \mathbf{0}. \quad (102)$$

Condition (102) satisfies the principle of material frame-indifference, it can serve as a constitutive inequality for elastic shells.

13.3 Strong Ellipticity and Hadamard Inequality

In nonlinear elasticity, the strong ellipticity condition and its weak form, the Hadamard inequality, are other known constitutive restrictions. Following the partial differential equations theory (PDE) (Lions and Magenes 1968; Fichera 1972; Hörmander 1976) we formulate the strong ellipticity condition of the equilibrium equations (38). For dead loads, the linearized equilibrium equations are

$$\nabla_s \cdot \mathbf{D}^\cdot = \mathbf{0}, \quad \nabla_s \cdot \mathbf{G}^\cdot + [\mathbf{F}^T \cdot \mathbf{D}^\cdot + (\nabla_s \mathbf{u})^T \cdot \mathbf{D}^\cdot]_{,x} = \mathbf{0}, \quad (103)$$

where \mathbf{D}^\cdot and \mathbf{G}^\cdot are defined by the formulae similar to (94). Equations (103) constitute a system of linear PDE of second order with respect to \mathbf{u} and $\boldsymbol{\theta}$. The second order parts of the differential operators in Eqs. (103) are

$$\begin{aligned} & \nabla_s \cdot \left\{ \left[\frac{\partial^2 W}{\partial \mathbf{E} \partial \mathbf{E}} : ((\nabla_s \mathbf{u}) \cdot \mathbf{Q}^T) + \frac{\partial^2 W}{\partial \mathbf{E} \partial \mathbf{K}} : ((\nabla_s \boldsymbol{\theta}) \cdot \mathbf{Q}^T) \right] \cdot \mathbf{Q} \right\}, \\ & \nabla_s \cdot \left\{ \left[\frac{\partial^2 W}{\partial \mathbf{K} \partial \mathbf{E}} : ((\nabla_s \mathbf{u}) \cdot \mathbf{Q}^T) + \frac{\partial^2 W}{\partial \mathbf{K} \partial \mathbf{K}} : ((\nabla_s \boldsymbol{\theta}) \cdot \mathbf{Q}^T) \right] \cdot \mathbf{Q} \right\}. \end{aligned}$$

Now we can formulate the condition of strong ellipticity for system (103). Following a formal procedure from Fichera (1972), we replace the differential operators ∇_s by the unit vector \mathbf{v} tangential to surface Σ and vector fields \mathbf{u} and $\boldsymbol{\theta}$ by vectors \mathbf{a} and \mathbf{b} , respectively. Thus, we get the algebraic expressions

$$\begin{aligned} & \mathbf{v} \cdot \left\{ \left[\frac{\partial^2 W}{\partial \mathbf{E} \partial \mathbf{E}} : (\mathbf{v} \otimes \mathbf{a} \cdot \mathbf{Q}^T) + \frac{\partial^2 W}{\partial \mathbf{E} \partial \mathbf{K}} : (\mathbf{v} \otimes \mathbf{b} \cdot \mathbf{Q}^T) \right] \cdot \mathbf{Q} \right\}, \\ & \mathbf{v} \cdot \left\{ \left[\frac{\partial^2 W}{\partial \mathbf{K} \partial \mathbf{E}} : (\mathbf{v} \otimes \mathbf{a} \cdot \mathbf{Q}^T) + \frac{\partial^2 W}{\partial \mathbf{K} \partial \mathbf{K}} : (\mathbf{v} \otimes \mathbf{b} \cdot \mathbf{Q}^T) \right] \cdot \mathbf{Q} \right\}. \end{aligned}$$

Multiply the first equation by vector \mathbf{a} , the second equation by \mathbf{b} and add the results. Then we get the strong ellipticity condition of Eqs. (103):

$$\begin{aligned} & \mathbf{v} \cdot \left\{ \left[\frac{\partial^2 W}{\partial \mathbf{E} \partial \mathbf{E}} : (\mathbf{v} \otimes \mathbf{a} \cdot \mathbf{Q}^T) + \frac{\partial^2 W}{\partial \mathbf{E} \partial \mathbf{K}} : (\mathbf{v} \otimes \mathbf{b} \cdot \mathbf{Q}^T) \right] \cdot \mathbf{Q} \right\} \cdot \mathbf{a} \\ & + \mathbf{v} \cdot \left\{ \left[\frac{\partial^2 W}{\partial \mathbf{K} \partial \mathbf{E}} : (\mathbf{v} \otimes \mathbf{a} \cdot \mathbf{Q}^T) + \frac{\partial^2 W}{\partial \mathbf{K} \partial \mathbf{K}} : (\mathbf{v} \otimes \mathbf{b} \cdot \mathbf{Q}^T) \right] \cdot \mathbf{Q} \right\} \cdot \mathbf{b} > 0, \\ & \quad \forall \mathbf{a}, \mathbf{b} \neq \mathbf{0}. \end{aligned}$$

Replacing dot product by the operation “:”, we transform the inequality into a symmetric form

$$\begin{aligned} & (\mathbf{v} \otimes \mathbf{a} \cdot \mathbf{Q}^T) : \frac{\partial^2 W}{\partial \mathbf{E} \partial \mathbf{E}} : (\mathbf{v} \otimes \mathbf{a} \cdot \mathbf{Q}^T) + 2 (\mathbf{v} \otimes \mathbf{a} \cdot \mathbf{Q}^T) : \frac{\partial^2 W}{\partial \mathbf{E} \partial \mathbf{K}} : (\mathbf{v} \otimes \mathbf{b} \cdot \mathbf{Q}^T) \\ & + (\mathbf{v} \otimes \mathbf{b} \cdot \mathbf{Q}^T) : \frac{\partial^2 W}{\partial \mathbf{K} \partial \mathbf{K}} : (\mathbf{v} \otimes \mathbf{b} \cdot \mathbf{Q}^T) > 0, \quad \forall \mathbf{a}, \mathbf{b} \neq \mathbf{0}. \end{aligned}$$

In matrix notations, we rewrite this in a compact form

$$\boldsymbol{\xi} \cdot \mathbf{A}(\mathbf{v}) \cdot \boldsymbol{\xi} > 0, \quad \forall \mathbf{v} \neq \mathbf{0}, \quad \mathbf{v} \cdot \mathbf{N} = 0, \quad \forall \boldsymbol{\xi} \in \mathbb{R}^6, \quad \boldsymbol{\xi} \neq \mathbf{0}, \quad (104)$$

where $\boldsymbol{\xi} = (\mathbf{a}', \mathbf{b}') \in \mathbb{R}^6$, $\mathbf{a}' = \mathbf{a} \cdot \mathbf{Q}^T$, $\mathbf{b}' = \mathbf{b} \cdot \mathbf{Q}^T$, and matrix $\mathbf{A}(\mathbf{v})$ is

$$\mathbf{A}(\mathbf{v}) \triangleq \begin{bmatrix} \frac{\partial^2 W}{\partial \mathbf{E} \partial \mathbf{E}} \{\mathbf{v}\} & \frac{\partial^2 W}{\partial \mathbf{E} \partial \mathbf{K}} \{\mathbf{v}\} \\ \frac{\partial^2 W}{\partial \mathbf{K} \partial \mathbf{E}} \{\mathbf{v}\} & \frac{\partial^2 W}{\partial \mathbf{K} \partial \mathbf{K}} \{\mathbf{v}\} \end{bmatrix},$$

where for any fourth-order tensor \mathbf{K} and vector \mathbf{v} we denote

$$\mathbf{K}\{\mathbf{v}\} \triangleq K_{klmn} \nu_k \nu_m \mathbf{i}_l \otimes \mathbf{i}_n.$$

Inequality (104) is the *strong ellipticity condition* of the equilibrium equations (38) for the elastic shell. A weak form of inequality (104) is an analogue of the *Hadamard inequality*. These inequalities are examples of possible restrictions of the constitutive equations of elastic shells under finite deformations. As for the theory of simple materials, a failure in inequality (104) can lead to the existence of non-smooth solutions to equilibrium equations (38), see Lurie (1990).

The strong ellipticity condition can be written in the equivalent form

$$\left. \frac{d^2}{d\tau^2} W(\mathbf{E} + \tau \mathbf{v} \otimes \mathbf{a}', \mathbf{K} + \tau \mathbf{v} \otimes \mathbf{b}') \right|_{\tau=0} > 0 \quad \forall \mathbf{v}, \mathbf{a}', \mathbf{b}' \neq \mathbf{0}. \quad (105)$$

Comparing the strong ellipticity condition (105) and the Coleman-Noll inequality (102) one can see that the latter implies the former. Indeed, inequality (102) holds for any tensors $\boldsymbol{\varepsilon}$ and $\boldsymbol{\kappa}$. Note that $\boldsymbol{\varepsilon}$ and $\boldsymbol{\kappa}$ may be nonsymmetric tensors, in general.

Substituting relations $\boldsymbol{\varepsilon} = \mathbf{v} \otimes \mathbf{a}'$ and $\boldsymbol{\kappa} = \mathbf{v} \otimes \mathbf{b}'$ to inequality (102), we immediately obtain inequality (105). Thus, the strong ellipticity condition is a particular case of the Coleman–Noll inequality. We watch an essential difference between the micropolar shell theory and the theory of simple elastic materials (Truesdell and Noll 1965; Truesdell 1977): in the latter these two properties are independent in the sense that neither of them implies the other.

In the shell theory, the following particular constitutive relation is widely used

$$W(\mathbf{E}, \mathbf{K}) = W_1(\mathbf{E}) + W_2(\mathbf{K}). \quad (106)$$

For example, Eq. (33) has the form of (106). Now condition (104) is equivalent to two simpler inequalities

$$\mathbf{a} \cdot \frac{\partial^2 W_1}{\partial \mathbf{E} \partial \mathbf{E}} \{\mathbf{v}\} \cdot \mathbf{a} > 0, \quad \mathbf{b} \cdot \frac{\partial^2 W_2}{\partial \mathbf{K} \partial \mathbf{K}} \{\mathbf{v}\} \cdot \mathbf{b} > 0.$$

As an example, let us consider consequences of conditions (104) for constitutive equation (33). In this case we have

$$\begin{aligned} \frac{\partial^2 W_1}{\partial \mathbf{E} \partial \mathbf{E}} \{\mathbf{v}\} &= \alpha_3 \mathbf{A} + (\alpha_1 + \alpha_2) \mathbf{v} \otimes \mathbf{v} + \alpha_4 \mathbf{N} \otimes \mathbf{N}, \\ \frac{\partial^2 W_2}{\partial \mathbf{K} \partial \mathbf{K}} \{\mathbf{v}\} &= \beta_3 \mathbf{A} + (\beta_1 + \beta_2) \mathbf{v} \otimes \mathbf{v} + \beta_4 \mathbf{N} \otimes \mathbf{N}. \end{aligned} \quad (107)$$

Now inequality (104) is valid under the following conditions

$$\begin{aligned} \alpha_3 > 0, \quad \alpha_1 + \alpha_2 + \alpha_3 > 0, \quad \alpha_4 > 0, \\ \beta_3 > 0, \quad \beta_1 + \beta_2 + \beta_3 > 0, \quad \beta_4 > 0. \end{aligned} \quad (108)$$

For a linear isotropic shell, inequalities (108) provide the strong ellipticity of equilibrium equation (59), they are weaker than the conditions of positive definiteness (93). Considering the constitutive equations of an isotropic micropolar shell (33) we have reduced inequality (104) to the inequalities (108).

13.4 Strong Ellipticity Condition and Acceleration Waves

Using the approach of Eremeyev (2005b), Eremeyev and Zubov (2007), Altenbach et al. (2010b), we will show that inequality (104) coincides with the conditions of the propagation of acceleration waves in a shell. We consider a motion when on a smooth curve $\mathcal{C}(t) \subset \Sigma$ called *singular* (Fig. 4), continuous kinematic and dynamic quantities can jump. We assume that the limit values of these quantities exist on \mathcal{C} being different from the opposite sides of \mathcal{C} in general. The jump of quantity $\boldsymbol{\psi}$ on

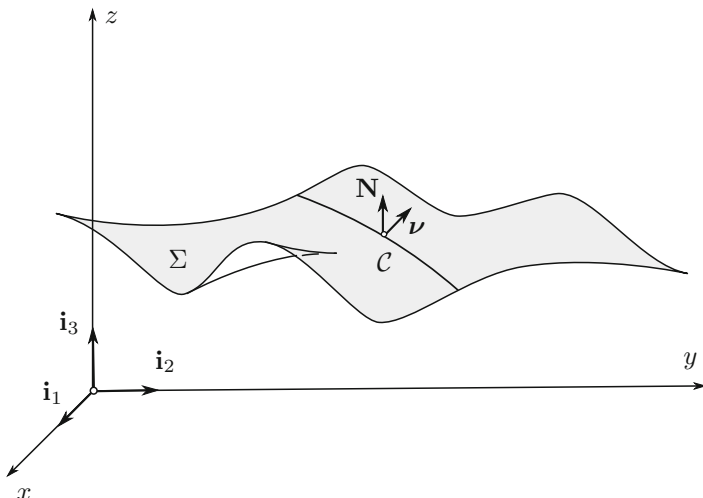


Fig. 4 Shell with a singular curve

\mathcal{C} will be denoted by the double brackets: $[[\psi]] = \psi^+ - \psi^-$, where ψ^\pm are one-side limits of ψ .

An *acceleration wave* (a *weak-discontinuity wave* or *second-order singular curve*) is a moving singular curve \mathcal{C} on which the second derivatives of the radius-vector $\boldsymbol{\rho}$ and the microrotation tensor \mathbf{Q} with respect to the spatial coordinates and time are discontinuous, while $\boldsymbol{\rho}$, \mathbf{Q} and their first derivatives are continuous that means that on \mathcal{C}

$$[[\mathbf{F}]] = \mathbf{0}, \quad [[\nabla_s \mathbf{Q}]] = \mathbf{0}, \quad [[\mathbf{v}]] = \mathbf{0}, \quad [[\boldsymbol{\omega}]] = \mathbf{0}. \quad (109)$$

By Eqs. (29), the stretch measure \mathbf{E} and the wryness tensor \mathbf{K} are continuous on \mathcal{C} . By constitutive equations (39), the jumps of tensors \mathbf{D} and \mathbf{G} are absent. Applying the Maxwell theorem formulated by Truesdell (1977) to continuous fields of velocities \mathbf{v} and $\boldsymbol{\omega}$, surface stress tensor \mathbf{D} , and the surface couple stress tensor \mathbf{G} , we deduce a system of equations that relates the jumps of the derivatives of these quantities with respect to the spatial coordinates and time

$$\begin{aligned} \left[\frac{d\mathbf{v}}{dt} \right] &= -V\mathbf{a}, \quad [[\nabla_s \mathbf{v}]] = \mathbf{v} \otimes \mathbf{a}, \quad \left[\frac{d\boldsymbol{\omega}}{dt} \right] = -V\mathbf{b}, \quad [[\nabla_s \boldsymbol{\omega}]] = \mathbf{v} \otimes \mathbf{b}, \quad (110) \\ V [[\nabla_s \cdot \mathbf{D}]] &= -\mathbf{v} \cdot \left[\frac{d\mathbf{D}}{dt} \right], \quad V [[\nabla_s \cdot \mathbf{G}]] = -\mathbf{v} \cdot \left[\frac{d\mathbf{G}}{dt} \right]. \end{aligned}$$

Here \mathbf{a} and \mathbf{b} are the vectorial amplitudes of the jumps of the linear and angular accelerations, respectively, \mathbf{v} is the unit normal vector to \mathcal{C} such that $\mathbf{N} \cdot \mathbf{v} = 0$, and V

is the velocity of the surface \mathcal{C} in the direction \mathbf{v} . If the external forces and couples are continuous, the relations

$$\llbracket \nabla_s \cdot \mathbf{D} \rrbracket = \rho \left[\frac{d\mathbf{K}_1}{dt} \right], \quad \llbracket \nabla_s \cdot \mathbf{G} \rrbracket = \rho \left[\frac{d\mathbf{K}_2}{dt} \right]$$

follow immediately from the motion equations (28).

Differentiating constitutive equations (39) and using Eqs. (109) and (110), we express the last relations in terms of vector amplitudes \mathbf{a} and \mathbf{b}

$$\begin{aligned} \mathbf{v} \cdot \frac{\partial^2 W}{\partial \mathbf{E} \partial \mathbf{E}} : (\mathbf{v} \otimes \mathbf{a} \cdot \mathbf{Q}^T) + \mathbf{v} \cdot \frac{\partial^2 W}{\partial \mathbf{E} \partial \mathbf{K}} : (\mathbf{v} \otimes \mathbf{b} \cdot \mathbf{Q}^T) \\ = \rho V^2 [\mathbf{a} \cdot \mathbf{Q}^T + (\mathbf{Q} \cdot \boldsymbol{\Theta}_1^T \cdot \mathbf{Q}^T) \cdot (\mathbf{b} \cdot \mathbf{Q}^T)], \\ \mathbf{v} \cdot \frac{\partial^2 W}{\partial \mathbf{K} \partial \mathbf{E}} : (\mathbf{v} \otimes \mathbf{a} \cdot \mathbf{Q}^T) + \mathbf{v} \cdot \frac{\partial^2 W}{\partial \mathbf{K} \partial \mathbf{K}} : (\mathbf{v} \otimes \mathbf{b} \cdot \mathbf{Q}^T) \\ = \rho V^2 [(\mathbf{Q} \cdot \boldsymbol{\Theta}_1 \cdot \mathbf{Q}^T) \cdot (\mathbf{a} \cdot \mathbf{Q}^T) + (\mathbf{Q} \cdot \boldsymbol{\Theta}_2 \cdot \mathbf{Q}^T) \cdot (\mathbf{b} \cdot \mathbf{Q}^T)]. \end{aligned}$$

Hence the strong ellipticity condition can be written in a compact form

$$\mathbf{A}(\mathbf{v}) \cdot \boldsymbol{\xi} = \rho V^2 \mathbb{B} \cdot \boldsymbol{\xi}, \quad \mathbb{B} = \begin{bmatrix} \mathbf{I} & \mathbf{Q} \cdot \boldsymbol{\Theta}_1^T \cdot \mathbf{Q}^T \\ \mathbf{Q} \cdot \boldsymbol{\Theta}_1 \cdot \mathbf{Q}^T & \mathbf{Q} \cdot \boldsymbol{\Theta}_2 \cdot \mathbf{Q}^T \end{bmatrix}. \quad (111)$$

Thus, the problem of propagation of an acceleration wave in a shell is reduced to the spectral problem given by algebraic Eqs. (111). Existence of potential-energy function W implies that $\mathbf{A}(\mathbf{v})$ is symmetric. Matrix \mathbb{B} is also symmetric and positive definite. This enables us to formulate an analogue of the *Fresnel–Hadamard–Duhem theorem* for the elastic shell:

Theorem 13.1 *In an elastic shell, for any propagation direction specified by vector \mathbf{v} , the squared velocities of a second order singular curve (the acceleration wave) are real.*

Note that positive definiteness of $\mathbf{A}(\mathbf{v})$, which is necessary and sufficient for the wave velocity V to be real, coincides with the strong ellipticity inequality (104).

For a physically linear shell, we present an example of solution of the problem (111). Let $\boldsymbol{\Theta}_1$ be zero and $\boldsymbol{\Theta}_2$ be a spherical part of tensor (ball tensor), that is $\boldsymbol{\Theta}_2 = j \mathbf{I}$, where j is the rotatory inertia measure. Let the inequalities (108) hold. Then the solutions of Eq. (111) are

$$V_1 = \sqrt{\frac{\alpha_3}{\rho}}, \quad \boldsymbol{\xi}_1 = (\boldsymbol{\tau}, \mathbf{0}), \quad V_2 = \sqrt{\frac{\alpha_1 + \alpha_2 + \alpha_3}{\rho}}, \quad \boldsymbol{\xi}_2 = (\mathbf{v}, \mathbf{0}), \quad (112)$$

$$V_3 = \sqrt{\frac{\alpha_4}{\rho}}, \quad \xi_3 = (\mathbf{N}, \mathbf{0}), \quad V_4 = \sqrt{\frac{\beta_3}{\rho j}}, \quad \xi_4 = (\mathbf{0}, \boldsymbol{\tau}),$$

$$V_5 = \sqrt{\frac{\beta_1 + \beta_2 + \beta_3}{\rho j}}, \quad \xi_5 = (\mathbf{0}, \mathbf{v}), \quad V_6 = \sqrt{\frac{\beta_4}{\rho j}}, \quad \xi_6 = (\mathbf{0}, \mathbf{N}).$$

The solutions (112) are similar to the 3D case Eremeyev (2005b), Altenbach et al. (2010b) and describe the *transverse and longitudinal acceleration waves* and *transverse and longitudinal acceleration waves of microrotation*, respectively.

13.5 Ordinary Ellipticity

If the equilibrium equations are not elliptic the continuity of solutions can fail. Let us consider this in more detail. We will assume the singular curves to be time-independent. Suppose on the shell surface Σ there exists a curve \mathcal{C} on which there happen a jump in the values of second derivatives of position vector $\boldsymbol{\rho}$ or microrotation tensor \mathbf{Q} . Such a jump will be called the *weak discontinuity*. As the curvature of Σ is determined through second derivatives of $\boldsymbol{\rho}$, such discontinuity can be exhibited as wrinkling of the shell surface.

From the equilibrium equations it follows $[[\nabla_s \cdot \mathbf{D}]] = \mathbf{0}$, $[[\nabla_s \cdot \mathbf{G}]] = \mathbf{0}$. Repeating the transformations of the previous section, we transform these to

$$\mathbf{A}(\mathbf{v}) \cdot \xi = \mathbf{0}, \quad \xi = (\mathbf{a}', \mathbf{b}') \in \mathbb{R}^6. \quad (113)$$

Existence of nontrivial solutions of Eq. (113) means that the weak discontinuities arise. The nontrivial solutions exist if the determinant of matrix $\mathbf{A}(\mathbf{v})$ is zero. If

$$\det \mathbf{A}(\mathbf{v}) \neq 0, \quad (114)$$

the weak discontinuities are impossible.

For the constitutive relation $W = W_1(\mathbf{E}) + W_2(\mathbf{K})$, condition (114) splits into two conditions

$$\det \frac{\partial^2 W_1}{\partial \mathbf{E} \partial \mathbf{E}} \{\mathbf{v}\} \neq 0, \quad \det \frac{\partial^2 W_2}{\partial \mathbf{K} \partial \mathbf{K}} \{\mathbf{v}\} \neq 0. \quad (115)$$

As an example, we consider conditions (115) for the constitutive relations of a physically linear shell (33). Using Eqs. (107) we can show that conditions (115) reduce to the inequalities

$$\alpha_3 \neq 0, \quad \alpha_1 + \alpha_2 + \alpha_3 \neq 0, \quad \alpha_4 \neq 0, \quad \beta_3 \neq 0, \quad \beta_1 + \beta_2 + \beta_3 \neq 0, \quad \beta_4 \neq 0.$$

Condition (114) is the *ellipticity condition* of the equilibrium equations of shell theory (ellipticity in the Petrovsky sense). The condition follows from the general definition

of ellipticity in PDE theory (Agranovich 1997; Hörmander 1976; Nirenberg 2001). Condition (114) is also called the *ordinary ellipticity condition*, it is weaker than the strong ellipticity condition (104).

14 Applications

The recent progress in material technology of materials extends the field of application of classical and non-classical theories of plates and shells towards the new phenomena which should be taken into account. In this section we discuss some applications and extensions of the presented above theory.

14.1 Surface Stresses

One example of phenomena which are significant at the micro- and nanoscales is the surface effects. For example, nanomaterials have physical properties which are different from the bulk material. The classical elasticity can be extended to the nanoscale by taking into account the surface stresses, cf. Duan et al. (2008), Wang et al. (2010, 2011), Javili et al. (2012), Altenbach and Morozov (2013). In particular, the surface stresses are responsible for the size-effect, that means the apparent material properties of a specimen depend on its size. For example, Young's modulus of a rod-like specimen increases significantly, when the cross-section area becomes very small. The surface stresses are the generalization of the scalar surface tension which is a well-known phenomenon in the theory of capillarity. The investigations of the surface phenomena were initiated by Laplace, Young and Gibbs within the sharp interface model, see original papers Laplace (1805), Laplace (1806), Young (1805), Longley and Name (1928), and extended by van der Waals (1893), Korteweg (1901) using the second-gradient models, see also Rowlinson and Widom (2003), Finn (1986), de Gennes et al. (2004), Javili et al. (2013). Rational mechanics of nonlinear elastic solids with surface stresses is developed in Gurtin and Murdoch (1975), Steigmann and Ogden (1999). The theory of elasticity with surface stresses is applied to the modifications of the two-dimensional theories of nanosized plates, see, for example, Altenbach and Eremeyev (2011b), Altenbach et al. (2012b) and the reference therein.

Using six-parameter theory of shells the modification of the constitutive equations taking into account surface stresses is proposed in Altenbach and Eremeyev (2011b). It is shown that both the stress resultant and the couple stress tensors are represented as a sum of two terms as follows

$$\mathbf{T}^* = \mathbf{T} + \mathbf{T}_S \quad \mathbf{M}^* = \mathbf{M} + \mathbf{M}_S, \quad (116)$$

where \mathbf{T} and \mathbf{M} are the classical stress resultant tensors presented for example in Lebedev et al. (2010), Libai and Simmonds (1998), while \mathbf{T}_S and \mathbf{M}_S are the resultant

tensors induced by the surface stresses

$$\mathbf{T}_S = G_+ \mathbf{S}_+ + G_- \mathbf{S}_-, \quad (117)$$

$$\mathbf{M}_S = -h/2 [G_+ \mathbf{S}_+ \times \mathbf{z}_+ - G_- \mathbf{S}_- \times \mathbf{z}_-]. \quad (118)$$

Here \mathbf{S}_\pm are the tensors of surface stresses acting on the shell faces, \mathbf{z}_\pm and $G = \det \mathbf{G}$ are the deviation and the geometric scale factor defined in Libai and Simmonds (1998), and $(\dots)_\pm = (\dots)|_{\pm h/2}$.

The first term in Eqs. (116) is the volume stress resultant while the second one determined by the surface stresses and the shell geometry. In the linear case this modification reduces to the addition of new terms to the elastic stiffness parameters, see Eremeyev et al. (2009), Altenbach et al. (2009, 2010a)

$$\alpha_1 = C\nu + 2\lambda_S, \quad \alpha_3 = C(1 - \nu) + 4\mu_S,$$

$$\alpha_4 = \alpha_s C(1 - \nu),$$

$$\beta_1 = D\nu + h^2\lambda_S/2, \quad \beta_3 = D(1 - \nu) + h^2\mu_S,$$

$$\beta_4 = \alpha_t D(1 - \nu),$$

$$C^* = C + 4\mu_S + 2\lambda_S,$$

$$D^* = D + h^2\mu_S + h^2\lambda_S/2.$$

Here λ_S and μ_S are the surface elastic moduli, C^* and D^* are the effective in-plane and bending stiffness of the plate with surface stresses. It is clear that $C^* > C$ and $D^* > D$, i.e. the plate with surface stresses is stiffer. The elastic moduli α_4 and β_4 do not depend on the surface stresses.

The model of plates and shells with the surface elasticity was extended for the case of surface viscoelasticity by Altenbach et al. (2012b).

14.2 Thin-Walled Structures Made of Micropolar Materials

The interest to the theory of thin-walled structures made of a micropolar material is based on prospective applications of this theory to mechanics of plates and shells made of materials with complex inner structure, such as, for example, cellular materials and foams, see Lakes (1986), Diebels and Steeb (2003), Bigoni and Drugan (2007), Goda et al. (2012), Reda et al. (2016), Eremeyev et al. (2013). In the literature theories of plates and shells and theories based on the reduction of the three-dimensional equations of the micropolar continuum are also known, see Eringen

(1967a), Eringen (1999), Reissner (1977), Altenbach and Eremeyev (2009c), Zubov (2009), Sargsyan (2011), Steinberg and Kvasov (2013) and the review Altenbach et al. (2010c), where various averaging procedures in the thickness direction together with the approximation of the displacements and rotations or the stresses and couple stresses in the thickness direction are discussed. As it is shown by Altenbach and Eremeyev (2009c) the 3D to 2D reduction procedure leads to Eqs. (58) and (59) with modified stiffness parameters α_k and β_k . The nonlinear case is considered by Zubov (2009). On the other hand there reduction procedure leading to the more complicated structure of governing equations, than the presented in this paper, see for example, Eringen (1967a), Sargsyan (2011). The model of micropolar shells can be used for modelling of thin structures made of certain composites, see dell'Isola et al. (2016a, b), Giorgio et al. (2015).

14.3 Thin-Walled Structures Made of Viscoelastic Materials

The two-dimensional constitutive equations for resultant force and couple stress tensors are derived from the constitutive equations of three-dimensional viscoelastic Cosserat continuum. For the linear theory of viscoelasticity given in Eringen (1967b) the application of the correspondence principle gives the possibility to derive the theory of viscoelasticity in the case of thin-walled structures such as plates and shells. The presented here results demonstrate how the viscoelastic properties of three-dimensional continuum inherit in the constitutive equations for plates and shells. Within framework of the linear micropolar viscoelasticity with the constitutive equations of differential type it is shown that 2D relaxation functions of shells have more complicated structures than the relaxation function of the bulk material. In particular, even for homogeneous shells the spectrum of relaxation time do not coincide with the spectrum of the bulk material. For nonhomogeneous shells the spectrum may depend also on the structure of the shell in the thickness direction and its curvature. The basics of such a theory considering general linear viscoelastic behavior are given by Altenbach and Eremeyev (2008, 2009a, b, 2011a) within the framework of five-parameter theory of shells and by Altenbach and Eremeyev (2015) for the six-parameter theory of shells. It is shown how the effective viscoelastic properties reflect the properties in the thickness direction.

14.4 Shells and Plates with Phase Transitions (PT)

The interest to thin-walled structures undergoing PT grows recently with perspective applications of martensite films in engineering, see e.g. Miyazaki et al. (2009). The major known theories of PT in deformable solids relate to the three-dimensional thermoelasticity, see Bhattacharya (2003), Abeyaratne and Knowles (2006), Berezovski et al. (2008) and references cited there.

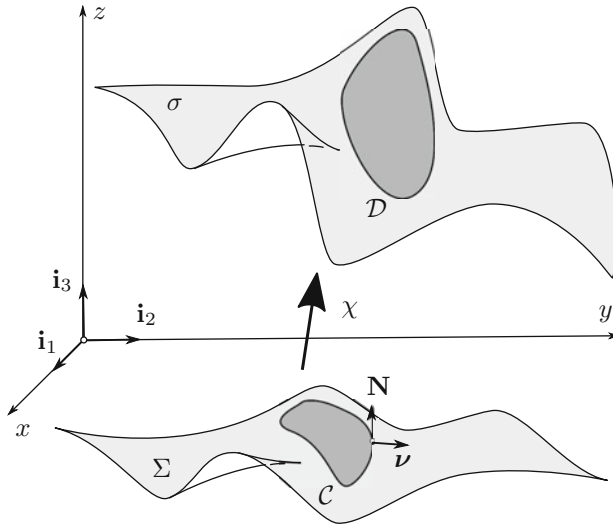


Fig. 5 Two-phase shell with phase interface in reference and actual configurations

The first two-dimensional (2D) mechanical models of PT in thin films are proposed by Bhattacharya and James (1999), James and Rizzoni (2000), see also Bhattacharya (2003), Miyazaki et al. (2009). Alternative 2D models of PT with applications to biomembrane modeling are suggested by Boulbitch (1999), Agrawal and Steigmann (2008), Elliott and Stinner (2010). The model of shell with PT discussed by Shkutin (2007) relates with phase-field models in the continuum mechanics.

The non-linear equilibrium conditions of elastic shells undergoing PT of martensitic type are formulated by Eremeyev and Pietraszkiewicz (2004) and extended in Pietraszkiewicz et al. (2007) taking into account the line tension energy. By analogy to the 3D case, the two-phase shell is regarded as a Cosserat surface consisting of two material phases divided by a sufficiently smooth surface singular curve (phase interface). The existence of such a curve is confirmed by several experiments on thin-walled samples, see e.g. He and Sun (2009, 2010) and the discussion in Eremeyev and Pietraszkiewicz (2011). The quasistatic behavior of two-phase shells is analyzed by Eremeyev and Pietraszkiewicz (2009, 2010, 2011). It is assumed that in the actual configuration of the shell consists of different material phases occupying different complementary subregions separated by the curvilinear phase interface $\mathcal{D} \in \sigma$ (Fig. 5). For a piecewise differentiable mapping $\chi : \Sigma \rightarrow \sigma$ one can introduce on Σ a singular image curve $\mathcal{C} = \chi^{-1}(\mathcal{D})$. The a priori unknown curves \mathcal{D} and \mathcal{C} are called phase interfaces in the reference and actual configurations, respectively.

The two-dimensional local laws of shell thermomechanics can be derived by direct and exact through-the-thickness integration of global three-dimensional balances of forces, moments, energy and the entropy inequality, see Eremeyev and Pietraszkiewicz (2009, 2011) for details. After appropriate transformations the

resulting 2D local Lagrangian laws contain also the surface temperature deviation, the extra surface heat flux, and dual entropy-type quantities in addition to the mean surface temperature and entropy fields. Other versions of the thermodynamics of shells and two-dimensional structures can be found in Green and Naghdi (1970), Green and Naghdi (1979), Murdoch (1976a,b), Zhilin (1976), Simmonds (1984, 2005, 2011), Makowski and Pietraszkiewicz (2002), Steinmann and Häsner (2005).

There are two types of phase interfaces: the coherent in rotations phase interface and the incoherent in rotations one (Eremeyev and Pietraszkiewicz 2004). Using the integral balance laws, the local balance equations along the coherent and incoherent phase interfaces \mathcal{C} , i.e. Lagrangian dynamic compatibility conditions, the local energy balance equation, and the local entropy inequality, the kinetic equation describing motion of the phase interface for all quasistatic processes, is formulated in the form

$$V = -\mathcal{F}(\boldsymbol{\nu} \cdot \llbracket \mathbf{C} \rrbracket \cdot \boldsymbol{\nu}), \quad (119)$$

where V is the velocity of the phase interface, the double brackets stand for the jump of \mathbf{C} across \mathcal{C} , \mathcal{F} is the non-negative definite kinetic function depending on the jump of \mathbf{C} at \mathcal{C} , i.e. $\mathcal{F}(x) \geq 0$ for $x > 0$, and \mathbf{C} is the Eshelby tensor in the non-linear shell theory introduced by Eremeyev and Pietraszkiewicz (2004). For the coherent phase interface \mathbf{C} is given by the formula

$$\mathbf{C} = \mathbf{C}_c \equiv W\mathbf{A} - \mathbf{T} \cdot \mathbf{F}^T - \mathbf{M} \cdot \mathbf{K}^T,$$

and for the phase interface incoherent in rotations by

$$\mathbf{C} = \mathbf{C}_i \equiv W\mathbf{A} - \mathbf{T} \cdot \mathbf{F}^T.$$

For the sake of simplicity these formulas are restricted by pure mechanical theory.

After Berezovski et al. (2008) $\mathcal{F}(x)$ is assumed in the form

$$\mathcal{F}(x) = \begin{cases} \frac{k(x - \varsigma_0)}{1 + a(x - \varsigma_0)} & x \geq \varsigma_0, \\ 0 & -\varsigma_0 < x < \varsigma_0, \\ \frac{k(x + \varsigma_0)}{1 - a(x + \varsigma_0)} & x \leq -\varsigma_0. \end{cases} \quad (120)$$

Here ς_0 describes the effects associated with nucleation of the new phase, a is a parameter describing the limit value of PT, and k is a positive kinetic factor.

Equation (120) with the appropriate boundary conditions and constitutive equations constitute the non-linear boundary-value problem for a shell with PT with respect to unknown surface fields, as well as the position of the phase interface \mathcal{C} . Considering the model s one observes the existence of hysteresis loop characteristic to the behaviour of phase transitions in martensitic materials. The size of the loop depends upon the values of several loading and material parameters.

14.5 Beams and Rods

The presented here direct approach based on Cosserat models can be easily transformed for more technically simple cases of beams and rods. For this purposes we refer to Altenbach et al. (2012a, 2013), Bîrsan et al. (2012) and the reference therein.

15 Conclusions

We presented here the basic equations of the micropolar shell theory using the concept of deformable directed surfaces as a model of a shell. The model coincides kinematically with the general six-parameter resultant shell theory. The presented theory is full analogues to the three-dimensional Cosserat or micropolar theory of elastic solids. The main peculiarity of the model that the interaction between the parts of the shell is determined only by the force and moment tensors including drilling moment. As the consequence the translations and the rotations of the material points of the deformable surface are kinematically independent.

References

- Abeyaratne, R., & Knowles, J. K. (2006). *Evolution of phase transitions: A continuum theory*. Cambridge: Cambridge University Press.
- Agranovich, M. (1997). Elliptic boundary problems. In M. Agranovich, Y. Egorov, & M. Shubin (Eds.), *Partial differential equations IX: Elliptic boundary problems* (pp. 1–144)., Encyclopaedia of Mathematical Sciences, volume 79 Berlin: Springer.
- Agrawal, A., & Steigmann, D. J. (2008). Coexistent fluid-phase equilibria in biomembranes with bending elasticity. *The Journal of Elasticity*, 93(1), 63–80.
- Akay, A., Xu, Z., Carcaterra, A., & Koç, I. M. (2005). Experiments on vibration absorption using energy sinks. *The Journal of the Acoustical Society of America*, 118(5), 3043–3049.
- Alijani, F., & Amabili, M. (2014). Non-linear vibrations of shells: A literature review from 2003 to 2013. *International Journal of Non-Linear Mechanics*, 58, 233–257.
- Altenbach, H., & Eremeyev, V. A. (2010). On the effective stiffness of plates made of hyperelastic materials with initial stresses. *International Journal of Non-Linear Mechanics*, 45(10), 976–981.
- Altenbach, H., & Eremeyev, V. A. (2011a) Mechanics of viscoelastic plates made of FGMs. In J. Murín, V. Kompiš, & V. Kutiš (Eds.), *Computational modelling and advanced simulations* (pp. 33–48), volume 24 of *Computational Methods in Applied Sciences*. Springer.
- Altenbach, H., & Eremeyev, V. A. (Eds.). (2013a) *Generalized continua from the theory to engineering applications*, volume 541 of *CISM International Centre for Mechanical Sciences*. Springer Vienna.
- Altenbach, H., & Eremeyev, V. A. (2014a). Vibration analysis of non-linear 6-parameter prestressed shells. *Meccanica*, 49, 1751–1761.
- Altenbach, H., & Eremeyev, V. A. (2008). On the analysis of viscoelastic plates made of functionally graded materials. *ZAMM*, 88(5), 332–341.
- Altenbach, H., & Eremeyev, V. A. (2009a). On the bending of viscoelastic plates made of polymer foams. *Acta Mechanica*, 204(3–4), 137–154.

- Altenbach, H., & Eremeyev, V. A. (2009b). On the time-dependent behavior of FGM plates. *Key Engineering Materials*, 399, 63–70.
- Altenbach, H., & Eremeyev, V. A. (2011b). On the shell theory on the nanoscale with surface stresses. *The International Journal of Engineering Science*, 49, 1294–1301.
- Altenbach, H., & Eremeyev, V. A. (2009c). On the linear theory of micropolar plates. *ZAMM*, 89(4), 242–256.
- Altenbach, H., & Eremeyev, V. A. (2011c). *Shell-like Structures: Non-classical Theories and Applications*, volume 15 of *Advanced Structured Materials*. Springer.
- Altenbach, H., & Eremeyev, V. A. (2013b). Cosserat-type shells. In H. Altenbach & V. A. Eremeyev (Eds.), *Generalized continua from the theory to engineering applications* (Vol. 541, pp. 131–178). CISM Courses and Lectures Wien: Springer.
- Altenbach, H., & Eremeyev, V. A. (2014b). Actual developments in the nonlinear shell theory—state of the art and new applications of the six-parameter shell theory. In W. Pietraszkiewicz & J. Górski (Eds.), *Shell structures: Theory and applications* (Vol. 3, pp. 3–12). Taylor & Francis.
- Altenbach, H., & Eremeyev, V. A. (2015). On the constitutive equations of viscoelastic micropolar plates and shells of differential type. *Mathematics and Mechanics of Complex Systems*, 3(3), 273–283.
- Altenbach, H., & Mikhasev, G. (Eds.). (2014). *Shell and Membrane Theories in Mechanics and Biology: From Macro-to Nanoscale Structures*, volume 45 of *Advanced Structured Materials*. Springer.
- Altenbach, H., & Morozov, N. F. (Eds.). (2013). *Surface Effects in Solid Mechanics—Models, Simulations and Applications*. Heidelberg: Springer.
- Altenbach, H., Eremeyev, V. A., & Morozov, N. F. (2009). Linear theory of shells taking into account surface stresses. *Doklady Physics*, 54(12), 531–535.
- Altenbach, H., Eremeyev, V. A., & Morozov, N. F. (2010a). On equations of the linear theory of shells with surface stresses taken into account. *Mechanics of Solids*, 45(3), 331–342.
- Altenbach, H., Eremeyev, V. A., Lebedev, L. P., & Rendón, L. A. (2010b). Acceleration waves and ellipticity in thermoelastic micropolar media. *Archive of Applied Mechanics*, 80(3), 217–227.
- Altenbach, H., Birsan, M., & Eremeyev, V. A. (2012a). On a thermodynamic theory of rods with two temperature fields. *Acta Mechanica*, 223(8), 1583–1596.
- Altenbach, H., Eremeyev, V. A., & Morozov, N. F. (2012b). Surface viscoelasticity and effective properties of thin-walled structures at the nanoscale. *The International Journal of Engineering Science*, 59, 83–89.
- Altenbach, H., Birsan, M., & Eremeyev, V. A. (2013). Cosserat-type rods. In H. Altenbach & V. A. Eremeyev (Eds.), *Generalized Continua from the Theory to Engineering Applications* (Vol. 541, pp. 179–248). CISM Courses and Lectures Wien: Springer.
- Altenbach, J., Altenbach, H., & Eremeyev, V. A. (2010c). On generalized Cosserat-type theories of plates and shells: A short review and bibliography. *Archive of Applied Mechanics*, 80, 73–92.
- Amabili, M. (2008). *Nonlinear vibrations and stability of shells and plates*. Cambridge: Cambridge University Press.
- Ambartsumyan, S. A. (1970). *Theory of anisotropic plates: Strength, stability, vibration*. Stamford: Technomic.
- Andreus, U., dell’Isola, F., & Porfiri, M. (2004). Piezoelectric passive distributed controllers for beam flexural vibrations. *Journal of Vibration and Control*, 10(5), 625–659.
- Bauchau, O. A. (2010). *Flexible Multibody Dynamics* (Vol. 176). Solid Mechanics and its Applications Dordrecht: Springer.
- Bauchau, O. A., & Trainelli, L. (2003). The vectorial parameterization of rotation. *Nonlinear Dynamics*, 32(1), 71–92.
- Berdichevsky, V. L. (2009). *Variational principles of continuum mechanics. I. Fundamentals*. Heidelberg: Springer.
- Berezovski, A., Engelbrecht, J., & Maugin, G. A. (2008). *Numerical simulation of waves and fronts in inhomogeneous solids*. New Jersey: World Scientific.

- Bhattacharya, K. (2003). *Microstructure of martensite: Why it forms and how it gives rise to the shape-memory effect*. Oxford: Oxford University Press.
- Bhattacharya, K., & James, R. D. (1999). A theory of thin films of martensitic materials with applications to microactuators. *Journal of the Mechanics and Physics of Solids*, 36(3), 531–576.
- Bigoni, D., & Drugan, W. J. (2007). Analytical derivation of Cosserat moduli via homogenization of heterogeneous elastic materials. *Transactions of ASME. Journal of Applied Mechanics*, 74(4), 741–753.
- Bîrsan, M., Altenbach, H., Sadowski, T., Eremeyev, V. A., & Pietras, D. (2012). Deformation analysis of functionally graded beams by the direct approach. *Composites B: Engineering*, 43(3), 1315–1328.
- Boulbitch, A. A. (1999). Equations of heterophase equilibrium of a biomembrane. *Archive of Applied Mechanics*, 69(2), 83–93.
- Carcatera, A., Akay, A., & Bernardini, C. (2012). Trapping of vibration energy into a set of resonators: Theory and application to aerospace structures. *Mechanical Systems and Signal Processing*, 26, 1–14.
- Carrera, E., Brischetto, S., & Nali, P. (2011). *Plates and shells for smart structures: Classical and advanced theories for modeling and analysis*. Chichester: Wiley.
- Chróścielewski, J., & Witkowski, W. (2010). On some constitutive equations for micropolar plates. *ZAMM*, 90(1), 53–64.
- Chróścielewski, J., Makowski, J., & Pietraszkiewicz, W. (2004a). *Statics and dynamics of multi-folded shells: Nonlinear theory and finite element method*. Warsaw: IPPT PAN.
- Chróścielewski, J., Makowski, J., & Pietraszkiewicz, W. (2004b). *Statics and dynamics of multi-folded shells: Nonlinear theory and finite element method (in Polish)*. Warszawa: Wydawnictwo IPPT PAN.
- Chróścielewski, J., Pietraszkiewicz, W., & Witkowski, W. (2010). On shear correction factors in the non-linear theory of elastic shells. *International Journal of Solids and Structures*, 47(25–26), 3537–3545.
- Ciarlet, Ph. (1997). *Mathematical elasticity, Volume II: Theory of plates*. Amsterdam: Elsevier.
- Ciarlet, Ph. (2000). *Mathematical elasticity, Volume III: Theory of shells*. Amsterdam: Elsevier.
- Courant, R., & Hilbert, D. (1991). *Methods of mathematical physics (Vol. 1)*. New York: Wiley.
- de Gennes, P. G., Brochard-Wyart, F., & Quéré, D. (2004). *Capillarity and wetting phenomena: Drops, bubbles, pearls, waves*. New York: Springer.
- dell’Isola, F., & Vidoli, S. (1998). Damping of bending waves in truss beams by electrical transmission lines with PZT actuators. *Archive of Applied Mechanics*, 68(9), 626–636.
- dell’Isola, F., Porfiri, M., & Vidoli, S. (2003). Piezo-ElectroMechanical (PEM) structures: passive vibration control using distributed piezoelectric transducers. *Comptes Rendus Mécanique*, 331(1), 69–76.
- dell’Isola, F., Della Corte, A., Greco, L., & Luongo, A. (2016a). Plane bias extension test for a continuum with two inextensible families of fibers: A variational treatment with lagrange multipliers and a perturbation solution. *International Journal of Solids and Structures*, 81, 1–12.
- dell’Isola, F., Giorgio, I., Pawlikowski, M., & Rizzi, N. L. (2016b). Large deformations of planar extensible beams and pantographic lattices: heuristic homogenization, experimental and numerical examples of equilibrium. *Proceedings of the Royal Society of London. Series A*, 472(2185), 20150790.
- Diebels, S., & Steeb, H. (2003). Stress and couple stress in foams. *Computational Materials Science*, 28(3), 714–722.
- Duan, H. L., Wang, J., & Karihaloo, B. L. (2008). Theory of elasticity at the nanoscale. In *Advances in applied mechanics (Vol. 42, pp. 1–68)*. Elsevier.
- Elliott, C. M., & Stinner, B. (2010). A surface phase field model for two-phase biological membranes. *SIAM Journal on Applied Mathematics*, 70(8), 2904–2928.

- Eremeyev, V. A. (2005a). Nonlinear micropolar shells: Theory and applications. In W. Pietraszkiewicz & C. Szymczak (Eds.), *Shell structures: Theory and applications* (pp. 11–18). London: Taylor & Francis.
- Eremeyev, V. A. (2005b). Acceleration waves in micropolar elastic media. *Doklady Physics*, 50(4), 204–206.
- Eremeyev, V. A., & Lebedev, L. P. (2011). Existence theorems in the linear theory of micropolar shells. *ZAMM*, 91(6), 468–476.
- Eremeyev, V. A., & Pietraszkiewicz, W. (2006). Local symmetry group in the general theory of elastic shells. *Journal of Elasticity*, 85(2), 125–152.
- Eremeyev, V. A., & Pietraszkiewicz, W. (2011). Thermomechanics of shells undergoing phase transition. *Journal of the Mechanics and Physics of Solids*, 59(7), 1395–1412.
- Eremeyev, V. A., & Pietraszkiewicz, W. (2004). The non-linear theory of elastic shells with phase transitions. *The Journal of Elasticity*, 74(1), 67–86.
- Eremeyev, V. A., & Pietraszkiewicz, W. (2010). On tension of a two-phase elastic tube. In W. Pietraszkiewicz & I. Kreja (Eds.), *Shell structures: Theory and applications* (Vol. 2, pp. 63–66). Boca Raton: CRC Press.
- Eremeyev, V. A., & Pietraszkiewicz, W. (2009). Phase transitions in thermoelastic and thermoviscoelastic shells. *Archives of Mechanics*, 61(1), 41–67.
- Eremeyev, V. A., & Pietraszkiewicz, W. (2012). Material symmetry group of the non-linear polar-elastic continuum. *International Journal of Solids and Structures*, 49(14), 1993–2005.
- Eremeyev, V. A., & Pietraszkiewicz, W. (2014). Editorial: Refined theories of plates and shells. *ZAMM*, 94(1–2), 5–6.
- Eremeyev, V. A., & Pietraszkiewicz, W. (2016). Material symmetry group and constitutive equations of micropolar anisotropic elastic solids. *Mathematics and Mechanics of Solids*, 21(2), 210–221.
- Eremeyev, V. A., & Zubov, L. M. (1994). On the stability of elastic bodies with couple stresses. *Mechanics of Solids*, 29(3), 172–181.
- Eremeyev, V. A., & Zubov, L. M. (2007). On constitutive inequalities in nonlinear theory of elastic shells. *ZAMM*, 87(2), 94–101.
- Eremeyev, V. A., & Zubov, L. M. (2008). *Mechanics of elastic shells (in Russian)*. Moscow: Nauka.
- Eremeyev, V. A., Altenbach, H., & Morozov, N. F. (2009). The influence of surface tension on the effective stiffness of nanosize plates. *Doklady Physics*, 54(2), 98–100.
- Eremeyev, V. A., Lebedev, L. P., & Altenbach, H. (2013). *Foundations of micropolar mechanics*. Heidelberg: Springer.
- Eremeyev, V. A., Ivanova, E. A., & Morozov, N. F. (2015a). On free oscillations of an elastic solids with ordered arrays of nano-sized objects. *Continuum Mechanics and Thermodynamics*, 27(4–5), 583–607.
- Eremeyev, V. A., Lebedev, L. P., & Cloud, M. J. (2015b). The Rayleigh and Courant variational principles in the six-parameter shell theory. *Mathematics and Mechanics of Solids*, 20(7), 806–822.
- Eringen, A. C. (1967a). Theory of micropolar plates. *ZAMP*, 18(1), 12–30.
- Eringen, A. C. (1967b). Linear theory of micropolar viscoelasticity. *International Journal of Engineering Science*, 5(2), 191–204.
- Eringen, A. C. (1999). *Microcontinuum field theory. I: Foundations and solids*. New York: Springer.
- Eringen, A. C., & Maugin, G. A. (1990). *Electrodynamics of continua*. New York: Springer.
- Fichera, G. (1972). Existence theorems in elasticity. In S. Flügge (Ed.), *Handbuch der Physik* (pp. 347–389), volume VIa/2 Berlin: Springer.
- Finn, R. (1986). *Equilibrium capillary surfaces*. New York: Springer.
- Fu, Y. B., & Ogden, R. W. (1999). Nonlinear stability analysis of pre-stressed elastic bodies. *Continuum Mechanics and Thermodynamics*, 11, 141–172.
- Germain, P. (1973a). La méthode des puissances virtuelles en mécanique des milieux continus - première partie, théorie du second gradient. *Journal de Mécanique*, 12, 235–274.
- Germain, P. (1973b). The method of virtual power in continuum mechanics. part 2: Microstructure. *SIAM Journal on Applied Mathematics*, 25(3), 556–575.

- Giorgio, I., Grygoruk, R., dell'Isola, F., & Steigmann, D. J. (2015). Pattern formation in the three-dimensional deformations of fibered sheets. *Mechanics Research Communications*, 69, 164–171.
- Goda, I., Assidi, M., Belouettar, S., & Ganghoffer, J. F. (2012). A micropolar anisotropic constitutive model of cancellous bone from discrete homogenization. *Journal of the Mechanical Behavior of Biomedical Materials*, 16, 87–108.
- Goldenevizer, A. L. (1976). *Theory of thin elastic shells (in Russ.)*. Moscow: Nauka.
- Green, A. E., & Naghdi, P. M. (1979). On thermal effects in the theory of shells. *Proceedings of the Royal Society of London Series A*, 365(1721), 161–190.
- Green, A. E., & Naghdi, P. M. (1970). Non-isothermal theory of rods, plates and shells. *International Journal of Solids and Structures*, 6, 209–244.
- Gurtin, M. E., & Murdoch, A. I. (1975). A continuum theory of elastic material surfaces. *The Archive for Rational Mechanics and Analysis*, 57(4), 291–323.
- He, Y. J., & Sun, Q. P. (2009). Effects of structural and material length scales on stress-induced martensite macro-domain patterns in tube configurations. *The International Journal of Solids and Structures*, 46(16), 3045–3060.
- He, Y. J., & Sun, Q. P. (2010). Macroscopic equilibrium domain structure and geometric compatibility in elastic phase transition of thin plates. *The International Journal of Mechanical Sciences*, 52(2), 198–211.
- Hörmander, L. (1976). *Linear partial differential equations* (4th ed., Vol. 116). A Series of Comprehensive Studies in Mathematics Berlin: Springer.
- Jaiani, G. (2011). *Cusped shell-like structures*. Heidelberg: Springer.
- Jaiani, G., & Podio-Guidugli, P. (2008). *IUTAM Symposium on Relations of Shell, Plate, Beam and 3D Models: Proceedings of the IUTAM Symposium on the Relations of Shell, Plate, Beam, and 3D Models Dedicated to the Centenary of Ilia Vekua's Birth, held Tbilisi, Georgia, April 23–27, 2007*, Vol. 9. Springer.
- James, R. D., & Rizzoni, R. (2000). Pressurized shape memory thin films. *The Journal of Elasticity*, 59(1–3), 399–436.
- Javili, A., McBride, A., & Steinmann, P. (2012). Thermomechanics of solids with lower-dimensional energetics: On the importance of surface, interface, and curve structures at the nanoscale. A unifying review. *Applied Mechanics Reviews*, 65, 010802–1–31.
- Javili, A., dell'Isola, F., & Steinmann, P. (2013). Geometrically nonlinear higher-gradient elasticity with energetic boundaries. *Journal of the Mechanics and Physics of Solids*, 61(12), 2381–2401.
- Jemielita, G. (2001). Meandry teorii płyt i powłok. In Cz. Woźniak (Ed.), *Mechanics of elastic plates and shells (in Polish)*, volume VIII of *Mechanika Techniczna*. PWN, Warszawa.
- Kabrits, S. A., Mikhailovskiy, E. I., Tovstik, P. E., Chernykh, K. F., & Shamina, V. A. (2002). *General nonlinear theory of elastic shells (in Russ.)*. St. Petersburg State University, St. Petersburg.
- Koç, I. M., Carcaterra, A., Xu, Z., & Akay, A. (2005). Energy sinks: Vibration absorption by an optimal set of undamped oscillators. *The Journal of the Acoustical Society of America*, 118(5), 3031–3042.
- Konopińska, V., & Pietraszkiewicz, W. (2007). Exact resultant equilibrium conditions in the nonlinear theory of branching and self-intersecting shells. *The International Journal of Solids and Structures*, 44(1), 352–369.
- Korteweg, D. J. (1901). Sur la forme que prennent les équations des mouvements des fluides si l'on tient compte des forces capillaires par des variations de densité. *Archives Néerlandaises des sciences exactes et naturelles, Sér. II*(6), 1–24.
- Kreja, I. (2007). *Geometrically non-linear analysis of layered composite plates and shells*. Gdańsk: Gdańsk University of Technology.
- Lakes, R. S. (1986). Experimental microelasticity of two porous solids. *The International Journal of Solids and Structures*, 22(1), 55–63.
- Laplace, P. S. (1805). Sur l'action capillaire. supplément à la théorie de l'action capillaire. *Traité de mécanique céleste* (Vol. 4, pp. 771–777). Supplement 1, Livre X Paris: Gauthier-Villars et fils.

- Laplace, P. S. (1806). À la théorie de l' action capillaire. supplément à la théorie de l' action capillaire. *Traité de mécanique céleste* (Vol. 4, pp. 909–945). Supplement 2, Livre X Paris: Gauthier-Villars et fils.
- Lebedev, L. P., Cloud, M. J., & Eremeyev, V. A. (2010). *Tensor analysis with applications in mechanics*. New Jersey: World Scientific.
- Libai, A., & Simmonds, J. G. (1983). Nonlinear elastic shell theory. *Advances in Applied Mechanics*, 23, 271–371.
- Libai, A., & Simmonds, J. G. (1998). *The nonlinear theory of elastic shells* (2nd ed.). Cambridge: Cambridge University Press.
- Lions, J.-L., & Magenes, E. (1968). *Problèmes aux limites non homogènes et applications*. Paris: Dunod.
- Longley, W. R. & Van Name, R. G. (Eds.). (1928). *The collected works of J. Willard Gibbs, PH.D., LL.D. Vol. I Thermodynamics*. Longmans, New York.
- Lurie, A. I. (1990). *Nonlinear theory of elasticity*. Amsterdam: North-Holland.
- Lurie, A. I. (2001). *Analytical mechanics*. Berlin: Springer.
- Makowski, J., & Pietraszkiewicz, W. (2002). *Thermomechanics of shells with singular curves*. Zesz. Nauk. No 528/1487/2002, IMP PAN, Gdańsk.
- Maugin, G. A. (1988). *Continuum mechanics of electromagnetic solids*. Oxford: Elsevier.
- Maurini, C., dell'Isola, F., & Del Vescovo, D. (2004). Comparison of piezoelectronic networks acting as distributed vibration absorbers. *Mechanical Systems and Signal Processing*, 18(5), 1243–1271.
- Mindlin, R. D. (1951). Influence of rotatory inertia and shear on flexural motions of isotropic elastic plates. Transactions of ASME. *Journal of Applied Mechanics*, 18, 31–38.
- Miyazaki, S., Fu, Y. Q., & Huang, W. M. (Eds.). (2009). *Thin film shape memory alloys: Fundamentals and device applications*. Cambridge: Cambridge University Press.
- Murdoch, A. I. (1976a). A thermodynamical theory of elastic material interfaces. *The Quarterly Journal of Mechanics and Applied Mathematics*, 29(3), 245–274.
- Murdoch, A. I. (1976b). On the entropy inequality for material interfaces. *ZAMP*, 27(5), 599–605.
- Naghdi, P. M. (1972). The theory of plates and shells. In S. Flügge (Ed.), *Handbuch der Physik* (pp. 425–640), volume VIa/2 Heidelberg: Springer.
- Nirenberg, L. (2001). *Topics in nonlinear functional analysis*. New York: American Mathematical Society.
- Novozhilov, V. V., Chernykh, K. F., & Mikhailovskiy, E. I. (1991). *Linear theory of thin shells (in Russ.)*. Politekhnik, Leningrad.
- Ogden, R. W. (1997). *Non-linear elastic deformations*. Mineola: Dover.
- Pietraszkiewicz, W. (2011). Refined resultant thermomechanics of shells. *International Journal of Engineering Science*, 49(10), 1112–1124.
- Pietraszkiewicz, W. (1979a). *Finite rotations and langrangian description in the non-linear theory of shells*. Warszawa-Poznań: Polish Sci. Publ.
- Pietraszkiewicz, W. (1979b). Consistent second approximation to the elastic strain energy of a shell. *ZAMM*, 59, 206–208.
- Pietraszkiewicz, W. (1989). Geometrically nonlinear theories of thin elastic shells. *Uspekhi Mehaniki (Advances in Mechanics)*, 12(1), 51–130.
- Pietraszkiewicz, W. (2015). The resultant linear six-field theory of elastic shells: What it brings to the classical linear shell models? *ZAMM*, 10.1002/zamm.201500184.
- Pietraszkiewicz, W., & Eremeyev, V. A. (2009a). On natural strain measures of the non-linear micropolar continuum. *International Journal of Solids and Structures*, 46(3–4), 774–787.
- Pietraszkiewicz, W., & Eremeyev, V. A. (2009b). On vectorially parameterized natural strain measures of the non-linear Cosserat continuum. *International Journal of Solids and Structures*, 46 (11–12), 2477–2480.
- Pietraszkiewicz, W., & Górski, J. (Eds.). (2014). *Shell structures: Theory and applications* (Vol. 3). Boca Raton: CRC Press.

- Pietraszkiewicz, W., & Konopińska, V. (2015). Junctions in shell structures: A review. *Thin-Walled Structures*, 95, 310–334.
- Pietraszkiewicz, W., & Konopińska, V. (2011). On unique kinematics for the branching shells. *The International Journal of Solids and Structures*, 48(14), 2238–2244.
- Pietraszkiewicz, W., & Kreja, I. (Eds.). (2010). *Shell structures: Theory and applications* (Vol. 2). Boca Raton: CRC Press.
- Pietraszkiewicz, W., & Szymczak, C. (Eds.). (2005). *Shell structures: Theory and applications*. London: Taylor & Francis.
- Pietraszkiewicz, W., Eremeyev, V. A., & Konopińska, V. (2007). Extended non-linear relations of elastic shells undergoing phase transitions. *ZAMM*, 87(2), 150–159.
- Reda, H., Rahali, Y., Ganghoffer, J. F., & Lakiss, H. (2016). Wave propagation in 3d viscoelastic auxetic and textile materials by homogenized continuum micropolar models. *Composite Structures*, 141, 328–345.
- Reddy, J. N. (2003). *Mechanics of laminated composite plates and shells: Theory and analysis* (2nd ed.). Boca Raton: CRC Press.
- Reissner, E. (1944). On the theory of bending of elastic plates. *Journal of Mathematical Physics*, 23, 184–194.
- Reissner, E. (1985). Reflection on the theory of elastic plates. *Applied Mechanics Reviews*, 38(11), 1453–1464.
- Reissner, E. (1977). A note on generating generalized two-dimensional plate and shell theories. *ZAMP*, 28(4), 633–642.
- Rowlinson, J. S., & Widom, B. (2003). *Molecular theory of capillarity*. New York: Dover.
- Sargsyan, S. H. (2011). The general dynamic theory of micropolar elastic thin shells. *Doklady Physics*, 56(1), 39–42.
- Sedov, L. I. (1968). Models of continuous media with internal degrees of freedom. *Journal of Applied Mathematics and Mechanics*, 32(5), 803–819.
- Shkutin, L. I. (2007). Analysis of axisymmetric phase strains in plates and shells. *Journal of Applied Mechanics and Technical Physics*, 48(2), 285–291.
- Simmonds, J. G. (2005). A simple nonlinear thermodynamic theory of arbitrary elastic beams. *The Journal of Elasticity*, 81(1), 51–62.
- Simmonds, J. G. (2011). A classical, nonlinear thermodynamic theory of elastic shells based on a single constitutive assumption. *The Journal of Elasticity*, 105(1–2), 305–312.
- Simmonds, J. G. (1984). The thermodynamical theory of shells: Descent from 3-dimensions without thickness expansions. In E. L. Axelrad & F. A. Emmerling (Eds.), *Flexible shells* (pp. 1–11). Theory and Applications Berlin: Springer.
- Steigmann, D. J., & Ogden, R. W. (1999). Elastic surface-substrate interactions. Proceedings of the Royal Society of London Series A: Mathematical, Physical and Engineering Science, 455(1982), 437–474.
- Steinberg, L., & Kvasov, R. (2013). Enhanced mathematical model for Cosserat plate bending. *Thin-Walled Structures*, 63, 51–62.
- Steinmann, P., & Häsner, O. (2005). On material interfaces in thermomechanical solids. *Archive of Applied Mechanics*, 75(1), 31–41.
- Tovstik, P. E., & Smirnov, A. L. (2001). *Asymptotic methods in the buckling theory of elastic shells*. Singapore: World Scientific.
- Truesdell, C. (1977). *A first course in rational continuum mechanics*. New York: Academic Press.
- Truesdell, C. (1984). *Rational thermodynamics* (2nd ed.). New York: Springer.
- Truesdell, C., & Noll, W. (1965). The nonlinear field theories of mechanics. In S. Flügge (Ed.), *Handbuch der Physik* (pp. 1–602). III(3) Berlin: Springer.
- van der Waals, J. D. (1893). The thermodynamic theory of capillarity under the hypothesis of a continuous variation of density (Engl. transl. by J. S. Rowlinson). *Journal of Statistical Physics*, 20, 200–244.
- Vidoli, S., & dell’Isola, F. (2001). Vibration control in plates by uniformly distributed PZT actuators interconnected via electric networks. *European Journal of Mechanics: A/Solids*, 20(3), 435–456.

- Wang, C. M., Reddy, J. N., & Lee, K. H. (2000). *Shear deformable beams and shells*. Amsterdam: Elsevier.
- Wang, J., Huang, Z., Duan, H., Yu, S., Feng, X., Wang, G., et al. (2011). Surface stress effect in mechanics of nanostructured materials. *Acta Mechanica Solida Sinica*, 24, 52–82.
- Wang, Z. Q., Zhao, Y.-P., & Huang, Z.-P. (2010). The effects of surface tension on the elastic properties of nano structures. *International Journal of Engineering Science*, 48(2), 140–150.
- Wiśniewski, K. (2010). *Finite rotation shells: Basic equations and finite elements for Reissner kinematics*. Berlin: Springer.
- Young, T. (1805). An essay on the cohesion of fluids. *Philosophical Transactions of the Royal Society of London*, 95, 65–87.
- Zhilin, P. A. (1976). Mechanics of deformable directed surfaces. *International Journals of Solids and Structures*, 12(9–10), 635–648.
- Zubov, L. M. (1997). *Nonlinear theory of dislocations and disclinations in elastic bodies*. Berlin: Springer.
- Zubov, L. M. (2009). Micropolar shell equilibrium equations. *Doklady Physics*, 54(6), 290–293.

The Bending-Gradient Theory for Laminates and In-Plane Periodic Plates

Arthur Lebéé and Karam Sab

Abstract In a recent work, a new plate theory for thick plates was suggested where the static unknowns are those of the Kirchhoff-Love theory, to which six components are added representing the gradient of the bending moment (Lebéé and Sab, *Int J Solids Struct*, 48(20):2878-2888, 2011a). This theory, called the Bending-Gradient theory, is the extension to multilayered plates and to in-plane periodic plates of the Reissner-Mindlin theory which appears as a special case when the plate is homogeneous. The Bending-Gradient theory was derived following the ideas from Reissner, *J Appl Mech*, 12(2):69-77, (1945). However, it is also possible to derive it through asymptotic expansions. In this lecture, the latter are applied one order higher than the leading order to a laminated plate following monoclinic symmetry. Using variational arguments, it is possible to derive the Bending-Gradient theory. Then, some applications are presented and the theory is finally extended to in-plane periodic plates.

1 Introduction

The classical theory of plates, known also as Kirchhoff-Love plate theory is based on the assumption that the normal to the mid-plane of the plate remains normal after transformation. This theory is also the first order of the asymptotic expansion with respect to the thickness (Ciarlet and Destuynder 1979). Thus, it presents a good theoretical justification and was soundly extended to the case of periodic plates (Caillerie 1984; Kohn and Vogelius 1984). It enables to have a first-order estimate of the macroscopic deflection as well as local stress fields. In most applications the first-order deflection is accurate enough. However, this theory does not capture the local effect of shear forces on the microstructure because shear forces are one higher-order derivative of the bending moment in equilibrium equations ($Q_\alpha = M_{\alpha\beta,\beta}$).

A. Lebéé · K. Sab (✉)

Université Paris-Est Laboratoire Navier (ENPC, IFSTTAR, CNRS), Paris, France
e-mail: karam.sab@enpc.fr

Because shear forces are part of the macroscopic equilibrium of the plate, their effect is also of great interest for engineers when designing structures. However, modeling properly the action of shear forces is still a controversial issue. Reissner (1945) suggested a model for homogeneous plates based on a parabolic distribution of transverse shear stress through the thickness (Reissner-Mindlin theory). This model performs well for homogeneous plates and gives more natural boundary conditions than those of Kirchhoff-Love theory. Thus, it is appreciated by engineers and broadly used in applied mechanics. However, the direct extension of this model to laminated plates raised many difficulties.

Two main paths were followed for deriving models suitable for laminated plates: axiomatic approaches and asymptotic approaches.

In asymptotic approaches, a plate model is derived directly from the full three-dimensional formulation of the problem, assuming the thickness of the plate goes to zero. In these approaches, the asymptotic expansion method plays a central role. As already mentioned, the leading order leads to Kirchhoff-Love plate theory (Ciarlet and Destuynder 1979; Caillerie 1984; Kohn and Vogelius 1984). Hence one needs to seek higher orders for bringing out the effect of shear forces. However, in the cases of laminated plates, this procedure does not lead to Reissner-Mindlin plate theory Lewiński (1991), Sutyryn and Hodges (1996).

In axiomatic approaches, 3D fields are assumed a priori and a plate theory is derived using integration through the thickness and variational tools. The reader can refer to the following reviews (Reddy 1989; Altenbach 1998; Noor and Malik 2000; Carrera 2002). Most suggestions leading to Reissner-Mindlin-like theories show discontinuous transverse shear stress through the thickness or are limited to some geometric configurations (orthotropy or cylindrical bending for instance). In this field, these limitations even led to the suggestion of “layerwise” models which give more satisfying results but are much more numerically intense than Reissner-Mindlin theory (Carrera 2002; Diaz Diaz 2001). Finally, let us point out that the theory suggested by Reissner (1945) is usually considered as an axiomatic approach since the parabolic transverse shear stress distribution of the stress was derived without asymptotic arguments. Consequently, some work took literally this distribution and applied it to laminated plates. Like in many unsuccessful axiomatic approaches this led to discontinuous displacement fields and raised an unjustified suspicion over the original work.

Revisiting the approach from Reissner (1945) directly with laminated plates, Lebée and Sab (2011a, b) showed that the transverse shear static variables which come out when the plate is heterogeneous are not shear forces Q_α but the full gradient of the bending moment $R_{\alpha\beta\gamma} = M_{\alpha\beta,\gamma}$. Using conventional variational tools, they derived a new plate theory—called Bending-Gradient theory—which is actually turned into Reissner-Mindlin theory when the plate is homogeneous. This new plate theory is seen by the authors as an extension of Reissner’s theory to heterogeneous plates which preserves most of its simplicity. It was applied to the cylindrical bending of carbon fibers laminated plates and compared to exact solutions in Lebée and Sab (2011b). Very good agreement for the transverse shear distribution as well as

in-plane displacement was pointed out and convergence with the slenderness was observed.

Originally designed for laminated plates, the Bending-Gradient theory was also extended to in-plane periodic plates using averaging considerations such as Hill-Mandel principle and successfully applied to sandwich panels (Lebée and Sab 2012a, b) as well as space frames Lebée and Sab (2013a).

Because the initial derivation of the Bending-Gradient theory followed the ideas from Reissner (1945), one can argue that it is basically an axiomatic approach. However, it is the intention of the present lecture to demonstrate that there is a close link between the derivation of the Bending-Gradient theory and the asymptotic expansion method (Lebée and Sab 2013b). Since the Bending-Gradient is turned into the Reissner-Mindlin theory when the plate is homogeneous, this link will be also demonstrated for the original work from Reissner (1945).

In order to derive the Bending-Gradient theory through asymptotic expansions, we first set in Sect. 2 the 3D problem, its symmetries and the asymptotic expansions framework. For the sake of simplicity we choose the constitutive material and the loadings of the plate such that the bending moment is fully uncoupled with the membrane stress. Then in Sect. 3 we perform the standard resolution of the auxiliary problems and conclude that bringing out transverse shear effects through this approach is not satisfying. Then, in Sect. 4 we derive the Bending-Gradient theory using variational considerations. In Sect. 5, the Bending-Gradient theory is applied to laminates under cylinder bending and its predictions are compared to closed-form solutions. Finally, Sect. 6 is dedicated to the extension of the theory to in-plane periodic plates.

2 The Asymptotic Expansion Framework

In this section, the asymptotic expansion framework is set in the special case of a laminated plate. This procedure was established by Sanchez-Palencia (1980) for linear dynamics of 3D continuum. It starts with the definition of the 3D problem of the laminated plate which is under consideration. Then this problem is scaled in order to separate the in-plane and the out-of-plane variables and we assume that the fields follow an expansion depending on a small parameter: the inverse of the plate slenderness. Finally, the equations are gathered for each order of this parameter.

2.1 Notations

Vectors and higher-order tensors, up to sixth order, are used in the following. When using short notation, several underlining styles are used: vectors are straight underlined, \underline{u} . Second order tensors are underlined with a tilde: $\underline{\underline{M}}$ and $\underline{\underline{K}}$. Third order tensors are underlined with a parenthesis: $\underline{\underline{\underline{R}}}$ and $\underline{\underline{\underline{\Gamma}}}$. Fourth order tensors are

doubly underlined with a tilde: $\underline{\underline{\mathbf{D}}}$ and $\underline{\underline{\mathbf{s}}}$. Sixth order tensors are doubly underlined with a parenthesis: $\underline{\underline{\mathbf{h}}}$ and $\underline{\underline{\mathbf{I}}}$. The full notation with indices is also used. Then we follow Einstein's notation on repeated indices. Furthermore, Greek indices $\alpha, \beta, \delta, \gamma = 1, 2$ denotes in-plane dimensions and Latin indices $i, j, k, l = 1, 2, 3$, all three dimensions.

The transpose operation ${}^t\bullet$ is applied to any order tensors as follows:

$$({}^t a)_{\alpha\beta\dots\psi\omega} = a_{\omega\psi\dots\beta\alpha}.$$

Three contraction products are defined, the usual dot product ($\underline{\mathbf{a}} \cdot \underline{\mathbf{b}} = a_i b_i$), the double contraction product ($\underline{\mathbf{a}} : \underline{\mathbf{b}} = a_{ij} b_{ji}$) and a triple contraction product ($\underline{\mathbf{a}} : \underline{\mathbf{a}} = a_{\alpha\beta\gamma} a_{\gamma\beta\alpha}$). The derivation operator $\underline{\nabla}$ is also formally represented as a vector: $\underline{\mathbf{a}} \cdot \underline{\nabla} = a_{ij} \nabla_j = a_{ij,j}$ is the divergence and $\underline{\mathbf{a}} \otimes \underline{\nabla} = a_{ij} \nabla_k = a_{ij,k}$ is the gradient. Here \otimes is the dyadic product.

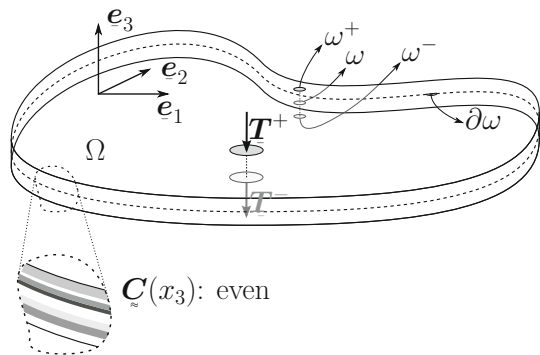
2.2 The 3D Problem

The laminated plate occupies a domain $\Omega' = \omega^t \times] - \frac{t}{2}, \frac{t}{2} [$ where ω^t is the middle surface of the plate (its typical size is L) and t its thickness (Fig. 1). The boundary of the plate, $\partial\Omega'$, is decomposed into three parts:

$$\begin{aligned} \partial\Omega' &= \partial\Omega_{\text{lat}} \cup \partial\Omega_3^+ \cup \partial\Omega_3^- \\ \text{with } \partial\Omega_{\text{lat}} &= \partial\omega^t \times] - \frac{t}{2}, \frac{t}{2} [\text{ and } \partial\Omega_3^\pm = \omega^t \times \left\{ \pm \frac{t}{2} \right\}. \end{aligned} \tag{1}$$

The plate is fully clamped on its lateral boundary, $\partial\Omega_{\text{lat}}$, and is submitted to the same distributed and purely transverse force $\underline{\mathbf{f}} = f_3(x_1, x_2)\mathbf{e}_3$ both on its upper and lower boundaries $\partial\Omega_3^+$ and $\partial\Omega_3^-$.

Fig. 1 The 3D plate problem



The fourth-order stiffness tensor $\underline{\underline{C}}'(x_3)$ characterizing the elastic properties of the constituent material at every point $\underline{x} = (x_1, x_2, x_3)$ of Ω' is introduced. We assume the following monoclinic symmetry: $C'_{3\alpha\beta\gamma} = C'_{\alpha 333} = 0$. In addition, $\underline{\underline{C}}'$ does not depend on (x_1, x_2) and is an even function of x_3 to ensure full uncoupling between in-plane and out-of-plane problems. Thus, the constitutive equation writes as:

$$\underline{\underline{\sigma}}'(\underline{x}) = \underline{\underline{C}}'(x_3) : \underline{\underline{\varepsilon}}'(\underline{x}) \quad (2)$$

where $\underline{\underline{\sigma}}' = (\sigma'_{ij}(\underline{x}))$ is the stress tensor and $\underline{\underline{\varepsilon}}' = (\varepsilon'_{ij}(\underline{x}))$ is the strain tensor at point \underline{x} . The tensor $\underline{\underline{C}}'$ follows the classical symmetries of linear elasticity and is positive definite. Its inverse, noted $\underline{\underline{S}}'$, is the compliance tensor and it has the same properties.

The full 3D elastic problem, \mathcal{P}^{3D} , is to find in Ω' a displacement vector field \underline{u}' , a strain tensor field $\underline{\underline{\varepsilon}}'$ and a stress tensor field $\underline{\underline{\sigma}}'$ such that the static conditions ($SC^{3D,t}$):

$$SC^{3D,t} : \begin{cases} \underline{\underline{\sigma}}' \cdot \underline{\nabla} = 0 \text{ on } \Omega' \\ \underline{\underline{\sigma}}' \cdot (\pm \underline{e}_3) = \underline{f} \text{ on } \partial\Omega_3^\pm, \end{cases} \quad (3a)$$

$$(3b)$$

the kinematic conditions ($KC^{3D,t}$):

$$KC^{3D,t} : \begin{cases} \underline{\underline{\varepsilon}}' = \underline{u}' \otimes^s \underline{\nabla} \text{ on } \Omega' \\ \underline{u}' = 0 \text{ on } \partial\Omega_{\text{lat}} \end{cases} \quad (4a)$$

$$(4b)$$

and the constitutive law (2) are satisfied. Here, $(\underline{e}_1, \underline{e}_2, \underline{e}_3)$ is the orthonormal basis associated with coordinates (x_1, x_2, x_3) and $\bullet \otimes^s \underline{\nabla}$ denotes the symmetric part of the gradient operator.

Variational Formulation of the 3D Problem The strain and stress energy density w^{3D} and w^{*3D} are respectively given by:

$$w^{3D}(\underline{\underline{\varepsilon}}) = \frac{1}{2} \underline{\underline{\varepsilon}} : \underline{\underline{C}}' : \underline{\underline{\varepsilon}}, \quad w^{*3D}(\underline{\underline{\sigma}}) = \frac{1}{2} \underline{\underline{\sigma}} : \underline{\underline{S}}' : \underline{\underline{\sigma}} \quad (5)$$

They are related by the following Legendre-Fenchel transform:

$$w^{*3D}(\underline{\underline{\sigma}}) = \sup_{\underline{\underline{\varepsilon}}} \{ \underline{\underline{\sigma}} : \underline{\underline{\varepsilon}} - w^{3D}(\underline{\underline{\varepsilon}}) \} \quad (6)$$

The kinematic variational approach states that the strain solution $\underline{\underline{\varepsilon}}'$ of \mathcal{P}^{3D} is the one that minimizes P^{3D} among all kinematically compatible strain fields:

$$P^{3D}(\underline{\underline{\varepsilon}}') = \min_{\underline{\underline{\varepsilon}} \in KC^{3D,t}} \{ P^{3D}(\underline{\underline{\varepsilon}}) \} \quad (7)$$

where P^{3D} is the potential energy given by:

$$P^{3D}(\underline{\varepsilon}) = \int_{\Omega'} w^{3D}(\underline{\varepsilon}) d\Omega' - \int_{\omega^L} \underline{f} \cdot \underline{u}^+ + \underline{f} \cdot \underline{u}^- d\omega^L \quad (8)$$

and $\underline{u}^\pm = \underline{u}(x_1, x_2, \pm t/2)$ are the 3D displacement fields on the upper and lower faces of the plate.

The static variational approach states that the stress solution $\underline{\sigma}'$ of \mathcal{P}^{3D} is the one that minimizes P^{*3D} among all statically compatible stress fields:

$$P^{*3D}(\underline{\sigma}') = \min_{\underline{\sigma} \in SC^{3D,t}} \{P^{*3D}(\underline{\sigma})\} \quad (9)$$

where P^{*3D} is the complementary potential energy given by:

$$P^{*3D}(\underline{\sigma}) = \int_{\Omega'} w^{*3D}(\underline{\sigma}) d\Omega' \quad (10)$$

Symmetries For the sake of simplicity, we chose the 3D plate problem such that only flexural part is involved and no membranal part.

The 3D problem \mathcal{P}^{3D} is skew-symmetric through a planar symmetry with respect to the mid-plane of the plate (known also as “mirror symmetry” in laminates engineering) because \underline{C}' is an even function of only x_3 . This means that, when applying the transformation $x_3 \rightarrow -x_3$ the problem remains unchanged but the applied external loading in (3b) changes its sign. Consequently the in-plane displacement $u'_\alpha(x_1, x_2, x_3)$ is an odd function of x_3 and the out-of-plane displacement $u'_3(x_1, x_2, x_3)$ is an even function of x_3 . Similarly, the in-plane stress $\sigma'_{\alpha\beta}(x_1, x_2, x_3)$ and transverse compression $\sigma'_{33}(x_1, x_2, x_3)$ are odd functions of x_3 and the transverse shear stress $\sigma'_{\alpha 3}(x_1, x_2, x_3)$ is an even function of x_3 .

In terms of resultants and averaged displacements, the integration through the thickness of u'_α and $\sigma'_{\alpha\beta}$ vanish and then the plate problem will be purely flexural. Of course, this result affects also the asymptotic expansion procedure and enables many simplifications.

2.3 Scaling

Once the 3D problem is set, we scale it for clearly separating the in-plane variables (which are related to macroscopic problems) and the out-of-plane variable (which is related to microscopic perturbations). Hence, L is the typical scale of the in-plane variables (e.g. the span and also the wavelength of the loadings). We introduce the following change of variable $Y_\alpha = L^{-1}x_\alpha$ for the in-plane variable where $Y_\alpha \in \omega$. The domain ω is the scaled mid-plane of the plate. Moreover we define $z = t^{-1}x_3$ for

the out-of-plane variable, $z \in] - \frac{1}{2}, \frac{1}{2}[$. Consequently, we define the small parameter as: $\eta = t/L$.

Based on this change of variables, the fourth-order elasticity tensor can be rewritten as:

$$\underset{\approx}{\mathbb{C}}'(x_3) = \underset{\approx}{\mathbb{C}}(t^{-1}x_3) = \underset{\approx}{\mathbb{C}}(z) \quad (11)$$

where $\underset{\approx}{\mathbb{C}}$ is a function of z . In the following, double-stroke fonts denote fields which are only function of the local variable z (i.e. localization fields).

The distributed forces are classically scaled in the following way as shown in Ciarlet and Destuynder (1979), Caillerie (1984), Dallot and Sab (2008):

$$\underline{\mathbf{f}}(x_1, x_2) = \eta^2 \frac{F_3(Y_1, Y_2)}{2} \mathbf{e}_3 \quad (12)$$

Similarly, in the following, fields with capital letters are only function of (Y_1, Y_2) (i.e. macroscopic fields).

Furthermore, from the fields of the 3D problem $(\underline{\mathbf{u}}', \underline{\boldsymbol{\varepsilon}}', \underline{\boldsymbol{\sigma}}')$ we define the non-dimensional fields $(\underline{\mathbf{u}}, \underline{\boldsymbol{\varepsilon}}, \underline{\boldsymbol{\sigma}})$ as follows:

$$\begin{cases} \underline{\mathbf{u}}'(x_1, x_2, x_3) = L \underline{\mathbf{u}}(x_1/L, x_2/L, x_3/t) = L \underline{\mathbf{u}}(Y_1, Y_2, z) \\ \underline{\boldsymbol{\varepsilon}}'(x_1, x_2, x_3) = \underline{\boldsymbol{\varepsilon}}(x_1/L, x_2/L, x_3/t) = \underline{\boldsymbol{\varepsilon}}(Y_1, Y_2, z) \\ \underline{\boldsymbol{\sigma}}'(x_1, x_2, x_3) = \underline{\boldsymbol{\sigma}}(x_1/L, x_2/L, x_3/t) = \underline{\boldsymbol{\sigma}}(Y_1, Y_2, z) \end{cases} \quad (13)$$

The derivation rule for those functions is:

$$\begin{aligned} \underline{\nabla} &= \left(\frac{d}{dx_1}, \frac{d}{dx_2}, \frac{d}{dx_3} \right) \\ &= L^{-1} \left(\frac{\partial}{\partial Y_1}, \frac{\partial}{\partial Y_2}, 0 \right) + t^{-1} \left(0, 0, \frac{\partial}{\partial z} \right) = L^{-1} \underline{\nabla}_y + t^{-1} \underline{\nabla}_z. \end{aligned} \quad (14)$$

We will also use the variational formulation of the 3D problem. Hence we provide here the scaled variational formulation. The set of statically compatible fields can be rewritten as:

$$\mathcal{SC}^{3D} : \begin{cases} \underline{\boldsymbol{\sigma}} \cdot \underline{\nabla}_{(Y,z)}^\eta = 0 \text{ on } \Omega = \omega \times] - \frac{1}{2}, + \frac{1}{2}[, & (15a) \\ \underline{\boldsymbol{\sigma}} \cdot (\pm \mathbf{e}_3) = \frac{\eta^2}{2} F_3 \mathbf{e}_3 \text{ on } \partial\Omega_3^\pm, & (15b) \end{cases}$$

where $\underline{\nabla}_{(Y,z)}^\eta = \underline{\nabla}_y + \frac{1}{\eta} \underline{\nabla}_z$. The kinematically compatible fields becomes (\mathcal{KC}^{3D}) :

$$\mathcal{KC}^{3D} : \begin{cases} \underline{\boldsymbol{\varepsilon}} = \underline{\mathbf{u}} \otimes^s \underline{\nabla}_{(Y,z)}^\eta \text{ on } \Omega, & (16a) \\ \underline{\mathbf{u}} = 0 \text{ on } \partial\omega \times] - \frac{1}{2}, + \frac{1}{2}[& (16b) \end{cases}$$

Then the potential energy can be rewritten as:

$$P^{3D}(\underline{\varepsilon}) = tL^2 \int_{\omega} \left(\langle w^{3D}(\underline{\varepsilon}) \rangle - \eta \frac{u_3^+ + u_3^-}{2} F_3 \right) d\omega \quad (17)$$

where $\langle \bullet \rangle$ is the integration through the thickness:

$$\langle \bullet \rangle = \int_{-\frac{1}{2}}^{\frac{1}{2}} \bullet dz.$$

The complementary energy becomes also:

$$P^{*3D}(\underline{\sigma}) = tL^2 \int_{\omega} \langle w^{*3D}(\underline{\sigma}) \rangle d\omega \quad (18)$$

Moreover, the non dimensional plate balance equation can be derived as follows. The bending moment and the shear force are defined as:

$$M_{\alpha\beta}(Y_1, Y_2) = \langle z\sigma_{\alpha\beta} \rangle, \quad \text{and} \quad Q_{\alpha}(Y_1, Y_2) = \eta^{-1} \langle \sigma_{3\alpha} \rangle. \quad (19)$$

Moment balance equations are:

$$\langle z(\sigma_{\alpha\beta,\beta} + \eta^{-1}\sigma_{\alpha 3,3}) \rangle = 0 = M_{\alpha\beta,\beta} - Q_{\alpha} \quad \text{or} \quad \underline{\underline{M}} \cdot \underline{\underline{\nabla}}_y - \underline{\underline{Q}} = 0 \quad (20)$$

And the out-of-plane balance equation writes:

$$\eta^{-1} \langle \sigma_{3\alpha,\alpha} + \eta^{-1}\sigma_{33,3} \rangle = 0 = Q_{\alpha,\alpha} + F_3 \quad \text{or} \quad \underline{\underline{Q}} \cdot \underline{\underline{\nabla}}_y + F_3 = 0 \quad (21)$$

Finally, we have the non dimensional plate balance equation:

$$M_{\alpha\beta,\beta\alpha} + F_3 = 0 \quad \text{or} \quad \underline{\underline{M}} : (\underline{\underline{\nabla}}_y \otimes \underline{\underline{\nabla}}_y) + F_3 = 0 \quad (22)$$

Now, $\underline{\underline{\mathbb{C}}}$, ω and F_3 being fixed, is to find a consistent approximation of the solution of the 3D problem \mathcal{P}^{3D} (2-3-4) assuming η is small.

2.4 Properties of the Non-Dimensional Solution

For given $(\omega, \underline{\underline{\mathbb{C}}}, F_3, \eta)$ where $\underline{\underline{\mathbb{C}}}$ is monoclinic and even in z , and under some regularity conditions, the solution of the non-dimensional problem is unique.

Obviously, due the change of variables $x_3 \rightarrow z$,

- u_3 and $\sigma_{\alpha 3}$ are even in z
- $u_\alpha, \sigma_{\alpha\beta}$ and σ_{33} are odd in z

We will establish the following knew properties

- u_3 and $\sigma_{\alpha 3}$ are odd in η
- $u_\alpha, \sigma_{\alpha\beta}$ and σ_{33} are even in η

Indeed, let $z' = -\frac{x_3}{t}$ be a new change of variable for the out-of-plane variable. The new non-dimensional fields $(\underline{u}', \underline{\varepsilon}', \underline{\sigma}')$ are defined by:

$$\begin{cases} \underline{u}'(x_1, x_2, x_3) = L \underline{u}'(x_1/L, x_2/L, -x_3/t) = L \underline{u}'(Y_1, Y_2, z') \\ \underline{\varepsilon}'(x_1, x_2, x_3) = \underline{\varepsilon}'(x_1/L, x_2/L, -x_3/t) = \underline{\varepsilon}'(Y_1, Y_2, z') \\ \underline{\sigma}'(x_1, x_2, x_3) = \underline{\sigma}'(x_1/L, x_2/L, -x_3/t) = \underline{\sigma}'(Y_1, Y_2, z') \end{cases} \quad (23)$$

The new derivation rule for these fields is:

$$\begin{aligned} \underline{\nabla} &= \left(\frac{d}{dx_1}, \frac{d}{dx_2}, \frac{d}{dx_3} \right) \\ &= L^{-1} \left(\frac{\partial}{\partial Y_1}, \frac{\partial}{\partial Y_2}, 0 \right) - t^{-1} \left(0, 0, \frac{\partial}{\partial z'} \right) = L^{-1} \underline{\nabla}_Y - t^{-1} \underline{\nabla}_{z'} \\ &= L^{-1} \underline{\nabla}_{(Y, z')}^{-\eta} \end{aligned} \quad (24)$$

where

$$\underline{\nabla}_{(Y, z')}^{-\eta} = \underline{\nabla}_Y - \frac{1}{\eta} \underline{\nabla}_{z'} \quad (25)$$

The new equations are:

$$\text{SC}^{3D'} : \begin{cases} \underline{\sigma}' \cdot \underline{\nabla}_{(Y, z')}^{-\eta} = 0 \text{ on } \Omega = \omega \times] -\frac{1}{2}, +\frac{1}{2}[\\ \underline{\sigma}' \cdot (\pm \underline{e}_3) = -\frac{\eta^2}{2} F_3 \underline{e}_3 \text{ on } \omega^\pm \end{cases} \quad (26a)$$

$$(26b)$$

$$\text{KC}^{3D'} : \begin{cases} \underline{\varepsilon}' = \underline{u}' \otimes^s \underline{\nabla}_{(Y, z')}^{-\eta} \text{ on } \Omega, \\ \underline{u}' = 0 \text{ on } \partial\omega \times] -\frac{1}{2}, +\frac{1}{2}[\end{cases} \quad (27a)$$

$$(27b)$$

$$\underline{\sigma}'(Y_1, Y_2, z') = \underline{\mathbb{C}}(z') : \underline{\varepsilon}'(Y_1, Y_2, z') \quad (28)$$

Therefore, the new non-dimensional fields $(\underline{u}', \underline{\varepsilon}', \underline{\sigma}')$ are solutions of the same equations as for $(\underline{u}, \underline{\varepsilon}, \underline{\sigma})$ where $F_3 \rightarrow -F_3$ and $\eta \rightarrow -\eta$:

$$(\underline{u}', \underline{\varepsilon}', \underline{\sigma}') (Y_1, Y_2, z') = (\underline{u}, \underline{\varepsilon}, \underline{\sigma})^{(-F_3, -\eta)} (Y_1, Y_2, z') \quad (29)$$

Moreover, by definition, the new non-dimensional fields coincide with the initial ones with $z = -z'$:

$$(\underline{u}', \underline{\varepsilon}', \underline{\sigma}') (Y_1, Y_2, z') = (\underline{u}, \underline{\varepsilon}, \underline{\sigma})^{(F_3, \eta)} (Y_1, Y_2, -z') \quad (30)$$

Hence, we have:

$$(\underline{u}, \underline{\varepsilon}, \underline{\sigma})^{(-\eta)} (Y_1, Y_2, z) = -(\underline{u}, \underline{\varepsilon}, \underline{\sigma})^{(\eta)} (Y_1, Y_2, -z) \quad (31)$$

This means that even components in z are odd in η and odd components in z are even in η .

2.5 Expansion

The asymptotic expansion method which is presented, for example, in Sanchez-Palencia (1980), Sanchez-Hubert and Sanchez-Palencia (1992) will be used to provide a formal justification of the Bending-Gradient theory. The starting point of the method is to assume that the solution to (2-3-4) can be written as a series in power of η in the following form:

$$\begin{cases} \underline{u} &= \eta^{-1} \underline{u}^{-1} + \eta^0 \underline{u}^0 + \eta^1 \underline{u}^1 + \dots \\ \underline{\varepsilon} &= \eta^0 \underline{\varepsilon}^0 + \eta^1 \underline{\varepsilon}^1 + \dots \\ \underline{\sigma} &= \eta^0 \underline{\sigma}^0 + \eta^1 \underline{\sigma}^1 + \dots \end{cases} \quad (32)$$

where \underline{u}^p , $\underline{\varepsilon}^p$ and $\underline{\sigma}^p$, $p = -1, 0, 1, 2, \dots$, are functions of (Y_1, Y_2, z) which have the following properties:

- u_3^p and $\sigma_{\alpha 3}^p$ are null for even p and even in z for odd p .
- u_α^p , $\sigma_{\alpha\beta}^p$ and σ_{33}^p are null for odd p and odd in z for even p .

The series are started from the order η^0 for $\underline{\sigma}$ and $\underline{\varepsilon}$, and from the order η^{-1} for \underline{u} . Then, the expansion (32)—taking into account the change of variable—must be inserted in the equations (2-3-4) and all the terms of the same order η^p must be identified.

Statically Admissible Fields The normalized 3D equilibrium equation becomes:

$$\underline{\sigma} \cdot \underline{\nabla}_{(Y,z)}^\eta = \eta^{-1} \left(\underline{\sigma}^0 \cdot \underline{\nabla}_z \right) + \eta^0 \left(\underline{\sigma}^0 \cdot \underline{\nabla}_y + \underline{\sigma}^1 \cdot \underline{\nabla}_z \right) + \dots = 0. \quad (33)$$

Identifying all the terms of the above series to be zero, we find:

$$\sigma_{i3,3}^0 = 0 \quad (34)$$

for the order η^{-1} and

$$\sigma_{i\alpha,\alpha}^p + \sigma_{i3,3}^{p+1} = 0 \quad (35)$$

for the order η^p with $p \geq 0$. The derivation \bullet_i is performed without ambiguity with respect to (Y_1, Y_2, z) . The static boundary conditions on ω^\pm writes:

$$\sigma_{i3}^p \left(Y_1, Y_2, \pm \frac{1}{2} \right) = 0 \quad (36)$$

for the order $p \geq 0$ and $p \neq 2$. When $p = 2$ we have:

$$\sigma_{\alpha 3}^2 \left(Y_1, Y_2, \pm \frac{1}{2} \right) = 0 \quad \text{and} \quad \sigma_{33}^2 \left(Y_1, Y_2, \pm \frac{1}{2} \right) = \pm \frac{1}{2} F_3(Y_1, Y_2) \quad (37)$$

Kinematically Compatible Fields The non-dimensional displacement field is:

$$\underline{\mathbf{u}} = \eta^{-1} \underline{\mathbf{u}}^{-1} + \eta^0 \underline{\mathbf{u}}^0 + \eta^1 \underline{\mathbf{u}}^1 + \dots \quad (38)$$

The non-dimensional strain field is:

$$\underline{\boldsymbol{\varepsilon}} = \underline{\mathbf{u}} \otimes^s \underline{\nabla}_{(Y,z)}^\eta = \eta^{-2} \underline{\boldsymbol{\varepsilon}}^{-2} + \eta^{-1} \underline{\boldsymbol{\varepsilon}}^{-1} + \eta^0 \underline{\boldsymbol{\varepsilon}}^0 + \dots \quad (39)$$

with:

$$\underline{\boldsymbol{\varepsilon}}^{-2} = \underline{\mathbf{u}}^{-1} \otimes^s \underline{\nabla}_z \quad \text{and} \quad \underline{\boldsymbol{\varepsilon}}^p = \underline{\mathbf{u}}^{p+1} \otimes^s \underline{\nabla}_z + \underline{\mathbf{u}}^p \otimes^s \underline{\nabla}_Y, \quad p \geq -1 \quad (40)$$

In components:

$$\varepsilon_{\alpha\beta}^{-2} = 0, \quad \varepsilon_{\alpha 3}^{-2} = \frac{1}{2} u_{\alpha,3}^{-1} \quad \text{and} \quad \varepsilon_{33}^{-2} = u_{3,3}^{-1} \quad (41)$$

and for all $p \geq -1$:

$$\varepsilon_{\alpha\beta}^p = \frac{1}{2} \left(u_{\alpha,\beta}^p + u_{\beta,\alpha}^p \right), \quad \varepsilon_{\alpha 3}^p = \frac{1}{2} \left(u_{\alpha,3}^{p+1} + u_{3,\alpha}^p \right) \quad \text{and} \quad \varepsilon_{33}^p = u_{3,3}^{p+1} \quad (42)$$

The kinematic condition on the lateral boundary leads to:

$$\forall p \geq -1 \quad \text{and} \quad \forall (Y_1, Y_2) \in \partial\omega, \quad \underline{\mathbf{u}}^p(Y_1, Y_2) = 0. \quad (43)$$

3 Explicit or Cascade Resolution

Now that the asymptotic expansion framework is set, we detail the explicit resolution which is classically performed (see Caillerie 1984; Lewinski 1991 for instance). Basically it starts with the derivation of low order displacements which do not generate local strain but are related to purely macroscopic displacement fields. Then the zeroth-order equations are gathered. They enable the definition of the first auxiliary problem and the construction of the well-known Kirchhoff-Love macroscopic plate model. Then the first-order is solved the same way. Of course it would be possible to carry on the process any order higher.

3.1 Low Order Displacement Fields

The assumption (32) provides the following equations:

$$\underline{\varepsilon}^{-2} = 0, \quad (44)$$

and

$$\underline{\varepsilon}^{-1} = 0, \quad (45)$$

From (44) it is deduced that \underline{u}^{-1} is a function of (Y_1, Y_2) . Moreover, u_α^{-1} being null, we write:

$$\underline{u}^{-1} = U_3^{-1}(Y_1, Y_2) \underline{e}_3. \quad (46)$$

Using (45), the boundary conditions (43) and the fact that u_3^0 is null, it can be found that \underline{u}^0 has the following form:

$$\underline{u}^0 = -z U_3^{-1} \otimes \nabla_Y = \begin{pmatrix} -z U_{3,1}^{-1} \\ -z U_{3,2}^{-1} \\ 0 \end{pmatrix}, \quad (47)$$

with the boundary conditions:

$$U_{3,\alpha}^{-1} = U_{3,\alpha}^{-1} n_\alpha = 0 \quad \forall (Y_1, Y_2) \in \partial\omega. \quad (48)$$

where \underline{n} is the outer normal to $\partial\omega$. Note that, since U_3^{-1} is null over $\partial\omega$, its tangential derivative will be also null over $\partial\omega$, hence only the normal gradient $U_{3,\alpha}^{-1} n_\alpha$ is required to be explicitly set to zero in this boundary condition.

3.2 Zeroth-Order Plate Model (Kirchhoff-Love)

Zeroth-Order Auxiliary Problem Gathering equilibrium equation for order -1 , compatibility equation, boundary conditions and constitutive equations of order 0 we get the zeroth-order auxiliary problem for $z \in [-\frac{1}{2}, \frac{1}{2}]$:

$$\begin{cases} \sigma_{i3,3}^0 = 0 & (49a) \\ \sigma_{ij}^0 = \mathbb{C}_{ijkl} \varepsilon_{kl}^0 & (49b) \\ \varepsilon_{\alpha\beta}^0 = z K_{\alpha\beta}^{-1}, \quad \varepsilon_{\alpha 3}^0 = \frac{1}{2} u_{\alpha,3}^1 \quad \text{and} \quad \varepsilon_{33}^0 = u_{3,3}^1 & (49c) \\ \sigma_{i3}^0 (z = \pm \frac{1}{2}) = 0 & (49d) \end{cases}$$

where we define the lowest-order curvature as:

$$K_{\alpha\beta}^{-1} = -U_{3,\alpha\beta}^{-1} \quad (50)$$

Solving this problem does not raise difficulty. Using short notation, the displacement field writes as:

$$\underline{\mathbf{u}}^1 = \underline{\mathbf{u}}^K : \underline{\mathbf{K}}^{-1} + U_3^1 \mathbf{e}_3 = \begin{pmatrix} 0 \\ 0 \\ \mathfrak{u}_{3\alpha\beta}^K K_{\beta\alpha}^{-1} + U_3^1 \end{pmatrix} \quad (51)$$

where the displacement localization tensor $\underline{\mathbf{u}}^K(z)$ related to the curvature is given by:

$$\mathfrak{u}_{3\alpha\beta}^K = - \left[\int_{-\frac{1}{2}}^z y \frac{\mathbb{C}_{33\alpha\beta}}{\mathbb{C}_{3333}} dy \right]^* \quad \text{and} \quad \mathfrak{u}_{\alpha\beta\gamma}^K = 0 \quad (52)$$

where $[\bullet]^*$ denotes the averaged-out distribution: $[\bullet]^* = \bullet - \langle \bullet \rangle$. Finally, U_3^1 appears as an integration constant which will load the next auxiliary problem. The stress localization writes as:

$$\underline{\boldsymbol{\sigma}}^0 = \underline{\mathfrak{s}}^K : \underline{\mathbf{K}}^{-1} \quad (53)$$

where the fourth-order stress localization tensor is:

$$\mathfrak{s}_{\alpha\beta\gamma\delta}^K = z \mathbb{C}_{\alpha\beta\gamma\delta}^\sigma \quad \text{and} \quad \mathfrak{s}_{i3\gamma\delta}^K = 0 \quad (54)$$

and $\mathbb{C}_{\alpha\beta\gamma\delta}^\sigma = \mathbb{C}_{\alpha\beta\gamma\delta} - \mathbb{C}_{\alpha\beta 33} \mathbb{C}_{33\gamma\delta} / \mathbb{C}_{3333}$ denotes the plane-stress elasticity tensor. Hence the plate is under pure *plane-stress* at this order.

The strain is derived using the local constitutive equation:

$$\varepsilon_{\alpha\beta}^0 = z K_{\alpha\beta}^{-1}, \quad \varepsilon_{\alpha 3}^0 = 0 \quad \text{and} \quad \varepsilon_{33}^0 = - \frac{z \mathbb{C}_{33\alpha\beta}}{\mathbb{C}_{3333}} K_{\alpha\beta}^{-1} \quad (55)$$

This confirms Kirchhoff's assumption regarding the in-plane strain. The reader's attention is drawn to the fact that the out-of-plane strain is not zero, as already mentioned in several works (Ciarlet and Destuynder 1979; Caillerie 1984) in contrast to the original assumption from Kirchhoff.

Hence, for given macroscopic field U_3^{-1} and its derivatives, the microscopic strain and stress are fully determined at this order. However, we also need U_3 for estimating the displacement field. This requires solving higher-order problems.

At this order, there remains to derive the macroscopic problem which enables the determination of U_3^{-1} .

Zeroth-Order Macroscopic Problem The macroscopic equilibrium is derived integrating the first two components of $z \times (35)$ for $p = 0$. This gives after integrating by parts over z :

$$M_{\alpha\beta,\beta}^0 - Q_\alpha^1 = 0 \quad (56)$$

where the zeroth-order bending moment is defined as:

$$M_{\alpha\beta}^0(Y_1, Y_2) = \langle z\sigma_{\alpha\beta}^0 \rangle, \quad (57)$$

and the first-order shear force is:

$$Q_\alpha^1(Y_1, Y_2) = \langle \sigma_{3\alpha}^1 \rangle. \quad (58)$$

It can be easily established that $\langle \sigma_{3\alpha}^0 \rangle = 0$ because of the equilibrium (34) and the boundary condition (36). Therefore, averaging the third component of (35) for $p = 0$ leads to a trivial equation. Using the second order boundary condition (37) for $p = 2$ and averaging the third component of the first-order equilibrium equation (35) for $p = 1$ gives:

$$Q_{\alpha,\alpha}^1 + F_3 = 0. \quad (59)$$

We obtain also the constitutive equation by plugging the local stress derived in (53) into the definition of $\underline{\underline{M}}^0$. This leads to the well-known Kirchhoff-Love constitutive equation:

$$\underline{\underline{M}}^0 = \underline{\underline{D}} : \underline{\underline{K}}^{-1} \quad \text{where:} \quad \underline{\underline{D}} = \langle z^2 \underline{\underline{C}}^\sigma \rangle \quad (60)$$

Gathering the preceding results leads to the definition of the Kirchhoff-Love plate problem:

$$\left\{ \begin{array}{l} \underline{\underline{M}}^0 : (\underline{\nabla}_y \otimes \underline{\nabla}_y) + F_3 = 0, \quad \text{on } \omega \quad (61a) \\ \underline{\underline{M}}^0 = \underline{\underline{D}} : \underline{\underline{K}}^{-1}, \quad \text{on } \omega \quad (61b) \\ \underline{\underline{K}}^{-1} = U_3^{-1} \underline{\nabla}_y \otimes \underline{\nabla}_y, \quad \text{on } \omega \quad (61c) \\ U_3^{-1} = 0 \quad \text{and} \quad (U_3^{-1} \otimes \underline{\nabla}_y) \cdot \underline{n} = 0 \quad \text{on } \partial\omega \quad (61d) \end{array} \right.$$

Finally, solving this macroscopic problem enables the derivation of the macroscopic displacement fields U_3^{-1} . However, U_3^1 remains unknown.

The well-known limitation of Kirchhoff-Love plate model is that it does not incorporate the effect of shear forces. In order to bring out the contribution of transverse shear, we need to go further in the expansion.

3.3 Higher-Order Analysis

First-Order Auxiliary Problem Gathering equilibrium equation for order 0, compatibility equation, boundary conditions and constitutive equations of order 1 we get the first-order auxiliary problem for $z \in [-\frac{1}{2}, \frac{1}{2}]$:

$$\begin{cases} \sigma_{i\alpha,\alpha}^0 + \sigma_{i3,3}^1 = 0 & (62a) \\ \sigma_{ij}^1 = \mathbb{C}_{ijkl} \varepsilon_{kl}^1 & (62b) \\ \varepsilon_{\alpha\beta}^1 = \frac{1}{2} (u_{\alpha,\beta}^1 + u_{\beta,\alpha}^1) = 0, \quad \varepsilon_{\alpha 3}^1 = \frac{1}{2} (u_{\alpha,3}^2 + u_{3,\alpha}^1), \quad \varepsilon_{33}^1 = u_{3,3}^2 = 0 & (62c) \\ \sigma_{i3}^1 (z = \pm \frac{1}{2}) = 0 & (62d) \end{cases}$$

In this auxiliary problem, the displacement field \mathbf{u}^1 (51) and the stress field $\boldsymbol{\sigma}^0$ (53) are local fields which depend linearly on \mathbf{K}^{-1} and U_3^1 . Hence, the displacement field \mathbf{u}^2 solution to the above problem (as well as $\boldsymbol{\varepsilon}^1$ and $\boldsymbol{\sigma}^1$) will be a linear superposition of localization fields which depend on the gradient of those macroscopic fields.

Taking into account the parity properties, the displacement field solution of this problem writes as:

$$\mathbf{u}^2 = \underline{\underline{\mathbf{u}}}^{K\nabla} : (\underline{\underline{\mathbf{K}}}^{-1} \otimes \underline{\underline{\nabla}}_y) - z U_3^1 \otimes \underline{\underline{\nabla}}_y = \begin{pmatrix} -z U_{3,1}^1 + \mathbf{u}_{1\beta\gamma\delta}^{K\nabla} K_{\delta\gamma,\beta}^{-1} \\ -z U_{3,2}^1 + \mathbf{u}_{2\beta\gamma\delta}^{K\nabla} K_{\delta\gamma,\beta}^{-1} \\ 0 \end{pmatrix} \quad (63)$$

where the displacement localization tensor $\underline{\underline{\mathbf{u}}}^{K\nabla}(z)$ related to the curvature gradient writes as:

$$\mathbf{u}_{\alpha\beta\gamma\delta}^{K\nabla} = - \left[\int_{-\frac{1}{2}}^z \left(4 \mathbb{S}_{\alpha 3 \eta 3} \int_{-\frac{1}{2}}^y v \mathbb{C}_{\eta\beta\gamma\delta}^\sigma dv + \delta_{\alpha\beta} \mathbf{u}_{3\gamma\delta}^K \right) dy \right]^* \quad \text{and} \quad \mathbf{u}_{3\beta\gamma\delta}^{K\nabla} = 0 \quad (64)$$

The first order stress writes as:

$$\boldsymbol{\sigma}^1 = \underline{\underline{\mathbf{s}}}^{K\nabla} : (\underline{\underline{\mathbf{K}}}^{-1} \otimes \underline{\underline{\nabla}}_y) \quad (65)$$

where we defined the fifth-order localization tensor $\underline{\underline{\mathfrak{s}}}^{K^\nabla}(z)$ as:

$$\mathfrak{s}_{\alpha\beta\gamma\delta\eta}^{K^\nabla} = 0, \quad \mathfrak{s}_{\alpha\beta\gamma\delta}^{K^\nabla} = - \int_{-\frac{1}{2}}^z y \mathbb{C}_{\alpha\beta\gamma\delta}^\sigma dy \quad \text{and} \quad \mathfrak{s}_{33\beta\gamma\delta}^{K^\nabla} = 0 \quad (66)$$

Hence, this order involves only transverse shear effects.

Note that $U_3^0 = 0$ because of parity considerations and

$$\underline{\underline{\mathfrak{M}}}^1 = \left((z\sigma_{\alpha\beta}^1) \right) = 0 \quad (67)$$

Thus, if we want to capture U_3^1 , we have to go one order higher. However, this will require the derivation of the second gradient of the curvature $\underline{\underline{\mathfrak{K}}}^{-1}$ and consequently the fourth derivative of $U_3^{-1} = 0$ which raises an issue in terms of physical meaning of this variable as well as of numerical implementation.

In contrast, it is remarkable that transverse shear effects are included in the localization field already at this order. Hence we suggest to stop at this order the asymptotic expansion and switch to variational arguments for deriving the Bending-Gradient theory.

Additional Remarks on the Asymptotic Expansion Approach Before going further in the derivation of the Bending-Gradient theory, let us point out some useful remarks regarding the asymptotic expansion procedure.

In the present paper, we performed the asymptotic expansion up to the very next order after the classical homogenization procedure. However, this formalism has already been studied up to “infinite order” in other elasticity problems (see Smyshlyaev and Cherednichenko (2000) for instance) and convergence results were derived (Bakhvalov and Panasenko 1989). Those works show that the fully reconstructed field \mathbf{u} is actually a double sum: a sum over orders, as expected because of the expansion, but also over degrees of derivative of the macroscopic displacement field. This is also the case in the present plate problem. If we gather all the fields derived in the cascade resolution we get the following:

$$\begin{aligned} \mathbf{u} = & \left(\frac{U_3^{-1}}{\eta} + \eta U_3^1 + \eta^3 U_3^3 + \dots \right) \mathbf{e}_3 - z (U_3^{-1} + \eta^2 U_3^1 + \dots) \otimes \underline{\underline{\nabla}}_y \\ & + \eta \left(\underline{\underline{\mathfrak{u}}}^K : (\underline{\underline{\mathfrak{K}}}^{-1} + \eta^2 \underline{\underline{\mathfrak{K}}}^1 + \dots) \right) + \eta^2 \left(\underline{\underline{\mathfrak{u}}}^{K^\nabla} : (\underline{\underline{\mathfrak{K}}}^{-1} \otimes \underline{\underline{\nabla}}_y + \dots) \right) + \dots \end{aligned} \quad (68)$$

Assuming that this double sum converges, it is legitimate to define:

$$U_3 = \sum_{p=-1}^{\infty} \eta^{p+1} U_3^p \quad (69)$$

and rewrite the total displacement field as:

$$\underline{\mathbf{u}} = \frac{U_3}{\eta} \underline{\mathbf{e}}_3 - z U_3 \otimes \underline{\nabla}_y + \eta \underline{\mathbf{u}}^K : \underline{\mathbf{K}} + \eta^2 \underline{\mathbf{u}}^{K\nabla} : \underline{\mathbf{K}} \otimes \underline{\nabla}_y + \dots \quad (70)$$

where $\underline{\mathbf{K}} = U_3 \underline{\nabla}_y \otimes \underline{\nabla}_y$. This was suggested by Boutin (1996) and further justified in Smyshlyaev and Cherednichenko (2000). We have also for the stress field:

$$\underline{\boldsymbol{\sigma}} = \underline{\mathfrak{s}}^K : \underline{\mathbf{K}} + \eta \underline{\mathfrak{s}}^{K\nabla} : \underline{\mathbf{K}} \otimes \underline{\nabla}_y + \dots \quad (71)$$

Hence, it seems that going higher-order in the asymptotic expansion only involves higher gradients of the displacement inside the constitutive equation. However, as already pointed out in these papers, the problem remains ill-posed as it stands here. Some caution must be taken when considering the constitutive equation as well as the boundary conditions if one wants to derive a mathematically sound problem.

First, in order to derive the constitutive equation it seems straightforward to take directly the elastic energy of the infinite order stress or strain (71) and to truncate this energy up to a given order *afterward*. However, this will lead to a non-positive quadratic form and makes the higher-order problem unstable. Hence, as pointed out by Smyshlyaev and Cherednichenko (2000) it is critical to truncate the expansion of the stress or strain *before* taking the related energy to ensure positivity.

Second, whereas the boundary conditions are set at each order in the cascade resolution of the asymptotic expansion (here Eq. (61d) at each order), in the format presented here, it is not possible to make distinction between orders and then the problem is not well-posed anymore. Here, variational tools will enable the derivation of consistent boundary conditions with the choice of macroscopic degrees of freedom.

4 The Bending-Gradient Theory

Keeping in mind the difficulties mentioned regarding the asymptotic expansion, the Bending-Gradient theory is derived as follows. The starting point is the exact balance equation (22) on the bending moment ($M_{\alpha\beta} = \langle \langle z\sigma_{\alpha\beta} \rangle \rangle$). The Bending-Gradient theory is based on the following two main ideas:

The first idea is that the stress field can be accurately approximated by:

$$\underline{\boldsymbol{\sigma}}^{BG} = \underline{\mathfrak{s}}^K : \underline{\boldsymbol{\chi}} + \eta \underline{\mathfrak{s}}^{K\nabla} : \underline{\boldsymbol{\chi}} \otimes \underline{\nabla}_y \quad (72)$$

where $\underline{\boldsymbol{\chi}} = (\chi_{\alpha\beta}) (Y_1, Y_2)$ is an unknown symmetric second-order tensor field.

The second idea is to find the best possible choice of $\underline{\boldsymbol{\chi}}$ by optimizing

$$P^{*3D}(\underline{\boldsymbol{\sigma}}^{BG}) = tL^2 \int_{\omega} \langle w^{*3D}(\underline{\boldsymbol{\sigma}}^{BG}) \rangle d\omega \quad (73)$$

over all $\underline{\chi}$ such that the balance equation on the bending moment \underline{M}^{BG} associated to $\underline{\sigma}^{BG}$ holds true. Actually, we have:

$$\underline{M}^{BG} = \underline{D} : \underline{\chi} \quad \text{where} \quad \underline{D} = \left\langle z^2 \underline{\mathbb{C}}^\sigma \right\rangle \quad \text{and} \quad \underline{d} = \underline{D}^{-1} \quad (74)$$

Its gradient is:

$$\underline{R} = \underline{M}^{BG} \otimes \underline{\nabla}_y \quad \text{or} \quad R_{\alpha\beta\gamma} = M_{\alpha\beta,\gamma}^{BG} \quad \text{with} \quad R_{\alpha\beta\gamma} = R_{\beta\alpha\gamma} \quad (75)$$

It is possible to rewrite $\underline{\sigma}^{BG}$ in terms of \underline{M}^{BG} and \underline{R} :

$$\underline{\sigma}^{BG} = \underline{\mathbb{S}}^K : \left(\underline{d} : \underline{M}^{BG} \right) + \eta \underline{\mathbb{S}}^{K\nabla} : \left(\underline{d} : \underline{M}^{BG} \right) \otimes \underline{\nabla}_y \quad (76)$$

and

$$\underline{\sigma}^{BG} = \underline{\mathbb{S}}^M : \underline{M}^{BG} + \eta \underline{\mathbb{S}}^R : \underline{R} \quad (77)$$

where the localizations tensors are given by:

$$\underline{\mathbb{S}}^M = \underline{\mathbb{S}}^K : \underline{d}, \quad \underline{\mathbb{S}}^R = \underline{\mathbb{S}}^{K\nabla} : \underline{d} \quad (78)$$

It is easy to check that if \underline{M}^{BG} satisfies balance equation (22), then the stress field $\underline{\sigma}^{BG}$ defined by (77) will satisfy the 3D equilibrium equation (15), as well as the $z = \pm 1/2$ face boundary conditions, up to the order η^1 . Hence, even if the set of such $\underline{\sigma}^{BG}$ does not define properly a restriction of SC^{3D} , it remains a good approximation in the sense of the asymptotic expansion. Let us introduce the following set of statically compatible fields for the Bending-Gradient theory:

$$SC^{BG} : \begin{cases} \underline{R} = \underline{M}^{BG} \otimes \underline{\nabla}_y \quad \text{or} \quad R_{\alpha\beta\gamma} = M_{\alpha\beta,\gamma}^{BG} & (79a) \\ \left(\underline{i} : \underline{R} \right) \cdot \underline{\nabla}_y + F_3 = 0 \quad \text{or} \quad R_{\alpha\beta\beta,\alpha} + F_3 = 0 & (79b) \end{cases}$$

where the shear forces were substituted and we used the following relation:

$$\underline{i} : \underline{R} = \underline{M}^{BG} \cdot \underline{\nabla}_y = \underline{Q}^{BG} \quad \text{or} \quad R_{\alpha\beta\beta} = M_{\alpha\beta,\beta}^{BG} = Q_\alpha^{BG} \quad (80)$$

where $i_{\alpha\beta\gamma\delta} = \frac{1}{2} (\delta_{\alpha\gamma}\delta_{\beta\delta} + \delta_{\alpha\delta}\delta_{\beta\gamma})$ is the identity for in-plane fourth-order tensors following the symmetries of linear elasticity.

Plugging $\underline{\sigma}^{BG}$ into the complementary energy of the full 3D problem leads to the following functional:

$$P^{*BG}(\underline{M}^{BG}, \underline{R}) = \int_{\omega} w^{*KL}(\underline{M}^{BG}) + \eta^2 w^{*BG}(\underline{R}) d\omega \quad (81)$$

where the stress elastic energies are defined as:

$$w^{*KL}(\underline{\underline{\mathbf{M}}}^{BG}) = \frac{1}{2} \underline{\underline{\mathbf{M}}}^{BG} : \underline{\underline{\mathbf{d}}} : \underline{\underline{\mathbf{M}}}^{BG} \quad \text{and} \quad w^{*BG}(\underline{\underline{\mathbf{R}}}) = \frac{1}{2} {}^T \underline{\underline{\mathbf{R}}} : \underline{\underline{\mathbf{h}}} : \underline{\underline{\mathbf{R}}} \quad (82)$$

with:

$$\underline{\underline{\mathbf{h}}} = \left\langle {}^T \underline{\underline{\mathbf{s}}}^R : \underline{\underline{\mathbf{s}}} : \underline{\underline{\mathbf{s}}}^R \right\rangle \quad (83)$$

This sixth-order tensor is the compliance related to the transverse shear of the plate. It is strictly identical to the one derived in Lebée and Sab (2011a). Let us recall here that it is positive, symmetric, but not definite in the general case. More details about $\underline{\underline{\mathbf{h}}}$ properties were discussed in Lebée and Sab (2011a).

NB: There is no uncoupling in the complementary energy (81) between $\underline{\underline{\mathbf{M}}}^{BG}$ and $\underline{\underline{\mathbf{R}}}$ because of the monoclinic symmetry of the local constitutive equation. In the auxiliary problems, this symmetry enforces the localization related to $\underline{\underline{\mathbf{M}}}$ to be purely in-plane and the one related to $\underline{\underline{\mathbf{R}}}$ to be pure transverse shear. Hence the cross terms in the 3D elastic energy vanish.

Now we define the generalized strains as:

$$\underline{\underline{\chi}} = \frac{\partial w^{*KL}}{\partial \underline{\underline{\mathbf{M}}}^{BG}} \quad \text{and} \quad \underline{\underline{\Gamma}} = \frac{\partial w^{*BG}}{\partial \underline{\underline{\mathbf{R}}}} \quad (84)$$

which leads to the following constitutive equations:

$$\left\{ \begin{array}{l} \underline{\underline{\chi}} = \underline{\underline{\mathbf{d}}} : \underline{\underline{\mathbf{M}}}^{BG} \\ \underline{\underline{\Gamma}} = \underline{\underline{\mathbf{h}}} : \underline{\underline{\mathbf{R}}} \end{array} \right. \quad (85a)$$

$$\quad (85b)$$

Introducing respectively $\Phi_{\alpha\beta\gamma}$, U_3^{BG} as Lagrange multipliers of Eqs. (79a), (79b) and taking the variations with respect to the static variables leads to the following definition for the strains:

$$KC^{BG} : \left\{ \begin{array}{l} \underline{\underline{\chi}} = \underline{\underline{\Phi}} \cdot \underline{\underline{\nabla}}_y \\ \eta^2 \underline{\underline{\Gamma}} = \underline{\underline{\Phi}} + \underline{\underline{\mathbf{i}}} \cdot \underline{\underline{\nabla}}_y U_3^{BG} \end{array} \right. \quad (86a)$$

$$\quad (86b)$$

where both $\underline{\underline{\Phi}}$ and $\underline{\underline{\Gamma}}$ are third-order tensors which follows the same index symmetry as $\underline{\underline{\mathbf{R}}}$. Setting $\eta^2 = 0$ in those definitions leads exactly to Kirchhoff-Love strains. Hence, the Bending-Gradient curvature is slightly different from the one of the asymptotic expansion and Eq. (86a) rewrites:

$$\underline{\underline{\chi}} = \underline{\underline{\mathbf{K}}}^{BG} + \eta^2 \underline{\underline{\Gamma}} \cdot \underline{\underline{\nabla}}_y \quad \text{where} \quad \underline{\underline{\mathbf{K}}}^{BG} = -U_3^{BG} \underline{\underline{\nabla}}_y \otimes \underline{\underline{\nabla}}_y \quad (87)$$

Namely it is the sum of the conventional curvature and a small correction term which relaxes this compatibility relation.

Considering the variations of the Lagrangian on the edges leads also to the following clamped boundary conditions:

$$U_3^{BG} = 0 \quad \text{and} \quad \underline{\Phi} \cdot \underline{n} = 0 \quad \text{on} \quad \partial\omega \quad (88)$$

Finally we have a well-posed plate theory.

Once the exact solution of the macroscopic problem is derived, it is possible to reconstruct the local displacement field. We suggest the following 3D displacement field where U_3^{BG} , $\underline{\Phi}$ are the fields solution of the plate problem:

$$\underline{u}^{BG} = \frac{U_3^{BG}}{\eta} \underline{e}_3 - z U_3^{BG} \otimes \underline{\nabla}_y + \eta \underline{u}^K : \underline{\chi} + \eta^2 \underline{u}^{K\nabla} : \left(\underline{\chi} \otimes \underline{\nabla}_y \right) \quad (89)$$

Defining the strain as

$$\underline{\varepsilon}^{BG} = \underline{\mathbb{S}} : \underline{\sigma}^{BG} \quad (90)$$

it is possible to check that:

$$\varepsilon \left(\underline{u}^{BG} \right)_{(Y,z)} - \underline{\varepsilon}^{BG} = \eta^2 \left(\left(\underline{\delta} \otimes^s \underline{u}^{K\nabla} \right) :: \left(\underline{\chi} \otimes \underline{\nabla}_y^2 \right) + z \underline{\Gamma} \cdot \underline{\nabla}_y \right) \quad (91)$$

which shows that the compatibility equation between the reconstructed displacement field \underline{u}^{BG} and strain localization $\underline{\varepsilon}^{BG}$ is satisfied up to the η^2 order.

The Original Work of Reissner for Homogeneous Plates Originally, Reissner started from the assumption that the in-plane stress distribution related to the bending moment is linearly distributed through the thickness for a homogeneous and isotropic plate. Then, integrating successively the in-plane and the out of plane equilibrium equations he built a statically admissible 3D stress field. It turns out that this field has exactly the form of $\underline{\sigma}^{BG}$ except for the σ_{33} component.

Indeed, for a homogeneous plate, we have¹: $\underline{D}' = \frac{1}{12} \underline{\mathbb{C}}^\sigma$. Hence, we have:

$$\underline{\sigma}^{BG} = \begin{cases} \sigma_{\alpha\beta}^{BG} = z \mathbb{C}_{\alpha\beta\gamma\delta}^\sigma \chi_{\delta\gamma} = 12z M_{\alpha\beta}^{BG} \\ \sigma_{\alpha 3}^{BG} = -\eta \int_{-\frac{1}{2}}^z y \mathbb{C}_{\alpha\beta\gamma\delta}^\sigma dy \chi_{\delta\gamma,\beta} = \eta \frac{3}{2} (1 - 4z^2) Q_\alpha^{BG} \\ \sigma_{33}^{BG} = 0 \end{cases} \quad (92)$$

which is a function of \underline{M}^{BG} and $\underline{Q}^{BG} = \underline{i} : \underline{R}$ instead of the whole \underline{R} . In the above expression, the equilibrium equation (79b) were used to define the shear forces as:

¹ $\underline{D}' = \frac{t^3}{12} \underline{\mathbb{C}}^{t,\sigma}$ in physical variables.

$\underline{Q}_{\alpha}^{BG} = M_{\alpha\beta,\beta}^{BG}$. It should be mentioned that in its original work, Reissner used the following expression $\sigma_{33} = \eta^2 \frac{3z}{2} \left(1 - \frac{4z^2}{3}\right) F_3$ for the out-of-plane traction instead of $\sigma_{33}^{BG} = 0$ in order to ensure the statical compatibility of the stress field. Therefore, $\underline{\sigma}^{BG}$ coincides with the stress proposed by Reissner up to the first order in η . Moreover, since shear stresses are only functions of shear forces when the plate is homogeneous, then the Bending-Gradient part of the stress elastic energy is actually a quadratic form of these shear forces:

$$w^{*BG}(\underline{\mathbf{R}}) = \frac{1}{2} {}^T \underline{\mathbf{R}} : \underline{\mathbf{h}} : \underline{\mathbf{R}} = \frac{1}{2} \underline{\mathbf{Q}}^{BG} \cdot \underline{\mathbf{h}}^{RM} \cdot \underline{\mathbf{Q}}^{BG} \quad (93)$$

with:

$$\underline{\mathbf{h}} = \underline{\mathbf{i}} \cdot \underline{\mathbf{h}}^{RM} \cdot \underline{\mathbf{i}} \quad (94)$$

and

$$h_{\alpha\beta}^{RM} = \frac{6}{5} \mathbb{S}_{\alpha 3 \beta 3} \quad (95)$$

is Reissner's shear forces stiffness (when the plate is isotropic one retrieve: $h_{\alpha\beta}^{RM} = \frac{6}{5G} \delta_{\alpha\beta}$ with G the shear modulus).

Inserting the above expression for $\underline{\mathbf{h}}$ in the constitutive equation (85b) gives:

$$\underline{\mathbf{\Gamma}} = \underline{\mathbf{h}} : \underline{\mathbf{R}} = \underline{\mathbf{i}} \cdot \underline{\mathbf{\gamma}} \quad (96)$$

with

$$\underline{\mathbf{\gamma}} = \underline{\mathbf{h}} \cdot \underline{\mathbf{Q}}^{BG} \quad (97)$$

Using the kinematic compatibility (86b), we find that $\underline{\mathbf{\Phi}}$ is also of the form:

$$\underline{\mathbf{\Phi}} = \underline{\mathbf{i}} \cdot \underline{\varphi} \quad (98)$$

where $\underline{\varphi}$ is the classical rotation vector of the Reissner theory.

In summary, when the plate is homogeneous and according to the Bending-Gradient theory, the kinematic unknowns are U_3^{BG} and $\underline{\varphi}$, the generalized strains and the constitutive equations are:

$$\begin{cases} \underline{\mathbf{\chi}} &= \underline{\varphi} \otimes^s \underline{\nabla}_y &= \underline{\mathbf{d}} : \underline{\mathbf{M}}^{BG} \\ \eta^2 \underline{\mathbf{\gamma}} &= \underline{\varphi} + U_3^{BG} \otimes \underline{\nabla}_y &= \eta^2 \underline{\mathbf{h}} \cdot \underline{\mathbf{Q}}^{BG} \end{cases} \quad (99)$$

and finally, the balance equations are:

$$\begin{cases} \underline{\underline{M}}^{BG} \cdot \underline{\underline{\nabla}}_y - \underline{\underline{Q}}^{BG} = 0 & \text{on } \omega \\ \underline{\underline{Q}}^{BG} \cdot \underline{\underline{\nabla}}_y + F_3 = 0 & \text{on } \omega \end{cases} \quad \begin{matrix} (100a) \\ (100b) \end{matrix}$$

This means that the Bending-Gradient theory completely coincides for homogeneous plates with the Reissner-Mindlin model. It is interesting to note that the Reissner-Mindlin curvature may be rewritten as the sum of the geometrically exact curvature and a correction term related to transverse shear effects which relaxes Kirchhoff-Love theory compatibility equation:

$$\underline{\underline{\chi}} = -U_3^{BG} \underline{\underline{\nabla}}_y \otimes \underline{\underline{\nabla}}_y + \eta^2 \underline{\underline{\gamma}} \otimes \underline{\underline{\nabla}}_y \quad (101)$$

In summary, we derived a plate model which enables the full description of local 3D fields ($\underline{\underline{u}}^{BG}$, $\underline{\underline{\varepsilon}}^{BG}$ and $\underline{\underline{\sigma}}^{BG}$) including the effects of transverse shear. Compared to the classical theory from Reissner (1945), we just add four macroscopic variables included into the generalized rotation $\underline{\underline{\Phi}}$ and which are related to transverse shear warping. Contrary to the asymptotic expansions approach or the approach suggested in Smyshlyaev and Cherednichenko (2000), our theory does not require the derivation of the first or even the second gradient of the curvature. Actually, when looking at the definition of strains in Eq. (86), only the first derivatives of U_3^{BG} and $\underline{\underline{\Phi}}$ are involved. Having low-order interpolation is a serious advantage compared to “strain-gradient-like” approaches given in Lewiński (1991), Smyshlyaev and Cherednichenko (2000).

Now, let us recall that the derivation of the Bending-Gradient theory through asymptotic expansions was purely formal. The small parameter η was essentially used for discriminating between orders. More precisely, the 3D local fields chosen for the Bending-Gradient theory satisfy the 3D compatibility equation and the 3D equilibrium equation one order higher than the Kirchhoff-Love fields. However, this is not a proof of convergence even if the good results in Lebée and Sab (2011b) are clearly encouraging. Especially, it is broadly acknowledged that the boundary have a critical role on that matter when going in higher orders. This question raises already with asymptotic expansions: it was demonstrated that the approximation which is derived in the bulk is not compatible with the actual 3D boundary condition and can only be fulfilled weakly (see Berdichevsky (1979), Buannic and Cartraud (2001a, b) for a clear illustration in the case of beams). In the case of the Bending-Gradient theory the boundary conditions are different from the asymptotic expansions and requires further analysis which is out of the scope of this lecture.

5 Application of the Bending-Gradient Theory to Laminates

The purpose of this Section is to derive closed-form solutions for the Bending-Gradient model in the case of cylindrical bending and compare them to the exact solutions from Pagano (1969, 1970a, b). In what follows, for simplicity, we drop the exponent term BG in the notation of the mechanical fields of the Bending-Gradient model.

5.1 Voigt Notations

In this subsection, we introduce Voigt notation in order to turn contraction products into conventional matrix products. Brackets $[\bullet]$ are used to denote that a tensor is considered in a matrix form. Thus $[\bullet]$ is a linear operator, reallocating tensor components.

For instance, the bending moment is reallocated in a vector form:

$$[\underline{\mathbf{M}}] = \begin{pmatrix} M_{11} \\ M_{22} \\ \sqrt{2}M_{12} \end{pmatrix} \quad (102)$$

as well as $\underline{\chi}$, and the fourth-order compliance tensor $\underline{\underline{\mathbf{d}}}$ is reallocated in a matrix form so that constitutive equation (85a) becomes a vector-matrix product:

$$[\underline{\underline{\mathbf{d}}}] = \begin{pmatrix} d_{1111} & d_{2211} & \sqrt{2}d_{1211} \\ d_{2211} & d_{2222} & \sqrt{2}d_{1222} \\ \sqrt{2}d_{1211} & \sqrt{2}d_{1222} & 2d_{1212} \end{pmatrix} \quad (103)$$

as well as the stiffness tensor $\underline{\underline{\mathbf{D}}}$. This is also done to the plane-stress stiffness tensor $\underline{\underline{\mathbf{C}}}^\sigma$.

The same procedure is applied to shear variables and the corresponding constitutive equation. Shear static unknowns are reallocated in a vector form,

$$[\underline{\mathbf{R}}] = \begin{pmatrix} R_{111} \\ R_{221} \\ \sqrt{2}R_{121} \\ R_{112} \\ R_{222} \\ \sqrt{2}R_{122} \end{pmatrix} \quad (104)$$

as well as $\underline{\Gamma}$ and $\underline{\Phi}$; and the constitutive sixth-order tensor is turned into a 6×6 matrix:

$$\left[\underline{\underline{h}} \right] = \begin{pmatrix} h_{111111} & h_{111122} & \sqrt{2}h_{111121} & h_{111211} & h_{111222} & \sqrt{2}h_{111221} \\ h_{221111} & h_{221122} & \sqrt{2}h_{221121} & h_{221211} & h_{221222} & \sqrt{2}h_{221221} \\ \sqrt{2}h_{121111} & \sqrt{2}h_{121122} & 2h_{121121} & \sqrt{2}h_{121211} & \sqrt{2}h_{121222} & 2h_{121221} \\ h_{112111} & h_{112122} & \sqrt{2}h_{112121} & h_{112211} & h_{112222} & \sqrt{2}h_{112221} \\ h_{222111} & h_{222122} & \sqrt{2}h_{222121} & h_{222211} & h_{222222} & \sqrt{2}h_{222221} \\ \sqrt{2}h_{122111} & \sqrt{2}h_{122122} & 2h_{122121} & \sqrt{2}h_{122211} & \sqrt{2}h_{122222} & 2h_{122221} \end{pmatrix} \quad (105)$$

Finally, when using Voigt matrices components, the same typeface is used. The number of indexes indicates unambiguously whether it is the tensor component or the matrix component: h_{222221} is the tensor component of $\underline{\underline{h}}$ and $h_{56} = \sqrt{2}h_{222221}$ is the matrix component of $\left[\underline{\underline{h}} \right]$.

5.2 Closed-Form Solution for Pagano’s Configuration

Pagano (1969) gives an exact solution for cylindrical bending of simply supported composite laminates. We choose the same configuration for the Bending-Gradient model. The plate is invariant and infinite in x_2 direction. The span is $L = 1$. Hence, $Y_\alpha = x_\alpha$ and η coincides with the plate’s thickness t . The plate is out-of-plane loaded with $F_3(x_1) = -F_0 \sin \kappa x_1$ in (12) where $\lambda = 1/\kappa = \frac{L}{n\pi}$, $n \in \mathbb{N}^{+*}$ is the wavelength of the loading (Fig. 2).

The plate is simply supported at $x_1 = 0$ and $x_1 = L$ with traction free edges:

$$U_3(0) = 0, \quad U_3(L) = 0, \quad \underline{\underline{M}}(0) = \underline{\underline{0}}, \quad \underline{\underline{M}}(L) = \underline{\underline{0}}. \quad (106)$$

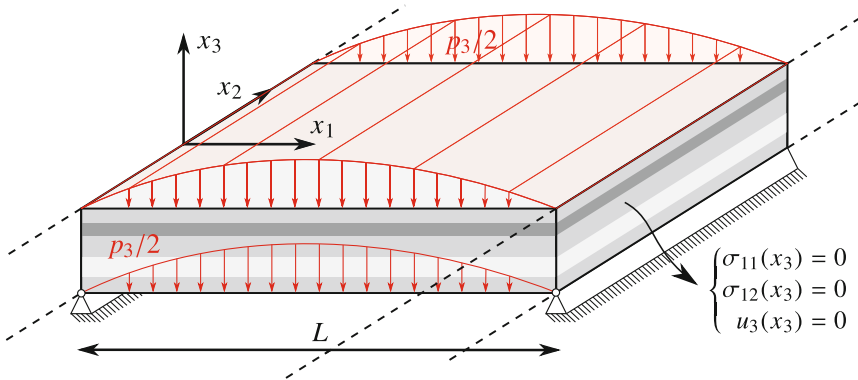


Fig. 2 Laminated plate configuration for Pagano’s cylindrical bending exact solution

In these boundary conditions, $M_{22}(0) = M_{22}(L) = 0$ is the additional boundary condition compared to the Reissner-Mindlin plate model. This boundary condition is very similar to the one which applies to the bimoment on a free subsection in Vlasov (1961) beam theory. This additional boundary condition takes into account free edge effects similar to those described in Lebée and Sab (2010) for periodically layered laminate.

The solution is obtained as follows: First, the x_2 -invariance leads to several simplifications and some unknowns vanish. Second, relevant equations and unknowns are gathered into a differential system and the closed-form solution is derived.

Curvatures Curvatures are defined by Eq. (86a): $\chi_{\alpha\beta} = \Phi_{\alpha\beta\gamma,\gamma}$. Taking into account x_2 invariance leads to:

$$\begin{bmatrix} \chi \\ \approx \end{bmatrix} = \begin{pmatrix} \chi_{11} \\ \chi_{22} \\ \sqrt{2}\chi_{12} \end{pmatrix} = \begin{pmatrix} \Phi_{111,1} \\ \Phi_{221,1} \\ \sqrt{2}\Phi_{121,1} \end{pmatrix} = \begin{pmatrix} \Phi_{1,1} \\ \Phi_{2,1} \\ \Phi_{3,1} \end{pmatrix} \quad (107)$$

Bending Constitutive Equation Bending constitutive Eqs. (85a) are written with Voigt notation as:

$$\begin{bmatrix} \chi \\ \approx \end{bmatrix} = \begin{bmatrix} d \\ \approx \end{bmatrix} \cdot \begin{bmatrix} M \\ \approx \end{bmatrix} \quad (108)$$

Equilibrium The x_2 invariance in the bending gradient equilibrium equation (79a) enforces:

$$\begin{pmatrix} R_1 \\ R_2 \\ R_3 \\ R_4 \\ R_5 \\ R_6 \end{pmatrix} = \begin{pmatrix} M_{11,1} \\ M_{22,1} \\ \sqrt{2}M_{12,1} \\ 0 \\ 0 \\ 0 \end{pmatrix} \quad (109)$$

and transverse loading equilibrium equation (79b) becomes:

$$M_{11,11} = -F_3(x_1) \quad (110)$$

Shear Constitutive Equation Taking into account $R_4 = R_5 = R_6 = 0$, $U_{3,2} = 0$ and generalized shear strain definition (86b), Shear constitutive equation (85b) is rewritten in two parts.

A first part with unknowns involving active boundary conditions:

$$\begin{pmatrix} \Phi_1 \\ \Phi_2 \\ \Phi_3 \end{pmatrix} = \eta^2 \begin{pmatrix} h_{11} & h_{12} & h_{13} \\ h_{12} & h_{22} & h_{23} \\ h_{13} & h_{23} & h_{33} \end{pmatrix} \cdot \begin{pmatrix} M_{11,1} \\ M_{22,1} \\ \sqrt{2}M_{12,1} \end{pmatrix} - \begin{pmatrix} U_{3,1} \\ 0 \\ 0 \end{pmatrix} \quad (111)$$

and a second part which enables the derivation of Φ_4 , Φ_5 , Φ_6 on which no boundary condition applies:

$$\begin{pmatrix} \Phi_4 \\ \Phi_5 \\ \Phi_6 \end{pmatrix} = \eta^2 \begin{pmatrix} h_{41} & h_{42} & h_{43} \\ h_{51} & h_{52} & h_{53} \\ h_{61} & h_{62} & h_{63} \end{pmatrix} \cdot \begin{pmatrix} M_{11,1} \\ M_{22,1} \\ \sqrt{2}M_{12,1} \end{pmatrix} - \begin{pmatrix} 0 \\ 0 \\ U_{3,1}/\sqrt{2} \end{pmatrix} \quad (112)$$

Final System Finally, combining Eqs. (106), (107), (110) and (111), leads to the following set of equations which fully determines the problem:

$$\begin{cases} M_{11,11} = F_0 \sin \kappa x_1 & (113a) \\ \left[\underset{\approx}{\mathbf{d}} \right] \cdot \left[\underset{\approx}{\mathbf{M}} \right] - \eta^2 \hat{\mathbf{h}} \cdot \left[\underset{\approx}{\mathbf{M}} \right]_{,11} = \begin{pmatrix} U_{3,11} \\ 0 \\ 0 \end{pmatrix} & (113b) \\ \left[\underset{\approx}{\mathbf{M}} \right] = 0 \text{ for } x_1 = 0 \text{ and } x_1 = L & (113c) \\ U_3 = 0 \text{ for } x_1 = 0 \text{ and } x_1 = L & (113d) \end{cases}$$

where for convenience, $\hat{\mathbf{h}}$ is the 3×3 submatrix of $\left[\underset{\approx}{\mathbf{h}} \right]$:

$$\hat{\mathbf{h}} = \begin{pmatrix} h_{11} & h_{12} & h_{13} \\ h_{12} & h_{22} & h_{23} \\ h_{13} & h_{23} & h_{33} \end{pmatrix}$$

Once $\left[\underset{\approx}{\mathbf{M}} \right]$ is derived, the non-zero unknowns are derived using Eqs. (109) and (112).

Solution Since $\hat{\mathbf{h}}$ is positive and $\left[\underset{\approx}{\mathbf{d}} \right]$ is positive definite, the differential system (113) is well-posed and the solution is the sum of a particular solution and hyperbolic solutions of the homogeneous equation. Boundary conditions applied to $\underset{\approx}{\mathbf{M}}$ vanish hyperbolic solutions. There remains the particular solution:

$$\left[\underset{\approx}{\mathbf{M}} \right] = \begin{pmatrix} -1 \\ \underset{\approx}{\mathbf{g}}^{-1} \cdot \underset{\approx}{\mathbf{g}} \end{pmatrix} F_0 \lambda^2 \sin \kappa x_1 \quad \text{and} \quad U_3 = -F_0 \lambda^4 \left(g_{11} - {}^t \underset{\approx}{\mathbf{g}} \cdot \underset{\approx}{\mathbf{g}}^{-1} \cdot \underset{\approx}{\mathbf{g}} \right) \sin \kappa x_1 \quad (114)$$

where

$$\underset{\approx}{\hat{\mathbf{g}}} = \left[\underset{\approx}{\mathbf{d}} \right] + \kappa^2 \eta^2 \hat{\mathbf{f}}, \quad \underset{\approx}{\hat{\mathbf{g}}} = \begin{pmatrix} \hat{g}_{22} & \hat{g}_{23} \\ \hat{g}_{23} & \hat{g}_{33} \end{pmatrix}, \quad \underset{\approx}{\mathbf{g}} = \begin{pmatrix} \hat{g}_{12} \\ \hat{g}_{13} \end{pmatrix}. \quad (115)$$

The matrix $\underset{\approx}{\hat{\mathbf{g}}}$ appears to be the effective flexural stiffness for cylindrical bending, corrected with shear effects. When $\kappa \eta \rightarrow 0$, $\underset{\approx}{\hat{\mathbf{g}}} = \left[\underset{\approx}{\mathbf{d}} \right]$ which yields exactly the Kirchhoff-Love solution.

Localization Once the generalized stresses are derived, it is possible to reconstruct local 3D fields, using Eqs. (77), (90) and (89).

5.3 Numerical Applications

Plate Configuration We consider angle-ply laminates. Each ply is made of unidirectional fiber-reinforced material oriented at θ relative to the bending direction x_1 . All plies have the same thickness and are perfectly bounded. A laminate is denoted between brackets by the successive ply-orientations along the thickness. For instance $[0^\circ, 90^\circ]$ denotes a 2-ply laminate where the lower ply fibers are oriented in the bending direction. When the laminate follows mirror symmetry, only half of the stack is given and the subscript s is added. Thus $[30^\circ, -30^\circ]_s$ means $[30^\circ, -30^\circ, -30^\circ, 30^\circ]$.

The constitutive behavior of a ply is assumed to be transversely isotropic along the direction of the fibers and engineering constants are chosen similar to those of Pagano (1969):

$$E_L = 25 \times 10^6 \text{ psi}, \quad E_T = E_N = 1 \times 10^6 \text{ psi}, \quad G_{LT} = G_{LN} = 0.5 \times 10^6 \text{ psi},$$

$$G_{NT} = \frac{E_T}{2(1 + \nu_{NT})} = 0.4 \times 10^6 \text{ psi}, \quad \nu_{LT} = \nu_{LN} = \nu_{NT} = 0.25$$

where G_{NT} has been changed to preserve transversely isotropic symmetry. L is the longitudinal direction oriented in the (x_1, x_2) plane at θ with respect to \underline{e}_1 , T is the transverse direction and N is the normal direction coinciding with \underline{e}_3 .

Localization Fields Shear forces are related to the bending gradient as follows: $Q_1 = R_{111} + R_{122}$ and $Q_2 = R_{121} + R_{222}$. Thus we suggest the following signification for the bending gradient components:

$R_{111} - R_1$: Cylindrical Bending part of Q_1

$R_{221} - R_2$: Pure warping

$R_{121} - R_3$: Torsional part of Q_2

$R_{112} - R_4$: Pure warping

$R_{222} - R_5$: Cylindrical Bending part of Q_2

$R_{122} - R_6$: Torsional part of Q_1

In Fig. 3 are plotted localization shear stress distributions corresponding to each components of \mathbf{R} in both directions for a quasi-isotropic laminate $[0^\circ, -45^\circ, 90^\circ, 45^\circ]_s$. All stress distributions are continuous and fulfill traction free boundary conditions on the upper and lower faces of the plate. For each direction there are four self-equilibrated stress distribution ($\langle \sigma_{\alpha 3} \rangle = 0$) associated to R_2, R_3, R_4 and R_5 for Direction 1 and R_1, R_2, R_4 and R_6 for Direction 2. This explains the suggested signification for shear variables. We draw the reader's attention to the fact that, even if there are self-equilibrated stress distributions, all distributions have comparable amplitude and none can be neglected at this stage. Moreover, it is clear that torsion generates different distributions than pure cylindrical bending, except in the homogeneous case.

Results In Fig. 4 are plotted the transverse distributions of all stress fields for the exact solution from Pagano, the Kirchhoff-Love and the Bending-Gradient solutions

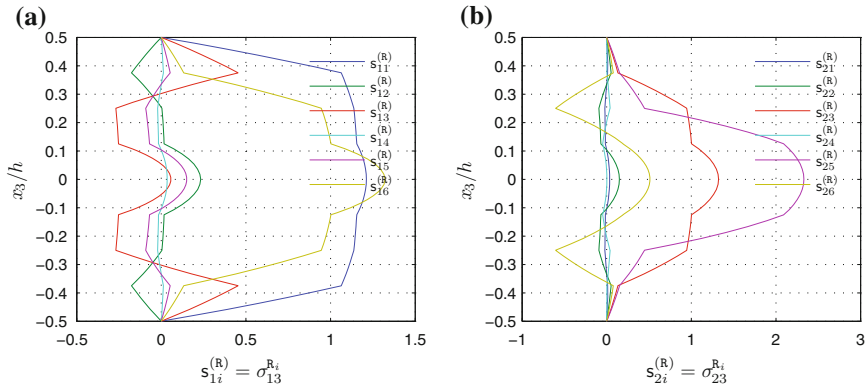


Fig. 3 Localization transverse shear distributions for each component of the bending gradient

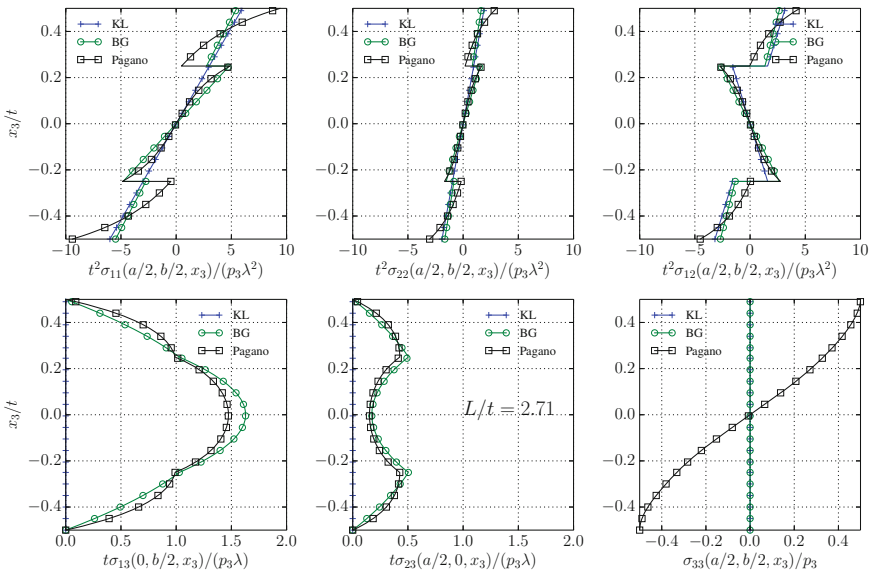


Fig. 4 Comparison of stress distributions under cylindrical bending for a $[-30^\circ, 30^\circ]_s$ ply and $L/t = 2.71$

after relocation. The ply under consideration is a $[-30^\circ, 30^\circ]_s$ for a slenderness $L/t = 2.71$. Even for this very low slenderness, the field reconstruction is quite good for the Bending-Gradient theory. The Kirchhoff-Love theory gives also a good estimate of in-plane stress field but does not enable the reconstruction of transverse shear stress. In Fig. 5 are plotted the transverse distributions of the displacement fields for the same configuration. The out-of plane deflection of the Bending-Gradient theory matches already extremely well the exact one whereas the Kirchhoff-Love deflection is not large enough. This because transverse shear effects are not included

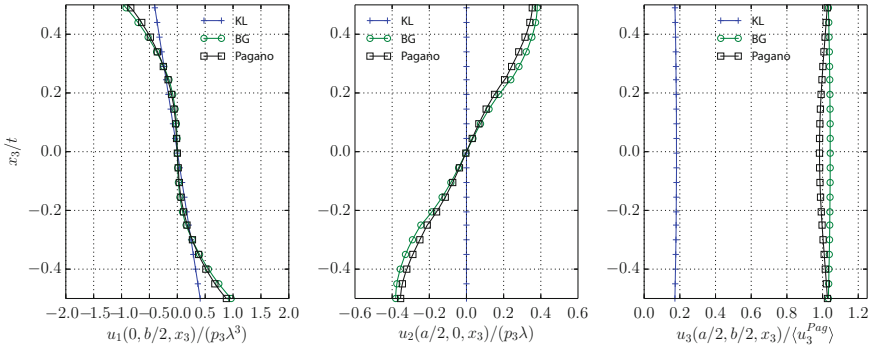


Fig. 5 Comparison of displacement distributions under cylindrical bending for a $[-30^\circ, 30^\circ]_s$ ply and $L/t = 2.71$

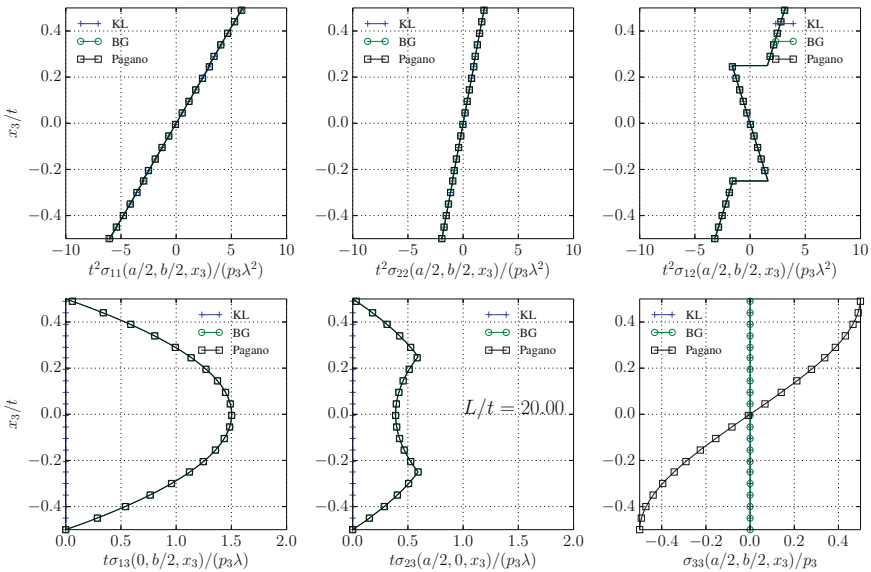


Fig. 6 Comparison of stress distributions under cylindrical bending for a $[-30^\circ, 30^\circ]_s$ ply and $L/t = 20$

in this theory whereas they are dominating for such slenderness. The displacement u_1 illustrate clearly the “rotation of the section”. For Kirchhoff-Love section remains straight whereas shear warping is allowed with the Bending-Gradient model. Because the plate is not orthotropic, there is also a displacement in Direction 2.

In Figs. 6 and 7, the slenderness was simply turned to $L/t = 20$. One can clearly observe the convergence of the fields between the exact and the approximated solutions. However, even at this rather larger slenderness, the Kirchhoff-Love deflection is still to stiff (about 8%) compared to the Bending-Gradient deflection.

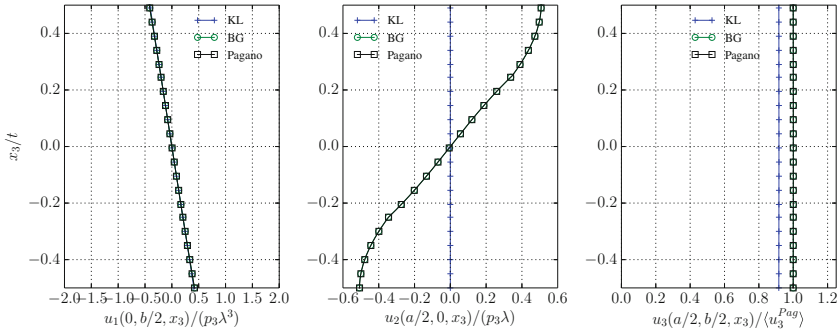


Fig. 7 Comparison of displacement distributions under cylindrical bending for a $[-30^\circ, 30^\circ]_s$ ply and $L/t = 20$

Distance Between the Reissner-Mindlin and the Bending-Gradient Model We introduce the relative distance between the Bending-Gradient model and a Reissner-Mindlin model, $\Delta^{RM/BG}$:

$$\Delta^{RM/BG} = \frac{\|\underline{\underline{\mathbf{h}}}^W\|}{\|\underline{\underline{\mathbf{h}}}\|} \quad (116)$$

where

$$\|\underline{\underline{\mathbf{h}}}\| = \sqrt{{}^T[\underline{\underline{\mathbf{h}}}] : [\underline{\underline{\mathbf{h}}]}} \quad (117)$$

is the norm for Bending-Gradient compliance tensors and $\underline{\underline{\mathbf{h}}}^W$ is the pure warping part of $\underline{\underline{\mathbf{h}}}$:

$$[\underline{\underline{\mathbf{h}}}]^W = [\underline{\underline{\mathbf{h}}}] - \frac{4}{9} {}^T[\underline{\underline{\mathbf{i}}}] \cdot [\underline{\underline{\mathbf{i}}}] \cdot [\underline{\underline{\mathbf{h}}}] \cdot {}^T[\underline{\underline{\mathbf{i}}}] \cdot [\underline{\underline{\mathbf{i}}}] \quad (118)$$

$\Delta^{RM/BG}$ gives an estimate of the pure warping fraction of the shear stress energy. When the plate constitutive equation is restricted to a Reissner-Mindlin one we have exactly $\Delta^{RM/BG} = 0$.

In Table 1, are given the values of $\Delta^{RM/BG}$ for the laminates considered in this work. For a single ply, the criterion is zero since we demonstrated that the Bending-Gradient model is exactly a Reissner-Mindlin model in this case. However, when there are several plies, the distance can be greater than 10%. Thus with these laminates, the shear constitutive equation cannot be reduced to a Reissner-Mindlin behavior.

Table 1 The criterion $\Delta^{RM/BG}$ for several laminates

Stack	$[0^\circ]$	$[30^\circ, -30^\circ]_s$	$[0^\circ, -45^\circ, 90^\circ, 45^\circ]_s$
$\Delta^{RM/BG}$	0	16.0 %	12.4 %

6 Periodic Plates

The derivation of the Bending-Gradient plate model can be extended to periodic plates. For these plates, the 3D problem is still the same but the fourth-order elasticity tensor is now a function of $\mathbf{x} = (x_1, x_2, x_3)$ which is periodic in the two first coordinates (x_1, x_2) (Fig. 8). It is assumed that the in-plane size of the period is comparable to its thickness, t , and that t is small with respect to L , the typical length of the in-plane variables (the span of the plate and the wavelength of the loadings). The change of variable $Y_\alpha = L^{-1}x_\alpha$ where $Y_\alpha \in \omega$ is still the same for the macroscopic global (in-plane) variables. Moreover, we introduce the microscopic local variables as $\underline{\mathbf{z}} = (z_1, z_2, z_3) = t^{-1}\mathbf{x} = (t^{-1}x_1, t^{-1}x_2, t^{-1}x_3)$. The normalized unit cell is noted Z , the small parameter of the asymptotic expansion is still $\eta = t/L$ and the external loading is still given by (61d).

Based on this change of variables, the fourth-order elasticity tensor can be rewritten as:

$$\underset{\approx}{\mathbb{C}}^t(\mathbf{x}) = \underset{\approx}{\mathbb{C}}(t^{-1}\mathbf{x}) = \underset{\approx}{\mathbb{C}}(\underline{\mathbf{z}}) \tag{119}$$

where $\underset{\approx}{\mathbb{C}}$ is a function of $\underline{\mathbf{z}}$ which is Z -periodic in the two first coordinates. In the following, double-stroke fonts denote fields which are only Z -periodic functions of the local variables $\underline{\mathbf{z}}$.

Following the asymptotic expansion method, it is assumed that that the solution to the 3D problem can be written as a series in power of η in the following form:

$$\begin{cases} \underline{\mathbf{u}}^t &= L(\eta^{-1}\underline{\mathbf{u}}^{-1} + \eta^0\underline{\mathbf{u}}^0 + \eta^1\underline{\mathbf{u}}^1 + \dots) \\ \underline{\boldsymbol{\varepsilon}}^t &= \eta^0\underline{\boldsymbol{\varepsilon}}^0 + \eta^1\underline{\boldsymbol{\varepsilon}}^1 + \dots \\ \underline{\boldsymbol{\sigma}}^t &= \eta^0\underline{\boldsymbol{\sigma}}^0 + \eta^1\underline{\boldsymbol{\sigma}}^1 + \dots \end{cases} \tag{120}$$

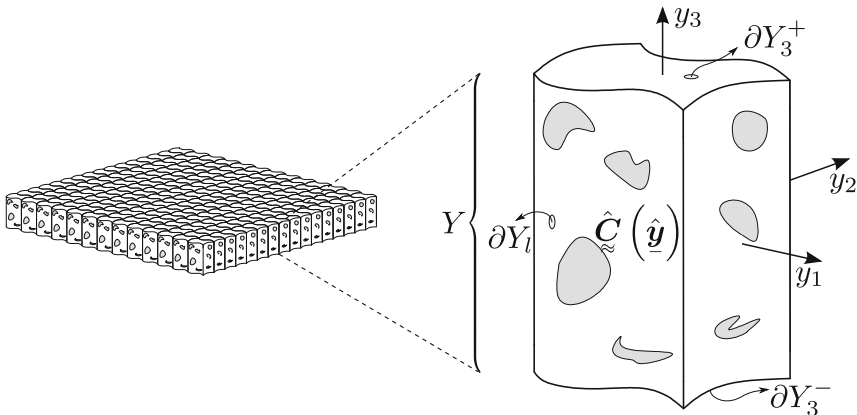


Fig. 8 The periodic plate and its unit-cell

where $p = -1, 0, 1, 2, \dots$ and $\underline{\mathbf{u}}^p$, $\underline{\underline{\boldsymbol{\varepsilon}}}^p$ and $\underline{\underline{\boldsymbol{\sigma}}}^p$ are functions of $(Y_1, Y_2, z_1, z_2, z_3)$ which are Z -periodic in the (z_1, z_2) coordinates. The derivation rule for these functions is:

$$\begin{aligned} \underline{\nabla} &= \left(\frac{d}{dx_1}, \frac{d}{dx_2}, \frac{d}{dx_3} \right) \\ &= L^{-1} \left(\frac{\partial}{\partial Y_1}, \frac{\partial}{\partial Y_2}, 0 \right) + t^{-1} \left(\frac{\partial}{\partial z_1}, \frac{\partial}{\partial z_2}, \frac{\partial}{\partial z_3} \right) = L^{-1} \underline{\nabla}_Y + t^{-1} \underline{\nabla}_z. \end{aligned} \quad (121)$$

Using this derivation rule in the compatibility condition $\underline{\underline{\boldsymbol{\varepsilon}}}^t = \underline{\mathbf{u}}^t \otimes^s \underline{\nabla}$ and identifying all the terms of the same order η^p , it is found from boundary conditions (43) and Eqs. (44), (45) that $\underline{\mathbf{u}}^{-1}$ and $\underline{\mathbf{u}}^0$ have the following form where fields with capital letters (like U, K, E, \dots) are only function of the macroscopic global variables (Y_1, Y_2) :

$$\underline{\mathbf{u}}^{-1} = U_3^{-1} \underline{\mathbf{e}}_3. \quad (122)$$

and

$$\underline{\mathbf{u}}^0 = -z_3 U_3^{-1} \otimes \underline{\nabla}_Y + \underline{\mathbf{U}}^0 = \begin{pmatrix} U_1^0 - z_3 U_{3,1}^{-1} \\ U_2^0 - z_3 U_{3,2}^{-1} \\ U_3^0 \end{pmatrix}, \quad (123)$$

with the boundary conditions:

$$U_3^{-1} = U_{3,\alpha}^{-1} n_\alpha = U_j^0 = 0 \quad \forall (Y_1, Y_2) \in \partial\omega \quad (124)$$

where $\underline{\mathbf{n}}$ is the outer normal to $\partial\omega$.

Moreover, the zeroth-order strain is given by:

$$\underline{\underline{\boldsymbol{\varepsilon}}}^0 = \underline{\underline{\mathbf{E}}}^0 + z_3 \underline{\underline{\mathbf{K}}}^{-1} + \underline{\mathbf{v}}^1 \otimes^s \underline{\nabla}_z \quad (125)$$

where

$$\underline{\underline{\mathbf{E}}}^0 = (U_\alpha^0) \otimes^s \underline{\nabla}_Y \quad \text{and} \quad \underline{\underline{\mathbf{K}}}^{-1} = U_3^{-1} \underline{\nabla}_Y \otimes \underline{\nabla}_Y \quad (126)$$

or equivalently in components:

$$E_{\alpha\beta}^0 = \frac{1}{2} (U_{\alpha,\beta}^0 + U_{\beta,\alpha}^0), \quad E_{i3}^0 = 0, \quad (127)$$

$$K_{\alpha\beta}^{-1} = -U_{3,\alpha\beta}^{-1}, \quad K_{i3}^{-1} = 0, \quad (128)$$

and $\underline{\mathbf{v}}^1$ is the Z -periodic displacement field function of $(Y_1, Y_2, z_1, z_2, z_3)$ defined by:

$$\underline{\mathbf{v}}^1 = \underline{\mathbf{u}}^1 + z_3 U_3^0 \otimes \underline{\nabla}_Y = \begin{pmatrix} u_1^1 + z_3 U_{3,1}^0 \\ u_2^1 + z_3 U_{3,2}^0 \\ u_3^1 \end{pmatrix} \quad (129)$$

Inserting the asymptotic expansion of the stress field into the 3D equilibrium equation, $\underline{\sigma}^t \cdot \underline{\nabla} = 0$ on Ω' , and identifying to zero the terms of this series in η^p gives:

$$\underline{\sigma}^0 \cdot \underline{\nabla}_z = 0 \quad (130)$$

for $p = -1$, and

$$\underline{\sigma}^p \cdot \underline{\nabla}_y + \underline{\sigma}^{p+1} \cdot \underline{\nabla}_z = 0 \quad (131)$$

for $p \geq 0$. The boundary condition, $\underline{\sigma}^t \cdot \underline{e}_3 = \pm \underline{f}$ on $\partial\Omega_3^\pm$, gives the following equations:

$$\sigma_{i3}^p \left(Y_1, Y_2, z_1, z_2, \pm \frac{1}{2} \right) = 0 \quad (132)$$

for the order $p \geq 0$ and $p \neq 2$. When $p = 2$ we have:

$$\sigma_{\alpha 3}^2 \left(Y_1, Y_2, z_1, z_2, \pm \frac{1}{2} \right) = 0 \quad \text{and} \quad \sigma_{33}^2 \left(Y_1, Y_2, z_1, z_2, \pm \frac{1}{2} \right) = \pm \frac{1}{2} F_3(Y_1, Y_2) \quad (133)$$

For given \underline{E}^0 and \underline{K}^{-1} , the zeroth-order auxiliary elasticity problem on the unit cell Z is to find Z -periodic stress field $\underline{\sigma}^0$ satisfying the local balance equation (130) and the constitutive law $\sigma_{ij}^0 = \mathbb{C}_{ijkl} \varepsilon_{kl}^0$ where ε^0 is given by (125). The solution of this problem is linearly dependent on \underline{E}^0 and \underline{K}^{-1} , and \underline{v}^1 is uniquely determined in terms of \underline{E}^0 and \underline{K}^{-1} up to a macroscopic field \underline{U}^1 only function of (Y_1, Y_2) . Therefore, we can write:

$$\underline{u}^1 = \underline{u}^E : \underline{E}^0 + \underline{u}^K : \underline{K}^{-1} - z_3 U_3^0 \otimes \underline{\nabla}_y + \underline{U}^1 \quad (134)$$

where \underline{u}^E and \underline{u}^K are third-order localisation tensors depending only on the local variable \underline{z} , and

$$\underline{\sigma}^0 = \underline{s}^E : \underline{E}^0 + \underline{s}^K : \underline{K}^{-1} \quad (135)$$

where \underline{s}^E and \underline{s}^K are fourth-order localisation tensors depending only on the local variable \underline{z} .

Except for the case of laminates, the determination of these localisation tensors should be numerically performed by solving at most 6 auxiliary zeroth-order problems on the unit cell (3 components for \underline{E}^0 and 3 components for \underline{K}^{-1}). The zeroth-order normal stress tensor and moment tensor are respectively defined by:

$$N_{\alpha\beta}^0(Y_1, Y_2) = \langle \sigma_{\alpha\beta}^0 \rangle, \quad M_{\alpha\beta}^0(Y_1, Y_2) = \langle z_3 \sigma_{\alpha\beta}^0 \rangle, \quad (136)$$

where $\langle \bullet \rangle$ is the volume-average over the unit cell Z : $\langle \bullet \rangle = \frac{1}{|Z|} \int_{\underline{z}} \bullet \, dz_1 dz_2 dz_3$.

Using Eq. (135) and the above definitions, the Love-Kirchhoff constitutive equation is derived:

$$\begin{aligned}\tilde{N}^0 &= \tilde{A} : \tilde{E}^0 + \tilde{B} : \tilde{K}^{-1} \\ \tilde{M}^0 &= \tilde{G} : \tilde{E}^0 + \tilde{D} : \tilde{K}^{-1}\end{aligned}\quad (137)$$

with:

$$A_{\alpha\beta\gamma\delta} = \langle \mathbb{s}_{\alpha\beta\gamma\delta}^E \rangle \quad B_{\alpha\beta\gamma\delta} = \langle \mathbb{s}_{\alpha\beta\gamma\delta}^K \rangle \quad G_{\alpha\beta\gamma\delta} = \langle z_3 \mathbb{s}_{\alpha\beta\gamma\delta}^E \rangle \quad D_{\alpha\beta\gamma\delta} = \langle z_3 \mathbb{s}_{\alpha\beta\gamma\delta}^K \rangle \quad (138)$$

It can be shown that \tilde{G} is the transpose tensor of \tilde{B} in the sense $G_{\alpha\beta\gamma\delta} = B_{\gamma\delta\alpha\beta}$ and that these two tensors are null if the unit cell Z is centro-symmetric, that is:

$$\tilde{\mathbb{C}}(\underline{z}) = \tilde{\mathbb{C}}(-\underline{z}) \quad \forall \underline{z} \quad (139)$$

In this case, the in-plane (stretching) and the out-of-plane (bending) behaviors of the plate are uncoupled. The centro-symmetric property of the unit cell will be assumed in the sequel. As for the laminates, the local balance equations (130) and (131) for $p = 1$ and the boundary conditions can be used to derive the macroscopic balance equations. We end up with the same bending Love-Kirchhoff plate problem (61) as for laminates to which the following in-plate Love-Kirchhoff must be added:

$$\left\{ \begin{array}{l} \tilde{N}^0 \cdot \underline{\nabla}_y = 0, \quad \text{on } \omega \\ \tilde{N}^0 = \tilde{A} : \tilde{E}^0, \quad \text{on } \omega \\ \tilde{E}^0 = (U_\alpha^0) \otimes^s \underline{\nabla}_y, \quad \text{on } \omega \\ U_\alpha^0 = 0 \quad \text{on } \partial\omega \end{array} \right. \quad (140a)$$

$$\quad (140b)$$

$$\quad (140c)$$

$$\quad (140d)$$

Note that there is no (in-plane) loading in this problem. Therefore, its solution is null: $U_\alpha^0 = N_{\alpha\beta}^0 = E_{\alpha\beta}^0 = 0$.

Gathering equilibrium equation for order 0, compatibility equation, boundary conditions and constitutive equations of order 1 we get the first-order auxiliary problem on the unit cell Z :

$$\left\{ \begin{array}{l} \underline{\sigma}^0 \cdot \underline{\nabla}_y + \underline{\sigma}^1 \cdot \underline{\nabla}_z = 0 \\ \underline{\sigma}^1 = \tilde{\mathbb{C}} : \underline{\varepsilon}^1 \end{array} \right. \quad (141a)$$

$$\quad (141b)$$

$$\left\{ \begin{array}{l} \underline{\varepsilon}^1 = \underline{u}^1 \otimes^s \underline{\nabla}_y + \underline{u}^2 \otimes^s \underline{\nabla}_z \\ \sigma_{i3}^1(z = \pm \frac{1}{2}) = 0 \end{array} \right. \quad (141c)$$

$$\quad (141d)$$

In this auxiliary problem, the zeroth-order displacement field \underline{u}^1 (134) and stress field $\underline{\sigma}^0$ (135) are local fields which depend linearly on \tilde{K}^{-1} , $U_{3,\alpha}^0$ and \underline{U}^1 . Hence, the first-order solution $\underline{\varepsilon}^1$, $\underline{\sigma}^1$ and \underline{u}^2 will be a linear superposition of localization fields which depend on the gradient of those macroscopic fields. We can write with obvious notations:

$$\underline{u}^2 = \underline{\mathbb{u}}^{K\nabla} : (\tilde{K}^{-1} \otimes \underline{\nabla}_y) + \underline{\mathbb{u}}^E : \tilde{E}^1 + \underline{\mathbb{u}}^K : \tilde{K}^0 - z_3 U_3^1 \otimes \underline{\nabla}_y + \underline{U}^2 \quad (142)$$

and

$$\underline{\underline{\sigma}}^1 = \underline{\underline{s}}^{K^\nabla} : (\underline{\underline{K}}^{-1} \otimes \underline{\underline{\nabla}}_y) + \underline{\underline{s}}^E : \underline{\underline{E}}^1 + \underline{\underline{s}}^K : \underline{\underline{K}}^0 \quad (143)$$

where the third-order localization tensor $\underline{\underline{u}}^{K^\nabla}$: and the fifth-order localization tensor $\underline{\underline{s}}^{K^\nabla}$: have to be computed by solving the above described first-order auxiliary problem on the unit cell Z .

It can be proved that if the unit cell Z is π -invariant along direction 3 (i.e. with respect to a rotation of 180° around axis 3), then the first-order normal and moment tensor fields are not coupled with $\underline{\underline{K}}^{-1} \otimes \underline{\underline{\nabla}}_y$. We have again:

$$\underline{\underline{N}}^1 = ((\sigma_{\alpha\beta}^1)) = \underline{\underline{A}} : \underline{\underline{E}}^1, \quad \underline{\underline{M}}^1 = (z_3 \sigma_{\alpha\beta}^1) = \underline{\underline{D}} : \underline{\underline{K}}^0 \quad (144)$$

Similarly to the case of laminates, the first-order macroscopic (plate) problem that determines $\underline{\underline{N}}^1$ and $\underline{\underline{M}}^1$ is unloaded which means that these fields are null as well as the displacement fields U_α^1 and U_3^0 .

In conclusion, if we assume both centro-symmetry and π -invariance along direction 3 of the unit cell Z , the asymptotic expansion of the 3D solution has exactly the same structure for periodic plates as for laminates. Therefore, all the equations of the Bending-Gradient theory described in Sect. 4 remain valid except that the localization tensors $\underline{\underline{s}}^K$ and $\underline{\underline{s}}^{K^\nabla}$: are Z -periodic functions which must be computed by solving auxiliary problems on the unit cell Z , and that the definition of the plate elastic tensors $\underline{\underline{D}}$, $\underline{\underline{d}}$ and $\underline{\underline{h}}$ involves volume-averaging on the unit cell instead of integration over z_3 for laminates. The Bending-Gradient theory was successfully applied to sandwich panels (Lebée and Sab 2012a, b) as well as space frames Lebée and Sab (2013a).

References

- Altenbach, H. (1998). Theories for laminated and sandwich plates. *Mechanics of Composite Materials*, 34(3), 243–252.
- Bakhvalov, N. S., & Panasenko, G. P. (1989). *Homogenization: Averaging processes in periodic media*. Dordrecht-Boston-London: Kluwer Academic Publishers.
- Berdichevsky, V. L. (1979). Variational-asymptotic method of constructing a theory of shells. *Journal of Applied Mathematics and Mechanics*, 43(4), 711–736.
- Boutin, C. (1996). Microstructural effects in elastic composites. *International Journal of Solids and Structures*, 33(7), 1023–1051.
- Buannic, N., & Cartraud, P. (2001a). Higher-order effective modeling of periodic heterogeneous beams. I. Asymptotic expansion method. *International Journal of Solids and Structures*, 38(40–41), 7139–7161.
- Buannic, N., & Cartraud, P. (2001b). Higher-order effective modeling of periodic heterogeneous beams. II. Derivation of the proper boundary conditions for the interior asymptotic solution. *International Journal of Solids and Structures*, 38(40–41), 7163–7180.
- Caillerie, D. (1984). Thin elastic and periodic plates. *Mathematical Methods in the Applied Sciences*, 6(1), 159–191.

- Carrera, E. (2002). Theories and finite elements for multilayered, anisotropic, composite plates and shells. *Archives of Computational Methods in Engineering*, 9(2), 87–140.
- Ciarlet, P. G., & Destuynder, P. (1979). Justification of the 2-Dimensional linear plate model. *Journal de Mécanique*, 18(2), 315–344.
- Dallot, J., & Sab, K. (2008). Limit analysis of multi-layered plates. Part I: The homogenized Kirchhoff-Love model. *Journal of the Mechanics and Physics of Solids*, 56(2), 561–580.
- Diaz Diaz, A. (2001). Un modèle de stratifiés. *Comptes Rendus de l'Académie des Sciences - Series IIB - Mechanics*, 329(12), 873–879.
- Kohn, R. V., & Vogelius, M. (1984). A new model for thin plates with rapidly varying thickness. *International Journal of Solids and Structures*, 20(4), 333–350.
- Lebée, A., & Sab, K. (2010). A Cosserat multiparticle model for periodically layered materials. *Mechanics Research Communications*, 37(3), 293–297.
- Lebée, A., & Sab, K. (2011a). A Bending-Gradient model for thick plates. Part I: Theory. *International Journal of Solids and Structures*, 48(20), 2878–2888.
- Lebée, A., & Sab, K. (2011b). A Bending-Gradient model for thick plates, Part II: Closed-form solutions for cylindrical bending of laminates. *International Journal of Solids and Structures*, 48(20), 2889–2901.
- Lebée, A., & Sab, K. (2012a). Homogenization of thick periodic plates: Application of the Bending-Gradient plate theory to a folded core sandwich panel. *International Journal of Solids and Structures*, 49(19–20), 2778–2792.
- Lebée, A., & Sab, K. (2012b). Homogenization of cellular sandwich panels. *Comptes Rendus Mécanique*, 340(4–5), 320–337.
- Lebée, A., & Sab, K. (2013a). Homogenization of a space frame as a thick plate: Application of the Bending-Gradient theory to a beam lattice. *Computers & Structures*, 127, 88–101.
- Lebée, A., & Sab, K. (2013b). Justification of the bending-gradient plate model through asymptotic expansions. In H. Altenbach, S. Forest, & A. Krivtsov (Eds.), *Generalized continua as models for materials* (pp. 217–236). Berlin, Heidelberg: Springer-Verlag.
- Lewiński, T. (1991). Effective models of composite periodic plates-I. Asymptotic solution. *International Journal of Solids and Structures*, 27(9), 1155–1172.
- Noor, A. K., Malik, M. (2000). An assessment of five modeling approaches for thermo-mechanical stress analysis of laminated composite panels. *Computational Mechanics*, 25(1), 43–58. ISSN 0178-7675.
- Pagano, N. J. (1969). Exact solutions for composite laminates in cylindrical bending. *Journal of Composite Materials*, 3(3), 398–411.
- Pagano, N. J. (1970a). Exact solutions for rectangular bidirectional composites and sandwich plates. *Journal of Composite Materials*, 4(1), 20–34.
- Pagano, N. J. (1970b). Influence of shear coupling in cylindrical bending of anisotropic laminates. *Journal of Composite Materials*, 4(3), 330–343.
- Reddy, J. N. (1989). On refined computational models of composite laminates. *International Journal for Numerical Methods in Engineering*, 27(2), 361–382.
- Reissner, E. (1945). The effect of transverse shear deformation on the bending of elastic plates. *Journal of Applied Mechanics*, 12(2), 69–77.
- Sanchez-Hubert, J., & Sanchez-Palencia, É. (1992). *Introduction aux méthodes asymptotiques et à l'homogénéisation: application à la mécanique des milieux continus*. Paris: Masson.
- Sanchez-Palencia, É. (1980). *Non-homogeneous media and vibration theory* (Vol. 127). Lecture Notes in Physics Berlin, Heidelberg: Springer.
- Smyshlyaev, V. P., & Cherednichenko, K. D. (2000). On rigorous derivation of strain gradient effects in the overall behaviour of periodic heterogeneous media. *Journal of the Mechanics and Physics of Solids*, 48(6–7), 1325–1357.
- Sutyrin, V. G., & Hodges, D. H. (1996). On asymptotically correct linear laminated plate theory. *International Journal of Solids and Structures*, 33(25), 3649–3671.
- Vlasov, V. Z. (1961). *Thin-walled elastic beams*. Jerusalem: National Technical Information Service.

Some Problems on Localized Vibrations and Waves in Thin Shells

Gennadi Mikhasev

Abstract Some problems on localized vibrations and waves in thin isotropic and laminated cylindrical shells are considered in this Chapter. To study vibrations of thin laminated shells, the equivalent single layer model for the whole packet of a sandwich is proposed. The basic goal of this paper is to demonstrate two asymptotic approaches for studying localized vibrations of thin shells. At first, the asymptotic method of Tovstik is applied to study free stationary vibrations localized in a neighbourhood of a fixed generatrix or parallel called the weakest one. As an interesting example, free localized vibrations of a laminated cylindrical shell containing polarized magnetorheological elastomer and affected by an external magnetic field are analyzed. Then the asymptotic method for investigation of running localized waves (wave packets) in thin shells is stated. The solution of governing equations is constructed in the form of a superposition of wave packets running in a thin non-circular prestressed cylinder in the circumferential direction. The influence of non-uniform stationary and dynamic pressures on running wave packets is briefly studied.

1 Introduction

Localization of vibrations in thin-walled structures is undesirable phenomenon because it results in a concentration of destructive stresses and may lead to the damage accumulation in a structure. That is why, when designing and calculating a shell-like structure experiencing external dynamic loads, it is very important to establish the reasons inducing localization of vibrations and waves, find out the spots where natural modes may concentrate, and predict dynamic behavior of the shell in a neighbourhood of some lines or points.

The factors resulting in localization of eigenmodes may be subdivided into the following three groups:

G. Mikhasev (✉)
Belarusian State University, Minsk, Belarus
e-mail: mikhasev@bsu.by

- variable geometrical parameters (curvature, thickness, initial imperfections, generator length);
- inhomogeneity of the prestressed state caused by a nonuniform or combined load;
- variable physical characteristics (Young's modulus, density, temperature).

For instance, low-frequency free vibrations of a thin medium-length cylindrical shell with a slanted edge are concentrated near the longest generatrix (Tovstik 1983a), and a thin laminated cylinder being under action of nonuniform axial forces has eigenmodes localized in a vicinity of the most compressed generatrix (Korchevskaya and Mikhasev 2006). Another interesting example considered in the recently published paper (Mikhasev et al. 2014) concerns the influence of a magnetic field on eigenmodes of a laminated cylindrical shell containing magnetorheological elastomer (MRE): an applied magnetic field may cause the inhomogeneity in mechanical and rheological properties of the MRE composing a sandwich and, as a result, lead to the strong distortion of eigenmodes some of which are found to be localized in places where shears reach their extremum values.

By definition of Tovstik (Tovstik 1983a; Tovstik and Smirnov 2001), the line in a neighbourhood of which buckling or vibration modes are localized is called the “weakest” one. Wave processes in shells with the weakest lines are, as a rule, very complicated and have the transitional character. As shown in papers (Mikhasev 1998a, 2002), the dynamic response of a cylindrical shell on the initial localized perturbations is the family of localized bending and tangential waves running in the circumferential and/or axial directions. If a shell has the weakest generatrix, then non-stationary localized vibrations in the form of wave packets (WPs) trend to run to the region containing this generatrix. The running WPs having small energy may be reflected from some generatrix, these reflections being accompanied by focusing and growing wave amplitudes (Mikhasev 2002).

The problems mentioned above are very complicated because the differential equations governing a localized motion of a shell do not admit solutions in the explicit form. The effective mathematical tool for studying similar problems is the asymptotic method called the WKB one (for instance, see Fröman and Fröman 1965). This name comes from the first letters of the authors' names: Wentzel, Kramers and Brillouin, who first applied this approach to problems of quantum mechanics. The WKB approximation is also used in mechanics of solids, acoustics, diffraction problems for studying high-frequency vibrations or short waves, and often called as short-wave asymptotics (Babich and Buldyrev 1991). The significant contribution to the further development of this method has been made by Maslov (1977) and Babich et al. (1985) who have constructed stationary and non-stationary solutions exponentially decreasing far from fixed or moving points. The new method has become known as the complex WKB method, and in acoustics, non-stationary solutions localized in a vicinity of a space-time ray were named as “quasiphotons”. It should be noticed that similar solutions (Maslov 1977; Babich et al. 1985) were mainly found for unbounded mediums. Studying stationary problems on localized buckling and free vibrations of thin shells, Tovstik (1983a) has proposed another variant of the complex WKB approach taking into account boundary conditions.

The method of Tovstik permits one to reduce the 2D boundary-value problem into a sequence of the 1D problems at the weakest (fixed) generatrix at the surface of a cylindrical or conical shell. Afterwards, this method has been generalized for studying non-stationary localized waves in shells (Mikhasev 2002). The basic concepts of this modification lie in introducing the center of the running wave packet and a local coordinate system connected with this center. According to the new approach, the phase function in the complex WKB expansion is sought in an explicit form and the initial 2D problem is reduced to the system of the 1D boundary-value problems at the moving generatrix.

The basic goals of this article are:

- the introduction to the asymptotic method of Tovstik for studying localized free (stationary) vibrations of thin shells;
- the introduction to the asymptotic approach which permits one to study non-stationary running localized vibrations (wave packets) in thin shells;
- to consider the series of problems (called non-classical ones here) on highly localized free vibrations and running wave packets in thin isotropic and composite laminated shells.

Because some of problems to be studied below are related to thin sandwich structures, Sect. 2 will be devoted to the principle hypothesis and governing equations for thin laminated shells. In Sects. 3–6, using the asymptotic method of Tovstik, the stationary vibrations localized near the weakest generatrix and parallel in medium-length and infinitely long cylindrical shells will be studied. Herewith, the asymptotic method details are considered in Sect. 3. And Sects. 4–5 concern problems on free vibrations of laminated viscoelastic and elastic shells. In particular, Sect. 4 demonstrates an interesting effect of the influence of an applied magnetic field on eigenmodes of a sandwich cylinder with MRE-core. Finally, the new asymptotic approach for studying running WPs in thin shells is stated in Sect. 7.

2 The Equivalent Single Layer Model for Thin Laminated Shells

2.1 Different Approaches in Modelling of Laminated Shells

By now, there exist a lot of different theories and models for studying dynamics of thin laminated shells. Basic available approaches for modelling of sandwich structures may be found in the survey articles of Quat et al. (2010, 2013). These theories can be subdivided into the following basic approaches. The first one is based on stress analysis and rigid-body motions (for instance, see Kulikov and Plotnikova 2013) and rather complicated when presented in curvilinear shell coordinates. New high accurate layer-wise theories developed by Bolotin and Novichkov (1980), Carrera (1999, 2002, 2003), Ferreira et al. (2011) and others (see in the survey articles, Qatu

et al. 2010; Qu et al. 2013) presuppose a satisfaction of boundary conditions on the interface surfaces. And if a sandwich is assembled from a large number of layers, these approaches become rather sophisticated in the theoretical formulations and numerical computations, thus preventing their general use in modeling practical shell vibration problems. In our opinion, the equivalent single layer (ESL) models are more perspective for dynamic simulation of thin multi-layered shells and, particularly, for tunable laminated thin-walled structures containing smart materials. Survey articles and monographs devoted to ESL theories are, e.g., (Grigolyuk and Kulikov 1988; Toorani and Lakis 2000; Carrera 2002; Reddy 2003; Qatu 2004; Qatu et al. 2010).

The attempt to apply one of ESL models for the dynamic analysis of a thin laminated shells containing smart viscoelastic material has been recently done by Mikhasev et al. (2011). Based on the assumptions of the generalized kinematic hypothesis of Timoshenko for the whole sandwich, the governing equations derived earlier (Grigolyuk and Kulikov 1988) were adapted to the description of dynamics of an adaptive sandwich cylindrical shell with magnetorheological layers. The principle equations of this ESL model will be considered in this Section and used later in Sects. 3 and 4 for studying localized vibrations of composite laminated shells.

2.2 Sandwich Structure

Consider a thin non-circular cylindrical sandwich shell (see Fig. 1) consisting of N transversely isotropic layers characterized by length L , thickness h_k , density ρ_k , Young's modulus E_k , and Poisson's ratio ν_k , where $k = 1, 2, \dots, N$. The middle surface of any fixed layer is taken as the original surface. The coordinate system α_1, α_2 is illustrated in Fig. 1, where α_1, α_2 are the axial and circumferential coordinates, respectively. The radius of curvature of the middle surface is $R_2 = R/k(\varphi)$, where R is the characteristic dimension of the shell surface. The shell is bounded by the two not necessary plane edges

$$L_1(\alpha_2) \leq \alpha_1 \leq L_2(\alpha_2).$$

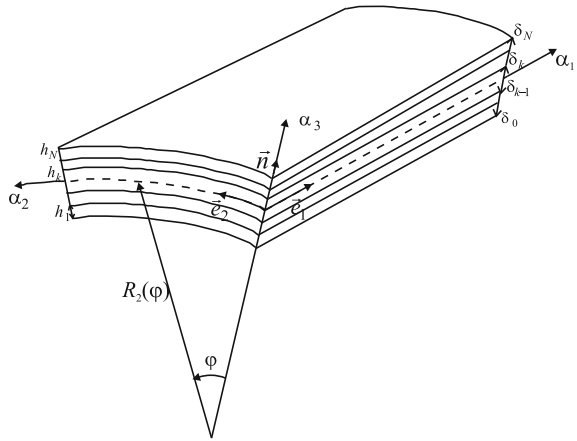
If every layer is made of elastic and homogeneous material, the parameters E_k as well as the shear moduli G_k are real constants for any k . When the sandwich is formed by embedding viscoelastic materials between elastic layers, some of these parameters corresponding to the viscoelastic lamina with adaptive rheological properties are assumed to be complex functions

$$E_k = E'_k + iE''_k, \quad G_k = G'_k + iG''_k, \quad i = \sqrt{-1}. \quad (1)$$

2.3 Basic Hypotheses

We introduce some additional notations. Let δ_k be the distance between the original surface and the upper bound of the k th layer, u_i and w the tangential and normal

Fig. 1 Laminated cylindrical shell with a curvilinear coordinate system



displacements of the original surface points, respectively, $u_i^{(k)}$ the tangential displacements of points of the k th layer, σ_{i3} the transverse shear stresses, θ_i the angles of rotation of the normal \mathbf{n} about the vector \mathbf{e}_i (see Fig. 1). Here $i = 1, 2; k = 1, 2, \dots, N$.

The following hypothesis of the laminated shell theory (Grigolyuk and Kulikov 1988) are assumed here:

- The distribution law of the transverse tangent stresses across the thickness of the k th layer is assumed to be in the form of

$$\sigma_{i3} = f_0(z)\mu_i^{(0)}(\alpha_1, \alpha_2) + f_k(z)\mu_i^{(k)}(\alpha_1, \alpha_2) ,$$

where continuous functions $f_0(z), f_k(z)$ are introduced as follows

$$f_0(z) = \frac{1}{h^2}(z - \delta_0)(\delta_N - z),$$

$$f_k(z) = \frac{1}{h_k^2}(z - \delta_{k-1})(\delta_k - z).$$

- Normal stresses acting on the element area parallel to the original one are negligible with respect to the other components of the stress tensor.
- The normal deflection w does not depend on the coordinate z .
- The tangential displacements are distributed across thickness of the layer packet according to the generalised kinematic hypothesis of Timoshenko:

$$u_i^{(k)}(\alpha_1, \alpha_2, z) = u_i(\alpha_1, \alpha_2) + z\theta_i(\alpha_1, \alpha_2) + g(z)\psi_i(\alpha_1, \alpha_2). \tag{2}$$

where

$$g(z) = \int_0^z f_0(x)dx.$$

The functions $\mu_i^{(0)}$, $\mu_i^{(k)}$ may be found in paper of Grigolyuk and Kulikov (1988). It should be noted that $\mu_i^{(0)}$, $\mu_i^{(k)}$ depend on the elements of the matrix characterizing the transverse shifted pliability of the k th layer.

Hypothesis (2) describes the non-linear dependence of the tangential displacements on the z coordinate; at $g \equiv 0$ it turns into the classical Kirchhoff-Love hypothesis.

2.4 Governing Equations

In the case when E_k, G_k, R_2 are constant, the system of five differential equations with respect to u_i, w, ψ_i , based on the stated above hypotheses, has been derived by Grigolyuk and Kulikov (1988). In paper (Mikhasev et al. 2011) these equations have been generalized for the more common case when E_k, G_k are dependent on curvilinear coordinates and time. If vibrations occur with formation of large number of waves although in one direction at shell surface, these equations may be essentially simplified. Introducing functions ψ_i appearing in (2) by

$$\psi_1 = a_{,1} + \phi_{,2}, \quad \psi_2 = a_{,2} - \phi_{,1}, \quad (3)$$

where a, ϕ are the shear functions defined from equations

$$a = -\frac{\eta_2 h^2}{\eta_1 \beta} \Delta \chi \quad (4)$$

and

$$\frac{1 - \nu}{2} \frac{h^2}{\beta} \Delta \phi = \phi, \quad (5)$$

the following compact system is reduced in study (Grigolyuk and Kulikov 1988)

$$\begin{aligned} \frac{Eh^3 \eta_3}{12(1 - \nu^2)} \left(1 - \frac{\theta h^2}{\beta} \Delta\right) \Delta^2 \chi + \frac{1}{R_2(\alpha_2)} \frac{\partial^2 \Phi}{\partial \alpha_1^2} + \rho h \frac{\partial^2}{\partial t^2} \left(1 - \frac{h^2}{\beta} \Delta\right) \chi = 0, \\ \Delta^2 \Phi - \frac{Eh}{R_2(\alpha_2)} \frac{\partial^2}{\partial \alpha_1^2} \left(1 - \frac{h^2}{\beta} \Delta\right) \chi = 0 \end{aligned} \quad (6)$$

with respect to the displacement and stress functions χ and Φ , respectively. Here χ is linked with the normal displacement w by the equation

$$w = \left(1 - \frac{h^2}{\beta} \Delta\right) \chi, \quad (7)$$

and the function Φ permits to find the specific membrane stress resultants

$$T_{ij} = \delta_{ij} \Delta \Phi - \Phi_{,ij}, \tag{8}$$

where $\Delta = \partial^2/\partial\alpha_1^2 + \partial^2/\partial\alpha_2^2$ is the Laplace operator in the curvilinear co-ordinates α_1, α_2 , and δ_{ij} is Kronecker's symbol ($\delta_{ii} = 1; \delta_{ij} = 0, i \neq j$). In (8), T_{ij} are the reduced stress resultants for the sandwich which are expressed in the standard way as

$$T_{ij} = \sum_{k=1}^N \int_{\delta_{k-1}}^{\delta_k} \sigma_{ij} dz.$$

In Eqs. (6), t is time, E, ν, ρ are the reduced modulus of elasticity, Poisson's ratio and density respectively, and the last parameters η_3, θ, β characterize the reduced shear stiffness of the sandwich. All the reduced parameters appearing in Eqs. (6) are calculated as follows

$$\begin{aligned} \nu &= \sum_{k=1}^N \frac{E_k h_k \nu_k}{1 - \nu_k^2} \left(\sum_{k=1}^N \frac{E_k h_k}{1 - \nu_k^2} \right)^{-1}, \quad E = \frac{1 - \nu^2}{h} \sum_{k=1}^N \frac{E_k h_k}{1 - \nu_k^2}, \quad \rho = \sum_{k=1}^N \rho_k \xi_k, \\ \beta &= \frac{12(1 - \nu^2)}{Eh\eta_1} q_{44}, \quad q_{44} = \frac{\left[\sum_{k=1}^N \left(\lambda_k - \frac{\lambda_{k0}^2}{\lambda_{kk}} \right) \right]^2}{\sum_{k=1}^N \left(\lambda_k - \frac{\lambda_{k0}^2}{\lambda_{kk}} \right) G_k^{-1}} + \sum_{k=1}^N \frac{\lambda_{k0}^2}{\lambda_{kk}} G_k, \\ \lambda_{kk} &= \int_{\delta_{k-1}}^{\delta_k} f_0^2(z) dz, \quad \lambda_{kn} = \int_{\delta_{k-1}}^{\delta_k} f_k(z) f_n(z) dz, \quad \theta = 1 - \eta_2^2 / (\eta_1 \eta_3), \\ \eta_1 &= \sum_{k=1}^N \xi_k^{-1} \pi_{1k} \gamma_k - 3c_{12}^2, \quad \eta_2 = \sum_{k=1}^N \xi_k^{-1} \pi_{2k} \gamma_k - 3c_{12}c_{13}, \\ \eta_3 &= 4 \sum_{k=1}^N (\xi_k^2 + 3\zeta_{k-1} \zeta_k) \gamma_k - 3c_{13}^2, \quad h\xi_k = h_k, \quad h\zeta_n = \delta_n \quad (n = 0, k), \\ \frac{1}{12} h^2 \pi_{1k} &= \int_{\delta_{k-1}}^{\delta_k} g^2(z) dz, \quad \frac{1}{12} h^2 \pi_{2k} = \int_{\delta_{k-1}}^{\delta_k} z g(z) dz, \\ \frac{1}{12} h^2 \pi_{3k} &= \int_{\delta_{k-1}}^{\delta_k} g(z) dz, \quad c_{13} = \sum_{k=1}^N (\zeta_{k-1} + \zeta_k) \gamma_k, \quad c_{12} = \sum_{k=1}^N \xi_k^{-1} \pi_{3k} \gamma_k, \\ \gamma_k &= \frac{E_k h_k}{1 - \nu_k^2} \left(\sum_{k=1}^N \frac{E_k h_k}{1 - \nu_k^2} \right)^{-1}. \end{aligned} \tag{9}$$

Remark 1 Equations (5), (6) have been derived (Grigolyuk and Kulikov 1988) for elastic laminated shells with constant parameters $E, \nu, \theta, \beta, \eta_k$. However, at some assumptions with respect to unknown functions χ, Φ and moduli E_k, G_k these equations may be used for prediction of vibrations of laminated viscoelastic shells with variable physical characteristics (Mikhasev et al. 2011). Let $h_* = h/R$ be a natural small parameter characterizing the shell thinness and $y(\alpha_j, t)$ any of the unknown functions χ, Φ .

Let the following conditions

$$R \frac{\partial}{\partial \alpha_j} (E_k, G_k) \sim (E_k, G_k),$$

$$R \frac{\partial}{\partial \alpha_1} (\chi, \Phi) \sim (\chi, \Phi), \quad R \frac{\partial}{\partial \alpha_2} (\chi, \Phi) \sim h_*^{-1/4} (\chi, \Phi)$$

be valid at $h_* \rightarrow 0$. Then solutions of Eqs. (5), (6) will satisfy the full system of differential equations with respect to u_i, w, ψ_i (Grigolyuk and Kulikov 1988) up to values of the order $h_*^{1/2}$ (Mikhasev et al. 2011).

Let the shell edges be simply supported. In terms of the displacement, stress and shear functions, the appropriate boundary conditions will be as follows (Grigolyuk and Kulikov 1988)

$$\chi = \Delta \chi = \Delta^2 \chi = \Phi = \Delta \Phi = 0, \quad \frac{\partial \phi}{\partial \alpha_1} = 0 \quad \text{at} \quad \alpha_1 = L_i(\alpha_2). \quad (10)$$

It may be seen from Eqs. (5), (6), (10) that the function ϕ is defined independently from χ and Φ . It has the sense of the edge integral which decreases rapidly far from the edges. So, in approximated calculations Eq. (5) may be eliminated, and the function ϕ should be set equal zero.

If $1/\beta \rightarrow 0$, then Eqs. (6) are reduced to the known equations

$$\begin{aligned} \frac{Eh^3}{12(1-\nu^2)} \Delta^2 w + \frac{1}{R_2(\alpha_2)} \frac{\partial^2 \Phi}{\partial \alpha_1^2} + \rho h \frac{\partial^2 w}{\partial t^2} &= 0, \\ \Delta^2 \Phi - \frac{Eh}{R_2(\alpha_2)} \frac{\partial^2 w}{\partial \alpha_1^2} &= 0 \end{aligned} \quad (11)$$

based on the classical Kirchhoff-Love hypotheses.

Equations (6) and (11) will be used in what follows for studying localized stationary and not-stationary vibrations of thin laminated and single layer shells, respectively.

3 Free Localized Vibrations of Thin Cylindrical Shells: Asymptotic Approach

The objective of this Section is to demonstrate the asymptotic method of Tovstik for studying free localized vibrations of thin elastic shells of the zeroth Gaussian curvature (Tovstik 1983a). As opposed to the complex WKB method or Maslov-WKB method (Maslov 1977) developed earlier for constructing localized solutions of the quantum mechanics equations, this approach is based on the presentation of the phase function in the WKB approximation in an explicit form and reduction of the initial two-dimensional boundary-value problem to a sequence of one-dimensional problems being considered at a fixed generatrix called the weakest one.

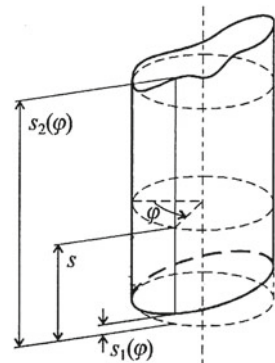
3.1 Statement of a Problem

We consider an elastic one-layered thin non-circular medium length cylindrical shell of thickness h . Let ρ be the density, E Young's modulus, and ν Poisson ratio of the material. A dimensionless coordinates $s = \alpha_1/R$, $\varphi = \alpha_2/R$ as illustrated in Fig. 2 are chosen at the middle surface of the cylinder. The radius of curvature is $R_2 = R/k(\varphi)$, where R is the characteristic dimension of the shell surface.

Up to values of the order h_* , low frequency free vibrations of the medium-length thin cylinder may be governed by Eqs. (11). In the dimensionless form these equations are rewritten as follows:

$$\begin{aligned} \varepsilon^4 \Delta^2 W + k(\varphi) \Phi_{,ss} - \lambda W &= 0, \\ \varepsilon^4 \Delta^2 \Phi - k(\varphi) W_{,ss} &= 0. \end{aligned} \tag{12}$$

Fig. 2 Neutral surface of thin cylindrical shell with non-plane edges and coordinate system



where $\Delta = (\cdot)_{,\varphi\varphi} + (\cdot)_{,ss}$, $\varepsilon = \{h^2/[12R^2(1 - \nu^2)]\}^{1/8}$ is a small parameter, $\lambda = R^3\rho(Eh)^{-1}[(12(1 - \nu^2))]^{1/2}\omega^2$ is the frequency parameter, ω is the natural frequency, and $W = w/R$, $\Phi = F/(\varepsilon^4 R^2 Eh)$ are the dimensionless magnitudes.

We will consider two variants of boundary conditions at both edges, namely:

$$\begin{aligned} W = W_{,ss} = 0 & \quad \text{for the joint supported edges } s = s_j(\varphi), \\ W = W_{,s} = 0 & \quad \text{for the rigid clamped edges } s = s_j(\varphi), \end{aligned} \quad (13)$$

where $s_j(\varphi) = L_j(\alpha_2/R)$, $j = 1, 2$.

The problem is to find positive values of λ for which the boundary-value problem (12), (13) has nontrivial solutions. It may be seen that in the common case this problem does not admit an explicit form of a solution. To solve it we will follow the idea stated by Tovstik (1983a).

Let $\varphi = \varphi_0$ be the weakest generator which is the center of more extensive localized vibrations. The position of this line on the shell surface is unknown.

We change the periodic conditions in the circumferential direction φ for the following ones

$$|W|, |\Phi| \rightarrow 0 \quad \text{as } |\varphi - \varphi_0| \rightarrow \infty. \quad (14)$$

3.2 Asymptotic Method of Tovstik

The formal asymptotic solution of the boundary-value problem (12)–(14) is assumed to be in the form of (Tovstik 1983a)

$$\begin{aligned} W(s, \varphi, \varepsilon) &\cong w_* \exp\{i[\varepsilon^{-1/2}p\xi + (1/2)b\xi^2]\}, \\ i = \sqrt{-1}, \quad w_* &= \sum_{j=0}^{\infty} \varepsilon^{j/2} w_j(s, \xi), \\ \lambda &= \lambda_0 + \varepsilon\lambda_1 + \varepsilon^2\lambda_2 + \dots, \\ \xi &= \varepsilon^{-1/2}(\varphi - \varphi_0), \quad \lambda_j, p, |b|, |w_j| \sim 1, \quad \text{Im}b > 0. \end{aligned} \quad (15)$$

where $w_j(s, \xi)$ are polynomials in ξ , the value of parameter p which determines the number of waves in the direction of φ is real, and a parameter b characterizes the rate of decrease of the wave amplitudes when going away from the weakest generatrix $\varphi = \varphi_0$. The function Φ is sought in the same form as (15), where W , w_* , w_j are replaced by Φ , Φ_* , Φ_j , respectively.

Otherwise, solutions of type (15) are called the complex WKB approximations.

To determine unknown functions w_j , Φ_j and parameters p , b , φ_0 , λ_j , we substitute ansatz (15) into system (12) and equalize the coefficients by the same powers of $\varepsilon^{1/2}$. All the coefficients of Eqs. (12) and functions s_j depending on φ are expanded in a power series of $\varphi - \varphi_0 = \varepsilon^{1/2}\xi$.

First, it is convenient to express Φ_* through w_* by virtue of second Eq. (12):

$$\begin{aligned} \Phi_* = & -\Delta_s \left[\frac{w_*}{p^4} - \frac{4\varepsilon^{1/2}}{p^5} \left(b\xi w_* - i \frac{\partial w_*}{\partial \xi} \right) \right. \\ & \left. + \frac{10\varepsilon}{p^6} \left(b^2 \xi^2 w_* - 2ib\xi \frac{\partial w_*}{\partial \xi} - ibw_* - \frac{\partial^2 w_*}{\partial \xi^2} \right) \right] + O(\varepsilon^{3/2}) \end{aligned}$$

with

$$\Delta_s = s^3 \frac{\partial^2}{\partial s^2}.$$

Now, taking into account the foregoing equation, the first equation of (12) gives the sequence of differential equations with respect to w_j , which may be written in the form

$$\mathbf{L}_0 w_0 = 0, \mathbf{L}_0 w_1 + \mathbf{L}_1 w_0 = 0, \mathbf{L}_0 w_2 + \mathbf{L}_1 w_1 + \mathbf{L}_2 w_0 = 0, \dots \quad (16)$$

where

$$\begin{aligned} \mathbf{L}_0 z &= \frac{k^2(\varphi_0)}{p^4} \frac{d^4 z}{ds^4} + (p^4 - \lambda_0)z = 0, \\ \mathbf{L}_1 z &= \left(b \frac{\partial \mathbf{L}_0}{\partial p} + \frac{\partial \mathbf{L}_0}{\partial \varphi_0} \right) \xi z - i \frac{\partial \mathbf{L}_0}{\partial p} \frac{\partial z}{\partial \xi}, \\ \mathbf{L}_2 z &= \frac{1}{2} \left(b^2 \frac{\partial^2 \mathbf{L}_0}{\partial p^2} + 2b \frac{\partial^2 \mathbf{L}_0}{\partial p \partial \varphi_0} + \frac{\partial^2 \mathbf{L}_0}{\partial \varphi_0^2} \right) \xi^2 z - \frac{1}{2} \frac{\partial^2 \mathbf{L}_0}{\partial p \partial \varphi_0} z \\ &\quad - \frac{1}{2} \frac{\partial^2 \mathbf{L}_0}{\partial p^2} \left(iz + \frac{\partial^2 z}{\partial \xi^2} \right) - i \left(b \frac{\partial^2 \mathbf{L}_0}{\partial p^2} + \frac{\partial^2 \mathbf{L}_0}{\partial p \partial \varphi_0} \right) \xi \frac{\partial z}{\partial \xi} + \mathbf{N}z \end{aligned} \quad (17)$$

with

$$\mathbf{N} = -\lambda_1.$$

The substitution of ansatz (15) into the boundary conditions produces the sequence of the boundary conditions for w_j . For instance, for the simply supported edges $s = s_j(\varphi_0)$, it is as follows:

$$\begin{aligned} w_0 = 0, \quad \frac{\partial^2 w_0}{\partial s^2} = 0, \\ w_1 + \xi s'_i \frac{\partial w_0}{\partial s} = 0, \quad \frac{\partial^2 w_1}{\partial s^2} + \xi s'_i \frac{\partial^3 w_0}{\partial s^3} = 0, \\ w_2 + \xi s'_i \frac{\partial w_1}{\partial s} + \frac{1}{2} \xi^2 \left(s''_i \frac{\partial w_0}{\partial s} + s'^2_i \frac{\partial^3 w_0}{\partial s^3} \right) = 0, \\ \frac{\partial^2 w_2}{\partial s^2} + \xi s'_i \frac{\partial^3 w_1}{\partial s^3} + \frac{1}{2} \xi^2 \left(s''_i \frac{\partial^3 w_0}{\partial s^3} + s'^2_i \frac{\partial^4 w_0}{\partial s^4} \right) - \frac{4is'_i}{p} \frac{\partial^3 w_0}{\partial s^3} = 0, \dots \end{aligned} \quad (18)$$

The prime ()' means differentiation of $s_i(\varphi)$ with respect to φ .

Note that Eqs. (18) guarantee a realization of the boundary conditions merely in the small vicinity of the weakest generator $s = s_i(\varphi_0)$. However, there is no sense to satisfy the boundary conditions on the entire surface of the shell.

The sequence of one-dimensional boundary-value problems (16), (18) serves to determine unknown functions $w_j(s, \xi)$ and parameters λ_j, p, b . The details of seeking these magnitudes are omitted here (see Tovstik 1983a; Mikhasev and Tovstik 2009). We will outline here only principle equations.

Let us consider the boundary-value problems (16), (18) step-by-step for $j = 0, 1, 2, \dots$. We will call these problems as BVP0, BVP1, BVP2, ...

Zerth order approximation (BVP0). In the zeroth order approximation, one has the homogeneous equation

$$\mathbf{L}_0 w_0 \equiv \frac{k^2(\varphi_0)}{p^4} \frac{d^4 w_0}{ds^4} + (p^4 - \lambda_0) w_0 = 0 \quad (19)$$

with the homogeneous boundary conditions

$$w_0 = 0, \quad \frac{d^2 w_0}{ds^2} = 0 \quad \text{at } s = s_i(\varphi_0). \quad (20)$$

Its solution may be presented in the form

$$w_0(s, \xi) = P(\xi) w^\circ(s, \varphi_0; p), \quad (21)$$

where w° is any solution of Eq. (19), and $P(\xi)$ is an unknown polynomial in ξ .

Substituting Eq. (21) into Eq. (19) results in the relation for the parameter

$$\lambda_0 = f(p, \varphi_0, m) \equiv p^4 + \frac{2\delta^4 m^4 k^2(\varphi_0)}{p^4 l^4(\varphi_0)}, \quad (22)$$

where $l(\varphi_0) = s_2(\varphi_0) - s_1(\varphi_0)$, and m is a natural number. The parameter δ depends on the variant of boundary conditions. For instance, if both edges are simply supported, then $\delta = \pi$, and for the clamped edges $\delta = 4.730$.

We will study low-frequency vibrations. Then $m \sim 1$, and $m = 1$ corresponds to the minimum eigenfrequency. Minimizing function (22), one gets

$$\lambda_0^\circ = \min_{p, \varphi_0, m} f(p, \varphi_0, m) = f(p^\circ, \varphi_0^\circ, 1) = \frac{2\delta^4 k(\varphi_0^\circ)}{l^2(\varphi_0^\circ)}, \quad (23)$$

where the parameter $p^\circ = \sqrt[4]{\lambda_0^\circ/2}$ and the weakest line $\varphi = \varphi_0^\circ$ are found from the following equations

$$\frac{\partial \lambda_0}{\partial p} = 0, \quad \frac{\partial \lambda_0}{\partial \varphi_0} = 0. \quad (24)$$

The last equation in (24) is reduced to

$$\left[\frac{k(\varphi_0)}{l^2(\varphi_0)} \right]' = 0.$$

Then $w_0 = P_0(\xi)w^\circ(s, \varphi_0^\circ; p^\circ)$ in what follows, where the polynomial $P_0(\xi)$ remains unknown in this approximation.

First order approximation (BVP1). In the first order approximation, one has the non-homogeneous differential Eq. (16). Taking into account the solution of the boundary-value problem in the previous step, this equation is as follows

$$\begin{aligned} \mathbf{L}_0 w_1 + G_1 &= 0, \\ G_1 &= [b\xi P_0(\xi) - iP'_0(\xi)] \frac{\partial \mathbf{L}_0}{\partial p} w^\circ + \xi P_0(\xi) \frac{\partial \mathbf{L}_0}{\partial \varphi_0} w^\circ. \end{aligned} \tag{25}$$

The appropriate boundary conditions at $s = s_i(\varphi_0)$ are

$$w_1 + \xi P_0(\xi) s'_i(\varphi_0^\circ) \frac{dw^\circ}{ds} = 0, \quad \frac{d^2 w_1}{ds^2} + \xi P_0(\xi) s'_i(\varphi_0^\circ) \frac{d^3 w^\circ}{ds^3} = 0. \tag{26}$$

We have got the non-homogeneous boundary-value problem **BVP1** (25), (26) “on spectrum”. Taking into account the self-conjugancy of the BVP0, the equality

$$\int_{s_1}^{s_2} w^\circ G_1 ds = 0 \tag{27}$$

serves as the condition for existence of a solution of the BVP1.

The function G_1 is defined by the operators $\frac{\partial \mathbf{L}_0}{\partial p}, \frac{\partial \mathbf{L}_0}{\partial \varphi_0}$ (see Eq. (17)). To define these operators, the BVP0 should be differentiated over the parameters p, φ_0 . For example,

$$\begin{aligned} \mathbf{L}_0 w_p + \frac{\partial \mathbf{L}_0}{\partial p} w^\circ - \frac{\partial \lambda_0}{\partial p} w^\circ &= 0, \\ w_p = \frac{\partial^2 w_p}{\partial s^2} &= 0 \quad \text{at } s = s_j(\varphi_0). \end{aligned} \tag{28}$$

Taking into account the self-conjugancy of the BVP0, one has

$$\begin{aligned} \int_{s_1}^{s_2} w^\circ \mathbf{L}_0 w_p ds &= \int_{s_1}^{s_2} w_p \mathbf{L}_0 w^\circ ds = 0, \\ \int_{s_1}^{s_2} w^\circ \mathbf{L}_0 w_\varphi ds &= \int_{s_1}^{s_2} w_\varphi \mathbf{L}_0 w^\circ ds = 0. \end{aligned} \tag{29}$$

Then, due to Eqs. (25), (28) and (29), condition (27) may be rewritten as follows:

$$\left\{ [b\xi P_0(\xi) - iP'_0(\xi)] \frac{\partial \lambda_0}{\partial p} + \xi P_0(\xi) \frac{\partial \lambda_0}{\partial \varphi_0} \right\} \int_{s_1}^{s_2} (w^\circ)^2 ds = 0. \tag{30}$$

Because

$$\int_{s_1}^{s_2} (w^\circ)^2 ds \neq 0$$

and $P_0(\xi)$ is a polynomial in ξ , Eq. 30 implies the known conditions (24) derived above.

Now, the solution of the BVP1 may be written as follows:

$$w_1 = P_1(\xi)w^\circ + \xi P_0(\xi)(bw_p + w_\varphi) - iP'_0(\xi)w_p,$$

where w_p, w_φ are solutions of the boundary-value problem (28) and similar problem for w_φ , and $P_1(\xi)$ is an unknown polynomial in ξ .

Second order approximation (BVP2). In the second order approximation, the non-homogeneous boundary-value problem (16), (18) arises again. The compatibility conditions for this problem may be deduced from the equation

$$\int_{s_1}^{s_2} w^\circ \{ \mathbf{L}_1 [P_1(\xi)w^\circ + \xi P_0(\xi)(bw_p + w_\varphi) - iP'_0(\xi)w_p] + \mathbf{L}_2 P_0 w^\circ \} ds = 0. \tag{31}$$

Omitting details for calculation of operators

$$\frac{\partial^2 \mathbf{L}_0}{\partial p^2}, \frac{\partial^2 \mathbf{L}_0}{\partial \varphi^2}, \frac{\partial^2 \mathbf{L}_0}{\partial p \partial \varphi}$$

appearing in \mathbf{L}_2 , we reduce relation (31) to the following differential equation with respect to the polynomial $P_0(\xi)$:

$$\mathcal{L}P_0 \equiv -\frac{1}{2}f_{pp}P_0'' - i(bf_{p\varphi} + f_{p\varphi}) \left(\xi P_0' + \frac{1}{2}P_0 \right) - \lambda_1 P_0 + c\xi^2 P_0 = 0, \tag{32}$$

where

$$2c = b^2 f_{pp} + 2b f_{p\varphi} + f_{\varphi\varphi}.$$

Condition $c = 0$ is necessary for the existence of a polynomial form solution of Eq. (32). From the square equation $c = 0$ we find the unique value of b such that $\text{Im}b > 0$:

$$b = (-f_{p\varphi} + ir)/f_{pp}, \quad r = \sqrt{d}, \quad d = f_{pp}f_{\varphi\varphi} - (f_{p\varphi})^2. \tag{33}$$

It may be seen from Eq. (33) that inequality $\text{Im}b > 0$ is valid if inequalities $f_{pp} > 0$ and $d > 0$ hold simultaneously.

For $c = 0$ and

$$\lambda_1 = \lambda_1^{(n)} = \left(n + \frac{1}{2}\right)r, \quad n = 0, 1, 2, \dots \tag{34}$$

Eq. (32) has the solution

$$P_0(\xi) = \mathcal{H}_n(\zeta), \quad \zeta = \sqrt{\frac{r}{f_{pp}}}\xi, \tag{35}$$

where \mathcal{H}_n are n th degree Hermite polynomials.

Higher approximations. The following approximations may be constructed in a similar way. We note that $w_j(s, \xi)$ are either even or odd polynomials in ξ . The existence conditions for w_{2j+2} give

$$\mathcal{L}P_{2j} + \lambda_j P_0 + \mathcal{F}_{2j}(\xi) = 0, \quad j > 0, \tag{36}$$

where \mathcal{L} is the operator in the left side of Eq. (32) at $c = 0$, and $\mathcal{F}_{2j}(\xi)$ is expressed in terms of the polynomials $P_{2j-1}, P_{2j-2}, \dots$ found in the previous steps.

The value λ_j is found from the existence conditions for polynomial form solution of (36). If the polynomials P_j are even, then the polynomials P_{j+1} and \mathcal{F}_{k+1} are odd and vice-versa.

In fact, the values of $\lambda_j (j \geq 2)$ are not found here because they depend on the terms which were omitted in the governing equations for cylindrical shells.

Natural frequencies and modes. Finally, the asymptotic equation for the set of the eigenvalues is obtained as follows

$$\lambda^{(m,n)} = \lambda_0^{(m)} + \varepsilon r \left(n + \frac{1}{2}\right) + O(\varepsilon^2), \quad n = 0, 1, 2, \dots \tag{37}$$

where m is the number of semi-waves in the axial direction, and n is the degree of Hermite polynomial \mathcal{H}_n .

Separating the real and imaginary parts in (15) we find that each eigenvalue (37) is asymptotically double. One of the natural modes has the form

$$\begin{aligned}
 w &= w_* \cos z \exp \left\{ -\frac{1}{2} \text{Im} b \xi^2 \right\}, \\
 w_*(s, \xi; \varepsilon) &= \left\{ \mathcal{H}_n \left[\sqrt{r f_{pp}^{-1}} \xi \right] w^\circ(s) + O(\varepsilon^{1/2}) \right\}, \\
 z &= \varepsilon^{-1/2} p^\circ \xi + \frac{1}{2} \text{Re} b \xi^2 + \varrho, \quad \xi = \varepsilon^{-1/2} (\varphi - \varphi_0),
 \end{aligned}
 \tag{38}$$

where ϱ is the initial phase. The method used here does not permit the determination of $\varrho = \text{const}$ which is equal to $0 \leq \varrho_1, \varrho_2 < 2\pi$.

3.3 Examples

Example 3.3.1 We consider a circular cylindrical shell with a slanted edge (see Fig. 3). Here

$$k = 1, s_1 = 0, s_2(\varphi) = l_0 + (\cos \varphi - 1) \tan \beta.$$

Then the longest generatrix $\varphi = \varphi_0^\circ = 0$ will be the weakest one.

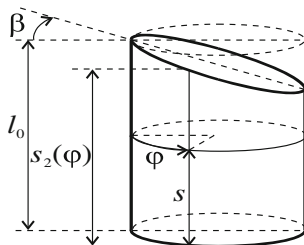
Let both edges be simply supported. Then the calculations give the formula for the first set (with one semi-wave $m = 1$ in the axial direction) of the natural frequencies:

$$(\omega^{(n)})^2 = \frac{\pi^2 E h}{\rho R L^2 \sqrt{3(1 - \nu^2)}} \left[1 + 4\varepsilon \left(n + \frac{1}{2} \right) \sqrt{\frac{2 \sin \beta}{\pi}} + O(\varepsilon^2) \right].$$

The pattern of the even (with respect to the line $\varphi = 0$) eigenmode is shown in Fig. 4.

Example 3.3.2 Consider a non-circular cylindrical shell of the constant generatrix length having the elliptic cross-section with semi-axes a_0 and b_0 ($a_0 < b_0$) (see Fig. 5). The ellipse curvature is the function

Fig. 3 Circular cylindrical shell with slanted edge



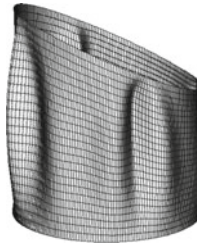


Fig. 4 Pattern of even eigenmode

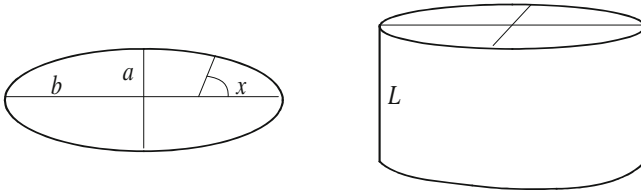


Fig. 5 Elliptical cylindrical shell

$$k(x) = \frac{dx}{d\varphi} = e^{-2}(\sin x^2 + e^2 \cos x^2)^{3/2}, \quad e = \frac{b_0}{a_0}.$$

Here, there are two the weakest lines $x = \pi/2$ and $x = 3\pi/2$ where the curvature $k(x)$ has the minimum value. In this case the naturel frequencies are asymptotically fourfold. Let the shell edges $s = 0, L$ be simply supported. Then, for these close frequencies the following common asymptotic formula is valid:

$$\lambda^{(n)} = \frac{2}{e^2} \left[1 + \varepsilon_0 \sqrt{\frac{48(e^2 - 1)}{e^3}} \left(n + \frac{1}{2} \right) + O(\varepsilon_0^2) \right], \quad n = 0, 1, 2, \dots,$$

where

$$\varepsilon_0^8 = \frac{h^2 L^4}{12(1 - \nu^2) a_0^6}$$

is a new small parameter.

Similar problems on free low-frequency localized vibrations of a thin medium-length cylindrical shell taking into account viscoelastic properties have been studied in paper (Mikhasev 1992).

4 On Localized Eigenmodes of Thin Laminated Shell Containing Magnetorheological Elastomer

4.1 Motivation

Thin composite laminated shells have a wide range of applications in many engineering structures (airborne/spaceborne vehicles, underwater objects, cars, etc.) Applying materials with different properties one can design sandwich structures fulfilling many requirements. One of up-to-date requirements is the noiselessness of similar structures. The vibroprotection is of great practical interest for mechanical engineers developing and modeling thin-walled vehicles. The appearance of new multifunctional composite materials with active and adaptive properties (so-called smart materials) opens new possibilities (Deng and Gong 2008; Gibson 2010). Some of them are magnetorheological (MR) composites and, particularly, magnetorheological elastomers (MREs). They belong to the group of active materials which physical properties such as viscosity and shear modulus can vary when subjected to different magnetic field levels (Ginder et al. 2001; Farshad and Benine 2004; Sorokin et al. 2014). It is expected that MREs embedded between elastic layers will provide for a sandwich a wide range of rheological properties which may be controlled rapidly by the application of an external magnetic field (Yancheng et al. 2014).

What is the MRE? This is a composite material composed of magnetizable particles molded in either rubbery polymers or deformed inorganic polymer matrices (Farshad and Benine 2004). The properties of MREs depend on its components. The optimum weight/density ratio of magnetic particles, carrier viscous liquid and polymer determines shear modulus and viscosity of smart materials (Ginder et al. 2001; Korobko et al. 2012). The basic ones, revealed in above and many other papers, are the following: increasing the magnetic field intensity leads to the ordering of magnetic particles in the matrix and finally results in increasing both the storage and the loss moduli, G'_{MR} and G''_{MR} (the real and imaginary parts of the complex shear modulus G_{MR} , respectively).

Properties of MRE show also a strong dependence on the manufacturing technology. If samples are embedded into sandwich mold and cooled down to room temperature without acting magnetic field, one gets a sandwich without preferred orientation (the iron particles are distributed in a chaotic manner). On the contrary, if the polymerization reaction is carried out in an external homogeneous magnetic field, then MRE becomes highly polarized (Korobko et al. 2009) and has anisotropic properties (Stepanov et al. 2007). In polarized MREs, the magnetizable particles align into the directions of the force lines of a magnetic field. Experimental research by Boczkowska et al. (2012) has revealed a specific property of polarized MREs: the maximum increase in the storage modulus G'_{MR} under homogeneous magnetic field action strongly depends on the particles arrangement within the matrix with respect to the magnetic field. So, studying the urethane MRE consisting of carbonyl-iron particles in a polyurethane matrix, it was found out (Boczkowska et al. 2012) that the maximum value of the modulus $G'_{MR} = 0.5$ MPa corresponded to samples

with particles orientated at 30° with respect to the lines of magnetic field, whereas the minimum magnitude $G'_{MR} = 0.1$ MPa did to samples with angle 90° between the magnetic force lines and the particle alignment. Thus, even through the magnetic field is uniform, its impact on different parts of the polarized MRE may differ considerably.

Recently, based on properties of polarized MREs, we have analysed (Mikhasev et al. 2014) the influence of a magnetic field on eigenmodes of thin laminated cylindrical shells containing a polarized MRE. Motivated by these study, we aim to demonstrate in this Section that an applied magnetic field may lead to localization of eigenmodes in a thin cylindrical sandwich containing the MRE-core.

4.2 Setting a Problem

We consider a thin non-circular laminated cylindrical shell consisting of N transversely isotropic layers, where N is an odd number (see Fig. 1). All notations of the geometrical and physical parameters are the same as in Sect. 2. Let the layers with the odd numbers be made of elastic material which is not affected by external magnetic field, and the layers with the even numbers be fabricated from a MRE. For elastic layers the Young's and shear moduli E_k and G_k are real constants for any k , and for the viscoelastic layers made from MRE these parameters are assumed to be complex functions (1) depending on the magnetic field induction B .

In our study we consider the polarized MRE consisting of a deformed polymer matrix prepared from bentonite clay and synthetic oil, and carbonyl iron particles having a size about $20\mu\text{m}$. The properties of this elastomer at different levels of applied magnetic field have been described by Korobko et al. (2012). As shown in paper (Mikhasev et al. 2011), in the pre-yield regime at $B < 200$ mT, the following linear approximations

$$\begin{aligned} E'_{MR} &= 13.230 + 45.040B, & E''_{MR} &= 50.000 + 10.920B, \\ G'_{MR} &= 4.500 + 14.978B, & G''_{MR} &= 17.000 + 3.680B \end{aligned} \quad (39)$$

are valid for this MRE with $\nu_{MR} = 0.4$.

Let the shell be under action of the uniform magnetic field whose the force lines have different angels with the alignment of magnetic particles in the polarized MRE. Then, as follows from experimental research by Boczkowska et al. (2012), the impact of the magnetic field on different parts of the MRE-based layer will be distinct. In this case it is necessary to introduce the relation between the moduli G_{MR} , E_{MR} and the circumferential coordinate α_2 on the sandwich.

We consider Eqs. (6) as the governing ones, where all magneto-sensitive complex magnitudes ν , η_3 , E , θ , β are assumed to be functions of the circumferential coordinate α_2 . Let us introduce a small parameter

$$\varepsilon^8 = \frac{h_*^2 \eta_{3r}^{(0)}}{12[1 - (\nu_r^{(0)})^2]}, \quad (40)$$

and consider sufficiently thin shells for which parameter h_* is a quantity of the order ~ 0.01 or less. In Eq. (40) and below, the superscript (0) means that an appropriate parameter is calculated at $B = 0$. Here, $\eta_{3r} = \text{Re } \eta_3$, $\nu_r = \text{Re } \nu$, $\nu_r^{(0)} \approx 0.4$. It is assumed that the total thickness of the MR layers is not less than 70 % from the total thickness h of the sandwich. Then, as shown in paper (Mikhasev et al. 2014), the following asymptotic estimations

$$\begin{aligned} \nu &= \nu_r^{(0)}[1 + \varepsilon^4 \delta\nu(\varphi)], & \theta_r &\sim \varepsilon^3, & \theta_i &\sim \varepsilon^4, \\ \eta_3 &= \eta_{3r}^{(0)}[1 + \varepsilon^2 \delta\eta_3(\varphi)], & \eta_{3r}^{(0)} &= \pi^{-4} \eta_r^{(0)}[1 - (\nu_r^{(0)})^2], \\ E_r &= E_r^{(0)} d(\varphi) = E_r^{(0)}[1 + \varepsilon d_1(\varphi)], & E_i/E_r^{(0)} &\sim \varepsilon^4, \\ h_*^2 \beta^{-1} &= \varepsilon^2 \kappa(\varphi) = \varepsilon^2[\kappa_0(\varphi) + i\varepsilon \kappa_1(\varphi)] \end{aligned} \quad (41)$$

are valid at $\varepsilon \rightarrow 0$. In Eqs. (41), $\delta\nu$, $\delta\eta_3$ and d_1 , κ_0 , κ_1 are complex and real functions of an angle $\varphi = \alpha_2/R$, respectively, so that their absolute magnitudes are quantities of the order $O(1)$ at $\varepsilon \rightarrow 0$. For any geometrical parameters (chosen in such way that the above assumptions for the total thickness of the MR layers and h_* hold) and a fixed value of the induction B , these functions are easily calculated by Eqs. (9).

The solution of Eqs. (6) describing free vibrations are assumed to be of the form

$$\chi = \varepsilon^{-4} R \chi^*(s, \varphi) \exp(i\Omega t), \quad \Phi = E_r^{(0)} h R^2 \Phi^*(s, \varphi) \exp(i\Omega t), \quad (42)$$

where $s = \alpha_1/R$ is the dimensionless axial coordinate, Ω is an unknown complex natural frequency, and χ^* , Φ^* are dimensionless displacement and stress functions.

The substitution of Eqs. (42) into Eqs. (6) results in the differential equations

$$\begin{aligned} \varepsilon^4 d(\varphi) \Delta^2 \chi^* + k(\varphi) \frac{\partial^2 \Phi^*}{\partial s^2} - \lambda[1 - \varepsilon^2 \kappa(\varphi) \Delta] \chi^* &= 0, \\ \varepsilon^4 \Delta^2 \Phi^* - k(\varphi) \frac{\partial^2}{\partial s^2} [1 - \varepsilon^2 \kappa(\varphi) \Delta] \chi^* &= 0 \end{aligned} \quad (43)$$

written in the dimensionless form, where $k(\varphi) = R/R_2$ is the variable dimensionless curvature, and $\lambda = \rho R^2 \Omega^2 / (\varepsilon^4 E_r^{(0)})$ is the dimensionless frequency parameter. When deriving Eqs. (43) from Eqs. (6), we have omitted the operator $\Delta^3 \chi$ because of smallness of the coefficient $\theta h^2 \beta^{-1}$ and disregarded by very small dimensionless parameters $\varepsilon^4 \delta\nu$, $\varepsilon^2 \delta\eta_3$, $E_i/E_r^{(0)}$. It should be noticed that when studying low-frequency eigenmodes this simplification leads to an error of the order h_* which is

comparable with the error of Eqs. (6). In Eqs. (43), $\kappa = \kappa_0(\varphi) + \varepsilon i \kappa_1(\varphi)$ is the principle complex shear parameter depending on both a coordinate φ and the magnetic field induction B .

Let the shell will be simply supported. Then appropriate boundary conditions are as follows

$$\chi^* = \Delta \chi^* = \Delta^2 \chi^* = \Phi^* = \Delta \Phi^* = 0 \quad \text{at } s = 0, l, \tag{44}$$

where $l = L/R$.

We aim to study low-frequency free vibrations. Then the problem will be to find the minimum eigenvalue $\text{Re } \lambda$ for the boundary value problem (43), (44).

4.3 Asymptotic Solution

Due to the variability of both the parameters $\kappa(\varphi)$, $d(\varphi)$ and the curvature $k(\varphi)$, the boundary value problem (43), (44) does not admit a solution in the explicit form. Let y be any of the foregoing parameters depending on φ . It is assumed that $dy/d\varphi \sim y$ at $\varepsilon \rightarrow 0$. Then, under some additional conditions for the functions $\kappa_0(\varphi)$, $k(\varphi)$ (which will be specified below), the boundary value problem (43), (44) may have a solution localized in the neighbourhood of some generatrix $\varphi = \varphi_0$. Following the approach stated in Sect. 3, we will seek the solution of the boundary value problem (43), (44) in the following form

$$\begin{aligned} \chi^* &= \sin \frac{\pi ns}{l} \sum_{j=0}^{\infty} \varepsilon^{j/2} \chi_j(\xi) \exp \{i(\varepsilon^{-1/2} p \xi + 1/2 b \xi^2)\}, \\ \Phi^* &= \sin \frac{\pi ns}{l} \sum_{j=0}^{\infty} \varepsilon^{j/2} \Phi_j(\xi) \exp \{i(\varepsilon^{-1/2} p \xi + 1/2 b \xi^2)\}, \end{aligned} \tag{45}$$

$$\lambda = \lambda_0 + \varepsilon \lambda_1 + \dots,$$

where $\xi = \varepsilon^{-1/2}(\varphi - \varphi_0)$, p is the real wave parameter, b is the imaginary parameter so that $\text{Im } b > 0$, and χ_j , Φ_j are polynomials in ξ .

The functions $\kappa_0(\varphi)$, $\kappa_1(\varphi)$, $k(\varphi)$, $d_1(\varphi)$ are expanded into series in a neighbourhood of the generator $\varphi = \varphi_0$.

The procedure for seeking all unknown parameters and functions appearing in (45) are as stated in Sect. 3. Omitting its details, we outline only the principal equations here. The substitution of (45) into (43) produces the sequence of algebraic equations

$$\sum_{j=0}^{\varsigma} \mathbf{L}_j \mathbf{X}_{\varsigma-j}^T, \quad \varsigma = 0, 1, 2, \dots, \tag{46}$$

where $\mathbf{X}_j = (\chi_j, \Phi_j)$ are two-dimensional vectors, the superscript T denotes a transposition, and \mathbf{L}_0 is the 2×2 matrix with the elements

$$l_{11} = p^4 - \lambda_0[1 + \kappa_0(\varphi_0)p^2], \quad l_{12} = -k(\varphi_0)\pi^2 n^2 l^{-2},$$

$$l_{21} = k(\varphi_0)[1 + \kappa_0(\varphi_0)p^2]\pi^2 n^2 l^{-2}, \quad l_{22} = p^4,$$

and the matrix operators \mathbf{L}_j for $j \geq 1$ are expressed by the matrix \mathbf{L}_0 by Eqs. (17), where

$$\mathbf{N} = \lambda_1 + i\lambda_0 \frac{\kappa_1(\varphi_0)p^2}{1 + \kappa_0(\varphi_0)p^2} - d_1(\varphi_0)p^4.$$

Considering the homogeneous system (46) at $\varsigma = 0$, one obtains

$$\Phi_0 = -\frac{g_n^{1/2}(\varphi_0)}{p^4}[1 + p^2\kappa_0(\varphi_0)], \quad (47)$$

$$\lambda_0 = f(p, \varphi_0) = \frac{g_n(\varphi_0)}{p^4} + \frac{p^4}{1 + \kappa_0(\varphi_0)p^2}, \quad (48)$$

where $g_n(\varphi_0) = \pi^4 n^4 l^{-4} k^2(\varphi_0)$. It may be seen from (47) that $p \neq 0$. The compatibility condition for system (46) at $\varsigma = 1$ implies the equations

$$f_p = 0, \quad f_\varphi = 0, \quad (49)$$

which may be rewritten as follows

$$\kappa_0(\varphi_0)p^{10} + 2p^8 - 2g_n(\varphi_0)\kappa_0^2 p^4 - 4g_n(\varphi_0)\kappa_0 p^2 - 2g_n(\varphi_0) = 0, \quad (50)$$

$$g'_n(\varphi_0)[1 + \kappa_0(\varphi_0)p^2] - p^{10}\kappa'_0(\varphi_0) = 0, \quad (51)$$

where the subscripts p, φ denote the partial derivatives of the function with respect to the corresponding variables p, φ_0 , and the prime (') means differentiation with respect to φ_0 . These equations allow to find the wave number p° and the weakest generator $\varphi_0 = \varphi_0^\circ$. Finally, the compatibility condition for system (46) at $\varsigma = 2$ yields the following equations

$$f_{pp}b^2 + 2f_{p\varphi}b + f_{\varphi\varphi} = 0, \quad (52)$$

$$\lambda_1 = -i(m + 1/2)(f_{pp}b + f_{p\varphi}) - i\lambda_0 \frac{p^2\kappa_1(\varphi_0)}{1 + \kappa_0(\varphi_0)p^2} + p^4 d_1(\varphi_0), \quad (53)$$

$$\chi_0 = \mathcal{H}_m(z), \quad z = [f_{\varphi\varphi}f_{pp}^{-1} - f_{p\varphi}f_{pp}^{-1}]^{1/4}\zeta, \quad (54)$$

where $\mathcal{H}_m(z)$ is the Hermitian polynomial of the m th degree. In Eqs. (52)–(54), the second derivatives of f with respect to p and φ_0 are calculated at $p = p^\circ, \varphi_0 = \varphi_0^\circ$.

Equation (52) is used for definition of b . It may be seen that the inequality $\text{Im}b > 0$ holds if the second differential of the function f at point $p = p^\circ$, $\varphi_0 = \varphi_0^\circ$ is a positive definite quadratic form, i.e.

$$d^2f = f_{pp}^\circ dp^2 + 2f_{p\varphi}^\circ dpd\varphi_0 + f_{\varphi\varphi}^\circ d\varphi_0^2 > 0. \quad (55)$$

The superscribe $^\circ$ denotes that the function f and its partial derivatives are calculated at $p = p^\circ$, $\varphi_0 = \varphi_0^\circ$. The conditions (49), (55) indicate that only eigenmodes corresponding to the lowest spectrum are considered here.

In Eq. (53), the second term containing parameter κ_1 is the frequency correction taking into account viscoelastic properties of MRE at different levels of magnetic field. For the inequality (55) to be hold, a solution of Eq. (50) should be chosen in such a way that $f_{pp}^\circ = f_{pp}(p^\circ, \varphi_0^\circ) > 0$.

4.4 Circular Cylinder with Nonuniform Physical Properties of the MR Layer

Now we consider an example that demonstrates how magnetic field can skew eigenmodes of a shell consisting the MR layers. Let all geometrical parameters of the cylindrical shell to be constant, but the magnetorheological properties of the MRE composing the sandwich are nonuniform in the circumferential direction. Here $k \equiv 1$, and κ_0 , κ_1 , d_1 are functions of φ . Similar inhomogeneity of the elastic and viscoelastic parameters may be observed if the magnetic field is spatially nonuniform or/and the MRE embedded in between the elastic layers is polarized and the angle between the magnetic force lines and the alignment of magnetic particles depends on a coordinate φ .

Here, as follows from Eqs. (51), (55), the weakest generator $\varphi = \varphi_0^\circ$ is the one at which the reduced shear parameter κ_0 approaches the maximum:

$$\kappa_0'(\varphi_0^\circ) = 0, \quad \kappa_0''(\varphi_0^\circ) < 0.$$

Then Eqs. (48), (52), (53) result in the following equations for the natural frequency, damping ratio and parameter b° :

$$\begin{aligned} \omega &= \text{Re}\Omega = \omega_c \omega^*, \quad \alpha = \text{Im}\Omega = \omega_c \alpha^*, \\ \omega^* &= (f^\circ)^{1/2} + \frac{\varepsilon}{2(f^\circ)^{1/2}} \left[\frac{(1+2m)(p^\circ)^3 \sqrt{-f_{pp}^\circ \kappa_0''(\varphi_0^\circ)}}{2[1+(p^\circ)^2 \kappa_0(\varphi_0^\circ)]} + d_1(\varphi_0^\circ)(p^\circ)^4 \right], \quad (56) \\ \alpha^* &= -\frac{\varepsilon(f^\circ)^{1/2} \kappa_1(\varphi_0^\circ)(p^\circ)^2}{2[1+\kappa_0(\varphi_0^\circ)(p^\circ)^2]}, \quad b^\circ = \frac{i(p^\circ)^3}{1+(p^\circ)^2 \kappa_0(\varphi_0^\circ)} \sqrt{-\frac{\kappa_0''(\varphi_0^\circ)}{f_{pp}^\circ}}, \end{aligned}$$

where $\omega_c = \varepsilon^2 R^{-1} (E_r(0)_r / \rho)^{1/2}$ is the characteristic frequency.

Tables 1 and 2 show the dependence of the parameters p° , ω_0^* , ω^* , α^* and $\text{Im } b^\circ$ on the induction B for the three-layered cylinder with the external layers made of ABS-plastic SD-0170 and the internal layer fabricated of MRE. The calculations have been performed at $n = 1$ for the parameters $R = 1$ m, $L = 1.5$ m, $h_1 = h_3 = 0.5$ mm and thicknesses $h_2 = 8; 11$ mm of the MR layer. The parameter $\kappa_0''(\varphi_0^\circ)$ characterizing the variability of the reduced shear modulus in a neighborhood of the weakest generator $\varphi = \varphi_0^\circ$ has been taken as $\kappa_0'' = -1.5$ for both cases. This is the approximate magnitude estimated proceeding from the experimental data from (Boczkowska et al., 2012). The parameters $\kappa_0(\varphi_0^\circ)$, $\kappa_1(\varphi_0^\circ)$, $d_1(\varphi_0^\circ)$ were found from Eqs. (41), (9). When comparing the third and fourth columns (the parameters ω_0^* and ω^*) in both tables, one concludes that accounting inhomogeneity of the reduced shear parameter K may result in increasing the natural frequency up to 20 %. Increasing the level of the magnetic field from $B = 0$ to $B = 200$ mT leads to increasing the natural frequency ω^* up to 9 % (from $3.304\omega_c$ at $B = 0$ mT to $3.606\omega_c$ at $B = 200$ mT) and minor decreasing the number of waves in the circumferential direction (the parameter p°). The dependence of the damping ratio α^* upon the induction is more

Table 1 Parameters p° , ω_0^* , ω^* , α^* , $\text{Im } b^\circ$ for the circular cylinder with nonuniform physical properties versus the magnetic induction B at $h_2 = 8$ mm, $\varepsilon = 0.231$, $\omega_c = 13.828$ Hz

B , mT	p°	ω_0^*	ω^*	α^*	$\text{Im } b^\circ$
0	1.479	2.876	3.438	0.0025	0.498
25	1.471	2.898	3.472	0.0091	0.487
50	1.466	2.911	3.494	0.0107	0.480
75	1.463	2.919	3.511	0.0108	0.475
100	1.461	2.925	3.523	0.0104	0.472
125	1.459	2.930	3.534	0.0098	0.470
150	1.458	2.934	3.543	0.0093	0.468
175	1.457	2.936	3.552	0.0087	0.466
200	1.456	2.939	3.559	0.0082	0.465

Table 2 Parameters p° , ω_0^* , ω^* , α^* , $\text{Im } b^\circ$ for the circular cylinder with nonuniform physical properties versus the magnetic induction B at $h_2 = 11$ mm, $\varepsilon = 0.248$, $\omega_c = 13.704$ Hz

B , mT	p°	ω_0^*	ω^*	α^*	$\text{Im } b^\circ$
0	1.532	2.745	3.304	0.0133	0.573
25	1.494	2.837	3.436	0.0291	0.519
50	1.480	2.875	3.493	0.0266	0.499
75	1.472	2.895	3.527	0.0231	0.488
100	1.467	2.907	3.550	0.0201	0.481
125	1.464	2.916	3.568	0.0177	0.477
150	1.462	2.922	3.582	0.0157	0.474
175	1.460	2.927	3.595	0.0142	0.471
200	1.459	2.931	3.606	0.0129	0.469

complicated and appreciable. It is also influenced by the thickness h_2 of the MR layer. In our cases, for $h_2 = 8$ mm and $h_2 = 11$ mm, the best passive suppression of the eigenmodes takes place at $B = 75$ mT and $B = 25$ mT respectively. In particular, applying the magnetic field of the intensity $B = 75$ mT (at $h_2 = 8$ mm) gives the three-fold increase in the damping ratio. Decreasing the parameter $\text{Im } b^\circ$ when increasing the induction B indicates that applying the strong magnetic field results in some spreading of localized modes over the shell surface.

5 Localized Eigenmodes of a Sandwich Cylindrical Shell Prestressed by Axial Forces

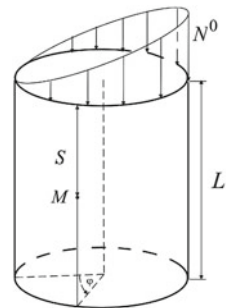
5.1 Setting a Problem

In this Section, we will study free localized vibrations of a thin, axially prestressed, circular cylindrical sandwich shell consisting of N transversely isotropic layers. The geometrical and physical characteristics of both the shell and layers are the same as in Sect. 2 (see Fig. 1). Let $s = \alpha_1/R$, $\varphi = \alpha_2/R$ be dimensionless coordinates at the neutral surface of the sandwich as shown in Fig. 6, where R is the radius of the middle surface. It is assumed that the simply supported edges are under action of the nonuniform axial forces $N^0(\alpha_2)$ (see Fig. 6).

To describe free vibrations of the axially prestressed laminated cylindrical shell, the following system of differential equations may be used:

$$\begin{aligned} & \frac{Eh^3\eta_3}{12(1-\nu^2)} \left(1 - \frac{\theta h^2}{\beta} \Delta\right) \Delta^2 \chi + \frac{1}{R} \frac{\partial^2 \Phi}{\partial \alpha_1^2} + T_1^0(\alpha_2) \frac{\partial^2 w}{\partial \alpha_1^2} \\ & \quad + \rho h \frac{\partial^2}{\partial t^2} \left(1 - \frac{h^2}{\beta} \Delta\right) \chi = 0, \\ & \Delta^2 \Phi - \frac{Eh}{R} \frac{\partial^2}{\partial \alpha_1^2} \left(1 - \frac{h^2}{\beta} \Delta\right) \chi = 0, \quad w = \left(1 - \frac{h^2}{\beta} \Delta\right) \chi. \end{aligned} \tag{57}$$

Fig. 6 Neutral surface of laminated cylinder and nonuniform axial forces



Here χ and Φ are the displacement and stress functions, respectively, h is the total thickness of the cylinder, E , ν are the reduced Young's modules and Poisson ratio for the whole sandwich, and θ , β , η_3 are parameters taking into account the transverse shears (see in Sect. 2). When comparing Eqs. (6) from Sect. 2 and the above equations, the first equation in (57) contains the additional term due to the axial stress resultant $T_1^\circ = N^0(\alpha_2)/R$.

In terms of the displacement and stress functions, the boundary conditions for simply supported edges are as follows:

$$\chi = \Delta\chi = \Delta^2\chi = \Phi = \Delta\Phi = 0. \quad (58)$$

To take into account the influence of shear parameters in the zeroth order approximation, we assume the following relations

$$\frac{K}{\pi^2} = \mu^2\kappa, \quad \frac{K\theta}{\pi^2} = \mu^3\tau, \quad \kappa, \tau \sim 1 \text{ as } \mu \rightarrow 0,$$

which are valid for sufficiently thin shell (Korchevskaya and Mikhasev 2006). Here

$$K = \frac{\pi^2 h^2}{R^2 \beta}, \quad \mu^4 = \frac{h^2 \eta_3}{12 R^2 (1 - \nu^2)}$$

Unknown functions χ and Φ are sought in the form

$$\begin{aligned} \chi &= R\hat{\chi}(s, \varphi) \sin \omega t, \\ \Phi &= \mu^2 E h R \hat{\Phi}(s, \varphi) \sin \omega t. \end{aligned}$$

Then Eqs. (57) can be rewritten as follows

$$\begin{aligned} \mu^4(1 - \mu^3\tau\Delta)\Delta^2\hat{\chi} + \mu^2\frac{\partial^2\hat{\Phi}}{\partial s^2} + \mu^2 t_1(\varphi)\frac{\partial^2}{\partial s^2}(1 - \mu^2\kappa\Delta)\hat{\chi} \\ - \Lambda(1 - \mu^2\kappa\Delta)\hat{\chi} = 0, \end{aligned} \quad (59)$$

$$\mu^2\Delta^2\hat{\Phi} - \frac{\partial^2}{\partial s^2}(1 - \mu^2\kappa\Delta)\hat{\chi} = 0,$$

where

$$l = \frac{L}{R}, \quad t_1(\varphi) = \frac{T_1^\circ(R\varphi)}{\mu^2 E h}, \quad \Lambda = \frac{R^2 \rho}{E} \omega^2,$$

and the boundary conditions for functions $\hat{\chi}$, $\hat{\Phi}$ will be:

$$\hat{\chi} = \Delta\hat{\chi} = \Delta^2\hat{\chi} = \hat{\Phi} = \Delta\hat{\Phi} = 0. \quad (60)$$

The problem is to find a positive value of Λ for which the system of Eqs. (59) has a nontrivial solution satisfying the boundary conditions (60). Due to the presence of the function $t_1(\varphi)$, this boundary-value problem does not have a solution in the explicit form. However, at some assumptions for the axial stress resultant, there exist eigenmodes which will be localized in a neighborhood of some generatrix.

5.2 Asymptotic Solution

A formal asymptotic solution of the boundary-value problem (59), (60) is constructed in the following form:

$$\hat{\chi} = \sin \frac{r_m S}{\mu} \chi_m(\xi, \mu), \tag{61}$$

$$\chi_m = \sum_{j=0}^{\infty} \mu^{j/2} \chi_{mj}(\xi) \exp \left[i \left(\mu^{-1/2} p \xi + \frac{1}{2} b \xi^2 \right) \right], \tag{62}$$

$$\Lambda = \Lambda_0 + \mu \Lambda_1 + \mu^2 \Lambda_2 + \dots$$

where $(\hat{\chi} \Rightarrow \hat{\Phi}, \chi_m \Rightarrow \Phi_m, \chi_{mj} \Rightarrow \Phi_{mj})$

$$\begin{aligned} \xi &= \mu^{-1/2}(\varphi - \varphi_0), \quad \text{Im} b > 0, \\ |\chi_{mj}|, |\Phi_{mj}|, \Lambda_j, p, |b|, r_m &= \frac{\mu \pi m}{l} \sim 1 \quad \text{as } \mu \rightarrow 0, \end{aligned} \tag{63}$$

and $\chi_{mj}(\xi), \Phi_{mj}(\xi)$ are polynomials in ξ . Here $\varphi = \varphi_0$ is a weakest generatrix which is unknown. Function (62) approximates the eigenmode localized in a vicinity of the line $\varphi = \varphi_0$.

The substitution of Eqs. (61), (62), (63) into the governing Eqs. (59) produces the sequence of algebraic equations:

$$\sum_{k=0}^j \mathbf{L}_k \mathbf{X}_{j-k} = 0, \quad j = 0, 1, 2, \dots \tag{64}$$

where $\mathbf{X}_j = (\xi_{mj}, \Phi_{mj})^T$, and \mathbf{L}_0 is the 2×2 matrix with the elements

$$\begin{aligned} l_{11} &= (r_m^2 + p^2)^2 - [1 + \kappa(r_m^2 + p^2)][r_m^2 t_1(\varphi_0) + \Lambda_0], \\ l_{12} &= -r_m^2, \quad l_{21} = r_m^2 [1 + \kappa(r_m^2 + p^2)], \quad l_{22} = (r_m^2 + p^2)^2, \end{aligned}$$

and the matrix operators \mathbf{L}_j for $j \geq 1$ are expressed by the matrix \mathbf{L}_0 in the same way as in Sect. 2 (see Eqs. (17)), but now the operator \mathbf{N} is 2×2 matrix with the unique nonzero element ($n_{12} = n_{21} = n_{22} = 0$):

$$n_{11} = \tau(r_m^2 + p^2)^3 - \Lambda_1[1 + \kappa(r_m^2 + p^2)].$$

The sequence of Eqs. (64) serves to determine all unknown functions and parameters appearing in (62), (63). Because the procedure for seeking these magnitudes are the same as in Sect. 2, we will omit transitional calculations and give here only the principle equations.

Considering the homogeneous system of algebraic Eqs. (64) for $j = 0$, one obtains the zeroth approximation for the frequency parameter:

$$\Lambda_0 = f(p, r_m, \varphi_0) = \frac{(r_m^2 + p^2)^2}{[1 + \kappa(r_m^2 + p^2)]} + \frac{r_m^4}{(r_m^2 + p^2)^2} - t_1(\varphi_0)r_m^2. \quad (65)$$

Holding a number m (and so, a parameter r_m) fixed, we will minimize the function (65) over p and φ . We have the following equations

$$\frac{\partial f}{\partial p} = 0, \quad \frac{\partial f}{\partial \varphi_0} = 0 \quad (66)$$

which serve for a determination of p° and φ_0° .

When solving Eqs. (66), three different cases appear:

- $r_m > z_0$ (case A)
- $r_m < z_0$ (case B)
- $r_m \approx z_0$, (case C)

where z_0 is a root of the algebraic equation

$$-2(1 + \kappa r_m z)^2 + z^4(2 + \kappa r_m z) = 0 \quad (67)$$

with respect to z .

Equation (67) contains a parameter κ which takes into account shears in the sandwich. If shears are disregarded ($\kappa = 0$), this root $z_0 = 1$.

At first we consider cases (A) and (B). For $r_m > z_0$ (case A), we derive

$$\Lambda_0^\circ = \min_{p, \varphi_0} f(p, r_m, \varphi_0) = 1 - t_1(\varphi_0^\circ)r_m^2 + \frac{r_m^4}{1 + \kappa r_m^2}, \quad p^\circ = 0, \quad (68)$$

and for $r_m < z_0$ (case B), one has

$$\Lambda_0^\circ = \min_{p, \varphi_0} f(p, r_m, \varphi_0) = \frac{z_0^2 r_m^2}{1 + \kappa r_m z_0} + \frac{r_m^2}{z_0^2} - t_1(\varphi_0^\circ)r_m^2, \quad (69)$$

$$p^\circ = \sqrt{r_m(z_0 - r_m)}.$$

Note that Eqs. (68), (69) are identical at $r_m = z_0$. For both cases the weakest generatrix $\varphi = \varphi_0^\circ$ is determined from the following conditions:

$$t_1'(\varphi_0^\circ) = 0, \quad t_1''(\varphi_0^\circ) < 0.$$

Now, a solution of the homogeneous system of Eqs. (64) at $j = 0$ may be written as

$$\mathbf{X}_0 = P_0(\xi)\mathbf{Y}_0,$$

where $P_0(\xi)$ is an unknown polynomial in ξ , and $\mathbf{Y}_0 = (1, -l_{11}/l_{12})$ is the vector.

In the first order approximation ($j = 1$), one has the nonhomogeneous system of Eqs. (64). When taking Eqs. (66) into account, these system turns into identities.

Consider the nonhomogeneous system of Eqs. (64) in the second order approximation ($j = 2$). The compatibility condition for this system generates the formula

$$b = i\sqrt{f_{\varphi\varphi}/f_{pp}}$$

and the equation for P_0 :

$$\frac{d^2 P_0}{d\xi^2} + ib \left(2\xi \frac{dP_0}{dxi} \right) + \frac{2\Lambda_1}{f_{pp}} P_0 + I_{A(B)} = 0,$$

where

$$I_A = \frac{2\tau r_m^6}{f_{pp}(1 + \kappa r_m^2)} P_0 \quad \text{at } r_m > z_0 \text{ (case A)}$$

$$I_B = \frac{2\tau r_m^3 z_0^3}{f_{pp}(1 + \kappa r_m z_0)} P_0 \quad \text{at } r_m < z_0 \text{ (case B)}$$

If $r_m = z_0$, then $I_A = I_B$. For both cases

$$P_0(\xi) = \mathcal{H}_n \left(\sqrt{f_{\varphi\varphi}/f_{pp}} \xi \right).$$

Now we can calculate the complex parameter b characterizing the rate of the amplitude decrement far from the generatrix $\varphi = \varphi_0^\circ$.

If $r_m > z_0$ (case A), then

$$b = i\sqrt{\frac{r_m^4(1 + \kappa r_m^2)^2[-t_1''(\varphi_0^\circ)]}{2r_m^4(2 + \kappa r_m^2) - 4(1 + \kappa r_m^2)^2}},$$

and for $r_m > z_0$ (case B), one obtains

$$b = i \sqrt{\frac{r_m(1 + \kappa r_m^2)^3 [-t_1''(\varphi_0^\circ)]}{4(z_0 - r_m)[8 + 9\kappa r_m z_0 + 3(\kappa r_m z_0)^2]}}.$$

It may be seen that $\lim_{r_m \rightarrow z_0} |b| = +\infty$ for both cases (A) and (B). Thus, requirement (63) for b does not hold if a root r_m is close to z_0 .

We will not consider higher order approximations because system (59) is not sufficiently accurate since it does not contain some terms which effect the third and subsequent approximations.

Now we can write equations for the set of eigenvalues. If $r_m > z_0$, we derive

$$\begin{aligned} \Lambda^{(n,m)} &= 1 - t_1(\varphi_0^\circ) r_m^2 + \frac{r_m^4}{1 + \kappa r_m^2} \\ &+ \mu \left\{ \frac{(1 + 2n) \sqrt{-2t''(\varphi_0^\circ) [r_m^4 (2 + \kappa r_m^2) - 2(1 + \kappa r_m^2)^2]}}{2(1 + \kappa r_m^2)} + \frac{\tau r_m^6}{1 + \kappa r_m^2} \right\} + O(\mu^2), \end{aligned} \quad (70)$$

and for $r_m < z_0$, one has

$$\begin{aligned} \Lambda^{(n,m)} &= \frac{z_0^2 r_m^2}{1 + \kappa r_m z_0} + \frac{r_m^2}{z_0^2} - t_1(\varphi_0^\circ) r_m^2 \\ &+ \mu \left\{ \frac{(1 + 2n) \sqrt{-t''(\varphi_0^\circ) r_m^3 (z_0 - r_m) [8 + 9\kappa r_m z_0 + 3(\kappa r_m z_0)^2]}}{(1 + \kappa r_m^2)^3} \right. \\ &\quad \left. + \frac{\tau r_m^3 z_0^3}{1 + \kappa r_m^2} \right\} + O(\mu^2). \end{aligned} \quad (71)$$

The corresponding eigenmodes will be the following: if $r_m > z_0$, then

$$\begin{aligned} \chi^{(n,m)} &= \sin \frac{r_m s}{\mu} \exp \left\{ \frac{ib(\varphi - \varphi_0^\circ)^2}{2\mu} \right\} \left\{ \mathcal{H}_n \left[\sqrt{\frac{ib}{\mu}} (\varphi - \varphi_0^\circ) \right] \right. \\ &\quad \left. + O(\mu^{1/2}) \right\}, \end{aligned} \quad (72)$$

and for $r_m < z_0$, one obtains

$$\begin{aligned} \chi^{(n,m)} &= \sin \frac{r_m s}{\mu} \exp \left\{ \frac{i}{\mu} \left[\sqrt{r_m(z_0 - r_m)} (\varphi - \varphi_0^\circ) \right] \right\} \\ &\times \exp \left\{ \frac{ib(\varphi - \varphi_0^\circ)^2}{2\mu} \right\} \left\{ \mathcal{H}_n \left[\sqrt{\frac{ib}{\mu}} (\varphi - \varphi_0^\circ) \right] + O(\mu^{1/2}) \right\}. \end{aligned} \quad (73)$$

It may be seen that eigenmodes (72) and (73) are different for the cases (A) and (B). If $r_m > z_0$ (case A), the eigenfunctions decay exponentially without oscillations ($p^\circ = 0$), and for $r_m < z_0$ (case B) the localized eigenmodes have a large number (of the order μ^{-1}) of waves.

If r_m is close to z_0 , then Eqs. (72) and (73) are not applicable. The case (C) when $r_m \simeq z_0$ deserves the special consideration.

5.3 Reconstruction of Asymptotic Expansions

Let parameter r_m be close to a root z_0 of Eq. (67). In this case a solution of the boundary-value problem (59), (60) is found again in form (61). The substitution of (61) into Eqs. (59) results in the following system of ordinary differential equations:

$$\begin{aligned} (1 - \mu\tau\Delta_m)\Delta_m^2\chi_m - r_m\Phi_m - (t_1r_m^2 + \Lambda)(1 - \kappa\Delta_m)\chi_m - \Lambda &= 0, \\ \Delta_m^2\Phi_m + r_m^2(1 - \kappa\Delta_m)\chi_m &= 0, \end{aligned} \tag{74}$$

where

$$\Delta_m = \mu^2 \frac{d^2}{d\varphi^2} - r_m^2$$

is the differential operator.

Consider Eq. (67) again. At $r_m = z_0$ it is reduced to the following algebraic equation

$$\kappa r_m^6 + 2r_m^4 - 2(1 + \kappa r_m^2)^2 = 0.$$

Let $r_m = r_*$ be its root. We introduce the following estimations:

$$\begin{aligned} r_m &= r_* + \tilde{\mu}r', \quad \Lambda = \Lambda_* + \tilde{\mu}^2\Lambda', \quad \varphi - \varphi_0^\circ = \tilde{\mu}\eta, \\ t_1(\varphi) &= t_1(\varphi_0^\circ) + \frac{1}{2}\tilde{\mu}^2 t_1''(\varphi_0^\circ)\eta^2 + \dots \end{aligned} \tag{75}$$

where $r', \Lambda' \sim 1$ as $\tilde{\mu} \rightarrow 0$, and

$$\tilde{\mu} = \mu^{2/3} = \left[\frac{h^2\eta_3}{12R^2(1 - \nu^2)} \right]^{1/6}$$

is a new small parameter.

We will seek a solution of Eqs. (74) in the form of series

$$\chi_m = \sum_{k=0}^{\infty} \tilde{\mu}^k \chi_m^{(k)}(\eta), \quad \Phi_m = \sum_{k=0}^{\infty} \tilde{\mu}^k \Phi_m^{(k)}(\eta), \tag{76}$$

where

$$\chi_m^{(k)}, \Phi_m^{(k)} \sim 1, \quad \text{and} \quad \chi_m^{(k)}, \Phi_m^{(k)} \rightarrow 0 \quad \text{as} \quad \eta \rightarrow \pm\infty.$$

In the zeroth and first order approximations, Eqs. (74) turn into identities if the following condition holds:

$$\Lambda_* = 1 - t_1(\varphi_0^\circ)r_*^2 + \frac{r_*^4}{1 + \kappa r_*^2}. \quad (77)$$

Note that Eq. (77) coincides with Eqs. (68) and (69) at $r_m = r_* = z_0$.

Equation (77) gives the zero approximation for the eigenvalue Λ . The eigenfunctions $\chi_m^{(0)}$ and $\Phi_m^{(0)}$ remain undefined at this step.

Let us consider the second order approximation. When taking Eq. (77) into consideration, one gets the following equation with respect to $\chi_m^{(0)}$:

$$a_4 \frac{d^4 \chi_m^{(0)}}{d\eta^4} + a_2(r') \frac{d^2 \chi_m^{(0)}}{d\eta^2} + [a_0(r') - a_\eta \eta^2 - \Lambda' a_\lambda] \chi_m^{(0)} = 0, \quad (78)$$

where

$$\begin{aligned} a_4 &= 1 + \frac{\kappa}{r_*^2} + \frac{3}{r_*^4}, \quad a_2(r') = -4r_*r' + 2\kappa r_*r' - \frac{4r'}{r_*}, \\ a_0(r') &= (r')^2 \left[6r_*^2 - 1 - \kappa r_*^2 \left(5 + \frac{r_*^2}{1 + \kappa r_*^2} \right) \right], \\ a_\eta &= \frac{1}{2} r_*^2 (1 + \kappa r_*^2) t_1''(\varphi_0^\circ), \quad a_\lambda = (1 + \kappa r_*^2). \end{aligned}$$

The problem is to find such values of r' , $\Lambda'(r')$ as to satisfy the following condition:

$$\chi_m^{(0)} \rightarrow 0 \quad \text{as} \quad \eta \rightarrow \pm\infty.$$

Applying Fourier transform

$$\chi_m^{(0)}(\eta) = \frac{1}{\sqrt{2\pi}} \int_{-\infty}^{+\infty} \chi^F(\tilde{\omega}) \exp(i\tilde{\omega}\eta) d\tilde{\omega}.$$

we come to a second order equation for function χ^F :

$$\frac{d^2 \chi^F}{dx^2} + \left\{ \tilde{\Lambda} - [x^4 + 2\gamma x^2 + \gamma^2 Q(\kappa)] \right\} \chi^F = 0, \quad (79)$$

where

$$\begin{aligned}
 x &= \frac{\tilde{\omega}}{\alpha(\kappa)}, \quad \gamma = C(\kappa)r', \\
 \tilde{\Lambda} &= \Lambda' \left\{ \frac{1 + \kappa r_*^2}{(r_*^4 + \kappa r_*^2 + 3)[-t_1''(\varphi_0^\circ)]^{1/2}} \right\}^{1/3}, \\
 \alpha(\kappa) &= \left[-\frac{t_1''(\varphi_0^\circ)r_*^6(1 + \kappa r_*^2)}{2(r_*^4 + \kappa r_*^2 + 3)} \right]^{1/6}, \\
 C(\kappa) &= \frac{2 + 2r_*^4 - \kappa r_*^4}{r_* \left[-\frac{1}{2}t_1''(\varphi_0^\circ)(1 + \kappa r_*^2)(r_*^4 + \kappa r_*^2 + 3) \right]^{1/3}}, \\
 Q(\kappa) &= 1 + \frac{2A(\kappa)\alpha^2(\kappa)}{C^2(\kappa)t_1''(\varphi_0^\circ)r_*^2(1 + \kappa r_*^2)}, \\
 A(\kappa) &= \frac{1 - (1 - \kappa)r_*^2(6 + 5\kappa r_*^2)}{1 + \kappa r_*^2} + \frac{(2 + 2r_*^4 - \kappa r_*^4)^2}{r_*^2(r_*^4 + \kappa r_*^2 + 3)}.
 \end{aligned} \tag{80}$$

For each γ there exists the countable set of values $\tilde{\Lambda}_j (j = 0, 1, \dots)$ of $\tilde{\Lambda}$, for which there exist non-trivial solutions of Eq. (79) such that:

$$\chi^F \rightarrow 0 \quad \text{as} \quad x \rightarrow \pm\infty.$$

It may be seen from Eqs. (79), (80) that eigenvalues $\tilde{\Lambda}_j$ depend on both the fixed value of the shear parameter κ and the axis stress resultant t_1 .

In Fig. 7, the first two eigenvalues $\tilde{\Lambda}_0, \tilde{\Lambda}_1$ versus a parameter γ are presented for $\kappa = 0.5$ and $t_1(\varphi) = 0.5(1 + \cos \varphi)$.

Fig. 7 First two eigenvalues $\tilde{\Lambda}_0, \tilde{\Lambda}_1$ versus parameter γ

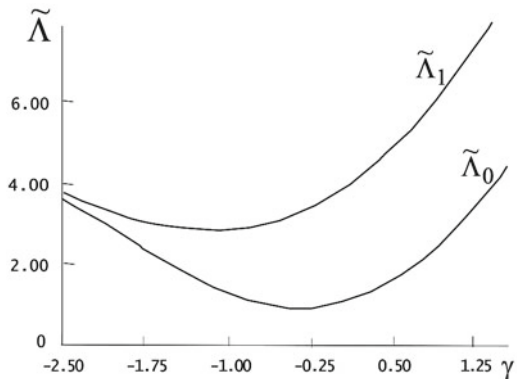


Table 3 Minimum eigenvalue Λ versus κ at $r_m \approx z_0$

κ	r_m	z_0	Λ_*	Λ'	Λ_{min}
0.037	0.993	1.014	0.990	0.590	1.005
0.100	1.017	1.039	0.972	0.586	0.986
0.250	1.077	1.102	0.917	0.575	0.931
0.400	1.142	1.171	0.843	0.563	0.857
0.500	1.186	1.220	0.782	0.553	0.796
0.600	1.229	1.271	0.710	0.539	0.723

As seen from Fig. 7, for parameters accepted above the function $\tilde{\Lambda}$ has the minimum value $\tilde{\Lambda}_0 \approx 0.924$ at $\gamma \approx -0.380$. Here $r_* \approx 1.220$, $\Lambda_* \approx 0.782$, and not complicated calculations by Eqs. (80) give $\Lambda'_{min} \approx 0.553$, $r' \approx -0.217$. Then the wave parameter r_m from Eq. (61) and the minimum eigenvalue Λ will be as follows (see Eqs. (75)):

$$r_m \approx 1.22 - 0.217e^{2/3}, \quad \Lambda_{min} \approx 0.782 + 0.553e^{4/3}.$$

Table 3 shows parameters r_m , z_0 , Λ_* , Λ' and Λ_{min} versus κ for the case (C) when $r_m \approx z_0$. It may be seen that increasing the shear parameter κ leads to decreasing the minimum natural frequency of the laminated cylindrical shell.

5.4 Examples

Example 5.4.1 We consider the three-layered cylinder of the radius $R = 150$ mm and length $L = 450$ mm. The first and third layers have the same thickness $h_1 = h_3 = 0.3$ mm and made of aluminium with the Young's modulus $E_1 = E_3 = 70,300$ N/mm², Poisson's ratio $\nu_1 = \nu_3 = 0.345$ and density $\rho_1 = \rho_3 = 2.7 \cdot 10^{-6}$ kg/mm³, and the second one is an epoxy matrix with $h_2 = 0.8$ mm, $E_2 = 3450$ N/mm², $\nu_2 = 0.3$, $\rho_2 = 1.2 \cdot 10^{-6}$ kg/mm³.

The dimensionless axial membrane stress resultant is assumed as follows:

$$t_1(\varphi) = \frac{1}{2}(1 + \varrho \cos \varphi).$$

Then the generatrix $\varphi = \varphi_0^0 = 0$ will be the weakest one.

Figure 8 shows the dependence of the zero approximation of the eigenvalue Λ_0 upon both the shear parameter κ and parameter ϱ at $m = 20$ ($r_m = 1.3$). In this case $r_m > z_0$ and all calculations were performed by equations corresponding to the variant (A). It may be seen that the eigenvalue Λ_0 is the monotonically decreasing function of both the axial force (in a neighbourhood of the weakest generatrix) and the shear parameter κ .

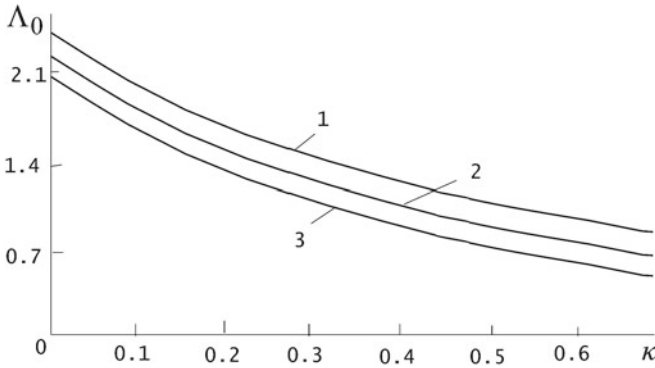


Fig. 8 Zero approximation Λ_0 of the eigenvalue Λ versus the shear parameter κ for various $\rho = 0.8, 1, 1.2$ (curves 1, 2 and 3, respectively)

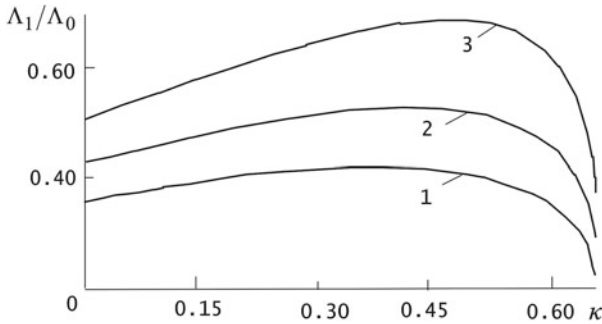


Fig. 9 Normalized correction Λ_1/Λ_0 versus the shear parameter κ for various $\rho = 0.8, 1, 1.2$ (curves 1, 2 and 3, respectively)

Figure 9 demonstrates the nonlinear behavior of the relative correction Λ_1/Λ_0 for the eigenvalue Λ at varying the shear parameter κ for different values of ρ . As accepted, the increase in parameter ρ characterizing inhomogeneity of loading involves the increase in the correction Λ_1/Λ_0 for any fixed κ . But for any fixed ρ there exists the maximum of Λ_1/Λ_0 being the function of κ . Approximately at $\kappa > 0.65$ the influence of inhomogeneity in loading on the natural frequencies becomes negligible.

Example 5.4.2 Let us consider again the three-layered cylinder with the same geometrical and physical parameters as in the previous Example. In Table 4, the dependence of the parameters $\text{Re}b$, Λ_0 (or Λ_* at $r_m \approx z_0$) and Λ_1/Λ_0 (or Λ'/Λ_* for $r_m \approx z_0$) on the wave parameter r_m found by two different asymptotic approaches is presented. The calculations have been performed at $\kappa = 0.5$ for the nonuniform dimensionless stress resultant $t_1(\varphi) = 0.5(1 + \cos \varphi)$. It may be seen that Λ_1/Λ_0 decreases and $\text{Im}b$ increases as $r_m \rightarrow z_0 = 1.077$.

Table 4 Parameters Reb , Λ_0 (or Λ_*), Λ_1/Λ_0 (or Λ'/Λ_*) versus r_m

Cases (A, B or C)	r_m	Imb	$\Lambda_0(\Lambda_*)$	$\Lambda_1/\Lambda_0(\Lambda'/\Lambda_*)$
B	0.844	0.285	0.575	1.117
B	0.909	0.347	0.656	0.942
B	0.974	0.448	0.741	0.752
C	1.077	–	0.917	0.627
A	1.360	1.588	1.490	0.552
A	1.490	1.026	1.949	0.564

6 Eigenmodes Localized Near Parallel in Long Axially Prestressed Cylindrical Shells

6.1 Setting a Problem

Consider a long thin one-layered isotropic cylindrical shell of the radius R with variable thickness $h(x)$, Young's modulus $E(x)$, Poisson's ratio $\nu(x)$, and density $\rho(x)$, where x is the axial coordinate at the shell surface.

The shell is assumed to be embedded in non-homogeneous elastic medium with the spring constant (Winkler foundation modulus) $c_f(x)$ and prestressed by the membrane stress resultants T_1° , T_2° .

We aim to study free axisymmetric vibrations localized in a neighbourhood of some parallel $x = x_0$ (see Fig. 10).

We consider the Flügge type equations (Flügge 1962) as the governing ones:

$$\begin{aligned} \frac{\partial T_1}{\partial x} + T_1^\circ \frac{\partial^2 u_1}{\partial x^2} - \rho h \frac{\partial^2 u_1}{\partial t_*^2} &= 0, \\ \frac{\partial^2 M_1}{\partial x^2} + \frac{1}{R} T_2 + T_1^\circ \frac{\partial^2 u_3}{\partial x^2} - \frac{1}{R^2} T_2^\circ u_3 + c_f u_3 + \rho h \frac{\partial^2 u_3}{\partial t_*^2} &= 0. \end{aligned} \quad (81)$$

where u_1 and u_3 are the longitudinal and normal displacements, T_1 , T_2 and M_1 are the additional stress resultants and bending moment, respectively, and t_* is time.

Fig. 10 Pattern of an eigenmode localized in a vicinity of the weakest parallel



For axisymmetric vibrations of isotropic shell the following stress-displacement relations are assumed:

$$\begin{aligned} T_1 &= \frac{Eh}{1 - \nu^2} \left(\frac{\partial u_1}{\partial x} + \frac{\nu}{R} u_3 \right), \\ T_2 &= \frac{Eh}{1 - \nu^2} \left(\nu \frac{\partial u_1}{\partial x} + \frac{1}{R} u_3 \right), \\ M_1 &= \frac{Eh}{12(1 - \nu^2)} \frac{\partial^2 u_3}{\partial x^2}. \end{aligned} \tag{82}$$

We introduce the dimensionless magnitudes as follows:

$$\begin{aligned} s &= \frac{x}{R}, \quad d(s) = \frac{Eh^3}{E_0 h_0^3 (1 - \nu^2)}, \quad g(s) = \frac{Eh}{E_0 h_0 (1 - \nu^2)}, \\ \gamma(s) &= \frac{\rho h}{\rho_0 h_0}, \quad c(s) = \frac{R^2 c_f}{E_0 h_0}, \quad \lambda = \frac{\rho_0 R^2}{E_0} \omega^2, \\ T_1^\circ &= \mu_1^2 E_0 h_0 t_1, \quad T_2^\circ = E_0 h_0 t_2, \quad \mu_1^4 = \frac{h_0^2}{12R^2}, \end{aligned}$$

where h_0, E_0, ρ_0 are the characteristic values of h, E, ρ , and ω is the natural frequency. It is assumed that

$$t_2 \leq 0, \quad t_1 < t_1^* \equiv \frac{2}{\sqrt{1 - \nu^2}}, \quad \frac{L^2}{R^2} < \frac{\pi^2 \sqrt{3(1 - \nu^2)}}{2} \frac{R}{h_0}, \tag{83}$$

where t_1^* is the critical value of the axial force resulting in a buckling of a very long thin cylinder (Tovstik and Smirnov 2001), and conditions (83) guarantee a subcritical stress state in the shell. The first inequality in (83) means that the shell may be prestressed by only stretching hoop stresses, and the second inequality points out that the shell may experience a compressing axial load which is less then the critical one.

We seek the displacements in the form:

$$u_1 = RU(s) \cos \omega t^*, \quad u_3 = RW(s) \cos \omega t^*.$$

Then the governing equations may be rewritten as follows:

$$\begin{aligned} \frac{d}{ds} \left[g(s) \left(\frac{dU}{ds} \nu W \right) \right] + \mu_1^2 t_1 \frac{d^2 U}{ds^2} + \lambda \gamma(s) U &= 0, \\ \mu_1^4 \frac{d^2}{ds^2} \left[d(s) \frac{d^2 W}{ds^2} \right] + \nu g(s) \frac{dU}{ds} & \\ + [g(s) - t_2 + c(s)] W + \mu_1^2 t_1 \frac{d^2 W}{ds^2} - \lambda \gamma(s) W &= 0. \end{aligned} \tag{84}$$

It is assumed that among all possible solutions of Eqs. (84) there are such eigenmodes which satisfy the following conditions

$$|U|, |W| \rightarrow 0 \quad \text{as} \quad |s - s_0| \rightarrow +\infty, \tag{85}$$

where $s = s_0$ is an unknown weakest parallel at the cylinder surface.

6.2 Asymptotic Solution

For small axisymmetric flexural vibrations of a long cylindrical shell the following asymptotic estimations are valid (Mikhasev 1998a)

$$W = w \sim 1, \quad U = \mu_1 u, \quad \frac{d}{ds} \sim \mu_1^{-1}, \quad \text{where} \quad u \sim 1.$$

The formal asymptotic solution of Eqs. (84) with conditions (85) is assumed to be in the form of (Mikhasev and Tovstik 2009)

$$\begin{aligned} \mathbf{X}(s, \mu_1) &= \sum_{k=0}^{\infty} \mu_1^{k/2} \mathbf{X}_k(\xi) \exp \left[i \left(\mu_1^{-1/2} p \xi + \frac{1}{2} b \xi^2 \right) \right], \\ \xi &= \mu_1^{-1/2} (s - s_0), \quad \lambda = \lambda_0 + \mu_1 \lambda_1 + \dots, \quad \text{Im} b > 0, \end{aligned} \tag{86}$$

where $s = s_0$ is the weakest parallel, $\mathbf{X} = (u, w)$, $\mathbf{X}_k = (u_k, w_k)$ are two-dimensional vectors, and u_k, w_k are polynomials in ξ with complex coefficients.

The substitution of Eq. (86) into Eqs. (84) yields the sequence of algebraic equations:

$$\sum_{k=0}^j \mathbf{L}_k \mathbf{X}_{j-k} = 0, \quad j = 0, 1, 2, \dots, \tag{87}$$

where \mathbf{L}_0 is the 2×2 matrix with the elements

$$\begin{aligned} l_{11} &= -g(s_0)p^2, \quad l_{12} = i\nu(s_0)g(s_0)p, \\ l_{21} &= l_{12}, \quad l_{22} = d(s_0)p^4 + g(s_0) - t_2 + c - t_1 p^2 - \lambda_0 \gamma(s_0), \end{aligned}$$

and the matrix operators \mathbf{L}_j at $j \geq 1$ are defined by Eqs. (17).

Considering the homogeneous system of algebraic Eqs. (87) in the zeroth approximation ($j = 0$), one derives

$$u_0 = i \frac{\nu(s_0)}{p} w_0(\xi), \tag{88}$$

and

$$\lambda_0 = f(p, s_0) = \gamma^{-1}(s_0) \{d(s_0)p^4 + [1 - \nu^2(s_0)]g(s_0) + c(s_0) - t_2 - t_1p^2\}. \quad (89)$$

The existence condition for a solution of the nonhomogeneous system (87) in the first approximation ($j = 1$) results in the formula for the wave parameter

$$p^\circ = \sqrt{\frac{t_1}{2d(s_0^\circ)}} \quad (90)$$

and the equation

$$\gamma \left[\frac{d'}{4d^2} t_1^2 + c' - (\nu^2 g)' \right] - \gamma' \left[91 - \nu^2 g + c - t_2 - \frac{t_1^2}{4d} \right] = 0,$$

which is used to determine the weakest parallel $s = s_0^\circ$.

It may be seen from (88) that $p^\circ \neq 0$. Then, as follows from Eq. (90), $t_1 > 0$. Thus, a localization of eigenmodes in a neighbourhood of a parallel in an infinity cylindrical shell is possible if and only if the shell is *prestressed* by axial *compressive* forces.

When the parameter p° and the generatrix $s = s_0^\circ$ are determined, one can calculate the zero approximation for the eigenvalue:

$$\lambda_0^\circ = \frac{1}{\gamma(s_0^\circ)} \left\{ [1 - \nu^2(s_0^\circ)]g(s_0^\circ) - \frac{t_1^2}{4d(s_0^\circ)} + c(s_0^\circ) - t_2 \right\}.$$

In the second approximation ($j = 2$) we have again the nonhomogeneous system (87). The existence condition for a solution of this system implies the quadratic equation

$$f_{pp}^\circ b^2 + 2f_{ps}^\circ b + f_{ss}^\circ = 0,$$

the correction

$$\lambda_1^{(n)} = -i \left(n + \frac{1}{2} \right) (f_{pp}^\circ b^\circ + f_{ps}^\circ) + \eta, \quad \eta = \frac{2d'(s_0^\circ)(p^\circ)^3}{\gamma(s_0^\circ)}.$$

for the eigenvalue λ , and the eigenfunction

$$w_0 = \mathcal{H}_n(r\xi), \quad r = \begin{bmatrix} f_{ss}^\circ \\ f_{pp}^\circ \end{bmatrix} - \begin{bmatrix} f_{ps}^\circ \\ f_{pp}^\circ \end{bmatrix},$$

where \mathcal{H}_n are n th degree Hermite polynomials, and the superscript $^\circ$ means that the second derivatives of the function f are calculated at $s = s_0^\circ$, $p = p^\circ$.

6.3 Examples

In the following examples we evaluate both the parameter b and the natural frequency ω with an accuracy up to values $O(\mu_1^2)$ for some particular cases.

Example 6.3.1 Let $h(s) = h_0(1 + as^2/2)$ be the function, and all other characteristics are constant parameters. Then $s = s_0^o \equiv 0$ is the weak parallel, and the inequality $\text{Im}b > 0$ is equivalent to the following one

$$a[t_2 - c + (1 - \nu^2)t_1^2] > 0.$$

It may be seen that there exist two different cases:

1. If $c < t_2 + (1 - \nu^2)t_1^2$ (small stiffness of the foundation), then $a > 0$, that is, free vibrations are localized near the parallel at which the shell thickness is minimum.
2. When the inequality $c > t_2 + (1 - \nu^2)t_1^2$ is valid (large stiffness of the foundation), then $a < 0$ and localization takes place in a vicinity of the line where a thickness is maximum.

For both cases we obtain the following equations:

$$b = \frac{i}{2} \sqrt{\frac{a[t_2 - c + (1 - \nu^2)t_1^2]}{t_1}},$$

$$\omega^2 = \frac{E}{R^2 \rho} \left\{ \left[1 - t_2 + c - \frac{1}{4}(1 - \nu^2)t_1^2 \right] + 2\mu_1 \left(n + \frac{1}{2} \right) \sqrt{a[t_2 - c + (1 - \nu^2)t_1]t_1} + O(\mu_1^2) \right\},$$

where $n = 0, 1, 2, \dots$

Example 6.3.2 It is assumed that $E(s) = E_0(1 + es^2/2)$ is variable, and all other characteristics are constant parameters. Here a localization is possible if and only if $e > 0$, that is, the weakest parallel is the line $s = 0$ where the modulus E is minimum. Then we obtain

$$b = \frac{i}{2} \sqrt{\frac{e[4 + (1 - \nu^2)t_1^2]}{6t_1}},$$

$$\omega^2 = \frac{E}{R^2 \rho} \left\{ \left[1 - t_2 + c - \frac{1}{4}(1 - \nu^2)t_1^2 \right] + 3\mu_1 (n + 1/2) \sqrt{(1/6)e[4 + (1 - \nu^2)t_1^2]t_1} + O(\mu_1^2) \right\}.$$

As seen from this example, both the parameter b and the correction to the natural frequency (due to inhomogeneity of the modulus E) are not influenced by the hoop stress resultant t_2 and the spring constant c as well.

Example 6.3.3 Let the Winkler foundation modulus $c(s) = c_0 + c_1 s^2/2$ be the function, and all other characteristics are constant parameters. In this case the localization takes the place in a vicinity of the parallel $s = 0$ at which the Winkler foundation modulus has the minimum value. Then

$$\begin{aligned}
 b &= \frac{i}{2} \sqrt{\frac{c_1}{t_1}}, \\
 \omega^2 &= \frac{E}{R^2 \rho} \left\{ \left[1 - t_2 + c - \frac{1}{4} (1 - \nu^2) t_1^2 \right] \right. \\
 &\quad \left. + 2\mu_1 (n + 1/2) \sqrt{c_1 t_1} + O(\mu_1^2) \right\}.
 \end{aligned}
 \tag{91}$$

The first equation in (91) shows that increasing the rate of inhomogeneity of a surrounding medium (parameter c_1) leads to increasing the rate of localization of eigenmodes.

The examples considered above showed that inhomogeneity in either thickness or Young’s modulus of a shell or the Winkler foundation spring constant may result in localization of eigenmodes in a vicinity of some parallel in an infinitely long cylindrical shell. We note that localized eigenmodes in the form of (86) exist if and only if the shell is compressed by axial forces. When axial forces are absent or tensile, the stated asymptotic method does not reveal similar modes in macro-scaled cylindrical shells (Mikhasev and Tovstik 2009). The recent study (Mikhasev 2014) on free vibrations of a single-walled carbone nanotube (presented by a nanoscale cylindrical shell) embedded in a nonhomogeneous elastic medium showed that introducing the internal nanoscale parameter into the continuum model of a nanotube permitted us to reveal the eigenmodes like (86) even through a nanoshell was tensile by axial forces.

7 Wave Packets in Thin Cylindrical Shells

7.1 Localized Stationary and Quasi-Stationary Vibrations

Free vibrations considered above are characterized by the localization of eigenmodes in a vicinity of a *fixed* line (generatrix or parallel) called the weakest one. Another peculiarity of the constructed complex WKB solutions is that all parameters and functions appearing in an ansatz (for instance, in (15)) are independent of time. According to the classification introduced in Sect. 1, similar vibrations are called localized *stationary* ones.

Another type of quasi-stationary vibrations localized near a *fixed* generatrix with constant parameters p, b in expansion (15) and slowly varying in time amplitude

functions w_j were investigated in studies (Mikhasev 1997; Mikhasev and Kuntsevich 2002). For instance, a non-uniform periodical axial load (Mikhasev 1997) applied to a non-circular cylindrical shell may result in parametric instability a shell in a vicinity of the weakest generatrix. And the paper (Mikhasev and Kuntsevich 2002) shows that the response of a non-circular conical shell to a non-uniform pulsing pressure may be also quasi-stationary vibrations localized near the *fixed* generatrix.

In this Section, *non-stationary* localized vibrations running over the shell surface will be considered. As opposed to problems considered in the previous Sections and papers (Mikhasev 1997; Mikhasev and Kuntsevich 2002), *running* vibrations called here *wave packets* (WPs) are assumed to be localized in a neighbourhood of a moving generatrix being the WP center (Mikhasev 2002). We propose the non-stationary variant of the complex WKB approximation (Mikhasev 1998a; Mikhasev and Tovstik 2009). According to this approach, magnitudes p , b and amplitude functions w_j in an ansatz (for instance, in Eq. (15)) are considered to be functions of time.

7.2 Setting a Problem

Considering an elastic single layer thin non-circular medium-length cylindrical shell. Let h be the shell thickness, ρ density, E Young's modulus, and ν Poisson ratio. A coordinate system s, φ as illustrated in Fig. 2 is chosen. The radius of curvature is $R_2 = R/k(\varphi)$, where R is the characteristic dimension of the shell surface. The shell is bounded by the two not necessary plane edges

$$s_1(\varphi) \leq s \leq s_2(\varphi).$$

Let the shell be under the external non-uniform dynamic load \mathbf{Q}^* . It is assumed that \mathbf{Q}^* is slowly varying vector function with respect to both space coordinates and time so that the dynamic stress state of the shell due to the load may be specified only by the axial, hoop and shear stress resultants

$$T_j^* = -Eh\varepsilon^6 \overline{T_j}(s, \varphi, t)$$

for $j = 1, 2, 3$, respectively. Here, $\varepsilon = \{h^2/[12R^2(1 - \nu^2)]\}^{1/8}$ is a small parameter, and $t = t^*/t_c$, $t_c^* = \sqrt{R^2\rho/(E\varepsilon^6)}$ are dimensionless and characteristic times, respectively.

It is assumed that all functions are infinitely differentiable ones with respect to φ , and $T_1(s, \varphi, t)$, $T_3(s, \varphi, t)$ are twice differentiable with respect to s and t so that

$$k, \quad s_i, \quad \frac{\partial^m k}{\partial \varphi^m}, \quad \frac{\partial^m s_i}{\partial \varphi^m} = O(1),$$

$$\frac{\partial^m T_j}{\partial \varphi^m}, \quad \frac{\partial^n T_\zeta}{\partial s^n}, \quad \frac{\partial^n T_\zeta}{\partial t^n} = O(1),$$

where $m = 1, 2, \dots$; $i, n = 1, 2$; $\zeta = 1, 3$; $j = 1, 2, 3$.

Governing equations in dimensionless form, including the effect of the initial stresses, are as follows

$$\begin{aligned}\varepsilon^4 \Delta^2 W + k(\varphi) \frac{\partial^2 \Phi}{\partial s^2} + \varepsilon^2 \Delta_T W + \varepsilon^2 \frac{\partial^2 W}{\partial t^2} &= 0, \\ \varepsilon^4 \Delta^2 \Phi - k(\varphi) \frac{\partial^2 W}{\partial s^2} &= 0.\end{aligned}\tag{92}$$

Here

$$\begin{aligned}\Delta &= \frac{\partial^2}{\partial s^2} + \frac{\partial^2}{\partial \varphi^2}, \\ \Delta_T W &= \frac{\partial}{\partial \varphi} \left(T_2 \frac{\partial W}{\partial \varphi} \right) + \frac{\partial}{\partial s} \left(T_3 \frac{\partial W}{\partial \varphi} \right) + \frac{\partial}{\partial \varphi} \left(T_3 \frac{\partial W}{\partial s} \right) + \frac{\partial}{\partial s} \left(T_1 \frac{\partial W}{\partial s} \right), \\ W &= W^*/R, \quad \Phi = \Phi^*/(\varepsilon^4 R^2 hE).\end{aligned}$$

The dynamic stress state of the shell consists of the basic dynamic stress state and the dynamic edge-effect integrals describing the shell behavior in a small neighborhood of each edge (Gol'denveizer 1961). To study the basic state on each edge, one only needs to satisfy two basic conditions. Apart from terms of the order ε^2 these conditions have the form (13) for the joint supported and rigid clamped edges, respectively.

Let us consider the following initial displacements and velocities

$$\begin{aligned}W|_{t=0} &= W^\circ(s, \varphi; \varepsilon) \exp \{i\varepsilon^{-1} S^\circ(\varphi)\}, \\ \dot{W}|_{t=0} &= i\varepsilon^{-1} V^\circ(s, \varphi; \varepsilon) \exp \{i\varepsilon^{-1} S^\circ(\varphi)\},\end{aligned}\tag{93}$$

where

$$\begin{aligned}i &= \sqrt{-1}, \quad S^\circ(\varphi) = a^\circ \varphi + \frac{1}{2} b^\circ \varphi^2, \quad a^\circ > 0, \quad \text{Im} b^\circ > 0, \\ a^\circ, |b^\circ|, |W^\circ|, |V^\circ|, |\partial W^\circ / \partial s|, |\partial V^\circ / \partial s| &= O(1) \quad \text{as } \varepsilon \rightarrow 0.\end{aligned}$$

The real and imaginary parts of Eq. (93) define the two initial WPs localized near the line $\varphi = 0$.

7.3 Asymptotic Approach

Splitting of the initial WP. Let $y_1(s, \varphi), y_2(s, \varphi), \dots, y_n(s, \varphi), \dots$ be an infinite orthonormal system of eigenfunctions of the equation

$$\frac{d^4 y}{ds^4} - \lambda y = 0\tag{94}$$

with one of the two variants of boundary conditions

$$\begin{aligned} y = \frac{d^2y}{ds^2} = 0 \quad \text{at } s = s_i(\varphi), \\ y = \frac{dy}{ds} = 0 \quad \text{at } s = s_i(\varphi), \end{aligned} \tag{95}$$

and $\lambda_1(\varphi), \lambda_2(\varphi), \dots, \lambda_n(\varphi), \dots$ be a corresponding sequence of eigenvalues. For instance, for the joint supported edges

$$y_n(s, \varphi) = \sin \frac{\pi n[s - s_1(\varphi)]}{l(\varphi)}, \quad \lambda_n(\varphi) = \left[\frac{\pi n}{l(\varphi)} \right]^4.$$

where $l(\varphi) = s_2(\varphi) - s_1(\varphi)$.

Suppose that the functions W°, V° appearing in the initial conditions (93) satisfy the boundary conditions (13). Then

$$\begin{aligned} W^\circ &= \sum_{n=1}^{\infty} w_n^\circ(\varphi; \varepsilon) y_n(s, \varphi), \\ V^\circ &= \sum_{n=1}^{\infty} v_n^\circ(\varphi; \varepsilon) y_n(s, \varphi), \end{aligned} \tag{96}$$

where

$$\begin{aligned} w_n^\circ &= \int_{s_1(\varphi)}^{s_2(\varphi)} W^\circ(s, \varphi; \varepsilon) y_n(s, \varphi) ds, \\ v_n^\circ &= \int_{s_1(\varphi)}^{s_2(\varphi)} V^\circ(s, \varphi; \varepsilon) y_n(s, \varphi) ds \end{aligned} \tag{97}$$

are assumed to be polynomials in $\zeta = \varepsilon^{-1/2}\varphi$ whose coefficients are regular functions of ε .

Running WP and its center. Taking into account the linearity of the governing equations and expansions (96) as well, the solution of the boundary-value problem (13), (92), (93) may be presented in the form

$$W = \sum_{n=1}^{\infty} \tilde{W}_n(s, \varphi, t; \varepsilon), \quad \Phi = \sum_{n=1}^{\infty} \tilde{\Phi}_n(s, \varphi, t; \varepsilon),$$

where $\tilde{W}_n, \tilde{\Phi}_n (n = 1, 2, 3, \dots)$ are the required functions localized in a neighborhood of a generatrix $\varphi = q_n(t)$.

Here $q_n(t)$ is a twice differential function such that

$$q_n(0) = 0. \tag{98}$$

The pair $\tilde{W}_n, \tilde{\Phi}_n$ will be called the n th WP with the center $\varphi = q_n(t)$ running in the circumferential direction.

Boundary-value problem in the local coordinate system. We hold the number n fixed and study the behavior of the n th WP. It is convenient to go over to a local moving coordinate system

$$\varphi = q_n(t) + \varepsilon^{1/2}\xi_n$$

with the center $\varphi = q_n(t)$.

Here parameters ξ_n, s define the position of a point on the shell surface with respect to the moving generatrix $\varphi = q_n(t)$.

Then the governing equations may be rewritten in the new coordinate system as follows:

$$\begin{aligned} &\varepsilon^2 \frac{\partial^4 \tilde{W}_n}{\partial \xi_n^4} + 2\varepsilon^3 \frac{\partial^4 \tilde{W}_n}{\partial \xi_n^2 \partial s^2} + \varepsilon^4 \frac{\partial^4 \tilde{W}_n}{\partial s^4} + k \frac{\partial^2 \tilde{\Phi}_n}{\partial s^2} + \varepsilon \frac{\partial}{\partial \xi_n} \left(T_2 \frac{\partial \tilde{W}_n}{\partial \xi_n} \right) \\ &+ \varepsilon^{3/2} \frac{\partial}{\partial s} \left(T_3 \frac{\partial \tilde{W}_n}{\partial \xi_n} \right) + \varepsilon^{3/2} \frac{\partial}{\partial \xi_n} \left(T_3 \frac{\partial \tilde{W}_n}{\partial s} \right) + \varepsilon^2 \frac{\partial}{\partial s} \left(T_1 \frac{\partial \tilde{W}_n}{\partial s} \right) \\ &+ \varepsilon^2 \frac{\partial^2 \tilde{W}_n}{\partial t^2} - \varepsilon^{3/2} \dot{q}_n \frac{\partial^2 \tilde{W}_n}{\partial \xi_n \partial t} + \varepsilon \dot{q}_n^2 \frac{\partial^2 \tilde{W}_n}{\partial \xi_n^2} - \varepsilon^{3/2} \ddot{q}_n \frac{\partial \tilde{W}_n}{\partial \xi_n} = 0, \\ &\varepsilon^2 \frac{\partial^4 \tilde{\Phi}_n}{\partial \xi_n^4} + 2\varepsilon^3 \frac{\partial^4 \tilde{\Phi}_n}{\partial \xi_n^2 \partial s^2} + \varepsilon^4 \frac{\partial^4 \tilde{\Phi}_n}{\partial s^4} - k \frac{\partial^2 \tilde{W}_n}{\partial s^2} = 0, \end{aligned} \tag{99}$$

where the dots(\cdot) denote differentiation with respect to the dimensionless time t .

The initial conditions for the n th WP take the form

$$\begin{aligned} \tilde{W}_n|_{t=0} &= w_n^\circ(\varphi, \varepsilon) y_n(s, \varphi) \exp [i\varepsilon^{-1} S^\circ(\varphi)], \\ \dot{\tilde{W}}_n|_{t=0} &= i\varepsilon^{-1} v_n^\circ(\varphi, \varepsilon) y_n(s, \varphi) \exp [i\varepsilon^{-1} S^\circ(\varphi)], \end{aligned} \tag{100}$$

and the boundary conditions for the simply supported and clamped edges are defined by Eqs. (95), where y should be replaced by \tilde{W}_n .

The functions $k(\varphi), s_i(\varphi), T_j(\varphi), y_n(s, \varphi), \lambda_n(\varphi)$ are expanded into a series in a neighborhood of the moving center $q(t)$. In particular,

$$T_2(\varphi, t) = T_2[q_n(t), t] + \varepsilon^{1/2} T_2'[q_n(t), t] \xi_n + \frac{1}{2} \varepsilon T_2''[q_n(t), t] \xi_n^2 + \dots$$

To avoid inconvenience the subscript n is omitted in what follows.

Ansatz for the n th WP. The formal asymptotic solution of the initial-boundary-value problem (99), (100), (95) for the n th WP is assumed to be in the form of (Mikhasev 2002)

$$\begin{aligned}\tilde{W} &\cong \sum_{m=0}^{\infty} \varepsilon^{m/2} w_m(s, \xi, t) \exp [i\varepsilon^{-1} S(\xi, t, \varepsilon)], \\ \tilde{\Phi} &\cong \sum_{m=0}^{\infty} \varepsilon^{m/2} f_m(s, \xi, t) \exp [i\varepsilon^{-1} S(\xi, t, \varepsilon)], \\ S &= \int_0^t \omega(\tau) d\tau + \varepsilon^{1/2} p(t) \xi + \frac{1}{2} \varepsilon b(t) \xi^2,\end{aligned}\tag{101}$$

where

$$\text{Im} b(t) > 0 \quad \text{for any } t \geq 0,\tag{102}$$

w_m, f_m are polynomials in ξ with complex coefficients being functions of t and s , $|\omega|$ is the momentary frequency of the shell in a neighbourhood of the center $\varphi = q(t)$, $p(t)$ is the wave number determining the variability of waves in the circumferential direction, and the function $b(t)$ characterizing the width of the n th wave packet. Inequality (102) guarantees attenuation of wave amplitudes far from the WP center.

It may be seen that in the case when $q = 0$, and ω, p, b, w_m, f_m are independent of time t , expansions (102) are degenerated into the stationary WP (15) describing free localized vibrations in a vicinity of the fixed (weakest) generatrix (Tovstik 1983a).

Sequence of boundary-value problems. The substitution of expansions (101) into Eqs. (99) results in the sequence of differential equations

$$\sum_{j=0}^m \mathbf{L}_j w_{m-j} = 0, \quad m = 0, 1, 2, \dots\tag{103}$$

where

$$\begin{aligned}\mathbf{L}_0 z &= \frac{k^2[q(t)]}{p^4(t)} \frac{\partial^4 z}{\partial s^4} + \{p^4(t) - T_2[q(t), t] p^2(t) - [\omega(t) - \dot{q}(t) p(t)]^2\} z, \\ \mathbf{L}_1 &= (b \mathbf{L}_p + \mathbf{L}_q + \dot{p} \mathbf{L}_\omega) \xi - i \mathbf{L}_p \frac{\partial}{\partial \xi}, \\ \mathbf{L}_2 &= (b^2 \mathbf{L}_{pp} + 2b \mathbf{L}_{pq} + \mathbf{L}_{qq} + \dot{p}^2 \mathbf{L}_{\omega\omega} + 2\dot{p} \mathbf{L}_{\omega q} \\ &\quad + 2\dot{p} b \mathbf{L}_{\omega p} + \dot{b} \mathbf{L}_\omega) \xi^2 - \frac{1}{2} \mathbf{L}_{pp} \frac{\partial^2}{\partial \xi^2} \\ &\quad - i (b \mathbf{L}_{pp} + \mathbf{L}_{pq} + \dot{p} \mathbf{L}_{\omega p}) \xi \frac{\partial}{\partial \xi} - i \mathbf{L}_\omega \frac{\partial}{\partial t} \\ &\quad - i \left(\frac{1}{2} b \mathbf{L}_{pp} + \frac{1}{2} \dot{\omega} \mathbf{L}_{\omega\omega} + \dot{p} \mathbf{L}_{\omega p} + \ddot{q} p + \mathbf{N} \right), \dots,\end{aligned}\tag{104}$$

$$\mathbf{N} = -\frac{4k[q(t)]k'[q(t)]}{p^5(t)} \frac{\partial^4}{\partial s^4} - 2p(t) \left\{ T_3[s, q(t), t] \frac{\partial}{\partial s} \frac{\partial T_3}{\partial s}[s, q(t), t] \right\}.$$

Substituting Eqs. (101) into (95), where y is replaced by w , produces the sequence of boundary conditions for w_m . For instance, for the simply supported edges they are defined by Eqs. (18), but considered at $s = s_i[q(t)]$, $i = 1, 2$.

Note that Eqs. (18) at $s = s_i[q(t)]$ guarantee a realization of the boundary conditions merely in a small vicinity of the moving center $\varphi = q(t)$. There is no sense to satisfy the boundary conditions on the whole segment $0 \leq \varphi < \pi$ because of the exponential decay of the wave amplitude far from the line $\varphi = q(t)$.

The sequence of one-dimensional boundary-value problems (103), (18) is used for the determination of unknown time-dependent functions $p(t)$, $q(t)$, $\omega(t)$, $b(t)$ and polynomials $w_j(s, \xi, t)$. As in Sect. 2, we will call these problems as BVP0, BVP1, BVP2, ..., respectively. Let us consider them step-by-step for $j = 0, 1, 2, \dots$

Zerth order approximation (BVP0). In the zeroth order approximation ($m = 0$), one has the homogeneous ordinary differential equation

$$\mathbf{L}_0 w_0 \equiv \frac{k^2[q(t)]}{p^4(t)} \frac{\partial^4 w_0}{\partial s^4} + \{p^4(t) - T_2[q(t), t]p^2(t) - [\omega(t) - \dot{q}(t)p(t)]^2\} w_0 = 0. \tag{105}$$

with the homogeneous boundary conditions

$$w_0 = 0, \quad \frac{d^2 w_0}{ds^2} = 0, \quad \text{at } s = s_i[q(t)]. \tag{106}$$

Its solution may be presented in the form

$$w_0(s, \xi) = P_0(\xi, t)y[s, q(t)], \tag{107}$$

where $P_0(\xi, t)$ is an unknown polynomial in ξ with coefficients being smooth functions of time t . Then $f_0 = P_0 k(q)p^{-4} \partial^2 y / \partial s^2$.

Substituting Eq. (107) into Eq. (105) yields the relation

$$\omega = \dot{q}(t)p(t) - H^\pm[p(t), q(t)], \tag{108}$$

linking the momentary frequency $\omega(t)$ to the wave parameter $p(t)$ and the grope velocity $v(t) = \dot{q}(t)$ of the n th WP, where

$$H^\pm(p, q, t) = \pm \sqrt{p^4 + \frac{\lambda(q)k^2(q)}{p^4} - T_2(q, t)p^4} \tag{109}$$

are Hamilton functions.

The signs \pm in Eqs. (109) indicate the availability of two branches (positive and negative) of the solutions corresponding to the functions H^\pm . These signs are omitted in what follows, and all further constructions are fulfilled for the function H^+ .

In this approximation, the polynomial $P_0(\xi, t)$ remains unknown.

Fist order approximation (BVP1). In the first order approximation ($m = 1$), the non-homogeneous differential equation

$$\mathbf{L}_0 w_1 = -\mathbf{L}_1 w_0 \quad (110)$$

with the non-homogeneous boundary conditions

$$w_1 + \xi s'_i \frac{\partial w_0}{\partial s} = 0, \quad \frac{\partial^2 w_1}{\partial s^2} + \xi s'_i \frac{\partial^3 w_0}{\partial s^3} = 0, \quad (111)$$

are derived.

Its solution is presented in the form of

$$w_1 = P_1(\xi, t)y[s, q(t)] + w_1^{(p)}(s, \xi, t), \quad (112)$$

where $P_1(\xi, t)$ is a new unknown polynomial in ξ , and $w_1^{(p)}(s, \xi, t)$ is a partial solution of Eq. (110).

Taking into account the self-conjugacy of the BVP1, we derive the equality

$$\int_{s_1[q(t)]}^{s_2[q(t)]} y(\mathbf{L}_0 w_1 + \mathbf{L}_1 P_0 y) ds = 0 \quad (113)$$

which serves as the condition for existence of a solution of the BVP1.

The operator \mathbf{L}_1 is defined by the operators \mathbf{L}_p and \mathbf{L}_q (see Eq. (104)). To define these operators, the BVP0 should be differentiated over the parameters p and q :

$$\begin{aligned} \mathbf{L}_0 w_p + \mathbf{L}_p w_0 + 2H(\dot{q} - H_p)w_0 &= 0, \\ w_p &= 0, \quad \frac{\partial^2 w_p}{\partial s^2} = 0 \quad \text{for } s = s_i[q(t)]; \\ \mathbf{L}_0 w_q + \mathbf{L}_q w_0 - 2HH_q w_0 &= 0, \\ w_q + s'_i \frac{\partial w_0}{\partial s}, \quad \frac{\partial^2 w_q}{\partial s^2} &= 0, \quad \frac{\partial^2 w_q}{\partial s^2} + s'_i \frac{\partial^3 w_0}{\partial s^3} = 0. \end{aligned} \quad (114)$$

Now Eq. (113) can be rewritten as the differential one

$$b(\dot{q} - H_p)\xi P_0 + (\dot{p} + H_q)\xi P_0 - i(\dot{q} - H_p) \frac{\partial P_0}{\partial \xi} = 0 \quad (115)$$

with respect to P_0 .

It may be seen from (115) that P_0 is the polynomial in ξ , if the functions $p(t)$, $q(t)$ satisfy the Hamiltonian system

$$\dot{q} = \frac{\partial H}{\partial p}, \quad \dot{p} = -\frac{\partial H}{\partial q} \quad \text{or} \quad \dot{q} = -\frac{\partial H}{\partial p}, \quad \dot{p} = +\frac{\partial H}{\partial q}. \tag{116}$$

In (116), the first and second systems correspond to the positive and negative branches of the solution, respectively.

Comparison of Eqs. (93) and (101), with Eq. (98) in mind, gives the initial conditions

$$p(0) = a^\circ, \quad q(0) = 0. \tag{117}$$

When taking Eqs. (116) into account, the operator \mathbf{L}_1 in (110) will be simplified:

$$\mathbf{L}_1 = (\mathbf{L}_q + \dot{p}\mathbf{L}_\omega) \xi.$$

Then the solution of the BVP1 may be written as follows

$$w_1 = P_1(\xi, t)y[s, q(t)] + \xi P_0(\xi, t) \frac{\partial y}{\partial q}, \tag{118}$$

where the polynomials P_0, P_1 remain undefined.

Second order approximation (BVP2). In the second order approximation, the non-homogeneous differential equation

$$\mathbf{L}_0 w_2 = -\mathbf{L}_1 w_1 - \mathbf{L}_2 w_0 \tag{119}$$

with the non-homogeneous boundary conditions

$$\begin{aligned} w_2 + \xi s'_i \frac{\partial w_1}{\partial s} + \frac{1}{2} \xi^2 \left(s''_i \frac{\partial w_0}{\partial s} + s'^2_i \frac{\partial^3 w_0}{\partial s^3} \right) &= 0, \\ \frac{\partial^2 w_2}{\partial s^2} + \xi s'_i \frac{\partial^3 w_1}{\partial s^3} + \frac{1}{2} \xi^2 \left(s''_i \frac{\partial^3 w_0}{\partial s^3} + s'^2_i \frac{\partial^4 w_0}{\partial s^4} \right) - \frac{4i s'_i}{p} \frac{\partial^3 w_0}{\partial s^3} &= 0, \end{aligned} \tag{120}$$

at $s = s_i[q(t)]$ arises again. The compatibility conditions for this boundary-value problem may be derived from the equation

$$\int_{s_1[q(t)]}^{s_2[q(t)]} y[\mathbf{L}_0 w_2 + \mathbf{L}_1(P_1 y + \xi P_0 y_q) + \mathbf{L}_2 P_0 y] ds = 0. \tag{121}$$

To define operators $\mathbf{L}_{pp}, \mathbf{L}_{pq}, \mathbf{L}_{qq}$ being the part of \mathbf{L}_2 in Eq. (121), it is necessary to differentiate the boundary-value problems (114) with respect to the parameters p and q once more. For instance, one gets the non-homogeneous differential equation

$$\begin{aligned} \mathbf{L}_0 w_{qq} + 2\mathbf{L}_q w_q - 2\mathbf{L}_\omega H_q w_q + \mathbf{L}_{qq} w_0 - 2\mathbf{L}_{\omega q} H_q w_0 \\ + \mathbf{L}_{\omega\omega} H_q^2 w_0 - \mathbf{L}_\omega H_{qq} w_0 = 0 \end{aligned}$$

with respect to the function w_{qq} and the non-homogeneous boundary conditions

$$\begin{aligned} w_{qq} + 2s'_i \frac{\partial w_q}{\partial s} + s''_i \frac{\partial w_0}{\partial s} + s_i'^2 \frac{\partial^2 w_0}{\partial s^2} = 0, \\ \frac{\partial w_{qq}}{\partial s^2} + 2s'_i \frac{\partial^3 w_q}{\partial s^3} + s''_i \frac{\partial^3 w_0}{\partial s^3} + s_i'^2 \frac{\partial^4 w_0}{\partial s^4} = 0 \quad \text{at } s = s_i[q(t)]. \end{aligned}$$

Other two supplementary problems for functions w_{pp} , w_{qp} are not written out here.

The substitution of $\mathbf{L}_{pp} w_0$, $\mathbf{L}_{pq} w_0$, $\mathbf{L}_{qq} w_0$ into the compatibility condition (121) results in the differential equation for P_0 :

$$(\xi^2 \mathbf{D}_b - 2\mathbf{D}_{\xi t}) P_0 = 0, \tag{122}$$

where

$$\begin{aligned} \mathbf{D}_b &= \dot{b} + H_{pp} b^2 + 2H_{pq} b + H_{qq}, \\ \mathbf{D}_{\xi t} &= h_0 \frac{\partial^2}{\partial \xi^2} + h_1 \xi \frac{\partial}{\partial \xi} + h_2 \frac{\partial}{\partial t} + h_3, \\ h_0(t) &= \frac{1}{2} H_{pp}, \quad h_1(t) = i(bH_{pp} + H_{pq}), \quad h_2 = i, \\ h_3(t) &= \frac{i}{2H} \left\{ bHH_{pp} - \dot{\omega} - 2H_q H_p + \ddot{q}p + \frac{1}{\eta} \int_{s_1}^{s_2} \mathbf{L}_\omega \dot{y} y ds + \Gamma \right\}, \\ \Gamma(t) &= -\frac{4k[q(t)]k'[q(t)]\lambda[q(t)]}{p^5(t)} - p(t) \frac{\partial T_2}{\partial \varphi}[q(t)] \\ &\quad - \frac{p(t)}{\eta(t)} T_3[s, q(t), t] y^2|_{s_1}^{s_2}, \quad \eta(t) = \int_{s_1}^{s_2} y^2 ds. \end{aligned}$$

Equation (122) has a solution of polynomial form if and only if the function $b(t)$ satisfies the Riccati equation

$$\dot{b} + H_{pp} b^2 + 2H_{pq} b + H_{qq} = 0. \tag{123}$$

The comparison of the initial conditions (100) and ansatz (101) gives the initial condition

$$b(0) = b^\circ \tag{124}$$

for the Riccati equation.

When taking the Riccati equation into account, Eq. (122) is reduced to the following equation

$$\mathbf{D}_{\xi t} P_0 = h_0 \frac{\partial^2 P_0}{\partial \xi^2} + h_1 \xi \frac{\partial P_0}{\partial \xi} + h_2 \frac{\partial P_0}{\partial t} + h_3 P_0 = 0 \tag{125}$$

called as the amplitude one. A solution of this equation may be presented in the following form (Mikhasev 2002):

$$P_0 = \Theta_m(t) \mathcal{H}_m(x), \tag{126}$$

where $\mathcal{H}_m(x)$ is the Hermite polynomials in x of the m th degree, and

$$x = \varrho(t)\xi, \quad \varrho(t) = \frac{\exp\left[-\int \frac{h_1(t)dt}{h_2(t)}\right]}{\sqrt{4 \int \frac{h_0(t)}{h_2(t)} \exp\left[-2 \int \frac{h_1(t)dt}{h_2(t)}\right] dt}}, \tag{127}$$

$$\Theta_m(t) = \frac{\left\{4 \int (h_0/h_2) \exp\left[-2 \int (h_1/h_2)dt\right] dt\right\}^{m/2}}{\exp\left[\int (h_3/h_2)dt\right]}.$$

It is evident that the polynomial

$$P_0(\xi, t; c_m) = \sum_{m=0}^M c_m \Theta_m(t) \mathcal{H}_m[\varrho(t)\xi] \tag{128}$$

of the M th degree is also the solution of the amplitude Eq. (125). Arbitrary constants c_m are found from the initial conditions.

Remark 2 The procedure for constructing the functions w_m, f_m appearing in (101) at $m \geq 1$ may be formally continued. It should be however noticed that higher approximations become asymptotically incorrect for $m \geq 4$ because the correction introduced by the boundary-value problem into the general solution (101) at the sixth step is of the order ε^2 at the shell edges, which is the same as the errors of both the original boundary conditions (13) and governing Eqs. (92).

The function

$$\tilde{W} = [w_0(s, \xi, t) + O(\varepsilon^{1/2})] \exp[i\varepsilon^{-1}S(s, \xi, t; \varepsilon)] \tag{129}$$

found from the first three approximations is the main term in the asymptotic expansion (101).

Determination of constants. Taking into account the availability of positive and negative branches of solution (1.30), we denote by

$$p^\pm, q^\pm, \omega^\pm, b^\pm, P_0^\pm, w_0^\pm, \Theta^\pm, \varrho^\pm$$

the appropriate functions corresponding to the Hamiltonians H^+ and H^- .

Consider the superposition

$$\tilde{W} = \tilde{W}^+ + \tilde{W}^-, \tag{130}$$

where

$$\begin{aligned} \tilde{W}^\pm &= \{P_0^\pm(\xi^\pm, t; c_m^\pm)y[s, q^\pm(t)] + O(\varepsilon^{1/2})\} \exp[i\varepsilon^{-1}S^\pm(s, \xi^\pm, t; \varepsilon)], \\ S^\pm &= \int_0^t \omega^\pm(\tau) d\tau + \varepsilon^{1/2}p^\pm(t)\xi^\pm + \frac{1}{2}\varepsilon b^\pm(t)\xi^{\pm 2}, \\ \xi^\pm &= \varepsilon^{-1/2}[\varphi - q^\pm(t)]. \end{aligned} \tag{131}$$

Function (130) contains $2(M + 1)$ constants c^\pm (see Eq. (128)).

Substituting Eqs. (130), (131) into the initial conditions (100) for the n th WP results in the following formulas for constants:

$$c_m^\pm = \frac{1}{2^{m+1}m!\sqrt{\pi}\Theta_m^\pm(0)} \int_{-\infty}^{+\infty} e^{-\zeta^2} \mathcal{H}_m[\varrho^\pm(0)\zeta] \left[w_0^\circ(\zeta) \mp \frac{v_0^\circ(\zeta)}{H^\circ} \right],$$

where

$$\zeta = \varepsilon^{-1/2}\varphi, \quad H^\circ = H(a^\circ, 0, 0),$$

and $w_0^\circ(\zeta)$, $v_0^\circ(\zeta)$ are the polynomials in ζ from Eqs. (96).

Remark 3 Solution (130), (131) is correct in the asymptotic seance at some segment $0 \leq t \leq t'$, where the following conditions hold:

$$\begin{aligned} \text{Im}b^\pm(t) &> 0, \\ \omega^\pm, p^\pm, b^\pm, \dot{\omega}^\pm, \dot{p}^\pm, \dot{b}^\pm, \dot{q}^\pm, w_j^\pm, f_j^\pm, \frac{\partial w_j^\pm}{\partial x}, \frac{\partial f_j^\pm}{\partial x} &= O(1) \quad \text{at } \varepsilon \rightarrow 0. \end{aligned} \tag{132}$$

In (132), x denotes any of the variables s, ξ, t .

7.4 Examples

Example 7.4.1 Consider the joint-supported circular cylindrical shell, for which $k = 1$, $s_1 = 0$, $s_2 = l$, $\lambda = (\pi n/l)^4$, being under the non-uniform hoop stresses

$$T_2(\varphi) = \Lambda(1 + \delta \cos \varphi), \quad 0 < \delta < 1, \quad \Lambda > 0.$$

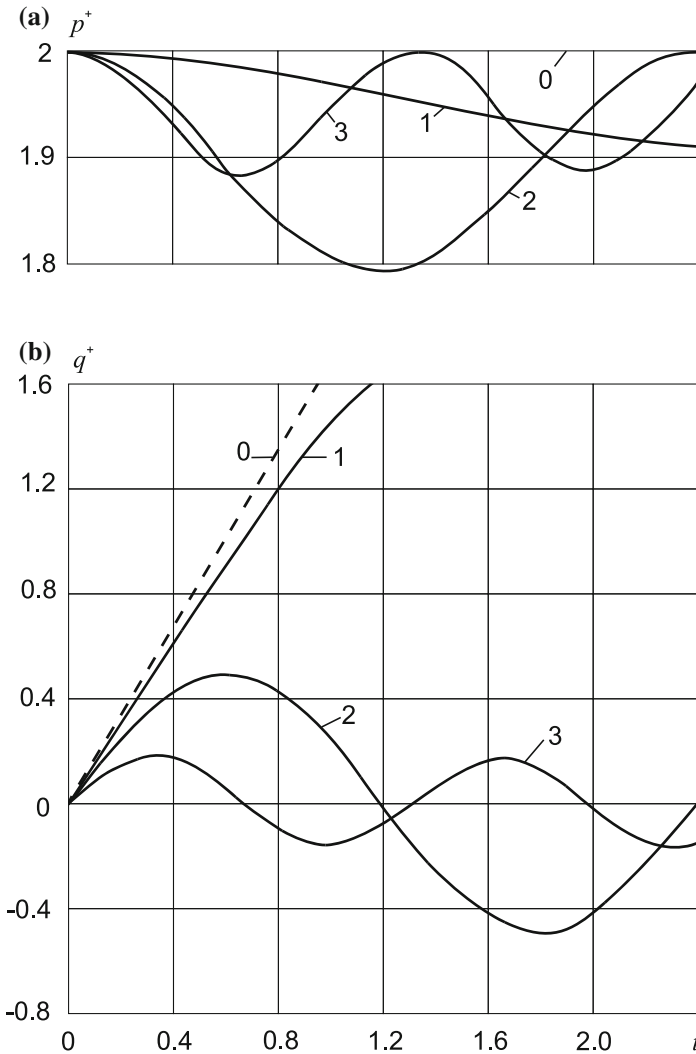


Fig. 11 Parameters p^+ (a) and centers q^+ (b) of running WP versus dimensionless time t for various δ : curve 0 ($\delta = 0$), curve 1 ($\delta = 0.05$), curve 2 ($\delta = 0.5$), curve 3 ($\delta = 1$)

Such stresses are caused by the external “wind” normal pressure. Here the generator $\varphi = 0$ is the weakest one. We assume that the center of the initial WP coincides with this line. We performed computations for $l = 1, n = 1, a^\circ = 2, b^\circ = i, w_1^\circ = 1, v_1^\circ = 0$ (see Eq. (97)), $\Lambda = 2$ and for various values of a parameter δ . Figure 11 shows the solutions of the Hamiltonian system. It may be seen that, in the cases of uniform and non-uniform pressure with the low non-homogeneity ($\delta = 0, 0.05$), the 1⁺st packet runs in the direction of pressure diminution without obstacles, whereas for $\delta = 0.5, 1$ there are the effects of reflection of the 1⁺st packet from the generators $\varphi = q_r^+ = 0.16$ and $\varphi = q_r^+ = 0.48$, respectively. Figure 12 demonstrates the manner in which the dimensionless momentary frequency ω^+ and the group velocity $v_g^+ = \dot{q}^+$ of the running WP vary with the course of time, for the uniform pressure these magnitudes staying constant. In Fig. 13, the parameter $\text{Im}b^+$ and the maximum amplitude w_{max}^+ of waves in the 1⁺st WP are plotted as functions of time t . When analyzing the behaviour of these functions, one can conclude: for small parameters δ characterizing the pressure non-homogeneity, the running WPs become dissolved, and for large parameters δ the effects of reflecting packets are accompanied by focusing and growing amplitudes as well; moreover, the larger the parameter δ is, the higher the power of focusing is and greater the magnitude of maximum amplitude becomes.

Example 7.4.2 Now, we consider the simply supported circular cylindrical shell with the sloping edge as shown in Fig. 3. Here

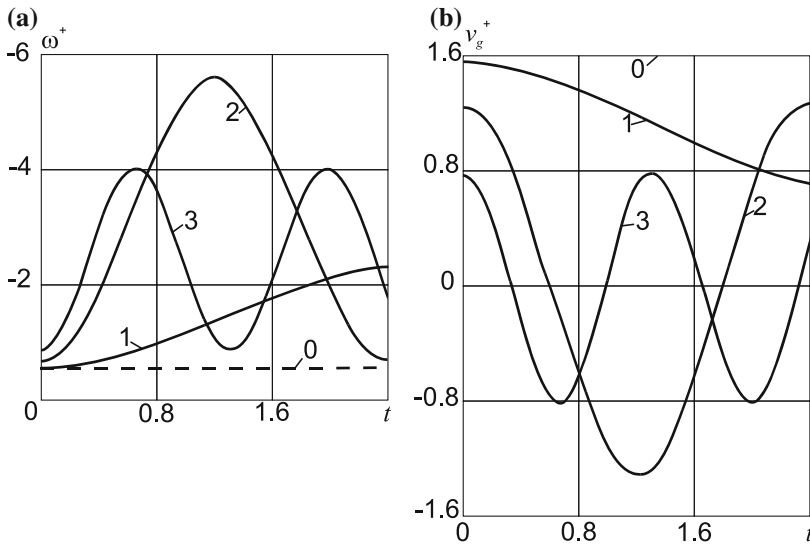


Fig. 12 Dimensionless frequencies ω^+ (a) and group velocities $v_g^+ = \dot{q}^+$ (b) of running WP versus dimensionless time t for various δ : curve 1 ($\delta = 0$), curve 1 ($\delta = 0.05$), curve 2 ($\delta = 0.5$), curve 3 ($\delta = 1$)

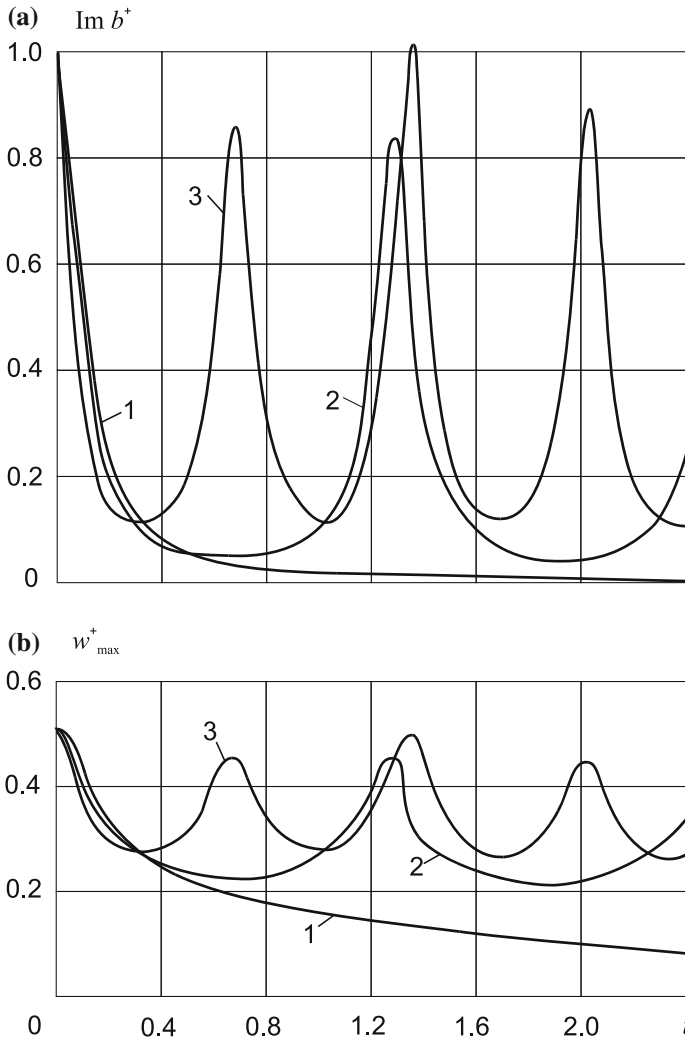


Fig. 13 Parameters $\text{Im} b^+$ (a) and maximum amplitudes w_{\max}^+ (b) of running WP versus dimensionless time t for various δ : curve 1 ($\delta = 0$), curve 1 ($\delta = 0.05$), curve 2 ($\delta = 0.5$), curve 3 ($\delta = 1$)

$$k = 1, \quad s_1 = 0, \quad s_2(\varphi) = l_0 + (\cos \varphi - 1) \tan \beta,$$

$$\lambda_n(\varphi) = \pi^4 n^4 / s_2^4(\varphi), \quad y_n(s, \varphi) = \sin [\pi n s / s_2(\varphi)]$$

and the longest generator $\varphi = 0$ will be the weakest one.

It is assumed that the shell is under the action of the slowly increasing normal pressure $Q_3^* = \varepsilon^6 R^{-1} E h c_t^* t^*$, where $c_t^* = c_t / t_c^*$, $c_t \sim 1$, t_c^* is the characteristic time introduced earlier. Then the dimensionless hoop stress-resultant $T_2 = \Lambda(t) = c_t t$ is also increasing function of time.

Let the initial WP (93) coincide with one of eigenmodes (38), where $a^\circ = p^\circ = \sqrt{\pi n/l_0}$, $b^\circ = i\sqrt{H_{qq}/H_{pp}}$, $w_0^\circ = \mathcal{H}_0 = 1$, $v_0^\circ = 0$.

Graphs of the functions $p^\pm(t)$, $q^\pm(t)$, $\omega^\pm(t)$, $\text{Im}b^\pm(t)$, $w_{max}^\pm(t)$ are shown in Figs. 14, 15 and 16. Calculations were performed at $l_0 = 2$, $\beta = 30^\circ$, $n = 1$ and different values of a parameter c_t . In the case of an external pressure ($c_t > 0$) computations were conducted at the segment $0 < t < t_b$, where the inequality $\Lambda(t) < \Lambda_b$ is valid, with Λ_b corresponding to the external buckling pressure

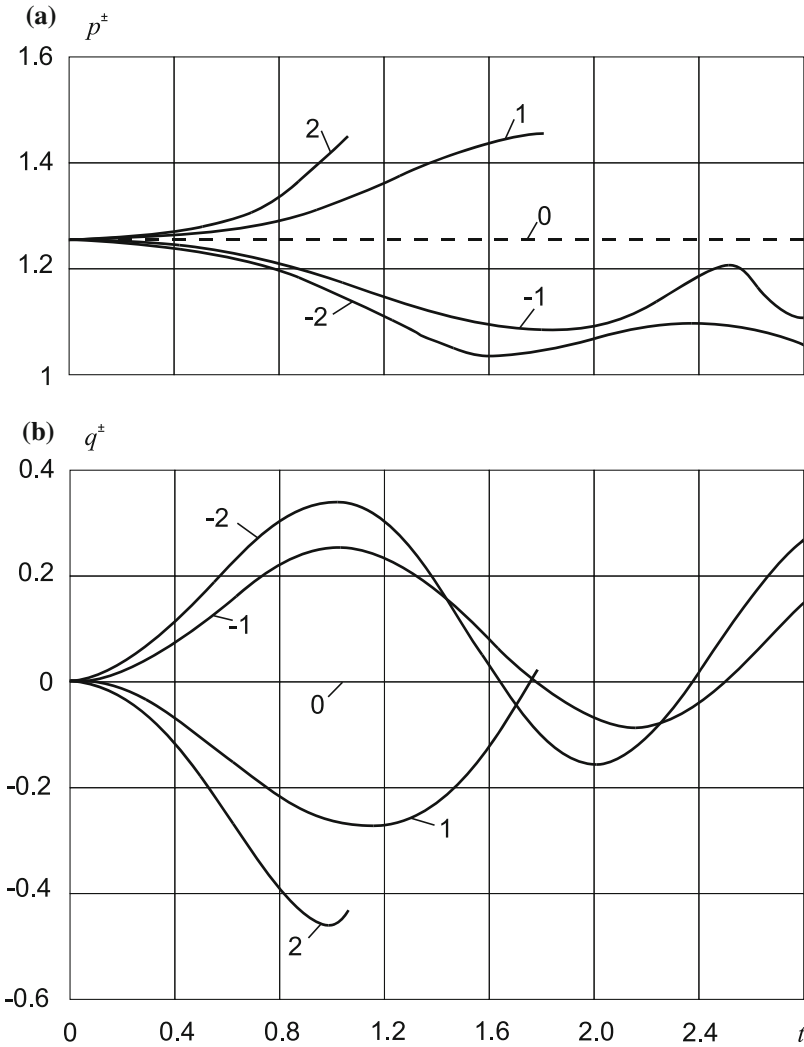


Fig. 14 Parameters $\text{Im}b^+$ (a) and maximum amplitudes w_{max}^+ (b) of running WP versus dimensionless time t for various δ : curve 1 ($\delta = 0$), curve 1 ($\delta = 0.05$), curve 2 ($\delta = 0.5$), curve 3 ($\delta = 1$)

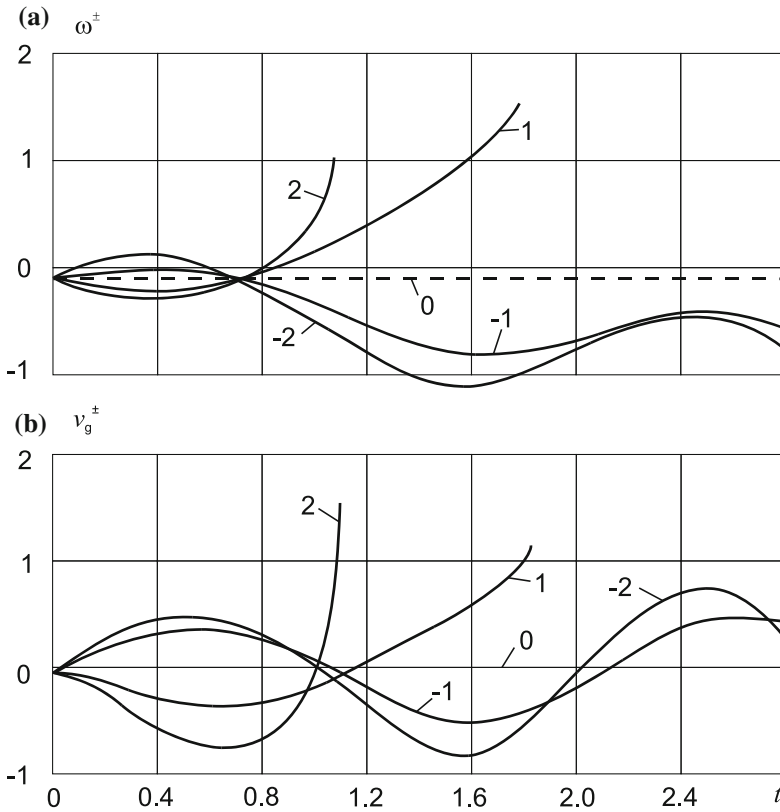


Fig. 15 Parameters $\text{Im}b^\pm$ (a) and maximum amplitudes w_{max}^\pm (b) of running WP versus dimensionless time t for various δ : curve 1 ($\delta = 0$), curve 1 ($\delta = 0.05$), curve 2 ($\delta = 0.5$), curve 3 ($\delta = 1$)

(Tovstik 1983b; Tovstik and Smirnov 2001). Here $t_b \approx 1.833$ and $t_b \approx 1.020$ for $c_t = 1.5$ and $c_t = 2.5$, respectively.

It may be seen from figures that growing pressure (both internal and external ones) leads to splitting the initial WP into the pair of the non-stationary WPs which run in the opposite directions. But for all that, the character of wave processes under internal and external pressures are different. So, under internal pressure, one observes the multiple reflections of the WPs from certain generatrix, these reflections being accompanied by strong focusing of the WPs and slight creasing the wave amplitudes. If the pressure is external, the reflection of the WPs are also possible, but in this case, running localized vibrations are accompanied by the very quick increase of the functions $|\omega^\pm(t)|$, $|v_g^\pm(t)|$, $|w_{max}^\pm(t)|$ as $t \rightarrow t_b$. It should be noted however that the unlimited growth of these functions contradicts conditions (132). Thus, solution (130), (131) should be considered at some interval $0 \leq t < t_b$ as long as the asymptotic correlations (132) are valid.

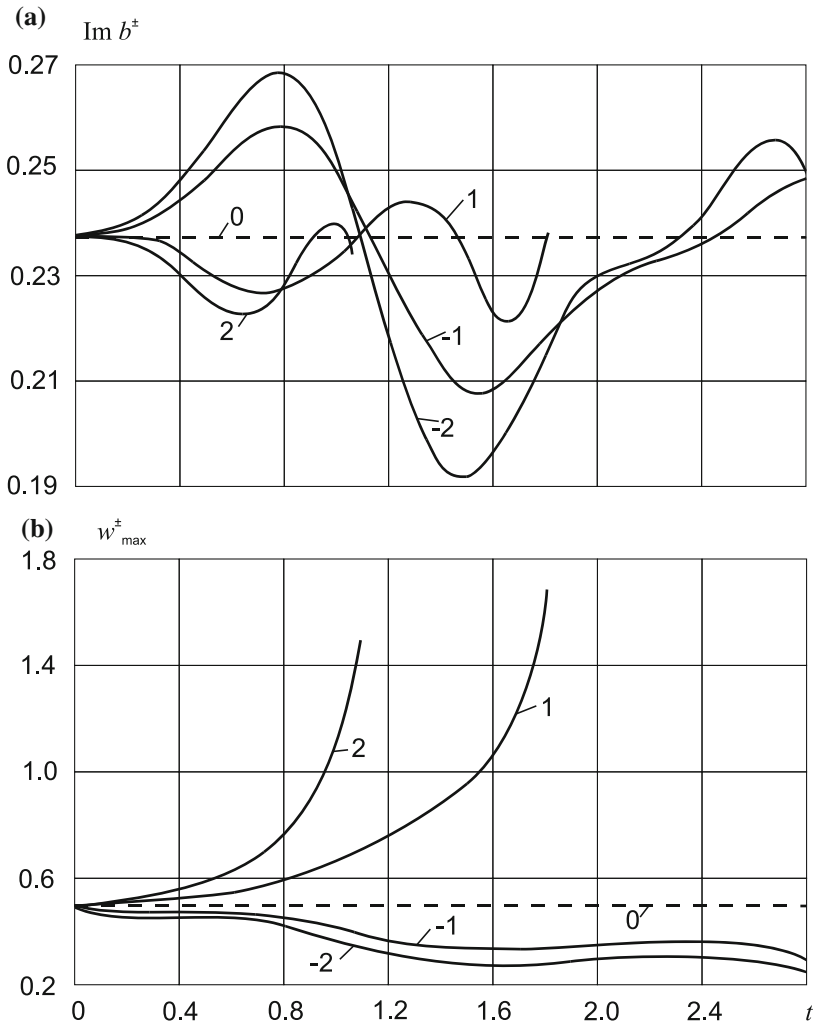


Fig. 16 Parameters $\text{Im } b^+$ (a) and maximum amplitudes w_{\max}^+ (b) of running WP versus dimensionless time t for various δ : curve 1 ($\delta = 0$), curve 1 ($\delta = 0.05$), curve 2 ($\delta = 0.5$), curve 3 ($\delta = 1$)

The examples considered above have revealed the following mechanical effects:

- The presence of the weakest generatrix on the shell surface due to variable generatrix length or pressure non-homogeneity may result in strong localization of the running packets of bending waves and their reflections from some generatrix which are accompanied by strong focusing and growing amplitudes.
- The initial local perturbations of the cylindrical shell having the weakest line and being under action of increasing external pressure may lead to very quick growing

amplitudes of the running WPs, and as a result, to dynamic buckling at the value of pressure which is lower than the critical static pressure.

At the end of the section, we refer to other papers, (Mikhasev 1996, 1998a,b; Avdoshka and Mikhasev 2001) devoted to propagation of WPs in thin shells. So, in paper of Avdoshka and Mikhasev (2001), the influence of nonuniform axial stationary and dynamic forces on WPs travelling in the circumferential direction of a thin elastic cylindrical shell was analyzed. Solutions for infinitely long cylindrical shells (Mikhasev 1998a) and shells of revolution (Mikhasev 1996) as well were constructed in the form of superposition of packets of bending, longitudinal and torsional waves running in the axial direction. And finally, two-dimensional WPs with centers in points running over the shell surface of an arbitrary shape were studied in reference (Mikhasev 1998b).

8 Conclusions

The scope of this Chapter on vibrations of thin shells demonstrates the variety of factors resulting in localization of eigenmodes. The differential equations governing the localized motion of shells do not admit, as a rule, a solution in an explicit form. The more effective approach for studying similar non-classical problems may be the complex WKB method. As shown, the asymptotic method of Tovstik permits one to examine highly localized vibrations in a vicinity of a fixed lines (called the weakest ones) at the shell surface. And the generalized variants of this approach (Mikhasev 2002; Mikhasev and Tovstik 2009) proved to be an effective mathematical tool for investigation of unsteady localized wave processes. In particular, the non-stationary complex WKB approximation permits one to study such mechanical effects as reflections of running wave packets, their strong focusing and increasing amplitudes which are difficult to be revealed by numerical methods.

References

- Avdoshka, I. V., & Mikhasev, G. I. (2001). Wave packets in a thin cylindrical shell under a non-uniform axial load. *Journal of Applied Mathematics and Mechanics*, 65(2), 301–309.
- Babich, V. M., & Buldyrev, V. S. (1991). *Asymptotic method in short-waves diffraction theory*. Berlin: Springer.
- Babich, V. M., Buldyrev, V. S., & Molotkov, I. A. (1985). *Space time ray method, linear and nonlinear waves*. Leningrad: Leningrad University Press.
- Boczkowska, A., Awietjan, S. F., Pietrzko, S., & Kurzydowski, K. J. (2012). Mechanical properties of magnetorheological elastomers under shear deformation. *Composites: Part B*, 43, 636–640.
- Bolotin, V. V., & Novichkov, Yu N. (1980). *Mechanics of multilayer structures*. Moscow: Mashinostroenie.
- Carrera, E. (1999). Multilayered shell theories accounting for layerwise mixed description. part 1: Governing equations. *AIAA Journal*, 37(9), 1107–1116.

- Carrera, E. (2002). Theories and finite elements for multilayered, anisotropic, composite plates and shells. *Archives of Computational Methods in Engineering*, 9, 1–60.
- Carrera, E. (2003). Theories and finite elements for multilayered plates and shells: a unified compact formulation with numerical assessment and benchmarking. *Archives of Computational Methods in Engineering*, 10, 215–96.
- Deng, H.-X., & Gong, X.-L. (2008). Application of magnetorheological elastomer to vibration absorber. *Communications in Nonlinear Science and Numerical Simulation*, 13, 1938–1947.
- Farshad, M., & Benine, A. (2004). Magnetoactive elastomer composites. *Polymer Testing*, 23, 347–353.
- Ferreira, A. J. M., Carrera, E., Cinefra, M., & Roque, C. M. C. (2011). Analysis of laminated doublycurved shells by a layerwise theory and radial basis functions collocation, accounting for through-the-thickness deformations. *Computational Mechanics*, 48(1), 13–25.
- Flügge, W. (1962). *Stresses in shells*. Berlin, Göttingen, Heidelberg: Springer.
- Fröman, N., & Fröman, P. O. (1965). *JWKB-Approximation. Contributions to the theory*. Amsterdam: North-Holland.
- Gibson, R. F. (2010). A review of recent research on mechanics of multifunctional composite materials and structures. *Composite Structures*, 92, 2793–2810.
- J.M. Ginder, W.F. Schlotter, & M.E. Nichols. Magneto-rheological elastomers in tunable vibration absorbers. In *Proceedings of the SPIE*, pp. 418–424, (2001).
- Gol'denveizer, A. L. (1961). *Theory of elastic thin shell*. London: Pergamon Press.
- Grigolyuk, E. I., & Kulikov, G. M. (1988). *Multilayer reinforced shells: Calculation of pneumatic tires*. Moscow: Mashinostroenie.
- Korchevskaya, E., & Mikhasev, G. (2006). Free vibrations of laminated cylindrical shell under action of non-uniformly distributed axial forces. *Mechanics of Solids*, 41(5), 130–138.
- Korobko, E. V., Zhuravski, M. A., Novikova, Z. A., & Kuzmin, V. A. (2009). Rheological properties of magneto-electrorheological fluids with complex disperse phase. *Journal of Physics: Conference Series*, 149, 12–65.
- Korobko, E. V., Mikhasev, G. I., Novikova, Z. A., & Zurauski, M. A. (2012). On damping vibrations of three-layered beam containing magnetorheological elastomer. *Journal of Intelligent Material Systems and Structures*, 23(9), 1019–1023.
- Kulikov, G. M., & Plotnikova, S. V. (2013). Advanced formulation for laminated composite shells: 3d stress analysis and rigid-body motions. *Composite Structures*, 95(3), 236–246.
- Maslov, V. P. (1977). *Complex WKB method in nonlinear equations*. Moscow: Nauka.
- Mikhasev, G. (1997). Free and parametric vibrations of cylindrical shell under static and periodic axial loads. *Technische Mechanik*, 17(3), 209–216.
- Mikhasev, G. (1998a). Travelling wave packets in an infinite thin cylindrical shell under internal pressure. *Journal of Sound and Vibration*, 209(4), 543–559.
- Mikhasev, G. (2014). On localized modes of free vibrations of single-walled carbon nanotubes embedded in nonhomogeneous elastic medium. *ZAMM*, 94(1–2), 130–141.
- Mikhasev, G. I. (1992). Low-frequency free vibrations of viscoelastic cylindrical shells. *International Applied Mechanics*, 28(9), 586–590.
- Mikhasev, G. I. (1996). Localized wave forms of motion of an infinite shell of revolution. *Journal of Applied Mathematics and Mechanics*, 60(5), 813–820.
- Mikhasev, G. I. (2002). Localized families of bending waves in a thin medium-length cylindrical shell under pressure. *Journal of Sound and Vibration*, 253(4), 833–857.
- Mikhasev G. I. (1998b). Asymptotic solutions of a system of equations of shallow shells in the form of two-dimensional wave packets. *Russian Mathematics (Izvestiya VUZ. Matematika)*, 42(2), 44–50.
- Mikhasev, G. I., & Kuntsevich, S. P. (2002). Local parametric vibrations of noncircular conical shell under action of non-uniform pulsing pressure. *Mechanics of Solids*, 37(3), 134–139.
- Mikhasev, G. I., & Tovstik, P. E. (2009). *Localized vibrations and waves in thin shells. Asymptotic methods*. Moscow: FIZMATLIT.

- Mikhasev, G. I., Botogova, M. G., & Korobko, E. V. (2011). Theory of thin adaptive laminated shells based on magnetorheological materials and its application in problems on vibration suppression. In H. Altenbach & V. A. Eremeyev (Eds.), *Shell-like structures* (Vol. 15, pp. 727–750). Advanced Structured Materials Berlin: Springer.
- Mikhasev, G. I., Altenbach, H., & Korchevskaya, E. A. (2014). On the influence of the magnetic field on the eigenmodes of thin laminated cylindrical shells containing magnetorheological elastomer. *Composite Structures*, *113*, 186–196.
- Qatu, M. S. (2004). *Vibration of laminated shells and plates*. San Diego: Elsevier.
- Qatu, M. S., Sullivan, R. W., & Wang, W. (2010). Recent research advances on the dynamic analysis of composite shells: 2000–2009. *Composite Structures*, *93*, 14–31.
- Qu, Y., Long, X., Wu, S., & Meng, G. (2013). A unified formulation for vibration analysis of composite laminated shells of revolution including shear deformation and rotary inertia. *Composite Structures*, *98*, 169–191.
- Reddy, J. N. (2003). *Mechanics of laminated composite plates and shells: Theory and analysis*. Florida: CRC Press.
- Sorokin, V. V., Ecker, E., Stepanov, G. V., Shamonin, M., Monkman, G. J., Kramarenko, E Yu., et al. (2014). Experimental study of the magnetic field enhanced payne effect in magnetorheological elastomers. *Soft Matter*, *10*, 8765–8776.
- Stepanov, G. V., Abramchuk, S. S., Grishin, D. A., Nikitin, L. V., Kramarenko, E Yu., & Khokhlov, A. R. (2007). Effect of a homogeneous magnetic field on the viscoelastic behavior of magnetic elastomers. *Polymer*, *48*, 488–495.
- Toorani, M. H., & Lakis, A. A. (2000). General equations of anisotropic plates and shells including transverse shear deformations, rotary inertia and initial curvature effects. *Journal of Sound and Vibration*, *237*(4), 561–615.
- Tovstik, P. E. (1983a). Two-dimensional problems of buckling and vibrations of the shells of zero gaussian curvature. *Soviet Physics Doklady*, *28*(7), 593–594.
- Tovstik, P. E. (1983b). Some problems in cylindrical and conical shell buckling. *Journal of Applied Mathematics and Mechanics*, *47*(5), 657–663.
- Tovstik, P. E., & Smirnov, A. L. (2001). *Asymptotic methods in the buckling theory of elastic shells*. Singapore: World Scientific.
- Yanchen, L., Jianchun, L., Weihua, L., & Haiping, D. (2014). A state-of-the-art review on magnetorheological elastomer devices. *Smart Materials and Structures*, *23*(12), 123001.

Six Lectures in the Mechanics of Elastic Structures

Paolo Podio-Guidugli

Abstract This document consists of six sections, one for each of my lectures. All lectures but the fourth consisted in slide presentations; in each section, the subsection sequence reproduces the slide sequence. The blackboard-and-chalk delivery of Lecture 4 is here accounted for in standard written form. The contents of all lectures were largely based on some papers of mine, mostly published, quoted in the opening lines of the sections; the interested reader is urged to consult the reference lists therein, let alone to find more complete and detailed expositions of the matters.

1 Generalities on the Validation of Theories of Thin Elastic Structures

This lecture was based on

- P. Podio-Guidugli, On the validation of theories of thin elastic structures. *Meccanica*, 49(6):1343–1352 (2014).
- P. Podio-Guidugli, Inertia and Invariance. *Ann. Mat. Pura Appl. (IV)*, CLXXII, 103–124 (1997).
- P. Podio-Guidugli, Concepts in the mechanics of thin structures. Pp. 77–110 of CISM Volume 503, A. Morassi and R. Paroni (Eds.) *Classical and Advanced Theories of Thin Structures*, Springer (2008).

P. Podio-Guidugli (✉)
Accademia Nazionale dei Lincei, Roma, Italy
e-mail: ppg@uniroma2.it

P. Podio-Guidugli
Department of Mathematics, University of Rome TorVergata, Roma, Italy

© CISM International Centre for Mechanical Sciences 2017
H. Altenbach and V. Eremeyev (eds.), *Shell-like Structures*,
CISM International Centre for Mechanical Sciences 572,
DOI 10.1007/978-3-319-42277-0_5

1.1 Prologue

“Thin Elastic Structures”: what are they? To answer this question, we should agree on what is meant by ‘structure’ and on what adscititious characters make a structure ‘elastic’ and ‘thin’. But this is not all: assuming that ‘mathematical simulation model’ is an acceptance of ‘theory’ appropriate to our context, we should also agree on what do we mean by ‘validating a theory’.

Structures, elastic or not, thin or not. ‘Structure’ is a word of manifold uses with manifold meanings. To a modelist, *mass points* and *rigid bodies* are structures, as much as *strings, beams, arches, plates, shells, ...*, because both mass points and rigid bodies compose *classes of continuous material bodies characterized by especially simple descriptions of their inertial and kinematical properties*; that is, both mass points and rigid bodies are *structures*.

Neither mass points nor rigid bodies are *elastic*, although they all can be in some sense *thin*. It would seem that ‘thinness’ and ‘elasticity’ should be regarded as independent properties. This leads me to make an attempt to

Disentangling thinness from elasticity. Unfortunately, both the classical theories of beams and plates and their modern variational counterparts are formulated in such a way as to make it impossible to separate thinness from elasticity.

There is more to thinness than *marked slenderness* in the case of beams or *modest thickness* in the case of plates: in fact, *thinness is a mixed property*, both geometrical and constitutive in nature. The adopted notion of thinness is at the conceptual core of any structure theory, so much so that *to assess the validity of a structure theory* amounts to judge *whether it is based on a convincing thinness notion*.

1.2 Generalities on Theory Validation

Uncertainty assessment. Assessing Uncertainty (UA) is “...crucial for *natural hazard risk management*, facilitating risk communication and informing strategies to successfully mitigate our society’s vulnerability to natural disasters”.¹ UA decreases when either accuracy or precision increase. But, its aim is to evaluate the outcome of a complex phenomenon, whose ingredients are mostly *stochastic*: having to deal with *deterministic* theories, we can forget about it.

Validation versus verification. Here is what one finds on browsing the computer version of a standard English dictionary:

¹See, e.g.,

– C.A. Schenk and G. I. Schuëller, *Uncertainty Assessment of Large Finite Element Systems*. Springer (2005).

- **validate**
check or prove the validity or **accuracy** of something (*these estimates have been validated by periodic surveys*).
 - demonstrate or support the truth or value of
 - make or declare legally valid.
- **verify**
make sure or demonstrate that something is true, **accurate**, or justified (*his conclusions have been verified by later experiments*).

NOTE For mathematical theories, ‘*verification*’ seems more apt a procedure than ‘*validation*’. Curiously enough, K. Popper proposed ‘*falsification*’ (or rather, ‘*falsifiability*’) as a basic criterion for verification. Yet, science philosophers seem to prefer ‘*validation*’ to ‘*verification*’, when they take up ‘*simulation models*’, such as, in particular, mathematical theories.

1.3 Validation Methodologies

There are two extreme approaches, namely, *objectivism* (aka *foundationalism*, *justificationism*) and *relativism* (aka *anti-foundationalism*, *anti-justificationism*), and various intermediate declinations, among which we pick: *instrumentalism*.²

According to this last approach, the validation criteria to be used are *esthetic value*, *simplicity*, and *predictive success*. Says M. Friedman:

- a *simulation model* of a real system is “...to serve as a *filing system* for organizing empirical material.”
- “Only factual evidence can show whether [a simulation model] is ‘*right*’ or ‘*wrong*’, or better, tentatively ‘*accepted*’ as valid or ‘*rejected*.’ ”
- “...the only relevant test of the validity of a hypothesis is *comparison of its predictions with experience*.”

Would you regard your favorite plate theory as “a filing system for organizing empirical material”?

I doubt it, for a number of reasons: because the same body of empirical evidences can be ‘filed’ according to many plate theories; because more than one theory

²See, e.g.,

- Kleindorfer, G.B., O’Neill, L, and Ganeshan, R., Validation in simulation: various positions in the philosophy of science. *Management Sci.*, 44 (8), 1087–1099 (1998).
- Friedman, M., *The Methodology of Positive Economics. Essays in Positive Economics*. University of Chicago Press, Chicago, II, 3–43 (1953).

can come out ‘right’—if one prefers to go for a cavalier *either/or* decision—or be ‘accepted’ as valid; and because *predictive success* is not the same as *predictive power*.

I maintain that the axiomatic format of a simulation model (\equiv mathematical theory) should be judged on the basis of

- its esthetic value: simplicity, elegance, whatever is at bottom a matter of taste counts; at times, even ethic value counts;
- its predictive power, i.e., its ability to give “...guidance to the gaps that sometimes *analogy* and *imagination* leave open in the process of generalizing an existing branch of the theory, or creating a new one.”³

Ultimately, for me, the *physical content* of an axiomatic scheme resides in its *discovery potential*, and is measured by its *persistence in form* when a broader or new theory is aimed at.

1.4 Computational Validation

I call a theory *approximate* when it is meant to be a *simplified version* of another accepted theory, but it is *not a special case* of it. Commonly, an approximate theory is validated when the discrepancy between its predictions and those of the accepted theory is found conveniently small.

Oftentimes, discrepancy is measured by comparing computational outcomes. When this is the case, *validation of approximate theories* depends on *reliableness of numerical schemes and computer codes*. Since such schemes and codes are indeed more and more reliable, the interest for explicit solutions, which simpler theories are more likely to allow for, is progressively evaporating. My reasons to believe that this trend should be resisted are listed here below.

1.5 Breaking a Lance for Simple Model Theories

My first and most important reason is that “...explicit solutions not only find a *quantitative* use, in that they allow for computing specific unknowns, but also a *qualitative* use, in that they help to interpret certain experimental findings in the light of the theory within which they were derived. Often, ...there is not a clear-cut distinction between quantitative and qualitative uses: for example, *benchmarking of algorithms and codes* entails a not purely quantitative use of explicit solutions.”⁴

³This quote is taken from the second of the papers listed in the beginning of this section.

⁴This quote and all the other to follow are taken from the third paper listed in the beginning of this section.

As a matter of fact, “...much current work in structure theory consists of computational developments, at times pertaining more to numerical analysis than to mechanics ...a relatively new discipline, Computational Mechanics, has acquired identity and dignity.” CM complements the program implicit in a Hadamard-like well-posedness cliché, by constructing solutions pointwise, with arbitrary precision, for each pointwise assignment of boundary data.”

Should we fear, with S.S. Antman, that “...a day will come when rod and shell theories will loose their distinctive identities within CM and be subsumed under a general theory for the numerical treatment of three-dimensional problems, endowed with useful error estimates”?

My answer to [this] question parallels Antman’s, and is definitely negative: “rather than furnishing approximations useful in applications—something that CM does better—structural mechanics should pose and study classes of meaningful problems amenable to qualitative analysis—something that is out of the scope of CM.”

“CM cannot treat *at one time* classes of shapes, loads, and materials: for example, in the case of Saint-Venant Problem ..., CM can compute with great precision the solution for *one* cylinder, *one* system of end loads, *one* material; but it cannot treat at one time a class of shapes (e.g., strictly speaking, it cannot predict what happens when a cylinder of given cross section becomes slender and slender), let alone treating classes of loads and classes of materials. Neither CM can establish the position of a given structure theory with respect to a parent, more general mechanical theory.”

2 Validation via Variational Convergence

This lecture was based on

- R. Paroni and P. Podio-Guidugli, On variational dimension reduction in structure mechanics. *J. Elasticity*, 118:1–13, 2015.
- P. Podio-Guidugli, On the validation of theories of thin elastic structures. *Meccanica*, 49(6):1343–1352, 2014.

2.1 Dimension-Reduction Methods

A *Dimension-Reduction Method* (DRM) is a method to show that, given a *real problem* \mathcal{P}^r and a $(3 - n)$ D *approximate problem* \mathcal{P}^a ($n \in \{1, 2, 3\}$), \mathcal{P}^a can be induced from \mathcal{P}^r . A *Variational DRM* (VDRM) is a DRM where both problems \mathcal{P}^r and \mathcal{P}^a admit a *variational formulation*, and where a *variational argument* is used.

Here, in the interest of time and definiteness, we take $n = 1$ and we let \mathcal{P}^r concern a linearly elastic *plate-like body*; moreover, we choose \mathcal{P}^a to be a *plate problem*, Kirchhoff-Love’s or Reissner-Mindlin’s. We briefly recall the kinematical assumptions at the base of those two classic 2D theories. In this connection, I find appropriate to offer a word of advice: make good use of the intuition of modelers of that caliber!

The K-L and R-M *Ansätze* both specify how fibers transversal to the mid surface of a plate-like body deform. In both cases,

(a) *transversal fibers preserve their length*;

in addition,

(b) *transversal fibers remain orthogonal to mid surface* (K-L);

(c) *transversal fibers remain straight* (R-M).

Mechanical DRMs. We mention two such methods:

- according to the *method of internal constraints*, the K-L and R-M *Ansätze* are regarded as *restrictions on admissible strain fields*, enforced by suitable *reactive stress fields*⁵;
- when the *scaling method* is adopted, the following steps are taken:
 - (i) data (\equiv domain, elastic moduli, applied forces) and solution are scaled in terms of integer powers of a *thickness parameters* ε ;
 - (ii) sets of scaling exponents are chosen, on the basis of one requirement: that the *scaled total-energy functional stay finite when $\varepsilon \rightarrow 0$* ;
 - (iii) backward-scaling of limit functionals yields K-L and R-M functionals (and many others!).⁶

Analytical DRMs. Once again we mention two methods of this type.

One is the *method of asymptotic expansions*, which is expounded with rigor and detail in

- P.G. Ciarlet, *Mathematical elasticity. Vol. II.* North-Holland Publishing Co., Amsterdam, 1997.

The other method is Γ -convergence; we distinguish it in *standard* and *improved*. For the standard method, a couple of relevant references are:

- G. Anzellotti, S. Baldo, and D. Percivale, Dimension reduction in variational problems, asymptotic development in Γ -convergence and thin structures in elasticity. *Asymptotic Anal.*, 9(1):61–100 (1994).
- F. Bourquin, P.G. Ciarlet, G. Geymonat, and A. Raoult, Γ -convergence et analyse asymptotique des plaques minces. *C. R. Acad. Sci. Paris Sér. I Math.*, 315(9):1017–1024 (1992).

The improved Γ -convergence method to be soon delineated has been proposed in the first paper quoted at the beginning of this lecture.

⁵This idea was first put forward and exploited in

- P. Podio-Guidugli, An exact derivation of the thin plate equation. *J. Elasticity*, 22:121–133 (1989).

See also the third paper quoted in the beginning of the previous section.

⁶See

- B. Miara and P. Podio-Guidugli, Deduction by scaling: a unified approach to classic plate and rod theories. *Asymptotic Anal.*, 51(2):113–131 (2007).

2.2 Standard Γ -Convergence, Stripped to the Bone

Given a family $\{P_\varepsilon\}$ of minimum problems:

$$P_\varepsilon : \quad \text{find } u_\varepsilon = \underset{u \in X_\varepsilon}{\operatorname{argmin}} F_\varepsilon(u),$$

it may happen that a minimum problem P_0 is found:

$$P_0 : \quad \text{find } u_0 = \underset{u \in X}{\operatorname{argmin}} F_0(u),$$

such that *problem convergence implies solution convergence*:

$$\{P_\varepsilon\} \rightarrow P_0 \Rightarrow \{u_\varepsilon\} \rightarrow u_0.$$

Under these circumstances, one says that *the family of problems P_ε (functionals F_ε) Γ -converges to the limit problem P_0 (functional F_0)*.

NOTE Standard Γ -convergence is more a method to justify and validate a given structure model than a method to deduce it, and even less to propose a new one.

2.3 Standard Γ -Convergence Validation of an Approximate Problem

Let a 3D real problem P^r and a 2D approximate problem P^a be given. Then, problem P^a is regarded as a valid approximation of problem P^r whenever, for ε the thickness parameter,

- (i) an ε -family F_ε of 3D functionals, such that $F^r = F_{\varepsilon^r}$ is found, and
- (ii) it can be shown that the family F_ε Γ -converges to a limit functional F_0 being in tight kinship (in a sense that needs to be made explicit) with the approximate functional F^a .

We now give an example of successful validation by way of this procedure. One begins by choosing

Problem P^r to be the equilibrium problem of a 3D plate-like body

- with square mid-section ω^r of side l^r and of thickness $2h^r$:

$$\Omega^r = \omega^r \times (-h^r, +h^r), \quad \varepsilon^r = h^r/l^r;$$

- clamped on the Dirichlet part $\partial_D \Omega^r = \partial_D \omega^r \times (-h^r, +h^r)$ of its boundary;

- subject to null contact loads on the Neumann part and to a distance-force field b^r over Ω^r ;
- comprised of a linearly elastic material, with elasticity tensor \mathbb{C}^r .

Next, one chooses

Functionals F^r and F_ε to be, respectively,

- the *total-energy functional of classic 3D elasticity*:

$$F^r(v) := \int_{\Omega^r} \left(\frac{1}{2} \mathbb{C}^r [E(v)] \cdot E(v) - b^r \cdot v \right) dx,$$

defined over the space

$$H_D^1(\Omega^r; \mathbb{R}^3) := \{v \in H^1(\Omega^r; \mathbb{R}^3) : v = 0 \text{ on } \partial_D \Omega^r\};$$

- the Γ -convergent sequence of functionals:

$$F_\varepsilon(v) := \int_{\Omega_\varepsilon} \left(\frac{1}{2} \mathbb{C}^r [E(v)] \cdot E(v) - b_\varepsilon \cdot v \right) dx,$$

defined over the space

$$H_D^1(\Omega_\varepsilon; \mathbb{R}^3), \text{ for } \Omega_\varepsilon = \omega^r \times \varepsilon(-h^r, +h^r), \varepsilon \in (0, 1].$$

Finally, as to

Functional F^a , one picks the *Kirchhoff-Love functional*:

$$F^a(w) := \int_{\omega^r} \left(\frac{1}{2} \left(\bar{D}^a (\Delta w)^2 - \bar{d}^a (w_{,11} w_{,22} - (w_{,12})^2) - \bar{b}^a w \right) \right) dx,$$

$$\bar{D}^a = D^a (h^r)^3, \bar{d}^a = d^a (h^r)^3, \bar{b}^a := \int_{-h^r}^{+h^r} b^r(x_1, x_2, x_3) dx_3,$$

defined over the space

$$H_0^2(\omega^r; \mathbb{R}) := \{w \in H^2(\omega^r; \mathbb{R}) : w = 0 \text{ and } w_{,n} = 0 \text{ on } \partial \omega^r\}.$$

So far so good. Now,

can the R-M functional too be squeezed out of 3D elasticity by standard Γ -convergence?

Many have tried, but nobody succeeded.

“Therefore, R-M’s must be an invalid model”, says the lazy variationalist.

“Not quite!”, his friend the astute mechanicist tells him, “You have to pick up the ‘right’ F^r and $\{F_\varepsilon\}$ ”. To do so, he continues, “the internal-constraints approach shows that you may

- either add in a bit of *second-gradient energy*, as is done in
 - R. Paroni, G. Tomassetti, and P. Podio-Guidugli, A justification of the Reissner-Mindlin plate theory through variational convergence. *Anal. Appl.* 5(2):165–182 (2007).
- or develop a notion of *fiberwise constraint*, as is done in
 - D. Percivale and P. Podio-Guidugli, A general linear theory of elastic plates and its variational validation. *Boll. Un. Mat. Ital.* (9), 2(2):321–341 (2009).

Alternatively, you can make use of an improved problem sequence.”

Here is how this, and much more, can be done.

2.4 Improved Γ -Convergence Validation of an Approximate Problem

Given a real problem P^r , we look for a problem P_0

- easier to solve than P^r ,
- whose solution u_0 is ‘close’ in some reasonable sense to the solution u^r of problem P^r ,
- which can be obtained via variational convergence.

Here is a two-step sequence of operations that open the way to achieving this goal.

STEP 1. Choose a *sequence of domains* Ω_ε such that

- (i) Ω_ε approaches ω^r as ε goes to zero;
- (ii) $\Omega_{\varepsilon^r} = \Omega^r$.

STEP 2. Choose a *sequence of problems* P_ε defined over Ω_ε , such that

- (i) $\{P_\varepsilon\}$ variationally converges;
- (ii) $P_{\varepsilon^r} = P^r$.

It is for the analyst and the modelist together to exploit efficiently the noticeable amount of remaining freedom in the choices of both domain and problem sequence: we give two examples of such improved Γ -convergence validation set-ups (both examples are taken from the first of the two papers quoted at the onset of this lecture, where a complete derivation of the results quoted here below can be found).

One domain sequence, two energy sequences: Kirchhoff-Love and Reissner-Mindlin plates. Consider a plate-like body of thickness $2h^r$ and mid cross-section $\omega^r = (-\ell^r, +\ell^r) \times (-\ell^r, +\ell^r)$, and identify the body point-wise with the region

$\Omega^r = \omega^r \times (-h^r, +h^r)$ it occupies in a reference configuration. Moreover, let Ω^r be clamped on the Dirichlet part $\partial_D \Omega^r = \partial_D \omega^r \times (-h^r, +h^r)$ of its boundary, subject to null contact loads on the complementary Neumann part, the only applied load being a distance-force field b^r over Ω^r . Finally, let Ω^r be comprised of a linearly elastic isotropic material.

We formulate the real problem

$$P^r : \quad \text{find } u^r = \arg \min_{u \in H_D^1(\Omega^r; \mathbb{R}^3)} \int_{\Omega^r} \left(W^r(E(u)) - b^r \cdot u \right) dx,$$

$$W^r(E) = \mu |E|^2 + \frac{\lambda}{2} (\text{tr } E)^2.$$

Next, we take

STEP 1. (choice of a domain sequence):

$$\Omega_\varepsilon = \omega^r \times \frac{\varepsilon}{\varepsilon^r} (-h^r, +h^r), \quad \varepsilon \in (0, \varepsilon^r].$$

STEP 2. (choice of a problem sequence):

(a) we observe that W^r can be re-written as follows:

$$W^r(E) = \frac{2\mu + \lambda}{2} (E_{11} + E_{22})^2 - 2\mu(E_{11}E_{22} - E_{12}^2)$$

$$+ \frac{2\mu + \lambda}{2} E_{33}^2 + \lambda(E_{11} + E_{22})E_{33} + 2\mu(E_{13}^2 + E_{23}^2);$$

(b) for $\kappa \geq 0$, we define

$$W_\varepsilon(u; \kappa) := \frac{2\mu + \lambda}{2} (E_{11} + E_{22})^2 - 2\mu(E_{11}E_{22} - E_{12}^2)$$

$$+ \frac{2\mu + \lambda}{2} \left(1 - \kappa + \kappa \left(\frac{\varepsilon^r}{\varepsilon} \right)^2 \right) E_{33}^2$$

$$+ \lambda \left(1 - \kappa + \kappa \left(\frac{\varepsilon^r}{\varepsilon} \right) \right) (E_{11} + E_{22})E_{33} + 2\mu(E_{13}^2 + E_{23}^2)$$

$$+ \kappa \left(\frac{\varepsilon^r - \varepsilon}{\varepsilon} \right)^2 ((u_{1,33})^2 + (u_{2,33})^2);$$

(c) we set

$$P_\varepsilon(\kappa) : \quad \text{find } u_\varepsilon = \arg \min_{u \in H_D^1(\Omega_\varepsilon; \mathbb{R}^3)} \frac{1}{\varepsilon} \int_{\Omega_\varepsilon} \left(W_\varepsilon(u; \kappa) - b_\varepsilon \cdot u \right) dx.$$

It is then not too difficult to show that

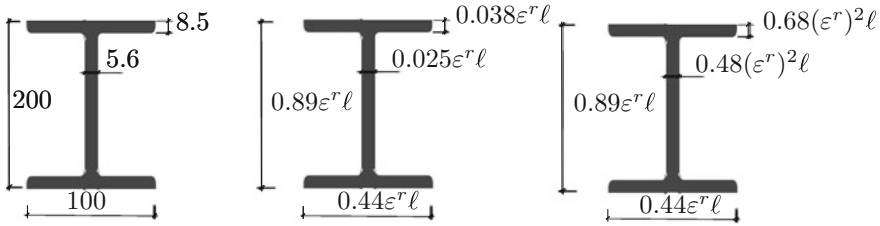


Fig. 1 Slender beam

- for $\kappa = 0$, the setting of the standard Γ -convergence validation is recovered; in fact, *problem sequence* $\{P_\varepsilon(0)\}$ leads to *Kirchhoff-Love plate theory*, and the limit displacement u_0 belongs to the *space of Kirchhoff-Love displacements*:

$$u_0 \in \mathcal{KL} := \{w^a \mathbf{e}_3 + \mathbf{v}^a - x_3 \nabla w^a : \mathbf{v}^a \in H_D^1(\omega^r; \mathbb{R}^2), w^a \in H^2(\omega^r), w^a = w^a_{,n} = 0 \text{ on } \partial_D \omega^r\}.$$

- for $\kappa > 0$, *problem sequence* $\{P_\varepsilon(\kappa)\}$ leads to a *theory of shearable plates*, and the limit displacement u_0 belongs to the *space of Reissner-Mindlin displacements*:

$$u_0 \in \mathcal{RM} := \{w^a \mathbf{e}_3 + \mathbf{v}^a + x_3 \varphi^a; \mathbf{v}^a, \varphi^a \in H_D^1(\omega^r; \mathbb{R}^2), w^a \in H_D^1(\omega^r)\}.$$

Two domain sequences, one energy sequence: Bernoulli-Navier and Vlassov beams. As to the real problem, consider a slender beam with “double-T” cross-section (item (i) of Fig. 1; the dimensions shown are those of a IPE200 steel beam), and let it be 4 m long, say, so that

$$\varepsilon^r = \sqrt{(100^2 + 200^2)}/4000 \approx 0.056.$$

Note that, on accepting the implicit and quite standard slenderness notion, a beam with a rectangular 100×200 cross-section would be considered equally slender.

Two domain sequences can be considered: the first (item (ii) of the figure) reflects the standard slenderness notion; the second (item (iii)) takes into account the higher-order thinness of both flanges and web. Were the beam in question bent, the first notion would be appropriate, in that the shape of the cross-section would make very little difference in the relevant stiffness; not so if it were twisted. Interestingly, choosing the second domain sequence leads to the Vlassov theory, which accurately accommodates both bending and twisting, whereas the other sequence yields the cruder Bernoulli-Navier theory for essentially bent beams.

These examples prompt me to jot down the following

Take-Home Message: In its improved version, Γ -convergence is a powerful validation tool, but it takes knowledgeable modelers to use it well.

3 The Virtual Power Principle

This lecture was meant to show that the Virtual Power Principle (the VPP) is for the theoretical mechanist kind of a Swiss Army knife, in that it has many blades and many accessories one can make good use of. In this connection, it seemed to me appropriate to begin by stating what the VPP is not. I decided to give no references: there are too many (discussable anticipations of the VPP can be traced in certain fragments of Aristotle's), and the contents to be expounded are all rather well-known in continuum and structure mechanics circles.

3.1 The VPP is not a Variational Statement

When recourse is made to the VPP, there is no energy functional to minimize in order to find equilibria. As a matter of fact, the VPP is much more general a tool than Euler-Lagrange equation, because

- it neither obscures nor precludes the contribution of *dissipative forces*, and because
- once constitutive choices singling out inertia forces are made, the *balances* it yields take the form of *evolution equations* for the relevant kinematical fields.

3.2 The Standard VPP

Let B denote a so-called *simple* (or *Cauchy's*) continuous body, which we identify point-wise with a domain in \mathcal{E}^N , with nice boundary ∂B , acted upon by *external distance forces* \mathbf{d}_o at its interior points and by *external contact forces* \mathbf{c}_o at its boundary points, where a *stress field* \mathbf{S} is induced by the loads at equilibrium. Moreover, let $Virt$ denote the space of *test* (\equiv *virtual*) *velocities* $\delta \mathbf{u}$, a collection of fields over B including all *realizable* velocities and being closed under translational observer changes.

The *Standard Virtual Power Principle* amounts to the following statement: for each $\delta \mathbf{u} \in Virt$,

$$\delta \Pi^i(B)[\delta \mathbf{u}] =: \boxed{\int_B \mathbf{S} \cdot \nabla \delta \mathbf{u} = \int_B \mathbf{d}_o \cdot \delta \mathbf{u} + \int_{\partial B} \mathbf{c}_o \cdot \delta \mathbf{u}} := \delta \Pi^e(B)[\delta \mathbf{u}], \quad (1)$$

i.e., the *internal* and *external virtual power expenditures* $\delta \Pi^i(B)$ and $\delta \Pi^e(B)$ should be equal for whatever virtual velocity field $\delta \mathbf{u}$.

As is well-known, via *test invariance* this global statement has two point-wise consequences, the *balance equation*:

$$\text{Div } \mathbf{S} + \mathbf{d}_o = \mathbf{0} \quad \text{in } B, \quad (2)$$

and the *boundary condition*:

$$\mathbf{S}\mathbf{n} = \mathbf{c}_o \quad \text{in } \partial B. \quad (3)$$

Thus, the Standard VPP is basically nothing but a balance statement in a weak form.

NOTE *Translation invariance* of (1) implies a global condition on the load data that is necessary for equilibrium, namely,

$$\int_B \mathbf{d}_o + \int_{\partial B} \mathbf{c}_o = \mathbf{0};$$

needless to say, this condition can be deduced from (2) and (3).

3.3 A Strengthened Version of the VPP

The basic mechanical structure of simple continua can be introduced under form of a *part-wise* VPP; here is how.

Forces can be formally introduced as dual of velocities, and *stresses* as dual of velocity gradients, by laying down two linear, continuous and bounded *power-expenditure functionals*:

$$\begin{aligned} \delta\Pi^e(P)[\delta\mathbf{u}] &:= \int_P \mathbf{d} \cdot \delta\mathbf{u} + \int_{\partial P} \mathbf{c} \cdot \delta\mathbf{u}, \\ \delta\Pi^i(P)[\delta\mathbf{u}] &:= \int_P \mathbf{S} \cdot \nabla\delta\mathbf{u}, \end{aligned} \quad (4)$$

defined for all *body parts* $P \subset B$ and for all $\delta\mathbf{u} \in \text{Virt}$. In so doing, the only *primitive object* is *Virt*, *forces* and *stresses* are *secondary notions*; specification of the two Riesz-duality relations (4) may be regarded as the ‘degré zero’ of the constitutive theory of simple bodies.

The mutual consistency of the stress and contact-force fields is a consequence of postulating the following *Strengthened Virtual Power Principle*:

for each $P \subset B$ and for each $\delta\mathbf{u} \in \text{Virt}$,

$$\delta\Pi^i(P)[\delta\mathbf{u}] = \delta\Pi^e(P)[\delta\mathbf{u}]. \quad (5)$$

Note the twofold quantification: asking that (5) holds for each body part makes (5) much stronger a requirement than (1), which holds for the whole body. This

additional strength connects the values taken by \mathbf{S} and \mathbf{c} at all points of B , and not only at its boundary points, as (3) does. Indeed, beside (3) and the point-wise balance (2)—which, as we know, both follow from (1) test invariance—via part invariance we can arrive from (5) at the *representation formulae*

$$\mathbf{c} = \widehat{\mathbf{c}}(p, \mathbf{n}) := \widehat{\mathbf{S}}(p)\mathbf{n}, \quad \widehat{\mathbf{S}}(p) := \sum_{i=1}^3 \widehat{\mathbf{c}}(p, \mathbf{n}^{(i)}) \otimes \mathbf{n}^{(i)}, \quad (p, \mathbf{n}) \in B \times \mathcal{U},^7$$

from⁷ which we can conclude that *contact interactions and stress convey the same information*.

3.4 The PVP as a Dimension-Reduction Tool

We now want to show how the balance equations of both beam and plate theories can be derived from the Standard VPP, provided the specialty in shape of the body classes in question is exploited.⁸

In an attempt to avoid unnecessary technical complications so as to let the essential conceptual features emerge, we consider the right cylinder shown in Fig. 2, for which, on taking all contact loads null for simplicity, the Standard VPP reads:

$$\int_{S \times (0, l)} \mathbf{S} \cdot \nabla \delta \mathbf{u} = \int_{S \times (0, l)} \mathbf{d} \cdot \delta \mathbf{u}, \quad \text{for all test fields } \delta \mathbf{u}. \quad (6)$$

From 3D to 1D: Beam Theory. Pick the *test fields*

$$\delta \mathbf{u}_R = v(z)\mathbf{e}_2 + (w(z) + y\varphi(z))\mathbf{e}_3,$$

and restrict attention to *load fields* of the form

$$\mathbf{d} = \tilde{p}(x, y, z)\mathbf{e}_2 + \tilde{q}(x, y, z)\mathbf{e}_3.$$

Then, (6) reduces to the following *1D Standard VPP*:

for all scalar test fields v , w , and φ ,

$$\int_0^l (T v' + \tilde{T} \varphi + N w' + M \varphi') = \int_0^l (p v + q w + c \varphi),$$

⁷Here \mathcal{U} is the collection of all unit vectors.

⁸See pp. 214–215 of

– P. Podio-Guidugli, *Lezioni di Scienza delle Costruzioni. II edizione, corretta, riveduta e ampliata*. Aracne, Roma (2009).

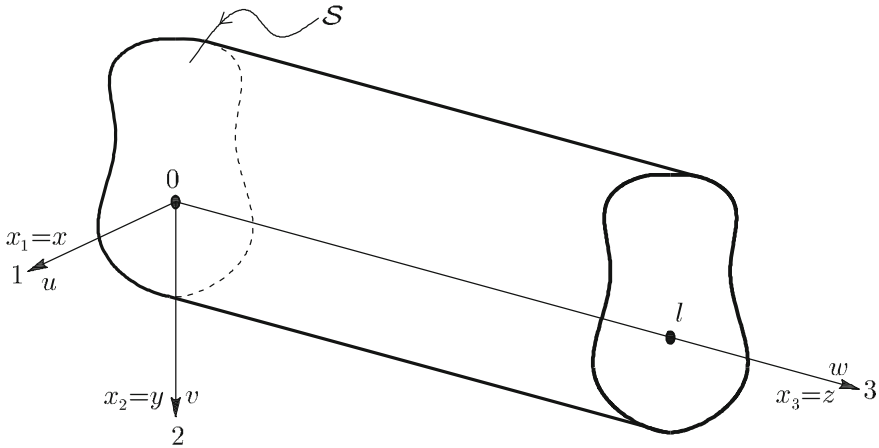


Fig. 2 Cylindrical body

where

$$T := \int_S S_{23}, \quad \tilde{T} := \int_S S_{32}, \quad N := \int_S S_{33}, \quad \text{and} \quad M := \int_S y S_{33},$$

are called, respectively, the *shear forces* T, \tilde{T} , the *normal force* N , and the *bending moment* M , and where

$$p := \int_S \tilde{p}, \quad q := \int_S \tilde{q}, \quad \text{and} \quad \int_S y \tilde{q},$$

are the *transverse load*, the *axial load*, and the *bending couple*, per unit length.

Test invariance of this statement yields both the *balance equations* prevailing at each point $z \in (0, l)$:

$$-T' = p, \quad -N' = q, \quad -M' + \tilde{T} = c$$

and the *boundary conditions* at $z = 0$ and $z = l$, which consist of assignments of

$$\text{either } \left\{ \begin{array}{l} \text{shear force } T \\ \text{normal force } N \\ \text{bending moment } M \end{array} \right\} \text{ or } \left\{ \begin{array}{l} \text{vertical displacement} \\ \text{axial displacement} \\ \text{rotation about } \mathbf{e}_1 \end{array} \right\}.$$

NOTE Our standard version of the 1D VPP is not powerful enough to imply that the shear forces T and \tilde{T} are equal, just as the standard 3D VPP does not imply that the stress field is symmetric.

From 3D to 2D: Plate Theory. This time, all one has to do is:

- (i) to pick the test fields

$$\delta \mathbf{u}_P = w(x, y) \mathbf{e}_3 + z \varphi(x, y), \quad \varphi \perp \mathbf{e}_3$$

and the load fields:

$$\mathbf{d} = \tilde{q}(x, y, z) \mathbf{e}_3;$$

- (ii) to insert these fields into (6);
 (iii) to exploit the inherent test-field quantification.

NOTE Needless to say, the plate test-fields $\delta \mathbf{u}_P$ are ‘Reissner-Mindlin inspired’, just as the beam-test field $\delta \mathbf{u}_R$ are ‘Timoshenko inspired’.

4 A Modicum of Continuum Mechanics

This section offers an enlarged account of the contents of Lecture 4; in particular, Sects. 4.1 and 4.2 are based on material taken, respectively, from

- P. Podio-Guidugli, *Sparse Notes in Continuum and Statistical Thermodynamics*. In preparation, 2006.
- P. Podio-Guidugli, *A Primer in Elasticity*. Kluwer, 2000.

4.1 Kinematics

Space-time structure, deformations, motions. We observe a body against the background of a chosen *space-time structure*. We presume to be able to observe a body ‘atomwise’—that is to say, material point by material point—and that material points can be persistently labelled once and for all.

SPACE STRUCTURE. The first mathematical objects we need are a *three-dimensional Euclidean point space* \mathcal{E} , with typical point x , and a *three-dimensional vector space* \mathcal{V} , with typical vector \mathbf{v} , endowed with an inner product. We think of both \mathcal{E} and \mathcal{V} as *counterclockwise oriented*; hence, in particular, the operation of vector product is unambiguously defined.⁹ The orientation-preserving *isometries* of \mathcal{E} onto itself consist of *translations*:

$$x \mapsto x' = x + \mathbf{v}, \quad \mathbf{v} \in \mathcal{V},$$

⁹Provided we specify what type of analogic watch we use!

and *rotations* about a chosen *origin* o :

$$x \mapsto x' = o + \mathbf{R}(x - o), \quad o \in \mathcal{E}, \quad \mathbf{R} \in \text{Rot}.$$

Here *Rot* denotes the group of all proper orthogonal elements of *Lin*, the linear space of all (second-order) *tensors*, i.e., of all linear transformations of \mathcal{V} into itself.¹⁰ We identify \mathcal{V} with the collection of all translations, and call it the *translation space* of \mathcal{E} .

TIME STRUCTURE. By *time* t we mean a point in a *one-dimensional time manifold* that we identify with the oriented real line $\overrightarrow{\mathbb{R}}$.

DEFORMATIONS. To study body deformations, we need two copies of the pair $(\mathcal{E}, \mathcal{V})$, namely, the *referential* pair $(\mathcal{E}, \mathcal{V})_{ref}$ and the *current* pair $(\mathcal{E}, \mathcal{V})_{cur}$. The referential pair serves the purpose of labelling material points by means of the space points they occupy in \mathcal{E}_{ref} and, in addition, of identifying *material fibers* $(x, \mathbf{e}) \in \mathcal{E}_{ref} \times \mathcal{V}_{ref}$, $|\mathbf{e}| = 1$. The current pair provides the background against which the images of a body and its material fibers are observed at the current time t .

By *image of a material body* $B \subset \mathcal{E}_{ref}$ under a *deformation*—that is, the restriction to B of a smooth invertible mapping

$$f_t : x \mapsto y = f_t(x)$$

from \mathcal{E}_{ref} into \mathcal{E}_{cur} —we mean the set $B_t = f_t(B) \subset \mathcal{E}_{cur}$. By *image of a material fiber* (x, \mathbf{e}) we mean a pair (y, \mathbf{f}) , where $y = f_t(x)$ and $\mathbf{f} = \partial_{\mathbf{e}} f_t(x)$ is the derivative of f_t in the direction \mathbf{e} , evaluated at x , that is to say,

$$\partial_{\mathbf{e}} f_t(x) := \lim_{\varepsilon \rightarrow 0} \frac{f_t(x + \varepsilon \mathbf{e}) - f_t(x)}{\varepsilon}. \quad (7)$$

The notion of material fiber is central to a local analysis of deformation and strain.

MOTIONS. A *body motion* is a one-parameter family of deformations of the form

$$\{f_t \mid f_t = \text{a deformation, } t \in \mathbb{R}\}.$$

To observe body motions, a one-parameter family of copies of $(\mathcal{E}, \mathcal{V})$ is needed; note that the referential pair may but need not be a member of this family.

Deformation gradient. The notion of *deformation gradient* is best introduced as follows:

$$\partial_{\mathbf{e}} f_t(x) =: \mathbf{F}(x, t)\mathbf{e} \quad \text{for all unit vectors } \mathbf{e}. \quad (8)$$

¹⁰Let $\mathbf{1}$ denote the unit element of *Lin*, that is, the identical transformation of \mathcal{V} . The orthogonal elements of *Lin* form the group *Orth*; each element $\mathbf{Q} \in \text{Orth}$ either is an element of *Rot* or has the representations $\mathbf{Q} = \mathbf{IR} = \mathbf{RI}$, with $\mathbf{R} \in \text{Rot}$ and $\mathbf{I} := -\mathbf{1}$ the *central inversion* of \mathcal{V} .

This definition makes evident that, at the present time t , the deformation gradient $\mathbf{F}(x, t)$ at a point $x \in B \subset \mathcal{E}_{ref}$ is a linear mapping from the unit sphere of \mathcal{V}_{ref} into \mathcal{V}_{cur} . This explains why the tensor-like object \mathbf{F} was once upon a time customarily called a *double vector*. This nomenclature is also suggested by the *dyadic representation* of \mathbf{F} , that we now introduce; as a necessary premiss, we recall the notions of dyadic product and curvilinear coordinates.

DYADIC PRODUCT. Given two inner-product vector spaces \mathcal{V}_α ($\alpha = 1, 2$), the *dyadic product* of vectors $\mathbf{a} \in \mathcal{V}_2$ and $\mathbf{b} \in \mathcal{V}_1$ is a linear transformation $\mathbf{a} \otimes \mathbf{b}$ of \mathcal{V}_1 into \mathcal{V}_2 , which is defined as follows:

$$(\mathbf{a} \otimes \mathbf{b})[\mathbf{c}] := (\mathbf{b} \cdot \mathbf{c})\mathbf{a} \quad \text{for all } \mathbf{c} \in \mathcal{V}_1.$$

Now, for \mathbf{A} a linear transformation of \mathcal{V}_1 into \mathcal{V}_2 , the *transpose* \mathbf{A}^T of \mathbf{A} is defined by the following condition:

$$\mathbf{A}\mathbf{b} \cdot \mathbf{a} := \mathbf{b} \cdot \mathbf{A}^T \mathbf{a} \quad \text{for all } \mathbf{a} \in \mathcal{V}_2 \quad \text{and for all } \mathbf{b} \in \mathcal{V}_1.$$

This definition establishes \mathbf{A}^T as a linear transformation of \mathcal{V}_2 into \mathcal{V}_1 ; in particular, it allows to show that¹¹

$$(\mathbf{a} \otimes \mathbf{b})^T = \mathbf{b} \otimes \mathbf{a}.$$

CURVILINEAR COORDINATES. A triplet of real numbers ζ^i ($i = 1, 2, 3$) is a set of *curvilinear coordinates* for a typical point $x \in \mathcal{E}_{ref}$ if it so happens that

$$(\zeta^1, \zeta^2, \zeta^3) \mapsto x = \hat{x}(\zeta^1, \zeta^2, \zeta^3), \quad x \mapsto \zeta^i = \hat{\zeta}^i(x) \quad (i = 1, 2, 3),$$

with

$$\hat{x}(\hat{\zeta}^1(x), \hat{\zeta}^2(x), \hat{\zeta}^3(x)) = x.$$

For each given deformation f_t , we may consider the mapping $f_t \circ \hat{x}$, and write the deformation gradient as:

$$\mathbf{F} = \mathbf{h}_i \otimes \mathbf{g}^i, \quad \mathbf{h}_i := \partial_{\zeta^i} y \quad \mathbf{g}^i := \partial_x \zeta^i, \quad (9)$$

where the vectors \mathbf{g}^i compose the so-called *contravariant base* in the reference placement and the vectors \mathbf{h}_i compose the *covariant base* in the current placement. For \mathbf{g}_i the referential covariant base vectors, it is easy to see that

$$\mathbf{g}^i \cdot \mathbf{g}_j = \begin{cases} 0 & \text{if } i \neq j \\ 1 & \text{if } i = j \end{cases}$$

¹¹Note that, to formulate the definition of transpose, both the inner-product of \mathcal{V}_1 and \mathcal{V}_2 are needed, and that, with slight notational abuse, they both have been denoted by a centered dot.

(and similarly for the vectors of the current covariant and contravariant bases). Hence,

$$\mathbf{F}\mathbf{g}_i = \mathbf{h}_i, \quad (10)$$

so that \mathbf{F} transforms the covariant base in \mathcal{V}_{ref} into the covariant base in \mathcal{V}_{cur} . As anticipated, formula (9) offers another perhaps more explicit way of seeing why \mathbf{F} is called a double vector (as is \mathbf{F}^T , that has the dyadic representation

$$\mathbf{F}^T = \mathbf{g}^i \otimes \mathbf{h}_i \quad (11)$$

and maps linearly \mathcal{V}_{cur} into \mathcal{V}_{ref}). We also have that

$$\mathbf{F}^{-1} = \mathbf{g}_i \otimes \mathbf{h}^i, \quad (12)$$

whence

$$\mathbf{F}^{-T} = \mathbf{h}^i \otimes \mathbf{g}_i, \quad (13)$$

$$\mathbf{F}\mathbf{F}^{-1} = \mathbf{1}_{cur} = \mathbf{h}^i \otimes \mathbf{h}_i = \mathbf{F}^{-T}\mathbf{F}^T, \quad \mathbf{F}^{-1}\mathbf{F} = \mathbf{g}_i \otimes \mathbf{g}^i = \mathbf{1}_{ref}, \quad (14)$$

where $\mathbf{1}_{cur}$ and $\mathbf{1}_{ref}$ are the *metric tensors* in the spaces \mathcal{E}_{cur} and \mathcal{E}_{ref} .¹² Thus, for any given material fiber (x, \mathbf{e}) ,

$$\begin{aligned} \mathbf{F}\mathbf{e} &= (\mathbf{h}_i \otimes \mathbf{g}^i)\mathbf{e} = (\mathbf{g}^i \cdot \mathbf{e})\mathbf{h}_i, \\ \mathbf{F}^{-T}\mathbf{e} &= (\mathbf{h}^i \otimes \mathbf{g}_i)\mathbf{e} = (\mathbf{g}_i \cdot \mathbf{e})\mathbf{h}^i. \end{aligned} \quad (15)$$

In that both \mathcal{E}_{ref} and \mathcal{E}_{cur} are copies of one and the same oriented Euclidean space, a *deformation must preserve local orientation*, in the sense that

$$\det \mathbf{F} > 0 \quad \text{everywhere in } B;$$

the relation

$$\mathbf{h}_1 \times \mathbf{h}_2 \cdot \mathbf{h}_3 =: (\det \mathbf{F}) \mathbf{g}_1 \times \mathbf{g}_2 \cdot \mathbf{g}_3,$$

where \times denotes the vector-product operation, conveniently defines $\det \mathbf{F}$.

Displacement, displacement gradient. The field

$$\mathbf{u}(x, t) := f_t(x) - x$$

¹²Metric tensors specify the outcome of inner products between elements of a given vector space. For example, for $\mathbf{a}, \mathbf{b} \in \mathcal{V}_{ref}$,

$$\mathbf{a} \cdot \mathbf{b} = a^i \mathbf{g}_i \cdot b_j \mathbf{g}^j = a^i b_i = (\mathbf{a} \cdot \mathbf{g}^i)(\mathbf{b} \cdot \mathbf{g}_i) = \mathbf{a} \otimes \mathbf{b} \cdot \mathbf{g}^i \otimes \mathbf{g}_i,$$

a relation that displays the necessary consistency between the inner products in \mathcal{V}_{ref} and Lin_{ref} .

is the *displacement* induced by the motion f_t . In that $f_t(x)$ is a point of \mathcal{E}_{cur} and x of \mathcal{E}_{ref} , the classification of displacement as a vector field requires an *identification* of \mathcal{V}_{ref} and \mathcal{V}_{cur} which is usually left tacit.

The *displacement gradient* $\mathbf{H} := \partial_x \mathbf{u}$ satisfies:

$$\mathbf{F} = \mathbf{H} + \mathbf{1}_{ref};$$

the following representation holds:

$$\mathbf{H} = \mathbf{u}_{,i} \otimes \mathbf{g}^i, \quad \mathbf{u}_{,i} = \partial_{\zeta^i} \mathbf{u}.$$

Strain measures. In the local analysis of a deformation, various \mathbf{F} -based constructs are encountered whose nature is fully tensorial.

Direct applications of definition (8)₂ yield that the *left Cauchy-Green strain measure* $\mathbf{B} := \mathbf{F}\mathbf{F}^T$ is an element of Lin_{cur} , and that the *right Cauchy-Green strain measure* $\mathbf{C} := \mathbf{F}^T\mathbf{F}$ is an element of Lin_{ref} . With the use of (9), we find that:

$$\mathbf{B} = \mathbf{F}\mathbf{F}^T = (\mathbf{g}^i \cdot \mathbf{g}^j) \mathbf{h}_i \otimes \mathbf{h}_j, \quad \mathbf{C} = \mathbf{F}^T\mathbf{F} = (\mathbf{h}_i \cdot \mathbf{h}_j) \mathbf{g}^i \otimes \mathbf{g}^j; \quad (16)$$

these formulae confirm that \mathbf{B} (\mathbf{C}) is a linear transformation of \mathcal{V}_{cur} (\mathcal{V}_{ref}) in itself.

The strain measures are so called because they tell us how the local measures of length, area, and volume, are changed by a deformation, and how the mutual angle of material fibers is changed. To exemplify the role of \mathbf{C} , let (x, \mathbf{e}) and $(x, \bar{\mathbf{e}})$ be two noncollinear material fibers through a point $x \in B$, and let (x, \mathbf{f}) and $(x, \bar{\mathbf{f}})$ be their images under a deformation f_t . Then,

$$\delta l(x, \mathbf{e}) := |\mathbf{f}| - 1 = |\mathbf{F}\mathbf{e}| - 1 = (\mathbf{C} \cdot \mathbf{e} \otimes \mathbf{e})^{1/2} - 1 \quad (17)$$

measures the deformation-induced *length change* in the direction \mathbf{e} ; likewise,

$$\begin{aligned} \delta a(x, \mathbf{e}, \bar{\mathbf{e}}) &:= \arccos(\mathbf{e} \cdot \bar{\mathbf{e}}) - \arccos(|\mathbf{f}|^{-1} |\bar{\mathbf{f}}|^{-1} \mathbf{f} \cdot \bar{\mathbf{f}}) \\ &= \arccos(\mathbf{e} \cdot \bar{\mathbf{e}}) - \arccos \frac{\mathbf{C} \cdot \mathbf{e} \otimes \bar{\mathbf{e}}}{(\mathbf{C} \cdot \mathbf{e} \otimes \mathbf{e})^{1/2} (\mathbf{C} \cdot \bar{\mathbf{e}} \otimes \bar{\mathbf{e}})^{1/2}} \end{aligned} \quad (18)$$

measures the deformation-induced *angle change* of two material fibers directed along \mathbf{e} and $\bar{\mathbf{e}}$.

A deformation is regarded as *small* in a first-order neighborhood of a given material point when the displacement gradient is, in the following sense:

$$\varepsilon := |\mathbf{H} \cdot \mathbf{H}|^{1/2} \ll 1. \quad (19)$$

In this case, strain is measured by the tensor

$$\mathbf{E} := \frac{1}{2}(\mathbf{H} + \mathbf{H}^T).$$

It so happens that

$$\mathbf{E} = \frac{1}{2}(\mathbf{C} - \mathbf{1}_{ref}) - \frac{1}{2}\mathbf{H}^T\mathbf{H}; \quad (20)$$

thus, \mathbf{E} approximates the exact strain measure

$$\tilde{\mathbf{E}} := \frac{1}{2}(\mathbf{C} - \mathbf{1}_{ref}) \quad (21)$$

to within a term of order ε^2 .

4.2 Internal Constraints

In continuum mechanics the standard notion of an internal constraint, i.e., of a restriction on possible strains, is modelled on the notion of a bilateral, perfect and frictionless positional constraint in mass–point mechanics; we recapitulate the latter, as is done in the second reference given at the beginning of this section.

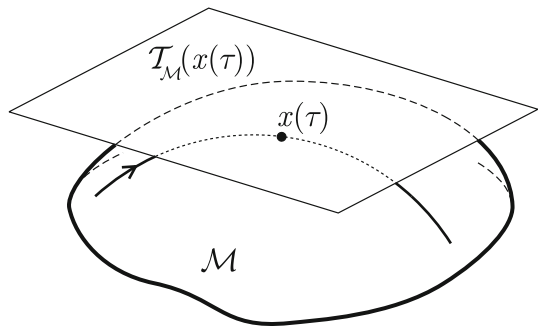
POSITIONAL CONSTRAINTS IN MASS–POINT MECHANICS. Let \mathcal{M} be a surface in \mathcal{E} (Fig. 3), viewed as the locus of zeroes of a smooth scalar mapping $x \mapsto \mu(x)$ on \mathcal{E} . We say that a mass point X , of mass $m > 0$, is constrained to move on \mathcal{M} , or that \mathcal{M} is a (bilateral, positional) *constraint manifold* for X , if all possible trajectories $\tau \mapsto x(\tau)$ in \mathcal{E} of X must lie in \mathcal{M} :

$$\mu(x(\tau)) = 0. \quad (22)$$

Differentiating (22) with respect to τ we have

$$\nabla\mu(x(\tau)) \cdot \mathbf{x}'(\tau) = 0, \quad (23)$$

Fig. 3 A constraint manifold and its tangent plane



where $\mathbf{x} := x - o$ denotes the position vector of a point $x \in \mathcal{M}$ with respect to a fixed origin o ; thus, as a direct *kinematical* consequence of a bilateral positional constraint, we see that, at a point $x(\tau) \in \mathcal{M}$, the possible velocities $\dot{\mathbf{x}}(\tau)$ are orthogonal to the gradient $\nabla\mu$ evaluated at $x(\tau)$, and therefore lie in the tangent plane $\mathcal{T}_{\mathcal{M}}(x(\tau))$ to \mathcal{M} at $x(\tau)$.

In addition to such a kinematical implication, the imposition that a mass point move on a prescribed surface is usually accompanied by the following dynamical stipulations:

1. the total force \mathbf{f} acting on X splits into a *reactive* and an *active* part:

$$\mathbf{f} = \mathbf{f}^{(R)} + \mathbf{f}^{(A)}; \tag{24}$$

2. the reactive part (briefly, the *reaction*) has the representation

$$\begin{aligned} \mathbf{f}^{(R)} &= \varphi^{(R)} \mathbf{n}, & \text{with } \varphi^{(R)}(x) \in \mathbb{R}, \\ \mathbf{n}(x) &:= \frac{\nabla\mu(x)}{|\nabla\mu(x)|} & \text{for } x \in \mathcal{M}, \end{aligned} \tag{25}$$

the scalar multiplier $\varphi^{(R)}$ being *indeterminate*, in the sense that it is not the object of a specific constitutive prescription;

3. the active part at $(x, \tau, \mathbf{v}) \in \mathcal{M} \times \mathbb{R} \times \mathcal{T}_{\mathcal{M}}(x)$ is given by a vector-valued mapping

$$(x, \tau, \mathbf{v}) \mapsto \mathbf{f}^{(A)}(x, \tau, \mathbf{v}). \tag{26}$$

The constraint we just described is termed *bilateral*, because the reaction multiplier $\varphi^{(R)}$ may have any sign; *perfect*, because the modulus of $\varphi^{(R)}$ can take any value may serve to satisfy the motion equations; and *frictionless*, because the reactive force expends no power in any admissible motion:

$$\mathbf{f}^{(R)}(x) \cdot \mathbf{v} = 0, \quad \text{for all } x \in \mathcal{M} \quad \text{and} \quad \mathbf{v} \in \mathcal{T}_{\mathcal{M}}(x). \tag{27}$$

In that it restricts the set of possible motions and specifies to some extent the forces that may accompany them, *the assignment of a constraint is constitutive by nature*. The associated evolution problem has peculiarities that make it different from the unconstrained problem (strictly speaking, the latter may be regarded as an important, but special, case of the former). From the motion equation

$$\mathbf{f}^{(R)} + \mathbf{f}^{(A)} = (m\dot{\mathbf{x}}) \tag{28}$$

and the initial conditions, one seeks to determine the trajectory of X , a curve on \mathcal{M} , and the reaction force as X travels along its trajectory. The two problems are solved in series: firstly, the “pure” (reaction-free) motion equation

$$\mathbf{N}\dot{\mathbf{x}}^{(A)} = \mathbf{N}(m\dot{\mathbf{x}}); \quad \mathbf{N}(x) := \mathbf{I} - \mathbf{n}(x) \otimes \mathbf{n}(x), \tag{29}$$

obtained by projecting (28) onto the current tangent plane, is used to find the trajectory; with this, (28) yields the reaction:

$$\mathbf{f}^{(R)} = (\mathbf{I} - \mathbf{N})[(m\mathbf{x}') - \mathbf{f}^{(A)}] = \{\mathbf{n} \cdot [(m\mathbf{x}') - \mathbf{f}^{(A)}]\}\mathbf{n}. \quad (30)$$

In (30), the constitutive prescription (26) is used to determine the active force at each point $x(\tau)$ of the trajectory:

$$\mathbf{f}^{(A)} = \mathbf{f}^{(A)}(x(\tau), \tau, \mathbf{x}(\tau)).$$

Thus, in particular, the reaction multiplier has the following expression:

$$\varphi^{(R)}(x(\tau)) = \mathbf{n}(x(\tau)) \cdot [(m\mathbf{x}'(\tau)) - \mathbf{f}^{(A)}(x(\tau), \tau, \mathbf{x}(\tau))].$$

CONSTRAINT MANIFOLDS. A *constraint manifold* is a connected C^1 -manifold $\mathcal{M} \subset Lin^+$ such that

- (i) $\mathbf{I} \in \mathcal{M}$;
- (ii) if $\mathbf{F} \in \mathcal{M}$ and $\mathbf{R} \in Rot$, then $\mathbf{R}\mathbf{F} \in \mathcal{M}$.

Constraint manifolds are studied in detail in the booklet quoted at the beginning of this section; those of interest have $dim(\mathcal{M}) \leq 8$; of the following well-known examples of unidimensional constraint manifold, the first play a relevant role in fluid mechanics, the other two in structure mechanics.

- **Incompressibility:**

$$\mathcal{M} = \{\mathbf{F} \in Lin^+ \mid \det \mathbf{F} = 1\};$$

accordingly, an incompressible material can only perform *isochoric* (volume-preserving) motions. In this case, $\mathcal{T}_{\mathcal{M}}(\mathbf{F}) = \{\dot{\mathbf{F}} \mid \dot{\mathbf{F}} \cdot \mathbf{F}^{-T} = 0\}$; consequently, $\mathcal{P}^{(R)} = \pi^{(R)}\mathbf{F}^{-T}$. The momentum balance equation:

$$Div \mathbf{P} + \bar{\mathbf{d}} = \mathbf{0},$$

where \mathbf{P} is Piola's stress and $\bar{\mathbf{d}}$ is the distance force per unit referential volume, becomes:

$$\nabla \pi^{(R)} + Div \mathbf{P}^{(A)} + \bar{\mathbf{d}} = \mathbf{0}; \quad (31)$$

its 'pure' consequence is:

$$Curl (Div \mathbf{P}^{(A)} + \bar{\mathbf{d}}) = \mathbf{0}. \quad (32)$$

- **Inextensibility** in the direction \mathbf{e} :

$$\mathcal{M} = \{\mathbf{F} \in Lin^+ \mid |\mathbf{F}\mathbf{e}| = 1\};$$

accordingly, whatever $x \in B$, material fibers (x, \mathbf{e}) cannot possibly change their length. In this case, $\mathcal{T}_{\mathcal{M}}(\mathbf{F}) = \{\dot{\mathbf{F}} \mid \dot{\mathbf{F}} \cdot (\mathbf{F}\mathbf{e} \otimes \mathbf{e}) = 0\}$; consequently, $\mathbf{P}^{(R)} = \lambda^{(R)}\mathbf{F}\mathbf{e} \otimes \mathbf{e}$.

- **Orthogonality** preserving in the orthogonal directions $\mathbf{e}, \bar{\mathbf{e}}$:

$$\mathcal{M} = \{\mathbf{F} \in Lin^+ \mid \mathbf{F}\mathbf{e} \cdot \mathbf{F}\bar{\mathbf{e}} = 0\};$$

accordingly, whatever $x \in B$, material fibers $(x, \mathbf{e}), (x, \bar{\mathbf{e}})$ must stay orthogonal in all possible deformations. In this case, $\mathcal{T}_{\mathcal{M}}(\mathbf{F}) = \{\dot{\mathbf{F}} \mid \dot{\mathbf{F}} \cdot \mathbf{F}(\mathbf{e} \otimes \bar{\mathbf{e}} + \bar{\mathbf{e}} \otimes \mathbf{e}) = 0\}$; consequently, $\mathbf{P}^{(R)} = \delta^{(R)}\mathbf{F}(\mathbf{e} \otimes \bar{\mathbf{e}} + \bar{\mathbf{e}} \otimes \mathbf{e})$.

The following combined constraint is of importance to arrive to interesting generalizations of the *Föppl-von Kármán* plate theory and to study of *buckling instabilities of von Kármán type*:

- *inextensibility* in the direction \mathbf{e} coupled with preservation of *orthogonality* of \mathbf{e} and all directions $\bar{\mathbf{e}}$ orthogonal to \mathbf{e} :

$$\mathcal{M} = \{\mathbf{F} \in Lin^+ \mid \mathbf{F}\mathbf{e} = \mathbf{F}^{-T}\}. \tag{33}$$

It is not difficult to check that (33) implies both extensibility in the direction \mathbf{e} (because $\mathbf{F}\mathbf{e} \cdot \mathbf{F}\mathbf{e} = \mathbf{F}\mathbf{e} \cdot \mathbf{F}^{-T}\mathbf{e} = 1$) and preservation of orthogonality for directions \mathbf{e} and $\bar{\mathbf{e}}$ (because $\mathbf{F}\bar{\mathbf{e}} \cdot \mathbf{F}\mathbf{e} = \mathbf{F}\bar{\mathbf{e}} \cdot \mathbf{F}^{-T}\mathbf{e} = 0$).

NOTE This internal constraint takes an especially simple form in terms of the exact strain measure $\tilde{\mathbf{E}}$ defined in (21); this expression is:

$$\tilde{\mathbf{E}}\mathbf{e} = \mathbf{0}.^{13} \tag{34}$$

Linearization¹³ of (34) with respect to the smallness parameter introduced in (19) yields the well-known constraint that, as we shall see, leads to the *Kirchhoff-Love theory of plates*, namely,

$$\mathbf{E}\mathbf{e} = \mathbf{0}. \tag{35}$$

In both its exact and linearized versions, \mathbf{e} is the direction orthogonal to the mid plane of the plate.

5 Plate Buckling, à la von Kármán, But Not Quite

This lecture was based on

- P. Podio-Guidugli, A new quasilinear model for plate buckling. *J. Elasticity*, Vol. 71, pp. 157–182 (2003).

¹³Indeed,

$$\mathbf{E}\mathbf{e} = \mathbf{0} \Leftrightarrow \mathbf{F}^T\mathbf{F}\mathbf{e} - \mathbf{e} = \mathbf{0} \Leftrightarrow \mathbf{F}\mathbf{e} = \mathbf{F}^{-T}\mathbf{e}.$$

5.1 The 3D Buckling Problem

Consider a plate-like body $\mathcal{C}(\varepsilon)$ of constant thickness, that is, a right cylinder of axis \mathbf{z} and cross-section \mathcal{P} , and identify it pointwise with the set $\mathcal{P} \times (-\varepsilon, +\varepsilon)$, with $2\varepsilon \ll \text{diam}(\mathcal{P})$ (the mid cross-section of $\mathcal{C}(\varepsilon)$ is depicted in Fig. 4). Let $\mathcal{C}(\varepsilon)$ be *weakly clamped* along its lateral boundary (see Fig. 5), and subject to in-plane compressive loads.

When the load attains a critical value, the plate ‘buckles’, that is, ceases to stay flat and assumes a bent shape. Although modelling the post-buckling behaviour is often of importance, the first and mostly wanted piece of information an engineer looks for is the *buckling load*, that is, the load value at the onset of buckling. This value is efficiently computed by solving a system of equations put together by Th. von Kármán in 1910. Instead of solving a rather formidable three-dimensional problem in nonlinear elasticity, he was able to devise a set of approximating assumptions, whose successful outcome convinced many for a long long while to trade intuitive plausibility for a rational justification.

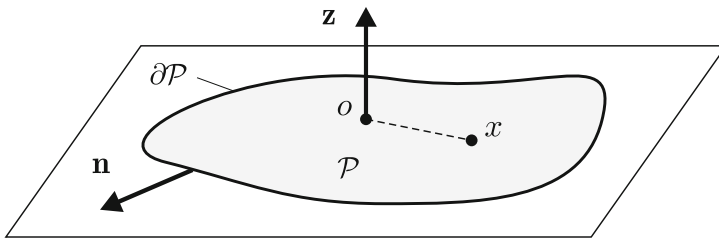


Fig. 4 Mid cross-section of a plate-like body

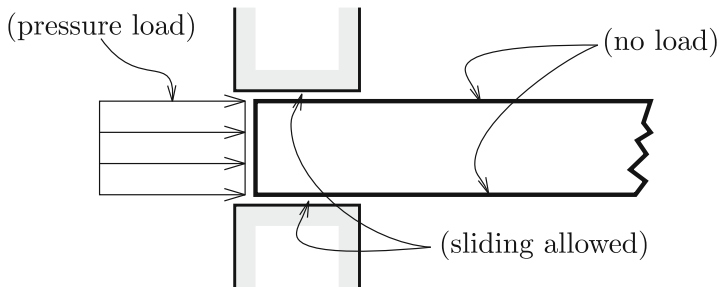


Fig. 5 Weakly-clamped boundary conditions

5.2 The 2D von Kármán Model

Let two scalar-valued fields φ_0, φ_1 over $\partial\mathcal{P}$ be given. One is due to find a real number λ and two scalar-valued fields φ, w over $\mathcal{P} \cup \partial\mathcal{P}$ such that

- in \mathcal{P} ,

$$\Delta \Delta \varphi - \frac{1}{2}[w, w]=0, \quad \kappa \Delta \Delta w - [\varphi, w]=0;$$

- in $\partial\mathcal{P}$,

$$\varphi = \lambda\varphi_0, \quad \partial_{\mathbf{n}}\varphi = \lambda\varphi_1, \quad w = 0, \quad \partial_{\mathbf{n}}w = 0.$$

Here,

- the *semilinear* problem to solve is governed by a system of two PDEs with *biharmonic* principal part;
- nonlinearity is brought in via the *Monge-Ampère differential “crochet”*:

$$[a, b] := a_{,11} b_{,22} + a_{,22} b_{,11} - 2a_{,12} b_{,12};$$

- φ is an Airy-type *stress function*;
- $w(x)\mathbf{c}$ is *transverse displacement* of $x \in \mathcal{P} \cup \partial\mathcal{P}$;
- $\kappa > 0$ is a *stiffness constant*, λ is a *load multiplier*.

We recall that a nonlinear differential problem is *semilinear* when its *principal part* (i.e., the collection of higher-order derivatives) is linear, with nonlinearity carried in through terms involving lower-order derivatives; and is *quasilinear* when its principal part is nonlinear. As a rule, semilinear problems are noticeably easier than quasilinear ones. Remarkably, given that *the 3D problem is quasilinear*, von Kármán’s modelling has suppressed a mathematically relevant difficulty.

We observe that the principal part of the second of von Kármán’s equations coincides with the operator of the classic linear theory of Kirchhoff-Love plates, suggesting an interpretation as an equilibrium equation under null transverse loads; an interpretation for the first von Kármán’s equation will be given in Sect. 5.4.

5.3 Back to the 3D Buckling Problem

We wish to put together an approximate 2D model that preserve the main mathematical character of the 3D problem, reduce to von Kármán’s in a mathematically explicit limit, and whose governing equations have a transparent interpretation. With a view toward this goal, we perform three preliminary steps.

i. Constrained Kinematics. We stipulate that *material fibers parallel to \mathbf{z} stay straight, do not change their length, and remain orthogonal to fibers orthogonal to \mathbf{z} :*

$$\tilde{\mathbf{E}}\mathbf{z} = \mathbf{0} \quad \text{in } \mathcal{C}(\varepsilon) \quad (36)$$

(recall (34)), where

$$\tilde{\mathbf{E}} = \frac{1}{2}((\nabla f)^T \nabla f - \mathbf{1}_{ref}).$$

Just as per (35), this is nonlinear counterpart of Kirchhoff-Love constraint:

$$\mathbf{E}\mathbf{z} = \mathbf{0},$$

a linear system of PDEs whose general solution is

$$\mathbf{u}_{KL}(x, \zeta) = \mathbf{v}(x) + w(x)\mathbf{z} - \zeta \nabla w(x), \quad \mathbf{v}(x) \cdot \mathbf{z} = 0. \quad (37)$$

Now, it turns out that that nonlinear PDE system (36) is solved by:

$$f(x, \zeta) = g(x) + \zeta \mathbf{m}(x), \quad (x, \zeta) \in \mathcal{P} \times (-\varepsilon, +\varepsilon), \quad (38)$$

where the point-valued function $g \equiv f|_{\mathcal{P}}$ delivers the *deformed cross section*, whose unit *normal* \mathbf{m} is computable in terms of g itself by a well-known formula from surface geometry. Note that the displacement field corresponding to (38) is:

$$\mathbf{u}_{vK}(x, \zeta) = f(x, \zeta) - x = g(x) - x + \zeta \mathbf{m}(x);$$

with slight abuse of notation, we set:

$$g(x) - x = \mathbf{v}(x) + w(x)\mathbf{c}.$$

Note also that the Kirchhoff-Love kinematics is recovered whenever

$$m_\alpha \simeq -w_{,\alpha} \quad \text{and} \quad m_3 \simeq 1.$$

ii. Constrained Elastic Response. We assume that the kinematical constraint (34) is maintained by a *powerless reactive Cosserat stress field*. In line with this assumption, we split the Cosserat stress \mathbf{S} additively:

$$\mathbf{S} = \mathbf{S}^{(A)} + \mathbf{S}^{(R)}, \quad \mathbf{S}^{(A)} \cdot \mathbf{S}^{(R)} = 0.$$

Given that

$$\tilde{\mathbf{E}}\mathbf{c} = \mathbf{0} \quad \Leftrightarrow \quad \tilde{\mathbf{E}} \cdot (\mathbf{a} \otimes \mathbf{c} + \mathbf{c} \otimes \mathbf{a}) = 0,$$

So we set

$$\mathcal{R} := \text{span}\{\mathbf{a} \otimes \mathbf{c} + \mathbf{c} \otimes \mathbf{a}\} \quad \forall \mathbf{a} \perp \mathbf{c}, \tag{39}$$

and stipulate that

$$\mathbf{S}^{(R)} \in \mathcal{R}, \quad \tilde{\mathbf{E}}, \mathbf{S}^{(A)} \in \mathcal{A} := \mathcal{R}^\perp. \tag{40}$$

As to the active stress $\mathbf{S}^{(A)}$, we choose a \mathbf{z} -transversely isotropic *St. Venant-Kirchhoff response*:

$$\mathbf{S}^{(A)} = \frac{E}{1 + \nu} \left(\tilde{\mathbf{E}} + \frac{\nu}{1 - \nu} (\text{tr} \tilde{\mathbf{E}}) \mathbf{1} \right), \tag{41}$$

or rather, equivalently,

$$\tilde{\mathbf{E}} = \frac{1 + \nu}{E} \left(\mathbf{S}^{(A)} - \frac{\nu}{1 + \nu} (\text{tr} \mathbf{S}^{(A)}) \mathbf{1} \right).$$

iii. Boundary Conditions. The stress boundary conditions are expressed in terms of Piola’s stress. Given the relationship between Piola’s and Cosserat’s stress measures:

$$\mathbf{S} = \mathbf{F}^{-1} \mathbf{P},$$

we have:

- top and bottom of $\mathcal{C}(\varepsilon)$:

$$\mathbf{Pz} = \mathbf{0} \quad \Leftrightarrow \quad \mathbf{S}^{(R)} \mathbf{c} = \mathbf{0};$$

- lateral mantel of $\mathcal{C}(\varepsilon)$:

$$\mathbf{Pn} = -\lambda \mathbf{n} \quad \Leftrightarrow \quad \mathbf{S}^{(R)} \mathbf{n} = \mathbf{0} \quad \& \quad \mathbf{S}^{(A)} \mathbf{n} = -\lambda \mathbf{F}^{-1} \mathbf{n};$$

- weak-clamping condition:

$$w = 0 \quad \& \quad \mathbf{m} = \mathbf{z} \quad \Leftrightarrow \quad w = 0 \quad \& \quad \partial_n w = 0 \quad \text{in } \partial \mathcal{P}.$$

We are now in a position to derive an exact 2D antecedent for each of the two v. Kármán’s equations. The interested reader is referred to the quoted paper for their rather complex derivation.

5.4 Compatibility and v. K’s 1st Equation

It can be shown that the following PDE, which is *an exact consequence of St. Venant-Beltrami compatibility conditions*, must hold in \mathcal{P} :

$$\Delta \Delta \varphi - \frac{1}{2}[w, w] + \frac{1}{2}\left([v_\alpha, v_\alpha] + \frac{1}{3}\varepsilon^2[m_i, m_i]\right) = 0. \quad (42)$$

This compatibility condition insures, roughly speaking, that a suitably defined plane strain field allows for the construction of a displacement field consistent with the internal constraint (36).

Recall now *v. K.'s 1st Equation*:

$$\Delta \Delta \varphi - \frac{1}{2}[w, w] = 0. \quad (43)$$

The obvious scaling

$$w^\varepsilon = \varepsilon w, \quad \mathbf{v}^\varepsilon = \varepsilon^2 \mathbf{v}, \quad \varphi^\varepsilon = \varepsilon^2 \varphi,$$

permits us to conclude that (42) is indeed an exact 2D antecedent of (43).

5.5 Equilibrium and *v. K.'s 2nd Equation*

At equilibrium, at each point of $\mathcal{C}(\varepsilon)$,

$$\text{Div } \mathbf{P} = \mathbf{0},$$

which can also be written in the form:

$$(\mathbf{P}\mathbf{c}_\alpha)_{,\alpha} + (\mathbf{P}\mathbf{z})_{,\zeta} = \mathbf{0}. \quad (44)$$

Combining (44) with (39) and (40) yields:

$$\begin{aligned} (S_{\beta\alpha}^{(A)} \mathbf{h}_\beta)_{,\alpha} \cdot \mathbf{h}_\gamma + P_{\gamma 3}^{(R)}_{,\zeta} &= 0, \\ (\mathbf{h}_{\beta,\alpha} \cdot \mathbf{m}) S_{\beta\alpha}^{(A)} + ((\mathbf{h}^\alpha \cdot \mathbf{h}^\beta) P_{\beta 3}^{(R)})_{,\alpha} + P_{33}^{(R)}_{,\zeta} &= 0, \end{aligned}$$

where $\mathbf{h}_\alpha, \mathbf{h}^\beta$ are, respectively, the *covariant* and *contravariant* base vectors associated with the *deformed* shape of $\mathcal{C}(\varepsilon)$. From this system, a ‘pure’ (\equiv reaction-free; recall the developments in Sect. 4.2) equation holding in \mathcal{P} can be deduced, namely,

$$\cdot \int_{-\varepsilon}^{+\varepsilon} \left((\mathbf{h}^\alpha \cdot \mathbf{h}^\beta) \int_{-\varepsilon}^{\zeta} (S_{\delta\gamma}^{(A)} \mathbf{h}_\delta)_{,\gamma} \cdot \mathbf{h}_\beta d\tau \right)_{,\alpha} d\zeta - \int_{-\varepsilon}^{+\varepsilon} (\mathbf{h}_{\beta,\alpha} \cdot \mathbf{m}) S_{\beta\alpha}^{(A)} d\zeta = 0$$

Combination with relation (41) specifying the active stress response yields a *4th-order quasilinear PDE*, whose *principal part* is:

$$p.p.(\varepsilon; w, \mathbf{v}) = \frac{E}{1 - \nu^2} (\mathbf{m} \cdot \mathbf{c}) B^{\alpha\delta}(\varepsilon; w, \mathbf{v}) (\Delta w)_{,\delta\alpha};$$

That equation is *an exact antecedent of v. K's 2nd equation*:

$$\kappa \Delta \Delta w - [\varphi, w] = 0,$$

whose

$$p.p.(\varepsilon; w) = \kappa(\varepsilon) \Delta \Delta w, \quad \kappa(\varepsilon) = \frac{E\varepsilon^2}{3(1-\nu^2)};$$

when coupled with (42), it can be casted under form of a nonlinear bifurcation problem, whose analysis is, at the moment of this writing, still wanted.

6 Mechanical Scaling

This lecture was based on

- B. Miara and P. Podio-Guidugli, Deduction by scaling: a unified approach to classic plate and rod theories. *Asymptotic Analysis*, Vol. 51 (2), pp. 113–131 (2007).

6.1 The Scaling Procedure in Summary

Just as we did in the previous lecture, we consider a body under form of a right cylinder of constant cross-section but, at variance with what we did there, we do not presume that the cylinder's length is much smaller than the diameter of its cross-section.

We begin by listing the sequence of steps of our deductive procedure:

- data (\equiv domain, elastic moduli, applied forces) and solution are scaled in terms of *integer powers of a parameter* ε ;
- the total (elastic + load) energy functional:

$$\Pi(\mathbf{u}, \varepsilon) = \Sigma(\mathbf{u}, \varepsilon) - \Delta(\mathbf{u}, \varepsilon),$$

where

$$\begin{aligned} \Sigma(\mathbf{u}, \varepsilon) &:= \int_{\mathcal{C}(\varepsilon)} \frac{1}{2} S_{ij}(\mathbf{E}(\mathbf{u})) E_{ij}(\mathbf{u}), \\ \Delta(\mathbf{u}, \varepsilon) &:= \int_{\mathcal{C}(\varepsilon)} \mathbf{b} \cdot \mathbf{u} + \int_{\mathcal{P}(\varepsilon)} \mathbf{c}^\pm \cdot \mathbf{u}^\pm, \end{aligned}$$

is scaled (here, $\mathcal{C}(\varepsilon) = \mathcal{P}(\varepsilon) \times]-\varepsilon h, +\varepsilon h[$, as a consequence of domain scaling; moreover, $(\mathbf{c}^+, \mathbf{u}^+)$ ($(\mathbf{c}^-, \mathbf{u}^-)$) denote the (applied load, displacement) pair at the top (bottom) end of $\mathcal{C}(\varepsilon)$);

- sets of *scaling exponents* are chosen, by requiring that the *scaled total-energy functional stays finite when $\varepsilon \rightarrow 0$* ;
- *backward-scaling of limit functionals* yields K-L and R-M functionals (and many others!).

6.2 Preparatory Scalings

Firstly, for each ε fixed in the half-open interval $]0, 1]$, we scale the *domain*:

$$x_\alpha = \varepsilon^p \bar{x}_\alpha \quad (\alpha = 1, 2), \quad x_3 = \varepsilon^q \bar{x}_3$$

and the *displacement*:

$$u_\alpha = \varepsilon^m \bar{u}_\alpha \quad (\alpha = 1, 2), \quad u_3 = \varepsilon^n \bar{u}_3,$$

whence the *strain scaling*:

$$\begin{aligned} \mathbf{E} &= \varepsilon^{\alpha_1} \bar{E}_{\alpha\beta} \operatorname{sym}(\mathbf{c}_\alpha \otimes \mathbf{c}_\beta) + \varepsilon^{\alpha_2} \bar{E}_{\alpha 3} \operatorname{sym}(\mathbf{c}_\alpha \otimes \mathbf{c}_3) + \varepsilon^{\alpha_3} \bar{E}_{33} \mathbf{c}_3 \otimes \mathbf{c}_3 \\ \alpha_1 &= -p + m, \quad \alpha_2 = -p + n, \quad \alpha_3 = -q + n. \end{aligned}$$

NOTE To derive plate equations either by *asymptotic analysis* or by *variational convergence*, the *standard (domain, displacement) scaling* is:

$$m = 1, \quad n = 0, \quad p = 0, \quad q = 1.$$

Secondly, we choose the material response to be that of a linearly elastic material, *transversely isotropic* with respect to the axial direction:

$$\begin{aligned} S_{\alpha\beta} &= 2\mu E_{\alpha\beta} + (\lambda(E_{11} + E_{22}) + \tau_2 E_{33}) \delta_{\alpha\beta}, \\ S_{3\alpha} &= 2\gamma E_{3\alpha}, \\ S_{33} &= \tau_1 E_{33} + \tau_2(E_{11} + E_{22}) \end{aligned}$$

$$\mu > 0, \quad \gamma > 0, \quad \tau_1 > 0, \quad \tau_1(\lambda + \mu) - \tau_2^2 > 0;$$

and we scale the *material moduli* as follows:

$$\bar{\lambda} = \varepsilon^{-r} \lambda, \quad \bar{\mu} = \varepsilon^{-r} \mu, \quad \bar{\gamma} = \varepsilon^{-u} \gamma, \quad \bar{\tau}_1 = \varepsilon^{-v} \tau_1, \quad \bar{\tau}_2 = \varepsilon^{-z} \tau_2.$$

6.3 The Scaled Load Potential

In principle, we wish to keep track of all pieces of the *load functional*

$$\Delta(\mathbf{u}, \varepsilon) := \int_{\mathcal{C}(\varepsilon)} \mathbf{b} \cdot \mathbf{u} + \int_{\mathcal{P}(\varepsilon)} \mathbf{c}^\pm \cdot \mathbf{u}^\pm,$$

Accordingly, we scale the loads as follows:

$$\begin{aligned} \text{distance loads: } \bar{b}_\alpha &= \varepsilon^{-s} b_\alpha, & \bar{b}_3 &= \varepsilon^{-t} b_3; \\ \text{contact loads: } \bar{c}_\alpha^\pm &= \varepsilon^{-y} c_\alpha^\pm, & \bar{c}_3^\pm &= \varepsilon^{-w} c_3^\pm, \end{aligned}$$

with

$$s + q = y, \quad t + q = w.$$

We find:

$$\widehat{\Delta}(\bar{\mathbf{u}}, \varepsilon; \hat{\delta}_1, \hat{\delta}_2) = \varepsilon^{\hat{\delta}_1} \Delta_1(\bar{\mathbf{u}}) + \varepsilon^{\hat{\delta}_2} \Delta_2(\bar{\mathbf{u}}),$$

with

$$\begin{aligned} \Delta_1(\bar{\mathbf{u}}) &= \int_{\mathcal{C}(1)} \bar{b}_\alpha \bar{u}_\alpha + \int_{\mathcal{P}(1)} \bar{c}_\alpha^\pm \bar{u}_\alpha^\pm, & \Delta_2(\bar{\mathbf{u}}) &= \int_{\mathcal{C}(1)} \bar{b}_3 \bar{u}_3 + \int_{\mathcal{P}(1)} \bar{c}_3^\pm \bar{u}_3^\pm, \\ \hat{\delta}_1 &= m + 2p + q + s, & \hat{\delta}_2 &= n + 2p + q + t. \end{aligned}$$

6.4 The Scaled Total-Energy Functional

At the end of the day, the total (elastic + load) *energy functional*:

$$\Pi(\mathbf{u}, \varepsilon) = \Sigma(\mathbf{u}, \varepsilon) - \Delta(\mathbf{u}, \varepsilon)$$

turns out to be scaled as follows:

$$\begin{aligned} \widehat{\Pi}(\bar{\mathbf{u}}, \varepsilon; \hat{\alpha}, \dots, \hat{\delta}_2) &= \widehat{\Sigma}(\bar{\mathbf{u}}, \varepsilon; \hat{\alpha}, \hat{\beta}_1, \hat{\beta}_2, \hat{\gamma}) - \widehat{\Delta}(\bar{\mathbf{u}}, \varepsilon; \hat{\delta}_1, \hat{\delta}_2) \\ &= \varepsilon^{\hat{\alpha}} \mathbf{A}(\bar{\mathbf{u}}) + \varepsilon^{\hat{\beta}_1} \mathbf{B}_1(\bar{\mathbf{u}}) + \varepsilon^{\hat{\beta}_2} \mathbf{B}_2(\bar{\mathbf{u}}) + \varepsilon^{\hat{\gamma}} \Gamma(\bar{\mathbf{u}}) - \varepsilon^{\hat{\delta}_1} \Delta_1(\bar{\mathbf{u}}) - \varepsilon^{\hat{\delta}_2} \Delta_2(\bar{\mathbf{u}}), \end{aligned}$$

where

$$\begin{aligned} \hat{\alpha} &= -m + 3n + p + v, & \hat{\beta}_1 &= m + n + p + u, \\ \hat{\beta}_2 &= m + n + p + z, & \hat{\gamma} &= 3m - n + p + 2z - v, \\ \hat{\delta}_1 &= 2m - n + 3p + s, & \hat{\delta}_2 &= m + 3p + t, \end{aligned}$$

with the *consistency condition*:

$$\hat{\alpha} - 2\hat{\beta}_2 + \hat{\gamma} = 0.$$

6.5 A Mechanical Principle of Convergence in Energy

We stipulate that

energy exponents be such that the scaled energy functional stay bounded above under the scaling group action:

$$\lim_{\varepsilon \rightarrow 0^+} \widehat{\Pi}(\bar{\mathbf{u}}, \varepsilon; \hat{\ell}) = \widehat{\Pi}(\bar{\mathbf{u}}, 0; \hat{\ell}) < +\infty,$$

at whatever field $\bar{\mathbf{u}}$ keeps each of the integrals in $\widehat{\Pi}$ finite.

This finiteness requirement acts as a selection criterion, because

- whenever anyone of the energy exponents $\hat{\alpha}, \hat{\beta}_1, \dots, \hat{\delta}_2$ in

$$\begin{aligned} & \widehat{\Pi}(\bar{\mathbf{u}}, \varepsilon; \hat{\alpha}, \dots, \hat{\delta}_2) \\ &= \varepsilon^{\hat{\alpha}} \mathbf{A}(\bar{\mathbf{u}}) + \varepsilon^{\hat{\beta}_1} \mathbf{B}_1(\bar{\mathbf{u}}) + \varepsilon^{\hat{\beta}_2} \mathbf{B}_2(\bar{\mathbf{u}}) + \varepsilon^{\hat{\gamma}} \Gamma(\bar{\mathbf{u}}) - \varepsilon^{\hat{\delta}_1} \Delta_1(\bar{\mathbf{u}}) - \varepsilon^{\hat{\delta}_2} \Delta_2(\bar{\mathbf{u}}), \end{aligned}$$

is positive [null], then the corresponding functional $\mathbf{A}, \mathbf{B}_1, \dots, \Delta_2$ is eliminated from [remains in] the limit functional $\widehat{\Pi}(\bar{\mathbf{u}}, 0; \hat{\ell})$, and hence is eliminated from [remains in] the related version of the energy functional $\Pi(\mathbf{u}, \varepsilon)$, which is arrived at after inverse scaling;

- whenever any one of the energy exponents $\hat{\alpha}, \hat{\beta}_1, \hat{\gamma}$ is negative, then the corresponding functional $\mathbf{A}, \mathbf{B}_1, \Gamma$ must be made to vanish identically: since each of those functionals is positive definite, this can only be achieved by restricting the class of functions on which the energy functional Π is defined; hence, a corresponding *internal constraint must be imposed*.

6.6 Taxonomy of Energy Functionals

For simplicity, we take $\hat{\delta}_1 = \hat{\delta}_2 = 0$; in addition, to concentrate on *shearable* structures, we take $\hat{\beta}_1 = 0$.

- (*in-plane stretching and flexure of plate-like cylinders*)
for $\hat{\alpha} < 0$, $\hat{\gamma} = 0$, the scaled elastic potential takes the form:

$$\widehat{\Sigma}_P(\bar{\mathbf{u}}, \varepsilon; \hat{\beta}_1, \hat{\gamma}) = \varepsilon^{\hat{\beta}_1} \mathbf{B}_1(\bar{\mathbf{u}}) + \varepsilon^{\hat{\gamma}} \Gamma(\bar{\mathbf{u}}),$$

and hence the relative energy functional is

$$\begin{aligned} \Pi_P(\mathbf{u}, \varepsilon) &= \int_{C(\varepsilon)} 2\gamma(E_{13}^2(\mathbf{u}) + E_{23}^2(\mathbf{u})) \\ &+ \int_{C(\varepsilon)} \frac{1}{2} \left((\lambda + 2\mu)(E_{11}(\mathbf{u}) + E_{22}(\mathbf{u}))^2 - 4\mu(E_{11}(\mathbf{u})E_{22}(\mathbf{u}) - E_{12}^2(\mathbf{u})) \right), \end{aligned}$$

defined over displacement class $u_3 = \hat{u}_3(x_1, x_2)$.

- (axial stretching and flexure of rod-like cylinders)
for $\hat{\alpha} = 0$, $\hat{\gamma} < 0$,

$$\widehat{\Sigma}_R(\bar{\mathbf{u}}, \varepsilon; \hat{\alpha}, \hat{\beta}_1) = \varepsilon^{\hat{\alpha}} \mathbf{A}(\bar{\mathbf{u}}) + \varepsilon^{\hat{\beta}_1} \mathbf{B}_1(\bar{\mathbf{u}});$$

the associated energy functional reads:

$$\Pi_R(\mathbf{u}, \varepsilon) = \Sigma_R(\mathbf{u}, \varepsilon) - \Delta(\mathbf{u}, \varepsilon),$$

where

$$\Sigma_R(\mathbf{u}, \varepsilon) = \int_{C(\varepsilon)} \frac{1}{2} \tau_1 E_{33}^2(\mathbf{u}) + \int_{C(\varepsilon)} 2\gamma(E_{13}^2(\mathbf{u}) + E_{23}^2(\mathbf{u})).$$

and is defined over the displacement class

$$u_1 = \hat{v}_1(x_3) - x_2 \hat{\psi}_3(x_3), \quad u_2 = \hat{v}_2(x_3) + x_1 \hat{\psi}_3(x_3).$$

We list three more problems in the theory of linearly elastic structures, all ruled by one and the same elastic potential:

$$\Sigma_{AST}(\mathbf{u}, \varepsilon) = \int_{C(\varepsilon)} 2\gamma(E_{13}^2(\mathbf{u}) + E_{23}^2(\mathbf{u})),$$

defined over three different function classes:

- (antiplane shear)

$$\hat{\alpha} < 0, \quad \hat{\gamma} < 0;$$

$$u_1 = \hat{v}_1(x_3) - x_2 \hat{\psi}_3(x_3), \quad u_2 = \hat{v}_2(x_3) + x_1 \hat{\psi}_3(x_3), \quad u_3 = \hat{u}_3(x_1, x_2);$$

- (torsion of plate-like cylinders)

$$\hat{\alpha} < 0, \quad \hat{\gamma} > 0; \quad u_3 = \hat{u}_3(x_1, x_2);$$

- (*torsion of rod-like cylinders*)

$$\hat{\alpha} > 0, \quad \hat{\gamma} < 0; \quad u_1 = \hat{v}_1(x_3) - x_2 \hat{\psi}_3(x_3), \quad u_2 = \hat{v}_2(x_3) + x_1 \hat{\psi}_3(x_3).$$

6.7 Reissner-Mindlin's Plates

The functional

$$\begin{aligned} \Pi_P(\mathbf{u}, \varepsilon) = & \int_{\mathcal{C}(\varepsilon)} 2\gamma(E_{13}^2(\mathbf{u}) + E_{23}^2(\mathbf{u})) \\ & + \int_{\mathcal{C}(\varepsilon)} \frac{1}{2} \left((\lambda + 2\mu)(E_{11}(\mathbf{u}) + E_{22}(\mathbf{u}))^2 - 4\mu(E_{11}(\mathbf{u})E_{22}(\mathbf{u}) - E_{12}^2(\mathbf{u})) \right), \end{aligned}$$

generalizes the *Reissner-Mindlin plate functional*, because it is defined over the displacement class

$$u_\alpha = \hat{u}_\alpha(x_1, x_2, x_3), \quad u_3 = \hat{u}_3(x_1, x_2),$$

that is, over the collection of all solutions of

$$u_{3,3} = 0, \quad u_{\alpha,33} = 0,$$

whereas Reissner-Mindlin's is the restriction of Π_P to the subclass:

$$u_\alpha = \hat{v}_\alpha(x_1, x_2) + x_3 \hat{\varphi}_\alpha(x_1, x_2), \quad u_3 = \hat{u}_3(x_1, x_2).$$

Now, *both PDEs*

$$u_{3,3} = 0 \quad \text{and} \quad u_{\alpha,33} = 0$$

are interpretable as *internal constraints*. We know the first-order constraint well; the second-order one can be set in the form:

$$u_{\alpha,33} = 0 \quad \Leftrightarrow \quad \nabla^{(2)} \mathbf{u} \cdot (\mathbf{e}_\alpha \otimes \mathbf{z} \otimes \mathbf{z}) = 0.$$

Suppose you do the following

- you include in the energy functional a term (say, $\frac{1}{2} \int_{\mathcal{C}(\varepsilon)} \tau_P (u_{\alpha,33})^2$, with $\tau_P > 0$) adding in elastic energy associated with the second-order displacement gradient;
- you insist in enforcing the mechanical principle of convergence in energy.

Do it, and you go home with your Reissner-Mindlin plate theory.

Selected Topics on Mixed/Enhanced Four-Node Shell Elements with Drilling Rotation

K. Wisniewski and E. Turska

Abstract In these lecture notes, we describe basic features of the mixed/ enhanced four-node shell elements with six dofs/node based on the Hu-Washizu (HW) functional, developed for Green strain. The focus is on the following features:

1. Derivation of the so-called incomplete (partial) HW functionals for shells, with different treatment of the bending/twisting part and the transverse shear part of strain energy. This is an alternative to the derivation from the three-dimensional HW functional, and it allows to reduce the number of elemental parameters.
2. Selection of parameters of the assumed fields and selection of an enhancements for the HW shell elements, with the purpose to improve accuracy for distorted meshes. This includes also the use of the so-called skew coordinates, which are associated with the natural basis at the element center.
3. Numerical treatment of the drilling Rotation Constraint equation by the Perturbed Lagrange method. The faulty term resulting from the equal-order approximations of displacements and the drilling rotation is eliminated and one spurious mode is stabilized using the gamma method.
4. A simple additive/multiplicative scheme of treating finite rotations is described and tested on numerical examples. This simplified scheme is consistent with the typical update scheme used by FE codes.

The quality of the proposed formulation is demonstrated using the Hu-Washizu shell element with 29 parameters (HW29), which has a very good accuracy and is insensitive to the shape distortions for coarse meshes. Besides, it exhibits an excellent convergence and robustness in nonlinear examples.

K. Wisniewski (✉)

IFTR, Polish Academy of Sciences (IPPT PAN), Warsaw, Poland
e-mail: kwisn@ippt.pan.pl

E. Turska

Polish Japanese Institute of Information Technology (PJWSTK),
Warsaw, Poland

1 Introduction

The aim of these lecture notes is to provide an introduction to mixed/ enhanced shell finite elements with drilling rotations. We consider shell equations derived from the Cauchy (non-polar) continuum by application of the Reissner-Mindlin kinematical hypothesis. For this class of shells, the strain energy depends on three types of strain: membrane, bending/twisting and transverse shear strains, which, in turn, are expressed in terms of displacements and 2-parameter rotations of a reference surface. The notes are based on several recent works which are cited in the sequel.

1.1 Drilling Rotation

The drilling rotation is defined as an elementary rotation about the vector normal to the reference surface, and it does not appear in shell equations for the Reissner-Mindlin kinematical hypothesis. This rotation is not necessary to describe the deformation of a shell when the shell reference surface is flat, but it is needed for curved or non-smooth (multi-branch) shells. So, it is needed in the general purpose shell elements, in which one of the following two strategies can be applied:

1. We can use 2 rotational parameters in smooth parts of a shell and 3 rotational parameters at intersections of shells, but then a complication arises with handling rotations, because:
 - (a) it must be automatically determined whether 2 or 3 rotational components are needed,
 - (b) additional transformations are required between bases, and
 - (c) different update schemes are applied at various nodes.

Nonetheless, many of the existing FE codes use this strategy.

2. We can use 3 rotational parameters, including the drilling rotation, at all nodes. It allows us to use three-parameter representations of rotations for an increment and to treat all rotational dofs in the same way. Then the intersections of multi-branch shells are naturally handled but we need to eliminate a singularity of the tangent matrix arising for co-planar elements. The simplest methods to fix this problem are as follows:
 - (a) to detect a singular equation and eliminate it,
 - (b) to provide an additional stiffness associated only with the drilling rotation dof, which is not coupled to in-plane displacements.

In both these methods, a physically meaningful value of the drilling rotation can be obtained only by an additional post-processing of the solution.

Other methods must be used when we expect the drilling rotation obtained as a solution to have a physical significance:

- (a) Using the so-called Allman shape functions, which interpolate the element's displacements in terms of nodal displacements \mathbf{u}_I and nodal drilling rotations ω_I . The Allman shape functions were first applied to 2D triangles in Allman (1984), Bergan and Felippa (1985) and subsequently to 2D quadrilaterals in Cook (1986), where a procedure of transforming an eight-node serendipity element to a four-node element with nodal drilling rotations was proposed. The classical Allman shape functions are valid only for small drilling rotations or for the rate-form equations; the version suitable for finite rotations and Automatic Differentiation was developed in Wisniewski and Turska (2006). The reader is referred to this paper for a review of earlier papers on this subject.
- (b) Using the drilling Rotation Constraint (RC) equation and standard bilinear shape functions. The scalar drilling RC equation is obtained as the (12) component of the three-dimensional RC equation, $\text{skew}(\mathbf{Q}^T \mathbf{F}) = \mathbf{0}$. The implementation of the drilling RC is a challenging task, involving several difficulties:
- i. The equal-order bi-linear interpolations of displacements and the drilling rotation render that the drilling RC equation is incorrectly approximated, which must be rectified. This, in turn, implies an additional zero eigenvalue of the tangent matrix, which needs a stabilization. We undertake this problem in Wisniewski (2010a) and provide a rectified solution in Wisniewski and Turska (2012).
 - ii. There is a question about the best method to incorporate the drilling RC equation into the governing functional, such as the Potential Energy, the Hellinger-Reissner and the Hu-Washizu functionals. A survey of such methods as the direct method, the penalty method, Lagrange Multiplier method and the Perturbed Lagrange Multiplier method, and our tests of them, are provided in Wisniewski (2010b, Sect. 12). We implemented and tested several methods of treatment of the drilling RC in order to select the one providing the best performance.
If the penalty method is used then a question comes up about the suitable value of the regularization parameter. In Hughes and Brezzi (1989), the theoretical value equal to the shear modulus is derived, but it seems to be too large when the element's shape is irregular (or when it is warped) and the penalty method is used. We show that using the Perturbed Lagrange Multiplier method, the theoretical value of the regularization parameter can be used.
 - iii. Pivotal to a good performance of elements with drilling rotation is the use of a proper type of an enhancement, namely the enhancement of the deformation gradient (EADG), because it affects also the drilling RC equation.

Chronologically, the approach based on the Allman shape functions was first, but our tests indicate that the elements based on the drilling RC equation perform better, i.e. yield more accurate solutions, are less cumbersome when the element is

warped, and can be also used to derive elements with a larger number of nodes, as, e.g., the nine-node elements with 6 dofs/node in Panasz and Wisniewski (2008).

Finally, we note that some of the above questions (for the shell equations derived from the Cauchy continuum) pertain also to the shell equations derived from the Cosserat (polar) media. The drilling rotation is naturally present in them but they require much more complicated constitutive equations, for details see, e.g., Altenbach et al. (2010), Eremeyev et al. (2012), Chróścielewski et al. (2011) Chróścielewski and Witkowski (2011).

1.2 Enhanced and Mixed/Enhanced Shell Elements

Regarding four-node shell elements, two classes of formulations are most popular:

1. *Enhanced Assumed Strain* shell elements, which use one of the three methods of enhancement of the element's kinematics:
 - (a) the *Incompatible Displacement* (ID) method,
 - (b) the *Enhanced Assumed Strain* (EAS) method, or
 - (c) the *Enhanced Assumed Displacement Gradient* (EADG) method.

This class is currently a standard but still some improvements are possible, especially for formulations with additional constraints.

2. *Mixed/Enhanced* shell elements, which are based on multi-field functionals, such as the two-field Hellinger-Reissner (HR) functional and the three-field Hu-Washizu (HW) functional. These functionals can be additionally enhanced using one of the above methods of enhancement.

Currently, the most promising seem to be the shell elements based on the Hu-Washizu (HW) functional. This is partly caused by the papers Wagner and Gruttmann (2005), Gruttmann and Wagner (2006), in which a new four-node shell HW element *without* the drilling rotation is derived, which shows significantly better convergence properties than the EAS shell element. The next reason is the progress in accuracy and robustness of the two-dimensional HW elements reported in Wisniewski and Turska (2009), Wisniewski et al. (2010). These two factors provided us the motivation for developing the HW shell elements *with* the drilling rotation, which have the following features:

- (a) The drilling rotation is introduced using the drilling RC, so an additional implementation related to this constraint is needed. Besides, different 'optimal' representations of the assumed stresses and strains must be selected. In particular, the 5-parameter stress representation of Pian-Sumihara, which was used in Wagner and Gruttmann (2005), Gruttmann and Wagner (2006), is not 'optimal' any longer.
- (b) Besides the full enhanced HW functional also the partial (incomplete) HW functionals, in which some strains are represented by the strain energy

functional, are tested. The purpose is to reduce the number of additional (elemental) parameters but still to retain the favorite convergence properties. The membrane part of a shell is treated by the HW functional, but we scrutinize the bending/twisting and the transverse shear strain energy.

- (c) In all these formulations, the parameters of the assumed fields (stresses, strains and Lagrange multipliers) are local (elemental) and discontinuous across the element's boundaries, and are eliminated (condensed out) on the element's level. Hence, externally, the HW elements have the same form as standard elements and no changes in the FE code are needed.

1.3 Algorithmic Treatment of Finite Rotations

The topic of finite rotations is very important in practice and often undertaken in the works on rigid-body dynamics, see Rosenberg (1977), Goldstein (1980) and on multi-body dynamics of rigid and flexible bodies, see Wittenburg (1977), Angeles (1988), Cardona and Geradin (1988), Geradin and Rixen (1995), Geradin and Cardona (2001), Atluri and Cazzani (1995). There are also mathematical works on rotations, such as, e.g., Stuelpnagel (1964), Cartan (1981), Altman (1986). This subject is also covered in the works on the Cosserat continuum and on the structures with rotational degrees of freedom, such as shells and 3D beams.

The rotations are described by a proper orthogonal tensor and its basic properties are presented first. However, in numerical implementations, we have to use some rotational parameters; for these lecture notes, we selected the canonical rotation vector.

2 Shell Kinematics and Drilling Rotation

In the case of Cosserat shells, the rotations are naturally present in the governing equations, but for the shells derived from the non-polar Cauchy continuum the drilling rotation is missing. Therefore, we define an extended configuration space, which uses an additional tensorial equation to introduce rotations; one of its equations is associated with the drilling rotation and is used for shells.

2.1 Extended Configuration Space

The classical configuration space of the non-polar Cauchy continuum is defined as: $\mathcal{C} \doteq \{\chi: B \rightarrow R^3\}$, where χ is the deformation function defined on the reference configuration of the body B . In the present work, we consider an *extended configuration space*, which is defined as

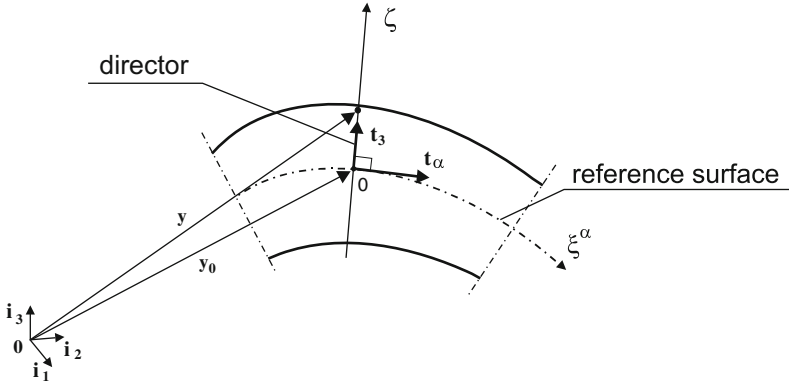


Fig. 1 Local Cartesian basis at a shell cross-section for initial configuration

$$\mathcal{C}_{\text{ext}} \doteq \{(\chi, \mathbf{Q}) : B \rightarrow R^3 \times SO(3) \mid \chi \in \mathcal{C}\}, \tag{1}$$

where χ is required to belong to the classical \mathcal{C} , see, e.g., Badur and Pietraszkiewicz (1986). The rotations $\mathbf{Q} \in SO(3)$ are constrained by the Rotation Constraint (RC) equation

$$\text{skew}(\mathbf{Q}^T \mathbf{F}) = \mathbf{0}, \tag{2}$$

where $\mathbf{F} \doteq \nabla \chi$ is the deformation gradient. The use of the RC equation was proposed in Simo et al. (1992) in conjunction with the potential energy functional, but, as we show in the present work, it can be used with the Hu-Washizu functional as well. Various forms of governing functionals modified by the RC are presented in Wisniewski (2010b).¹ The advantage of such a formulation is that it avoids the use of non-symmetric stresses, which was typical in the earlier papers, and currently are used in the so-called Cosserat-type approach, in which the rotations remain unconstrained, see, e.g., Chróścielewski et al. (1992).

2.2 Reissner-Mindlin Shell Kinematics

The position vector of an arbitrary point of a shell in the initial configuration is expressed as $\mathbf{y}(\zeta) = \mathbf{y}_0 + \zeta \mathbf{t}_3$, where \mathbf{y}_0 is a position of the reference surface and \mathbf{t}_3 is the shell director, normal to the reference surface (Fig. 1). Besides, $\zeta \in [-h/2, +h/2]$ is the coordinate in the direction normal to the reference surface, where h denotes the initial shell thickness. In the deformed configuration, the position vector is expressed by the Reissner-Mindlin’s kinematical hypothesis,

¹Note that the RC equation can also be used to constrain parameters of the 2nd order kinematics of shells, see Wisniewski and Turska (2000, 2001, 2002).

$$\mathbf{x}(\zeta) = \mathbf{x}_0 + \zeta \mathbf{Q}_0 \mathbf{t}_3, \quad (3)$$

where \mathbf{x}_0 is a position of the reference surface and $\mathbf{Q}_0 \in SO(3)$ is a rotation tensor. The rotation tensor, which is constant over ζ , can be parameterized by the canonical rotation vector $\boldsymbol{\psi}$; more details on the algorithmic treatment of rotations is given in Sect. 4. Note that all the vectors and tensors used above are functions of the natural coordinates $\xi, \eta \in [-1, +1]$, which parameterize the reference surface locally within a single finite element.

The deformation function $\boldsymbol{\chi} : \mathbf{x} = \boldsymbol{\chi}(\mathbf{y})$ maps the reference configuration of the shell onto the current (deformed) one, and the deformation gradient is obtained as

$$\mathbf{F} \doteq \frac{\partial \mathbf{x}}{\partial \mathbf{y}} = \left[\frac{\partial \mathbf{x}}{\partial \xi^k} \right] \left[\frac{\partial \mathbf{y}}{\partial \xi^k} \right]^{-1}, \quad k = 1, 2, 3, \quad (4)$$

where the natural coordinates are defined as $\xi^1 \doteq \xi$, $\xi^2 \doteq \eta$, $\xi^3 = 2\zeta/h$, and $\xi^k \in [-1, +1]$. Besides, \mathbf{y} is the position vector in the initial configuration.

The 3D Green strain can be transformed from the global reference basis to the local Cartesian basis at the element's center $\{\mathbf{t}_k^c\}$,

$$\mathbf{E} \doteq \frac{1}{2} (\mathbf{R}_{0c}^T \mathbf{F}^T \mathbf{F} \mathbf{R}_{0c} - \mathbf{I}), \quad (5)$$

where $\mathbf{R}_{0c} \in SO(3)$ describes the orientation of the vectors \mathbf{t}_k^c , i.e. at the element's center. We can split the deformation gradient \mathbf{F} into the constant and linear parts in ζ as follows: $\mathbf{F} = \mathbf{F}_0 + \zeta \mathbf{F}_1$. Then

$$\mathbf{F}^T \mathbf{F} = \underbrace{\mathbf{F}_0^T \mathbf{F}_0}_{\text{to } \boldsymbol{\varepsilon}} + \zeta \underbrace{(\mathbf{F}_0^T \mathbf{F}_1 + \mathbf{F}_1^T \mathbf{F}_0)}_{\text{to } \boldsymbol{\kappa}} + \dots, \quad (6)$$

and the Green strain can be expressed as a sum of the *0th order* and the *1st order* shell strains,

$$\mathbf{E}(\zeta) \approx \boldsymbol{\varepsilon} + \zeta \boldsymbol{\kappa}. \quad (7)$$

The *0th order* strain $\boldsymbol{\varepsilon}$ includes the membrane and transverse shear components, while the *1st order* strain $\boldsymbol{\kappa}$, the bending and twisting components. The transverse $\kappa_{\alpha 3}$ ($\alpha = 1, 2$) components are neglected.

2.3 Drilling Rotation Constraint

The drilling rotation ω is defined as the rotation about the vector normal to the reference surface \mathbf{t}_3 , see Fig. 2, so the (canonical) drilling rotation vector is $\boldsymbol{\psi} \doteq \omega \mathbf{t}_3$.

Fig. 2 Drilling rotation: the axis of rotation is perpendicular to the reference surface

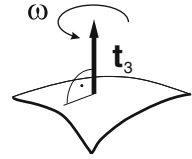
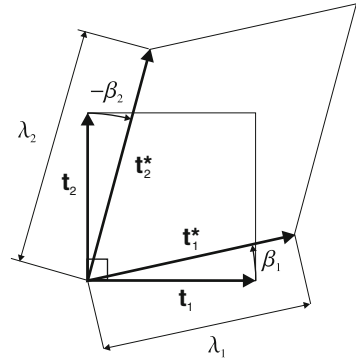


Fig. 3 Deformation of a pair of vectors \mathbf{t}_1 and \mathbf{t}_2



A magnitude of the drilling rotation is determined by the equation linking it to displacements. We consider the (12)-component of the RC of Eq. (2), which yields

$$c \doteq \frac{1}{2} [(\mathbf{F}\mathbf{t}_2) \cdot \mathbf{a}_1 - (\mathbf{F}\mathbf{t}_1) \cdot \mathbf{a}_2] = 0, \tag{8}$$

where $\mathbf{a}_\alpha \doteq \mathbf{Q}_0(\omega)\mathbf{t}_\alpha$ ($\alpha = 1, 2$) and \mathbf{t}_α are the initial tangent vectors. This equation is designated as the drilling Rotation Constraint (drilling RC).

A physical 2D interpretation of the drilling rotation ω can be established by considering, for simplicity, a planar deformation of a pair of ortho-normal vectors, \mathbf{t}_α . Each of these vectors is rotated and stretched,

$$\mathbf{t}_1^* = \mathbf{F}\mathbf{t}_1 = \lambda_1 \mathbf{Q}_1(\beta_1) \mathbf{t}_1, \quad \mathbf{t}_2^* = \mathbf{F}\mathbf{t}_2 = \lambda_2 \mathbf{Q}_2(\beta_2) \mathbf{t}_2, \tag{9}$$

where $\lambda_1, \lambda_2 > 0$ are scalar stretch parameters, and $\mathbf{Q}_1, \mathbf{Q}_2$ are rotation tensors, each depending on one rotation angle, β_α , see Fig. 3.

Using Eq. (9) and the drilling RC equation, we obtain

$$\omega \approx \frac{1}{2}(\beta_1 + \beta_2) + k\pi, \quad k = 0, \dots, K, \tag{10}$$

for $\cos \omega \neq 0, \lambda_1 c_1 + \lambda_2 c_2 \neq 0$ and $\lambda_\alpha \approx 1$, where $s_\alpha \doteq \sin \beta_\alpha$ and $c_\alpha \doteq \cos \beta_\alpha$. Hence, the drilling angle ω is an average of rotations of vectors \mathbf{t}_α , and this holds also for finite rotation angles. This interpretation is valid for shells when ω is a rotation about the director \mathbf{t}_3 and \mathbf{t}_α are the vectors tangent to the reference surface, for details see Wisniewski and Turska (2006, Appendix).

3 Shell Hu-Washizu Functional with Rotations

3.1 3D HW Functional with Rotations

Our formulation is based on the 2nd Piola-Kirchhoff stress \mathbf{S} and the Green strain

$$\mathbf{E} \doteq \frac{1}{2}(\mathbf{F}^T \mathbf{F} - \mathbf{I}).$$

The *standard* Hu-Washizu (HW) functional is mixed by definition and, besides the compatible displacements, it involves two additional independent fields, strains and stresses, where the latter play the role of the Lagrange multipliers. Consider the classical form of the three-field HW functional,

$$F_{\text{HW}}(\mathbf{u}, \mathbf{S}^*, \mathbf{E}^*) \doteq \int_V \{ \mathcal{W}(\mathbf{E}^*) + \mathbf{S}^* \cdot [\mathbf{E}(\nabla \mathbf{u}) - \mathbf{E}^*] \} dV - F_{\text{ext}}, \quad (11)$$

where $\mathcal{W}(\mathbf{E}^*)$ is the strain energy expressed by the independent strain \mathbf{E}^* , and the independent stress \mathbf{S}^* plays the role of the Lagrange multiplier of the relation between the independent strain \mathbf{E}^* and the Green strain $\mathbf{E}(\nabla \mathbf{u})$. The strain energy density \mathcal{W} is a function of the independent strain \mathbf{E}^* . F_{ext} is the potential of the external loads, the body force, and the displacement boundary conditions. V is the volume of the 3D body.

To incorporate the rotations into a 3D formulation, we constrain the governing HW functional of Eq. (11) by the weak form of the Rotation Constraint of Eq. (2) using the Lagrange multiplier method

$$\tilde{F}_5(\mathbf{u}, \mathbf{Q}, \mathbf{S}^*, \mathbf{E}^*, \mathbf{T}^*) \doteq \int_V \{ \mathcal{W}(\mathbf{E}^*) + \mathbf{S}^* \cdot [\mathbf{E}(\nabla \mathbf{u}) - \mathbf{E}^*] + F_{\text{RC}} \} dV - F_{\text{ext}}, \quad (12)$$

where the term related to the Rotation Constraint of Eq. (2) has the so-called Perturbed Lagrange (PL) form,

$$F_{\text{RC}}(\mathbf{u}, \mathbf{Q}, \mathbf{T}^*) \doteq \mathbf{T}^* \cdot \text{skew}(\mathbf{Q}^T \mathbf{F}) - \frac{1}{2\gamma} \underline{\underline{\mathbf{T}^* \cdot \mathbf{T}^*}}. \quad (13)$$

Here, \mathbf{T}^* is the skew-symmetric Lagrange multiplier for the RC equation and $\gamma \in (0, \infty)$ is the regularization parameter. The perturbation term in the above formula is underlined.

Penalty form of the RC term. Taking a variation of this functional w.r.t. \mathbf{T}^* , we obtain the Euler-Lagrange equation, from which we can calculate \mathbf{T}^* and eliminate

it from the formulation. This yields the four-field functional $\tilde{F}_4(\mathbf{u}, \mathbf{Q}, \mathbf{S}^*, \mathbf{E}^*)$, where the Rotation Constraint term has the penalty (P) form,

$$F_{RC}(\mathbf{u}, \mathbf{Q}) \doteq \frac{\gamma}{2} \text{skew}(\mathbf{Q}^T \mathbf{F}) \cdot \text{skew}(\mathbf{Q}^T \mathbf{F}). \tag{14}$$

However, we prefer the PL form to the P form because the corresponding formulation is less sensitive to the element’s distortions and implies a larger radius of convergence in non-linear problems.

3.2 Complete (Pure) HW Functional for Shells

To derive the HW functional for shells, we use the functional (12), approximate the strain as $\mathbf{E}(\zeta) \approx \varepsilon + \zeta \boldsymbol{\kappa}$, which is a result of the Reissner-Mindlin kinematical hypothesis and a linearization in ζ , see Eq. (7). Let us define the shell strain energy as

$$\mathcal{W}^{\text{sh}}(\varepsilon, \boldsymbol{\kappa}) \doteq \int_{-h/2}^{+h/2} \mathcal{W}(\mathbf{E}) \mu d\zeta, \tag{15}$$

where $\mu \doteq \det \mathbf{Z} \approx 1$, and \mathbf{Z} is the shifter tensor, see (Wisniewski 2010b, p. 54). For a particular case of the linear Saint Venant-Kirchhoff material, we obtain the well-known form,

$$\mathcal{W}^{\text{sh}}(h, \varepsilon, \boldsymbol{\kappa}) = h \mathcal{W}(\varepsilon) + \frac{h^3}{12} \mathcal{W}(\boldsymbol{\kappa}). \tag{16}$$

However, \mathcal{W}^{sh} can be much more complicated and, e.g., for the composites with a nonsymmetric layer stacking sequence, it also depends on the position of the reference surface. For non-symmetric cross-sections, the contributions of ε and $\boldsymbol{\kappa}$ cannot be separated in the strain energy and in constitutive equations.

Let us assume that the independent strain has the form: $\mathbf{E}^*(\zeta) \doteq \varepsilon^* + \zeta \boldsymbol{\kappa}^*$. By integration of the three-field HW functional of Eq. (11) over the shell thickness, we obtain its shell counterpart,

$$F_{\text{HW}}^{\text{sh}}(\mathbf{u}, \mathbf{Q}, \mathbf{N}^*, \mathbf{M}^*, \varepsilon^*, \boldsymbol{\kappa}^*) \doteq \int_A \{ \mathcal{W}^{\text{sh}}(\varepsilon^*, \boldsymbol{\kappa}^*) + \mathbf{N}^* \cdot [\varepsilon(\mathbf{u}, \mathbf{Q}) - \varepsilon^*] + \mathbf{M}^* \cdot [\boldsymbol{\kappa}(\mathbf{u}, \mathbf{Q}) - \boldsymbol{\kappa}^*] \} dA - F_{\text{ext}}^{\text{sh}}, \tag{17}$$

where

$$\mathbf{N}^* \doteq \int_{-h/2}^{+h/2} \mathbf{S}^* \mu d\zeta, \quad \mathbf{M}^* \doteq \int_{-h/2}^{+h/2} \zeta \mathbf{S}^* \mu d\zeta. \tag{18}$$

The independent cross-sectional force \mathbf{N}^* plays the role of the Lagrange multiplier for the relation between the independent strain $\boldsymbol{\varepsilon}^*$ and the shell *0th order* compatible strain $\boldsymbol{\varepsilon}(\mathbf{u}, \mathbf{Q})$. Similarly, the independent cross-sectional couple \mathbf{M}^* is the Lagrange multiplier for the relation between the independent strain $\boldsymbol{\kappa}^*$ and the *1st order* compatible strain $\boldsymbol{\kappa}(\mathbf{u}, \mathbf{Q})$. Besides, A is the area of the shell reference surface.

We note that the functional (17) involves the rotation \mathbf{Q} , but not the elementary rotation about the normal vector, the drilling rotation. To include the drilling rotation, we append the (12)-component of the Rotation Constraint of Eq. (2) to the functional of Eq. (17) using the Lagrange multiplier method. Then we obtain the seven-field functional,

$$\tilde{F}_7^{\text{sh}}(\mathbf{u}, \mathbf{Q}, \mathbf{N}^*, \mathbf{M}^*, \boldsymbol{\varepsilon}^*, \boldsymbol{\kappa}^*, T^*) \doteq F_{\text{HW}}^{\text{sh}} + F_{\text{RC}}^{\text{drill}}, \quad (19)$$

where the drilling rotation term has the Perturbed Lagrange (PL) form,

$$F_{\text{RC}}^{\text{drill}}(\mathbf{u}, \mathbf{Q}, T^*) \doteq \int_A \{T^*[\text{skew}(\mathbf{Q}^T \mathbf{F})]_{12} - \frac{1}{2\gamma}(T^*)^2\} dA, \quad (20)$$

where T^* is the Lagrange multiplier, and the (12)-component of the RC is specified by Eq. (8). Note that an analogous procedure was applied to the 3D case to obtain Eq. (12) from Eq. (11). Comparing the shell functional of Eq. (19) to the 3D functional of Eq. (12), we see the following correspondence between them:

$$\boldsymbol{\varepsilon}^*, \boldsymbol{\kappa}^* \leftrightarrow \mathbf{E}^*, \quad \mathbf{N}^*, \mathbf{M}^* \leftrightarrow \mathbf{S}^*, \quad T^* \leftrightarrow T^*. \quad (21)$$

3.3 Incomplete (Partial) HW Functionals for Shells

The derivation of Eq. (17) from Eq. (12) is restricted because the shell HW functional must be constructed for all strain components, which is not necessarily optimal. Below, we describe another method, which provides more flexibility, as the HW functional can be constructed for selected strain components; such a functional is called the incomplete (partial) HW functional.

Let us start the derivation from the 3D potential energy functional,

$$F_{\text{PE}}(\mathbf{u}) \doteq \int_V \mathcal{W}(\mathbf{E}(\nabla \mathbf{u})) dV - F_{\text{ext}}, \quad (22)$$

which, by the Reissner-Mindlin hypothesis and the integration over the thickness, yields the shell potential energy functional

$$F_{\text{PE}}^{\text{sh}}(\mathbf{u}, \mathbf{Q}) \doteq \int_A \mathcal{W}^{\text{sh}}(\boldsymbol{\varepsilon}, \boldsymbol{\kappa}) dA - F_{\text{ext}}^{\text{sh}}, \quad (23)$$

where \mathcal{W}^{sh} is defined by Eq. (15). Using $F_{\text{PE}}^{\text{sh}}$, we can construct the shell HW functional for a selected strain type only while still using the potential energy functional for the other type. For example, the incomplete (partial) HW functional for the 0th order shell strain only is

$$F_{\text{HW}}^{\text{sh}}(\mathbf{u}, \mathbf{Q}, \mathbf{N}^*, \varepsilon^*) \doteq \int_A \{ \mathcal{W}^{\text{sh}}(\varepsilon^*, \boldsymbol{\kappa}) + \mathbf{N}^* \cdot [\boldsymbol{\varepsilon}(\mathbf{u}, \mathbf{Q}) - \varepsilon^*] \} dA - F_{\text{ext}}^{\text{sh}}, \quad (24)$$

where \mathbf{N}^* is the Lagrange multiplier.² The above incomplete HW functional uses only 4 fields, compared to 6 fields in Eq. (17). The so-derived functionals can be used to develop finite elements with a reduced number of additional parameters, but still having good numerical properties. To obtain the shell HW functional with the drilling rotation, we proceed in the same way as when deriving Eq. (19) from Eq. (17).

Using the above described methodology, several HW functionals for shells were derived in Wisniewski and Turska (2012). For instance, the functionals which were used to develop the HW47 and HW29 elements were as follows:

1. The complete (pure) HW functional, which is used for the HW47 element,

$$\begin{aligned} \tilde{F}_{\text{HW}}^{\text{sh}} \doteq & \int_A \{ \mathcal{W}^{\text{sh}}(\varepsilon_{\alpha\beta}^*, \varepsilon_{\alpha 3}^*, \kappa_{\alpha\beta}^*) \\ & + N_{\alpha\beta}^* \cdot [\varepsilon_{\alpha\beta} - \varepsilon_{\alpha\beta}^*] + M_{\alpha\beta}^* \cdot [\kappa_{\alpha\beta} - \kappa_{\alpha\beta}^*] \\ & + N_{\alpha 3}^* \cdot [\varepsilon_{\alpha 3} - \varepsilon_{\alpha 3}^*] \} dA - F_{\text{ext}}^{\text{sh}} + F_{\text{RC}}^{\text{drill}}. \end{aligned} \quad (25)$$

2. The incomplete (partial) HW functional, which is used for the HW29 element,

$$\begin{aligned} \tilde{F}_{\text{HW}}^{\text{sh}} \doteq & \int_A \{ \mathcal{W}^{\text{sh}}(\varepsilon_{\alpha\beta}^*, \varepsilon_{\alpha 3}^*, \kappa_{\alpha\beta}) + N_{\alpha\beta}^* \cdot [\varepsilon_{\alpha\beta} - \varepsilon_{\alpha\beta}^*] \\ & + N_{\alpha 3}^* \cdot [\varepsilon_{\alpha 3} - \varepsilon_{\alpha 3}^*] \} dA - F_{\text{ext}}^{\text{sh}} + F_{\text{RC}}^{\text{drill}}, \end{aligned} \quad (26)$$

where the strain energy functional is used for $\kappa_{\alpha\beta}$, while the HW functional is used for all the other strain components.

In the above functionals, the tangent (in-plane) $\alpha\beta$ components ($\alpha, \beta = 1, 2$) and the transverse $\alpha 3$ components are distinguished. The transverse components $\kappa_{\alpha 3}$ are neglected in the developed finite elements.

²Note that the definition of Eq. (18) is not valid for the \mathbf{N}^* used here!

4 Finite Rotations: Simple Algorithmic Treatment

In this section, we describe the basic questions related to properties, parametrization and the algorithmic treatment of rotations.

4.1 Basic Definitions

Rotation Tensor Let us denote by \mathbf{R} the rotation tensor belonging to the special orthogonal group defined as follows

$$SO(3) := \{\mathbf{R} : \mathbb{R}^3 \rightarrow \mathbb{R}^3 \text{ is linear} \mid \mathbf{R}^T \mathbf{R} = \mathbf{I} \text{ and } \det \mathbf{R} = +1\}. \quad (27)$$

The orthogonality condition $\mathbf{R}^T \mathbf{R} = \mathbf{I}$ renders that preserved are:

- (i) the angle between two rotated vectors and
- (ii) the length of a rotated vector.

The condition $\det \mathbf{R} = +1$ ensures the handedness of a rotated triad of vectors. The eigenvalues of \mathbf{R} are: $\lambda_1 = +1$ and $\lambda_{2,3} = \cos \omega \pm i \sin \omega$. Note that for $\lambda_1 = +1$, the eigenequation $(\mathbf{R} - \lambda \mathbf{I})\mathbf{v} = \mathbf{0}$ becomes $\mathbf{R}\mathbf{v} = \mathbf{v}$. As the eigenvector \mathbf{v} is unaffected by \mathbf{R} so it defines the axis of rotation, which we designate by \mathbf{e} .

Canonical Parametrization of Rotation Tensor Consider a classical elementary problem of a rotation of a vector \mathbf{v} about the unit axis \mathbf{e} . The result can be written as $\mathbf{v}' = \mathbf{R}\mathbf{v}$, where

$$\mathbf{R} \doteq \mathbf{I} + \sin \omega \mathbf{S} + (1 - \cos \omega) \mathbf{S}^2. \quad (28)$$

Here, $\mathbf{S} \doteq \mathbf{e} \times \mathbf{I} \in so(3)$, where $so(3)$ is a linear space of skew-symmetric tensors such that

$$so(3) := \{\mathbf{S} : \mathbb{R}^3 \rightarrow \mathbb{R}^3 \text{ is linear} \mid \mathbf{S}^T = -\mathbf{S}\}. \quad (29)$$

The basic properties of \mathbf{R} and \mathbf{S} are defined in Wisniewski (2010b, p. 131). The above form of \mathbf{R} involves 4 parameters $\{\omega, \mathbf{e}\}$, which must be supplemented by the constraint $\|\mathbf{e}\| = 1$.

We have to assume some form (or parametrization) of \mathbf{R} to be used in shell equations; several such forms exist, see the survey in Wisniewski (2010b, Chap. 8.2), but these involving more than 3 parameters require additional constraints to ensure that \mathbf{R} is proper orthogonal, see Table 1.

The three parameters, forming the so-called rotation pseudo-vectors, do not require any additional constraints, which is very convenient. Several rotation pseudo-vectors were proposed in the literature; they all have the direction of the axis of rotation \mathbf{e} but differ in length. The basic relations, which are common to all these rotation vectors, are

Table 1 Number of constraints for various parameterizations

Number of rotation parameters	9	6	5	4	3
Number of orthogonality constraints	7	3	2	1	0

$$\tilde{\psi} = \psi \times \mathbf{I}, \quad \psi = \frac{1}{2}(\mathbf{I} \times \tilde{\psi}), \quad \|\psi\| = \sqrt{\psi \cdot \psi}, \quad \mathbf{e} = \frac{\psi}{\|\psi\|}, \quad (30)$$

where the tilde denotes the skew-symmetric tensor associated with the rotation vector and the cross-product of a vector and a tensor is defined as in deBoer (1982, p. 74).

Let us define the canonical rotation vector as $\psi \doteq \omega \mathbf{e}$, for which we have: $\tilde{\psi} = \omega \mathbf{S}$, $\tilde{\psi}^2 = \omega^2 \mathbf{S}^2$, $\psi \cdot \psi = \frac{1}{2} \tilde{\psi} \cdot \tilde{\psi} = \omega^2$. The rotation tensor, Eq. (28), can be rewritten in terms of ψ , as follows

$$\mathbf{R} \doteq \mathbf{I} + c_1 \tilde{\psi} + c_2 \tilde{\psi}^2, \quad (31)$$

where the scalar coefficients are

$$c_1 \doteq \frac{\sin \|\psi\|}{\|\psi\|}, \quad c_2 \doteq \frac{1 - \cos \|\psi\|}{\|\psi\|^2}. \quad (32)$$

The representation (31) is a periodic function of $\|\psi\|$, so we can restrict its range to $\omega \leq 2\pi$ by shortening the rotation vector. Note, however, that such an operation is incorrect for the tangent operator $\mathbf{T}(\psi)$, see Eq. (48), which is not periodic.

In numerical calculations involving (31), we encounter two problems:

1. Only c_1 converges correctly for $\|\psi\| \rightarrow 0$, while c_2 does not due to round-off errors. Using the identity $1 - \cos \|\psi\| = 2 \sin^2(\|\psi\|/2)$, we obtain

$$c_2 \doteq \frac{1 - \cos \|\psi\|}{\|\psi\|^2} = \frac{1}{2} \left[\frac{\sin(\|\psi\|/2)}{(\|\psi\|/2)} \right]^2, \quad (33)$$

which ensures a correct behavior for a wider range of $\|\psi\| \rightarrow 0$.

2. At exactly $\|\psi\| = 0$, both coefficients are indeterminate,

$$c_1 = \frac{\sin \|\psi\|}{\|\psi\|} \Big|_{\|\psi\|=0} = \frac{0}{0}, \quad c_2 = \frac{1}{2} \left[\frac{\sin(\|\psi\|/2)}{(\|\psi\|/2)} \right]^2 \Big|_{\|\psi\|=0} = \frac{0}{0}, \quad (34)$$

which indicates that $\|\psi\| = 0$ does not belong to their domains. However,

$$\lim_{\|\psi\| \rightarrow 0} c_1 = 1, \quad \lim_{\|\psi\| \rightarrow 0} c_2 = \frac{1}{2}, \quad (35)$$

which are finite, so we can define these coefficients as the limit values.

Nonetheless, then still remains the problem of derivatives of \mathbf{R} at $\|\psi\| = 0$, for which we also obtain indeterminate expressions. Two simple remedies can be used at $\|\psi\| = 0$:

1. the perturbation of $\|\psi\|$, i.e. the use $\|\psi\| = \sqrt{\psi \cdot \psi + \tau}$, where $\tau = 10^{-8}$ in calculations in double precision, or
2. the Taylor expansion of $\|\psi\|$.

By the first method, the values of derivatives are equal to the limits of derivatives, see Wisniewski (2010b, pp.149–150).

Euler Parameters (Quaternions) The set of four parameters $\{\omega, \mathbf{e}\}$ of Eq. (28) can be replaced by the so-called Euler parameters (or quaternions), Altman (1986), Spring (1986), defined as follows:

$$q_0 \doteq \cos(\omega/2), \quad \mathbf{q} \doteq \sin(\omega/2) \mathbf{e}. \tag{36}$$

The rotation tensor of Eq. (28), in terms of $\{q_0, \mathbf{q}\}$ is expressed as

$$\mathbf{R} \doteq (2q_0^2 - 1)\mathbf{I} + 2q_0\mathbf{q} \times \mathbf{I} + 2\mathbf{q} \otimes \mathbf{q}, \tag{37}$$

or, by using the skew-symmetric $\tilde{\mathbf{q}} \doteq \mathbf{q} \times \mathbf{I} = \sin(\omega/2) \mathbf{S}$, as

$$\mathbf{R} \doteq \mathbf{I} + 2q_0\tilde{\mathbf{q}} + 2\tilde{\mathbf{q}}^2, \tag{38}$$

and both these forms are never singular. The parameters $\{q_0, \mathbf{q}\}$ must satisfy the constraint equation, $q_0^2 + \mathbf{q} \cdot \mathbf{q} = 1$, to form a unit quaternion. If we try to eliminate this constraint equation, e.g. by calculating $q_0 = \sqrt{1 - \mathbf{q} \cdot \mathbf{q}}$ and inserting it into Eq. (37) or (39), then the expression for \mathbf{R} contains the square root, which causes a failure of the Newton method when solving the equilibrium equations.

Composition of quaternions. The quaternions are a very convenient tool to compose rotations. For the product of rotation tensors $\mathbf{R}_2 \mathbf{R}_1$, where

$$\begin{aligned} \mathbf{R}_1(r_0, \mathbf{r}) &\doteq (2r_0^2 - 1)\mathbf{I} + 2r_0\mathbf{r} \times \mathbf{I} + 2\mathbf{r} \otimes \mathbf{r}, \\ \mathbf{R}_2(p_0, \mathbf{p}) &\doteq (2p_0^2 - 1)\mathbf{I} + 2p_0\mathbf{p} \times \mathbf{I} + 2\mathbf{p} \otimes \mathbf{p}, \end{aligned} \tag{39}$$

the composition of the associated quaternions is defined as follows:

$$\{p_0, \mathbf{p}\} \circ \{r_0, \mathbf{r}\} \doteq \{p_0r_0 - \mathbf{p} \cdot \mathbf{r}, \quad p_0\mathbf{r} + r_0\mathbf{p} + \mathbf{p} \times \mathbf{r}\}. \tag{40}$$

Another advantage of a quaternion is that it can be easily re-normalized,

$$q_0 = q_0 / \sqrt{q_0^2 + \mathbf{q} \cdot \mathbf{q}}, \quad \mathbf{q} = \mathbf{q} / \sqrt{q_0^2 + \mathbf{q} \cdot \mathbf{q}}, \tag{41}$$

which is more convenient than in the case of rotation matrices, the re-orthogonalization of which is complicated.

Using the quaternion of Eq. (37), the rotated shell director of Eq. (3) can be expressed as

$$\mathbf{a}_3 \doteq \mathbf{Q}_0 \mathbf{t}_3 = (2q_0^2 - 1) \mathbf{t}_3 + 2q_0 \mathbf{q} \times \mathbf{t}_3 + 2(\mathbf{q} \cdot \mathbf{t}_3) \mathbf{q}, \quad (42)$$

where only the operations on scalars and vectors are performed.

Relations Between Quaternion and Canonical Rotation Vector. *Canonical rotation vector for given quaternion.* Having the quaternion $\{q_0, \mathbf{q}\}$, we can extract the axis of rotation and the rotation angle as follows

$$\mathbf{e} = \frac{\mathbf{q}}{\sqrt{\mathbf{q} \cdot \mathbf{q}}}, \quad \begin{array}{l} \omega = 2 \arcsin \sqrt{\mathbf{q} \cdot \mathbf{q}}, \quad \tau < \sqrt{\mathbf{q} \cdot \mathbf{q}} \leq 1, \\ \text{and} \\ \omega = 2\sqrt{\mathbf{q} \cdot \mathbf{q}}, \quad 0 \leq \sqrt{\mathbf{q} \cdot \mathbf{q}} \leq \tau, \end{array} \quad (43)$$

where the second formula for ω is a one-term Taylor series of the first formula and τ is a small value. To avoid arguments of the arcsin function greater than 1 (caused by round off errors), $\min(\sqrt{\mathbf{q} \cdot \mathbf{q}}, 1)$ is used instead of $\sqrt{\mathbf{q} \cdot \mathbf{q}}$. As the argument of the arcsin function is non-negative hence $0 \leq \omega \leq \pi$, which limits the step size when an algorithm uses the extraction of a rotation vector from a quaternion. Finally, we can calculate $\boldsymbol{\psi} \doteq \omega \mathbf{e}$.

Quaternion for given canonical rotation vector. Having the canonical rotation vector $\boldsymbol{\psi}$, we can calculate $\omega = \|\boldsymbol{\psi}\|$, $\mathbf{e} = \boldsymbol{\psi}/\|\boldsymbol{\psi}\| = \boldsymbol{\psi}/\omega$, and, then, the quaternion is obtained as follows:

$$q_0 \doteq \cos(\omega/2), \quad \mathbf{q} \doteq \sin(\omega/2) \mathbf{e} = \frac{1}{2} \frac{\sin(\omega/2)}{(\omega/2)} \boldsymbol{\psi}. \quad (44)$$

To avoid indeterminate expressions, we treat $\|\boldsymbol{\psi}\|$ similarly to the derivatives of \mathbf{R} at $\|\boldsymbol{\psi}\| = 0$.

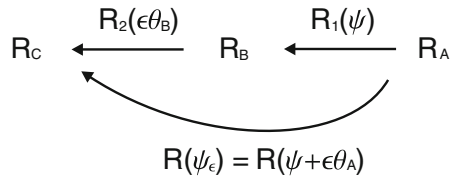
4.2 Variations of Rotation Tensor

Increments of Rotation Vectors in Various Tangent Planes We consider the tangent planes at two different rotations, \mathbf{R}_A and \mathbf{R}_B , and establish the relation between the infinitesimal rotation vectors belonging to these spaces using the left composition rule. The tangent operators \mathbf{T} and $\chi\mathbf{T}$ are defined, and used in the first and second variations of the rotation tensor for the canonical parametrization.

Tangent plane. The set of all infinitesimal rotations $\tilde{\boldsymbol{\theta}}$ superposed onto the finite rotation \mathbf{R} is referred to as the plane tangent to $SO(3)$ at \mathbf{R} , and denoted by $T_{\mathbf{R}}SO(3) \doteq \{\tilde{\boldsymbol{\theta}} \mathbf{R} \mid \text{for } \tilde{\boldsymbol{\theta}} \in so(3)\}$. At $\mathbf{R} = \mathbf{I}$, we have the initial tangent plane, $T_{\mathbf{I}}SO(3) \doteq \{\tilde{\boldsymbol{\theta}} \mid \text{for } \tilde{\boldsymbol{\theta}} \in so(3)\}$.³

³The tilde denotes the skew-symmetric tensor associated with the rotation vector, i.e. $\tilde{\boldsymbol{\theta}} \doteq \boldsymbol{\theta} \times \mathbf{I}$.

Fig. 4 Scheme of increments of rotations for the left composition rule



4.3 Operator **T**

We associate the tangent operator **T** with the left composition rule, see Fig. 4; note that in some papers this tangent operator is defined differently, see the comparison in Wisniewski (2010b, p. 179). The perturbed rotation **R_C** can be related either to **R_A** or to **R_B**,

$$\mathbf{R}_C = \mathbf{R}(\psi_\epsilon) \mathbf{R}_A, \quad \mathbf{R}_C = \mathbf{R}_2(\epsilon\theta_B) \mathbf{R}_B, \quad (45)$$

where $\psi_\epsilon \doteq \psi + \epsilon\theta_A$ and ϵ is a scalar parameter. Besides, θ_A and θ_B are infinitesimal rotation vectors, and

$$\tilde{\psi}_\epsilon \mathbf{R}_A = (\tilde{\psi} + \epsilon\tilde{\theta}_A) \mathbf{R}_A \in T_{\mathbf{R}_A}SO(3), \quad \epsilon\tilde{\theta}_B \mathbf{R}_B \in T_{\mathbf{R}_B}SO(3), \quad (46)$$

i.e. the perturbations $\epsilon\tilde{\theta}_A$ and $\epsilon\tilde{\theta}_B$ belong to different tangent planes. Because both relations (45) must yield the same **R_C**, we obtain

$$\mathbf{R}_2(\epsilon\theta_B) \mathbf{R}_B = \mathbf{R}(\psi_\epsilon) \mathbf{R}_A,$$

which, by using $\mathbf{R}_B = \mathbf{R}_1(\psi) \mathbf{R}_A$, is reduced to

$$\mathbf{R}_2(\epsilon\theta_B) = \mathbf{R}(\psi_\epsilon) \mathbf{R}_1^T(\psi). \quad (47)$$

This is a non-linear equation of θ_A and θ_B , from which we can find the relation between them using the condition that the differentials of both sides must be equal. Then we obtain

$$\theta_B = \mathbf{T}(\psi) \theta_A, \quad \mathbf{T} \doteq \frac{\partial \theta_B}{\partial \theta_A}, \quad (48)$$

where the tangent operator for the canonical rotation vectors is as follows

$$\mathbf{T}(\psi) = \mathbf{I} + c_2 \tilde{\psi} + c_3 \tilde{\psi}^2, \quad (49)$$

where $c_3 \doteq (1 - c_1) / \|\psi\|^2$, while c_1, c_2 were used in the definition of **R**, see Eqs. (32) and (33). The operator **T** has the following properties:

1. At $\|\psi\| = 0$, the coefficients of \mathbf{T} are numerically indeterminate, so we replace c_1 and c_2 by the limit values given in Eq. (35), while for c_3 we use the limit value $\lim_{\|\psi\| \rightarrow 0} c_3 = 1/6$. In consequence of such modifications, $\mathbf{T}(\|\psi\| = 0) = \mathbf{I}$.
2. $\mathbf{T}(\psi)$ is singular at $\|\psi\| = 2k\pi$, ($k = 1, 2, \dots$), at which the determinant $\det \mathbf{T} = 2(1 - \cos \|\psi\|)/\|\psi\|^2$ is equal to zero. This is not a problem in computation of shells as the step size always is $< 2\pi$.
3. $\mathbf{T}(\psi)$ is not a periodic function of $\|\psi\|$, so we cannot shorten ψ .
4. $\mathbf{T}(\psi)$ is singular for $\|\psi\| \rightarrow \infty$, as then $\mathbf{T}(\psi) \rightarrow \mathbf{e} \otimes \mathbf{e}$. Hence, it is not advisable to use very long rotation vectors.

Several other properties are discussed in Wisniewski (2010b, pp. 184–185).

4.4 Differential $\chi\mathbf{T}$

The directional derivative of the tangent operator \mathbf{T} is defined as follows

$$\chi\mathbf{T} \doteq D\mathbf{T}(\psi) \cdot \theta^+, \quad (50)$$

for $\tilde{\psi}^+ = \tilde{\psi} + \epsilon \tilde{\theta}^+ \in T_I SO(3)$, and is needed in calculations of the second variation of the rotation tensor. For the operator \mathbf{T} of Eq. (49), we obtain

$$\begin{aligned} \chi\mathbf{T}(\psi, \theta^+) &= a_1 (\mathbf{e} \cdot \theta^+) \mathbf{I} + a_2 (\theta^+ \otimes \mathbf{e} + \mathbf{e} \otimes \theta^+) \\ &\quad + a_3 (\mathbf{e} \cdot \theta^+) (\mathbf{e} \otimes \mathbf{e}) + a_4 (\mathbf{e} \cdot \theta^+) \tilde{\psi} + a_5 \tilde{\theta}^+, \end{aligned} \quad (51)$$

where the scalar coefficients are

$$\begin{aligned} a_1 &= b_2 - b_1, & a_2 &= b_3 - b_1, \\ a_3 &= 3b_1 - b_2 - 2b_3, & a_4 &= -b_3 b_4 + b_1, & a_5 &= \frac{1}{2} b_4, \\ b_1 &= \frac{\sin \omega}{\omega^2}, & b_2 &= \frac{\cos \omega}{\omega}, & b_3 &= \frac{1}{\omega}, & b_4 &= \left[\frac{\sin(\omega/2)}{(\omega/2)} \right]^2. \end{aligned} \quad (52)$$

We see that the coefficients b_i ($i = 1, \dots, 4$) are numerically indeterminate at $\omega = 0$. For $\psi \rightarrow \mathbf{0}$, $\chi\mathbf{T} \rightarrow \frac{1}{2} \tilde{\theta}^+ \in so(3)$. Correctness of Eq. (51) can be verified approximately using the difference formula

$$D\mathbf{T} \cdot \theta^+ \approx \mathbf{T}(\psi + \theta^+) - \mathbf{T}(\psi).$$

4.5 First Variation of Rotation Tensor for Canonical Parametrization

Below we derive the formulae for the variation of the rotation tensor using either the additive composition or the multiplicative (left) composition.

A. For the additive composition of the rotation parameters,

$$\tilde{\psi}_\epsilon = \tilde{\psi} + \epsilon \tilde{\theta}_A \in T_1SO(3),$$

we define the variation as the following directional derivative:

$$\delta_{\tilde{\theta}_A} \mathbf{R}(\psi) \doteq D\mathbf{R}(\psi) \cdot \tilde{\theta}_A = \frac{d}{d\epsilon} [\mathbf{R}(\psi_\epsilon)]_{\epsilon=0}, \tag{53}$$

where ϵ is a scalar parameter. This derivative can be calculated directly using a symbolic algebra program, such as *Mathematica* or *Maple*, but more concise formulas can be obtained using method B described below.

B. For the left multiplicative composition rule, the perturbed rotation is defined as $\mathbf{R}_{B\epsilon} \doteq \mathbf{R}_2(\epsilon \tilde{\theta}_B) \mathbf{R}_B$, where $\tilde{\theta}_B \in so(3)$. The variation of \mathbf{R}_B w.r.t. $\tilde{\theta}_B$ is defined as the derivative of \mathbf{R}_B in the direction $\tilde{\theta}_B$,

$$\delta_{\tilde{\theta}_B} \mathbf{R}_B \doteq D\mathbf{R}_B \cdot \tilde{\theta}_B = \frac{d}{d\epsilon} [\mathbf{R}_2(\epsilon \tilde{\theta}_B) \mathbf{R}_B]_{\epsilon=0} = \frac{d}{d\epsilon} [\mathbf{R}_2(\epsilon \tilde{\theta}_B)]_{\epsilon=0} \mathbf{R}_B, \tag{54}$$

where

$$\frac{d}{d\epsilon} [\mathbf{R}_2(\epsilon \tilde{\theta}_B)]_{\epsilon=0} = \tilde{\theta}_B, \tag{55}$$

on use of the exponential representation

$$\mathbf{R}_{B\epsilon} = \exp(\epsilon \tilde{\theta}_B) = \mathbf{I} + \epsilon \tilde{\theta}_B + \dots + \frac{1}{n!} (\epsilon \tilde{\theta}_B)^n + \dots$$

Note that at $\mathbf{R}_B = \mathbf{I}$, we obtain $\delta_{\tilde{\theta}_B} \mathbf{R}_B = \tilde{\theta}_B$.

Relations Between Variations for Various Composition Rules We can rewrite Eq. (47) as $\mathbf{R}(\psi_\epsilon) = \mathbf{R}_2(\epsilon \tilde{\theta}_B) \mathbf{R}_1(\psi)$, and, by using

$$\psi_\epsilon = \psi + \epsilon \theta_A$$

and $\mathbf{R}_1(\psi) \doteq \mathbf{R}(\psi)$, we obtain

$$\underbrace{\mathbf{R}(\psi + \epsilon \theta_A)}_{\text{additive}} = \underbrace{\mathbf{R}_2(\epsilon \tilde{\theta}_B) \mathbf{R}(\psi)}_{\text{multiplicative, left}}, \tag{56}$$

where the infinitesimal rotation vectors θ_A and θ_B are shown in Fig. 4. We can calculate the derivative of Eq. (56) in the direction $\tilde{\theta}_A \in T_1SO(3)$ in a standard manner and the derivatives of both sides of it are as follows:

- (a) For the additive composition, $\mathbf{R}(\psi + \epsilon\theta_A)$, the variation $\delta_{\tilde{\theta}_A} \mathbf{R}(\psi)$ is defined as the directional derivative of Eq. (53).
- (b) For the left multiplicative composition, $\mathbf{R}_2(\epsilon\tilde{\theta}_B) \mathbf{R}(\psi)$, we have

$$\delta_{\tilde{\theta}_A} \left[\mathbf{R}_2(\epsilon\tilde{\theta}_B) \mathbf{R}(\psi) \right] = \frac{d}{d\epsilon} \left[\mathbf{R}_2(\epsilon\tilde{\theta}_B) \mathbf{R}(\psi) \right]_{\epsilon=0}, \tag{57}$$

in which we must express $\tilde{\theta}_B$ as a function of $\tilde{\theta}_A$. Using $\theta_B = \mathbf{T}(\psi) \theta_A$, where \mathbf{T} is defined in Eq. (49), we obtain

$$\delta_{\tilde{\theta}_A} \left[\mathbf{R}_2(\epsilon\tilde{\theta}_B) \mathbf{R}(\psi) \right] = \underbrace{\{[\mathbf{T}(\psi) \theta_A] \times \mathbf{I}\}}_{\text{skew-symm.}} \mathbf{R}(\psi). \tag{58}$$

The above both derivatives can be written together as follows:

$$\delta_{\tilde{\theta}_A} \mathbf{R}(\psi) = \{[\mathbf{T}(\psi) \theta_A] \times \mathbf{I}\} \mathbf{R}(\psi), \tag{59}$$

where the r.h.s. has a concise form indeed.

Remark 4.1 When the above variation is multiplied by a vector, e.g. by the shell director \mathbf{t}_3 , then θ_A can be separated as follows:

$$\begin{aligned} \delta \mathbf{a}_3 &= \delta_{\tilde{\theta}_A} \mathbf{R}(\psi) \mathbf{t}_3 = \{[\mathbf{T}(\psi) \theta_A] \times \mathbf{I}\} \mathbf{R}(\psi) \mathbf{t}_3 = [\mathbf{T}(\psi) \theta_A] \times \mathbf{a}_3 \\ &= -\mathbf{a}_3 \times [\mathbf{T}(\psi) \theta_A] = -\underbrace{(\mathbf{a}_3 \times \mathbf{I})}_{3 \times 3 \text{ matrix}} \mathbf{T}(\psi) \theta_A, \end{aligned} \tag{60}$$

where $\mathbf{a}_3 \doteq \mathbf{R}(\psi) \mathbf{t}_3$ was used. This form is more suitable for numerical implementations, as it involves a product of the matrix and the vector θ_A .

Second Variation of Rotation Tensor for Canonical Parametrization The first variation is defined as the following directional derivative:

$$\delta \mathbf{R} \doteq D\mathbf{R}(\tilde{\psi}) \cdot \tilde{\theta}^- = \frac{d}{d\epsilon} [\mathbf{R}(\tilde{\psi}^-)]_{\epsilon=0}, \tag{61}$$

where $\tilde{\psi}^- = \tilde{\psi} + \epsilon \tilde{\theta}^- \in T_1SO(3)$, while the second variation is defined as the directional derivative of the first variation

$$\chi \delta \mathbf{R} \doteq D[\delta \mathbf{R}] \cdot \tilde{\theta}^+ = \frac{d}{d\epsilon} [\delta \mathbf{R}(\tilde{\psi}^+)]_{\epsilon=0}, \tag{62}$$

where $\tilde{\psi}^+ = \tilde{\psi} + \epsilon \tilde{\theta}^+ \in T_1SO(3)$. Note that we extended the notation used earlier, and, instead of θ_A , we use θ^- and θ^+ , and, instead of ψ_e , we use ψ^- and ψ^+ . Besides, the variations “ δ ” and “ χ ” are associated with $\tilde{\theta}^-$ and $\tilde{\theta}^+$, respectively. The above directional derivatives can be calculated using a symbolic manipulation program, or obtained by the multiplicative composition of rotation tensors.

For the multiplicative composition of the rotation parameters, we have Eq. (59), which, in the current notation, can be rewritten as follows:

$$\delta \mathbf{R} = \{[\mathbf{T}(\psi) \theta^-] \times \mathbf{I}\} \mathbf{R}(\psi), \quad (63)$$

while the second differential of \mathbf{R} is defined as the directional derivative of the first variation of Eq. (63) in direction θ^+ ,

$$\chi(\delta \mathbf{R}) \doteq \left. \frac{d}{d\epsilon} \{[\mathbf{T}(\psi + \epsilon\theta^+) \theta^-] \times \mathbf{I}\} \mathbf{R}(\psi + \epsilon\theta^+) \right|_{\epsilon=0}. \quad (64)$$

By the formula for the derivative of a cross-product of a vector and a tensor with respect to the scalar ϵ , the second derivative becomes

$$\chi(\delta \mathbf{R}) = \{(\chi \mathbf{T} \theta^-) \times \mathbf{I}\} \mathbf{R} + \{(\mathbf{T} \theta^-) \times \mathbf{I}\} \chi \mathbf{R}. \quad (65)$$

For $\chi \mathbf{R} = [(\mathbf{T} \theta^+) \times \mathbf{I}] \mathbf{R}$, this becomes

$$\chi(\delta \mathbf{R}) = \{[(\chi \mathbf{T} \theta^-) \times \mathbf{I}] + [(\mathbf{T} \theta^-) \times \mathbf{I}][(\mathbf{T} \theta^+) \times \mathbf{I}]\} \mathbf{R}, \quad (66)$$

where \mathbf{R} is factored out of the braces. The second component of this formula can be directly evaluated. Regarding the first component, the differential $\chi \mathbf{T}$ is defined in Eq. (51), and we can calculate the product

$$\begin{aligned} \chi \mathbf{T}(\psi, \theta^+) \theta^- &= a_1 (\mathbf{e} \cdot \theta^+) \theta^- + a_2 (\mathbf{e} \cdot \theta^-) \theta^+ + a_2 (\theta^+ \cdot \theta^-) \mathbf{e} \\ &+ a_3 (\mathbf{e} \cdot \theta^+) (\mathbf{e} \cdot \theta^-) \mathbf{e} + a_4 (\mathbf{e} \cdot \theta^+) \tilde{\psi} \theta^- + a_5 (\theta^+ \times \theta^-). \end{aligned} \quad (67)$$

The term $(\chi \mathbf{T} \theta^-) \times \mathbf{I}$ is the associated skew-symmetric tensor, and we see that only two terms (third and fourth) are symmetric with respect to θ^- and θ^+ . The symmetry of the tangent operator (stiffness matrix) for the Newton method affects the speed of computations; this issue was considered, e.g., in Simo and Vu-Quoc (1986), Cardona and Geradin (1988), Simo (1992), Buechter and Ramm (1992), Makowski and Stumpf (1995).

4.6 Simple Algorithm for Treating Finite Rotations

In this section we focus our attention on the simple scheme of treating finite rotations, which corresponds to the Updated Lagrangian description in computational mechanics.

We assume that the Newton method is used to solve the non-linear equilibrium equations of shells. The updates of rotational parameters are performed after each iteration and after each load step of the Newton method. Several update schemes can be considered and the question which one is optimal is not easy to answer theoretically; numerical tests indicate that they do not perform identically. Especially when the solution has bifurcation points then different branches of the solution can be followed for various update schemes.

Note that a good testing ground for the algorithmic issues related to finite rotations provide the equations of a 3D beam, which are much simpler than the shell equations yet they involve 3-parameter rotations. Similarly, the equations for the angular motion of a rigid body are relatively simple, although the questions of conservation of the angular momentum and the kinetic energy by a dynamic algorithm by no means are trivial, see Simo and Wong (1991). Dynamics, however, remains beyond the scope of this work.

Below we present a simple additive/multiplicative update algorithm based on the left composition rule of rotations, see Fig. 5. It is formulated in the plane tangent to $SO(3)$ at \mathbf{R}_A , where $\mathbf{R}_A = \mathbf{R}_n$ is the converged solution in the previous step n . Using the notation of Eq. (45), the total rotation \mathbf{R}_C is related to the rotation for the current step as follows:

$$\mathbf{R}_C = \underbrace{\mathbf{R}(\Delta\psi) \mathbf{R}(\psi)}_{\text{current step}} \mathbf{R}_A. \tag{68}$$

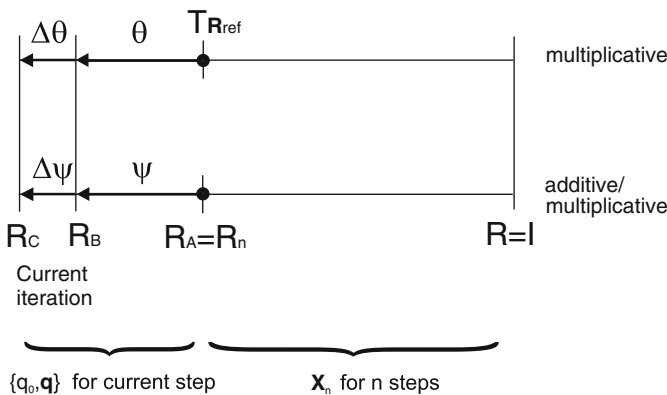


Fig. 5 Two schemes of treating finite rotations; the second one is described in this paper

Table 2 Additive/multiplicative scheme for rotations

Initialize \mathbf{X}	← total quaternion
Loop of Newton method	
$\mathbf{X}_n = \mathbf{X}$	
$\psi = \mathbf{0}$	
Iteration loop	
Form equilibrium equations using (\mathbf{X}, ψ) , solve for $\Delta\psi$	
Update	
$\psi = \psi + \Delta\psi$	← for increment (additive update)
End of Iteration loop	
Calculate quaternion for step	
$\psi \rightarrow \mathbf{q}$	
Update	
$\mathbf{X}_{n+1} = \{q_0, \mathbf{q}\} \circ \mathbf{X}_n$	← total (multiplicative update)
$\mathbf{X} = \mathbf{X}_{n+1}$	
End of Loop of Newton method	

We use the canonical rotation vector ψ associated with the step of the Newton method, (related to \mathbf{R}_A) as the rotational unknown. In a numerical implementation, we do not use rotation matrices but quaternions, because they require less storage and are easily re-normalized. The canonical rotation vectors and quaternions can be used together, as we can transform between them using Eqs. (43) and (44).

In the notation traditionally used in computational mechanics, the variations of the rotation tensor \mathbf{Q}_0 (which was used in the shell kinematical hypothesis of Eq. (3)) can be expressed as follows:

$$\delta\mathbf{Q}_0 = \text{Skew}[\mathbf{T}(\psi) \delta\psi] \mathbf{Q}_0, \quad \Delta\mathbf{Q}_0 = \text{Skew}[\mathbf{T}(\psi) \Delta\psi] \mathbf{Q}_0, \quad (69)$$

$$\Delta\delta\mathbf{Q}_0 = \{\text{Skew}[\chi\mathbf{T}(\psi, \Delta\psi) \delta\psi] + \text{Skew}[\mathbf{T}(\psi) \delta\psi] \text{Skew}[\mathbf{T}(\psi) \Delta\psi]\} \mathbf{Q}_0,$$

where Eqs. (63) and (66) were used. Besides, $\mathbf{Q}_0 \doteq \mathbf{Q}_0(\psi)$ is associated with the rotation vector ψ for the current step. $\text{Skew}[\mathbf{v}] \doteq \mathbf{v} \times \mathbf{I}$ is the skew-symmetric matrix associated with the axial vector \mathbf{v} , previously designated as $\tilde{\mathbf{v}}$, see, e.g., Eq. (30).

The simple additive/multiplicative update algorithm is shown in Table 2, and it has the following features:

1. Within the load step, we keep the total quaternion \mathbf{X} unchanged, where \mathbf{X} corresponds to $\mathbf{R}_A = \mathbf{R}_n$. However, in each iteration, we update the rotation vector accumulating additively the increments of rotation vector,

$$\psi = \psi + \Delta\psi, \quad (70)$$

where $\Delta\psi$ is the increment for iteration. Note that at the beginning of the load step $\psi = \mathbf{0}$.

2. When iterations of the Newton method for the step have converged then we convert ψ into the quaternion for the step $\{q_0, \mathbf{q}\}$ using Eq. (44). Then we multiplicatively compose the total quaternion \mathbf{X} and the quaternion for step $\{q_0, \mathbf{q}\}$ using Eq. (40). The whole sequence of operations is as follows:

$$\psi \rightarrow \mathbf{q} \rightarrow \mathbf{X}_{n+1} = \{q_0, \mathbf{q}\} \circ \mathbf{X}_n. \quad (71)$$

We must be aware that the composition rule for (finite) canonical rotation vectors, is not additive, in general, so Eq. (70) is only approximate! A more correct approach is to convert $\Delta\psi$ into a quaternion and compose it with the quaternion for the step in each iteration; such an algorithm is described as Scheme 2 in Wisniewski (2010b, p.205).

The simple algorithm of Table 2 has several advantages:

1. As the ψ for a step is stored anyhow by FE codes, additionally only 1 quaternion/node needs to be stored.
2. It conforms with a typical solution strategy implemented in incremental FE codes, in which a convergence within a step is controlled using vector quantities, e.g., in Taylor (2014).

We have verified on numerous examples that this simple algorithm performs very well in non-linear statics of shells.

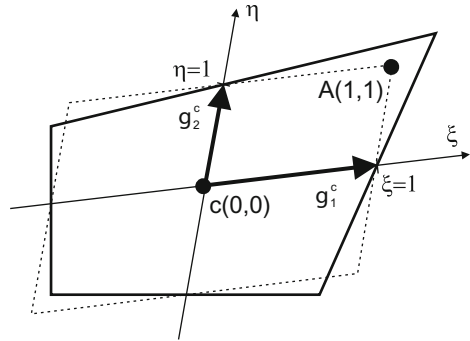
5 Enhanced/Mixed HW Shell Elements

In this section, we characterize the basic features of our 4-node HW shell elements, and we describe the treatment of independent fields in the shell HW functional. The standard bi-linear approximations are applied to compatible displacements and compatible rotational parameters. The assumed fields are expressed in terms of the skew coordinates.

5.1 Skew Coordinates

Defining the assumed representations of stress and strain in the 4-node HW elements, we use the skew coordinates instead of the natural ones coordinates. It is in accord with the results of Wisniewski and Turska (2008, 2009), where it is shown that this modification improves accuracy of mixed elements and renders that the homogenous equilibrium equations and the compatibility condition are satisfied pointwise for arbitrary shape of elements.

Fig. 6 Natural basis at the element's center and the 'fictitious' parallelogram (dotted line) obtained for $\bar{\mathbf{y}} = \xi \mathbf{g}_1^c + \eta \mathbf{g}_2^c$



Natural Basis at Element's Center The position vector of a 4-node element in the initial configuration is approximated as follows:

$$\mathbf{y}(\xi, \eta) = \sum_{I=1}^4 N_I(\xi, \eta) \mathbf{y}_I, \quad N_I(\xi, \eta) \doteq \frac{1}{4}(1 + \xi_I \xi)(1 + \eta_I \eta), \quad (72)$$

where N_I are the standard bi-linear shape functions, $\xi, \eta \in [-1, +1]$ are the natural coordinates and $\{\xi_I, \eta_I\}$ are the coordinates of nodes $I = 1, \dots, 4$.

The vectors of the natural basis are defined as

$$\mathbf{g}_1(\xi, \eta) \doteq \frac{\partial \mathbf{y}(\xi, \eta)}{\partial \xi}, \quad \mathbf{g}_2(\xi, \eta) \doteq \frac{\partial \mathbf{y}(\xi, \eta)}{\partial \eta}. \quad (73)$$

At the element's center, $\mathbf{g}_1^c \doteq \mathbf{g}_1|_{\xi, \eta=0}$ and $\mathbf{g}_2^c \doteq \mathbf{g}_2|_{\xi, \eta=0}$. In general, \mathbf{g}_1^c and \mathbf{g}_2^c are neither unit nor mutually orthogonal, see Fig. 6.

In the reference Cartesian basis $\{\mathbf{i}_1, \mathbf{i}_2\}$, the position vector is expressed as $\mathbf{y} = x\mathbf{i}_1 + y\mathbf{i}_2$. The Jacobian matrix is defined as

$$\mathbf{J} \doteq \begin{bmatrix} \frac{\partial x}{\partial \xi} & \frac{\partial x}{\partial \eta} \\ \frac{\partial y}{\partial \xi} & \frac{\partial y}{\partial \eta} \end{bmatrix} = \begin{bmatrix} \mathbf{g}_1 \cdot \mathbf{i}_1 & \mathbf{g}_2 \cdot \mathbf{i}_1 \\ \mathbf{g}_1 \cdot \mathbf{i}_2 & \mathbf{g}_2 \cdot \mathbf{i}_2 \end{bmatrix}, \quad (74)$$

and, at the element's center, $\mathbf{J}_c \doteq \mathbf{J}|_{\xi, \eta=0}$.

Skew Coordinates It is a common belief that the natural coordinates $\xi, \eta \in [-1, +1]$ are associated with the natural basis at the element's center $\{\mathbf{g}_1^c, \mathbf{g}_2^c\}$, see Fig. 6. This, however, is true only for parallelograms but not for irregular (trapezoidal) shapes. The coordinates which are associated with $\{\mathbf{g}_1^c, \mathbf{g}_2^c\}$ are designated as "skew" and can be derived as shown below.

Consider the position vector relative to the element's center, and express it the basis $\{\mathbf{g}_1^c, \mathbf{g}_2^c\}$ as

$$\bar{\mathbf{y}} \doteq \mathbf{y} - \mathbf{y}_c = x_S \mathbf{g}_1^c + y_S \mathbf{g}_2^c, \quad (75)$$

where x_S, y_S are the just-introduced skew coordinates. We see that these coordinates are defined similarly to the contravariant components of the position vector, but the elemental natural basis $\mathbf{g}_1^c, \mathbf{g}_2^c$ is used instead of the local natural basis $\mathbf{g}_1, \mathbf{g}_2$. Using Eq. (75), we can express the skew coordinates in terms of the natural coordinates in the following way.

First, we find the relation between the skew coordinates and the coordinates $\{x, y\}$ associated with the Cartesian reference basis $\{\mathbf{i}_1, \mathbf{i}_2\}$. The position vector can be written in the two basis as follows:

$$\bar{x} \mathbf{i}_1 + \bar{y} \mathbf{i}_2 = x_S \mathbf{g}_1^c + y_S \mathbf{g}_2^c. \quad (76)$$

Taking a scalar product of this equation with the vectors \mathbf{i}_1 and \mathbf{i}_2 , we obtain two equations, which are solved for the skew coordinates,

$$\begin{bmatrix} x_S \\ y_S \end{bmatrix} = \mathbf{J}_c^{-1} \begin{bmatrix} \bar{x} \\ \bar{y} \end{bmatrix}, \quad (77)$$

where \mathbf{J}_c is the Jacobian of Eq. (74) at the element's center.

Next, we find the relation between the skew coordinates and the natural coordinates. By approximations of Eq. (72), used in Eq. (77), we obtain the mapping between these two types of coordinates

$$\begin{bmatrix} x_S \\ y_S \end{bmatrix} = \begin{bmatrix} \xi + A \xi \eta \\ \eta + B \xi \eta \end{bmatrix}, \quad (78)$$

where A and B are functions of a_i, b_i . Alternatively, they can be expressed in terms of the determinant of the Jacobian \mathbf{J} of Eq. (74), the determinant of which can be expanded as $\det \mathbf{J} = j_c + (j, \xi)_c \xi + (j, \eta)_c \eta$, where $j_c = a_1 b_2 - a_2 b_1$, $(j, \xi)_c = a_1 b_3 - a_3 b_1$, and $(j, \eta)_c = a_3 b_2 - a_2 b_3$. It can be verified that

$$A = \frac{(j, \eta)_c}{j_c}, \quad B = \frac{(j, \xi)_c}{j_c}, \quad (79)$$

see Wisniewski and Turska (2008) for details. Hence, the skew coordinates are expressed in terms of the natural coordinates by Eqs. (78) and (79). Note that for parallelograms, $(j, \xi)_c = (j, \eta)_c = 0$, so $A = B = 0$, and then the skew coordinates are equal to the natural coordinates.

If we define the position of an irregular trapezoidal element using the formula with the natural coordinates, i.e. $\bar{\mathbf{y}} = \xi \mathbf{g}_1^c + \eta \mathbf{g}_2^c$, then the 'fictitious' parallelogram shown in Fig. 6 is obtained. On the other hand, $\bar{\mathbf{y}} = x_S \mathbf{g}_1^c + y_S \mathbf{g}_2^c$ reproduces the element's shape exactly.

Finally, the skew coordinates are used to define the assumed fields (stresses and strains) only, while for the compatible displacements/rotational parameters, the standard natural coordinates are used.

5.2 Assumed Stress or Couple Resultants and Assumed Shell Strains

Let us take the shell HW functional of Eq. (19) as a starting point. All the fields marked by the asterisk in this functional will be treated as the assumed fields, which is indicated by the superscript “a”,

$$\mathbf{N}^* \rightarrow \mathbf{N}^a, \quad \mathbf{M}^* \rightarrow \mathbf{M}^a, \quad \boldsymbol{\varepsilon}^* \rightarrow \boldsymbol{\varepsilon}^a, \quad \boldsymbol{\kappa}^* \rightarrow \boldsymbol{\kappa}^a. \quad (80)$$

Let us denote the shell stress/couple resultants as $\boldsymbol{\sigma}^a \in \{\mathbf{N}^a, \mathbf{M}^a\}$ and the shell strains as $\boldsymbol{\varepsilon}^a \in \{\boldsymbol{\varepsilon}^a, \boldsymbol{\kappa}^a\}$. The assumed $\boldsymbol{\sigma}^a$ and $\boldsymbol{\varepsilon}^a$ are defined in the natural basis at the element’s center $\{\mathbf{g}_k^c\}$,

$$\boldsymbol{\sigma}^a = \sigma^{kl} \mathbf{g}_k^c \otimes \mathbf{g}_l^c, \quad \boldsymbol{\varepsilon}^a = \epsilon^{kl} \mathbf{g}_k^c \otimes \mathbf{g}_l^c, \quad k, l = 1, 2, \quad (81)$$

where σ^{kl} and ϵ^{kl} are the contravariant components of shell stress and strains, respectively. Denote the matrices of assumed components as $\boldsymbol{\sigma}^\xi \doteq [\sigma^{kl}]$ and $\boldsymbol{\varepsilon}^\xi \doteq [\epsilon^{kl}]$. They are transformed to the Cartesian reference basis using the transformation rule for contravariant components,

$$\boldsymbol{\sigma}^{ref} = \mathbf{J}_c \boldsymbol{\sigma}^\xi \mathbf{J}_c^T, \quad \boldsymbol{\varepsilon}^{ref} = \mathbf{J}_c \boldsymbol{\varepsilon}^\xi \mathbf{J}_c^T, \quad (82)$$

where \mathbf{J}_c is the Jacobian matrix \mathbf{J} of Eq. (74) at the element’s center. Note that we use the contravariant rule for stress and strains, but in Wisniewski and Turska (2009), Wisniewski et al. (2010) also other combinations of rules are tested.

In the current paper, the following representations are used for the shell stress/couple resultants $\boldsymbol{\sigma}^a$ and the shell strains $\boldsymbol{\varepsilon}^a$.

1. For the assumed stress/couple resultants, we use the 7-parameter representation,

$$\boldsymbol{\sigma}^\xi \doteq \begin{bmatrix} q_1 + q_2 y_S & q_5 + q_6 x_S + q_7 y_S \\ \text{sym.} & q_3 + q_4 x_S \end{bmatrix}. \quad (83)$$

Compared to the well-known 5-parameter representation of Pian and Sumihara (1984):

- (1) the skew coordinates are used instead of the natural ones, and
- (2) the off-diagonal terms are not constant but linear in x_S, y_S .

In Wisniewski and Turska (2008), the linking transformations for several forms of another 7-parameter representation existing in the literature are given but our tests indicate that the representation of Eq. (83) is more accurate for the elements with drilling rotation.

2. For the assumed shell strains, we use the 9-parameter representation:

$$\boldsymbol{\epsilon}^\xi \doteq \begin{bmatrix} q_1 + q_2 y_S + q_3 x_S & q_7 + q_8 x_S + q_9 y_S \\ \text{sym.} & q_4 + q_5 x_S + q_6 y_S \end{bmatrix}, \quad (84)$$

in which all components are linear in the skew coordinates x_S, y_S .

Remark 5.1 The assumed representations can be verified symbolically as follows.

1. For the assumed representations of stress, we check whether they satisfy the homogenous equilibrium equations

$$\frac{\partial \sigma_{xx}}{\partial x} + \frac{\partial \sigma_{xy}}{\partial y} = 0, \quad \frac{\partial \sigma_{xy}}{\partial x} + \frac{\partial \sigma_{yy}}{\partial y} = 0. \quad (85)$$

2. For the assumed representations of strain, we check whether they satisfy the compatibility condition,

$$\frac{\partial^2 \epsilon_{xx}}{\partial y^2} + \frac{\partial^2 \epsilon_{yy}}{\partial x^2} = 2 \frac{\partial^2 \epsilon_{xy}}{\partial x \partial y}. \quad (86)$$

For the representations assumed in skew coordinates, these equations are satisfied pointwise, even for irregular trapezoidal shapes of an element. If we use the same representations but in the natural coordinates then these equations are satisfied pointwise only for parallelograms, for details see Wisniewski and Turska (2008, 2009).

5.3 *Enhanced Assumed Displacement Gradient (EADG) Method*

For elements with the drilling rotation we should enhance the displacement gradient rather than the strain, because the former enhancement affects also the drilling RC. The *Enhanced Assumed Displacement Gradient (EADG)* method is a generalization of the *Incompatible Displacement (ID)* method of Wilson et al. (1973), Taylor et al. (1976), and was proposed for 2D elements in Simo and Armero (1992). We find it particularly beneficial for the 2D elements with the drilling rotation. For shells, we further modify this method as described in the sequel.

In the *Incompatible Displacement* method, the assumed incompatible displacements \mathbf{u}^{inc} are added to the compatible displacements \mathbf{u}^c , so the enhanced displacements are defined as $\mathbf{u} \doteq \mathbf{u}^c + \mathbf{u}^{\text{inc}}$. Then the enhanced deformation gradient becomes

$$\mathbf{F} = \mathbf{F}^c + \tilde{\mathbf{H}}, \quad (87)$$

where the compatible deformation gradient \mathbf{F}^c is defined by Eq. (4) and the enhancing matrix is constructed as follows:

$$\tilde{\mathbf{H}} \doteq \left[\frac{\partial \mathbf{u}^{\text{inc}}}{\partial \xi^k} \right] \mathbf{J}^{-1} \approx \left[\frac{\partial \mathbf{u}^{\text{inc}}}{\partial \xi^k} \right] \mathbf{J}_c^{-1} \left(\frac{j_c}{j} \right). \quad (88)$$

Note that the 2×2 -point Gauss integration of \mathbf{J}_c^{-1} (j_c/j) yields exactly the result of the 1-point integration of \mathbf{J}^{-1} .

Let us define the incompatible displacements in the natural basis at the element's center $\{\mathbf{g}_1^c, \mathbf{g}_2^c\}$ of Fig. 6,

$$\mathbf{u}^{\text{inc}}(\xi, \eta) \doteq \mathbf{g}_1^c u^{\text{inc}}(\xi, \eta) + \mathbf{g}_2^c v^{\text{inc}}(\xi, \eta), \quad (89)$$

which can be rewritten as

$$\begin{bmatrix} u_C^{\text{inc}} \\ v_C^{\text{inc}} \end{bmatrix} = \mathbf{J}_c \begin{bmatrix} u^{\text{inc}} \\ v^{\text{inc}} \end{bmatrix}, \quad (90)$$

where \mathbf{J}_c is the Jacobian matrix of Eq. (74) at the element's center, and $u_C^{\text{inc}}, v_C^{\text{inc}}$ are the components in the Cartesian basis $\{\mathbf{i}_k\}$. Then

$$\tilde{\mathbf{H}} = \mathbf{J}_c \begin{bmatrix} \frac{\partial u^{\text{inc}}}{\partial \xi} & \frac{\partial u^{\text{inc}}}{\partial \eta} \\ \frac{\partial v^{\text{inc}}}{\partial \xi} & \frac{\partial v^{\text{inc}}}{\partial \eta} \end{bmatrix} \mathbf{J}_c^{-1} \left(\frac{j_c}{j} \right). \quad (91)$$

In the method of *Enhanced Assumed Displacement Gradient* (EADG), we replace the matrix of derivatives by the matrix \mathbf{G} , and directly assume its form, without resorting to the concept of incompatible displacements and without differentiation,

$$\tilde{\mathbf{H}} \doteq \mathbf{J}_c \mathbf{G} \mathbf{J}_c^{-1} \left(\frac{j_c}{j} \right). \quad (92)$$

We use the above formula for 2D problems, but for shells, the EADG method can be modified as follows. Define the natural basis in the deformed (current) configuration,

$$\mathbf{g}_1^*(\xi, \eta) \doteq \frac{\partial \mathbf{x}(\xi, \eta)}{\partial \xi}, \quad \mathbf{g}_2^*(\xi, \eta) \doteq \frac{\partial \mathbf{x}(\xi, \eta)}{\partial \eta}, \quad (93)$$

where $\mathbf{x}(\xi, \eta)$ is the current position vector. At the element's center, $\mathbf{g}_1^{*c} \doteq \mathbf{g}_1^*|_{\xi, \eta=0}$ and $\mathbf{g}_2^{*c} \doteq \mathbf{g}_2^*|_{\xi, \eta=0}$, where, in general, these vectors are neither unit nor mutually orthogonal.

These basis vectors can be used to define the incompatible displacements, and then, instead of Eq. (89), we have

$$\mathbf{u}^{\text{inc}}(\xi, \eta) \doteq \mathbf{g}_1^{*c} u^{\text{inc}}(\xi, \eta) + \mathbf{g}_2^{*c} v^{\text{inc}}(\xi, \eta), \quad (94)$$

which can be rewritten as

$$\begin{bmatrix} u_C^{\text{inc}} \\ v_C^{\text{inc}} \end{bmatrix} = \mathbf{J}_c^* \begin{bmatrix} u^{\text{inc}} \\ v^{\text{inc}} \end{bmatrix}, \quad (95)$$

where $\mathbf{J}_c^* \doteq \partial \mathbf{x} / \partial \xi^k |_{\xi, \eta=0}$ is the Jacobian matrix for the deformed (current) configuration. Proceeding as previously, we obtain

$$\tilde{\mathbf{H}} = \mathbf{J}_c^* \begin{bmatrix} \frac{\partial u^{\text{inc}}}{\partial \xi} & \frac{\partial u^{\text{inc}}}{\partial \eta} \\ \frac{\partial v^{\text{inc}}}{\partial \xi} & \frac{\partial v^{\text{inc}}}{\partial \eta} \end{bmatrix} \mathbf{J}_c^{-1} \begin{pmatrix} j_c \\ j \end{pmatrix}. \quad (96)$$

As previously, when constructing the EADG method, we replace the matrix of derivatives by the matrix \mathbf{G} , to obtain

$$\tilde{\mathbf{H}} \doteq \mathbf{J}_c^* \mathbf{G} \mathbf{J}_c^{-1} \begin{pmatrix} j_c \\ j \end{pmatrix}. \quad (97)$$

This formula used in our enhanced HW and EADG shell elements because, as we verified on benchmarks, for this formula the performance was better than for Eq. (92). On the other hand, the two-dimensional EADG elements perform identically for both Eqs. (92) and (97).

Finally, let us define the matrix \mathbf{G} , which must correspond to the selected representation of the assumed stress/couple resultants. For the 7-parameter representation of stresses of Eq. (83), the 2-parameter representation is as follows:

$$\mathbf{G} \doteq \begin{bmatrix} 0 & y_S q_1 \\ x_S q_2 & 0 \end{bmatrix}. \quad (98)$$

Besides, we also use the 4-parameter representation, which is a sum of the EADG2 enhancement plus an analogous enhancement depending on the through-the-thickness coordinate $\zeta \in [-h/2, +h/2]$,

$$\mathbf{G} \doteq \begin{bmatrix} 0 & y_S (q_1 + \zeta q_2) \\ x_S (q_3 + \zeta q_4) & 0 \end{bmatrix}. \quad (99)$$

5.4 Approximation of Drilling RC

For the equal-order bi-linear interpolations of the displacement components and the drilling rotation, the drilling RC is incorrectly approximated; this issue was discussed in Wisniewski (2010a), Wisniewski and Turska (2012).

For simplicity, we consider a 2D problem with drilling rotation. The linearized form of the drilling RC for a bi-unit square element is as follows:

$$c \doteq \omega + \frac{1}{2}(u_{,\eta} - v_{,\xi}) = 0,$$

where $u_{,\eta} \doteq u_{1,2}$ and $v_{,\xi} \doteq u_{2,1}$, and, for the equal-order bilinear interpolations, we obtain

$$c \doteq \left[\omega_0 + \frac{1}{2}(u_2 - v_1) \right] + \left[\omega_1 + \frac{1}{2}u_3 \right] \xi + \left[\omega_2 - \frac{1}{2}v_3 \right] \eta + \underline{\omega_3 \xi \eta} = 0, \quad (100)$$

where the coefficients of the bilinear shape function of the displacements and the drilling rotation are u_i , v_i , ω_i ($i = 0, \dots, 3$). These coefficients are functions of the nodal values of the respective components.

We see that the $\xi\eta$ -term (underlined) contains only the rotational parameter ω_3 but no displacement parameters, which is incorrect, as these two types of parameters should be linked.

For this reason, we omit this term using either a linear expansion of the drilling RC at the element's center, or sampling at mid-side points of element's edges, see Wisniewski (2010b, p.318). Either one of these methods can be used when the drilling RC is imposed using the penalty method. For the Perturbed Lagrange method of Eq. (19), the same can be achieved by omitting the bi-linear term in the representation of the Lagrange multiplier, see Eq. (102). Then, one additional zero-eigenvalue appears in the tangent matrix and must be stabilized.

Approximation of Lagrange Multiplier for Drilling RC The Lagrange multiplier of the functional F_{RC} of Eq. (13) is assumed in the elemental natural basis $\{\mathbf{g}_k^c\}$ and transformed to the Cartesian basis $\{\mathbf{t}_k^c\}$, both at the element center, using the transformation rule for contravariant components

$$\mathbf{T}^a = \mathbf{J}_{Lc} \begin{bmatrix} 0 & T^a \\ -T^a & 0 \end{bmatrix} \mathbf{J}_{Lc}^T, \quad (101)$$

where \mathbf{J}_{Lc} is the local Jacobian at element's center, and the assumed representation for the Lagrange multiplier, is as follows:

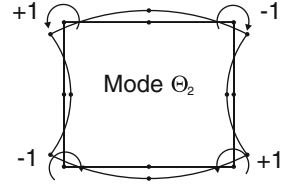
$$T^a(\xi, \eta) \doteq q_{15} + \xi q_{16} + \eta q_{17}, \quad (102)$$

We selected this representation in Wisniewski (2010a) as optimal for non-linear in-plane bending when the element is flat. For a warped element, we proposed in Wisniewski and Turska (2012) to modify this representation as follows:

$$T^a(\xi, \eta) \doteq q_{15} + \frac{1}{c}(\xi q_{16} + \eta q_{17}). \quad (103)$$

where $c \in (0, \infty)$ is a large number. Hence, effectively, the constant representation $T^a(\xi, \eta) \doteq q_{15}$ is used for warped elements, which is sufficient to provide a correct rank of the tangent matrix.

Fig. 7 Spurious mode Θ_2 for drilling rotation



Stabilization of the Spurious Mode Due to the omission of the $\xi\eta$ -term in Eq. (100), the tangent matrix for the drilling RC has one spurious zero eigenvalue, which can be eliminated using the stabilization function in the penalty form,

$$P_2 = 10^{-3} G V \Theta_2^2, \quad \Theta_2 \doteq \frac{1}{4}(\omega_1 - \omega_2 + \omega_3 - \omega_4), \quad (104)$$

where V is the element volume, and Θ_2 is the mode shown in Fig. 7. This form of the stabilization function was proposed in MacNeal and Harder (1988) for the Allman-type quadrilaterals, and it yields a stabilization matrix which has 1 non-zero eigenvalue.

This simple stabilization is sufficient for rectangular elements but not for irregular ones, as, e.g., it negatively affects the solution of the Cook's membrane test, compared to the solution for a non-stabilized element. Hence, we propose to improve the stabilization as follows. Let us re-write the spurious mode as

$$\Theta_2 \doteq \frac{1}{4} \mathbf{h}^T \boldsymbol{\omega}_I, \quad (105)$$

where $\boldsymbol{\omega}_I \doteq [\omega_1, \omega_2, \omega_3, \omega_4]^T$ are the nodal drilling rotations, and $\mathbf{h} \doteq [1, -1, 1, -1]^T$ is the hourglass vector. Then, instead of $\frac{1}{4}\mathbf{h}$, we can use the γ -vector, which was proposed to stabilize one-integration point elements in Flanagan and Belytschko (1981), and refined in numerous papers afterwards. Using the γ -vector, the Θ_2 mode is re-defined as

$$\Theta_2 \doteq \gamma^T \boldsymbol{\omega}_I, \quad (106)$$

where

$$\gamma \doteq \frac{1}{4} [\mathbf{h} - (\mathbf{h}^T \mathbf{S}^1) \mathbf{b}_1 - (\mathbf{h}^T \mathbf{S}^2) \mathbf{b}_2], \quad (107)$$

$$\mathbf{b}_1 \doteq \frac{1}{4A} [(\boldsymbol{\eta}^T \mathbf{S}^2) \boldsymbol{\xi} - (\boldsymbol{\xi}^T \mathbf{S}^2) \boldsymbol{\eta}], \quad \mathbf{b}_2 \doteq \frac{1}{4A} [-(\boldsymbol{\eta}^T \mathbf{S}^1) \boldsymbol{\xi} + (\boldsymbol{\xi}^T \mathbf{S}^1) \boldsymbol{\eta}],$$

$$\boldsymbol{\xi} \doteq [-1, 1, 1, -1]^T, \quad \boldsymbol{\eta} \doteq [-1, -1, 1, 1]^T.$$

Besides, \mathbf{S}^1 and \mathbf{S}^2 are the vectors of projections of the nodal relative position vectors on \mathbf{t}_1 and \mathbf{t}_2 , and $A = 4j_c$. The above modification is relatively simple to implement and clearly improves performance for irregular (skew, trapezoidal) shapes of the element.

6 Numerical Tests

In this section, we describe numerical tests of two four-node shell elements with 6 dofs/node listed in Table 3. They are based on the Green strain and are developed from the incremental form of the enhanced HW functionals of Eqs. (25)–(26). The assumed representations of stresses and strains are in terms of skew coordinates, see Sect. 5.2.

Both the tested HW elements have an identical membrane part (which was selected as ‘optimal’ in tests of the 2D+drill HW elements) and a transverse shear part. The differences are in the bending/twisting part, and they are as follows:

1. The HW47 element has the bending/twisting part fully analogous to the membrane part, see Sect. 3.2. It is a very good element but uses a considerable number of parameters.
2. The HW29 element has the bending/twisting part derived from the (non-enhanced) potential energy, see Sect. 3.2, otherwise it is identical to the HW47 element. This element has a reduced number of parameters and is faster than HW47.

In both these elements, the transverse shear part is treated by the HW functional with 8 (4 stress and 4 strain) parameters.

For the compatible transverse shear strain, we use the ANS method of Bathe and Dvorkin (1985). The related part of HW functional is constructed with the 2-parameter representations of the assumed stress and strain for each component, totally 8 parameters.

Regarding the drilling rotation part, it has the following features:

1. the perturbed Lagrange (PL) method is used with 3-parameter Lagrange multiplier \mathbf{T} , and
2. a stabilization based on the γ -vector is applied to eliminate 1 spurious mode, see Sect. 5.4. The regularization parameter $\gamma = G$ is used in both elements.

Table 3 Characteristics of the tested HW shell elements

Element	Assumed stresses			Assumed strains			Enhancement
	$N_{\alpha\beta}^a$	$M_{\alpha\beta}^a$	$N_{\alpha 3}^a$	$\varepsilon_{\alpha\beta}^a$	$\kappa_{\alpha\beta}^a$	$\varepsilon_{\alpha 3}^a$	
HW47	7p	7p	4p	9p	9p	4p	4p, Eq. (99)
HW29	7p	–	4p	9p	–	4p	2p, Eq. (98)

Drilling RC by PL with $\gamma = G$. “p” stands for “parameters”

The multipliers q_i of additional modes are eliminated on the element's level and updated by the scheme U2, see Wisniewski (2010b). In all elements, the 2×2 Gauss integration is used.

The elements are derived using the automatic differentiation program AceGen developed by Korelc (2002), and are tested within the finite element program FEAP developed by Taylor (2014), Zienkiewicz and Taylor (1989).⁴

All our elements have a correct number of zero eigenvalues and pass the constant strain patch tests, also with the drilling rotations unconstrained at boundary nodes, see Wisniewski and Turska (2006). Their performance is presented and compared with the enhanced EADG elements in Wisniewski and Turska (2012), where the following examples are presented:

- (1) Cook's membrane,
- (2) Pinched hemisphere with hole,
- (3) Twisted beam,
- (4) Short C-beam,
- (5) Pinched spherical shell,
- (6) Long C-beam and
- (7) L-shaped plate.

Two additional examples for the HW29 shell element are provided in Wisniewski and Turska (2014), and they are:

- (1) two one-element tests for non-zero drilling rotation, and
- (2) ring twisted by drilling rotations.

Below are presented two new examples:

- (1) the intersection of two perpendicular elements test, and
- (2) the cylindrical shell under wind load.

We also present additional results for the example of the long C-beam.

6.1 Intersection of Two Perpendicular Elements

Two square elements of the size 1×1 intersect at the right angle. The element 1 is clamped while two forces, $P = 1$, are applied at the free edge of the element 2, see Fig. 8. The forces are perpendicular to the element 2. The data is as follows: $E = 1.2 \times 10^7$, $\nu = 0.3$, and the thickness $h = 0.05$. The displacement in the direction of force P and the rotation at node A about the horizontal edge are monitored.

The linear analysis is performed, and the results at node A are presented in Table 4. Three our elements, the mixed/enhanced HW47, HW29 and the enhanced element EADG5A are compared to the element of Taylor (2014), which is the linear element (without the transverse shear) with 6 dofs/node described in Taylor (1988) and to the element S4 of N.N. (2013).

⁴The use of these programs is gratefully acknowledged.

Fig. 8 Intersection of two perpendicular elements. Initial geometry and load

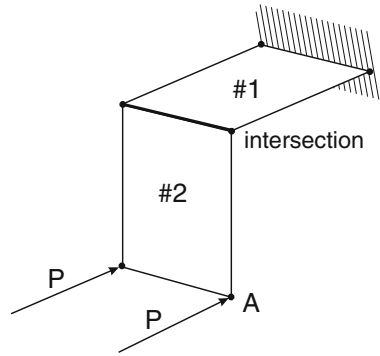


Table 4 Intersection of two perpendicular elements

Element	Displacement	Rotation
	$u_2 \times 10^2$	$\psi_1 \times 10^2$
HW47	1.9985	2.2548
HW29	1.9953	2.2488
EADG5A	1.9880	2.2415
FEAP 6 dofs/n	2.0515	2.3158
S4 ABAQUS	1.8760	2.2658

Linear solutions at A

6.2 Cylindrical Shell Under Wind Load

A vertical cylindrical shell is clamped at the bottom and has a free top edge. The data is as follows: $E = 3 \times 10^7$, $\nu = 0.3$, the length $L = 120$, the radius $R = 40$ and the thickness $h = 0.1064$. The wind pressure is constant in the axial direction but varies in the circumferential direction as follows:

$$q(\phi) = p_0 \sum_{n=0}^6 a_n \cos n\phi, \tag{108}$$

where p_0 is the load multiplier and the coefficients a_n have the values: $\{-0.220, -0.338, -0.533, -0.471, -0.166, 0.066, 0.055\}$. The distribution of pressure is shown by a broken line in Fig. 9, and the maximum $q = 1.607 p_0$ is at $\phi = 0^\circ$. Due to symmetry of loads and the shell, one half of the shell can be analyzed.

This example was computed in Brendel and Ramm (1980), where a non-uniform mesh of 4×8 shell elements S16 was used.⁵ We use our 4-node shell element HW29 and uniform meshes of $m \times 2m$ elements, where $m = 8, 16, 24, 32, 40$.⁶

⁵S16 is the 16-node shell element based on bi-cubic Lagrangian shape functions.

⁶ $2m$ is used in the circumferential direction.

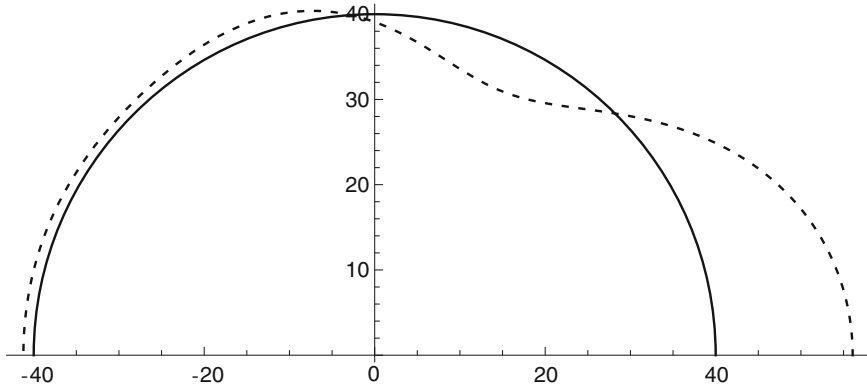


Fig. 9 Cylindrical shell under wind load. Pressure distribution

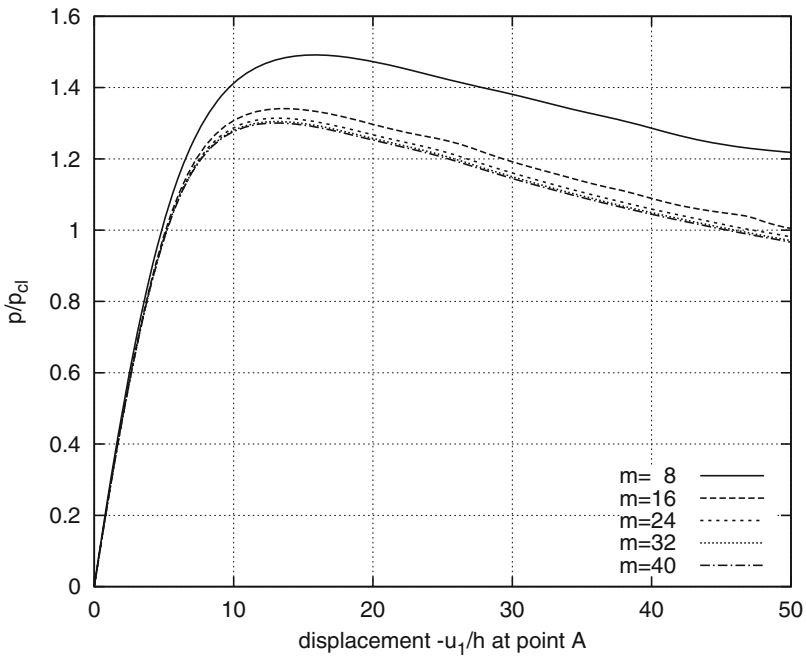


Fig. 10 Cylindrical shell under wind load. Mesh convergence

The arc-length method is used to compute the solution, and the results are presented in Fig. 10, where the plot of the radial displacement u_1/h (at top edge and $\phi = 0^\circ$) versus p/p_{cl} is shown.

Note that $p_{cl} = 2.03$ is a buckling load for a cylinder under uniform external pressure, see Brendel and Ramm (1980, p. 554). We see in Fig. 10 that the curves for $m = 24, 32, 40$ are close, which indicates the mesh convergence; therefore, we can

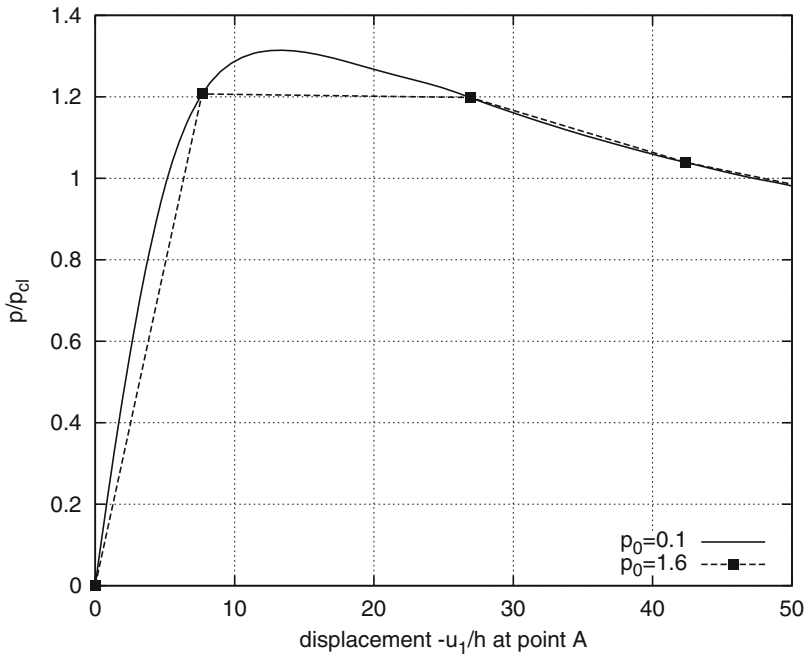


Fig. 11 Cylindrical shell under wind load. Nonlinear solution for large load increments

use $m = 24$ in further computations. The maximum pressure is 1.30, which is lower than 1.58 obtained in the cited paper.

To demonstrate very good convergence properties of the element HW29, we re-computed this example for large load increments $p_0 = 1.6$, and the convergence in the first 3 steps was achieved in 7, 11, and 8 iterations. The subsequent solution points are shown in Fig. 11.

The solutions in Figs. 10 and 11 were obtained for the so-called dead pressure (of a fixed direction and intensity) but we also tested the pressure acting in the direction of the *current* normal vector to the shell and of the intensity defined per *current* area of the shell. The virtual work of such a configuration-dependent pressure is

$$\delta F \doteq \int_A q \mathbf{n} \cdot \delta \mathbf{x}_0 dA, \tag{109}$$

where the current normal vector \mathbf{n} and the relation between the current area and initial area, dA and dA_0 , are defined as follows:

$$\mathbf{n} \doteq \frac{\mathbf{x}_{0,1} \times \mathbf{x}_{0,2}}{\|\mathbf{x}_{0,1} \times \mathbf{x}_{0,2}\|}, \quad dA = \frac{\|\mathbf{x}_{0,1} \times \mathbf{x}_{0,2}\|}{\|\mathbf{y}_{0,1} \times \mathbf{y}_{0,2}\|} dA_0. \tag{110}$$

Here $\mathbf{x}_0, \mathbf{y}_0$ are the position vectors of the reference surface for the deformed and non-deformed configurations, respectively. The linearization of Eq. (110) yields, in general, a nonsymmetric load tangent matrix, symmetrization of which is acceptable only when the free edge effects can be neglected and for a uniform pressure.

We re-computed this example for the so-defined configuration-dependent pressure, and the maximum load was only slightly lower than 1.30.

6.3 Long C-Beam

This test was proposed in Wagner and Gruttmann (2005). A long C-beam is fully clamped at one end and loaded by a vertical force P at the other end, see Fig. 12a. The material data is as follows: $E = 21000, \nu = 0.3$. Each flange is modeled by 36×2 elements and the web by 36×6 elements, totally 360 elements. At the clamped end, displacements and rotations are constrained.

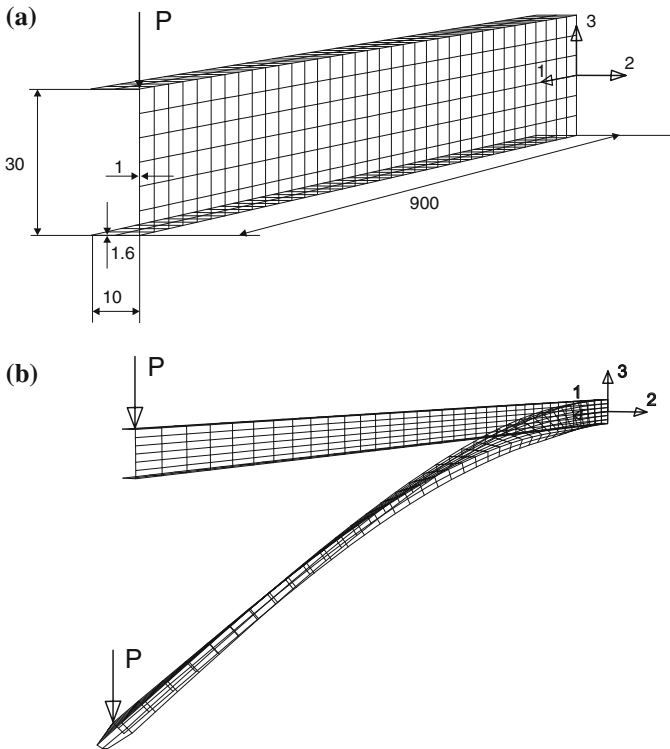


Fig. 12 Long C-beam. **a** Initial geometry and load. **b** Deformed configuration at $P = 20$

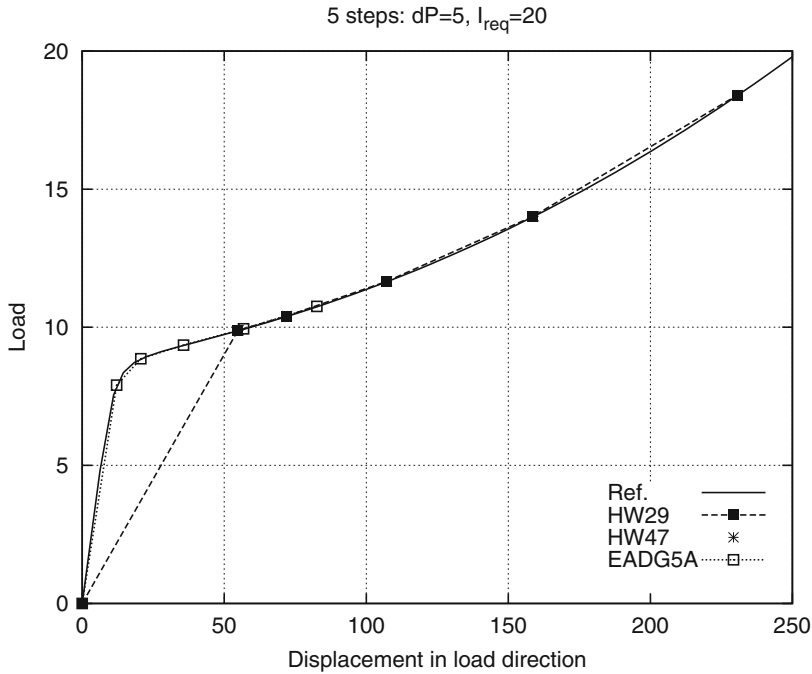


Fig. 13 Long C-beam. Non-linear solutions

The beam is slender and its response is mostly global, see Fig. 12b. The non-linear solution obtained by the arc-length method is shown in Fig. 13. The vertical displacement at the point where the force is applied is monitored. Only 5 steps are performed for the initial load increment $\Delta P = 11$ and the requested number of iterations per step $I_{req} = 20$. The HW29 element needed 53 iterations while the enhanced EADG5A element 77 iterations. Besides, for the HW29 element, the steps are longer and the final load is much higher than for the enhanced element. The solution for the element HW47 coincides with the solution for the HW29 element.

7 Final Remarks

These lecture notes describe several features of our mixed/enhanced four-node Hu-Washizu (HW) shell element *with* the drilling rotation.

1. In our HW29 element, which was developed in Wisniewski and Turska (2012), we applied the so-called incomplete (partial) HW functional, which reduces the number of elemental parameters from 47 to 29. The membrane part and the transverse shear part are treated by the HW functional, but the bending/twisting part is standard, i.e. derived from the strain energy. HW29 element is almost

equally accurate and has similar convergence properties to our reference element HW47, which is derived from the complete (pure) HW functional, but is faster.

2. For the membrane part, we selected the assumed fields which are different than the assumed fields of the HW elements *without* the drilling rotation. Besides, the representations of the assumed stresses and strains are in terms of the so-called skew coordinates and the EADG enhancement is applied, which affects positively also the drilling RC. These three modifications improved the accuracy of solutions for distorted meshes.
3. The drilling rotation is incorporated using the drilling part of the Rotation Constraint, and, in numerical implementation, we use the Perturbed Lagrange method and the 3-parameter (linear) interpolation of the multiplier field, which increases the radius of convergence. This, however, yields one spurious mode, which is identical to the Θ_2 -mode of the Allman/Cook's quadrilaterals of MacNeal and Harder (1988), where also a simple stabilization was proposed. This stabilization works correctly only for rectangular elements and we proposed to use the γ -stabilization, which is suitable for distorted meshes.

Concluding, the developed shell element *with* drilling rotation HW29, has an improved accuracy for coarse distorted meshes and superior convergence properties in non-linear problems, compared to the enhanced elements.

References

- Allman, D. J. (1984). A compatible triangular element including vertex rotations for plane elasticity analysis. *Computers & Structures*, 19(2), 1–8.
- Altenbach, J., Altenbach, H., & Eremeyev, V. A. (2010). On generalized Cosserat-type theories of plates and shells: a short review and bibliography. *Archive of Applied Mechanics*, 80, 73–92.
- Altman, S. L. (1986). *Rotations, quaternions and double groups*. Oxford: Clarendon Press.
- Angeles, J. (1988). *Rational kinematics* (Vol. 34). Springer Tracts in Natural Philosophy New York: Springer.
- Atluri, S. N., & Cazzani, A. (1995). Rotations in computational solid mechanics. *Archives of Computational Methods in Engineering*, 2(1), 49–138.
- Badur, J., & Pietraszkiewicz, W. (1986). On geometrically non-linear theory of elastic shells derived from pseudo-Cosserat continuum with constrained micro-rotations. In W. Pietraszkiewicz (Ed.), *Finite rotations in structural mechanics* (pp. 19–32). Berlin: Springer.
- Bathe, K.-J., & Dvorkin, E. N. (1985). A four-node plate bending element based on Mindlin-Reissner plate theory and mixed interpolation. *International Journal for Numerical Methods in Engineering*, 21, 367–383.
- Bergan, P. G., & Felippa, C. A. (1985). A triangular membrane element with rotational degrees of freedom. *Computer Methods in Applied Mechanics and Engineering*, 50, 25–60.
- Brendel, B., & Ramm, E. (1980). Linear and nonlinear stability analysis of cylindrical shell. *Computers & Structures*, 12, 549–558.
- Buechter, N., & Ramm, E. (1992). Shell theory versus degeneration—A comparison in large rotation finite element analysis. *International Journal for Numerical Methods in Engineering*, 34, 39–59.
- Cardona, A., & Geradin, M. (1988). A beam finite element nonlinear theory with finite rotations. *International Journal for Numerical Methods in Engineering*, 26, 2403–2438.
- Cartan, E. (1981). *The theory of spinors*. New York: Dover.

- Chróścielewski, J., & Witkowski, W. (2011). FEM analysis of Cosserat plates and shells based on some constitutive relations. *Z. Angew. Math. Mech.*, *91*, 400–412.
- Chróścielewski, J., Makowski, J., & Stumpf, H. (1992). Genuinely resultant shell finite elements accounting for geometric and material nonlinearity. *International Journal for Numerical Methods in Engineering*, *35*, 63–94.
- Chróścielewski, J., Kreja, I., & Sabik, A. (2011). Modeling of composite shells in 6-parameter nonlinear theory with drilling degree of freedom. *Mechanics of Advanced Materials and Structures*, *18*(6), 403–419.
- Cook, R. D. (1986). On the Allman triangle and a related quadrilateral element. A plane hybrid element with rotational d.o.f. and adjustable stiffness. *Computers & Structures*, *22*(6), 1065–1067.
- deBoer, R. (1982). *Vektor- und Tensorrechnung für Ingenieure*. Berlin: Springer.
- Eremeyev, V. A., Lebedev, L. P., & Altenbach, H. (2012). *Foundations of micropolar mechanics*. Heidelberg: Springer.
- Flanagan, D. P., & Belytschko, T. (1981). A uniform strain hexahedron and quadrilateral with orthogonal hourglass control. *International Journal for Numerical Methods in Engineering*, *17*, 679–706.
- Geradin, M., & Cardona, A. (2001). *Flexible multibody dynamics*. New York: Wiley.
- Geradin, M., & Rixen, D. (1995). Parametrization of finite rotations in computational dynamics. A review. *European Journal of Finite Elements*, *4*(Special Issue: Ibrahimbegovic A., Geradin M. (eds.)), 497–553.
- Goldstein, H. (1980). *Classical mechanics* (2nd ed.). Reading, MA: Addison Wesley.
- Gruttmann, F., & Wagner, W. (2006). Structural analysis of composite laminates using a mixed hybrid shell element. *Computer Methods*, *37*, 479–497.
- Hughes, T. J. R., & Brezzi, F. (1989). On drilling degrees of freedom. *Computer Methods in Applied Mechanics and Engineering*, *72*, 105–121.
- Korelc, J. (2002). Multi-language and multi-environment generation of nonlinear finite element codes. *Engineering with Computers*, *18*, 312–327.
- MacNeal, R. H., & Harder, R. L. (1988). A refined four-noded membrane element with rotational degrees of freedom. *Computers & Structures*, *28*(1), 75–84.
- Makowski, J., & Stumpf, H. (1995). On the “symmetry” of tangent operators in nonlinear mechanics. *Z. Angew. Math. Mech.*, *75*(3), 189–198.
- N.N. Abaqus Software, Ver. 6.13-3. Dassault Systemes Simulia, 2013.
- Panasz, P., & Wisniewski, K. (2008). Nine-node shell elements with 6 dofs/node based on two-level approximations. *Finite Elements in Analysis and Design*, *44*, 784–796.
- Pian, T. H. H., & Sumihara, K. (1984). Rational approach for assumed stress finite elements. *International Journal for Numerical Methods in Engineering*, *20*, 1685–1695.
- Rosenberg, R. M. (1977). *Analytical dynamics of discrete systems*. New York: Plenum Press.
- Simo, J. C. (1992). The (symmetric) Hessian for geometrically nonlinear models in solid mechanics: Intrinsic definition and geometric interpretation. *Computer Methods in Applied Mechanics and Engineering*, *96*, 189–200.
- Simo, J. C., & Armero, F. (1992). Geometrically non-linear enhanced strain mixed methods and the method of incompatible modes. *International Journal for Numerical Methods in Engineering*, *33*, 1413–1449.
- Simo, J. C., & Vu-Quoc, L. (1986). On the dynamics of 3-d finite strain rods. In *Finite element methods for plate and shell structures* (Vol. 2). Formulations and Algorithms (pp. 1–30). Swansea: Pineridge Press.
- Simo, J. C., & Wong, K. K. (1991). Unconditionally stable algorithms for rigid body dynamics that exactly preserve energy and momentum. *Computer Methods in Applied Mechanics and Engineering*, *31*, 19–52.
- Simo, J. C., Fox, D. D., & Hughes, T. J. R. (1992). Formulations of finite elasticity with independent rotations. *International Journal for Numerical Methods in Engineering*, *95*, 227–288.
- Spring, K. W. (1986). Euler parameters and the use of quaternion algebra in the manipulation of finite rotations: a review. *Mechanism and Machine Theory*, *21*(5), 365–373.

- Stuelpnagel, J. (1964). On the parametrization of three-dimensional rotational group. *SIAM Review*, 6(4), 422–430.
- Taylor, R. L. (2014). Program FEAP, Ver.8.4. Berkeley: University of California.
- Taylor, R. L. (1988). Finite element analysis of linear shell problems. In J. R. Whiteman (Ed.), *The mathematics of finite elements and applications VI* (pp. 191–203)., MAFELAP 1987 London: Academic Press.
- Taylor, R. L., Beresford, P. J., & Wilson, E. L. (1976). A non-conforming element for stress analysis. *International Journal for Numerical Methods in Engineering*, 10, 1211–1220.
- Wagner, W., & Gruttmann, F. (2005). A robust nonlinear mixed hybrid quadrilateral shell element. *International Journal for Numerical Methods in Engineering*, 64, 635–666.
- Wilson, E. L., Taylor, R. L., Doherty, W. P., & Ghaboussi, J. (1973). Incompatible displacement models. In S. J. Fennes, N. Perrone, A. R. Robinson, & W. C. Schnobrich (Eds.), *Numerical and computer methods in finite element analysis* (pp. 43–57). New York: Academic Press.
- Wisniewski, K. (2010a). Recent improvements in formulation of mixed and mixed/enhanced shell elements. In W. Pietraszkiewicz & I. Kreja (Eds.), *Shell structures. Theory and applications. Proceedings of 9th Conference SSTA'2009*, Jurata, October 14–16, 2009, pp. 35–44. Milton Park, Abingdon, Oxford, Taylor & Francis.
- Wisniewski, K. (2010b). *Finite rotation shells. Basic equations and finite elements for reissner kinematics*. Heidelberg: Springer.
- Wisniewski, K., & Turska, E. (2000). Kinematics of finite rotation shells with in-plane twist parameter. *Computer Methods in Applied Mechanics and Engineering*, 190(8–10), 1117–1135.
- Wisniewski, K., & Turska, E. (2001). Warping and in-plane twist parameter in kinematics of finite rotation shells. *Computer Methods in Applied Mechanics and Engineering*, 190(43–44), 5739–5758.
- Wisniewski, K., & Turska, E. (2002). Second order shell kinematics implied by rotation constraint equation. *Journal of Elasticity*, 67, 229–246.
- Wisniewski, K., & Turska, E. (2006). Enhanced Allman quadrilateral for finite drilling rotations. *Computer Methods in Applied Mechanics and Engineering*, 195(44–47), 6086–6109.
- Wisniewski, K., & Turska, E. (2008). Improved four-node Hellinger-Reissner elements based on skew coordinates. *International Journal for Numerical Methods in Engineering*, 76, 798–836.
- Wisniewski, K., & Turska, E. (2009). Improved four-node Hu-Washizu elements based on skew coordinates. *Computers & Structures*, 87, 407–424.
- Wisniewski, K., & Turska, E. (2012). Four-node mixed Hu-Washizu shell element with drilling rotation. *International Journal for Numerical Methods in Engineering*, 90, 506–536.
- Wisniewski, K., Turska, E. (2013). On mixed/enhanced Hu-Washizu shell elements with drilling rotation. In W. Pietraszkiewicz & J. Górski, (Eds.), *Shell structures. Theory and applications. Proceedings of 10th Conference SSTA'2013*, Gdańsk, October 16–18, Vol. 3, pp. 469–472, Milton Park, Abingdon, Oxford, 2014. CRC Press/Balkema, Taylor & Francis Group.
- Wisniewski, K., Wagner, W., Turska, E., & Gruttmann, F. (2010). Four-node Hu-Washizu elements based on skew coordinates and contravariant assumed strain. *Computers & Structures*, 88, 1278–1284.
- Wittenburg, J. (1977). *Dynamics of systems of rigid bodies*. Stuttgart: B.G. Teubner.
- Zienkiewicz, O. C., & Taylor, R. L. (1989). *The Finite element method* (4th edn., Vol. 1). Basic Formulation and Linear Problems. New York: McGraw-Hill.